Molecular and genetic characterisation of early aleurone development in barley (*Hordeum vulgare* L.)

Matthew Kevern Aubert

BSc. (Hons)

A thesis submitted to The University of Adelaide in fulfilment of the requirements for the degree of Doctor of Philosophy

The University of Adelaide

Faculty of Sciences

School of Agriculture, Food and Wine

THE UNIVERSITY of ADELAIDE

November 2018

Contents

Declaration

I certify that this work contains no material which has been accepted for the award of any other degree or diploma in my name, in any university or other tertiary institution and, to the best of my knowledge and belief, contains no material previously published or written by another person, except where due reference has been made in the text. In addition, I certify that no part of this work will, in the future, be used in a submission in my name, for any other degree or diploma in any university or other tertiary institution without the prior approval of the University of Adelaide and where applicable, any partner institution responsible for the joint-award of this degree.

I acknowledge that copyright of published works contained within this thesis resides with the copyright holder(s) of those works.

I also give permission for the digital version of my thesis to be made available on the web, via the University's digital research repository, the Library Search and also through web search engines, unless permission has been granted by the University to restrict access for a period of time.

I acknowledge the support I have received for my research through the provision of an Australian Government Research Training Program Scholarship.

Matthew Kevern Aubert

November 2018

Acknowledgments

Firstly, I would like to express deepest appreciation to my supervisors Matthew Tucker and Rachel Burton. Your continued support and endless assistance and advice during my candidature has been beyond helpful. Under your guidance and mentorship, I feel I have grown not only as a scientist and researcher, but as a person. Thank you for everything.

I would like to thank The University of Adelaide for awarding me a Faculty of Science Divisional Scholarship and the Grains Research & Development Corporation (GRDC) for further supporting me with a GRDC Grains Industry Research Scholarship. Further thanks must be extended to the Australian Research Council Centre of Excellence in Plant Cell Walls for the support and allowing me to travel and present my research around Australia.

I wish to express my sincere thanks to Neil Shirley for your guidance and valuable contributions to this thesis, without you the molecular component of this project would've been far more difficult. I am also greatly thankful to Kelly Houston and Ali Hassan for all the advice and input towards the GWAS component of this project. I would also like to thank Rohan Singh and Kylie Neumann for their expertise and technical support in transgenic generation and plant care.

Special shout out goes to the current, past and visiting Tucker Lab members! Laura Wilkinson, Dayton Bird, Cindy Callens, Jana Phan, Haoyu (Mia) Lou, Caterina Selva, Chao Ma, Weng Leong, Kum (Maple) Ang, Rosanna Petrella, Sara Pinto, Xiujuan Yang, Jorge Lora Cabrera, Ghazwan Karem and Susan Johnson. Each of you have contributed in some way to my PhD, whether that be through helping out with my project, developing ideas during our brain storming sessions we call lab meetings, or having long discussions about life, food, books, animals or games as we procrastinate

writing or figuring out what when wrong during experiments. Thank you for all the great times we've had together!

I would also like to thank past Plant Cell Wall members and current RabLab and Bulone Lab members, especially to Wai Li Lim, Trang Pham, Shi (Sandy) Khor, Natalie Betts, Helen Collins, Andrea Matros, Lisa O'Donovan, Robyn McBride, David Mathew, Natalie Kibble, Stav Manafis, Emma Drew, Alan Little, Julian Schwerdt, Suong Cu, Jake Parker, James Cowley, Jakob Schulz, Jelle Lahnstein, Juanita Lauer-Smith, Benjamin Keiller and George Dimitroff, for creating a warm, supportive, inspiring and motivating work environment.

To my closest friends who helped me find a healthy work-life balance through the countless breakfasts, lunches, dinners, parties, catch ups, holidays and endless banter while playing games together, I thank you. To Luke Oatway, Matthew Reynolds, Tom Fabian, Travis Fattori, Crishel Bauer, Kirstie Evans, Briony Roberts, Brad McCulloch, Kyle Brewer, Liam Tothill, Robert Yeomans, Isabella Johnson and Ada Chan, I sincerely thank you for helping me get through my PhD.

To my loving family, Cindy Aubert, Neville Aubert, Nathan Aubert, Prathet Dien and Spike, I am incredibly thankful for your unconditional love and support during this journey and encouraging me to pursue all my interests throughout my life. Thank you for being there for me through all my failures and success, I hope I can continue to make you proud with whatever comes next! I am also incredibly grateful to my extended family and all the support they have shown me.

I would like to thank my partner's family Rose Thomas, Ruby Thomas, Pippa Milroy, Paul Thomas and Griffin for everything you have done for us over the past few years and all the interest and support you have given me. Thank you for all the fun family gatherings, help and life advice you have provided.

Finally, last but not least, to my partner Hannah Thomas, thank you. With both of us undertaking a PhD, it has been a hectic couple of years and things haven't been easy. There have been many ups and downs, stress and excitement but all of it has been worth it. Words can't describe how important you have been to me during this time. Your intelligence, motivation, kindness and passion have inspired me to continuously better myself. I don't know if I could've survived this journey without you.

To all of you, thank you.

List of Publications and Expected Publications

1. Tucker MR, Lou H, **Aubert MK**, Wilkinson LG, Little A, Houston K, Pinto SC and Shirley NJ (2018) Exploring the Role of Cell Wall-Related Genes and Polysaccharides during Plant Development. **Plants** 7(2):42 (Published May 2018)
2. **Aubert MK**, Coventry S, Shirley NJ, Betts NS, Würschum T, Burton RA, Tucker MR (2018) Differences in hydrolytic enzyme activity accompany natural variation in mature aleurone morphology in barley (*Hordeum vulgare* L.). **Scientific Reports** 8:11025. (Published July 2018)
3. Shirley NJ, **Aubert MK**, Wilkinson LG, Bird DC, Lora J, Yang X and Tucker MR. Translating auxin responses into ovules, seeds and yield: insight from *Arabidopsis* and the cereals. **Journal of Integrative Plant Biology**. (Accepted October 2018)
4. Lim WL, Collins H, Byrt C, Lahnstein J, Shirley NJ, **Aubert MK**, Tucker MR, Peukert M, Matros A and Burton RA. Overexpression of *CslF6* gene in hull-less barley grain alters carbon partitioning endosperm development. **Journal of Experimental Botany** (Submitted November 2018)
5. **Aubert MK**, Houston K, Burton RA, Hassan AS, Würschum T, Shirley NJ and Tucker MR. Identification of candidate genes involved in barley (*Hordeum vulgare* L.) aleurone development by laser capture microdissection and genome wide association studies. (Unpublished)
6. **Aubert MK**, Johnson S, Wu D, Singh R, Davies C, Shirley NJ, Burton RA and Tucker MR. Aleurone development in barley (*Hordeum vulgare* L.) is regulated by auxin and homologues of the *Zea mays NAKED ENDOSPERM 1* and *SUPERNUMERARY ALEURONE LAYER 1* genes. (Unpublished)

Chapter 1

General Introduction

Thesis Introduction

Cultivation of cereals has been the cornerstone of the delevopment of civilisation around the world. Cereal grains are important for human health and nutrition and can be utilised for a number of processes in the brewing, fibre and food industries. One such cereal species important in these industries is barley (*Hordeum vulgare* L.), which is used as malt in brewing, as a major additive for animal feed and a component in various foods for human consumption. Within the barley grain, an outer tissue layer known as the aleurone contains high levels of dietary fibre, minerals and antioxidants, and is known to be crucial for grain germination. In barley and other cereal species, the aleurone releases enzymes during germination that stimulate the release of starch-derived energy reserves, and this is utilised in the production of malt for brewing. Barley is primarily used for malt production compared to other cereal species, potentially due to morphological differences in aleurone structure as a result of selective breeding. For example, in cereal grains such as maize (*Zea mays* L.) and wheat (*Triticum aestivum* L.), only a single layer of aleurone cells is present, whilst in barley, multilayered aleurones are observed. The significance of having more or less aleurone layers on germination or seed development still remains unclear. Despite the economic importance of barley aleurone, few details are available in regards to molecular cues controlling the differentiation of the aleurone from the inner starchy endosperm cells. Current research into aleurone morphology and development has primarily occurred in maize and rice (*Oryza sativa* L.). Therefore, the aims of this project were to investigate and characterise the molecular and genetic basis for aleurone development in barley.

Since barley is an important cereal crop, it has been selectively bred worldwide to produce many cultivars, each possessing various traits that support growth and productivity. The *Hordeum* genetic pool is therefore quite large, consisting of some

460,000 accessions, including cultivars, landraces, breeding lines and wild *Hordeum* species. With a large selection of barley accessions, barley transformation efficiency has also rapidly improved, making it easier to generate transgenic lines to study molecular factors involved in plant growth and development. Similarly, with the release of the barley genome, together with the barley accessions, many useful genetic tools can now be employed. For example, Genome Wide Association Studies utilise genetic diversity and a sequenced genome to investigate the genetic architecture of diverse traits. In this thesis, the genetic pool of the *Hordeum* species has been exploited in an attempt to identify candidate genes involved in aleurone development.

Thesis Structure

This thesis contains six chapters comprised of a general thesis introduction (Chapter 1), a review of the literature (Chapter 2), three research chapters in publication format (Chapters 3 – 5), one of which has been published (Chapter 4) and a final general discussion (Chapter 6). A schematic overview of the thesis structure is presented in Figure 1-1.

The literature review chapter, Chapter 2, aims to introduce the aleurone to the reader. The diversity of aleurone morphology within cereal species and its development in regard to endosperm development are discussed. Several genes and proteins known to influence development in a number of species are also summarised.

In Chapter 3, the complex pathway supporting barley aleurone development, involving both genetic and hormonal inputs, is described. This involved the development of barley transgenic lines targeting homologues of known maize aleurone genes, as well as examining the role of auxin in controlling sub-epidermal grain morphology. The

results suggest that factors influencing barley aleurone development are conserved, to a certain degree, across several cereal species.

Inter- and intra-species differences in aleurone layer number have been identified in the cereals but the significance of this variation during seed development and germination remains unclear. In Chapter 4, a published research paper (Aubert et al., 2018, *Scientific Reports*. 8: 1 – 14), describes the natural variation in mature aleurone features across a small panel of barley elite breeding lines. The paper identified correlations between aleurone traits and key germination enzymes, where genotypes with more aleurone showed increased levels of free β-amylase at grain maturity.

Following on from Chapter 4, the natural variation in aleurone morphology observed within this small panel suggested that a Genome Wide Association Study (GWAS) for genetic variation might be possible in a larger panel of genotypes. In Chapter 5, mature aleurone measurements from a larger panel were coupled with genotypic data and utilised for GWAS to identify regions of the barley genome associated with variation in aleurone morphology. Laser-capture microdissection, wholegrain and tissue-specific RNA sequencing were used to identify potential candidate genes influencing aleurone development in barley, as well as candidate cell-type specific marker genes.

The final chapter of this thesis presents a general discussion and explores future perspectives.

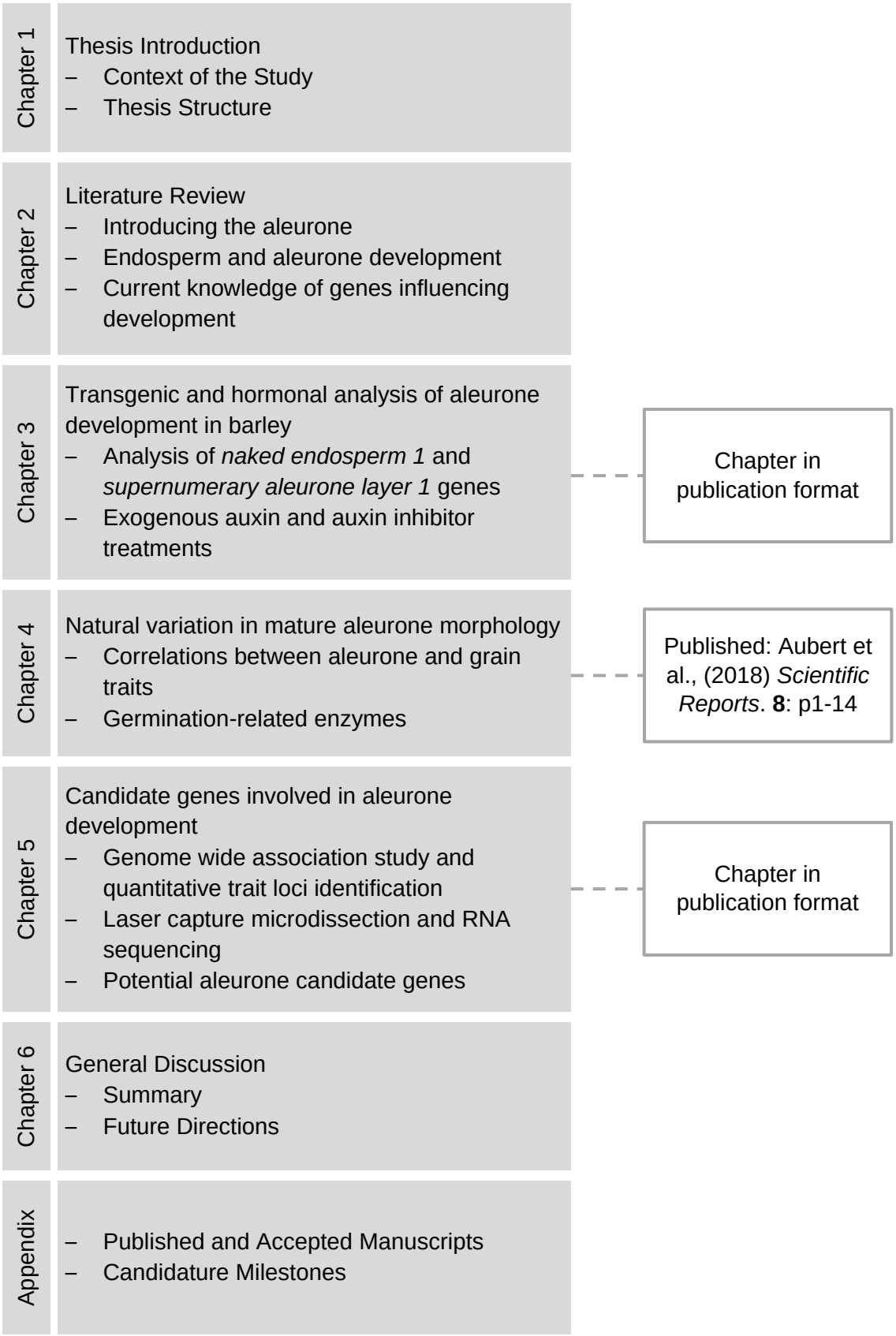

Figure 1-1: Schematic overview of thesis structure.

Chapter 2

Review of the Literature

Abbreviations

ABA	Abscisic acid
AP2TF	AP2 transcription factor
Chmp1	Charged multivesicular body protein 1/chromatin-modifying protein 1
CR4	CRINKLY 4
CSE	Central starchy endosperm
DAP	Days after pollination
DEK1	DEFECTIVE KERNEL 1
ESR	Embryo surrounding region
ETL	Endosperm transfer layer
EXP11	EXPANSIN 11
GA	Gibberellic acid
IDD	INTERMEDIATE1 domain
LTP3	LIPID TRANSFER PROTEIN 3
NKD	NAKED ENDOSPERM
NTM1	NAC with transmembrane motif1
PCD	Programmed cell death
PSV	Protein storing vacuoles
QTL	Quantitative trait loci
ROS1	REPRESSOR OF SILENCING 1
RPBF	Rice prolamin box binding factor
SAL1	SUPERNUMERARY ALEURONE LAYER 1
TA2	THICK ALEURONE 2
TF	Transcription factor
TNFR	Tumour Necrosis Factor Receptor
VP1	VIVIPAROUS 1

Introduction

Cereal grains represent a crucial human food source that also underpin a wide range of industrial applications such as beverage production, animal feed and biofuel production. Barley (*Hordeum vulgare* L.), an essential cereal crop with a worldwide production exceeding 141 million metric tonnes (2016 FAO statistics; http://faostat3.fao.org/download/Q/QC/E), has been widely studied in order to improve yield, quality and disease tolerance. Most of the human sought benefits of the barley grain are contained within the endosperm (Figure 2-1), a filial tissue that is not only essential in supporting embryonic growth, but is also crucial for contributing key components for human health, such as dietary fibre (Baik and Ullrich, 2008; Harris and Fincher, 2009) and antioxidants (Ragaee et al., 2006; Gamel and Abdel-Aal, 2012). Within the barley endosperm, different layers fulfil different functions; the inner starchy endosperm cells undergo multiple rounds of endoreduplication to increase their ploidy, accumulate starch as an energy storage product and undergo programmed cell death, while the peripheral aleurone layers are diploid, remain living for an extended period of time and release hydrolytic enzymes during germination to degrade the starchy endosperm thereby providing energy to the growing embryo. While the aleurone is known to be crucial for germination in cereals, it is unclear why the structure of the aleurone differs so significantly between species (i.e. aleurone cell layer(s) and aleurone cell size). Key factors and genes known to influence aleurone cell fate and differentiation have been identified in cereals such as maize (*Zea mays* L.); however, their molecular functions are often unclear. In order to further understand aleurone differences between species, gene activity and function of crucial developmental genes must be analysed.

This literature review will focus on cereal grain development with a particular emphasis on endosperm and aleurone development and differentiation. It is clear that variation

in aleurone cell structure and number of aleurone layers is observed between cultivars and species. This presents an opportunity to examine aleurone development in further detail to identify crucial genes controlling elements in the pathway, particularly in barley.

Barley: An important cereal crop

Cereal grains have been widely studied since they represent a crucial food source across the planet and contribute to the major calorie intake for an ever-growing human population. Likewise, at an industrial level, raw materials from cereal grain have been utilised for beverage production, such as beer and whisky, and are important for biofuel production (Becraft and Yi, 2011). Cereal grains, such as barley, are used as malt in brewing, as a major additive for animal feed and occasionally used as a component in various foods for human consumption, i.e. bread and pasta (Verardo et al., 2011). Barley is a member of the Poaceae family, a monocotyledonous family that includes many agriculturally important species such as maize, wheat (*Triticum aestivum* L.) and rice (*Oryza sativa* L.), and it is the fourth most important cereal grain worldwide (Mrízová et al., 2014). In 2016 worldwide production of barley exceeded 141 million metric tonnes, where approximately 9 million metric tonnes (~6%) was contributed by Australia worth $2.2 billion (FAO statistics; http://faostat3.fao.org/download/Q/QC/E). Of the 9 million metric tonnes, 64% was exported, 20% was used for malting and 11% was used for animal feed (FAO statistics; http://faostat3.fao.org/download/Q/QC/E). The remaining 5% was used for human consumption; the abundance of dietary fibre and antioxidants in barley grain contributes positively towards human health by decreasing cholesterol (Behall et al., 2004) and reducing symptoms of diabetes (Gamel and Abdel-Aal, 2012).

As barley is a valuable cereal crop, it has been bred worldwide to produce many useful cultivars, each possessing various traits that support growth and productivity, i.e. stress and disease tolerance, yield variation and flowering time. Similarly, some of these traits also affect end-use quality for malting and brewing. The genetic variation is large, consisting of some 460,000 accessions, including cultivars, landraces, breeding lines and wild *Hordeum* species (Sato et al., 2014). In recent years, the

accessibility of the barley genome (Mayer et al., 2012; Mascher et al., 2017) and improvements in barley transformation efficiency have made it easier to generate transgenic lines to study crucial factors involved in plant growth and development (Mrízová et al., 2014). This presents an opportunity to extend these resources to address fundamental details of cereal grain development, in particular, cell-type-specific pathways that may affect suitability of the barley grain for different end uses. The development of the barley endosperm and the importance of different endosperm cell types will be discussed in subsequent sections.

Endosperm development

Embryo sac formation

The barley endosperm is essential for supporting embryonic growth by supplying nutrients and protecting the embryo by providing a mechanical barrier during grain development (Yan et al., 2014). The precurser to endosperm formation in cereals is the female gametophyte, which is produced when a meiotically-reduced maternal megaspore undergoes mitotic division without cell wall formation between the nuclei. The resultant nuclei migrate to opposite ends of the immature embryo sac and undergo two more rounds of mitotic division, without cytokinesis. One of the four nuclei from each pole migrates to the centre of the syncytial embryo sac to become polar nuclei. Cell walls develop around the remaining nuclei and the result is a seven-celled, eight-nucleate female gametophyte (embryo sac) (Figure 2-2) (Drews et al., 1998; Olsen, 2004a). The endosperm results from a double fertilisation event between two maternal polar nuclei and one male sperm nucleus in the central cell of the embryo sac, which resides within the ovule of the flower (Olsen, 2004a; Becraft and Yi, 2011; Yan et al., 2014; Wilkinson and Tucker, 2017).

Post fertilisation; formation of the nuclear endosperm

The stages of endosperm development in cereals have been categorised into three types: coenocyte (Figure 2-3), cellularisation by alveolation (Figure 2-3) and differentiation (Figure 2-4) (Leroux et al., 2014; Yan et al., 2014). Upon fertilisation in cereals, the triploid endosperm nucleus in the central cell of the embryo sac undergoes several rounds of mitotic division. However, the formation of a cell plate between daughter cells does not occur, resulting in a multinucleated cell known as the endosperm coenocyte (Olsen, 2004a, 2004b; Yan et al., 2014). The nuclei repeatedly divide and disperse until they line the periphery of the central vacuole, thus ending the coenocyte stage (Leroux et al., 2014). The cellularisation stage initiates near the embryo with the formation of anticlinal cell walls separating the peripheral nuclei within tube-like structures known as alveoli. The nuclei then divide within each alveolus and become separated by new periclinal cell walls, with these cells continuing to divide until the central vacuole is fully cellularised (Figure 2-3) (Olsen, 2004a; Leroux et al., 2014).

Endosperm differentiation

Different seed components contribute to diverse biological functions (Lopes and Larkins, 1993; Olsen et al., 1999; Haughn and Chaudhury, 2005) and also display varied properties that can be utilised for different end uses. In the case of cereal endosperm, which is a structurally simple tissue, four key cell types are crucial for contributing these properties. These are the embryo surrounding region (ESR), endosperm transfer layer (ETL), central starchy endosperm (CSE) and aleurone cells, each of which confers different biological functions in grain maturation and in seed germination.

Embryo surrounding region

In maize, wheat, barley, *Arabidopsis* and other species, the endosperm adjacent to the embryo is cytologically different from the remaining endosperm. This region is the micropylar region or the more commonly known embryo surrounding region (ESR). In early grain development, the ESR is comprised of dense endosperm cells that surrounds the entire embryo. These cells are smaller than neighbouring cells, have a dense cytoplasm and contain a mass of highly ordered rough endoplasmic reticulum (Schel et al. 1984). During development, the ESR becomes restricted to the suspensor (cells connecting the embryo to the endosperm) before being succeeded by a liquid filled space around the embryo at later stages (Schel et al. 1984; Opsahl-Ferstad et al. 1997; Cosségal et al., 2007). Currently, the exact function of the ESR is unknown, however, it is hypothesised to play a role in embryo nutrition and/or in establishing an interface between the embryo and the endosperm (Cosségal et al., 2007). Several genes, such as sucrose transporter genes, have been found to be expressed in the ESR, potentially allowing direct sucrose transfer from the endosperm to the embryo (Bonello et al., 2000; Lafon-Placette and Köhler, 2014).

Endosperm transfer cells

The endosperm transfer layer (Figure 2-4 represented in green) cells within the developing endosperm are responsible for maternal to filial nutrient transfer. The ETL functions to facilitate transport across surfaces by developing cell wall ingrowths with plasma membranes enriched in transporter proteins (Vaughn et al., 2007; Thiel et al., 2008; Sreenivasulu et al., 2010). This increase in plasma membrane surface area and in the concentration of transporter proteins allows elevated rates of nutrient transport that is crucial for endosperm growth and development (Vaughn et al., 2007).

Starchy endosperm

The central starchy endosperm cells (Figure 2-4 represented in red/pink) accumulate starch and storage proteins. Cells comprising the CSE undergo a process of endoreduplication, meaning the genome replicates in the absence of cell division resulting in an elevated polyploidy (Sabelli, 2012). Endoreduplication is also associated with the rapid growth of endosperm cells and the biosynthesis and accumulation of starch and storage proteins. Therefore, endoreduplicated cells are typically large, highly metabolically active and have thin cell walls (Sabelli and Larkins, 2008). The benefits of endoreduplication may include: (1) Maximising allocated energy for synthesising storage products since cell walls do not assemble between daughter nuclei (Kowles, 2009), (2) undergoing fewer cell divisions to consume less energy (Sabelli, 2012), and (3) possibly boosting gene expression from the increased gene content (D'Amato, 1984; Kowles, 2009). The CSE cells accumulate storage products, such as starch, to act as energy reserves for germination and seedling establishment. Starch is the main compound synthesised in the barley endosperm and it is the primary energy reserve utilised during germination (Shaik et al., 2014).

As the grain matures, cells in the endosperm undergo programmed cell death (PCD). The PCD that occurs in the starchy endosperm is a different process compared to other tissues where the cells are degraded and the cellular constituents are recycled (Bozhkov and Lam, 2011). Here most cellular constituents remain in place (Fath et al., 2000). The starchy endosperm cells persist until hydrolytic enzymes degrade the cell walls and mobilise the internal starch reserves during germination. The remaining endosperm tissues such as the ETL and aleurone remain alive throughout grain maturity and do not undergo PCD until germination. Once germination is initiated by the uptake of water, hydrolytic enzymes are released to mobilise the endosperm

reserves. The enzymes primarily involved in starch degradation consist of amylases, which are synthesised in the aleurone and are controlled by hormones such as gibberellins (GA) and by sugar demand/starvation signals (Fath et al., 2000; Shaik et al., 2014).

Aleurone

The aleurone is a tissue layer present at the periphery of the endosperm that forms the epidermal layer of the endosperm. The aleurone cells are cubical in shape and are distinctly different to the large, irregularly shaped starchy endosperm cells (Figure 2-5 and Figure 2-6). Mature aleurone cells are characterised by thick autofluorescent cell walls and by aleurone granules (protein storage bodies) that form in protein storing vacuoles (PSVs) (Brown and Lemmon, 2007). Additionally, the aleurone may develop pigmentation due to the accumulation of anthocyanins (Becraft and Asuncion-Crabb, 2000; Yi et al., 2015). At grain maturity, the aleurone layer is crucial for metabolite mobilisation and germination initiation and consists of living cells compared to the dead starchy endosperm. The aleurone (Figure 2-4 represented in blue) is responsible for releasing lytic enzymes to degrade the starch granules within the starchy endosperm cells to support germination. Upon seed imbibition, the embryo synthesises and releases gibberellic acid (GA), which translocates to the aleurone where it can induce the transcription of these lytic enzymes (Fath et al., 2000). These enzymes consist of amylases, glucanases, xylanases, proteases and nucleases, which contribute to the degradation of the aleurone and starchy endosperm (Smith et al., 2005; Betts et al., 2017), providing the growing embryo with energy to support germination (Wang et al., 1998).

Differences in aleurone layer numbers and structure have been observed between cereal species. Most cereal grains such as maize and wheat have a single layer of

aleurone cells; however, barley has a multilayered aleurone (Figure 2-6) (Shapter et al., 2009). The significance of having more or less aleurone layers on germination or seed development still remains unclear. Currently, molecular models for cereal aleurone development are inferred from research in maize and rice while little is known for other cereal species.

Aleurone properties for human health

The aleurone from cereal grains possesses key nutrients that contribute to human health. By ingesting aleurone, human blood cholesterol can decrease (Behall et al., 2004) and diabetes symptoms can be reduced (Gamel and Abdel-Aal, 2012). For food production, the aleurone, along with the pericarp and testa, is considered part of the cereal bran. Bread and breakfast cereals that contain a large proportion of bran act to increase dietary fibre content. Similarly, the aleurone layer contributes vitamins, minerals and phenolic antioxidants to bran (Behall et al., 2004; Pins and Kaur, 2006; Kamal-Eldin et al., 2009; Gamel and Abdel-Aal, 2012; Hassan et al., 2017) and hence is beneficial to a variety of food products. Evidence also suggests that compounds within the aleurone may contribute to the prevention of certain chronic diseases such as cancer and cardiovascular disease (Zhou et al., 2004a; Del Rio et al., 2013). For example, phenolic antioxidants have favourable effects against these chronic diseases and are concentrated in the aleurone (Zhou et al., 2004b). Similarly, polysaccharides such as β-glucan are deposited in the aleurone and sub-aleurone cell walls (Charalampopoulos et al., 2002; Demirbas et al., 2005; Holtekjølen et al., 2006) and are highly fermentable (Topping et al., 2001), forming highly viscous solution in the human gut (Autio et al., 1996; Wood et al., 1998; Wood et al., 2000). These solutions have been found to reduce many metabolic syndromes as reviewed in Khoury et al. (2012).

The aleurone also incorporates potentially negative properties for consumption such as phytate (phytic acid). Phytate, the primary storage compound of phosphorus in seeds, can bind strongly to cations with high nutritional value such as potassium, magnesium and calcium. This binding renders these cations unavailable in the gut (Bohn et al., 2008). However, these harmful chemicals are far less concentrated in the aleurone compared to the abundance of dietary fibre, vitamins and minerals (Coulibaly et al., 2011). Another property of the aleurone that restricts nutritional quality is the presence of thick cell walls. Difficulties in obtaining nutritional benefits arise when the thick cell walls are unable to be digested, thus preventing the release of trapped nutrients. Hence this aspect also may decrease the putative benefit of consuming cereal aleurone, irrespective of the abundance of nutritionally beneficial components. Therefore, the aleurone represents an important factor for health applications as well as a key source of health-promoting compounds. The potential to increase availability of nutrients trapped in the thick cell walls during digestion could provide further health benefits.

Aleurone development

The aleurone does not initiate until after several rounds of periclinal and anticlinal cell division in the endosperm have taken place (Gillies et al., 2012). In maize, the aleurone typically appears at 6-10 days after pollination (DAP) depending on genetic and environmental factors (Sabelli and Larkins, 2009; Chen et al., 2014; Doll et al., 2017), while in rice, the aleurone can appear as early as 4-5 DAP (Ishimaru et al., 2015; Xu et al., 2016). However, in barley, aleurone development occurs at around 6-8 days DAP (Bosnes et al., 1992; Kalla et al., 1994; Wilson et al., 2006; Burton and Fincher, 2014). Various events influence aleurone and starchy endosperm cell fates. Internal cells formed from a division of a periclinal aleurone cell redifferentiate into starchy endosperm cells, indicating aleurone identity is position dependent (Geisler-Lee and

Gallie, 2005). Positional cues within the filial tissue are suspected to play a role in aleurone development rather than specific maternal signals, since the aleurone is the outmost cell layer of the endosperm (Geisler-Lee and Gallie, 2005; Gruis et al., 2006; Gillies et al., 2012). The starchy endosperm also appears to be the default cell type since in the absence of positional cues at the periphery, aleurone cells fail to develop and only starchy endosperm cells are observed (Becraft and Asuncion-Crabb, 2000; Gruis et al., 2006). These signals are thought to be hormonal.

Positional cues and hormones contributing to aleurone development

Positional cues that prompt and influence aleurone development may be driven by several hormones including auxin and cytokinin. It has been deduced that phytohormone gradients may be involved in establishing endosperm patterning and aleurone fate since the phenotype of maize mutants with phytohormone production under the regulation of senescence inducible promoters (inducible deterioration of function) gave rise to a mosaic aleurone (Geisler-Lee and Gallie, 2005). The molecular mechanisms by which these phytohormones influence aleurone cell fate are currently not well understood. However, auxin has been found to be most concentrated in the periphery of the endosperm and aleurone (Forestan et al., 2010; Pielot et al., 2015; Figueiredo and Kohler, 2018), and has been implicated in aleurone cell fate due to its regulatory nature in the entire embryo sac (Pagnussat et al., 2009; Locascio et al., 2014). Maize plants treated with an auxin transport inhibitor (N-1-naphthylphthalamic acid) produced kernels with multilayered aleurones, where kernels normally only have a single layer, suggesting a positive influence on aleurone cell fate by auxin (Forestan et al., 2010). In contrast, cytokinin stimulates cell division within endoreduplicated cells and has been found to have an inhibitory effect on aleurone differentiation, although it is currently unknown whether endogenous cytokinins function in controlling normal

aleurone differentiation (Becraft and Yi, 2011). It is thought that auxin accumulation counters cytokinin since the auxin gradient is high when the cytokinin gradient is low (Locascio et al., 2014).

Other hormones have also been found to be involved in the maintenance of aleurone cells. In grains, the dormancy-germination transition is regulated by hormones such as abscisic acid (ABA) and gibberellic acid (GA). These hormones act antagonistically where ABA is known to promote seed dormancy, desiccation tolerance and repress germination (Nguyen et al., 2007), while GA functions to trigger germination. Models suggest that GA is mainly synthesised in the embryo and scutellum and diffuses to the starchy endosperm. Upon diffusion, GA is perceived by aleurone cells located in the more distal part of the grain, which are prompted to be become metabolically active through a complex signalling cascade (Appleford and Lenton, 1997). When GA and ABA are exogenously applied to maize the aleurone cells respond almost synchronously; GA triggers the production of hydrolases to break down storage products whilst ABA prevents the synthesis of hydrolases inhibiting the breakdown of stored endosperm reserves (Chandler et al., 1984).

Molecular genetic basis for aleurone development

The pathways and molecular mechanisms that define aleurone or starchy endosperm cell fate are not well understood, however key factors have been identified. Various studies, the majority in maize, have identified positional cues and crucial genes, such as kinases and transcription factors, involved in aleurone development and differentiation (Becraft et al., 1996; Becraft and Asuncion-Crabb, 2000; Shen et al., 2003; Wisniewski and Rogowsky, 2004; Olsen, 2004a; Tian et al., 2007; Olsen et al., 2008; Yi et al., 2015; Liu et al., 2018). These include *naked endosperm* (*NKD*), *defective kernel 1* (*DEK1*), *crinkly 4* (*CR4*), *supernumerary aleurone layer 1* (*SAL1*),

thick aleurone 2 (*TA2*) and *viviparous 1* (*VP1*) and their mutants all appear to produce strong phenotypic effects on aleurone development and structure (Figure 2-7). Although much is known about cell differentiation in plants, the identification of genes controlling cell identity has been hampered in many cases by the difficulty in accessing tissues of interest within complex organs. Addressing these questions in cereal crops, such as barley, has also been hampered until only recently, when a genomic sequence was released (Brenchley et al., 2012; Mayer et al., 2012; Mascher et al., 2017). A fundamental requirement for investigating molecular mechanisms is to identify important genes, gene activity and function.

***Naked endosperm* (*nkd*)**

The *naked endosperm* (*nkd*) mutation in maize, produces kernels with no aleurone or a patchy aleurone (Becraft and Asuncion-Crabb, 2000; Yi et al., 2015). The phenotype can vary depending on the penetrance of the mutation, i.e. strong penetrance produces no aleurone and intermediate penetrance results in mosaic aleurone (Becraft and Asuncion-Crabb, 2000). There are two *NKD* genes present in maize, *NKD1* and *NKD2*, and both encode a transcription factor (TF) containing a conserved C2H2 zinc finger DNA-binding domain known as the INTERMEDIATE1 domain (IDD). In *nkd* double mutants, multiple cell layers are present at the periphery of the endosperm that show neither aleurone nor starchy endosperm cell characteristics (Figure 2-8). The aleurone cells usually have thick walls and dense cytoplasm, while starchy endosperm cells contain starch granules, which are absent from the aleurone (Yi et al., 2015). However, at intermediate NKD1 expression levels, aleurone cells sporadically develop within these peripheral layers producing the mosaic phenotype. Hence the *NKD* genes are suspected to be involved in aleurone differentiation and to restrict the number of cell layers (Yi et al., 2015). NKD is hypothesised to act as a repressor of aleurone cell

proliferation since it negatively regulates cell cycle-related genes including *retinoblastoma-related1* (*RBR1*) and mitotic *cyclin 3B-like* (*CYC3B*) (Gontarek et al., 2016). NKD also appears to influence many genes involved in aleurone cell fate, aleurone maturation, starch biosynthesis, anthocyanin biosynthesis and stress response (Yi et al., 2015; Gontarek and Becraft, 2017).

Defective kernel 1 (*dek1*)

Another mutation in maize known as *defective kernel 1* (*dek1*) also produces a varying phenotype depending on the type of mutation. Normally the *dek1* maize mutant kernels are lacking aleurone but less dominant mutations can produce mosaic aleurones. For example, a study by Becraft et al. (2002) found that the strong mutant allele *dek1-1394* eliminated the aleurone completely, while the weaker *dek1-D* mutant allele produced grains with a mosaic aleurone. Unlike the *nkd1* mutants, *dek1* mutant periphery endosperm cells show the histological attributes of starchy endosperm cells (Figure 2-9). *DEK1* encodes a putative cell-wall integrity sensor which possesses 21-24 predicted transmembrane helices, an extracellular loop region and a cytoplasmic calpain protease domain (Lid et al., 2002; Amanda et al., 2016). Calpains are calcium-dependent cysteine proteases and DEK1 undergoes autolytic cleavage, which has been shown to release the CALPAIN domain into the cytoplasm (Johnson et al., 2008; Tran et al., 2017). Although the exact function of DEK1 remains unclear, it has been postulated as a candidate protein for sensing and signalling surface cell position in diverse plant tissues (Figure 2-10) (Tian et al., 2007; Demko et al., 2014; Amanda et al., 2016; Malivert et al., 2018). This is consistent with its role in aleurone cell fate specification as it is surface position-dependent (Lid et al., 2002) and with axial pattern formation during embryogenesis, where *dek1* mutants show altered cell fate in the leaf epidermis (Neuffer et al., 1997). DEK1 is suspected to cleave an inactive cytoplasmic

substrate leading to activation, where this active substrate may influence aleurone and epidermal cell fate (Amanda et al., 2016) (Figure 2-10). This substrate may be a membrane bound TF such as NTM1 (NAC with transmembrane motif1), which has been implicated in cell division regulation (Kim et al., 2006). Other genes such as *Lipid transfer protein 3* (*LTP3*), *EXPANSIN 11* (*EXP11*) and *AP2 transcription factor* (*AP2TF*) may also be targets of DEK1 since their expression was found to be highly upregulated in plants constitutively expressing the CALPAIN domain of DEK1 (Johnson et al., 2008; Amanda et al., 2017). These genes may also respond to DEK1-induced physical/biochemical changes in the cell wall, potentially via other cell wall-sensing pathways (Wolf et al., 2012; Amanda et al., 2017).

Crinkly 4 (*cr4*)

Crinkly 4 (*cr4*) recessive mutations also found in maize seem to act similarly to the *dek1* mutation. The *cr4* mutation in maize endosperm shows an allele-dependent effect whereby homozygous mutant endosperm phenotypes range from kernels lacking small to large patches of aleurone (Figure 2-11) (Becraft et al., 1996; Jin et al., 2000; Tian et al., 2007). Similarly, *cr4* mutants also possess a visible phenotype where the kernel appears to be crinkly or wrinkled. In the region where the aleurone fails to develop, cells at the endosperm periphery have a starchy endosperm phenotype (Becraft and Asuncion-Crabb, 2000). Several studies have implicated CR4 in the development of other tissues (Czyzewicz et al., 2016). For example, in *Arabidopsis*, CR4 has been shown to regulate asymmetric cell division in the root, where *cr4* mutants display a disorganised and/or irregularly differentiating columella (De Smet et al., 2008; Stahl et al., 2013). Similarly, CR4 also functions to define epidermal identity since maize *cr4* mutants possess short ‘crinkly’ leaves due to the abnormal expansion and overabundant division of cells in regions of the shoot apical meristem epidermis (Jin,

et al., 2000; Becraft, et al., 2001; Kang, et al., 2002). Wart-like growths containing large, undifferentiated and disorganised cell structures, and abnormalities in neighbouring tissues are also observed in the leaves of *cr4* mutants (Jin, et al., 2000; Becraft, et al., 2001; Cao, et al., 2005). CR4 encodes a protein receptor-like Ser/Thr kinase with a Cys-rich region with a ligand binding domain in its extracellular domain (Becraft et al., 1996). It is suspected that CR4 regulates epidermal cell fate via ligand binding, since it contains a domain bearing similarity to the animal Tumour Necrosis Factor Receptor (TNFR) ligand binding motif, responsible for cell proliferation, differentiation and death (Li et al., 2009; Tarrats et al., 2011; Waters et al., 2013; Galletti and Ingram, 2015). CR4 protein also localises more at the plasma membrane of aleurone associated plasmodesmata than any other plasma membrane site (Jin et al., 2000; Tian et al., 2007), and may be key for allowing aleurone specific signals to pass through (Figure 2-10). Therefore, CR4 may function to recognise positional cues to specify aleurone cell identity, however, the mechanism by which CR4 is involved in aleurone and epidermal cell fate is currently unknown (Becraft et al., 2002; Tian et al., 2007).

***Supernumerary aleurone layer 1* (*sal1*)**

Another gene that appears to be crucial for aleurone cell layering in maize, and may regulate both CR4 and DEK1, is the *supernumerary aleurone layer 1* (*SAL1*) gene. The SAL1 protein is crucial for aleurone cell layering and mutations produce kernels with a multiple aleurone layer phenotype, consisting of up to seven layers (Figure 2-12) (Shen et al., 2003). *SAL1* encodes a class E vacuolar sorting protein implicated in membrane vesicle trafficking and is a homologue of the human *charged multivesicular body protein 1*/*chromatin-modifying protein 1* (*CHMP1*) gene, also a class E vacuolar sorting protein, functioning in targeting plasma membrane receptors and ligands to

lysosomes for proteolytic degradation (Shen et al., 2003). Currently, the molecular mechanism for SAL1 function is unknown, but it is suspected that the concentration of molecules responsible for aleurone cell specification may be controlled by the endosomal degradation pathway, where the *sal1* mutation results in their accumulation and hence the multilayered aleurone phenotype (Tian et al., 2007). SAL1 is hypothesised to act as a negative regulator of both aleurone cell fate together with CR4 and DEK1 functions since it was found to co-localise in endocytic vesicles with both CR4 and DEK1 (Tian et al., 2007; Yi et al., 2011). SAL1 appears to function upstream of DEK1 and CR4 to direct their cycling from the plasma membrane (i.e. internalising them for degradation) and hence reduces their capacity for signalling (Figure 2-10) (Yi et al., 2011). Therefore, *SAL1* would be an interesting gene to further analyse in other species since it appears to be crucial in regulating aleurone layer number and cell fate.

***Thick aleurone 2* (*ta2*)**

Recently, a mutant in rice was identified called *thick aleurone 2* (*ta2*), where mutant grains possessed four or more aleurone cell layers compared to typically single layered wild-type grains (Liu et al., 2018) (Figure 2-13). Not only did this mutation increase aleurone cell layer number, it also increased key nutritional factors such as lipids, proteins, vitamins, minerals and dietary fibres. Further analysis of *ta2* mutants revealed that *TA2* encodes a DNA demethylase, *repressor of silencing 1* (*OsROS1*) gene (Liu et al., 2018). DNA demethylases are crucial for regulating levels of DNA methylation, which plays an essential role in many biological processes, including growth, development, and stress responses (Zhang et al., 2018). DNA demethylases catalyse the release of 5-methylcytosine (5-meC) from DNA by a glycosylase/lyase mechanism (Morales-Ruiz et al., 2006). Several genes involved in DNA demethylation have been identified in *Arabidopsis thaliana*, such as the transcription activator *DEMETER* (*DME*).

DME is predominately expressed in the central cell of the female gametophyte and the early endosperm and is required for seed viability (Choi et al., 2002). ROS1 is a paralog of DME and regulates gene expression by preventing DNA methylation and transcriptional silencing from transposons (Gong et al., 2002; Tang et al., 2016). Knockout mutations in *OsROS1*, homologue of *AtROS1*, produce no progeny (Ono et al., 2012), however, weak mutations such as single amino acid substitutions in the non-conserved domain of *OsROS1*, induce increased aleurone cell layers but do not negatively affect yield-related traits (Liu et al., 2018). It was also found that transgenic overexpression of the alternative spliced transcript, *mOsROS1*, in wild type-rice induced the *ta2* mutant phenotype (Liu et al., 2018). Potential targets of OsROS1 may have reduced expression levels in *ta2* mutants since ROS1 may be unable to demethylate gene promotors effectively. Several potential target genes of OsROS1 causing the *ta2* phenotype were identified. The rice basic leucine zipper factor *RISBZ1* and *rice prolamin box binding factor* (*RPBF*), both possess multi-layered aleurone in knockdown rice seed (Kawakatsu et al., 2009), had hypermethylated promoter regions and substantially reduced expression levels in *ta2* mutants (Liu et al., 2018). However, at this stage it is unclear whether OsROS1 is influencing other aleurone genes; the promoter of NKD1 was examined and no hypermethylation was observed (Liu et al., 2018).

***Viviparous 1* (*vp1*)**

A gene involved in the maturation phase of aleurone development is *viviparous 1* (*VP1*). Mutations in the *VP1* gene or others involved in ABA biosynthesis and/or response lead to a viviparous phenotype, prompting precocious germination accompanied by the activation of lytic enzymes in the aleurone (Brown and Lemmon, 2007). *VP1* encodes a B3 domain TF that appears to be a central regulator of the grain

maturation process. VP1 functions to control the expression of ABA regulation and other maturation related genes, whilst inhibiting GA induced expression of hydrolyses in the aleurone (Jones et al., 1997; Hoecker et al., 1999). VP1 is also involved in transcriptional regulation of anthocyanin synthesis since *vp1* mutants lack anthocyanin pigmentation in the aleurone (Hoecker et al., 1995). The expression of VP1 is very high in the aleurone and hence can act as a marker for this tissue (Figure 2-14) (Cao et al., 2007), but the molecular mechanisms by which VP1 expression is spatially regulated in the endosperm are currently not known.

Questions relating to aleurone development

In cereals, fundamental understanding is lacking regarding aleurone development and the molecular mechanisms driving its differentiation. For example, DEK1 and CR4 are both crucial for the correct formation of the aleurone in maize, but the specific ligands or signalling mechanisms involved remain unclear. Similarly, NKD1/2 and VP1 are TFs involved in aleurone development but their specific target genes are still unclear (Gontarek et al., 2016; Gontarek and Becraft, 2017). Therefore, further research into aleurone development is required to uncover the molecular mechanisms involved. Unfortunately, even less information regarding these mechanisms is available in barley and wheat. Recent studies have produced a wheat aleurone transcriptome (Gillies et al., 2012) and proteome (Nadaud et al., 2015), but such a resource is lacking for barley. Several quantitative trait loci (QTL) associated with barley aleurone development have been mapped to chromosomes 2H, 5H and 7H, and these influence aleurone thickness and cell number (Jestin et al., 2008). A broader assessment of the genetic variation underlying aleurone development in barley would be important to pursue, since this might be utilised to select cultivars for specific end uses in the food, fibre and beverage

industries. Moreover, the degree of intraspecific variation might lead to the identification of key genes and mechanisms influencing aleurone development.

Conclusion

Summary

Understanding the development of the cereal endosperm is useful in order to improve industrial processes and to further contribute to food and malting practises. The outer layer of the endosperm, known as the aleurone, is an intriguing tissue since large differences in aleurone development and layers are observed across cereal species. Most cereal grains such as maize and wheat have a single layer of aleurone, while other species such as barley display a multi-layered aleurone. The aleurone is known to be essential for germination by releasing hydrolase enzymes to degrade the starchy endosperm, providing energy to the growing embryo, but it is currently unclear why the aleurone morphology would differ so largely between species. Several fundamental components of aleurone development have been identified in cereal species, but the molecular mechanisms involved still remain unclear. The key factors and genes known to influence aleurone cell fate and differentiation have predominantly been investigated in maize, but little is known in other cereal species. Therefore, further research into other cereal species, such as barley, is required to improve our fundamental understanding of regulatory processes.

Proposed Study

During this project, bioinformatic, microscopic, genetic, transgenic and transcriptomic profiling techniques were used to investigate and characterise aleurone development in barley. Transgenic barley plants were developed targeting orthologous candidate genes known to be involved in aleurone development in maize. Grains produced from these plants were compared to identify phenotypic differences in aleurone and endosperm development. In addition, the aleurone from various cultivars of barley was

analysed to identify any underlying natural variation. Differences between cultivars were assessed to identify naturally variable loci possibly involved in aleurone development. Finally, laser capture microdissection and RNAseq-based transcriptional profiling was employed to identify candidate genes associated with wild-type barley aleurone development. The integration of different datasets provided a comprehensive blueprint for barley aleurone specification and identified genes that might be the target of future strategies for tailored grain development.

References

Amanda D, Doblin MS, Galletti R, Bacic A, Ingram GC, Johnson KL (2016) DEFECTIVE KERNEL1 (DEK1) regulates cell walls in the leaf epidermis. Plant Physiology **172:** 2204-2218

Amanda D, Doblin MS, Galletti R, Bacic A, Ingram GC, Johnson KL (2017) Regulation of cell wall genes in response to DEFECTIVE KERNEL1 (DEK1)-induced cell wall changes. Plant Signaling & Behavior **12:** 1-4

Appleford NEJ and Lenton JR (1997) Hormonal regulation of α-amylase gene expression in germinating wheat (*Triticum aestivum*) grains. Physiol Plant. **100**: 534–542

Autio K (1996) Functional aspects of cell wall polysaccharides. *In*: Eliasson A-C, ed, Carbohydrates in food. Marcel Dekker, New York, USA, pp 227-264

Baik BK, Ullrich SE (2008) Barley for food: Characteristics, improvement, and renewed interest. Journal of Cereal Science **48:** 233-242

Becraft PW, Asuncion-Crabb Y (2000) Positional cues specify and maintain aleurone cell fate in maize endosperm development. Development **127:** 4039-4048

Becraft PW, Kang S, Suh S (2001) The maize CRINKLY4 receptor kinase controls a cell-autonomous differentiation response. Plant Physiology **127**: 486-496

Becraft PW, Li KJ, Dey N, Asuncion-Crabb Y (2002) The maize *dek1* gene functions in embryonic pattern formation and cell fate specification. Development **129:** 5217-5225

Becraft PW, Stinard PS, McCarty DR (1996) CRINKLY4: A TNFR-like receptor kinase involved in maize epidermal differentiation. Science **273:** 1406-1409

Becraft PW, Yi GB (2011) Regulation of aleurone development in cereal grains. Journal of Experimental Botany **62:** 1669-1675

Behall KM, Scholfield DJ, Hallfrisch J (2004) Diets containing barley significantly reduce lipids in mildly hypercholesterolemic men and women. American Journal of Clinical Nutrition **80:** 1185-1193

Betts NS, Wilkinson LG, Khor SF, Shirley NJ, Lok F, Skadhauge B, Burton RA, Fincher GB, Collins HM (2017) Morphology, carbohydrate distribution, gene expression, and enzymatic activities related to cell wall hydrolysis in four barley varieties during simulated malting. Frontiers in Plant Science **8:** 1-15

Bohn L, Meyer AS, Rasmussen SK (2008) Phytate: impact on environment and human nutrition. A challenge for molecular breeding. Journal of Zhejiang University-Science B **9:** 165-191

Bonello J-F, Opsahl-Ferstad H-G, Perez P, Dumas C, Rogowsky PM (2000) *Esr* genes show different levels of expression in the same region of maize endosperm. Gene **246**: 219-227

Bosnes M, Weideman F, Olsen OA (1992) Endosperm differentiation in barley wild-type and sex mutants. Plant Journal **2:** 661-674

Bozhkov PV, Lam E (2011) Green death: revealing programmed cell death in plants. Cell Death and Differentiation **18:** 1239-1240

Brenchley R, Spannagl M, Pfeifer M, Barker GLA, D'Amore R, Allen AM, McKenzie N, Kramer M, Kerhornou A, Bolser D, Kay S, Waite D, Trick M, Bancroft I, Gu Y, Huo N, Luo MC, Sehgal S, Gill B, Kianian S, Anderson O, Kersey P, Dvorak J, McCombie WR, Hall A, Mayer KFX, Edwards KJ, Bevan MW, Hall N (2012) Analysis of the breadwheat genome using whole-genome shotgun sequencing. Nature **491:** 705-710

Brown RC, Lemmon BE (2007) The developmental biology of cereal endosperm. *In* OA Olsen, ed, Plant cell monographs. Endosperm, Vol 8. Springer-Verlag, Berlin, Germany, pp 1–20

Burton RA, Fincher GB (2014) Evolution and development of cell walls in cereal grains. Frontiers in Plant Science **5:** 1-15

Cao XY, Costa LM, Biderre-Petit C, Kbhaya B, Dey N, Perez P, McCarty DR, Gutierrez-Marcos JF, Becraft PW (2007) Abscisic acid and stress signals induce *Viviparous1* expression in seed and vegetative tissues of maize. Plant Physiology **143:** 720-731

Cao XY, Li K, Suh SG, Guo T, Becraft PW (2005) Molecular analysis of the *CRINKLY4* gene family in *Arabidopsis thaliana*. Planta **220**: 645-657

Chandler PM, Zwar JA, Jacobsen JV, Higgins TJV, Inglis AS (1984) The effects of gibberellic-acid and abscisic-acid on α-amylase mRNA levels in barley aleurone layers studies using an α-amylase cdna clone. Plant Molecular Biology **3:** 407-418

Charalampopoulos D, Wang R, Pandiella SS Webb C (2002) Application of cereals and cereal components in functional foods: a review. International Journal of Food Microbiology **79**: 131-141

Chen J, Lausser A, Dresselhaus T (2014) Hormonal responses during early embryogenesis in maize. Biochem. Soc. Trans **42**: 325-331

Choi YH, Gehring M, Johnson L, Hannon M, Harada JJ, Goldberg RB, Jacobsen SE, Fischer RL (2002) DEMETER, a DNA glycosylase domain protein, is required for endosperm gene imprinting and seed viability in *Arabidopsis*. Cell **110:** 33-42

Cosségal M, Vernoud V, Depège N, Rogowsky PM (2007) The embryo surrounding region. *In* OA Olsen, ed, Endosperm. Springer-Verlag, Berlin, Heidelberg, pp 57-71

Coulibaly A, Kouakou B, Chen J (2011) Phytic acid in cereal grains: structure, healthy or harmful ways to reduce phytic acid in cereal grains and their effects on nutritional quality. American Journal of Plant Nutrition and Fertilization Technology **1:** 1-22

Czyzewicz N, Nikonorova N, Meyer MR, Sandal P, Shah S, Vu LD, Gevaert K, Rao AG, De Smet I (2016) The growing story of (ARABIDOPSIS) CRINKLY 4. Journal of Experimental Botany **67**: 4835-4847

D'Amato F (1984) Role of polyploidy in reproductive organs. *In* BM Johri, ed, Embryology of Angiosperms. Springer-Verlag, New York, pp 519-566

De Smet I, Vassileva V, De Rybel B, Levesque MP, Grunewald W, Van Damme D, Van Noorden G, Naudts M, Van Isterdael G, De Clercq R, Wang JY, Meuli N, Vanneste S, Friml J, Hilson P, Jürgens G, Ingram GC, Inzé D, Benfey PN, Beeckman T (2008) Receptor-like kinase ACR4 restricts formative cell divisions in the *Arabidopsis* root. Science **322**: 594-597

Del Rio D, Rodriguez-Mateos A, Spencer JPE, Tognolini M, Borges G, Crozier A (2013) Dietary (poly)phenolics in human health: Structures, bioavailability, and evidence of protective effects against chronic diseases. Antioxidants & Redox Signaling **18:** 1818-1892

Demirbas A (2005) β-Glucan and mineral nutrient contents of cereals grown in Turkey. Food Chemistry **90**: 773-777

Demko V, Perroud PF, Johansen W, Delwiche CF, Cooper ED, Remme P, Ako AE, Kugler KG, Mayer KFX, Quatrano R, Olsen OA (2014) Genetic analysis of *DEFECTIVE KERNEL1* loop function in three-dimensional body patterning in physcomitrella patens. Plant Physiology **166:** 903-U684

Doll NM, Depége-Fargeix N, Rogowsky PM, Widiez T (2017) Signaling in early maize kernel development. Molecular Plant **10**: 375-388

Drews GN, Lee D, Christensen GA (1998) Genetic analysis of female gametophyte development and function. Plant Cell **10:** 5-17

Fath A, Bethke P, Lonsdale J, Meza-Romero R, Jones R (2000) Programmed cell death in cereal aleurone. Plant Molecular Biology **44:** 255-266

Figueiredo DD, Kohler C (2018) Auxin: a molecular trigger of seed development. Genes & Development **32:** 479-490

Forestan C, Meda S, Varotto S (2010) ZmPIN1-mediated auxin transport is related to cellular differentiation during maize embryogenesis and endosperm development. Plant Physiology **152:** 1373-1390

Galletti R, Ingram GC (2015) Communication is key: Reducing DEK1 activity reveals a link between cell-cell contacts and epidermal cell differentiation status. Commun Integr Biol **8**: 1-4

Gamel TH, Abdel-Aal EM (2012) Phenolic acids and antioxidant properties of barley wholegrain and pearling fractions. Agricultural and Food Science **21:** 118-131

Geisler-Lee J, Gallie DR (2005) Aleurone cell identity is suppressed following connation in maize kernels. Plant Physiology **139:** 204-212

Gillies SA, Futardo A, Henry RJ (2012) Gene expression in the developing aleurone and starchy endosperm of wheat. Plant Biotechnology Journal **10:** 668-679

Gong ZH, Morales-Ruiz T, Ariza RR, Roldan-Arjona T, David L, Zhu JK (2002) *ROS1*, a repressor of transcriptional gene silencing in *Arabidopsis*, encodes a DNA glycosylase/lyase. Cell **111:** 803-814

Gontarek BC, Becraft PW (2017) Aleurone. *In* BA Larkin, ed, Maize kernel development. Centre for Agriculture and Bioscience International, Oxfordshire, UK, pp 68-80

Gontarek BC, Neelakandan AK, Wu H, Becraft PW (2016) NKD transcription factors are central regulators of maize endosperm development. Plant Cell **28:** 2916-2936

Gruis D, Guo HN, Selinger D, Tian Q, Olsen OA (2006) Surface position, not signaling from surrounding maternal tissues, specifies aleurone epidermal cell fate in maize. Plant Physiology **141:** 898-909

Harris PJ, Fincher GB (2009) Distribution, fine structure and function of (1,3;1,4)-β-glucans in the grasses and other taxa. *In* A Bacic, GB Fincher, BA Stone, eds, Chemistry, biochemistry, and biology of 1-3 beta glucans and related polysaccharides. Academic Press, Elsevier Inc, San Diego, USA, pp 621-654

Hassan AS, Houston K, Lahnstein J, Shirley N, Schwerdt JG, Gidley MJ, Waugh R, Little A, Burton RA (2017) A genome wide association study of arabinoxylan content in 2-row spring barley grain. Plos One **12:** e0182537

Haughn G, Chaudhury A (2005) Genetic analysis of seed coat development in *Arabidopsis*. Trends in Plant Science **10:** 472-477

Hoecker U, Vasil IK, McCarty DR (1995) Integrated control of seed maturation and germination programs by activator and repressor functions of *Viviparous-1* of maize. Genes & Development **9:** 2459-2469

Hoecker U, Vasil IK, McCarty DR (1999) Signaling from the embryo conditions *Vp1*-mediated repression of α-amylase genes in the aleurone of developing maize seeds. Plant Journal **19:** 371-377

Holtekjølen AK, Uhlen AK, Bråthen E, Sahlstrøm S, Knutsen SH (2006) Contents of starch and non-starch polysaccharides in barley varieties of different origin. Food Chemistry **94**: 348-358

Ishimaru T, Ida M, Hirose S, Shimamura S, Masumura T, Nishizawa NK, Nakazono M, Kondo M (2015) Laser microdissection-based gene expression analysis in the aleurone layer and starchy endosperm of developing rice caryopses in the early storage phase. Rice **8:** 1-15

Jestin L, Ravel C, Auroy S, Laubin B, Perretant MR, Pont C, Charmet G (2008) Inheritance of the number and thickness of cell layers in barley aleurone tissue (*Hordeum vulgare* L.): an approach using F2-F3 progeny. Theoretical and Applied Genetics **116:** 991-1002

Jin P, Guo T, Becraft PW (2000) The maize CR4 receptor-like kinase mediates a growth factor-like differentiation response. Genesis **27:** 104-116

Johnson KL, Faulkner C, Jeffree CE, Ingram GC (2008) The phytocalpain DEFECTIVE KERNEL 1 is a novel *Arabidopsis* growth regulator whose activity is regulated by proteolytic processing. Plant Cell **20:** 2619-2630

Jones HD, Peters NCB, Holdsworth MJ (1997) Genotype and environment interact to control dormancy and differential expression of the *VIVIPAROUS 1* homologue in embryos of *Avena fatua*. Plant Journal **12:** 911-920

Kalla R, Shimamoto K, Potter R, Nielsen PS, Linnestad C, Olsen OA (1994) The promoter of the barley aleurone-specific gene encoding a putative 7-kDa lipid transfer protein confers aleurone cell-specific expression in transgenic rice. Plant Journal **6:** 849-860

Kamal-Eldin A, Larke HN, Knudsen KEB, Lampi AM, Piironen V, Adlercreutz H, Katina K, Poutanen K, Aman P (2009) Physical, microscopic and chemical characterisation of industrial rye and wheat brans from the Nordic countries. Food & Nutrition Research **53:** 1-11

Kang S, Lee H, Suh S (2002) The maize *Crinkly4* gene is expressed spatially in vegetative and floral organs. Journal of Plant Biology **45**: 219-224

Kawakatsu T, Yamamoto MP, Touno SM, Yasuda H, Takaiwa F (2009) Compensation and interaction between RISBZ1 and RPBF during grain filling in rice. Plant Journal **59:** 908-920

Khoury DE, Cuda C, Luhovyy BL and Anderson GH (2012) Beta glucan: Health benefits in obesity and metabolic syndrome. J Nutr Metab **2012**: 1-28

Kim YS, Kim SG, Park JE, Park HY, Lim MH, Chua NH, Park CM (2006) A membrane-bound NAC transcription factor regulates cell division in *Arabidopsis*. Plant Cell **18:** 3132-3144

Kowles RV (2009) The importance of DNA endoreduplication in the developing endosperm of maize. Maydica **54:** 387-399

Lafon-Placette C, Köhler C (2014) Embryo and endosperm, partners in seed development. Current Opinion in Plant Biology **17**: 64-69

Leroux BM, Goodyke AJ, Schumacher KI, Abbott CP, Clore AM, Yadegari R, Larkins BA, Dannenhoffer JM (2014) Maize early endosperm growth and development: From fertilization through cell type differentiation. American Journal of Botany **101:** 1259-1274

Li B, Vincent A, Cates J, Brantley-Sieders DM, Polk DB, Young PP (2009) Low levels of tumor necrosis factor alpha increase tumor growth by inducing an endothelial phenotype of monocytes recruited to the tumor site. Cancer Research **69:** 338-348

Lid SE, Gruis D, Jung R, Lorentzen JA, Ananiev E, Chamberlin M, Niu XM, Meeley R, Nichols S, Olsen OA (2002) The *defective kernel 1* (*dek1*) gene required for aleurone cell development in the endosperm of maize grains encodes a membrane protein of the calpain gene superfamily. Proceedings of the National Academy of Sciences of the United States of America **99:** 5460-5465

Liu J, Wu X, Yao X, Yu R, Larkin PJ, Liu C-M (2018) Mutations in the DNA demethylase *OsROS1* result in a thickened aleurone and improved nutritional value in rice grains. PNAS**:** 1-6

Locascio A, Roig-Villanova I, Bernardi J, Varotto S (2014) Current perspectives on the hormonal control of seed development in *Arabidopsis* and maize: a focus on auxin. Frontiers in Plant Science **5:** 1-22

Lopes MA, Larkins BA (1993) Endosperm origin, development, and function. Plant Cell **5:** 1383-1399

Malivert A, Hamant O, Ingram GC (2018) The contribution of mechanosensing to epidermal cell fate specification. Current Opinion in Genetics and Development **51:** 52-58

Mascher M, Gundlach H, Himmelbach A, Beier S, Twardziok SO, Wicker T, Radchuk V, Dockter C, Hedley PE, Russell J, Bayer M, Ramsay L, Liu H, Haberer G, Zhang XQ, Zhang QS, Barrero RA, Li L, Taudien S, Groth M, Felder M, Hastie A, Simkova H, Stankova H, Vrana J, Chan S, Munoz-Amatrian M, Ounit R, Wanamaker S, Bolser D, Colmsee C, Schmutzer T, Aliyeva-Schnorr L, Grasso S, Tanskanen J, Chailyan A, Sampath D, Heavens D, Clissold L, Cao SJ, Chapman B, Dai F, Han Y, Li H, Li X, Lin CY, McCooke JK, Tan C, Wang PH, Wang SB, Yin SY, Zhou GF, Poland JA, Bellgard MI, Borisjuk L, Houben A, Dolezel J, Ayling S, Lonardi S, Kersey P, Lagridge P, Muehlbauer GJ, Clark MD, Caccamo M, Schulman AH, Mayer KFX, Platzer M, Close TJ, Scholz U, Hansson M, Zhang GP, Braumann I, Spannagl M, Li CD, Waugh R, Stein N (2017) A chromosome conformation capture ordered sequence of the barley genome. Nature **544:** 426-433

Mayer KFX, Waugh R, Langridge P, Close TJ, Wise RP, Graner A, Matsumoto T, Sato K, Schulman A, Muehlbauer GJ, Stein N, Ariyadasa R, Schulte D, Poursarebani N, Zhou RN, Steuernagel B, Mascher M, Scholz U, Shi BJ, Langridge P, Madishetty K, Svensson JT, Bhat P, Moscou M, Resnik J, Close TJ, Muehlbauer GJ, Hedley P, Liu H, Morris J, Waugh R, Frenkel Z, Korol A, Berges H, Graner A, Stein N, Steuernagel B, Taudien S, Groth M, Felder M, Lonardi S, Duma D, Alpert M, Cordero F, Beccuti M, Ciardo G, Ma Y, Wanamaker S, Stein N, Close TJ, Platzer M, Brown JWS, Schulman A, Platzer M, Fincher GB, Muehlbauer GJ, Sato K, Taudien S, Sampath D, Swarbreck D, Scalabrin S, Zuccolo A, Vendramin V, Morgante M, Schulman A, Int Barley Genome Sequencing C (2012) A physical, genetic and functional sequence assembly of the barley genome. Nature **491:** 711-716

McCartney L, Marcus SE and Knox JP (2005) Monoclonal antibodies to plant cell wall xylans and arabinoxylans. J. Histochem. Cytochem. **53**: 543-546

Morales-Ruiz T, Ortega-Galisteo AP, Ponferrada-Marin MI, Martinez-Macias MI, Ariza RR, Roldan-Arjona T (2006) *DEMETER* and *REPRESSOR OF SILENCING 1* encode 5-methylcytosine DNA glycosylases. PNAS **103:** 6853-6858

Mrízová K, Holasková E, Öz MT, Jiskrová E, Frébort I, Galuszka P (2014) Transgenic barley: A prospective tool for biotechnology and agriculture. Biotechnology Advances **32:** 137-157

Nadaud I, Tasleem-Tahir A, Chateigner-Boutin AL, Chambon C, Viala D, Branlard G (2015) Proteome evolution of wheat (*Triticum aestiuum* L.) aleurone layer at fifteen stages of grain development. Journal of Proteomics **123:** 29-41

Neuffer MG, Coe EH, Wessler SR (1997) Mutants of maize. Cold Spring Harbor Laboratory Press New York, USA, pp 1-468

Nguyen HN, Sabelli PA, Larkin BA (2007) Endoreduplication and programmed cell death in the cereal endosperm. *In* OA Olsen, ed, Plant Cell Monographs, Vol 8, pp 21-43

Olsen LT, Divon HH, Al R, Fosnes K, Lid SE, Opsahl-Sorteberg HG (2008) The *defective seed5* (*des5*) mutant: effects on barley seed development and *HvDek1*, *HvCr4*, and *HvSal1* gene regulation. Journal of Experimental Botany **59:** 3753-3765

Olsen OA (2004a) Nuclear endosperm development in cereals and *Arabidopsis thaliana*. Plant Cell **16:** S214-S227

Olsen OA (2004b) Dynamics of maize aleurone cell formation: The "surface-"rule. Maydica **49:** 37-40

Olsen OA, Linnestad C, Nichols SE (1999) Developmental biology of the cereal endosperm. Trends in Plant Science **4:** 253-257

Ono A, Yamaguchi K, Fukada-Tanaka S, Terada R, Mitsui T, Iida S (2012) A null mutation of *ROS1a* for DNA demethylation in rice is not transmittable to progeny. Plant Journal **71:** 564-574

Opsahl-Ferstad H-G, Le Deunff E, Dumas C, Rogowsky PM (1997) *ZmEsr*, a novel endosperm-specific gene expressed in a restricted region around the maize embryo. Plant J **12**: 235-246

Pagnussat GC, Alandete-Saez M, Bowman JL, Sundaresan V (2009) Auxin-dependent patterning and gamete specification in the *Arabidopsis* female gametophyte. Science **324:** 1684-1689

Pielot R, Kohl S, Manz B, Rutten T, Weier D, Tarkowska D, Rolcik J, Strnad M, Volke F, Weber H, Weschke W (2015) Hormone-mediated growth dynamics of the barley pericarp as revealed by magnetic resonance imaging and transcript profiling. Journal of Experimental Botany **66:** 6927-6943

Pins JJ, Kaur H (2006) A review of the effects of barley β-glucan on cardiovascular and diabetic risk. Cereal Foods World **51:** 8-11

Ragaee S, Abdel-Aal EM, Noaman M (2006) Antioxidant activity and nutrient composition of selected cereals for food use. Food Chemistry **98:** 32-38

Sabelli PA (2012) Replicate and die for your own good: Endoreduplication and cell death in the cereal endosperm. Journal of Cereal Science **56:** 9-20

Sabelli PA, Larkins BA (2008) The endoreduplication cell cycle: Regulation and function. *In* DPS Verma, Z Hong, eds, Plant Cell Monographs, Vol 9. Springer-Verlag, Berlin-Heidelberg, pp 75-100

Sabelli PA, Larkins BA (2009) The development of endosperm in grasses. Plant Physiology **149**: 14-26

Sato K, Flavell A, Russell J, Börner A, Valkoun J (2014) Genetic diversity and germplasm management - wild barley, landraces, breeding materials. *In* J Kumlehn, N Stein, eds, Biotechnological approaches to barley improvement. Springer-Verlag, Berlin Heidelberg, Germany, pp 21-36

Schel JHN, Kieft H, van Lammeren AAM (1984) Interactions between embryo and endosperm during early developmental stages of maize caryopses (*Zea mays*). Canad J Bot **62**: 2842-2853

Shaik SS, Carciofi M, Martens HJ, Hebelstrup KH, Blennow A (2014) Starch bioengineering affects cereal grain germination and seedling establishment. Journal of Experimental Botany **65:** 2257-2270

Shapter FM, Dawes MP, Lee LS, Henry RJ (2009) Aleurone and subaleurone morphology in native Australian wild cereal relatives. Australian Journal of Botany **57:** 688-696

Shen B, Li CJ, Min Z, Meeley RB, Tarczynski MC, Olsen OA (2003) *sal1* determines the number of aleurone cell layers in maize endosperm and encodes a class E vacuolar sorting protein. Proceedings of the National Academy of Sciences of the United States of America **100:** 6552-6557

Smith AM, Zeeman SC, Smith SM (2005) Starch degradation. Annual Review of Plant Biology **56:** 73-98

Sreenivasulu N, Borisjuk L, Junker BH, Mock HP, Rolletschek H, Seiffert U, Weschke W, Wobus U (2010) Barley grain development: Toward an integrative view. *In* KW Jeon, ed, International Review of Cell and Molecular Biology, Vol 281, pp 49-89

Stahl Y, Grabowski S, Bleckmann A, Kühnemuth R, Weidtkamp-Peters S, Pinto KG, Kirschner GK, Schmid JB, Wink RH, Hülsewede A, Felekyan S, Seidel CA, Simon R (2013) Moderation of *Arabidopsis* root stemness by CLAVATA1 and ARABIDOPSIS CRINKLY4 receptor kinase complexes. Curr Biol **23**: 362-371

Tang K, Lang ZB, Zhang H, Zhu JK (2016) The DNA demethylase ROS1 targets genomic regions with distinct chromatin modifications. Nature Plants **2:** 1-10

Tarrats N, Moles A, Morales A, Garcia-Ruiz C, Fernandez-Checa JC, Mari M (2011) Critical role of tumor necrosis factor receptor 1, but not 2, in hepatic stellate cell proliferation, extracellular matrix remodeling, and liver fibrogenesis. Hepatology **54:** 319-327

Thiel J, Weier D, Sreenivasulu N, Strickert M, Weichert N, Melzer M, Czauderna T, Wobus U, Weber H, Weschke W (2008) Different hormonal regulation of cellular differentiation and function in nucellar projection and endosperm transfer cells: A microdissection-based transcriptome study of young barley grains. Plant Physiology **148:** 1436-1452

Tian Q, Olsen L, Sun B, Lid SE, Brown RC, Lemmon BE, Fosnes K, Gruis DF, Opsahl-Sorteberg HG, Otegui MS, Olsen OA (2007) Subcellular localization and functional domain studies of DEFECTIVE KERNEL1 in maize and *Arabidopsis* suggest a model for aleurone cell fate specification involving CRINKLY4 and SUPERNUMERARY ALEURONE LAYER1. Plant Cell **19:** 3127-3145

Topping DL, Clifton PM (2001) Short-chain fatty acids and human colonic function: Roles of resistant starch and nonstarch polysaccharides. Physiological Reviews **81**: 1031-1064

Tran D, Galletti R, Neumann ED, Dubois A, Sharif-Naeini R, Geitmann A, Frachisse JM, Hamant O, Ingram GC (2017) A mechanosensitive Ca2+ channel activity is dependent on the developmental regulator DEK1. Nature Communications **8:** 1-8

Vaughn KC, Talbot MJ, Offler CE, McCurdy DW (2007) Wall ingrowths in epidermal transfer cells of Vicia faba cotyledons are modified primary walls marked by localized accumulations of arabinogalactan proteins. Plant and Cell Physiology **48:** 159-168

Verardo V, Gomez-Caravaca AM, Messia MC, Marconi E, Caboni MF (2011) Development of functional spaghetti enriched in bioactive compounds using barley coarse fraction obtained by air classification. Journal of Agricultural and Food Chemistry **59:** 9127-9134

Wang M, Oppedijk BJ, Caspers MPM, Lamers GEM, Boot MJ, Geerlings DNG, Bakhuizen B, Meijer AH, Van Duijn B (1998) Spatial and temporal regulation of DNA fragmentation in the aleurone of germinating barley. Journal of Experimental Botany **49:** 1293-1301

Waters JP, Pober JS, Bradley JR (2013) Tumour necrosis factor and cancer. Journal of Pathology **230:** 241-248

Wilkinson LG, Tucker MR (2017) An optimised clearing protocol for the quantitative assessment of sub-epidermal ovule tissues within whole cereal pistils. Plant Methods **13:** 67-77

Wilson SM, Burton RA, Doblin MS, Stone BA, Newbigin EJ, Fincher GB, Bacic A (2006) Temporal and spatial appearance of wall polysaccharides during cellularization of barley (*Hordeum vulgare*) endosperm. Planta **224:** 655-667

Wisniewski JP, Rogowsky PM (2004) Vacuolar H+-translocating inorganic pyrophosphatase (Vpp1) marks partial aleurone cell fate in cereal endosperm development. Plant Molecular Biology **56:** 325-337

Wolf S, Hematy K, Hofte H (2012) Growth control and cell wall signaling in plants. *In* SS Merchant, ed, Annual Review of Plant Biology, Vol 63, pp 381-407

Wood PJ, Beer MU (1998) Functional oat products. *In*: Mazza J, ed, Functional foods, biochemical and processing aspects, Vol 1. Technomic Publishing Company, Lancester, UK, pp 1-38

Wood PJ, Beer MU, Butler G (2000) Evaluation of role of concentration and molecular weight of oat β-glucan in determining effect of viscosity on plasma glucose and insulin following an oral glucose load. British Journal of Nutrition **84**: 19-23

Xu JJ, Zhang XF, Xue HW (2016) Rice aleurone layer specific OsNF-YB1 regulates grain filling and endosperm development by interacting with an ERF transcription factor. Journal of Experimental Botany **67:** 6399-6411

Yan D, Duermeyer L, Leoveanu C, Nambara E (2014) The functions of the endosperm during seed germination. Plant and Cell Physiology **55:** 1521-1533

Yi G, Lauter AM, Scott MP, Becraft PW (2011) The *thick aleurone1* mutant defines a negative regulation of maize aleurone cell fate that functions downstream of *defective kernel1*. Plant Physiology **156:** 1826-1836

Yi G, Neelakandan AK, Gontarek BC, Vollbrecht E, Becraft PW (2015) The *naked endosperm* genes encode duplicate indeterminate domain transcription factors required for maize endosperm cell patterning and differentiation. Plant Physiology **167:** 443-456

Zhang HM, Lang ZB, Zhu JK (2018) Dynamics and function of DNA methylation in plants. Nature Reviews Molecular Cell Biology **19:** 489-506

Zhou K, Su L, Yu LL (2004a) Phytochemicals and antioxidant properties in wheat bran. Journal of Agricultural and Food Chemistry **52:** 6108-6114

Zhou KQ, Laux JJ, Yu LL (2004b) Comparison of swiss red wheat grain and fractions for their antioxidant properties. Journal of Agricultural and Food Chemistry **52:** 1118-1123

Figures

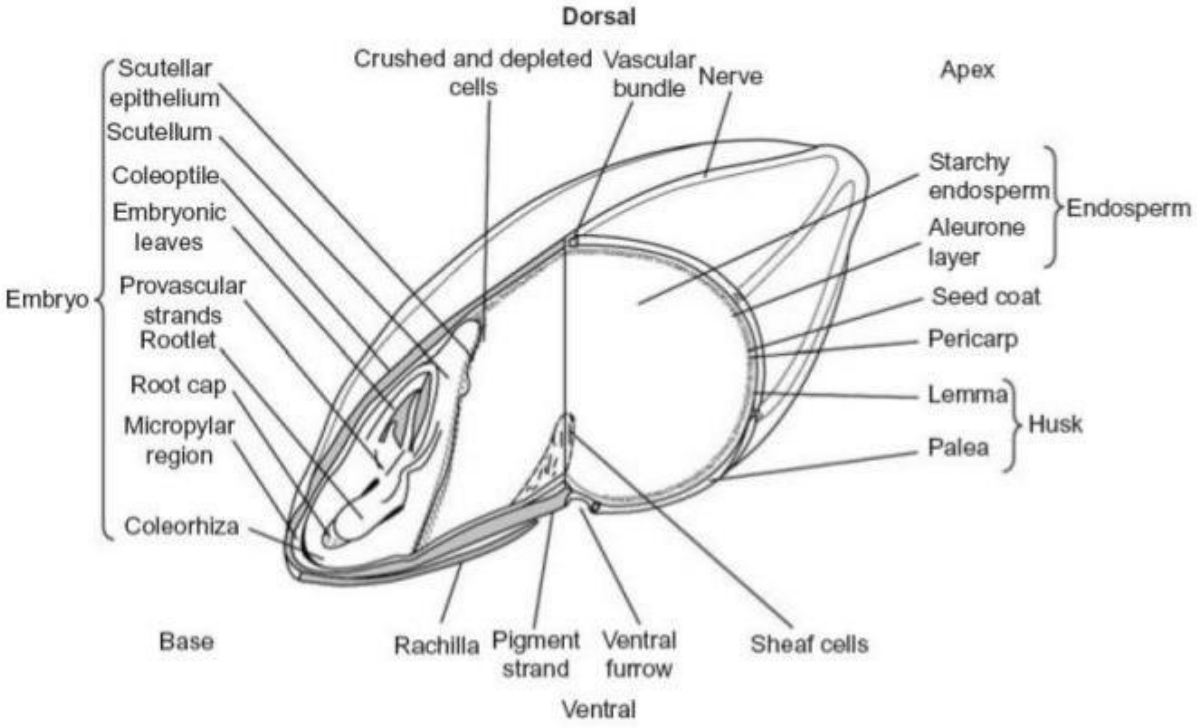

Figure 2-1. Diagram of the barley grain showing the different organs, tissues and cell types. Adapted from Harris and Fincher (2009).

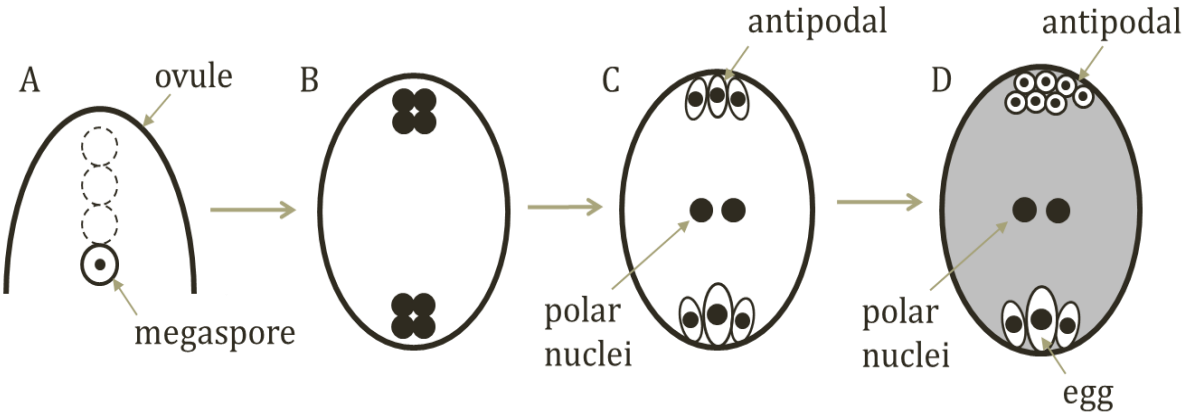

Figure 2-2. Development of the embryo sac in cereals and Arabidopsis. (A) The embryo sac forms within the ovule from a surviving maternal haploid megaspore. (B) Two groups of nuclei form at either pole of the cell after migration. (C) One nucleus from each pole migrates to the centre of the cell, thus becoming the two polar nuclei. Cell walls develop around the remaining nuclei, forming the egg and the antipodal cells. (D) Represents a barley embryo sac. The polar nuclei remain separate until fertilisation by one of the male haploid nuclei from the pollen tube. The shaded area of the embryo sac represents the central cell that develops into the endosperm after fertilisation. Modified from Olsen (2004a).

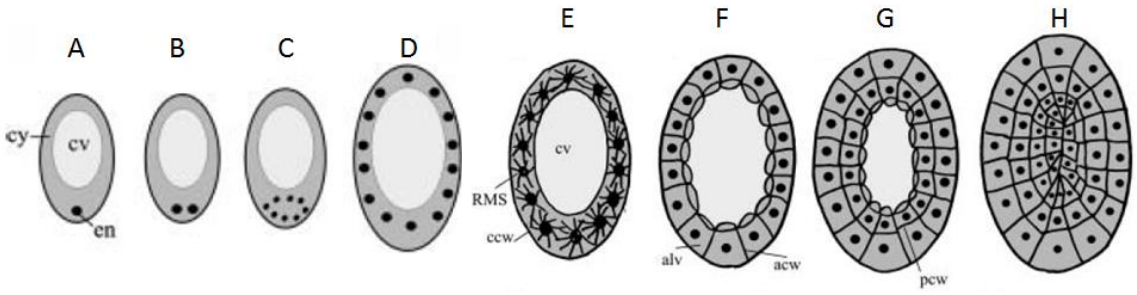

Figure 2-3. Cereal endosperm coenocyte (A–D) and cellularisation (E–H) stages. (A) Initial coenocyte stage with a large central vacuole (cv), thin cytoplasm (cy) and a triploid endosperm nucleus (en). (B) Endosperm nucleus divides with no cell plate forming between daughter nuclei. (C) Nuclei undergo three rounds of nuclear division. (D) Nuclei repeatedly divide and migrate evenly until the nuclei line the periphery of the central vacuole. (E) Radial microtubule system (RMS) forms on the surface of nuclear membranes (central cell wall; ccw). (F) Anticlinal cell walls (acw) separate the peripheral nuclei within tube-like structures known as alveoli (alv). (G) Nuclei divide and periclinal cell walls (pcw) form. (H) Periclinal divisions repeatedly occur until the endosperm is completely cellularised. Modified from Olsen (2004a).

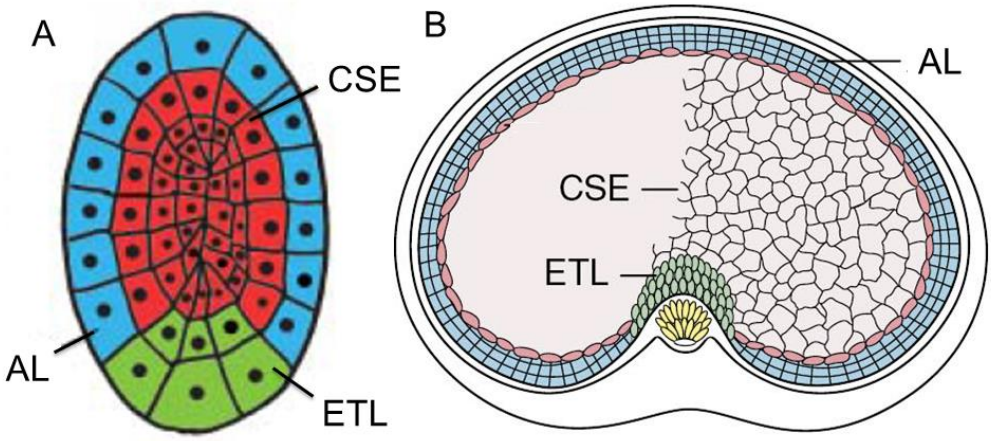

Figure 2-4. Diagram depicting barley endosperm cell types. (A) Domains in young cereal endosperm with colour coding. Aleurone layer (AL; blue), central starchy endosperm (CSE; red) and endosperm transfer layers (ETL; green). (B) Mature barley grain section showing the different domains and cell type with similar colour coding. Aleurone layer (AL; blue), central starchy endosperm (CSE; pink) and endosperm transfer layers (ETL; green). Modified from Olsen et al. (1999) and Olsen (2004a).

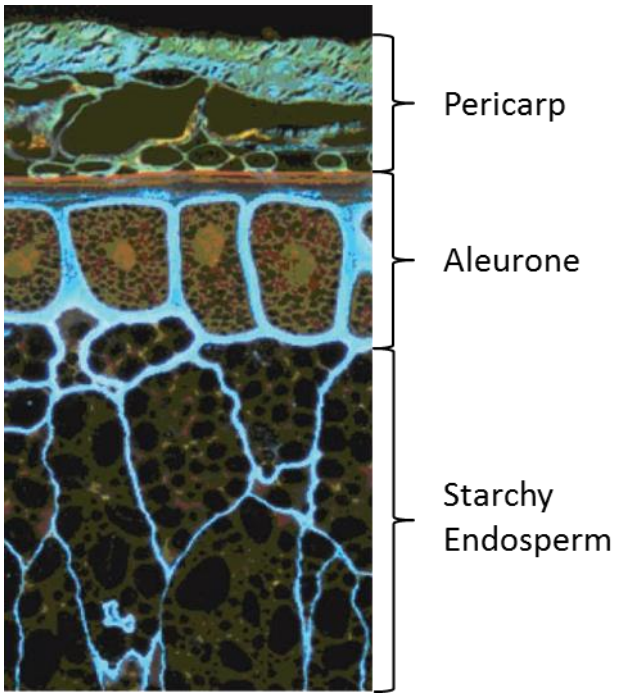

Figure 2-5. Section of a rye grain (*Secale cereale*) showing the single aleurone layer and irregular starchy endosperm cells. The section was stained with Acid Fuchsin and Calcofluor. Proteins appear red, the cell walls are light blue (rich in β-glucan) and lignified cell walls of the pericarp are yellowish-brown. Modified from Kamal-Eldin et al. (2009).

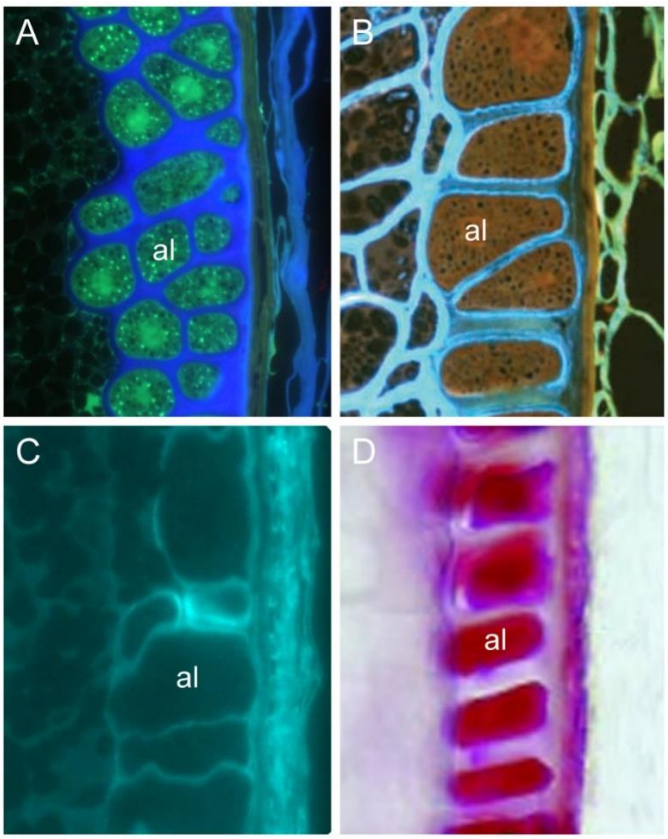

Figure 2-6. Grain sections from various cereal species displaying the structural differences observed in the aleurone, as well as different aleurone visualising techniques. (A) Transverse section of barley (*Hordeum vulgare* L.) showing multiple aleurone cell layers. Section was immunolabelled using the monoclonal antibody LM11 (green), which recognises an arabinoxylan epitope (McCartney et al., 2005), and stained with calcofluor white stain (blue). Image provided by Dr. Helen Collins (University of Adelaide). (B) Section of wheat (*Triticum aestivum* L.) showing the single aleurone layer. The section was stained with Acid Fuchsin and Calcofluor. Proteins appear red, the cell walls are light blue (rich in β-glucan) and lignified cell walls of the fruit husk are yellowish-brown. Modified from Kamal-Eldin et al. (2009). (C) Section of rice (*Oryza sativa* L.) section showing up to two layers of aleurone stained with calcofluor white stain. Image provided by Dr. Helen Collins (University of Adelaide). (D) Transverse section of a maize (*Zea mays* L.) kernel showing the single aleurone

layer. The section was stained with the lipid stain Sudan red, a dye that detects the characteristic oil bodies in the aleurone. Modified from Lid et al. (2002).

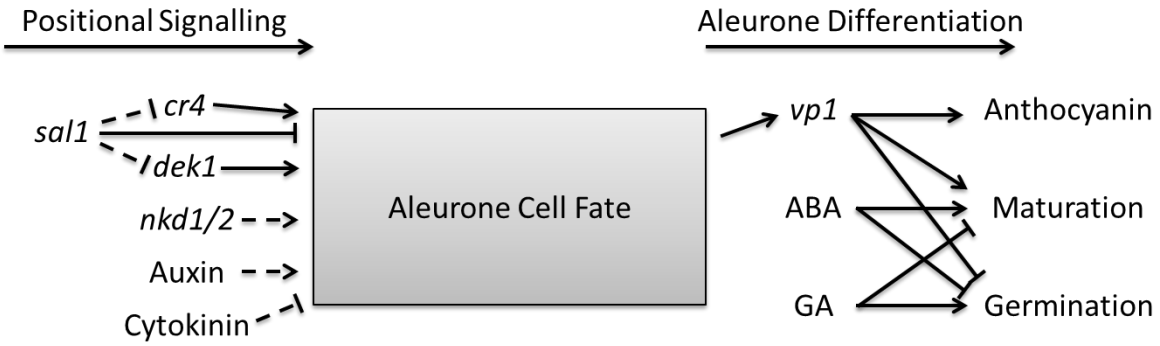

Figure 2-7. A model of the regulatory factors involved in the aleurone developmental process. Key genes critical to this study are represented in italics showing both positive and negative regulators of aleurone cell fate. Similarly, hormones implicated in aleurone cell fate are also shown. Established relationships are represented by solid lines and more hypothetical relationships with dashed lines. Modified from Becraft and Yi (2011).

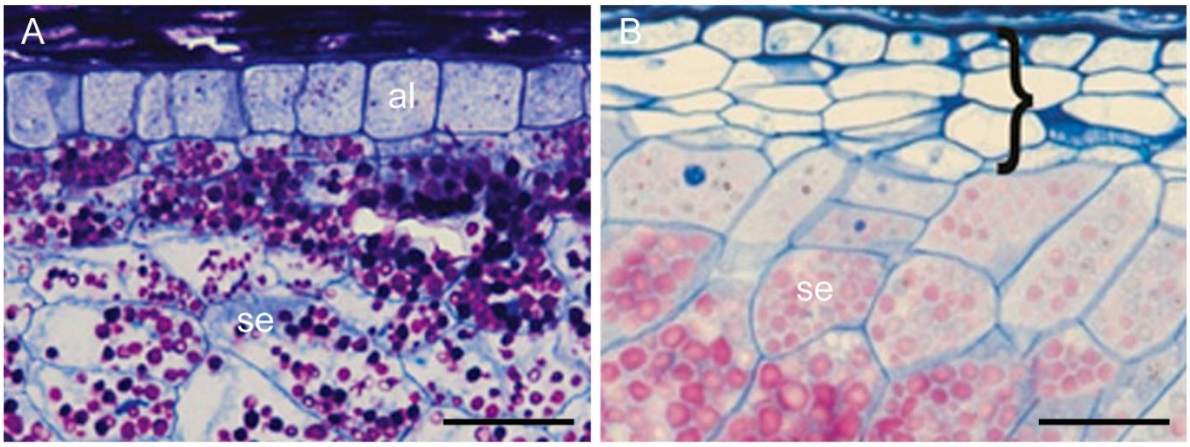

Figure 2-8. The *naked endosperm* (*nkd*) phenotype shows disruption in aleurone differentiation. (A) Wild-type maize endosperm containing a single layer of aleurone cells (al). (B) Maize *nkd* double mutant showing the multiple peripheral endosperm layers having neither characteristics of aleurone or starchy endosperm cells. Both A and B show histological stains with starchy endosperm cells (se) stained pink by periodic acid-Schiff and aleurone cells stained darkly with Toluidine Blue counterstain. Scale bars = 50 μm. Modified from Yi et al. (2015).

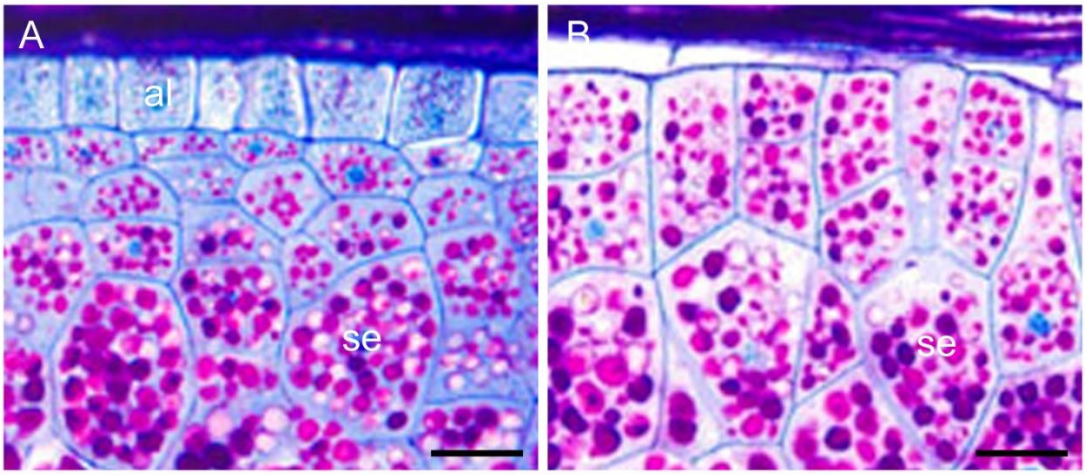

Figure 2-9. The *defective kernel 1* (*dek1*) mutant phenotype showing the absence of an aleurone. (A) Wild type maize endosperm containing a single layer of aleurone cells (al). (B) Maize dek1 mutant possessing no aleurone and the peripheral cell layer showing starchy endosperm (se) identity as revealed by histological stains with periodic acid-Schiff (pink se) and Toluidine Blue (dark al) counterstain. Scale bars = 25 μm. Modified from Becraft and Yi (2011).

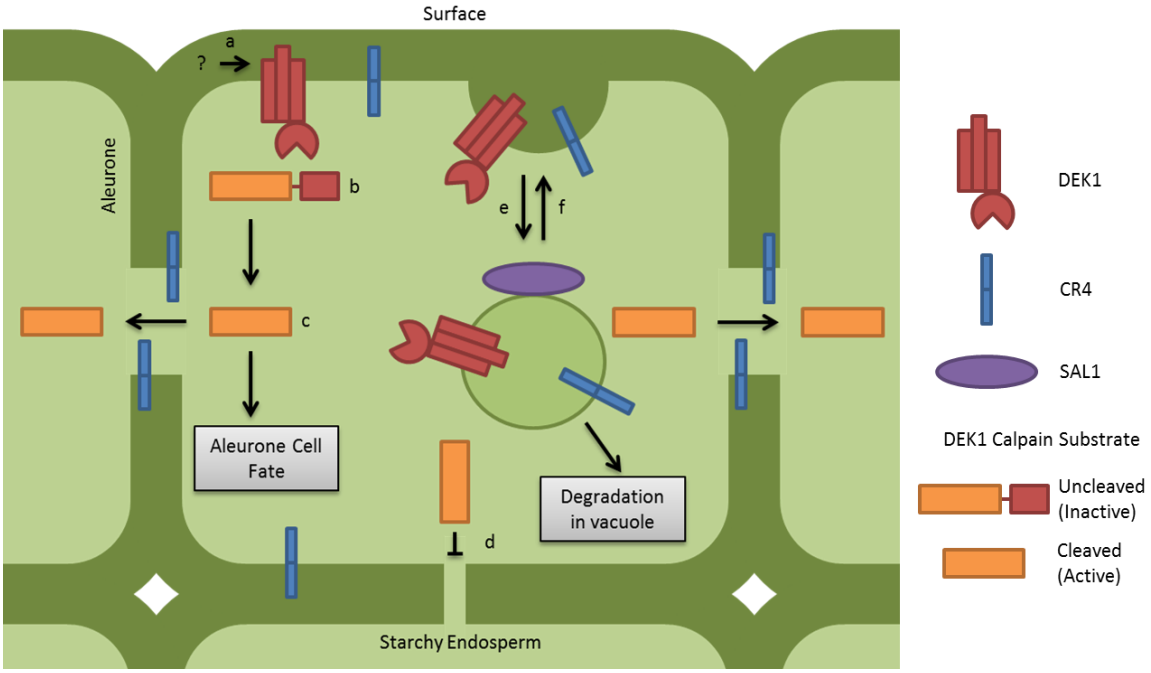

Figure 2-10. Proposed model for the involvement of DEK1, CR4 and SAL1 in aleurone cell specification. (a) Firstly, DEK1 present at the surface of the endosperm cell is activated through its perceptive function by an unknown mechanism. (b) The DEK1 calpain domain present in the cytoplasm is then able to cleave an unknown substrate. This active substrate is postulated from maize *in vitro* studies (Tian et al., 2007) and is essential for aleurone cell specification, but the mechanism of its involvement remains unclear. During DEK1 signalling, CR4 accumulates around the plasmodesmata between aleurone cells functioning to increase the exclusion limit and allow for signals to move through. This allows the active substrate to move between aleurone cells and strengthen the aleurone cell specification signal. (d) Plasmodesmata between aleurone and starchy endosperm cells are suspected to be too narrow for the active substrate to pass through or the exclusion limit remains too low due to the lack of surrounding CR4. (e) DEK1 and CR4 regulation occurs through endocytosis where the proteins can either be (f) recycled back to the plasma membrane or undergo degradation in the vacuole via SAL1. Modified from Tian et al. (2007).

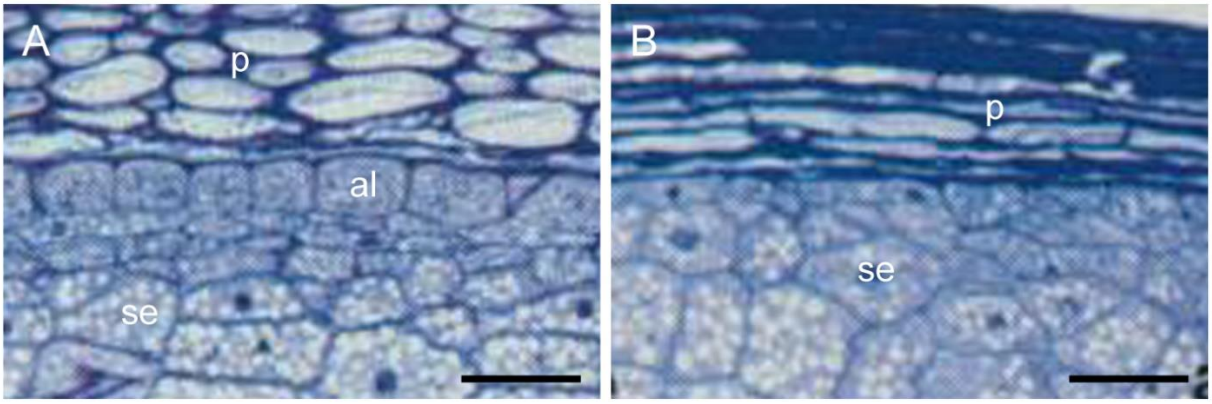

Figure 2-11. The *crinkly 4* (*cr4*) maize mutant phenotype showing the mosaic aleurone. (A) Section of wild type maize endosperm where the single densely stained peripheral layer is the aleurone (al) adjacent to the pericarp and large irregularly shaped cells are the starchy endosperm (se). (B) Section from a *cr4* mutant kernel showing both al and se at the most peripheral layer of the endosperm, producing a mosaic aleurone. Scale bar = 50 μm. Modified from Becraft et al. (1996).

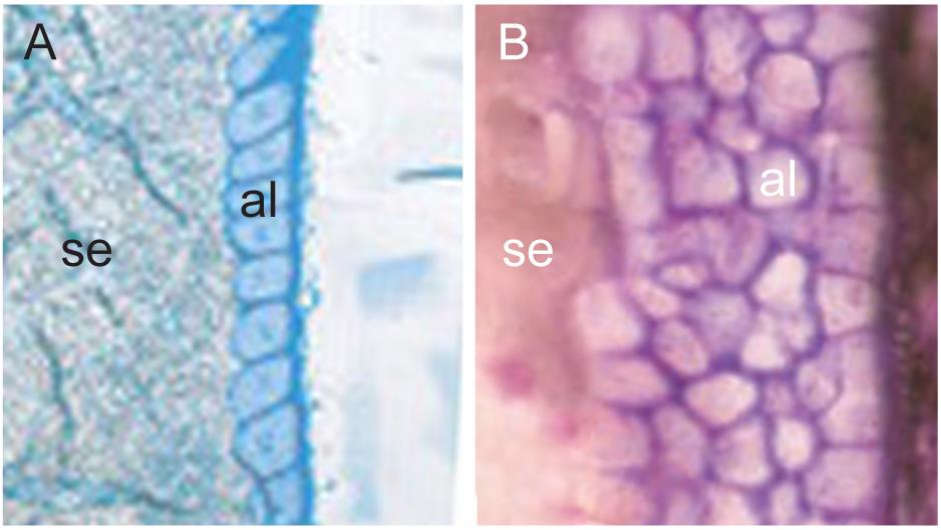

Figure 2-12. The *supernumerary aleurone layer 1* (*sal1*) mutant phenotype showing the increased number of aleurone layers in maize. (A) Wild-type kernel containing a single layer of aleurone cells (al). Section stained with Toluidine Blue O, modified from Geisler-Lee and Gallie (2005). (B) Maize *sal1* mutant possessing a multilayered aleurone, with up to five layers. Section was stained with Sudan red (staining neutral lipids) and Toluidine Blue counterstain, modified from Shen et al. (2003). al, aleurone; se, starchy endosperm.

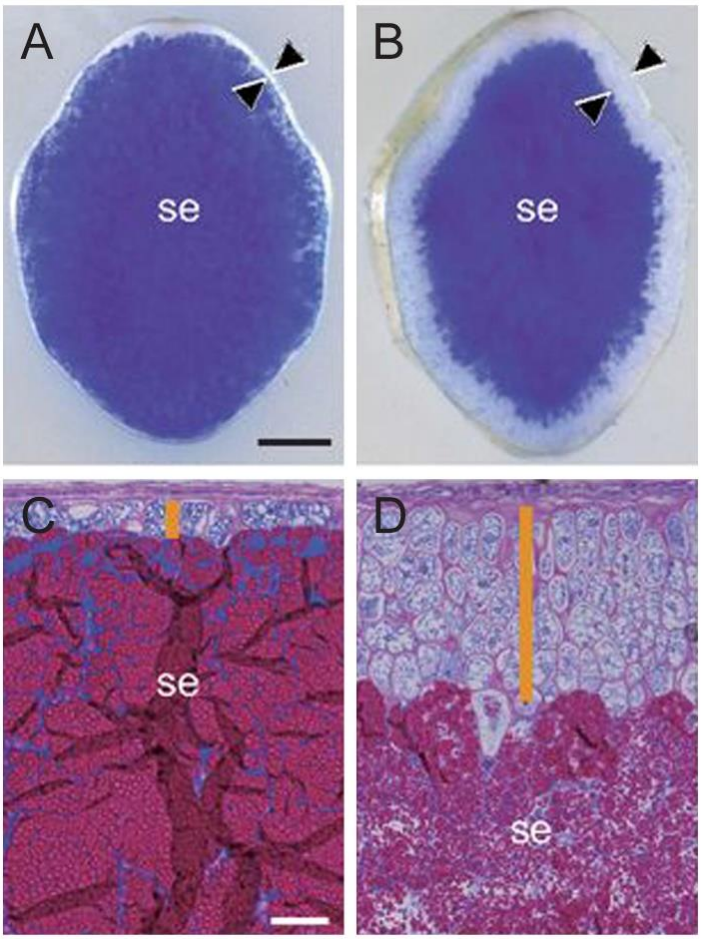

Figure 2-13. The *thick aleurone 2* (*ta2*) mutant phenotype showing increased aleurone tissue in rice. (A–B). Transverse sections of wild-type (A) and *ta2* (B) dehusked mature rice grains, stained with Evans blue, a dye that stains dead tissues by penetrating membranes with compromised integrity. Scale bar = 0.5 mm. (C–D) Morphology of the aleurone at the lateral positions of wild-type (C) and *ta2* (D) endosperms. Scale bar = 50 μm. Orange lines indicate aleurone. se, starchy endosperm. Modified from Liu et al. (2018).

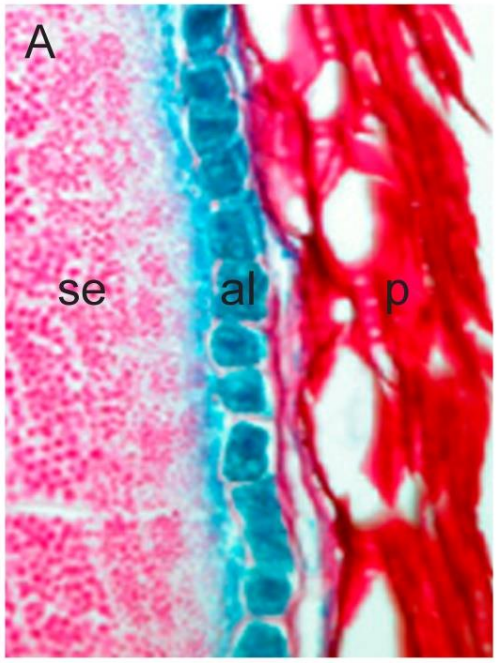

Figure 2-14. Cross section of a transgenic maize grain with *VP1* as a reporter gene marker for aleurone cells. The aleurone cell layer (al) is stained to detect *VP1::GUS* expression that can be observed in blue. Counterstains have been used to visualise the starchy endosperm (se) and pericarp (p) using periodic acid-Schiff seen in pink/red. Modified from Cao et al. (2007).

Chapter 3

Aleurone development in barley (*Hordeum vulgare* L.) is regulated by auxin and homologues of the Zea mays *NAKED ENDOSPERM 1* and *SUPERNUMERARY ALEURONE LAYER 1* genes

Statement of Authorship

Title of Paper	Aleurone development in barley (*Hordeum vulgare* L.) is regulated by auxin and homologues of the *Zea mays NAKED ENDOSPERM 1* and *SUPERNUMERARY ALEURONE 1* genes
Publication Status	☐ Published ☐ Accepted for Publication ☐ Submitted for Publication ☑ Unpublished and Unsubmitted work written in manuscript style
Publication Details	Matthew K. Aubert[1,2], Susan Johnson[1], Denghao Wu[1], Rohan Singh[1], Christopher Davies[3], Neil J. Shirley[1,2], Rachel A. Burton[2] and Matthew R Tucker[1]*.

Principal Author

Name of Principal Author (Candidate)	Matthew K. Aubert		
Contribution to the Paper	Performed experiments, analysed all samples, interpreted data and wrote manuscript.		
Overall percentage (%)	70%		
Certification:	This paper reports on original research I conducted during the period of my Higher Degree by Research candidature and is not subject to any obligations or contractual agreements with a third party that would constrain its inclusion in this thesis. I am the primary author of this paper.		
Signature		Date	21/11/2018

Co-Author Contributions

By signing the Statement of Authorship, each author certifies that:

i. the candidate's stated contribution to the publication is accurate (as detailed above);

ii. permission is granted for the candidate in include the publication in the thesis; and

iii. the sum of all co-author contributions is equal to 100% less the candidate's stated contribution.

Name of Co-Author	Susan Johnson		
Contribution to the Paper	Performed and helped with microscopy. I hereby certify that the statement of authorship is accurate.		
Signature		Date	20/11/2018

Name of Co-Author	Denghao Wu		
Contribution to the Paper	Performed microscopy and analysed samples. I hereby certify that the statement of authorship is accurate.		
Signature		Date	21/11/2018

Name of Co-Author	Rohan Singh		
Contribution to the Paper	Performed barley transformation work. I hereby certify that the statement of authorship is accurate.		
Signature		Date	20/11/2018.

Name of Co-Author	Christopher Davies		
Contribution to the Paper	Conceived part of the project and helped to design experiments. Provided NAA and TIBA. I hereby certify that the statement of authorship is accurate.		
Signature		Date	20/11/2018

Name of Co-Author	Neil J. Shirley		
Contribution to the Paper	Performed quantitative PCR, assembled RNA sequencing library and helped with sample analysis. I hereby certify that the statement of authorship is accurate.		
Signature		Date	21/11/18

Name of Co-Author	Rachel A. Burton		
Contribution to the Paper	Conceived project and helped to design experiments. Contributed to the preparation of the manuscript. I hereby certify that the statement of authorship is accurate.		
Signature		Date	22/11/2018

Name of Co-Author	Matthew R. Tucker		
Contribution to the Paper	Conceived project and designed experiments. Contributed to the preparation of the manuscript. I hereby certify that the statement of authorship is accurate.		
Signature		Date	20/11/18

Title Aleurone development in barley (*Hordeum vulgare* L.) is regulated by auxin and homologues of the *Zea mays NAKED ENDOSPERM 1* and *SUPERNUMERARY ALEURONE LAYER 1* genes

Authors Matthew K. Aubert[1,2], Susan Johnson[1], Denghao Wu[1], Rohan Singh[1], Christopher Davies[3], Neil J. Shirley[1,2], Rachel A. Burton[2] and Matthew R Tucker[1]*.

[1]School of Agriculture, Food and Wine, Waite Research Institute, The University of Adelaide, Glen Osmond, SA, Australia.

[2]Australian Research Council Centre of Excellence in Plant Cell Walls, The University of Adelaide, Adelaide, Australia.

[3]CSIRO Agriculture and Food, Glen Osmond, SA, Australia.

Keywords Barley, transgenic, aleurone, endosperm, development, nkd1, sal1, auxin, gene

Abbreviations

ABA	Abscisic acid
AGO	Argonaute
aMIR	Artificial micro-RNA
AUX	Auxin transporter protein 1
BMM	Butyl methyl methacrylate
CHMP1	Charged multivesicular body protein 1/chromatin-modifying protein 1
CR4	CRINKLY 4
cv	Cultivar
CYC3B	Mitotic cyclin 3B-like
DAP	Days after pollination
DEK1	DEFECTIVE KERNEL 1
DMSO	Dimethyl sulfoxide
DPA	Days post anthesis
DTT	1,4-Dithiothreitol
ESCRTs	Endosomal sorting complexes required for transport
GA	Gibberellic acid
HorB1	HORDEIN B1
IAA	Indole-3-acetic acid
IDD	INDETERMINATE1 domain
LCM	Laser capture microdissection
LTP2	LIPID TRANSFER PROTEIN 2
NAA	Naphthalene-1-acetic acid
NKD1	NAKED ENDOSPERM 1
NLS	Nuclear localising sequence

NPA	N-1-naphthylphthalamic acid
PBS	Phosphate-buffered saline
PIN	PIN-Formed
PROS	Positive regulator of SKD1
qPCR	quantitative Polymerase chain reaction
RBR1	Retinoblastoma-related1
RNAseq	RNA sequencing
SAL1	SUPERNUMERARY ALEURONE LAYER 1
TA2	THICK ALEURONE 2
TF	Transcription factor
THK1	THICK ALEURONE 1
TIBA	2,3,5-triiodobenzoic acid
UTR	Untranslated region
VSP	Vacuolar sorting protein
YFP	Yellow florescent protein

Abstract

The aleurone is a critical component of the cereal grain that acts as a repository for micronutrients and lipids as well as producing key enzymes required for germination. Differences in aleurone structure have been observed across the cereals; barley has a multilayered aleurone, while other cereal grains such as wheat produce a single layer of aleurone cells. The pathways and molecular mechanisms that define aleurone cell fate in barley are not well understood, however regulatory factors have been identified in several species. Genes such as *NAKED ENDOSPERM 1* (*NKD1*) and *SUPERNUMERARY ALEURONE LAYER 1* (*SAL1*) influence aleurone development in *Zea mays* (maize), with mutants showing defects in the number and organisation of aleurone layers. Phytohormones such as auxin also play a role in cereal grain development and appear to influence aleurone morphology. To date it is unclear whether these factors directly contribute to aleurone development in barley, particularly in the context of a multilayered aleurone. In this study, barley homologues of several maize genes implicated in aleurone development were examined to determine their temporal and spatial expression dynamics during grain formation. Transgenic knockdown and overexpression lines were developed to modify *NKD1* and *SAL1* expression in specific barley grain tissues, and results suggest that both genes fulfil key functions during aleurone development. In parallel, the role of auxin in controlling sub-epidermal grain morphology was examined through exogenous auxin (NAA) and auxin inhibitor (TIBA) treatments. Treated barley grain showed differences in tissue development, specifically in the aleurone and sub-aleurone, and in aleurone-related gene expression. Taken together, the results suggest that conserved factors influence barley aleurone development via a complex developmental pathway involving both genetic and hormonal inputs across the cereals.

Introduction

Cereal grains have been widely studied since they represent an important food source for animals and humans, and provide the major calorie intake for an ever-growing population. Although barley (*Hordeum vulgare* L.) fulfils a relatively minor role as a food for human consumption, barley grain is a major additive for animal feed (Verardo et al., 2011) and is heavily utilised to produce malt for brewing and distilling (Newman and Newman, 2006). The predominant tissue in the barley grain is the endosperm, which functions as a key source of complex carbohydrates and nutrients for embryo germination. During grain development, the endosperm also protects the embryo by providing a mechanical barrier against stress (Yan et al., 2014). In barley, endosperm formation begins within the embryo sac after fertilisation of the central cell, involving fusion of the two maternal polar nuclei with one male sperm cell (Olsen, 2004; Becraft and Yi, 2011; Yan et al., 2014; Wilkinson and Tucker, 2017). The primary triploid endosperm nucleus subsequently undergoes several rounds of mitotic division without cytokinesis, with nuclei repeatedly dividing and dispersing evenly around the periphery of the central cell (Leroux et al., 2014). This nuclear or syncytial phase of endosperm development is followed by cellularisation, when periclinal divisions and anticlinal wall formation occur until the endosperm is fully cellularised and endosperm differentiation can initiate (Olsen, 2004; Leroux et al., 2014). Differentiation produces four key tissues, the embryo surrounding region, endosperm transfer layer, starchy endosperm and aleurone. The transfer layer adjoins the nucellar projection and funnels nutrients into the starchy endosperm, which acts a storage tissue for protein and starch. The aleurone is a peripheral endosperm tissue that forms approximately 7 days after pollination (Wilson et al., 2006; Aubert et al., 2018) and exhibits a different cellular composition and morphology to the starchy endosperm, accumulating vitamins,

minerals, proteins and lipids in cube-shaped cells that develop thick walls reinforced with phenolic acids and polysaccharides such as arabinoxylan (Geisler-Lee and Gallie, 2005; Liu, 2011; Regvar et al., 2011; Gillies et al., 2012). The mature aleurone has been of particular interest for human health and industrial applications since it accumulates high levels of health promoting compounds and is crucial for metabolite mobilisation during grain germination.

Our current understanding of pathways involved in aleurone development in the cereals arises primarily from studies in maize (Qi et al., 2017). Aleurone fate in maize appears to be determined by positional cues, since aberrant periclinal divisions of aleurone cells produce daughters that differentiate into starchy endosperm cells (Olsen, 2004; Geisler-Lee and Gallie, 2005; Gruis et al., 2006). Moreover, starchy endosperm appears to be the default cell identity, since aleurone cells fail to develop at the endosperm periphery in the absence of several cues (Becraft et al., 1996; Becraft and Asuncion-Crabb, 2000; Lid et al., 2002; Shen et al., 2003; Gruis et al., 2006; Gillies et al., 2012). These cues include phytohormones, such as auxin and cytokinin, since maize mutants deficient in phytohormone production give rise to a mosaic aleurone (Geisler-Lee and Gallie, 2005). Auxin is transported and concentrated in the periphery of the maize endosperm and aleurone (Forestan et al., 2010; Figueiredo et al., 2015; Pielot et al., 2015), and has been implicated in both embryo sac and aleurone cell fate (Pagnussat et al., 2009; Locascio et al., 2014). Forestan et al. (2010) found that maize plants treated with an auxin transport inhibitor (N-1-naphthylphthalamic acid; NPA) produced kernels with a multilayered aleurone, whereas wild-type kernels normally have a single layer. This suggests that local auxin accumulation within the grain may induce aleurone cell fate. In contrast, cytokinin stimulates cell division within endoreduplicated cells and can have an inhibitory effect on aleurone differentiation

(Becraft and Yi, 2011). Auxin may act in opposition to cytokinin since the auxin concentration is high when the cytokinin concentration is low (Locascio et al., 2014). Other hormones have also been implicated in the maintenance of aleurone cells, these include abscisic acid (ABA) and gibberellic acid (GA) (Chandler et al., 1984; Nguyen et al., 2007).

Key genes that influence aleurone development have been identified through the analysis of mutants in maize and rice (Becraft and Asuncion-Crabb, 2000; Olsen, 2004; Wisniewski and Rogowsky, 2004; Liu et al., 2018). Homozygous mutants of several maize genes show pleiotropic phenotypic effects, most severe in epidermal structures including the aleurone (Olsen et al., 2008). In the *crinkly 4* (*cr4*) and *defective kernel 1* (*dek1*) mutants, the aleurone layer of mature kernels is defective or absent, indicating that these two genes are required for the perception or transmission of the signals specifying aleurone cell fate (Becraft et al., 1996; Becraft et al., 2002; Lid et al., 2002). *DEK1* encodes a putative cell-wall integrity sensor (Amanda et al., 2016) while *CR4* encodes a receptor-like kinase that accumulates near plasmodesmata (Jin et al., 2000). Recently, the *THICK ALEURONE 1* (*THK1*) gene, was found to negatively regulate aleurone cell fate in sub-aleurone cells and function downstream of DEK1, as suggested by *thk1/dek1* double mutant analysis (Yi et al., 2011; Qi et al., 2017). Similarly, a rice mutant called *thick aleurone* (*ta2*) was identified that produces four or more aleurone cell layers compared to a single layer in wild-type grains. *TA2* encodes a DNA demethylase, the *repressor of silencing 1* (*OsROS1*) gene that appears to be involved in epigenetic regulation of gene expression (Liu et al., 2018).

Another maize mutant, *naked endosperm* (*nkd*), displays altered aleurone differentiation with a mosaic aleurone phenotype of two to five layers of undifferentiated peripheral endosperm cells, which exhibit neither starchy endosperm nor aleurone

characteristics (Yi et al., 2015). There are two duplicate *NKD* genes present in maize, *NKD1* and *NKD2*, both encoding transcription factors (TF) containing a conserved C2H2 zinc finger DNA-binding domain known as the INTERMEDIATE1 domain (IDD). NKD is hypothesised to act as a repressor of aleurone cell proliferation since cell cycle-related genes including *RETINOBLASTOMA-RELATED1* (*RBR1*) and *mitotic cyclin 3B-like* (*CYC3B*) are predicted to be negatively regulated by NKD (Gontarek et al., 2016). Recent reports indicate that NKD influences many genes involved in aleurone cell fate, aleurone maturation, starch biosynthesis, anthocyanin biosynthesis and stress response (Yi et al., 2015; Gontarek and Becraft, 2017).

Another gene identified in maize that acts as a negative regulator of aleurone cell fate is the *SUPERNUMERARY ALEURONE LAYER 1* (*SAL1*) gene. In *sal1* mutants, up to seven layers of aleurone cells can be observed in the endosperm (Shen et al., 2003). SAL1 has been characterised as a vacuolar type E sorting protein, which is similar to human CHMP1 involved in vesicle trafficking. SAL1 is proposed to act upstream of DEK1 and CR4, inducers of aleurone cell fate, by directing their recycling from the plasma membrane and thus dampening their signalling activity (Tian et al., 2007).

In contrast to maize, relatively little is known about the molecular basis for aleurone development in barley, and it is unclear how or why the multilayered aleurone is produced. One possibility is that genes or hormonal pathways homologous to those influencing aleurone development in other cereals might function differently in barley. Given the importance of genes such as *NKD1* and *SAL1* in maize aleurone development, it is of considerable interest to determine whether homologous genes show a similar function during barley grain development.

In this study, the barley homologues of *ZmNKD1* and *ZmSAL1* were investigated to assess their role during aleurone development. Transgenic cell-type specific

knockdown and overexpression lines were developed using either aleurone-specific or starchy-endosperm specific promoters, driving expression of either artificial microRNAs or full-length coding sequences. To assess the mRNA localisation of *HvNKD1* and *HvSAL1* within the developing barley grain, laser capture microdissection (LCM) was utilised. In parallel, the response of barley grain, and the *HvNKD1* and *HvSAL1* genes, to exogenous application of auxin and an auxin transport inhibitor was investigated. Findings suggest that *HvNKD1* and *HvSAL1* are required for correct aleurone development in barley, but differ from maize in that an aleurone still develops with reduced *HvNKD1* and *HvSAL1* expression. This suggests that other factors are required for aleurone specification in barley and that *HvNKD1* and *HvSAL1* may function downstream of an aleurone promoting signal. Additionally, hormone balance and/or regulation, specifically auxin, influences aleurone and sub-aleurone cell fate.

Materials and Methods

Plant material and growth conditions

Two reference barley cultivars were used in this study. *Hordeum vulgare* cv. Sloop is an elite Australian 2-row spring barley that has been used in the past to characterise morphological features of early grain development (Wilson et al., 2006) and to document the expression of genes involved in endosperm cell wall formation (Burton et al., 2008). *Hordeum vulgare* WI4330 is a more recent elite Australian 2-row spring barley that shows high fertility, is optimised for Australian growth conditions and is compatible with transformation protocols. Transgenic lines were generated in the WI4330 background (MA017, MA019, MA024, MA026, MA033, MA034, MA065, MA069, MA089 and MA090). All plants were grown in The Plant Accelerator, Adelaide, Australia, at daytime and night time temperatures of 22°C and 15°C, respectively.

Vector Construction

Marker Lines

DNA fragments were synthesised by Genscript (USA) and inserted into the pUC57 vector. The 2.6kb *3xnls-YFP* gene (MA044) was adapted from Ueda et al. (2011) and codon optimized for *Hordeum vulgare* using the online tool at https://sg.idtdna.com/CodonOpt. The 807bp promoter sequence of the barley gene encoding *LIPID TRANSFER PROTEIN 2* (*LTP2*; HORVU4Hr1G089500; MA001) was previously published (Olsen and Kalla, 1993), and in this study the sequence was obtained from cv. Morex (contig_38354). The 1975bp barley *HORDEIN B1* (*HorB1*; HORVU1Hr1G001420) promoter sequence (MA004) was identified in a cv. Morex BAC contig (HVVMRXALLHA0620G07_C5) using MLOC_46003 and CUST_3883 as bait

in BLAST searches (Zhang et al., 2016) (http://webblast.ipk-gatersleben.de/barley_ibsc/). Both promoters were modified to include 5'-HindIII and 3'-KpnI restriction sites. The HindIII/KpnI pLTP2 fragment from MA001 and HindIII/KpnI pHorB1 fragment from MA004 were excised and inserted into the Gateway-compatible pMDC32 vector (Curtis and Grossniklaus, 2003) in place of the double 35S promoter, creating MA007 and MA010, respectively. The 3xnlsYFP sequence was amplified from pUC57 using pUC57-attL1_FWD (5'-ACCTCGCGAATGCATCTAGATCA-3') and SacI-attL2 REV (5'-CAAATAATGATTTTATTTTGACTGATAGTGACCTGTTCGTTGCAACAAATTGATGAGCAATTATTTTTTATAATGCCAACTTTGTACAAGAAAGCTGGGTTCATTATTTGGAGCTC-3') primers and HiFi Platinum Taq (ThermoFisher, Scoresby Vic, Australia) resulting in a PCR fragment flanked by attL1 and attL2 gateway compatible sites. The 3xnlsYFP insert was transferred into the MA007 (pLTP2:pMDC32) and MA010 (pHorB1:pMDC32) vectors using LR clonase II (ThermoFisher, Scoresby Vic, Australia) according to the manufacturer's instructions. The resulting vectors, MA021 (*pLTP2:3xnlsYFP*) and MA023 (*pHorB1:3xnlsYFP*), were transformed into *Agrobacterium tumefaciens* strain AGL1, becoming MA024 and MA026, respectively, prior to use in barley transformation.

Overexpression Lines

Full-length coding sequences for *HvNKD1* (1845bp) and *HvSAL1* (615bp) were identified by BLAST searches within MorexGenes (https://ics.hutton.ac.uk/morexGenes/index.html), EnsemblPlants (https://plants.ensembl.org/index.html) and IPK (http://webblast.ipk-gatersleben.de/barley_ibsc/) databases using the *ZmNKD1* and *ZmSAL1* genes as

bait. The best match for *ZmNKD1* was identified as MLOC_56120 / contig_40566 / HORVU2Hr1G095730. The genomic sequence of contig_40566 containing *HvNKD1* was examined using FGENESH (http://www.softberry.com) and *ZmNKD1* to identify a putative 1845bp coding sequence. This sequence was found to cover three HORVUs; HORVU2Hr1G095710, HORVU2Hr1G095720 and HORVU2Hr1G095730 as shown in Figure 3-1. This predicted ORF encodes a 614aa protein and is significantly longer than the 1184 bp coding sequence suggested for an almost identical *HvNKD1* gene from cv. Haruna nijo (AK374308), and the HORVU2Hr1G095730.7 model that encodes a predicted 556aa protein. The second-best match to *ZmNKD1* was MLOC_60958 / contig_44942 / HORVU6Hr1G064880. This gene appears to encode the barley orthologue of *ZmNKD2*. The putative *HvNKD1* and *HvNKD2* coding sequences are 72% identical over their length and have 70% protein sequence similarlity.

The best match for *ZmSAL1* was identified as MLOC_57384 / contig_41698 / HORVU7Hr1G115800, and no other matches of any significance were identified. The predicted coding sequences for *HvNKD1* and *HvSAL1* from cv. Morex were synthesised and inserted into the pUC57 vector. The *HvNKD1* and *HvSAL1* sequences were amplified from pUC57 using pUC57-attL1_FWD (5'-ACCTCGCGAATGCATCTAGATCA-3') and NKD1_attL2_REV (5'-CAAATAATGATTTTATTTTGACTGATAGTGACCTGTTCGTTGCAACAAATTGATGAGCAATTATTTTTTATAATGCCAACTTTGTACAAGAAAGCTGGGTTCATGGCATCCGGCCTCCGT-3') or SAL1_attL2_REV (5'-CAAATAATGATTTTATTTTGACTGATAGTGACCTGTTCGTTGCAACAAATTGATGAGCAATTATTTTTTATAATGCCAACTTTGTACAAGAAAGCTGGGTTCAGCCGCGGGCCTTGAGCT-3') primers, respectively, and HiFi Platinum Taq (ThermoFisher, Scoresby Vic, Australia) resulting in a PCR fragment flanked by attL1 and attL2

gateway compatible sites. Both *HvNKD1* and *HvSAL1* inserts were transferred into the MA007 (pLTP2:pMDC32) and MA010 (pHorB1:pMDC32) vectors using LR clonase II (ThermoFisher, Scoresby Vic, Australia) according to the manufacturer's instructions, respectively. The resulting vectors, MA049 (*pLTP2:HvNKD1*), MA051 (*pLTP2:HvSAL1*), MA054 (*pHorB1:HvNKD1*) and MA055 (*pHorB1:HvSAL1*), were transformed into *Agrobacterium tumefaciens* strain AGL1, becoming MA089, MA065, MA090 and MA069, respectively, prior to use in barley transformation.

Knockdown Lines

Artificial micro-RNA (aMIR) sequences targeting *HvNKD1* and *HvSAL1* were developed using the online predictor tool WMD3 (Warthmann et al., 2008) (http://wmd3.weigelworld.org/cgi-bin/webapp.cgi?page=Home;project=stdwmd) or P-SAMs (Fahlgren et al., 2016) (http://p-sams.carringtonlab.org/) integrated into the *OsMIR390-AtL* precursor (Carbonell et al., 2015) *in silico* and then synthesised by Genscript in the pUC57 vector flanked by LR cloning sites. Care was taken in the case of *HvNKD1* to ensure the amiRNA would not target the predicted *HvNKD2* sequence. The TAACTCGCTAACCTTACTCTG miRNA (amiR-NKD1) sequence used to target *HvNKD1* was the best predicted amiRNA from WMD3 and is located within the exon encoding the IDD domain, approximately 241bp upstream of the putative stop codon. The TCAGCTTCTCCGGGTTGCCCT miRNA (miR-SAL1) sequence used to target *HvSAL1* was predicted by P-SAMS and is located at position +2 in the coding sequence. The full length aMIR-NKD1 and aMIR-SAL1 precursor sequences were amplified from pUC57 using pUC57-attL1_FWD (5'-ACCTCGCGAATGCATCTAGATCA-3') and OsMIR390-attL2 REV (5'-CAAATAATGATTTTATTTTGACTGATAGTGACCTGTTCGTTGCAACAAATTGATGA

GCAATTATTTTTTATAATGCCAACTTTGTACAAGAAAGCTGGGTGAGACTAAAGA TGAGATCTA-3') primers and HiFi Platinum Taq (ThermoFisher, Scoresby Vic, Australia) resulting in a PCR fragment flanked by attL1 and attL2 gateway compatible sites. Both aMIR-NKD1 and aMIR-SAL1 inserts were transferred into the MA007 (pLTP2:pMDC32) and MA010 (pHorB1:pMDC32) vectors using LR clonase II (ThermoFisher, Scoresby Vic, Australia) according to the manufacturer's instructions, respectively. The resulting vectors, MA013 (*pLTP2:aMIR-NKD1*), MA015 (*pLTP2:aMIR-SAL1*), MA029 (*pHorB1:aMIR-NKD1*) and MA030 (*pHorB1:aMIR-SAL1*), were transformed into *Agrobacterium tumefaciens* strain AGL1, becoming MA017, MA019, MA033 and MA034, respectively, prior to use in barley transformation.

Agrobacterium-Mediated Barley Transformation

The transformation protocol was carried out as described in Tingay et al. (1997), but with modifications described by Matthews et al. (2001) and Burton et al. (2011). One modification was the replacement of *Hordeum vulgare* cv. Golden Promise with *Hordeum vulgare* WI4330. All plants were grown under standard glasshouse conditions following Burton et al. (2004).

Transverse grain and aleurone morphological trait analysis

To observe the aleurone in mature barley grain samples, approximately 10 grain were sectioned for each line and transverse grain measurements were recorded via UV autofluorescence and ZEN 2012 software as described in Aubert et al. (2018) (also see Chapter 4). Transverse endosperm area was measured by tracing the outline of whole endosperm, whist aleurone area was measured by tracing around the starchy

endosperm and subtracting from the total endosperm area. Transverse aleurone proportion was measured by taking the aleurone area as a percentage of the endosperm area. Aleurone layer number was recorded as an average where, in each section of barley grain, a maximum and minimum layer number was recorded at three different positions. Similarly, aleurone width was measured as the distance from the most peripheral autofluorescent aleurone wall to the starchy endosperm, the endpoint marked by the innermost autofluorescent aleurone cell wall.

Tissue Collection

Developing grains were staged at the beginning of anthesis; florets were opened to determine whether anthers had mature pollen present by tapping anthers on a fingernail. If pollen could be released after gentle application of pressure, then this was marked as 0 days post anthesis (DPA). Various developmental stages were collected for observation, including 7, 9, 11, 13, 15, 20 and 25 DPA. To observe aleurone morphology, staged samples were fixed in 0.25% glutaraldehyde, 4% paraformaldehyde and 4% sucrose in phosphate-buffered saline (PBS; pH 7.2), embedded in LR-White resin and sectioned to 1.0 µm as per Burton et al. (2011) and Betts et al. (2017). Sections were stained with Toluidine Blue (ProSciTech, Australia).

RNA extraction and cDNA synthesis

Developing barley grains were collected at the stages mentioned above (7 – 25 DPA) and embryo tissue was removed using a razor blade. Fresh tissue was placed into liquid nitrogen and stored at -80°C until required. Total RNA was extracted using the Spectrum™ Plant Total RNA kit (Sigma-Aldrich, USA). Post-extraction DNase

treatment with the Ambion® TURBO DNA-free™ kit was completed according to the manufacturer's instructions (Life Technologies Corporation, USA). The Superscript®III Reverse Transcriptase kit (Invitrogen, USA) was used to synthesise cDNA according to Burton et al. (2008).

Laser Capture Microdissection

Developing barley grains (cv. Sloop) were collected at the stages mentioned above (7 – 25 DPA) and were immediately fixed with an ice-cold mixture of 3:1 ethanol: acetic acid and 1mM 1,4-Dithiothreitol (DTT). Samples were stored at 4°C overnight then placed into 70% ethanol and maintained at -20°C until required. Samples were dehydrated with an ethanol series from 10%, 30%, 50%, 70 %, 80%, 90%, 95% and 100% ethanol (all containing 1mM DTT) and embedded in BMM resin containing 40mL n-butyl methacrylate, 10mL methyl methacrylate, 250mg benzoin methyl ether (ProSciTech, Australia) and 1mM DTT in BEEM capsules (ProSciTech, Australia). Samples were polymerised in a Cryo Chamber set at -20°C with UV light for 5 days. Transverse sections (5µm thick) were generated from the central part of the developing grain using an ultramicrotome (Leica microsystems, Germany) and placed onto a PEN-Membrane slide (Leica microsystems, Germany). Pericarp, aleurone and two different starchy endosperm tissues (inner and outer) were microdissected using a Leica LMD Microscope (Leica microsystems, Germany).

LCM RNA Extraction, Amplification and cDNA Synthesis

Total RNA was extracted with a Picopure RNA isolation kit (Thermo Fisher Scientific, USA) using DNase I. RNA integrity and concentration was determined using a

NanoDrop One (Thermo Fisher Scientific, USA). Total RNA was amplified twice using a MessageAmp II aRNA Amplification kit (Thermo Fisher Scientific, USA) as per Tucker et al. (2012). cDNA synthesis was performed using Superscript®III Reverse Transcriptase kit (Invitrogen, USA) according to Burton et al. (2008), however, random hexamer primers from the Roche Transcriptor First Strand cDNA Synthesis Kit (Roche Molecular Systems, Australia) were used instead of an Oligo dT Primer.

Application of auxin and an auxin inhibitor to barley plants

Selected barley plants (cv. Sloop and transgenic marker line MA024 (*pLTP2:3xnlsYFP*) in WI4330) were germinated and grown under standard conditions. From anthesis onwards, plants were watered for 14 days with 50µM Naphthalene-1-acetic acid (NAA, Sigma-Aldrich, USA) or 80µM 2,3,5-triiodobenzoic acid (TIBA, Sigma-Aldrich, USA) dissolved in dimethyl sulfoxide (DMSO; Sigma Aldrich, USA) and diluted to the appropriate concentration with water. Control plants were also watered with water containing an equal amount of DMSO. All plants were watered daily with 150 mL of solution as described in Wu and McSteen (2007). Three plants were used for each treatment, and developing grain were collected at the different stages of development described above.

Quantitative polymerase chain reaction (qPCR) primer design

Primers for *HvLTP2*, *HvHorB1*, *HvNKD1* and *HvSAL1* were designed to amplify a region including a small amount of coding sequence, the stop codon and the 3' untranslated region (UTR) of each gene using Primer3 (v.0.4.0) (Untergasser et al., 2012) and are shown in Table 3-S4. Primers were used in a blastn search against the

barley nucleotide sequence available on the NCBI database (http://blast.ncbi.nlm.nih.gov/Blast.cgi). Primer pairs with a single BLAST hit were used for qPCR. Best BLAST hit full-length gene sequences were downloaded and compared by BLAST against initial gene sequence in Geneious version 8.1.3. (Kearse et al., 2012).

Quantitative polymerase chain reaction

qPCR was conducted based on Burton et al. (2008) and the primers and PCR products are described in Table 3-S4. Two biological replicates of cDNAs from developing grains, 7 – 25 DPA, were used for each treatment. Normalisation factors from control genes (see Table 3-S4) were determined according to Vandesompele et al. (2002) and Burton et al. (2004). Normalisation factors were generated from the geometric means of control genes (Vandesompele et al., 2002; Burton et al., 2004).

Results

Identification of *NAKED ENDOSPERM 1* (*NKD1*) and *SUPERNUMERARY ALEURONE LAYER 1* (*SAL1*) homologues in barley

Full-length coding sequences for *HvNKD1* and *HvSAL1* were predicted by employing morexGenes, EnsemblPlants and IPK databases using the maize *ZmNKD1* gene and *ZmSAL1* genes as models. The best match for *ZmNKD1* was identified as MLOC_56120 / contig_40566 / HORVU2Hr1G095730 where the candidate *HvNKD1* gene has four exons encoding the C2H2-like zinc finger domain, three introns and is located on chromosome 2H (Figure 3-1A). However, due to poor gene models, the INTERMEDIATE DOMAIN (IDD) was not present within HORVU2Hr1G095730, but was located in the neighbouring gene HORVU2Hr1G095720, and the 5' region was present in the HORVU2Hr1G095710 gene. Therefore, a new gene model was constructed using the three genes, consisting of nine exons and six introns (Figure 3-1A). NKD1 was the sole focus during this study, rather than NKD2, due to time constraints and the difficulty in developing specific amiRNA knockdown lines targeting both NKD1 and NKD2. Furthermore, it was hypothesised that transgenics targeting NKD2 may not produce an altered aleurone since *nkd2* maize mutants generated by Yi et al. (2015) lacked any phenotypic defect when compared to wild-type and *nkd1* mutants. Similarly, whilst NKD2 showed a similar transcript pattern, the levels tended to be much lower than NKD1 in the endosperm and kernel (Yi et al., 2015). Based on these observations, NKD1 may contribute the majority of the genetic function required for normal endosperm development compared to NKD2. The best match for maize *ZmSAL1* gene was identified as MLOC_57384 / contig_41698 / HORVU7Hr1G115800, and no other matches of any significance were identified. The candidate *HvSAL1* gene has four exons, one intron and is located on chromosome 7H (Figure 3-1B). To confirm

whether these genes are expressed within the grain, published microarray data and tissue-specific RNA profiles were examined (Figure 3-1C and D) (Zhang et al., 2016). Oligonucleotide sequences present on the array showed homology to both genes; CUST_23722 for *NKD1* and CUST_19948 for *SAL1*. *HvNKD1* transcript abundance appeared to increase across early grain development (Figure 3-1C) and was highest in caryopsis (developing grain) tissue (Figure 3-1D). *HvSAL1* also appeared to increase during early grain development (Figure 3-1C), although transcript was detected in a number of tissues, with highest abundance in internode and early caryopsis tissue (Figure 3-1D). Expression patterns were also examined across mid to late stages of barley grain development (cv Sloop) using qPCR (Figure 3-1E). *HvNKD1* appeared to peak at nine days post anthesis (DPA) and decline across later stages of development. However, *HvSAL1* appeared to increase across grain development and peaked at 15 DPA. These results show that homologues of the maize *NKD1* and *SAL1* are present in barley and appear to be expressed in the grain during stages where aleurone is forming.

Generation of tissue-specific marker lines to assess promoter specificity in barley grain

In order to develop transgenic barley lines showing modified expression of candidate genes involved in aleurone development, suitable tissue-specific promotors were required. For the purposes of this study, two main tissue targets were identified; the aleurone and the starchy endosperm. The *LIPID TRANSFER PROTEIN 2* (*LTP2*) gene was selected since previous studies determined that the 5' upstream region (promoter) was sufficient to drive aleurone-specific expression in several cereal species (Kalla et al., 1994). Similarly, previous studies showed that various *HORDEIN* (*HOR*) genes are

specifically expressed in the endosperm and not in the aleurone (Onate et al., 1999; Cho et al., 2002; Furtado et al., 2009). Microarray analysis of a barley endosperm time course from anthesis to 8 days after pollination (DAP) (Zhang et al., 2016) confirmed that expression of *HvLTP2* and a putative *HvHorB1* gene coincides with the initiation and progression of endosperm cellularisation (Figure 3-2A). Additionally, both genes were specifically expressed in the developing caryopsis at 15 DAP according to a publicly available tissue RNAseq dataset (morexGenes) (IBGS, 2012) (Figure 3-2B). To assess the spatial location of *HvLTP2* and *HvHorB1* expression in the WI4330 background, transgenic marker lines were developed containing the promoter regions fused to a nuclear localised yellow fluorescent protein (3xnlsYFP). Transverse sections of developing grain from five independent transgenic lines showed that 3xnlsYFP fluorescence controlled by the *HvLTP2* promoter accumulated specifically in the aleurone, consistent with previous literature (Figure 3-2C). Fluorescence was observed as early as 7 DPA and persisted until at least 15 DPA (Figure 3-S3). Similarly, 3xnlsYFP fluorescence controlled by the *HvHorB1* promoter accumulated in the outer starchy endosperm tissue but not the aleurone from five examined *HvHorB1:3xnlsYFP* lines (Figure 3-2D). However, the pattern across development is unknown since only grains around 11-13 DPA were examined. These data suggest that the *HvLTP2* and *HvHorB1* promoters are suitable to drive tissue-specific expression of genes in the outer layers of the endosperm when the aleurone is developing.

Transgenic modification of candidate aleurone regulators using the *HvLTP2* and *HvHorB1* promoters

Transgenic barley lines were developed to modify expression of the barley homologues of *ZmNKD1*, which is reported to function as an inducer of aleurone fate

and a repressor of aleurone proliferation (Yi et al., 2015), and *ZmSAL1*, which is also reported to act as a repressor of aleurone proliferation (Shen et al., 2003). Knockdown lines were created using an artificial microRNA (aMIR) strategy (Carbonell et al., 2015), which was expected to induce post-transcriptional silencing in either the aleurone or outer starchy endosperm depending on the promoter used. Conversely, overexpression lines utilising the predicted full-length coding sequence of each gene, also under the control of the *HvLTP2* and *HvHorB1* promoters, were expected to contain higher amounts of transcript and protein in the aleurone or outer starchy endosperm respectively. In total, a minimum of eight and maximum of seventeen lines were generated for each construct and PCR was used to confirm the presence of the transgene in each line.

Mature grain samples from more than five T0 plants (i.e. T1 seed) were analysed by hand sectioning and UV autoflorescence microscopy to reveal potential differences in mature aleurone morphology (Figure 3-3). These grains were expected to segregate for the introduced transgenes, all of which are dominant in nature, and hence 75% of grain could potentially show a phenotype. Compared to control WI4330 plants, no significant differences in aleurone morphology were observed in transgenic knockdown or overexpression lines controlled by the *HvLTP2* promoter (Figure 3-4; Figure 3-S1; Figure 3-S2). In all cases, aleurone area, proportion, layer number and width appeared to be unchanged compared to grain produced by WI4330 controls. In contrast, lines expressing the various genes under the control of the *HvHorB1* promoter showed significant differences in aleurone morphology compared to each other and to wild-type WI4330 grain (Figure 3-3, Figure 3-4 and Table 3-S1). Aleurone differences were more prominent on the lateral side of the grain compared to the dorsal and ventral, thus lateral differences are reported here (Figure 3-3; Figure 3-S2; Table 3-S1; Table

3-S2; Table 3-S3). A significant decrease in aleurone cell layers was observed in grain produced from *pHorB1:aMIR-NKD1* (1.3 ± 0.5 layers; Figure 3-3A; Figure 3-4C) and *pHorB1:SAL1* plants (1.3 ± 0.5 layers; Figure 3-3F; Figure 3-4C), when compared to the WT (2.5 ± 0.5 layers; Figure 3-3E; Figure 3-4C). In addition, aleurone width was significantly decreased in both *pHorB1:aMIR-NKD1* (28.21 ± 7.35 µm) and *pHorB1:SAL1* (31.06 ± 8.04 µm) grain compared to the WT (47.42 ± 4.29 µm). Although the phenotypes were remarkably similar, aleurone cells appeared to be slightly larger in *pHorB1:SAL1* compared to *pHorB1:aMIR-NKD1* and WT (Figure 3-3). Importantly, no significant difference was observed in total transverse endosperm area between the transgenic lines and WI4330, suggesting that grain fill is not affected by the constructs and is unlikely to be a cause of the differences in aleurone morphology.

Aleurone traits were also modified in lines carrying the *pHorB1:NKD1* overexpression and *pHorB1:aMIR-SAL1* knockdown constructs (Figure 3-3D and 3-3C). In this case, aleurone area, proportion and width were affected. While WT grains exhibited an average transverse aleurone area of 0.55 ± 0.07 mm², *pHorB1:NKD1* and *pHorB1:aMIR-SAL1* appeared to produce significantly more aleurone with an area of 0.74 ± 0.07 mm² and 0.72 ± 0.09 mm², respectively (Table 3-S1 and Table 3-S2). Consistent with this, *pHorB1:aMIR-SAL1* grains produced a significantly higher proportion of aleurone (12.87 ± 2.63%) compared to WT (8.58 ± 1.29%; Figure 3-4 and Table 3-S1). However, unlike *pHorB1:aMIR-SAL1*, *pHorB1:NKD1* did not show a significantly higher aleurone proportion compared to the WT. Most likely, grain size, represented by transverse endosperm area, could be responsible for this difference. No significant difference in endosperm area was observed between *pHorB1:aMIR-SAL1* and *pHorB1:NKD1* when compared to the WT grain (5.68 ± 0.81 mm2 and 7.38 ± 0.56 mm2 compared to 6.49 ± 0.73 mm2, respectively), however, they were

significantly different from each other (Figure 3-S2A; Table 3-S1; Table 3-S2). *pHorB1:aMIR-SAL1* possessed a significantly higher proportion of aleurone due to less endosperm area and increased aleurone area, while *pHorB1:NKD1* was not significantly different due to possessing an initial large endosperm. The increase in aleurone area within the grains of *pHorB1:NKD1* and *pHorB1:aMIR-SAL1* appeared to be primarily caused by a significant increase in aleurone width (61.70 ± 10.95 µm and 70.33 ± 13.21 µm, respectively) compared to the WT (47.42 ± 4.29 µm), rather than aleurone layer number, which overall appeared to be unchanged (Figure 3-4 and Table 3-S1).

These data show that the *pHorB1:NKD1* and *pHorB1:aMIR-SAL1* constructs drive remarkably similar phenotypes, and have opposing effects on aleurone development compared to the *pHOR:aMIR-NKD1* and *pHorB1:SAL1* constructs. Taken together, the transgenic knockdown and overexpression lines under the control of the *pHorB1* promoter appeared to significantly affect aleurone morphology compared to the WT. Although molecular data confirming the over-expression and/or knockdown of the target genes is still to be finalised, these preliminary results are consistent with *HvNKD1* and *HvSAL1* playing important roles in barley grain development.

Tissue-specific expression analysis of *HvLTP2*, *HvHorB1* and other candidate aleurone genes

Phenotypic analysis of transgenic grain suggested that the modification of *HvNKD1* and *HvSAL1* expression in the starchy endosperm (driven by *pHorB1*) leads to altered aleurone development, while expression in the aleurone (driven by *pHvLTP2*) had no obvious effect. There are a number of possible explanations for this. First, it is unclear

whether the *pHvLTP2* constructs were effectively expressed during grain development. However, this would be inconsistent with the results of the *pHvLTP2:3xnlsYFP* transgene, which showed high levels of YFP expression during early grain development. Alternatively, *HvNKD1* and *HvSAL1* might not be expressed in the aleurone, but rather contribute to aleurone development from elsewhere in the grain. To assess where *HvNKD1* and *HvSAL1* are expressed in the developing grain, we utilised laser-capture microdissection followed by RNA sequencing. Thin transverse tissue sections of developing grain at two developmental time points (13 and 25 days post anthesis (DPA)) from cv. Sloop were dissected by laser-dissection to capture the outer starchy endosperm, inner starchy endosperm, pericarp and aleurone tissues from the midpoint of the grain (Figure 3-5A). RNA was extracted, amplified and sequenced to examine levels of *HvLTP2*, *HvHorB1*, *HvNKD1* and *HvSAL1* transcripts. Expression analysis confirmed that *HvLTP2* was aleurone specific at 13 and 25 DPA, while *HvHorB1* was predominantly expressed in the outer starchy endosperm (Figure 3-5B and 3-5C). These results generally support the YFP patterns observed in the *pHvLTP2* and *pHvHorB1* marker lines (Figure 3-2), although the *HvHorB1* mRNA profile at 13 DPA was somewhat broader than expected. This may indicate that additional cis-elements, absent from the *pHvHorB1* 5'upstream fragment, contribute to *HvHorB1* expression in other grain tissues, or that there is a small degree of starchy endosperm contamination in the different 13 DPA LCM tissues.

Transcripts for *HvNKD1* and *HvSAL1* were also detected in the LCM datasets although their relative abundance was lower than *HvLTP2* and *HvHorB1* (Figure 3-5D and 3-5E). In the case of *HvNKD1*, expression was detected in all four grain tissues with the highest levels in the aleurone and outer starchy endosperm. Expression of *HvSAL1* was most abundant in the pericarp at 13 DPA, but was also detected in filial tissues

including the aleurone at 13 DPA and 25 DPA. These profiles indicate both *HvNKD1* and *HvSAL1* are expressed widely in grain tissues including the aleurone. This may point to a complex interaction between the aleurone and adjoining cells that involves these genes and distinct functions in aleurone cell division and fate.

Exogenous application of auxin and an auxin-transport inhibitor induces changes in barley aleurone morphology

The transgenic approaches described above provide some evidence to support the conservation of molecular pathways regulating aleurone development between maize and barley. Another important regulator of endosperm development in plants is the phytohormone auxin (reviewed in Shirley et al. (2018), see Appendix III), which appears to influence the aleurone specification in maize (Forestan et al., 2010). Application of an auxin transport inhibitor to maize plants led to the formation of multiple aleurone layers in kernels, presumably due to the over-accumulation of auxin in kernel tissues. To determine if auxin contributes to aleurone development in barley, exogenous auxin (naphthalene-1-acetic acid; NAA) and an auxin transport inhibitor (2,3,5-triiodobenzoic acid; TIBA) were applied to cv. Sloop plants by daily watering from anthesis until 14 DPA. After fertilisation, developing grain samples were collected and sectioned at 7 DPA, 9 DPA and 15 DPA to characterise aleurone morphology.

Plants treated with NAA appeared to develop aleurone tissue faster than control or TIBA treated plants, since aleurone-like cells were already observed at the periphery of the starchy endosperm at 7 DPA (Compare Figure 3-6B with 3-6A-C). However, by 9 DPA, the aleurone was present and morphologically similar to grain from control, TIBA and NAA-treated plants (Figure 3-6D-F). The early formation of aleurone after

treatment with NAA was also confirmed in WI4330 plants containing the *pHvLTP2:3xnlsYFP* construct (Figure 3-S3). Although the staging differed slightly, *pHvLTP2:3xnlsYFP* was much more prominent at an earlier time point (9 DPA) in NAA-treated lines compared to control or TIBA-treated plants.

The main difference in morphology was observed at 15 DPA (Figure 3-6G-I). Grains from NAA-treated cv. Sloop plants contained a 3-4 layered aleurone, similar to the control, but the sub-aleurone cells appeared more cubical compared to the irregularly shaped sub-aleurone cells in control and TIBA plants. In grains from control plants, the sub-aleurone accumulated small starch granules and protein storage vesicles. These were also present in the sub-aleurone of NAA-treated samples, although less obvious, and the single nucleus appeared much more similar to the aleurone than starchy endosperm cells. Conversely, in the grains from TIBA-treated plants, differences were observed in the inner-most layer of the aleurone. This layer appeared to be under-developed compared to the outer 2-3 aleurone layers since the cell walls appeared to be thinner and fewer aleurone protein bodies were present (Figure 3-6I, indicated by the black arrow).

These results suggest that the application of NAA or TIBA to cv. Sloop plants via watering impacts grain development. It is unclear whether the early formation of aleurone in NAA-treated plants occurs as a consequence of overall faster reproductive development or grain-specific effects but the changes in sub-aleurone development appear to be consistent with specific effects of auxin within the developing grain. At grain maturity the aleurone from NAA treated and TIBA treated grain appeared similar to control grain (data not shown). This may suggest final aleurone morphology is unaffected, since the delay in aleurone development is overcome during subsequent stages of grain development.

Transcript levels of candidate barley aleurone regulating genes changes when exogenous auxin or inhibitor is applied

The morphological differences induced by NAA and TIBA could potentially result from the disruption of auxin transport within or around the grain. Based on the putative role of *HvNKD1* and *HvSAL1* in barley aleurone development (described above), it is possible that these genes respond to the modification of auxin signalling and contribute to the phenotypes in NAA and TIBA treated plants.

The response of *HvLTP2*, *HvHorB1*, *HvNKD1* and *HvSAL1* to exogenous NAA and TIBA treatment was investigated during grain development by quantitative PCR (qPCR; Figure 3-7). When assessing aleurone-specific *HvLTP2* expression (Figure 3-7A), transcripts were significantly higher at 7 DPA in grain from NAA-treated plants, which is consistent with the morphological data reported above (ie. Figure 3-6B). Similarly, at 13 and 15 DPA, *HvLTP2* was more abundant in grains from NAA-treated plants compared to TIBA-treated plants and controls. In contrast, grains from TIBA-treated plants showed the lowest *HvLTP2* transcript levels by 20 DPA, possibly indicating less aleurone tissue being developed. Curiously, grain from both NAA and TIBA-treated plants showed a reduction in *HvLTP2* expression relative to controls at this mature time point, perhaps indicating some late pleiotropic effects of continuous application of NAA or TIBA on grain development.

Differences were also observed in *HvHorB1* expression between the treatments. At 13 and 15 DPA, *HvHorB1* transcript was highest in NAA-treated plants, however, transcripts were more abundant in the control grains by 20 DPA (Figure 3-7B). In contrast to *HvLTP2*, the overall pattern of *HvHorB1* transcript accumulation was quite

similar between the treatments, arguing against a general de-regulation of grain development in the stages analysed.

In terms of the genes of interest, *HvNKD1* and *HvSAL1*, both exhibited high transcript levels in grain from NAA-treated plants at 7 DPA (Figure 3-7C and 3-7D). Similar to *HvLTP2*, this may result from the early appearance of aleurone tissue where both genes are expressed. More “aleurone-inducing signal” would potentially induce more *HvNKD1*, promoting aleurone cell fate, as well as *HvSAL1* to counteract or balance the aleurone signal. In contrast to NAA-treatments, TIBA appeared to reduce *HvNKD1* expression relative to both the control and NAA-treatment. Of the four genes analysed, *HvNKD1* was the most susceptible to NAA and TIBA treatments, with the overall profile appearing distinct from that in control plants. This may highlight *HvNKD1* as a gene that is particularly sensitive to fluctuations in hormone levels.

A key developmental time point was 13 DPA, where *HvNKD1* transcripts were high in grains from NAA-treated plants, while *HvSAL1* was high in grains from TIBA-treated plants. This was interesting since the higher abundance of *HvNKD1* may be sufficient to induce the physical changes observed in the sub-aleurone, as indicated by cytological observations, through either being transcribed in the sub-aleurone or an adjoining tissue. Likewise, the increase of *HvSAL1* at 13DPA in grains from TIBA-treated plants may impact the final stages in aleurone proliferation, causing the inner layer of sub-aleurone cells to remain under-developed.

Discussion

In this study, we combined several approaches to address the effect of two genes and the phytohormone auxin on aleurone development in barley. Transgenic studies suggest that *HvNKD1* and *HvSAL1,* similar to their orthologues in maize*,* fulfil key roles during aleurone development. Moreover, the application of auxin and an auxin transport inhibitor to barley plants induced changes in grain development, suggesting that endogenous auxin levels may contribute to aleurone formation. These findings are discussed below in terms of a basic model explaining molecular and physiological components of aleurone development in barley.

Transgenic knockdown and overexpression lines suggest that *HvNKD1* and *HvSAL1* are required for aleurone development in barley

A combination of mutants and transgenic lines have been utilised in previous studies of oat, wheat, maize and rice to investigate candidate genes involved in endosperm development (Kalla et al., 1994; Horvath et al., 2000; Lid et al., 2002; Perret et al., 2003; Thorneycroft et al., 2003; Qi et al., 2017). In regards to the aleurone, relatively little is known in cereal species other than maize, where a panel of mutants have been described that show defects in aleurone development (Becraft and Yi, 2011). The genes underlying these mutants have been cloned and characterised, found to encode a range of regulatory proteins, and linked to create models explaining aleurone specification and differentiation. Whether similar molecular pathways are involved in aleurone development in other cereal species has yet to be accurately addressed.

In this study, tissue-specific transgenic knockdown and overexpression lines were generated to assess whether homologues of characterised maize aleurone regulators

show similar function in barley (Figure 3-1). Promoters were chosen from candidate genes to drive aleurone-specific or endosperm-specific expression (Figure 3-2). The *LTP2* gene has been characterised as aleurone-specific in rice, maize and barley using fluorescent markers and *in situ* hybridisation (Kalla et al., 1994; Morino et al., 2004; Gruis et al., 2006). Similarly, the *HorB1* gene has been characterised as endosperm-specific (Brandt, 1976; Cho et al., 2002; Furtado et al., 2009). Here, using laser capture microdissection (LCM) in the Sloop cultivar, *HvLTP2* transcripts were almost uniquely detected within aleurone tissue (Figure 3-5) while *HvHorB1* transcripts were enriched in the outer starchy endosperm (Figure 3-5). Fusions to a barley codon-optimised *3xnlsYFP* gene confirmed the tissue-specificity of *pHvLTP2* (aleurone) and *pHvHorB1* (outer starchy endosperm; Figure 3-2) and their suitability for tissue-specific modification of barley grain gene expression. These promoter lines form a useful resource for further physiological and genetic studies of grain cell identity in barley. In addition, the laser capture datasets appear to be suitable for further study of tissue-specific gene expression in barley grain.

The *HvLTP2* and *HvHorB1* promoters were utilised in an attempt to modify the expression of *HvNKD1* and *HvSAL1*. In maize, *nkd* double mutant kernels show multiple layers of cells at the periphery of the endosperm; however, these cells have compromised identity and do not correctly differentiate into aleurone cells, hence the name naked endosperm (Yi et al., 2015). *NKD1* encodes an INDETERMINATE DOMAIN (IDD) transcription factor (TF), and IDD TFs have been found to regulate genes associated with cell cycle, cell growth and division (Yi et al., 2015). Hence, NKD1 most likely promotes aleurone cell fate through regulation of downstream target genes (Yi et al., 2015; Gontarek et al., 2016). In contrast, maize *sal1* mutant kernels exhibit an increased number of aleurone-like cell layers suggesting *SAL1* may act as

a negative regulator of aleurone proliferation (Shen et al., 2003; Tian et al., 2007). Homologues of both genes were identified in barley, and both *HvNKD1* and *HvSAL1* were found to be expressed in the developing endosperm by microarray analysis and qPCR (Figure 3-1), suggesting they may play a role in barley grain development.

Transgenic knockdown and overexpression lines targeting either *HvNKD1* or *HvSAL1* showed no obvious differences in aleurone morphology when controlled by the *HvLTP2* promoter (Figure 3-S2). One possibility is that the level of these genes in the aleurone was not significantly altered by the transgenic approaches. Artificial miRNAs require specific Argonaute (AGO) proteins to mediate silencing, and these genes may not be expressed within the aleurone. This could be analysed in future studies by examining the LCM RNA-seq datasets. One way to determine if correct aMIR knockdown has occurred would be to assess target gene expression across grain development via qPCR and compare to WT expression. However, preliminary results suggest that this may be difficult to confirm in wholegrain RNA samples when the amiRNA is targeted only to a subset of grain cells.

Another possible reason for the lack of any obvious effect of *pLTP2:aMIR-NKD1* and *pLTP2: aMIR-SAL1* on aleurone morphology is that *HvNKD1* and *HvSAL1* are not expressed or functioning in the aleurone but rather in neighbouring tissue. LCM data negates against the lack of expression model since both genes are detected in the aleurone, but *in situ* hybridisation will be required to confirm mRNA localisation of *HvNKD1* and *HvSAL1* in transgenic and WT lines. Whether both genes are required within the aleurone is more difficult to address. Several studies have shown the importance of intercellular signalling via plasmodesmata during aleurone development (Taiz and Jones, 1973; Tian et al., 2007), and one hypothesis could be that *HvNKD1* and *HvSAL1* are expressed at the periphery of the starchy endosperm and transported

into the aleurone. However, currently there is no evidence to support that HvNKD1 or HvSAL1 are mobile proteins. This might overcome any effect of amiRNA-mediated silencing of the genes in the aleurone itself. Support for such a model, whereby *HvNKD1* and *HvSAL1* contribute to aleurone development from tissues adjoining the aleurone, comes from the transgenic knockdown and overexpression lines controlled by the *HvHorB1* promoter, which induced dramatic changes in aleurone development. Artificial microRNA knockdown lines targeting either *HvNKD1* or *HvSAL1* showed inverse effects on aleurone morphology. Plants containing the *pHvHorB1:miR-NKD1* gene produced grain containing a thinner aleurone with less aleurone cell layers, while grain from *pHvHorB1:miR-SAL1* plants contained a thicker aleurone caused by an increase in aleurone cell size (Figure 3-3; Figure 3-4). Conversely, grain from *pHvHorB1:NKD1* plants tended to produce a thicker aleurone with larger aleurone cell size, whilst *pHvHorB1:SAL1* plants produced grain with a thinner aleurone with less aleurone cell layers (Figure 3-3; Figure 3-4). The opposite effects of the knockdown and over-expression constructs tend to suggest that *HvNKD1* and *HvSAL1* fulfil important opposing roles during barley endosperm development in the outer layers of the starchy endosperm.

A limitation of the transgenic analysis in this study is that aleurone morphology was scored based on mature aleurone localised phenolic acid autofluorescence phenotype. It is currently unclear when the phenotypes first appear, or if more cell layers have adopted an aleurone-like phenotype without accumulating phenolic acids, since developing grain sections were not examined. Therefore, grains will need to be collected and analysed across grain development in future experiments. Interestingly, all transgenic lines generated still develop an aleurone. This may indicate that *HvNKD1* and *HvSAL1* function downstream of the aleurone specification signal, while other

factors in the aleurone development pathway can still induce an aleurone phenotype. This result would need to be confirmed in future studies using CRISPR/Cas9 knockout lines since aMIR transgenic knockdown lines tend to create hypomorphic effects, rather than null mutations. Another limitation with the transgenics was that the level of knockdown and overexpression of *HvNKD1* and *HvSAL1* was not examined directly in the grain. This will need to be analysed during development of transgenic barley grains to determine the level of *HvNKD1*, *HvSAL1* and possible downstream target genes (Gontarek et al., 2016).

No previous studies appear to have reported a role for *HvNKD1* in barley grain development. Based on the findings presented here, *HvNKD1* appears to fulfil an important role, although there appear to be subtle differences between maize and barley. In maize, which usually contains a single layer of aleurone in each kernel, NKD1 is required to promote aleurone cell identity (Becraft and Asuncion-Crabb, 2000; Yi et al., 2015) but also to restrict the number of cell layers at the endosperm periphery, possibly as a result of de-regulated cell proliferation genes (Gontarek et al., 2016). In barley, the aleurone is already multilayered, with each layer accumulating diagnostic autofluorescent phenolic acids in the cell walls. *HvNKD1* appears to promote aleurone proliferation in barley, since fewer layers showed characteristic aleurone autofluorescence in amiRNA lines, but the aleurone was clearly still present. This suggests that the targets and/or the molecular mechanism of NKD1 may differ between maize and barley. This may be due to differences in grain morphology, target genes or other redundant factors. For example, it is possible that the *HvNKD2* gene fulfils some functions that overlap with *HvNKD1*. LCM data suggests that *HvNKD2* is expressed in multiple grain tissues but most abundant in the aleurone (Figure 3-S4), however, its contribution to grain development is currently unclear.

Unlike the *HvNKD1* gene, *HvSAL1* has been examined in previous studies of barley. Because SAL1 has been shown to act as a negative regulator of aleurone proliferation in maize (Shen et al., 2003; Tian et al., 2007), it was hypothesised that *HvSAL1* may contribute to the formation of increased number of aleurone cell layers in barley. *SAL1* encodes a class E vacuolar sorting protein (VSP), where VSPs form multimeric complexes called endosomal sorting complexes required for transport (ESCRTs) and have two major sorting functions: the recycling of vacuolar cargo receptors via endocytotic machinery and the sorting of membrane proteins for degradation (Hilscher et al., 2016). Decreased SAL1 activity is proposed to result in the accumulation of molecules regulating aleurone cell specification, such as HvDEK1 and HvCR4 at the plasma membrane (Shen et al., 2003), which are usually controlled by degradation through the endosomal pathway. This in turn results in an increased number of aleurone cell layers.

The results from this study suggest that *HvSAL1* is involved in grain development in barley. Transgenic overexpression of *HvSAL1* in the grain led to a significant decrease in aleurone layer number (down to a single layer in many grain), while expression of an *aMIR-SAL1* gene had no significant effect on layer number, but led to an increase in aleurone cell size (Figure 3-3; Figure 3-4). These results are intriguing, since they mimic a complementation-type effect that might be expected if WT barley was already a *sal1* mutant i.e. layer number can be rescued by overexpression but is insensitive to additional down-regulation. Although this is an attractive hypothesis, it is difficult to find additional support for the presence of a naturally hypomorphic *HvSAL1* pathway in barley. *HvSAL1* appears to be a single copy gene with few close homologues in barley; a full length *HvSAL1* sequence was identified in the cv Morex reference sequence (Figure 3-1) that shows high homology to maize *SAL1* and appears to encode a

functional protein. A near identical full-length sequence was identified in cv Sloop by RNAseq (data not shown). The gene is expressed at high levels in a number of tissues. A previous study examining variation in barley aleurone layer number (Jestin et al., 2008) identified a QTL close to the position of *HvSAL1* on chromosome 7H, but went on to state that polymorphisms in *HvSAL1* are not the underlying cause of detected variation. Further evidence to support or discount this theory is therefore required, either through the generation of CRISPR plants or analysis of natural variants.

One clear outcome is that *HvSAL1* down-regulation appears to impact cell expansion in the barley grain. Recently, a plant-specific ESCRT component known as *POSITIVE REGULATOR OF SKD1* (*PROS*) was found to be involved in cell expansion in *Arabidopsis thaliana* (Reyes et al., 2014). Other core ESCRT members HvSNF7a, HvVPS24 and HvVPS60a were examined by transient localisation studies in barley endosperm and expression was examined by RT-PCR from 12 DAP endosperm tissue (Hilscher et al., 2016). HvVPS24 was mainly localised in cytosolic regions in the aleurone and sub-aleurone, while HvVPS60a localised to the plasma membrane in aleurone cells and to a lesser extent in the plasma membrane and vacuolar membranes in sub-aleurone cells, suggesting that HvVPS60a may be involved in different cell layer-specific trafficking pathways. This may indicate that ESCRTs such as HvSAL1 are influenced by cell layer-specific protein deposition or trafficking and remodelling of the endomembrane system in endosperm tissues such as aleurone and sub-aleurone. This is consistent with the results in this study from LCM and transgenic analysis, and provides further support for a role of *HvSAL1* in the developing barley aleurone.

HvNKD1 and *HvSAL1* appear to respond to modified auxin signalling

Hormonal pathways are promising candidates that might act with, or in parallel to *HvNKD1* and *HvSAL1* genes during endosperm development in barley. It is currently hypothesised that aleurone cell differentiation occurs in response to surface position but the effect of maternal versus filial signals has been debated (Gruis et al., 2006; Reyes et al., 2010). Several studies suggest that phytohormones such as auxin fulfil a prominent role in this process (Geisler-Lee and Gallie, 2005; Bethke et al., 2006; Forestan et al., 2010). Genes expressed within the aleurone have previously been shown to respond to auxin. In maize endosperm, the auxin transporter ZmPIN-FORMED1 (ZmPIN1) is preferentially expressed in the aleurone, and treatment of developing kernels with the auxin transport inhibitor NPA induced alterations in aleurone cell layer number (Forestan et al., 2010). Furthermore, transgenic expression of isopentenyl transferase, a cytokinin-synthesising enzyme, showed a mosaic aleurone (Geisler-Lee and Gallie, 2005) suggesting that the auxin-cytokinin balance could be important for aleurone differentiation. To test the role of auxin in barley aleurone development, as well as the response of *HvNKD1* and *HvSAL1*, naphthalene-1-acetic acid (NAA) and 2,3,5-triiodobenzoic acid (TIBA) were applied to developing barley plants.

In maize, application of exogenous auxin inhibitor had various effects on kernel development (Wu and McSteen, 2007; Forestan et al., 2010). During normal maize development, the timing of developmental events and regulatory roles of auxin were examined and it was observed that auxin concentration, specifically indole-3-acetic acid (IAA), abruptly increased from 9 to 11 days after pollination (DAP). This increase in auxin levels directly induced cellular differentiation events, endoreduplication, and expression of particular zein storage proteins (Lur and Setter, 1993). High

accumulation of auxin was observed in the aleurone corresponding to the differentiation phase of endosperm development, while auxin levels decreased in the starchy endosperm (Forestan et al., 2010). Adopting the application method from Forestan et al. (2010), aleurone differentiation events appeared to occur earlier in the developing barley endosperm with the application of NAA, as well as inducing morphological changes in the sub-aleurone (Figure 3-6). When compared to the untreated grains, aleurone development occurred earlier, at 7 DPA compared to 9 DPA. Quantitative PCR results were consistent with more aleurone tissue being present earlier in NAA-treated grain (Figure 3-7A). Similarly, more cubical sub-aleurone cells were observed when compared to the untreated grain, suggesting auxin levels may affect sub-aleurone development. We hypothesise that accumulation of exogenous auxin may reach a certain threshold for the cells to start adopting aleurone cell fates, but not the maximum threshold to fully adopt an aleurone morphology.

Similar to *HvLTP2*, *HvNKD1* transcript appeared more abundant in NAA-treated grains during aleurone development indicating auxin may upregulate *HvNKD1* expression. This may be a result of early induction of the primary aleurone signal, resulting in faster aleurone development, specification and proliferation, thereby producing more aleurone tissue. As previously mentioned, *NKD1* encodes an IDD transcription factor, and several *Arabidopsis* IDD genes have been implicated in cellular patterning influenced by hormonal regulation (Cui et al., 2013; Yi et al., 2015). *Arabidopsis* IDD14-1A, IDD15, and IDD16 perform overlapping functions in directing auxin biosynthesis and transport (Cui et al., 2013). Similarly, *Arabidopsis* IDD proteins were also found to interact with proteins that mediate gibberellic acid (GA) induced gene expression and some IDD proteins also interacted with these genes directly (Feurtado et al., 2011; Yoshida et al., 2014; Yoshida and Ueguchi-Tanaka, 2014). Furthermore, maize *nkd1*

mutants show decreased expression of the *VP1* gene, required for ABA responses, including aleurone maturation (McCarty et al., 1989; McCarty et al., 1991; Cao et al., 2007). Therefore, increased *HvNKD1* expression during aleurone development, induced by exogenous NAA, may cause an auxin imbalance, allowing for more aleurone development. This could possibly occur through a cell division/proliferation pathway involving *SCL1*, *RBR1* and *CYC3B* genes and the *VP1* and ABA pathway, which controls aleurone maturation in maize (Yi et al., 2015; Gontarek et al., 2016).

In a parallel experiment, auxin distribution was modified with the auxin transport inhibitor 2,3,5-triiodobenzoic acid (TIBA) in order to investigate whether auxin transport has a role in barley endosperm patterning. Previous studies have examined treatments using the auxin transport inhibitor N-1-naphthylphthalamic acid (NPA), where NPA induced differentiation of up to four layers of aleurone cells in the maize endosperm (Forestan et al., 2010). The phenotypes may be due to auxin being trapped within the kernel, as observed in NPA-treated *Hieracium* ovules (Tucker et al., 2012). Differentiation of up to two layers of aleurone cells was observed in TIBA treated plants along with a third under-developed aleurone cell layer (Figure 3-6). This difference compared to wild-type may result from TIBA restricting auxin transport into or away from the developing grain and therefore causing an opposite effect to that observed in NAA treated plants. The difference between TIBA and NPA treatments may also result from TIBA being less effective than NPA at inhibiting auxin transport (Thomson et al., 1973; Katekar and Geissler, 1977). TIBA appears to act as a weak antagonist in stem tissue, being able to suppress auxin activity at high concentrations while having no significant auxin activity itself (Katekar and Geissler, 1980). TIBA has been shown to interfere with the most common auxin (IAA), by competing for the same binding sites as IAA (Thomson et al., 1973; Jablanovic and Nooden, 1974) and being capable of

polar transportation since it utilises the same transport channels as IAA (Thomson et al., 1973). Therefore, TIBA may act as an auxin antagonist (Katekar and Geissler, 1980), while NPA may act as a true auxin inhibitor (Lomax et al., 1995; Muday, 2000; Muday and Murphy, 2002; Wu and McSteen, 2007).

As a result of TIBA application, auxin levels required for correct aleurone differentiation may actually be decreased in the barley grain, blocking the innermost aleurone layer from adopting a complete aleurone cell identity and leading to accumulation of less protein storage bodies (Figure 3-6I). Consistent with delayed or inhibited aleurone development, *HvLTP2* transcripts were least abundant in TIBA treated samples compared to NAA and untreated grains, suggesting less aleurone has developed (Figure 3-7). TIBA applications also altered *HvSAL1* expression across grain development. In TIBA treated grain, *HvSAL1* transcript was abundant at 13 DPA, corresponding to the final phase of aleurone cell division and beginning of aleurone cell expansion. It is currently unclear how *HvSAL1* responds to auxin, but VSPs have been implicated in the auxin pathway (Spitzer et al., 2009). In recent years, studies have focused on the endosomal recycling and vesicular trafficking of plant plasma membrane proteins involved in auxin transport, such as the PIN and Auxin Transporter Protein 1 (AUX1) proteins (Spitzer et al., 2009). It was found that ESCRT proteins in *Arabidopsis* mediate the degradation and recycling of PIN and AUX from the plasma membrane. Disruptions in this process lead to the accumulation of PIN and AUX in vacuolar membranes which are unable to be recycled back to the plasma membrane (Spitzer et al., 2009). Therefore, TIBA treatments may have influenced this protein recycling pathway in the barley grain. The balance of degradation to recycling may have been disrupted, favouring the degradation pathway and thus inducing less

aleurone cell fate signal possibly due to decreases in CR4 and DEK1 being recycled back to the plasma membrane.

In future studies, the *HvNKD1* and *HvSAL1* transgenic lines might be used to confirm these responses to auxin modification. For example, transgenic lines that produce grain with altered aleurone morphology might be used in NAA and TIBA treatments to assess whether the effects are additive or suppressed. This would provide additional support to position *HvNKD1* and/or *HvSAL1* relative to auxin in the aleurone development pathway.

Auxin biosynthesis and transport appears to occur within the grain

Currently it is unknown how much of the exogenous NAA and TIBA is absorbed by the barley roots and transported into the developing grain. Local NAA and TIBA treatments directly to barley grains might also be employed in future studies to induce more severe developmental modifications, since it would not rely on root absorption or transport through the barley plant. In order to confirm if grains exhibit modified auxin accumulation compared to DMSO application within aleurone and sub-aleurone tissue, LC-ESI-MS (liquid chromotogrophy-electrospray ionisation-mass spectrometry) could be employed to quantify auxin levels in the barley grain (Böttcher et al., 2011). Another way to visualise auxin accumulation in the grain would be to utilise florescent reporters under the control of known auxin-responsive elements, such as *DR5* and *DR5v2* (Ulmasov et al., 1997). *DR5* and *DR5v2* have been commonly used in several species, such as *Arabidopsis*, rice and maize, to visualise auxin accumulation (Forestan et al., 2012; Liao et al., 2015; Yang et al., 2017). Multiple *pDR5v2:3xnlsYFP* reporter lines were developed in this study to visualise auxin accumulation in barley, and preliminary

evidence suggests they are expressed in reproductive tissues (Tucker et al., unpublished). However, a recent report using *DR5* and *DR5v2* suggests they are undetectable or unstably expressed in barley roots (Kirschner et al., 2018). It is clear that many components of the auxin biosynthetic and response pathways are expressed in the developing barley grain (Shirley et al., 2018), and their analysis may provide additional support for the role of auxin in barley aleurone development.

Taken together, the results from this study and others have been combined to construct a model of genes and hormones impacting aleurone development in barley (Figure 3-8). Although questions remain regarding how the balance of hormones and genes contribute to aleurone development, this model provides an opportunity to address individual components in the context of a larger network. Several genes identified and characterised in maize aleurone development appear to be playing a partially conserved role in barley aleurone development, but other key factors must exist and still remain unknown (Figure 3-8). In addition, factors that regulate the levels or response to hormones such as auxin must exist that contribute to correct aleurone and sub-aleurone differentiation. Further characterisation of the molecular mechanisms of *HvNKD1* and *HvSAL1*, including the transcriptional regulation of downstream gene networks, will provide additional understanding of the control of endosperm cell differentiation in barley.

References

Amanda D, Doblin MS, Galletti R, Bacic A, Ingram GC, Johnson KL (2016) *DEFECTIVE KERNEL1* (*DEK1*) regulates cell walls in the leaf epidermis. Plant Physiology **172:** 2204-2218

Aubert MK, Coventry S, Shirley NJ, Betts NS, Würschum T, Burton RA, Tucker MR (2018) Differences in hydrolytic enzyme activity accompany natural variation in mature aleurone morphology in barley (*Hordeum vulgare* L.). Scientific Reports **8:** 1-14

Becraft PW, Asuncion-Crabb Y (2000) Positional cues specify and maintain aleurone cell fate in maize endosperm development. Development **127:** 4039-4048

Becraft PW, Li KJ, Dey N, Asuncion-Crabb Y (2002) The maize *dek1* gene functions in embryonic pattern formation and cell fate specification. Development **129:** 5217-5225

Becraft PW, Stinard PS, McCarty DR (1996) CRINKLY4: A TNFR-like receptor kinase involved in maize epidermal differentiation. Science **273:** 1406-1409

Becraft PW, Yi GB (2011) Regulation of aleurone development in cereal grains. Journal of Experimental Botany **62:** 1669-1675

Bethke PC, Hwang YS, Zhu T, Jones RL (2006) Global patterns of gene expression in the aleurone of wild-type and *dwarf1* mutant rice. Plant Physiology **140:** 484-498

Betts NS, Berkowitz O, Liu R, Collins HM, Skadhauge B, Dockter C, Burton RA, Whelan J, Fincher GB (2017) Isolation of tissues and preservation of RNA from intact, germinated barley grain. The Plant Journal **91**:754-765

Böttcher C, Boss PK, Davies C (2011) Acyl substrate preferences of an IAA-amido synthetase account for variations in grape (*Vitis vinifera* L.) berry ripening caused by different auxinic compounds indicating the importance of auxin conjugation in plant development. Journal of Experimental Botany **62**:4267-4280

Brandt A (1976) Endosperm protein formation during kernel development of wild-type and a high-lysine barley mutant. Cereal Chemistry **53:** 890-901

Burton RA, Collins HM, Kibble NAJ, Smith JA, Shirley NJ, Jobling SA, Henderson M, Singh RR, Pettolino F, Wilson SM, Bird AR, Topping DL, Bacic A, Fincher GB (2011) Over-expression of specific *HvCslF* cellulose synthase-like genes in transgenic barley increases the levels of cell wall (1,3;1,4)-beta-D-glucans and alters their fine structure. Plant Biotechnology Journal **9:** 117-135

Burton RA, Jobling SA, Harvey AJ, Shirley NJ, Mather DE, Bacic A, Fincher GB (2008) The genetics and transcriptional profiles of the cellulose synthase-like *HvCslF* gene family in barley. Plant Physiology **146:** 1821-1833

Burton RA, Shirley NJ, King BJ, Harvey AJ, Fincher GB (2004) The *CesA* gene family of barley. Quantitative analysis of transcripts reveals two groups of co-expressed genes. Plant Physiology **134:** 224-236

Cao XY, Costa LM, Biderre-Petit C, Kbhaya B, Dey N, Perez P, McCarty DR, Gutierrez-Marcos JF, Becraft PW (2007) Abscisic acid and stress signals induce *Viviparous1* expression in seed and vegetative tissues of maize. Plant Physiology **143:** 720-731

Carbonell A, Fahlgren N, Mitchell S, Cox KL, Reilly KC, Mockler TC, Carrington JC (2015) Highly specific gene silencing in a monocot species by artificial microRNAs derived from chimeric miRNA precursors. Plant Journal **82:** 1061-1075

Chandler PM, Zwar JA, Jacobsen JV, Higgins TJV, Inglis AS (1984) The effects of gibberellic-acid and abscisic-acid on α-amylase messenger-RNA levels in barley aleurone layers studies using an α-amylase cDNA clone. Plant Molecular Biology **3:** 407-418

Cho MJ, Choi HW, Jiang W, Ha CD, Lemaux PG (2002) Endosperm-specific expression of green fluorescent protein driven by the hordein promoter is stably inherited in transgenic barley (*Hordeum vulgare*) plants. Physiologia Plantarum **115:** 144-154

Cui DY, Zhao JB, Jing YJ, Fan MZ, Liu J, Wang ZC, Xin W, Hu YX (2013) The *Arabidopsis* IDD14, IDD15, and IDD16 cooperatively regulate lateral organ morphogenesis and gravitropism by promoting auxin biosynthesis and transport. Plos Genetics **9:** 1-15

Curtis MD, Grossniklaus U (2003) A gateway cloning vector set for high-throughput functional analysis of genes in planta. Plant Physiology **133:** 462-469

Fahlgren N, Hill ST, Carrington JC, Carbonell A (2016) P-SAMS: a web site for plant artificial microRNA and synthetic trans-acting small interfering RNA design. Bioinformatics **32:** 157-158

Feurtado JA, Huang DQ, Wicki-Stordeur L, Hemstock LE, Potentier MS, Tsang EWT, Cutler AJ (2011) The *Arabidopsis* C2H2 zinc finger INDETERMINATE DOMAIN1/ENHYDROUS promotes the transition to germination by regulating light and hormonal signaling during seed maturation. Plant Cell **23:** 1772-1794

Figueiredo DD, Batista RA, Roszak PJ, Kohler C (2015) Auxin production couples endosperm development to fertilization. Nature Plants **1:** 1-6

Forestan C, Farinati S, Varotto S (2012) The maize *PIN* gene family of auxin transporters. Frontiers in Plant Science **3:** 1-23

Forestan C, Meda S, Varotto S (2010) ZmPIN1-mediated auxin transport is related to cellular differentiation during maize embryogenesis and endosperm development. Plant Physiology **152:** 1373-1390

Furtado A, Henry RJ, Pellegrineschi A (2009) Analysis of promoters in transgenic barley and wheat. Plant Biotechnology Journal **7:** 240-253

Geisler-Lee J, Gallie DR (2005) Aleurone cell identity is suppressed following connation in maize kernels. Plant Physiology **139:** 204-212

Gillies SA, Futardo A, Henry RJ (2012) Gene expression in the developing aleurone and starchy endosperm of wheat. Plant Biotechnology Journal **10:** 668-679

Gontarek BC, Becraft PW (2017) Aleurone. *In* BA Larkins, ed, Maize kernel development. Centre for Agriculture and Bioscience International, Oxfordshire, UK, pp 68-80

Gontarek BC, Neelakandan AK, Wu H, Becraft PW (2016) NKD transcription factors are central regulators of maize endosperm development. Plant Cell **28:** 2916-2936

Gruis D, Guo HN, Selinger D, Tian Q, Olsen OA (2006) Surface position, not signaling from surrounding maternal tissues, specifies aleurone epidermal cell fate in maize. Plant Physiology **141:** 898-909

Hilscher J, Kapusi E, Stoger E, Ibl V (2016) Cell layer-specific distribution of transiently expressed barley ESCRT-III component HvVPS60 in developing barley endosperm. Protoplasma **253:** 137-153

Horvath H, Huang JT, Wong O, Kohl E, Okita T, Kannangara CG, von Wettstein D (2000) The production of recombinant proteins in transgenic barley grains. Proceedings of the National Academy of Sciences of the United States of America **97:** 1914-1919

IBGS (2012) A physical, genetic and functional sequence assembly of the barley genome. Nature **491:** 711-716

Jablanovic M, Nooden LD (1974) Changes in compatible IAA binding in relation to bud development in pea-seedlings. Plant and Cell Physiology **15:** 687-692

Jestin L, Ravel C, Auroy S, Laubin B, Perretant MR, Pont C, Charmet G (2008) Inheritance of the number and thickness of cell layers in barley aleurone tissue (*Hordeum vulgare* L.): an approach using F2-F3 progeny. Theoretical and Applied Genetics **116:** 991-1002

Jin P, Guo T, Becraft PW (2000) The maize CR4 receptor-like kinase mediates a growth factor-like differentiation response. Genesis **27:** 104-116

Kalla R, Shimamoto K, Potter R, Nielsen PS, Linnestad C, Olsen OA (1994) The promoter of the barley aleurone-specific gene encoding a putative 7-kDa lipid transfer protein confers aleurone cell-specific expression in transgenic rice. Plant Journal **6:** 849-860

Katekar GF, Geissler AE (1977) Auxin transport inhibitors. 3. Chemical requirements of a class of auxin transport inhibitors. Plant Physiology **60:** 826-829

Katekar GF, Geissler AE (1980) Auxin transport inhibitors. 4. Evidence of a common-mode of action for a proposed class of auxin transport inhibitors - the phytotropins. Plant Physiology **66:** 1190-1195

Kearse M, Moir R, Wilson A, Stones-Havas S, Cheung M, Sturrock S, Buxton S, Cooper A, Markowitz S, Duran C, Thierer T, Ashton B, Meintjes P, Drummond A (2012) Geneious Basic: An integrated and extendable desktop software platform for the organization and analysis of sequence data. Bioinformatics **28:** 1647-1649

Kirschner GK, Stahl Y, Imani J, von Korff M, Simon R (2018) Fluorescent reporter lines for auxin and cytokinin signalling in barley (*Hordeum vulgare*). Plos One **13:** 1-25

Leroux BM, Goodyke AJ, Schumacher KI, Abbott CP, Clore AM, Yadegari R, Larkins BA, Dannenhoffer JM (2014) Maize early endosperm growth and development: From fertilization through cell type differentiation. American Journal of Botany **101:** 1259-1274

Liao CY, Smet W, Brunoud G, Yoshida S, Vernoux T, Weijers D (2015) Reporters for sensitive and quantitative measurement of auxin response. Nature Methods **12:** 207-210

Lid SE, Gruis D, Jung R, Lorentzen JA, Ananiev E, Chamberlin M, Niu XM, Meeley R, Nichols S, Olsen OA (2002) The *defective kernel 1* (*dek1*) gene required for aleurone cell development in the endosperm of maize grains encodes a membrane protein of the calpain gene superfamily. Proceedings of the National Academy of Sciences of the United States of America **99:** 5460-5465

Liu J, Wu X, Yao X, Yu R, Larkin PJ, Liu C-M (2018) Mutations in the DNA demethylase *OsROS1* result in a thickened aleurone and improved nutritional value in rice grains. PNAS**:** 1-6

Liu KS (2011) Comparison of lipid content and fatty acid composition and their distribution within seeds of 5 small grain species. Journal of Food Science **76:** C334-C342

Locascio A, Roig-Villanova I, Bernardi J, Varotto S (2014) Current perspectives on the hormonal control of seed development in *Arabidopsis* and maize: a focus on auxin. Frontiers in Plant Science **5:** 1-22

Lomax TL, Muday GK, Rubery PH (1995) Auxin transport. *In* PJ Davies, ed, Plant hormones: physiology, biochemistry and molecular biology. Kluwer, Dordrecht, Netherlands, pp 509–530

Lur HS, Setter TL (1993) Role of auxin in maize endosperm development - Timing of nuclear-DNA endoreduplication, zein expression, and cytokinin. Plant Physiology **103:** 273-280

Matthews PR, Wang MB, Waterhouse PM, Thornton S, Fieg SJ, Gubler F, Jacobsen JV (2001) Marker gene elimination from transgenic barley, using co-transformation with adjacent 'twin T-DNAs' on a standard *Agrobacterium* transformation vector. Molecular Breeding **7:** 195-202

McCarty DR, Carson CB, Stinard PS, Robertson DS (1989) Molecular analysis of *viviparous-1* - An abscisic acid-insensitive mutant of maize. Plant Cell **1:** 523-532

McCarty DR, Hattori T, Carson CB, Vasil V, Lazar M, Vasil IK (1991) The *Viviparous-1* developmental gene of maize encodes a novel transcriptional activator. Cell **66:** 895-905

Morino K, Olsen OA, Shimamoto K (2004) Silencing of the aleurone-specific *Ltp2-gus* gene in transgenic rice is reversed by transgene rearrangements and loss of aberrant transcripts. Plant and Cell Physiology **45:** 1500-1508

Muday GK (2000) Maintenance of asymmetric cellular localization of an auxin transport protein through interaction with the actin cytoskeleton. Journal of Plant Growth Regulation **19:** 385-396

Muday GK, Murphy AS (2002) An emerging model of auxin transport regulation. Plant Cell **14:** 293-299

Newman CW, Newman RK (2006) A brief history of barley foods. Cereal Foods World **51:** 4-7

Nguyen HN, Sabelli PA, Larkin BA (2007) Endoreduplication and programmed cell death in the cereal endosperm. *In* OA Olsen, ed, Plant Cell Monographs, Vol 8. Springer, Berlin, Heidelberg, pp 21-43

Olsen LT, Divon HH, Al R, Fosnes K, Lid SE, Opsahl-Sorteberg HG (2008) The *defective seed5* (*des5*) mutant: effects on barley seed development and *HvDek1*, *HvCr4*, and *HvSal1* gene regulation. Journal of Experimental Botany **59:** 3753-3765

Olsen OA (2004) Nuclear endosperm development in cereals and *Arabidopsis thaliana*. Plant Cell **16:** S214-S227

Olsen OA, Kalla R (1993) LTP2 promoter having aleurone-tissue-specific activity. *In*. Olsen, O. A., Kalla, R., ed, USA, pp 1-24

Onate L, Vicente-Carbajosa J, Lara P, Diaz I, Carbonero P (1999) Barley BLZ2, a seed-specific bZIP protein that interacts with BLZ1 *in vivo* and activates transcription from the GCN4-like motif of B-hordein promoters in barley endosperm. Journal of Biological Chemistry **274:** 9175-9182

Pagnussat GC, Alandete-Saez M, Bowman JL, Sundaresan V (2009) Auxin-dependent patterning and gamete specification in the *Arabidopsis* female gametophyte. Science **324:** 1684-1689

Perret SJ, Valentine J, Leggett JM, Morris P (2003) Integration, expression and inheritance of transgenes in hexaploid oat (*Avena sativa* L.). Journal of Plant Physiology **160:** 931-943

Pielot R, Kohl S, Manz B, Rutten T, Weier D, Tarkowska D, Rolcik J, Strnad M, Volke F, Weber H, Weschke W (2015) Hormone-mediated growth dynamics of the barley pericarp as revealed by magnetic resonance imaging and transcript profiling. Journal of Experimental Botany **66:** 6927-6943

Qi X, Li SX, Zhu YX, Zhao Q, Zhu DY, Yu JJ (2017) *ZmDof3*, a maize endosperm-specific Dof protein gene, regulates starch accumulation and aleurone development in maize endosperm. Plant Molecular Biology **93:** 7-20

Regvar M, Eichert D, Kaulich B, Gianoncelli A, Pongrac P, Vogel-Mikus K, Kreft I (2011) New insights into globoids of protein storage vacuoles in wheat aleurone using synchrotron soft X-ray microscopy. Journal of Experimental Botany **62:** 3929-3939

Reyes FC, Buono RA, Roschzttardtz H, Di Rubbo S, Yeun LH, Russinova E, Otegui MS (2014) A novel endosomal sorting complex required for transport (ESCRT) component in *Arabidopsis thaliana* controls cell expansion and development. Journal of Biological Chemistry **289:** 4980-4988

Reyes FC, Sun BM, Guo HN, Gruis D, Otegui MS (2010) *Agrobacterium tumefaciens*-mediated transformation of maize endosperm as a tool to study endosperm cell biology. Plant Physiology **153:** 624-631

Shen B, Li CJ, Min Z, Meeley RB, Tarczynski MC, Olsen OA (2003) *sal1* determines the number of aleurone cell layers in maize endosperm and encodes a class E vacuolar sorting protein. Proceedings of the National Academy of Sciences of the United States of America **100:** 6552-6557

Shirley NJ, Aubert MK, Wilkinson LG, Bird DC, Lora J, Yang X, Tucker MR (2018) Translating auxin responses into ovules, seeds and yield: insight from Arabidopsis and the cereals. Journal of Integrative Plant Biology**:** Accepted

Spitzer C, Reyes FC, Buono R, Sliwinski MK, Haas TJ, Otegui MS (2009) The ESCRT-related CHMP1A and B proteins mediate multivesicular body sorting of auxin carriers in *Arabidopsis* and are required for plant development. Plant Cell **21:** 749-766

Taiz L, Jones RL (1973) Plasmodesmata and an associated cell-wall component in barley aleurone tissue. American Journal of Botany **60:** 67-75

Thomson KS, Hertel R, Muller S, Tavares JE (1973) 1-N-naphthylphthalamic acid and 2,3,5-triiodobenzoic acid - *in vitro* binding to particulate cell fractions and action on auxin transport in corn coleoptiles. Planta **109:** 337-352

Thorneycroft D, Hosein F, Thangavelu M, Clark J, Vizir I, Burrell MM, Ainsworth C (2003) Characterization of a gene from chromosome 1B encoding the large subunit of ADPglucose pyrophosphorylase from wheat: evolutionary divergence and differential expression of *Agp2* genes between leaves and developing endosperm. Plant Biotechnology Journal **1:** 259-270

Tian Q, Olsen L, Sun B, Lid SE, Brown RC, Lemmon BE, Fosnes K, Gruis DF, Opsahl-Sorteberg HG, Otegui MS, Olsen OA (2007) Subcellular localization and functional domain studies of DEFECTIVE KERNEL1 in maize and *Arabidopsis* suggest a model for aleurone cell fate specification involving CRINKLY4 and SUPERNUMERARY ALEURONE LAYER1. Plant Cell **19:** 3127-3145

Tingay S, McElroy D, Kalla R, Fieg S, Wang MB, Thornton S, Brettell R (1997) *Agrobacterium tumefaciens*-mediated barley transformation. Plant Journal **11:** 1369-1376

Tucker MR, Okada T, Johnson SD, Takaiwa F, Koltunow AMG (2012) Sporophytic ovule tissues modulate the initiation and progression of apomixis in *Hieracium*. Journal of Experimental Botany **63:** 3229-3241

Ueda M, Zhang ZJ, Laux T (2011) Transcriptional activation of *Arabidopsis* axis patterning genes *WOX8/9* links zygote polarity to embryo development. Developmental Cell **20:** 264-270

Ulmasov T, Murfett J, Hagen G, Guilfoyle TJ (1997) Aux/IAA proteins repress expression of reporter genes containing natural and highly active synthetic auxin response elements. Plant Cell **9:** 1963-1971

Untergasser A, Cutcutache I, Koressaar T, Ye J, Faircloth BC, Remm M, Rozen SG (2012) Primer3-new capabilities and interfaces. Nucleic Acids Research **40:** e115

Vandesompele J, De Preter K, Pattyn F, Poppe B, Van Roy N, De Paepe A, Speleman F (2002) Accurate normalization of real-time quantitative RT-PCR data by geometric averaging of multiple internal control genes. Genome Biology **3:** 1-12

Verardo V, Gomez-Caravaca AM, Messia MC, Marconi E, Caboni MF (2011) Development of functional spaghetti enriched in bioactive compounds using barley coarse fraction obtained by air classification. Journal of Agricultural and Food Chemistry **59:** 9127-9134

Warthmann N, Chen H, Ossowski S, Weigel D, Herve P (2008) Highly Specific Gene Silencing by Artificial miRNAs in Rice. Plos One **3:** 1-10

Wilkinson LG, Tucker MR (2017) An optimised clearing protocol for the quantitative assessment of sub-epidermal ovule tissues within whole cereal pistils. Plant Methods **13:** 67-77

Wilson SM, Burton RA, Doblin MS, Stone BA, Newbigin EJ, Fincher GB, Bacic A (2006) Temporal and spatial appearance of wall polysaccharides during cellularization of barley (*Hordeum vulgare*) endosperm. Planta **224:** 655-667

Wisniewski JP, Rogowsky PM (2004) Vacuolar H+-translocating inorganic pyrophosphatase (Vpp1) marks partial aleurone cell fate in cereal endosperm development. Plant Molecular Biology **56:** 325-337

Wu XT, McSteen P (2007) The role of auxin transport during inflorescence development in maize (*Zea mays*, Poaceae). American Journal of Botany **94:** 1745-1755

Yan DW, Duermeyer L, Leoveanu C, Nambara E (2014) The functions of the endosperm during seed germination. Plant and Cell Physiology **55:** 1521-1533

Yang J, Yuan Z, Meng QC, Huang GQ, Perin C, Bureau C, Meunier AC, Ingouff M, Bennett MJ, Liang WQ, Zhang DB (2017) Dynamic regulation of auxin response during rice development revealed by newly established hormone biosensor markers. Frontiers in Plant Science **8:** 1-17

Yi G, Lauter AM, Scott MP, Becraft PW (2011) The *thick aleurone1* mutant defines a negative regulation of maize aleurone cell fate that functions downstream of *defective kernel1*. Plant Physiology **156:** 1826-1836

Yi G, Neelakandan AK, Gontarek BC, Vollbrecht E, Becraft PW (2015) The *naked endosperm* genes encode duplicate indeterminate domain transcription factors required for maize endosperm cell patterning and differentiation. Plant Physiology **167:** 443-456

Yoshida H, Hirano K, Sato T, Mitsuda N, Nomoto M, Maeo K, Koketsu E, Mitani R, Kawamura M, Ishiguro S, Tada Y, Ohme-Takagi M, Matsuoka M, Ueguchi-Tanaka M (2014) DELLA protein functions as a transcriptional activator through the DNA binding of the INDETERMINATE DOMAIN family proteins. Proceedings of the National Academy of Sciences of the United States of America **111:** 7861-7866

Yoshida H, Ueguchi-Tanaka M (2014) DELLA and SCL3 balance gibberellin feedback regulation by utilizing INDETERMINATE DOMAIN proteins as transcriptional scaffolds. Plant Signaling and Behavior **9:** 1-3

Zhang RX, Tucker MR, Burton RA, Shirley NJ, Little A, Morris J, Milne L, Houston K, Hedley PE, Waugh R, Fincher GB (2016) The dynamics of transcript abundance during cellularization of developing barley endosperm. Plant Physiology **170:** 1549-1565

Figures

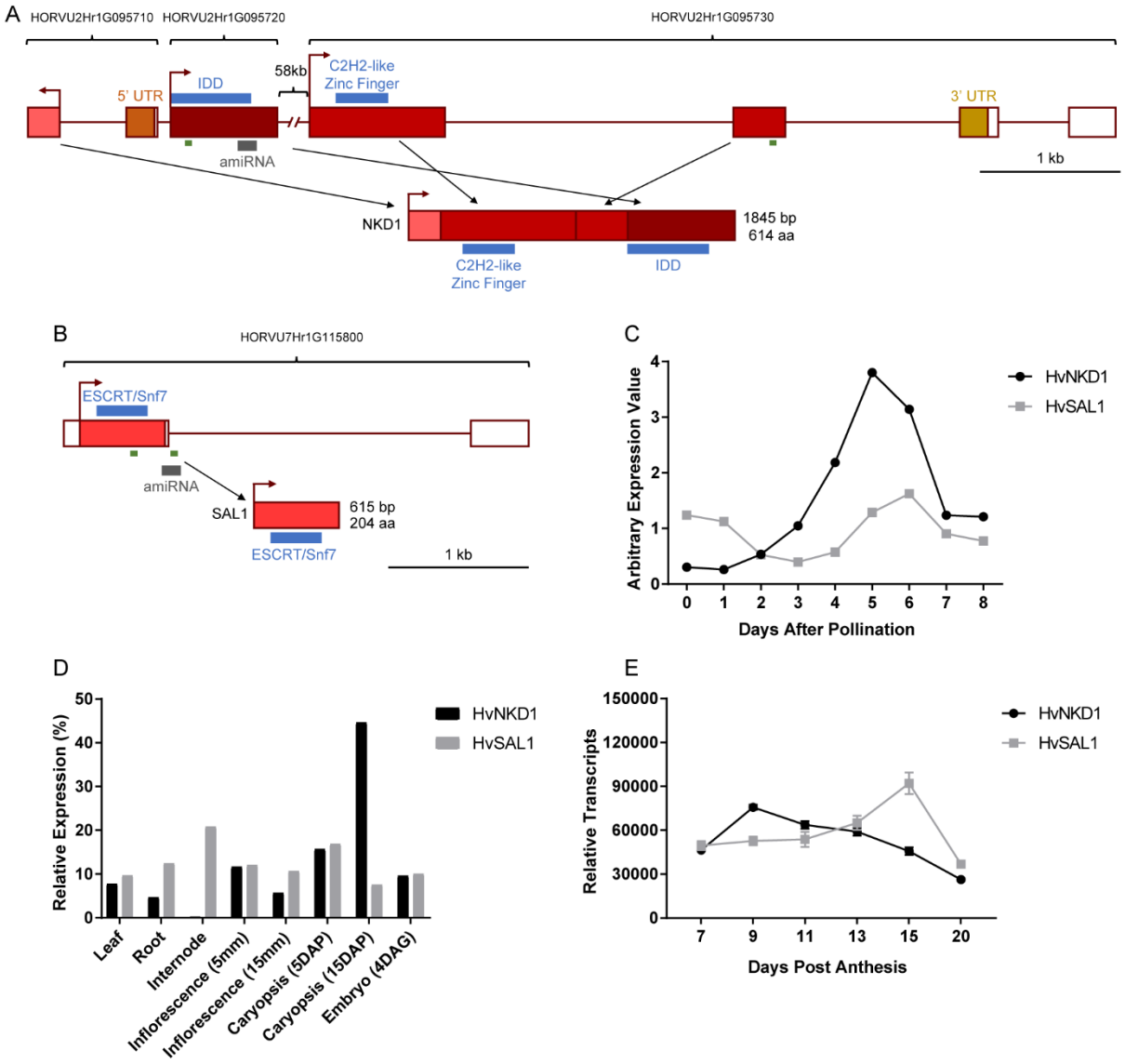

Figure 3-1: Genomic models of *HvNKD1* and *HvSAL1* with relative gene expression. (A) Genomic structure of *HvNKD1* consisting of three predicted genes: HORVU2Hr1G095710, HORVU2Hr1G095720 and HORVU2Hr1G095730. Protein domains are present within HORVU2Hr1G095720 (IDD domain) and HORVU2Hr1G095730 (C2H2-like zinc finger domain), respectively. The predicted *HvNKD1* transcript is assembled in the order of HORVU2Hr1G095710, HORVU2Hr1G095730 then HORVU2Hr1G095720. (B) Genomic structure of *HvSAL1* (HORVU7Hr1G115800) encompassing an ESCRT/Snf7 domain. Grey bars represent

artificial microRNA (amiRNA) target region. Green bars represent qPCR primers. (C) Normalised arbitrary expression across barley endosperm development from microarray data generated by Zhang et al., (2016). (D) Relative expression in various barley tissues using RNAseq profiles available on morexGenes (IBGS 2012). Days after pollination (DAP), days after germination (DAG). (E) qPCR transcript differences between *HvNKD1* and *HvSAL1* across grain development. Error bar represents standard deviation.

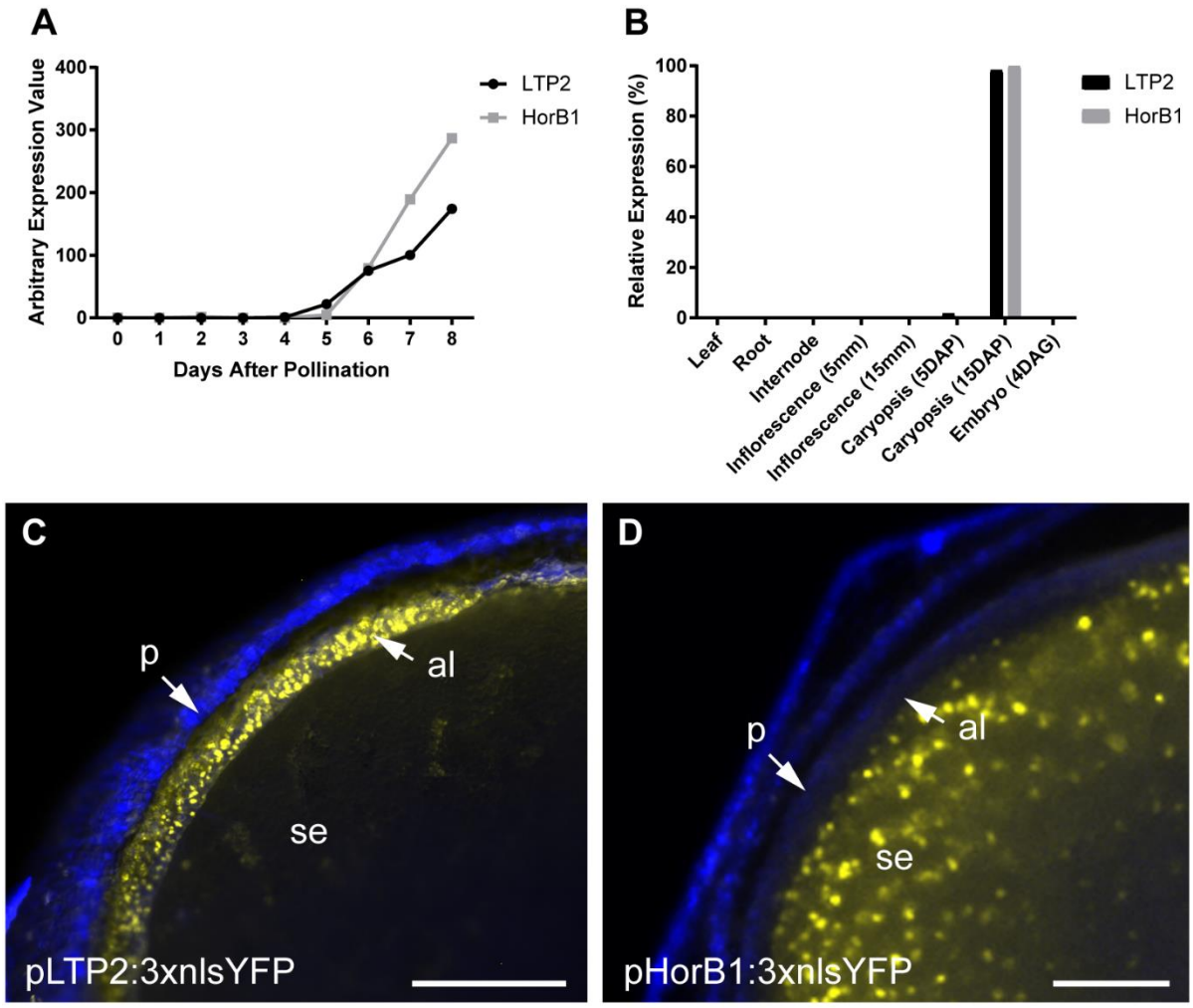

Figure 3-2: Relative expression of *LTP2* and *HorB1* across grain development and in various tissues. (A) Normalised arbitrary expression across barley endosperm development from microarray data generated by Zhang et al., (2016). (B) Relative expression in various barley tissues using RNAseq profiles available on morexGenes (IBGS 2012). Days after pollination (DAP), days after germination (DAG). (C) Aleurone-specific fluorescent line controlled by the LTP2 promoter (*pLTP2:3xnlsYFP*). (D) Endosperm-specific fluorescent line controlled by the HorB1 promoter (*pHorB1:3xnlsYFP*). Images taken using Zeiss Filter sets 49 (DAPI; false-coloured blue, TuYFP; false-coloured yellow). The pericarp (p), starchy endosperm (se) and aleurone (al) tissues are indicated. Scale bar = 250 µm.

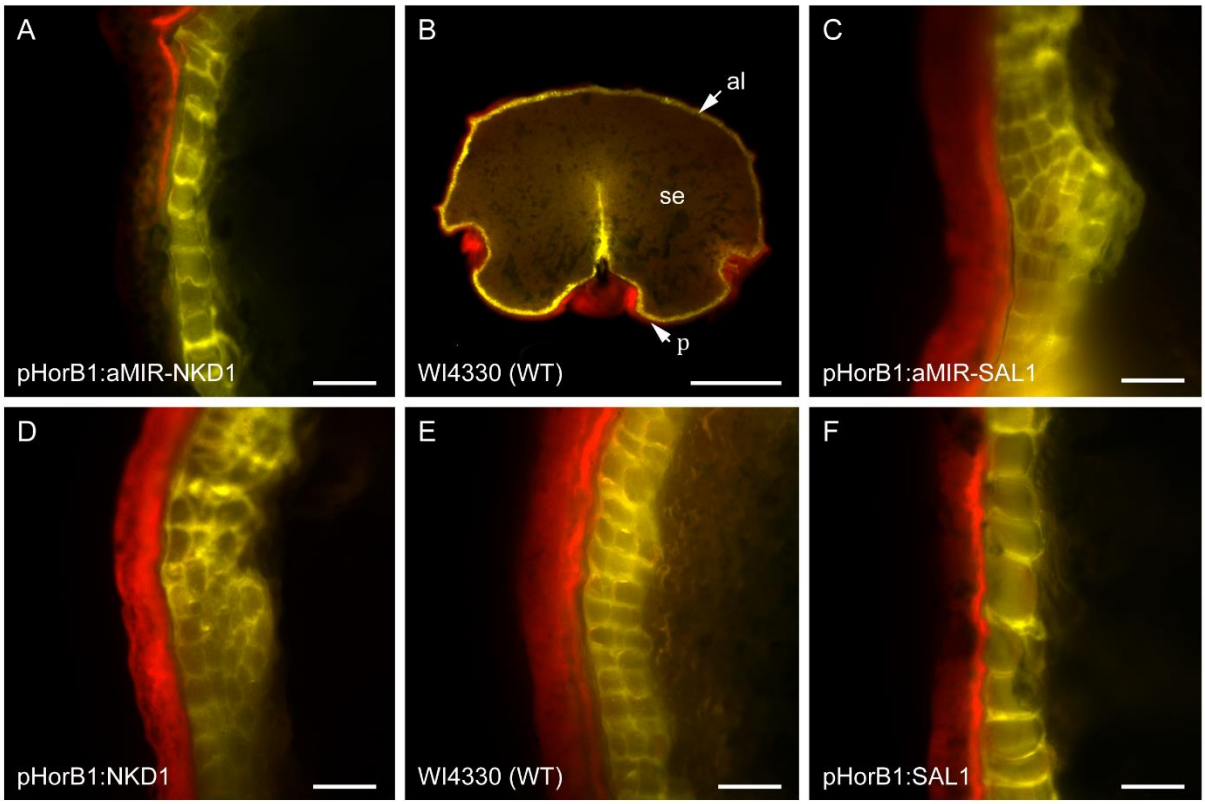

Figure 3-3: Aleurone differences observed from knockdown and overexpression lines under the control of the HorB1 promoter. (A) *pHorB1:aMIR-NKD1* knockdown line. (B) Wholegrain transverse section WI4330 (WT). The pericarp (p), starchy endosperm (se) and aleurone (al) tissues are indicated. (C) *pHorB1:aMIR-SAL1* knockdown line. (D) *pHorB1:NKD1* overexpression line. (E) Wild-type (WT) line WI4330. (F) *pHorB1:SAL1* overexpression line. Images taken using Zeiss Filter sets 46 (false-coloured red) and 49 (DAPI; false-coloured yellow). Scale bar in B = 1 mm and remaining images scale bar = 50 µm.

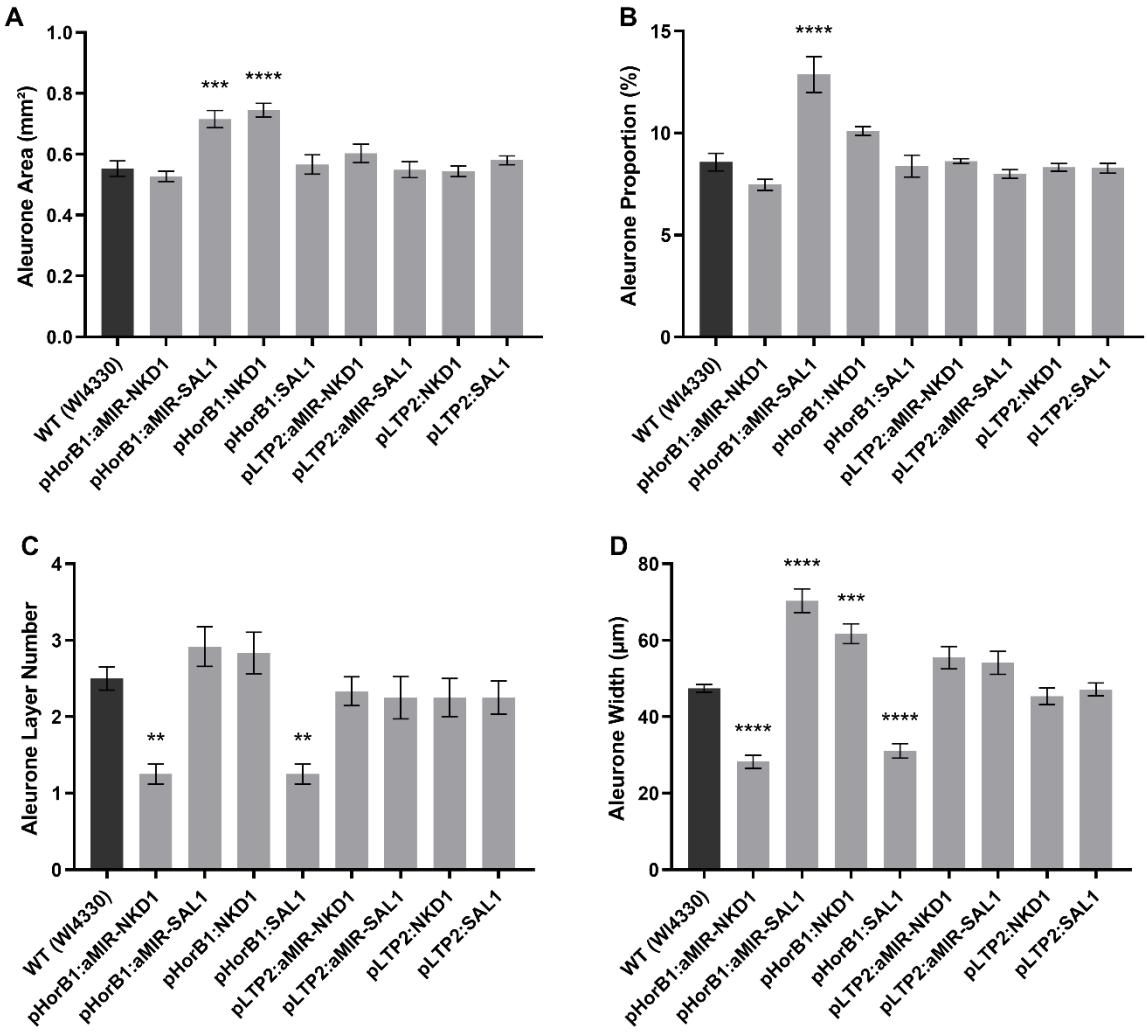

Figure 3-4: Lateral aleurone differences observed between WT and knockdown and overexpression lines under the control of the HorB1 and LTP2 promoters, respectively. For each construct, aleurone measurements were averaged from at least three transgenic lines and compared to the wild-type WI4330 line. (A) Aleurone area. (B) Aleurone proportion. (C) Aleurone layer number. (D) Aleurone width. Error bars represent standard error of the mean. n = 9 grains (three grain from three independent transgenic lines). Significance identified using a one-way ANOVA as compared to the WT; * = p≤0.0332, ** = p≤0.0021, *** = p≤0.0002, **** = p<0.0001.

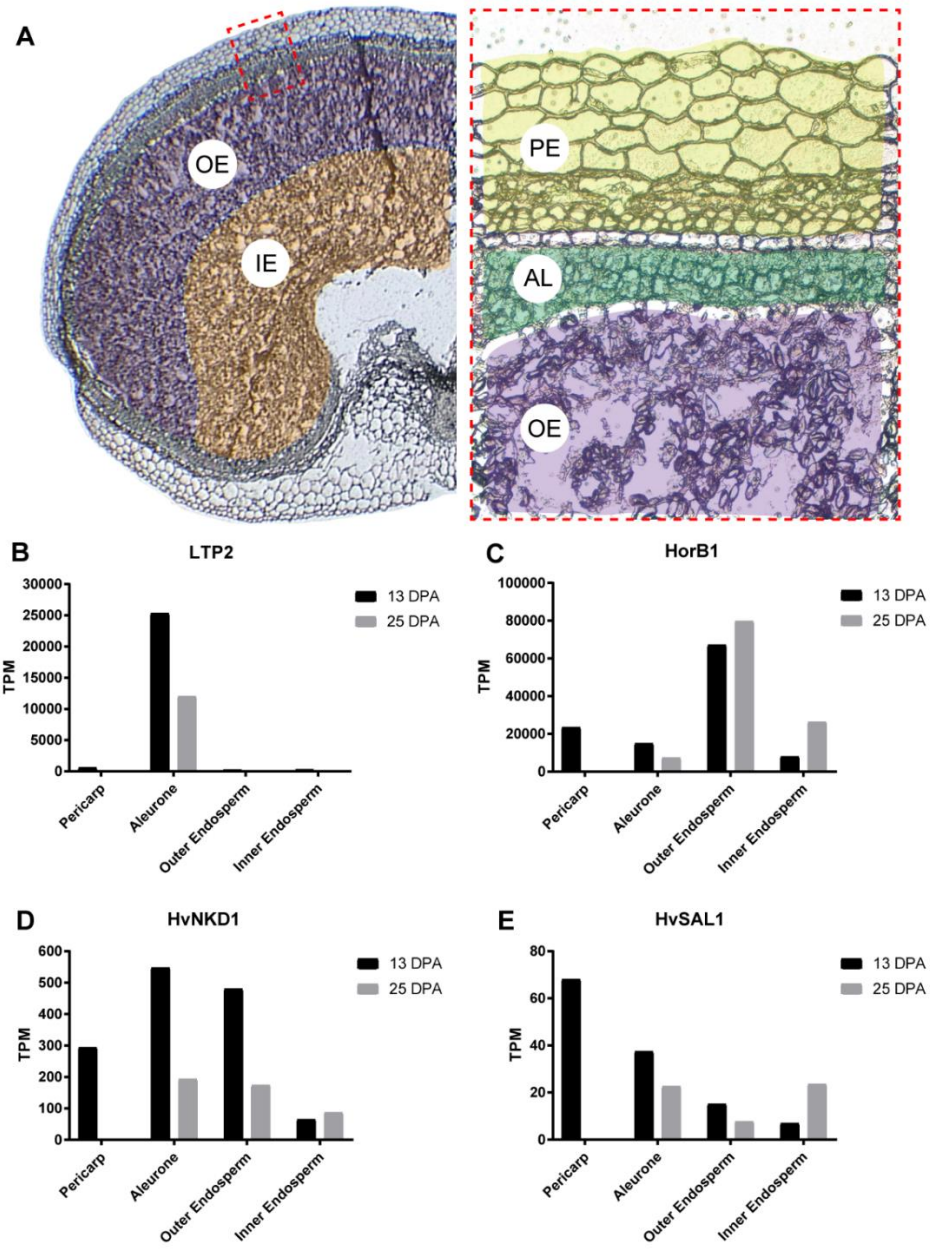

Figure 3-5: Laser-capture microdissected grain tissue collected for RNAseq analysis. (A) Thin butyl methyl methacrylate sections of cv Sloop barley grain showing the regions collected by laser microdissection. OE, outer starchy endosperm including sub-aleurone, purple; IE, inner starchy endosperm, orange; PE, pericarp, yellow; AL, aleurone, green. The red dashed box shows a magnified view of the outer grain layers. (B-E) RNAseq transcripts in transcripts per million (TPM) between barley grain development stages 13 and 25 DPA. Genes focussed on were (B) *LTP2*, (C) *HorB1*, (D) *HvNKD1* and (E) *HvSAL1*.

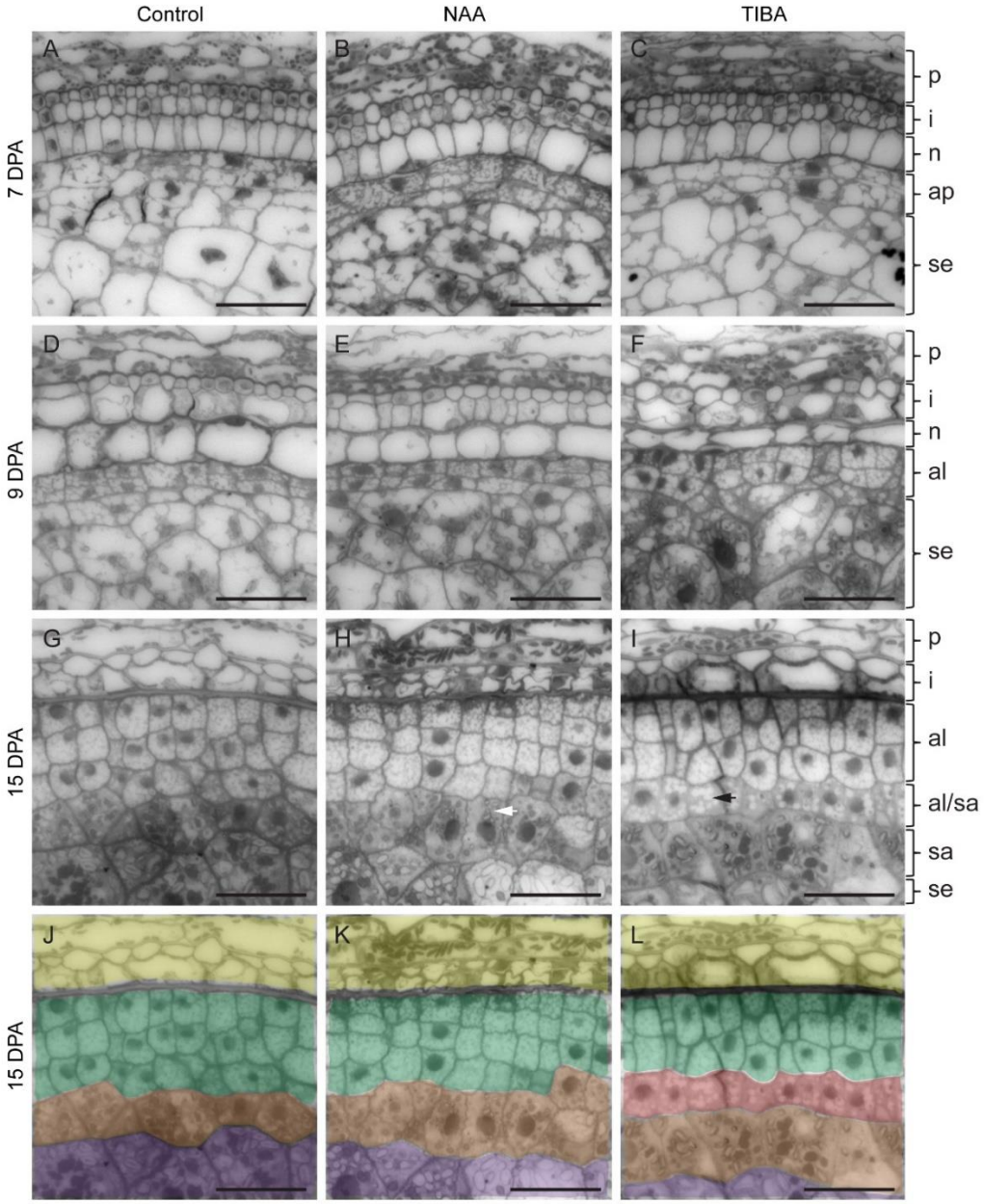

Figure 3-6: Developmental differences in aleurone development after treatment with exogenous auxin (NAA) and auxin inhibitor (TIBA). (A, D, G, J) Control treated grain. (B, E, H, K) NAA treated grain. (C, F, I, L) TIBA treated grain. White arrow depicting sub-aleurone layer adopting aleurone characteristics. Black arrow depicting aleurone layer adopting sub-aleurone characteristics. (J-I) false coloured images of 15 DPA: The pericarp (p; yellow), integument (I; yellow), nucellus (n), aleurone precursor (ap), aleurone (al; green), altered aleurone (red), sub-aleurone (sa; orange) and starchy endosperm (se; purple) tissues are indicated. Scale bar = 50 μm.

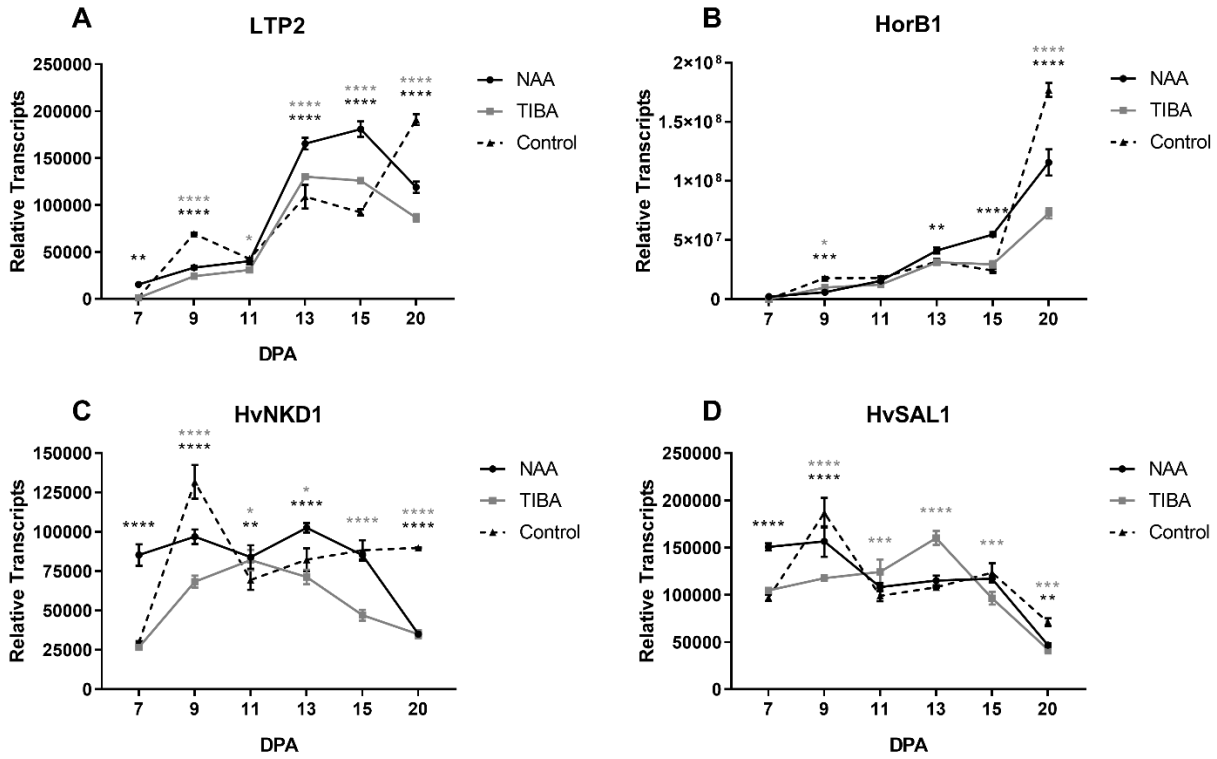

Figure 3-7: qPCR transcript differences of selected genes after auxin (NAA) and auxin inhibitor (TIBA) application. Genes of interest include (A) *LTP2*, (B) *HorB1*, (C) *HvNKD1* and (D) *HvSAL1*. Error bar represent standard deviation. Significance identified using a two-way ANOVA as compared to the control; * = p≤0.0332, ** = p≤0.0021, *** = p≤0.0002, **** = p<0.0001. Black * indicates NAA compared to the control. Grey * indicated TIBA compared to the control.

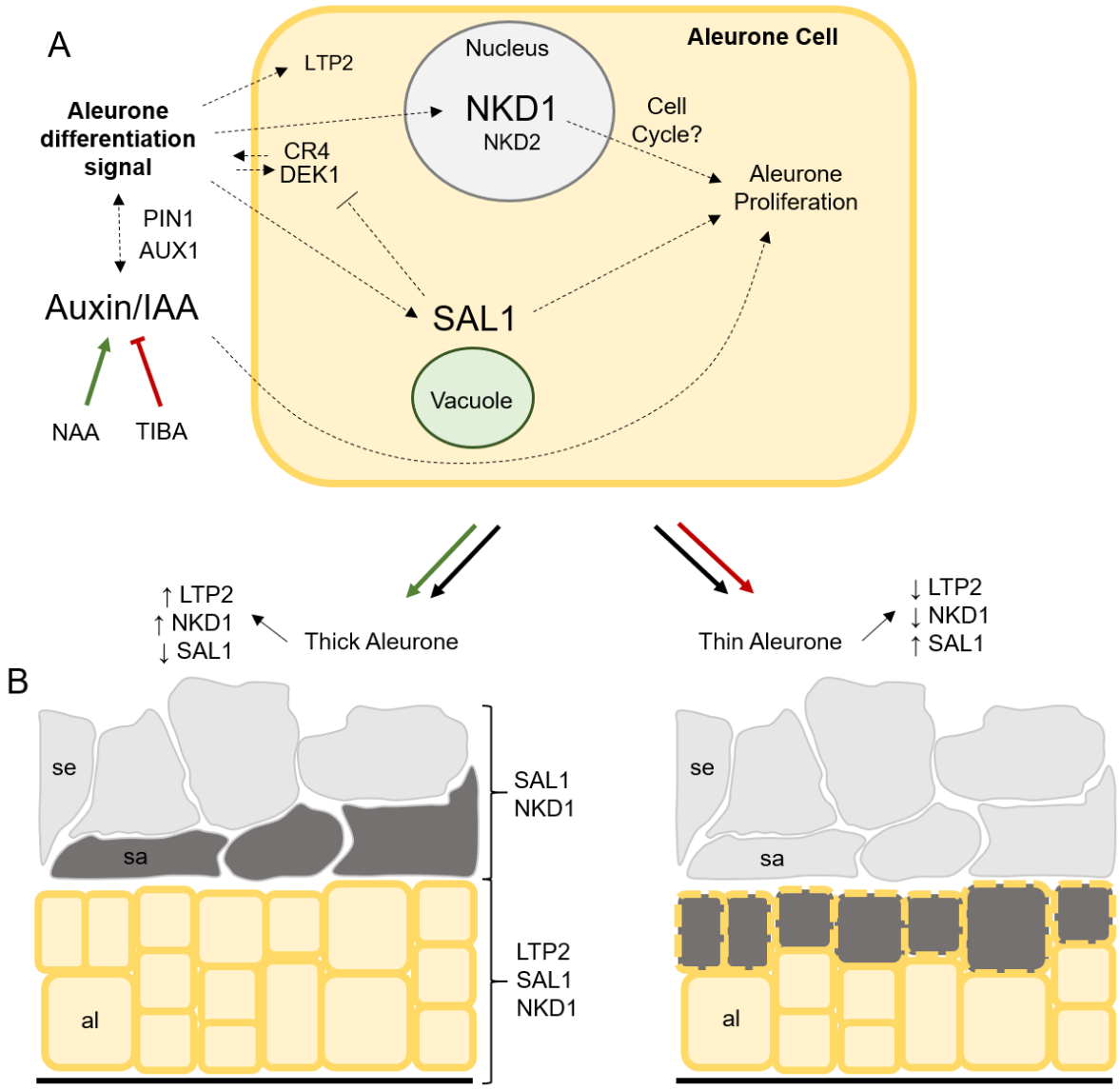

Figure 3-8: Proposed molecular model of aleurone development in barley. (A) Molecular pathway of key factors affecting aleurone development within the aleurone cell. Dashed arrows represent possible interactions within the aleurone but mechanisms are unknown. Green arrows represent the effect of NAA treatment while red arrows represent effect of TIBA treatment. (B) Possible aleurone morphological outcomes, a thick or thin aleurone. Dark grey cells represent morphological change in that layer due to NAA or TIBA treatment. Aleurone (al), sub-aleurone (sa) and starchy endosperm (se).

Supplementary Figures

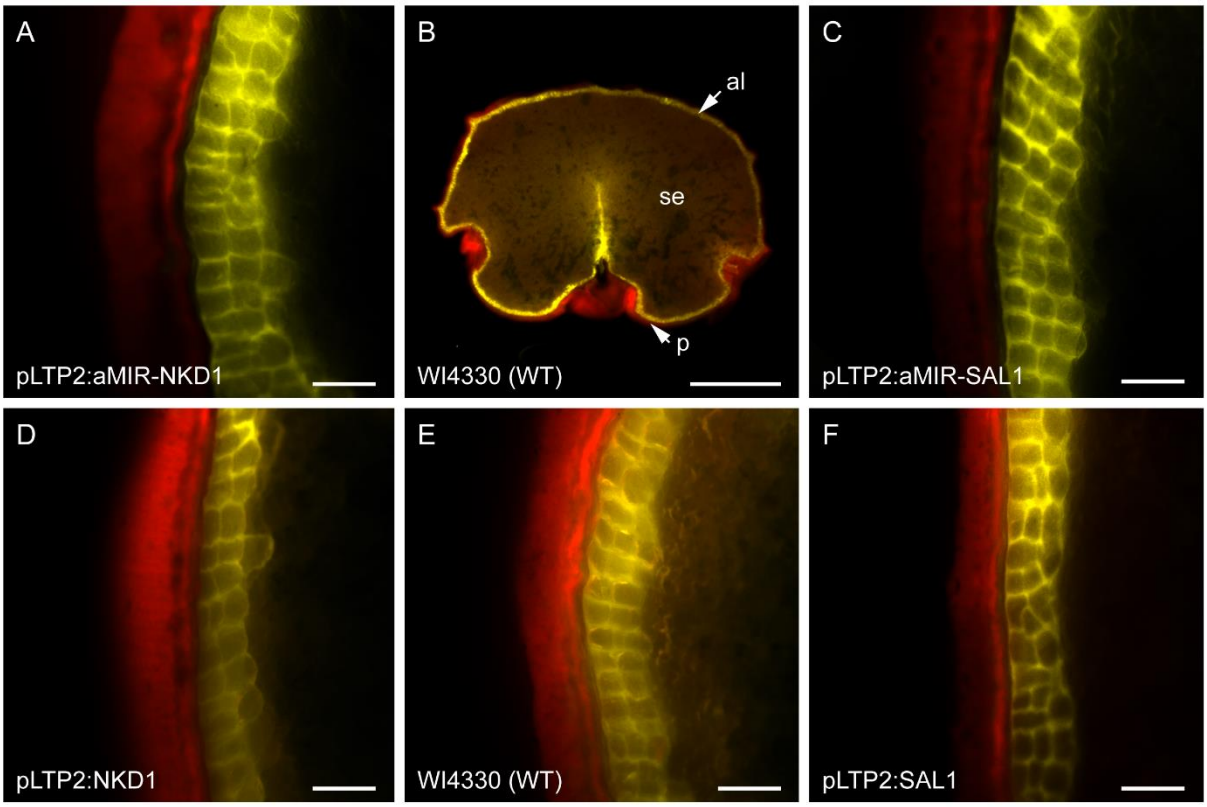

Figure 3-S1: Aleurone differences observed from knockdown and overexpression lines under the control of the LTP2 promoter. (A) *pLTP2:aMIR-NKD1* knockdown line. (B) Wholegrain transverse section WI4330 (WT). The pericarp (p), starchy endosperm (se) and aleurone (al) tissues are indicated. (C) *pLTP2:aMIR-SAL1* knockdown line. (D) *pLTP2:NKD1* overexpression line. (E) Wild-type (WT) line WI4330. (F) *pLTP2:SAL1* overexpression line. Images taken using Zeiss Filter sets 46 (false-coloured red) and 49 (DAPI; false-coloured yellow). Scale bar in B = 1 mm and remaining images scale bar = 50 µm.

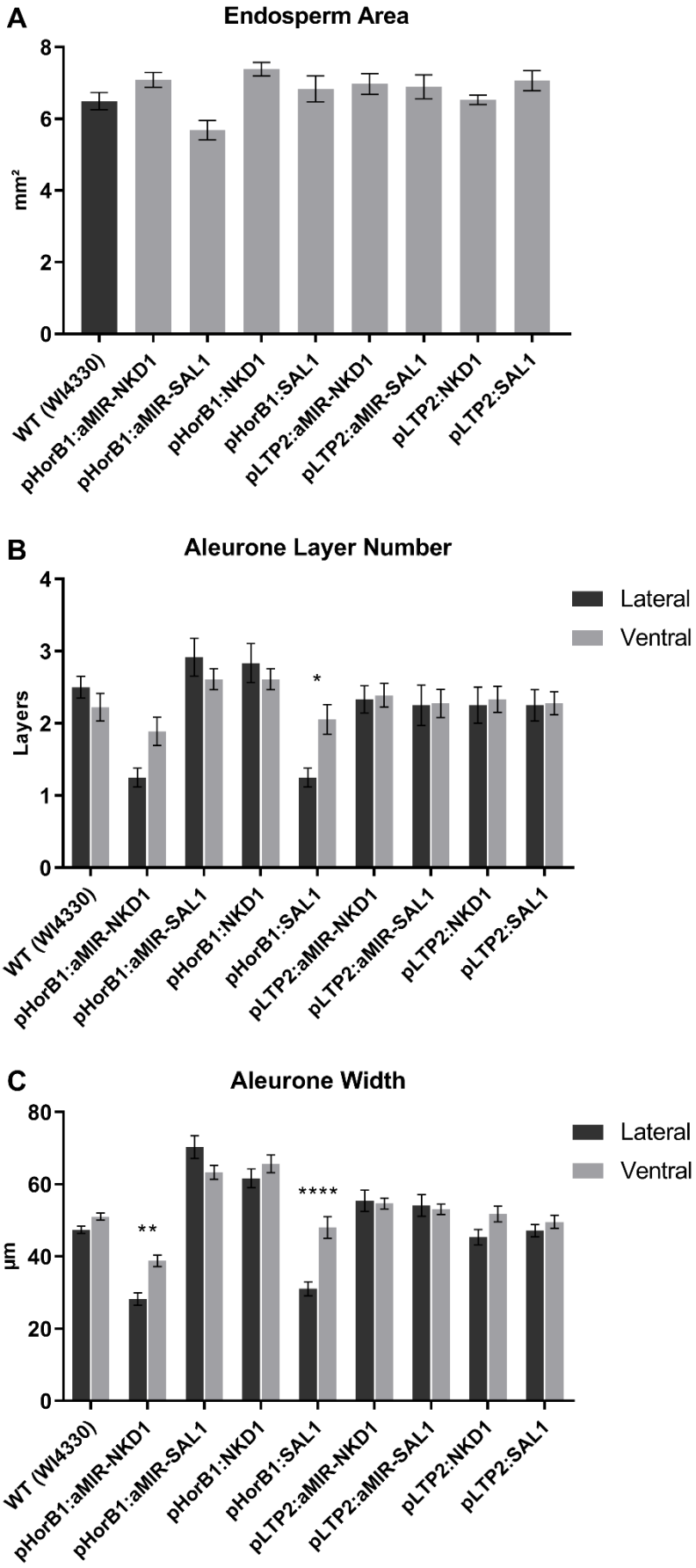
A
Endosperm Area
mm²
0
2
4
6
8
WT (WI4330)
pHorB1:aMIR-NKD1
pHorB1:aMIR-SAL1
pHorB1:NKD1
pHorB1:SAL1
pLTP2:aMIR-NKD1
pLTP2:aMIR-SAL1
pLTP2:NKD1
pLTP2:SAL1
B
Aleurone Layer Number
Layers
Lateral
Ventral
*
C
Aleurone Width
µm
**
****

Figure 3-S2: Comparsion of lateral and ventral aleurone traits between WT transgenic lines. (A) Endosperm area. No significant differences between the wild-type and transgenic lines were observed. (B) Aleurone layer number. A significant difference between lateral and ventral layers in *pHorB1:SAL1* lines was observed. (C) Aleurone width. A significant difference between lateral and ventral layers in *pHorB1:aMIR-NKD1* and *pHorB1:SAL1* lines was observed. Error bars represent standard error of the mean. Significance identified using a two-way ANOVA between lateral and ventral groups; * = p≤0.0332, ** = p≤0.0021, *** = p≤0.0002, **** = p<0.0001.

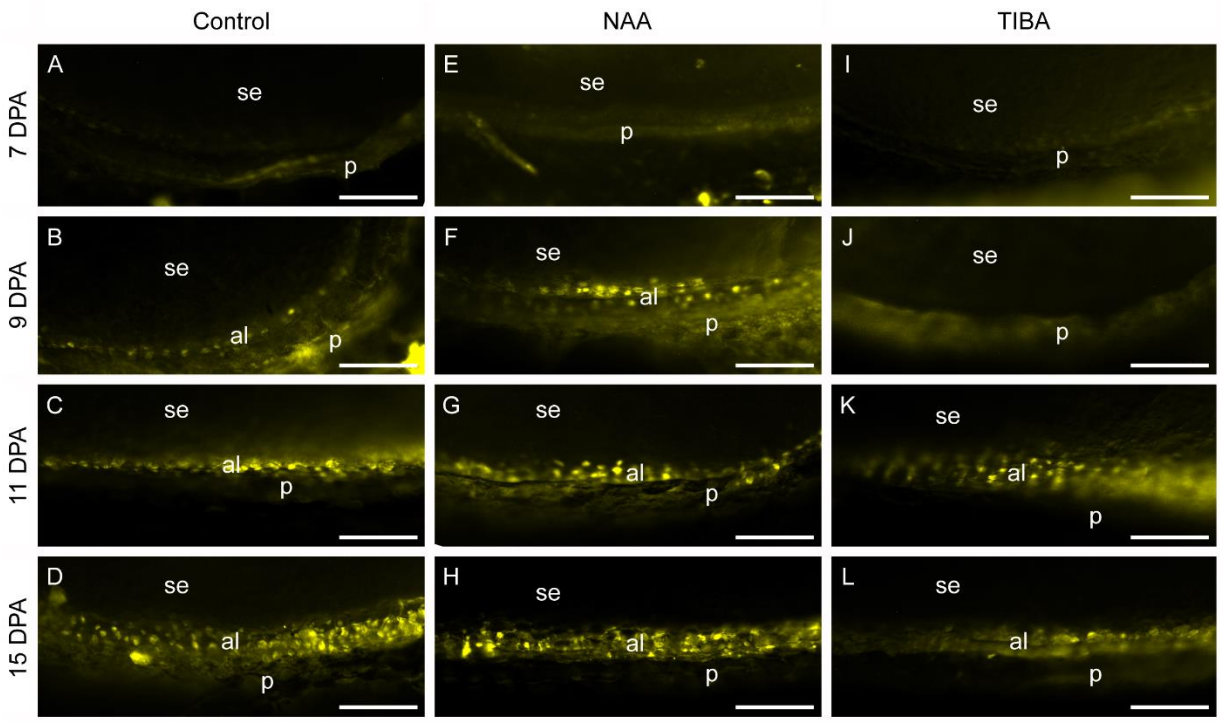

Figure 3-S3: Developing transgenic marker grain (*pLTP2:3xnlsYFP*) sections treated with an exogenous auxin (NAA) and auxin inhibitor (TIBA) visualised by autofluorescence. (A–D) Naphthalene-1-acetic acid (NAA) treated sections. (E–H) 2,3,5-triiodobenzoic acid (TIBA) treated sections. (I–L) Control (0.1% DMSO) treated sections. Scale bar = 100 µm. se, starchy endosperm; al, aleurone; p, pericarp.

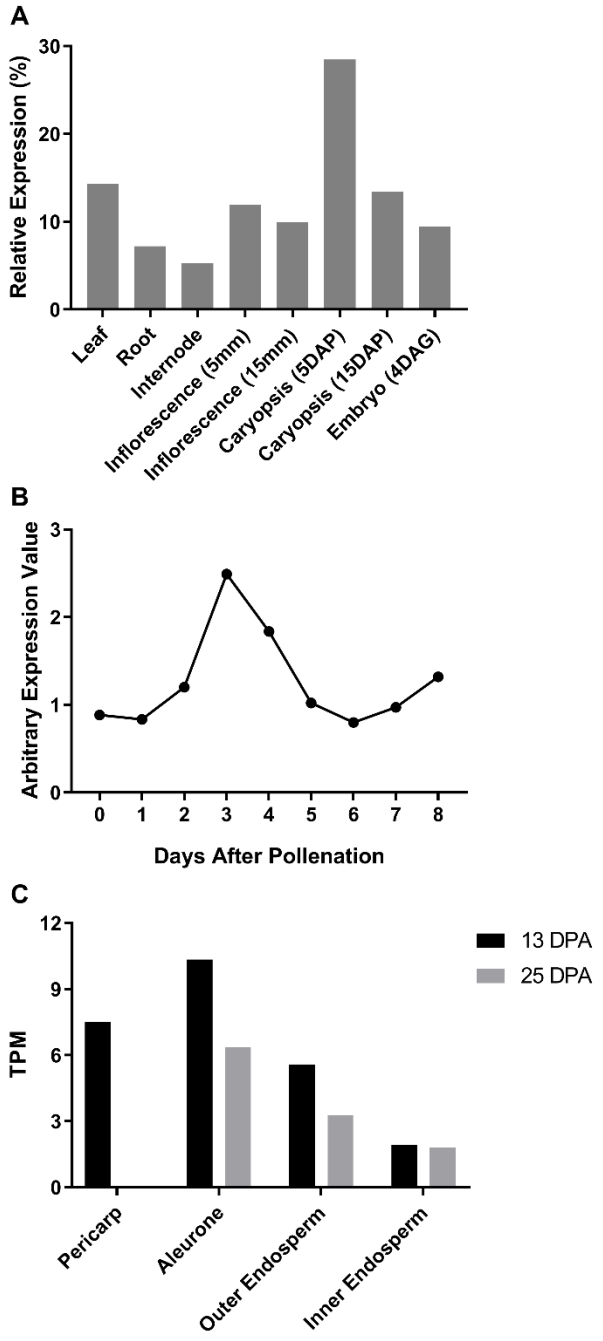

Figure 3-S4: Relative expression of *HvNKD2*. (A) Relative expression in various barley tissues using RNAseq profiles available on morexGenes (IBGS 2012). (B) Normalised arbitrary expression across barley endosperm development from microarray data generated by Zhang et al., (2016). (C) RNAseq transcripts from tissues isolated by LCM between barley grain development stages 13 and 25 DPA. Days after pollination (DAP); days after germination (DAG); transcripts per million (TPM).

Supplementary Tables

Table 3-S1: Average grain measurements across WT and transgenic lines.

A	Transverse sections							
Construct	**EA (mm²)**	**SEA (mm²)**	**AA (mm²)**	**AP (%)**	**DVW (µm)**	**LRW (µm)**	**ALN**	**AW (µm)**
WI4330 (WT)	6.49 ± 0.73	5.94 ± 0.70	0.55 ± 0.07	8.58 ± 1.29	2584 ± 162	3460 ± 228	2.3 ± 0.8	48.66 ± 5.34
pHorB1:aMIR-NKD1	7.09 ± 0.62	6.56 ± 0.61	0.53 ± 0.05	7.47 ± 0.80	2650 ± 177	3651 ± 199	1.7 ± 0.8	35.02 ± 9.38
pHorB1:aMIR-SAL1	5.68 ± 0.81	4.97 ± 0.83	0.72 ± 0.09	12.87 ± 2.63	2384 ± 258	3334 ± 212	2.7 ± 0.7	63.03 ± 13.18
pHorB1:NKD1	7.38 ± 0.56	6.64 ± 0.51	0.74 ± 0.07	10.10 ± 0.64	2802 ± 116	3577 ± 141	2.6 ± 0.8	63.06 ± 12.30
pHorB1:SAL1	6.84 ± 1.08	6.27 ± 1.05	0.57 ± 0.10	8.38 ± 1.61	2597 ± 273	3689 ± 206	1.8 ± 0.9	40.70 ± 14.26
pLTP2:aMIR-NKD1	6.97 ± 0.87	6.37 ± 0.78	0.60 ± 0.09	8.62 ± 0.35	2594 ± 199	3492 ± 204	2.4 ± 0.7	56.22 ± 10.59
pLTP2:aMIR-SAL1	6.89 ± 1.00	6.35 ± 0.94	0.55 ± 0.08	7.99 ± 0.65	2571 ± 240	3485 ± 180	2.4 ± 0.9	54.43 ± 9.94
pLTP2:NKD1	6.53 ± 0.40	5.99 ± 0.36	0.54 ± 0.05	8.32 ± 0.57	2591 ± 130	3458 ± 103	2.3 ± 0.8	48.45 ± 11.03
pLTP2:SAL1	7.06 ± 0.84	6.48 ± 0.81	0.58 ± 0.04	8.28 ± 0.74	2655 ± 170	3594 ± 141	2.3 ± 0.7	48.76 ± 8.21

B	Transverse sections							
Construct	**EA (mm²)**	**SEA (mm²)**	**AA (mm²)**	**AP (%)**	**DVW (µm)**	**LRW (µm)**	**ALN**	**AW (µm)**
WI4330 (WT)	6.49 ± 0.73	5.94 ± 0.70	0.55 ± 0.07	8.58 ± 1.29	2584 ± 162	3460 ± 228	2.5 ± 0.5	47.42 ± 4.29
pHorB1:aMIR-NKD1	7.09 ± 0.62	6.56 ± 0.61	0.53 ± 0.05	7.47 ± 0.80	2650 ± 177	3651 ± 199	1.3 ± 0.5	28.21 ± 7.35
pHorB1:aMIR-SAL1	5.68 ± 0.81	4.97 ± 0.83	0.72 ± 0.09	12.87 ± 2.63	2384 ± 258	3334 ± 212	2.9 ± 0.9	70.33 ± 13.21
pHorB1:NKD1	7.38 ± 0.56	6.64 ± 0.51	0.74 ± 0.07	10.10 ± 0.64	2802 ± 116	3577 ± 141	2.8 ± 0.9	61.70 ± 10.95
pHorB1:SAL1	6.84 ± 1.08	6.27 ± 1.05	0.57 ± 0.10	8.38 ± 1.61	2597 ± 273	3689 ± 206	1.3 ± 0.5	31.06 ± 8.04
pLTP2:aMIR-NKD1	6.97 ± 0.87	6.37 ± 0.78	0.60 ± 0.09	8.62 ± 0.35	2594 ± 199	3492 ± 204	2.3 ± 0.7	55.43 ± 12.41
pLTP2:aMIR-SAL1	6.89 ± 1.00	6.35 ± 0.94	0.55 ± 0.08	7.99 ± 0.65	2571 ± 240	3485 ± 180	2.3 ± 1.0	54.09 ± 12.69
pLTP2:NKD1	6.53 ± 0.40	5.99 ± 0.36	0.54 ± 0.05	8.32 ± 0.57	2591 ± 130	3458 ± 103	2.3 ± 0.9	45.35 ± 9.05
pLTP2:SAL1	7.06 ± 0.84	6.48 ± 0.81	0.58 ± 0.04	8.28 ± 0.74	2655 ± 170	3594 ± 141	2.3 ± 0.8	47.18 ± 7.12

C		Transverse sections							
Construct	**Transgenic Line**	**EA (mm²)**	**SEA (mm²)**	**AA (mm²)**	**AP (%)**	**DVW (µm)**	**LRW (µm)**	**ALN**	**AW (µm)**
WI4330 (WT)	WI4330-1	6.60 ± 0.80	6.10 ± 0.71	0.50 ± 0.09	7.49 ± 0.55	2609 ± 232	3500 ± 241	2.2 ± 0.7	47.62 ± 5.48
	WI4330-2	6.02 ± 0.95	5.44 ± 0.91	0.58 ± 0.08	9.70 ± 1.57	2512 ± 198	3284 ± 258	2.3 ± 0.8	48.30 ± 4.32
	WI4330-5	6.84 ± 0.19	6.26 ± 0.20	0.58 ± 0.02	8.54 ± 0.53	2632 ± 13	3596 ± 81	2.3 ± 0.9	50.06 ± 6.07
pHorB1:aMIR-NKD1	MA033-5	7.33 ± 0.43	6.79 ± 0.51	0.54 ± 0.08	7.43 ± 1.50	2704 ± 227	3658 ± 24	1.5 ± 0.8	32.06 ± 11.42
	MA033-8	7.18 ± 1.04	6.65 ± 0.99	0.54 ± 0.05	7.49 ± 0.53	2578 ± 241	3814 ± 273	1.8 ± 0.8	38.36 ± 8.04
	MA033-19	6.75 ± 0.10	6.25 ± 0.09	0.50 ± 0.02	7.48 ± 0.24	2668 ± 55	3482 ± 31	1.8 ± 0.8	34.63 ± 7.64
pHorB1:aMIR-SAL1	MA034-6	6.09 ± 1.02	5.44 ± 1.05	0.65 ± 0.10	10.88 ± 2.78	2536 ± 139	3350 ± 287	2.8 ± 0.9	53.98 ± 10.55
	MA034-9	5.60 ± 0.38	4.83 ± 0.41	0.77 ± 0.05	13.81 ± 1.62	2287 ± 220	3442 ± 171	2.5 ± 0.5	64.24 ± 12.58
	MA034-11	5.36 ± 1.01	4.63 ± 0.99	0.73 ± 0.07	13.91 ± 2.90	2331 ± 382	3209 ± 161	2.8 ± 0.7	70.86 ± 10.91
pHorB1:NKD1	MA090-13	7.40 ± 0.35	6.67 ± 0.34	0.73 ± 0.05	9.87 ± 0.74	2870 ± 16	3555 ± 76	2.8 ± 1.0	64.85 ± 10.44
	MA090-14	6.96 ± 0.55	6.26 ± 0.53	0.70 ± 0.04	10.04 ± 0.65	2663 ± 69	3546 ± 171	2.6 ± 0.7	60.78 ± 9.58
	MA090-15	7.78 ± 0.56	6.98 ± 0.52	0.81 ± 0.07	10.38 ± 0.70	2874 ± 74	3629 ± 196	2.5 ± 0.5	63.54 ± 16.17
pHorB1:SAL1	MA069-3	6.49 ± 0.92	6.00 ± 0.81	0.49 ± 0.13	7.49 ± 0.97	2504 ± 174	3581 ± 239	1.5 ± 0.8	30.49 ± 7.22

	MA069-9	5.97 ± 0.40	5.39 ± 0.46	0.59 ± 0.06	9.92 ± 1.73	2459 ± 173	3589 ± 26	2.0 ± 1.0	44.33 ± 11.96
	MA069-14	8.05 ± 0.41	7.43 ± 0.45	0.62 ± 0.05	7.73 ± 1.03	2830 ± 337	3898 ± 115	1.8 ± 0.8	47.29 ± 16.37
pLTP2:aMIR-NKD1	MA017-3-5	7.34 ± 0.22	6.69 ± 0.21	0.64 ± 0.02	8.79 ± 0.23	2683 ± 36	3630 ± 93	2.6 ± 0.8	60.31 ± 8.13
	MA017-9-5	7.63 ± 0.42	6.95 ± 0.37	0.67 ± 0.05	8.83 ± 0.15	2754 ± 92	3594 ± 103	2.5 ± 0.5	60.00 ± 8.86
	MA017-13	5.95 ± 0.63	5.46 ± 0.60	0.49 ± 0.04	8.26 ± 0.34	2345 ± 75	3253 ± 131	2.3 ± 0.8	48.36 ± 10.33
pLTP2:aMIR-SAL1	MA019-2	7.16 ± 0.17	6.56 ± 0.17	0.60 ± 0.04	8.36 ± 0.54	2630 ± 81	3570 ± 33	2.3 ± 1.0	57.55 ± 7.60
	MA019-5	5.81 ± 0.37	5.33 ± 0.34	0.48 ± 0.03	8.26 ± 0.23	2326 ± 90	3291 ± 106	2.3 ± 0.8	52.31 ± 8.30
	MA019-9-5	7.72 ± 0.99	7.15 ± 0.91	0.57 ± 0.10	7.37 ± 0.67	2756 ± 263	3595 ± 177	2.5 ± 1.0	53.42 ± 12.86
pLTP2:NKD1	MA089-8	6.66 ± 0.30	6.07 ± 0.28	0.59 ± 0.03	8.85 ± 0.07	2688 ± 58	3561 ± 65	2.6 ± 0.7	56.18 ± 11.94
	MA089-12	6.47 ± 0.65	5.95 ± 0.61	0.52 ± 0.05	7.99 ± 0.62	2537 ± 189	3373 ± 84	2.5 ± 0.9	47.85 ± 6.64
	MA089-13	6.47 ± 0.30	5.94 ± 0.25	0.53 ± 0.06	8.12 ± 0.50	2549 ± 88	3441 ± 59	1.8 ± 0.7	41.32 ± 8.67
pLTP2:SAL1	MA065-9	8.12 ± 0.31	7.50 ± 0.26	0.61 ± 0.04	7.55 ± 0.24	2865 ± 46	3755 ± 44	2.3 ± 0.7	48.65 ± 7.84
	MA065-13	6.47 ± 0.42	5.90 ± 0.41	0.57 ± 0.04	8.81 ± 0.62	2501 ± 79	3556 ± 93	2.2 ± 0.8	48.63 ± 10.72
	MA065-20	6.59 ± 0.18	6.03 ± 0.19	0.56 ± 0.04	8.47 ± 0.68	2600 ± 31	3471 ± 72	2.3 ± 0.7	49.01 ± 5.80

(A) Average grain measurements across the whole transverse sections for WT and transgenic lines. (B) Average grain measurements across lateral grain positions for WT and transgenic lines. (C) Individual WT and transgenic line grain measurements. n = 9 grains (three grain from three independent transgenic lines). Endosperm area (EA); starchy endosperm area (SEA); aleurone area (AA); aleurone proportion (AP); dorsal-ventral width (DVW); left-right width (LRW); aleurone layer number (ALN); aleurone width (AW).

Table 3-S2: One-way analysis of variance (ANOVA) for barley grain features WT and transgenics.

	Grain features				
Comparison	**EA**	**AA**	**AP**	**ALN**	**AW**
WT (WI4330) vs. pHorB1:aMIR-NKD1	-	-	-	**	****
WT (WI4330) vs. pHorB1:aMIR-SAL1	-	***	****	-	****
WT (WI4330) vs. pHorB1:NKD1	-	****	-	-	***
WT (WI4330) vs. pHorB1:SAL1	-	-	-	**	****
WT (WI4330) vs. pLTP2:aMIR-NKD1	-	-	-	-	-
WT (WI4330) vs. pLTP2:aMIR-SAL1	-	-	-	-	-
WT (WI4330) vs. pLTP2:NKD1	-	-	-	-	-
WT (WI4330) vs. pLTP2:SAL1	-	-	-	-	-
pHorB1:aMIR-NKD1 vs. pHorB1:aMIR-SAL1	**	****	****	****	****
pHorB1:aMIR-NKD1 vs. pHorB1:NKD1	-	****	***	****	****
pHorB1:aMIR-NKD1 vs. pHorB1:SAL1	-	-	-	-	-
pHorB1:aMIR-NKD1 vs. pLTP2:aMIR-NKD1	-	-	-	*	****
pHorB1:aMIR-NKD1 vs. pLTP2:aMIR-SAL1	-	-	-	*	****
pHorB1:aMIR-NKD1 vs. pLTP2:NKD1	-	-	-	*	****
pHorB1:aMIR-NKD1 vs. pLTP2:SAL1	-	-	-	*	****
pHorB1:aMIR-SAL1 vs. pHorB1:NKD1	***	-	***	-	-
pHorB1:aMIR-SAL1 vs. pHorB1:SAL1	-	**	****	****	****
pHorB1:aMIR-SAL1 vs. pLTP2:aMIR-NKD1	*	*	****	-	***
pHorB1:aMIR-SAL1 vs. pLTP2:aMIR-SAL1	*	***	****	-	****
pHorB1:aMIR-SAL1 vs. pLTP2:NKD1	-	***	****	-	****
pHorB1:aMIR-SAL1 vs. pLTP2:SAL1	*	**	****	-	****
pHorB1:NKD1 vs. pHorB1:SAL1	-	****	-	****	****
pHorB1:NKD1 vs. pLTP2:aMIR-NKD1	-	**	-	-	-
pHorB1:NKD1 vs. pLTP2:aMIR-SAL1	-	****	*	-	-
pHorB1:NKD1 vs. pLTP2:NKD1	-	****	-	-	****
pHorB1:NKD1 vs. pLTP2:SAL1	-	***	-	-	***
pHorB1:SAL1 vs. pLTP2:aMIR-NKD1	-	-	-	*	****
pHorB1:SAL1 vs. pLTP2:aMIR-SAL1	-	-	-	*	****
pHorB1:SAL1 vs. pLTP2:NKD1	-	-	-	*	***
pHorB1:SAL1 vs. pLTP2:SAL1	-	-	-	*	****
pLTP2:aMIR-NKD1 vs. pLTP2:aMIR-SAL1	-	-	-	-	-
pLTP2:aMIR-NKD1 vs. pLTP2:NKD1	-	-	-	-	-
pLTP2:aMIR-NKD1 vs. pLTP2:SAL1	-	-	-	-	-
pLTP2:aMIR-SAL1 vs. pLTP2:NKD1	-	-	-	-	-
pLTP2:aMIR-SAL1 vs. pLTP2:SAL1	-	-	-	-	-
pLTP2:NKD1 vs. pLTP2:SAL1	-	-	-	-	-

"*" indicates significant difference, while "-" indicates insignificance. * = p≤0.0332, ** = p≤0.0021, *** = p≤0.0002, **** = p<0.0001, - = p≥0.1234. n = 9 grains (three grain from three independent transgenic lines). EA, transverse endosperm area, AA, transverse aleurone area, AP, transverse aleurone proportion, ALN, aleurone layer number, AW, aleurone width.

Table 3-S3: Two-way analysis of variance (ANOVA) for dorsal and ventral aleurone features between WT and transgenics.

	Grain features				
Comparison	**EA**	**AA**	**AP**	**ALN**	**AW**
WT (WI4330) (Dorsal vs. Ventral)	NA	NA	NA	-	-
pHorB1:aMIR-NKD1 (Dorsal vs. Ventral)	NA	NA	NA	-	**
pHorB1:aMIR-SAL1 (Dorsal vs. Ventral)	NA	NA	NA	-	-
pHorB1:NKD1 (Dorsal vs. Ventral)	NA	NA	NA	-	-
pHorB1:SAL1 (Dorsal vs. Ventral)	NA	NA	NA	*	****
pLTP2:aMIR-NKD1 (Dorsal vs. Ventral)	NA	NA	NA	-	-
pLTP2:aMIR-SAL1 (Dorsal vs. Ventral)	NA	NA	NA	-	-
pLTP2:NKD1 (Dorsal vs. Ventral)	NA	NA	NA	-	-
pLTP2:SAL1 (Dorsal vs. Ventral)	NA	NA	NA	-	-

"*" indicates significant difference, while "-" indicates insignificance. * = p≤0.0332, ** = p≤0.0021, *** = p≤0.0002, **** = p<0.0001, - = p≥0.1234. n = 9 grains (three grain from three independent transgenic lines). EA, transverse endosperm area, AA, transverse aleurone area, AP, transverse aleurone proportion, ALN, aleurone layer number, AW, aleurone width, NA, not available since can't separate into dorsal and ventral.

Table 3-S4: Table of primer sequences for qPCR.

Gene	HORVU	Forward	Reverse	Product Size (bp)
HvLTP2	HORVU4Hr1G089500	TGTGCCAGTACGTCAAGGAC	GCTAGCCAGGAAGCAAGCTA	207
HvHorB1	HORVU1Hr1G001420	GCCTAGTGGAGCTTCTTCACA	TGGTTTGCTGGCAATGGAATG	278
HvNKD1	HORVU2Hr1G095720	GATGTTTGATCCGAGGATGTG	TACGGCTTGTGTAAGCTCGAT	297
HvSAL1	HORVU7Hr1G115800	CAGTTCGTCAACATGGAGGTC	GATCTGAAGCGTAAGCGTTTG	268
HvCR4	HORVU7Hr1G071390	AGCAGCATAGGAGATGGTCTG	TTTCAGCTGATCTTGGCATTT	113
HvGAP	HORVU7Hr1G074690	GTGAGGCTGGTGCTGATTACG	TGGTGCAGCTAGCATTTGAGAC	198
HvCyclophilin	HORVU6Hr1G012570	CCTGTCGTGTCGTCGGTCTAAA	ACGCAGATCCAGCAGCCTAAAG	122
HvTubulin	HORVU1Hr1G081280	AGTGTCCTGTCCACCCACTC	AGCATGAAGTGGATCCTTGG	248
HvHSP70	HORVU5Hr1G113180	CGACCAGGGCAACCGCACCAC	ACGGTGTTGATGGGGTTCATG	108

Chapter 4

Differences in hydrolytic enzyme activity accompany natural variation in mature aleurone morphology in barley (*Hordeum vulgare* L.)

Statement of Authorship

Title of Paper	Differences in hydrolytic enzyme activity accompany natural variation in mature aleurone morphology in barley (*Hordeum vulgare* L.)
Publication Status	☑ Published ☐ Accepted for Publication ☐ Submitted for Publication ☐ Unpublished and Unsubmitted work written in manuscript style
Publication Details	Matthew K. Aubert[1,2], Stewart Coventry[1], Neil J. Shirley[1,2], Natalie S. Betts[1], Tobias Würschum[3], Rachel A. Burton[2] & Matthew R. Tucker[1*]

Principal Author

Name of Principal Author (Candidate)	Matthew K. Aubert		
Contribution to the Paper	Performed experiments, analysed all samples, interpreted data and wrote manuscript.		
Overall percentage (%)	80%		
Certification:	This paper reports on original research I conducted during the period of my Higher Degree by Research candidature and is not subject to any obligations or contractual agreements with a third party that would constrain its inclusion in this thesis. I am the primary author of this paper.		
Signature		Date	21/11/2018

Co-Author Contributions

By signing the Statement of Authorship, each author certifies that:

i. the candidate's stated contribution to the publication is accurate (as detailed above);

ii. permission is granted for the candidate in include the publication in the thesis; and

iii. the sum of all co-author contributions is equal to 100% less the candidate's stated contribution.

Name of Co-Author	Stewart Coventry		
Contribution to the Paper	Helped conceived project and helped to design experiments. Provided samples for the project. Contributed to the preparation of the manuscript. I hereby certify that the statement of authorship is accurate.		
Signature		Date	22/11/18

Name of Co-Author	Neil J. Shirley		
Contribution to the Paper	Performed quantitative PCR, assembled RNA sequencing library and helped with sample analysis. Contributed to the preparation of the manuscript. I hereby certify that the statement of authorship is accurate.		
Signature		Date	21/11/18

Name of Co-Author	Natalie S. Betts		
Contribution to the Paper	Helped with hydrolytic enzyme analysis. Contributed to the preparation of the manuscript. I hereby certify that the statement of authorship is accurate.		
Signature		Date	21.11.18

Name of Co-Author	Tobias Würschum		
Contribution to the Paper	Assisted with statistical analysis and preparation. Contributed to the preparation of the manuscript. I hereby certify that the statement of authorship is accurate.		
Signature		Date	20. Nov. 2018

Name of Co-Author	Rachel A. Burton		
Contribution to the Paper	Conceived project and helped to design experiments. Contributed to the preparation of the manuscript. I hereby certify that the statement of authorship is accurate.		
Signature		Date	22/11/2018

Name of Co-Author	Matthew R. Tucker		
Contribution to the Paper	Conceived project and designed experiments. Contributed to the preparation of the manuscript. I hereby certify that the statement of authorship is accurate.		
Signature		Date	20/11/2018

Journal Nature Scientific Reports

In Press July 2018, **8**:11025, p1-14, doi: 10.1038/s41598-018-29068-4

Title Differences in hydrolytic enzyme activity accompany natural variation in mature aleurone morphology in barley (*Hordeum vulgare* L.)

Authors Matthew K. Aubert[1,2], Stewart Coventry[1], Neil J. Shirley[1,2], Natalie S. Betts[1], Tobias Würschum[3], Rachel A. Burton[2] & Matthew R. Tucker[1]

[1]School of Agriculture, Food and Wine, Waite Research Institute, the University of Adelaide, Glen Osmond, SA, Australia.

[2]Australian Research Council Centre of Excellence in Plant Cell Walls, the University of Adelaide, Adelaide, Australia.

[3]State Plant Breeding Institute, University of Hohenheim, Stuttgart, Germany.

Keywords Barley, aleurone, endosperm, development, grain, fluorescence, enzyme, β-amylase, germination

Abbreviations

β-glucanase	1,3;1,4-β-glucanase
BMM	Butyl methyl methacrylate
BMY	β-amylase
CR4	CRINKLY 4
DEK1	DEFECTIVE KERNEL 1
Des5	DEFECTIVE SEED 5
DPA	Days post anthesis
FG	Female gametophyte stage
GA	Gibberellic acid
GWAS	Genome wide association study
HINa	Hordoinoline
hpi	Hours post imbibition
LCM	Laser capture microdissection
LTP2	LIPID TRANSFER PROTEIN 2
NKD1	NAKED ENDOSPERM 1
NVT	National variety trials
PCA	Principal component analysis
qPCR	quantitative Polymerase chain reaction
QTL	Quantitative trait loci
SAL1	SUPERNUMERARY ALEURONE LAYER 1
SKCS	Single kernel characterisation system
TPM	Transcripts per million
UA	University of Adelaide

Abstract

The aleurone is a critical component of the cereal seed and is located at the periphery of the starchy endosperm. During germination, the aleurone is responsible for releasing hydrolytic enzymes that degrade cell wall polysaccharides and starch granules, which is a key requirement for barley malt production. Inter- and intra-species differences in aleurone layer number have been identified in the cereals but the significance of this variation during seed development and germination remains unclear. In this study, natural variation in mature aleurone features was examined in a panel of 33 *Hordeum vulgare* (barley) genotypes. Differences were identified in the number of aleurone cell layers, the transverse thickness of the aleurone and the proportion of aleurone relative to starchy endosperm. In addition, variation was identified in the activity of hydrolytic enzymes that are associated with germination. Notably, activity of the free fraction of β-amylase (BMY), but not the bound fraction, was increased at grain maturity in barley varieties possessing more aleurone. Laser capture microdissection (LCM) and transcriptional profiling confirmed that *HvBMY1* is the most abundant *BMY* gene in developing grain and accumulates in the aleurone during early stages of grain fill. The results reveal a link between molecular pathways influencing early aleurone development and increased levels of free β-amylase enzyme, potentially highlighting the aleurone as a repository of free β-amylase at grain maturity.

Introduction

Barley (*Hordeum vulgare* L.) is recorded as one of the first agricultural crops to be domesticated (Zohary et al., 2012) and is a major food source in both Asia and northern Africa. The highest economic value for the crop is in its use as a malting grain for whisky and beer production (Newman and Newman, 2006). Extensive worldwide cultivation has led to the development and identification of over 460,000 barley accessions, including cultivars, landraces, breeding lines and wild *Hordeum* relatives (Sato et al., 2014). Coupled with a diploid sequenced genome (Mayer et al., 2012; Mascher et al., 2017), these genetic resources provide excellent opportunities to study the fundamental details of barley growth and development, with potential to tailor barley varieties for specific end uses.

Barley grain contains many key nutrients, antioxidants and dietary fibres that benefit the human diet (Behall et al., 2004; Pins and Kaur, 2006; Gamel and Abdel-Aal, 2012). Most of these nutrients accumulate in the endosperm, a filial tissue that supports embryonic growth in addition to providing physical protection during seed development (Yan et al., 2014). The endosperm consists of three main cell types - the endosperm transfer cells, starchy endosperm and aleurone layer - each of which confer different biological functions during grain maturation and seed germination. Endosperm development begins after fertilisation of the central cell within the embryo sac (Wilkinson and Tucker, 2017), when successive nuclear divisions without cytokinesis lead to the formation of a nuclear syncytium. This mass of nuclei begins to cellularise at the embryo sac periphery at approximately 5 days post anthesis (DPA). The aleurone first appears as a single layer at approximately 7–10 DPA and divides to form multiple layers by around 12–15 DPA. At maturity, the aleurone layers separate the mass of inner starchy endosperm from outer maternal layers, which include the

nucellar epidermis, integuments and pericarp. The aleurone cells display a cuboid shape with reinforced cell walls (Brown and Lemmon, 2007) that are enriched in phenolic acids and polysaccharides such as arabinoxylan (Nordkvist et al., 1984; Wilson et al., 2012; Hassan et al., 2017). During germination, the embryo releases gibberellic acid (GA), which translocates to the aleurone where it induces the transcription of genes encoding hydrolytic enzymes (Fath et al., 2000). Enzymes, such as 1,3;1,4-β-glucanase (β-glucanase), α-amylase and β-amylase, are released to catalyse the breakdown of cell wall polysaccharides and starchy energy reserves that are essential for germination and the production of malt for brewing (Betts et al., 2017). β-glucanase hydrolyses 1,3;1,4-β-glucan, which is the predominant cell wall polysaccharide present in barley endosperm, α-amylase cleaves internal amylose and amylopectin residues, and the β-amylase exo-hydrolase liberates maltose from the non-reducing end of starch molecules (Betts et al., 2017). While α-amylase appears to be transcribed and translated *de novo* during germination, β-amylase is transcribed and translated during grain development (Radchuk et al., 2009). Some of the β-amylase enzyme is present in a free form, while most is present in an inactive bound form, purportedly linked through protein bridges to starch molecules (Tronier and Ory, 1970; Hara-Nishimura et al., 1986; Sopanen and Lauriere, 1989).

Seeds from mutants showing defects in aleurone development are often shrunken or misshapen (Becraft and Yi, 2011). However, natural differences in aleurone layer number and structure have been observed between cereal species. Cereal grains from species such as maize (*Zea mays* L.) and wheat (*Triticum aestivum* L.) have a single layer of aleurone cells while the barley aleurone is multilayered (Shapter et al., 2009). Intra-species variation has been found between barley cultivars, and several QTL were identified in an Erhard Frederichen × Criolla Negra population that influence the

number of aleurone layers (Jestin et al., 2008). Genes such as *NAKED ENDOSPERM 1*, *SUPERNUMERARY ALEURONE LAYER 1*, *DEFECTIVE KERNAL 1* and *CRINKLY 4* influence aleurone development in maize (Becraft et al., 1996; Lid et al., 2002; Shen et al., 2003; Yi et al., 2015), but whether similar genes influence variation in barley aleurone development has yet to be reported. Moreover, the significance of having more or fewer aleurone layers on seed development or germination, particularly in the context of barley, remains unclear.

In this study, 33 barley genotypes were surveyed to identify natural variation in aleurone phenotypes. A method was developed to measure features of the aleurone in mature grain based on UV-autofluoresence of the thick aleurone walls, and to assess correlations with wholegrain traits. Selected genotypes were examined in greater detail to assess the relationship between the aleurone and hydrolytic enzyme activities. Finally, transcriptional profiling of fresh and laser micro-dissected grain tissues was used to ascertain when and where key germination-related genes are transcribed during grain development.

Materials and methods

Plant material

A University of Adelaide (UA) barley diversity panel of 33 genotypes was grown in the field at Charlick, SA, in 2013. A partially overlapping set of genotypes was grown at Gooloogong, NSW, in 2015 and grain was obtained from the National Variety Trials (NVT; www.nvtonline.com.au). The UA panel was chosen to reflect a diverse array of genetic stocks and row-types (Table 4-S1), and consists of both 2-row (n = 30) and 6-row (n = 3) spring genotypes and breeding lines. Grain samples were sieved using a 2.5 mm screen to remove broken grain, long awns and foreign material prior to analysis. The majority of intact grain are retained using this method, allowing analyses to be performed on grains of varying sizes and shapes.

Grain sectioning and imaging

Mature grain were cut into quarters and fixed overnight in TEM fix (0.25% glutaraldehyde, 4% paraformaldehyde, 4% sucrose in phosphate buffered saline). Samples were rinsed with phosphate buffered saline (3 × 4 hour washes) and then dehydrated in an ethanol series (3 × 8 hours in 70%, 80%, 90%, 95% and 100%). This was followed by an overnight infiltration in a 50:50 mix of 100% ethanol/LR White resin, and 3 changes of pure LR White resin for 8 hours each. Infiltrated specimens were transferred to gelatin capsules in fresh LR White resin, covered with lids and polymerized in a 60 °C oven for at least 48 hours. Sections were prepared at a thickness of 1 µm using a Reichert Ultracut ultramicrotome (Leica, Wetzlar, Germany). For the anatomical study of aleurone cells, sections were stained with 0.01% (w/v)

Toluidine Blue and viewed using brightfield microscopy, or 0.001% (w/v) Calcofluor White and viewed using Zeiss Filter set 47 (BP 436/20, FT 455, BP 480/40; blue staining in Figure 4-S3) and Filter set 46 (BP 500/20, FT 515, BP 535/30; false coloured red in Figure 4-S3) on a Zeiss M2 AxioImager equipped with DIC optics and an Apotome.2 (Zeiss, Germany).

To observe the aleurone in fresh samples, mature grain were bisected by hand (transversely) using a reinforced single-edge razor blade (ProSciTech, Australia) and adhered to a microscopy slide using Blu-Tack® (Bostick, Australia) with the flat midpoint of the grain facing upwards. Between 3 and 10 grain from each cultivar were imaged using a Zeiss M2 AxioImager with an attached AxioCam MrM camera (Zeiss, Germany). Zeiss Filter set 46 (BP 500/20, FT 515, BP 535/30) was used to view pericarp and husk autofluorescence (false coloured red in Figure 4-1) and Filter set 49 (G365, FT395, BP445/50) was used to view aleurone wall autofluoresence (false coloured yellow in Figure 4-1). Images were processed using ZEN 2012 software (Zeiss, Germany).

Grain measurements were also recorded using ZEN 2012 software (Zeiss, Germany; Figure 4-S1). Transverse endosperm area was measured by tracing the outline of whole endosperm, while aleurone area was calculated by subtracting the starchy endosperm area from the total endosperm area. Aleurone proportion was measured by calculating the aleurone area as a percentage of the total transverse endosperm area. Aleurone layer number was recorded as an average where, in each section of barley grain, a maximum and minimum layer number was recorded at dorsal, left and right positions. Similarly, aleurone width was measured as the distance from the edge of the endosperm to the innermost autofluorescent aleurone cell wall.

Wholegrain phenotypic analysis

Barley grain weight and dimensions were determined using a SeedCountTM SC4 (Seed Count Australasia, Condell Park, Australia), following manufacturer's instructions. Single grain hardness, moisture content and diameter of 300 grain were analysed using a Single Kernel Characterisation System, SKCS 4100 (SKCS; Perten Instruments, Springfield, IL), following the manufacturer's instructions.

Grain germination and sample preparation for enzyme assays

Grain from selected barley genotypes was placed at 37 °C for two days to remove residual moisture. Dry grains were subsequently sprinkled onto 10 cm diameter No 1. Whatman® filter paper disks (×2), placed in a 10 cm diameter Petri dish and soaked with 4 mL sterilised water. For the germination assay, 70 sample grains were plated alongside 30 control Navigator grain. For the enzyme assays, 30 sample grains were used alongside 70 sacrificial Sloop and Navigator grains for standards and water saturation balances. The Petri dishes were sealed with Parafilm® (Bemis, USA) then placed in an incubator at 20 °C in the dark for 6, 12, 24, 48 or 96 hours. For the germination assay, plates were removed and scored visually to determine the frequency of grain germination at each time point. For the enzyme assays, grain were removed from the incubator and all 30 germinating grains placed into 10 mL tubes (for each variety) and freeze dried for 96 hours to remove residual moisture. Mature grain and dried germinated grains were ground to flour with a Retsch MM400 Mixer Mill (Retsch GmbH, Haan, Germany).

Hydrolytic enzyme assays

Enzyme assays were performed on both mature grain and dried germinated grain flour, respectively, using downscaled methods (approximately four-fold) from Megazyme (Ireland). The β-Glucanase Assay Kit (K-MBGL) (McCleary and Shameer, 1987), the α-Amylase Assay Kit (K-CERA) (McCleary et al., 2002) and the Betamyl-3; β-Amylase Kit (K-BETA3) (McCleary and Codd, 1989) were all used following manufacturer's instructions.

Correlation analysis and figure preparation

All correlation and PCA analyses were carried out in RStudio using the 'corrplot' package. (RStudio®, Boston, USA; https://cran.r-project.org/web/packages/corrplot/corrplot.pdf). Selected graphs were prepared in SigmaPlot or Microsoft Excel. Statistical differences were determined using one-way ANOVA followed by the Tukey-Kramer test. Figures were assembled in Adobe Photoshop CS6 and Adobe Illustrator CS6.

RNAseq analysis

Developing grain were collected from *H. vulgare* cv. Sloop plants at 7, 9, 11, 13, 15 and 20 days post anthesis (DPA). The embryo was discarded and all remaining (wholegrain) tissues were snap frozen in liquid nitrogen. At least six grain from three independent plants were collected and pooled to form a single composite sample at each time point. RNA for all samples was extracted using the SpectrumTM Plant Total RNA kit (Sigma-Aldrich, Darmstadt, Germany). Samples were submitted for

sequencing using the Illumina Hiseq Platform (AGRF, Australia), and reads were assembled against the most recent barley reference sequence using CLC Genomics (Mascher et al., 2017). Normalised read counts (transcripts per million; TPM) were determined for each HORVU sequence and used to determine the abundance of each transcript in each sample. For RNAseq analysis of pre-fertilisation stages, developing ovaries (pistils) were harvested from *H. vulgare* cv. Golden Promise at female gametophyte stage 4 (FG4), FG8, FG mature and FG anthesis and processed in a similar manner to that described above. The two different genotypes (Sloop and Golden Promise) were used for historical reasons; we have previously used Golden Promise as a resource for studies of floral organ fertility while Sloop has been used for studies of grain development and seedling growth.

Laser Capture Microdissection and Quantitative PCR

Grain samples from *H. vulgare* cv. Sloop were collected at 11 and 25 DPA, bisected transversely and fixed in ethanol:acetic acid as described previously (Tucker et al., 2012). Tissues were embedded in butyl methyl methacrylate (BMM) and polymerised at −20 °C under UV light (Tucker et al., 2012; Okada et al., 2013). Samples were sectioned to 5 µm using a Leica Ultracut microtome, adhered to Leica PEN membrane slides and dissected using a Leica LMD microscope (Leica, Wetzlar, Germany; Adelaide Microscopy, Adelaide; Figure 4-S2). Approximately 6–10 sections from three grain were collected from the outer grain layers (predominantly pericarp), aleurone, outer-starchy endosperm (incorporating sub-aleurone and some adjoining starchy cells) and inner starchy endosperm (incorporating starchy endosperm cells and the grain cavity) and stored at −80 °C. Total RNA was isolated using the PicoPure kit

(ThermoFisher, Australia) and converted to cDNA using SuperscriptTM III reverse transcriptase (ThermoFisher, Australia) and oligodT primer with a 2 hour synthesis step at 37 °C. For the 25 DPA samples, RNA was amplified twice using the MessageAmpTM II kit (ThermoFisher, Australia) before converting to cDNA using Superscript III and random hexamers (Yi et al., 2015). Multiple control genes were used to normalise samples (Aditya et al., 2015) and primer sequences are included in Table 4-S5.

Results

Sub-epidermal grain features are revealed by autofluorescence microscopy

The aleurone layers and cell structure present at the periphery of the barley endosperm were examined by hand-sectioning (Figure 4-1A) and autofluorescence microscopy (Figure 4-1B–J). UV-light revealed different types of autofluorescence depending on the filter set and clearly distinguished the pericarp (false coloured red) and aleurone cells (false-coloured yellow). Hand sections provided sufficient detail to measure transverse features of the aleurone, starchy endosperm and pericarp/husk using a 1× objective (Figures 4-1B–D and 4-S1), while the number of aleurone layers and aleurone thickness could be determined using a 20× objective (Figures 4-1E–J and 4-S1). To assess whether these measurements were consistent with those generated by thin sections, mature grain samples from two genotypes showing differences (Golden Promise and Flagship) were embedded in resin and sectioned prior to staining with Calcofluor White. Staining revealed differences between the genotypes, with Flagship tending to show fewer aleurone layers (Figure 4-S3A) than Golden Promise (Figure 4-S3B). A similar result was obtained by hand-sectioning (Figure 4-S3C,D), suggesting that the hand-sectioning method is appropriate to measure differences in aleurone phenotypes.

Transverse grain sections were generated for 33 different barley genotypes and significant differences in aleurone phenotypes were identified (Figures 4-1 and 4-2, Table 4-S1). Aleurone layer number was not identical around the entire grain periphery, but the average number of layers from three regions (dorsal, left and right) in each grain provided a representative measurement for comparisons between genotypes. The average number of aleurone layers for all genotypes was 2.4 ± 0.2,

but showed genotype-dependent variation. Clipper (2.8 ± 0.01; Table 4-S1) and Franklin (2.8 ± 0.01; Figure 4-1E, Table 4-S1) typically possessed more aleurone layers, Dhow showed an intermediate number of layers (2.5 ± 0.02; Figure 4-1F) and Hindmarsh possessed significantly fewer layers (1.8 ± 0.05; Figure 4-1G). Additionally, genotypes differed in regards to aleurone width, which was on average 53.2 ± 6.5 µm. The YU6472 genotype showed a thick aleurone (65.4 ± 6.2 µm; Figure 4-1H), Mundah was intermediate (60.4 ± 4.2 µm; Figure 4-1I) and Harrington possessed a thinner aleurone (40.6 ± 2.8 µm; Figure 4-1J). The variation in each measurement across the panel was normalised to the average trait value, which was assigned a value of 1 (Figure 4-2A). The largest variation was observed in transverse endosperm area, followed by aleurone area, aleurone layer number and aleurone width, whilst aleurone proportion and transverse grain width were less variable (Figure 4-2A). The lack of variation in grain width is likely to be a result of grain screening. When focussing on aleurone-specific measurements, the values appeared to display normal distributions (Figure 4-2B).

Principal component analysis (PCA) separated the genotypes based on the seven transverse grain measurements (Figures 4-2C and 4-S4A). Genotypes such as CM72, Morex, Barque-73, Hindmarsh, Franklin, Harrington and YU6472 showed distinct differences.

Differences in aleurone measurements at grain maturity correlate with other grain features

The relationship between mature grain and aleurone measurements was examined across the 33 different genotypes by correlation analysis (Figures 4-3, 4-S4 and 4-S5).

While some traits appeared unrelated across the panel, others showed strong correlations, and in the following sections significance indicators are included as follows: ***p ≤ 0.001, **p ≤ 0.01 and *p ≤ 0.05. For example, aleurone area was positively correlated with endosperm area (0.79***; Figures 4-3A and 4-S4B), while aleurone proportion negatively correlated with endosperm area (−0.53***; Figures 4-3B and 4-S4B). These results suggest that although bigger grains contain more aleurone, the increase in grain size is driven by the starchy endosperm, and aleurone proliferation/expansion is compromised proportionally. Increased aleurone area was driven by increased aleurone width (0.75***; Figures 4-3C and 4-S4B) but was independent of layer number, while an increased proportion of aleurone was partly due to more aleurone layers (0.41***; Figure 4-S4B). Aleurone width only showed a weak correlation with aleurone layer number (0.41**; Figure 4-S4B). Thus, larger grains contain more aleurone, mainly as a result of increased aleurone width (i.e., thickness), but smaller grains contain more aleurone layers with a higher proportion of aleurone relative to starchy endosperm. Together, these results indicate that mature aleurone morphology in barley is determined by the number and size of aleurone cells, which are in turn influenced by starchy endosperm development, and the contribution of each feature can vary depending on the genotype.

Comparisons between wholegrain and transverse section measurements were examined in greater detail for the 2-row genotypes (n = 30; Figures 4-3D–F and 4-S5, Table 4-S1). Increased transverse endosperm area was positively correlated with wholegrain measurements including grain width (0.64**; Figures 4-3D and 4-S5) and grain weight (0.59**; Figures 4-3E and 4-S5), confirming that some of the transverse measurements relate directly to overall grain features. Several aleurone measurements showed similar correlations to grain size; for example, aleurone area

was positively correlated with grain width, thickness, area, diameter and weight (Figure 4-S5). Interestingly, the only transverse grain measurements to show a correlation with grain hardness were aleurone proportion (0.49**; Figures 4-3F and 4-S5) and aleurone layer number (0.37*; Figure 4-S5). This indicates that in this panel, some 2-row genotypes producing harder grains tend to contain more aleurone layers and a higher proportion of aleurone relative to starchy endosperm.

Differences in aleurone development are maintained across different field sites

To determine how consistent the transverse grain measurements were across different environments and years, grain from eight genotypes including Barque, Baudin, Commander, Flagship, Hindmarsh, Keel, Mundah and Shepherd were compared from Charlick, UA, in 2013 (UA), and Gooloogong, NSW, in 2015 (NVT). The aleurone and wholegrain measurements were recorded and compared as a ratio between the different environments and years, i.e., NVT value / UA value (Table 4-S2; Figure 4-S6). The majority of genotypes showed less than 10% variation for all transverse measurements between environments; for example, the least variable transverse measurement was grain width (Figure 4-S6A) while the most variable measurements were aleurone layer number and proportion (Figure 4-S6A). The variation in aleurone layer number was most obvious in Barque and Hindmarsh, which tend to have more layers in the NVT samples (1.83 UA vs 2.44 NVT and 1.88 UA vs 2.38 NVT, respectively), while the variation in aleurone proportion was most obvious in Flagship, which showed more endosperm overall but less aleurone in the NVT samples. Although this reveals an effect of environment on transverse grain features, particularly with regard to the aleurone, correlation analysis indicated that the aleurone

measurements generally show a similar trend between environments. For example, measurements of aleurone proportion (0.67*; Figure 4-S6B) and width (0.79*; Figure 4-S6C) were significantly correlated despite the different environments. Although this analysis is limited to a small number of genotypes, it suggests there is some degree of stability in aleurone measurements between distinct environments.

Identification of barley genotypes for downstream analysis

Genotypes showing distinct grain phenotypes were selected for more detailed analysis based on transverse grain measurements and PCA (Figures 4-2C and 4-S4A). Shepherd tended to be at the high extreme for most measurements, while Morex and Barque-73 tended to be at the low extreme (Table 4-S1). Other genotypes were chosen to specifically examine differences in aleurone development, with the aim of avoiding confounding factors such as starchy endosperm area and grain size. For example, endosperm area in Mundah, YU6472, WI2585, WI4262 (Navigator), WI4191 and Steptoe was similar, but aleurone features such as area, proportion and width were distinct. The Mundah and YU6472 genotypes appeared to be “high” genotypes for these characteristics, WI2585 was “average”, while Flagship, WI4191 and Steptoe were “low” (Figure 4-2C and Table 4-S1). It is important to note that unlike most of the barley genotypes examined here, Morex and Steptoe are 6-row barleys. Based on the small number of 6-row genotypes in the panel, it is currently unclear whether the 6-row phenotype contributes directly to differences in aleurone development.

Hydrolytic enzyme activities differ between genotypes with different aleurone phenotypes

The distinct genotypes were examined to determine whether grain with more aleurone might display increased enzyme activity during germination. The results of β-glucanase, α-amylase, total and free β-amylase activity assays for the nine genotypes of interest are shown for two time points in Figure 4-4, with some genotypes showing significant differences (Table 4-S3). One of the two time points was grain maturity, allowing detection of enzymes that had been synthesised and stored during grain development, and the other was 96 hours post imbibition (hpi), which detects enzymes that have been synthesised during germination. The total β-amylase assay used a reducing agent to liberate bound enzyme before activity analysis, while the free β-amylase assay measured activity of unbound enzyme.

Consistent with previous studies, β-glucanase (Figure 4-4A) and α-amylase (Figure 4-4B) activity was barely detectable in mature grain, while total (Figure 4-4C) and free β-amylase (Figure 4-4D) activity was detectable at grain maturity. By 96 hpi, activity could be detected for all enzymes in the selected genotypes and clear differences were observed. For example, at 96 hpi, WI4191 (2-row), Steptoe (6-row) and Morex (6-row) showed relatively low β-glucanase and α-amylase activity compared to the other varieties (Figure 4-4A,B). Conversely, WI4191 and Morex showed relatively high total and free β-amylase activity compared to the other varieties (Figure 4-4C,D). Average total β-amylase activity was similar at grain maturity and germination for most of the varieties (Figure 4-4C), although free β-amylase levels tended to be lower at grain maturity compared to the 96 hpi samples, presumably as more enzyme is released through proteolytic cleavage from starch bodies.

Correlation analysis was used to assess the relationships between aleurone morphology and enzyme activity (Figure 4-4E). Significant correlations ($p \leq 0.05$) were identified between (1) β-glucanase and α-amylase activity after germination (0.98*), (2) total β-amylase activity at grain maturity and free β-amylase after germination (0.78*) and (3) total β-amylase and free β-amylase after germination (0.76*). By contrast, none of the transverse endosperm or aleurone measurements showed a significant correlation with β-glucanase or α-amylase activity at maturity or 96 hpi (Figure 4-4E). Also, differences in total β-amylase activity did not correlate with differences in any of the transverse grain measurements (Figure 4-4E).

Conversely, free β-amylase activity showed a significant correlation ($p \leq 0.05$) with transverse aleurone area (0.77*), aleurone proportion (0.87*) and aleurone width (0.86*) at grain maturity (Figure 4-4E). Furthermore, although aleurone area and endosperm area were correlated (0.90*), endosperm area itself did not directly correlate with free β-amylase activity. This suggests that direct variation in aleurone cell size or area, or perhaps indirect features of the starchy endosperm that influence aleurone development, may contribute to differential abundance of free β-amylase in different barley genotypes.

To assess if variation in enzyme levels, particularly free β-amylase, might contribute to the rate of grain germination we utilised an *in vitro* germination assay (Figure 4-S7). Differences were observed between genotypes, particularly in the case of WI4262 (Navigator) and YU6472 (Figure 4-S7). Comparisons between grain features, germination frequency and enzyme levels revealed significant correlations between the number of germinated seedlings at 12 hours post imbibition (hpi) and β-glucanase and α-amylase levels at 96hpi (0.72*), and the frequency of germinated seedlings at 24 hpi and 48 hpi (0.71*). However, no significant correlation was detected between

any transverse mature grain features or β-amylase activity compared to the frequency of germination at the time points analysed. Therefore, it seems unlikely that the varying aleurone features, and their association with free β-amylase activity, relate directly to the rate of germination from 12 hpi onwards.

β-amylase transcript abundance varies in specific grain cell-types

To address how variation in aleurone features might directly contribute to increased wholegrain free β-amylase levels at grain maturity, we considered the spatial and temporal dynamics of *β-amylase* transcript abundance. Previous studies have shown that *β-amylase* genes are transcribed and translated during barley grain development (Radchuk et al., 2009; Betts et al., 2017), with some enrichment in sub-aleurone or aleurone tissues. In this study, several datasets were generated to examine the abundance of 11 putative barley *β-amylase*-encoding genes identified in the latest release of the barley genome (Table 4-S4). First, a developmental series of early grain development was generated from Sloop wholegrain samples (minus embryo) at 7, 9, 11, 13, 15 and 20 days post anthesis (DPA), which covers the main stages of aleurone differentiation and development (Figure 4-S8). This overlaps with datasets from several studies (Sreenivasulu et al., 2006; Radchuk et al., 2009; Thiel et al., 2011; Zhang et al., 2016). Analysis confirmed that *HvBMY1* was the most abundant *β-amylase* gene in the developing grain, increasing in abundance from 9 DPA onwards (Table 4-S4; Figure 4-5A). This pattern was distinct from that of the *lipid transfer protein 2* (*HvLTP2*) gene, a specific marker for aleurone tissue, although transcripts for both genes accumulated over time (Figure 4-5A). *HvBMY2* was the second most abundant *β-amylase* transcript in the developing grain, but showed a significant decrease in

abundance from 7 DPA onwards (Table 4-S4; Figure 4-5A). The expression at 7 DPA may correspond to residual expression from vegetative tissues, since in a separate dataset generated from pre-fertilisation pistil tissues (from the Golden Promise cultivar), *HvBMY2* was most abundant *β-amylase* gene (Table 4-S4).

Next, we utilised laser microdissection to precisely separate the pericarp, aleurone, outer starchy endosperm (including sub-aleurone) and inner starchy endosperm tissues from transverse mid-point grain sections at 11 DPA (Figure 4-5B) and 25 DPA (Figure 4-S9). RNA from these specific regions was analysed by quantitative PCR (qPCR) using known markers of grain development. At 11 DPA, transcript from the *HvLTP2* aleurone marker was barely detected in the pericarp, outer starchy endosperm and inner starchy endosperm cells, but was abundant in the aleurone (Figure 4-5C). In contrast, transcript from the barley *hordoinoline* (*HvHINa*) gene that influences grain hardness and accumulates in the endosperm was predominantly detected in the outer starchy endosperm and inner starchy endosperm tissues (Figure 4-5D). Unlike *HvLTP2* and *HvHINa*, *HvBMY2* transcript was predominantly detected in the pericarp and outer starchy endosperm samples, and not in the aleurone or inner starchy endosperm (Figure 4-5E). *HvBMY1* transcript was detected in the aleurone, outer starchy endosperm and inner starchy endosperm samples. On average, expression was ~4 fold higher in the inner starchy endosperm tissues compared to the aleurone (Figure 4-5E) and the ratio of aleurone: outer starchy endosperm: inner starchy endosperm was approximately 1:3:4. Transcript patterns were similar at 25 DPA (Figure 4-S9A–D), although the aleurone appeared to contribute only 3% of the total detected *HvBMY1* transcript. Taken together, these data suggest that the inner and outer starchy endosperm are the major sites of *HvBMY1* expression. However, an increase in *HvBMY1* transcript during grain development is driven by expression in

multiple tissues, with the aleurone contributing up to 13% of the overall grain transcript levels depending on the developmental stage. Therefore, the increase in free β-amylase levels at grain maturity in genotypes exhibiting a larger aleurone may be partly due to expression of *HvBMY1* in aleurone tissues.

Discussion

The cereal aleurone is a multifunctional tissue with important roles in grain development and germination, and applications in the health and brewing industries (Burton and Fincher, 2014). In this study, we utilised autofluorescence microscopy to identify differences in aleurone morphology within a panel of diverse barley genotypes, and considered how these differences relate to grain biology and the amount of germination-related enzyme activity.

Within the cereal grain, the aleurone and starchy endosperm are both derived from the fertilised central cell and only begin to differentiate around 7–10 days after pollination (Burton and Fincher, 2014). Unsurprisingly, analysis of 33 barley genotypes confirmed that development of the starchy endosperm and aleurone are intimately linked; as radial starchy endosperm area increased, so too did the radial area of aleurone. Genotypes producing grain with more aleurone layers also tended to show a thicker aleurone, and aleurone width contributed directly to aleurone area. However, the number of aleurone layers shared no direct relationship with aleurone area, suggesting that factors determining aleurone cell expansion have a greater impact on this trait. A reduced proportion of aleurone was typically linked to an increase in starchy endosperm area, while an increased proportion correlated with increased aleurone layer number. These data indicate that pathways promoting increased grain fill (i.e., starchy endosperm cell division and/or cell expansion) are (1) unlikely to be perceived by aleurone cells, (2) may inhibit the formation / maintenance of additional inner aleurone layers and (3) may indirectly impact the size of aleurone cells, possibly due to physical constraints imparted by the pericarp.

Of all the aleurone and grain features measured in this study, aleurone layer number appeared to be the most independent (see Figure 4-S4B). This may be due to difficulty

in collecting precise measurements or perhaps a unique mechanism underlying layer formation. In maize, specific pathways appear to prevent an increase in aleurone layer number, since aberrant periclinal divisions of aleurone cells result in them adopting starchy endosperm fate (Becraft and Yi, 2011). A similar mechanism may contribute to subtle variations in aleurone layer number in barley. Genotypes such as Barque-73 and Hindmarsh, which produce fewer aleurone layers (~1.8 on average), may be more sensitive to differentiation signals that promote starchy endosperm identity compared to genotypes such as Clipper and Franklin, which produce more aleurone layers (~2.8 on average). The source and temporal activity of the fate-determining signals is unclear (Becraft and Yi, 2011); one possibility is that aleurone cells perceive a stimulatory cue at the periphery of the grain that only reaches a certain radial depth. Similar basic mechanisms have been identified in Arabidopsis, where diffusible epidermal signals control sub-epidermal cell identity during shoot meristem development (Tucker et al., 2012; Knauer et al., 2013). Alternatively, the starchy endosperm generates signals that do not reach or are not perceived by the aleurone. The diversity of aleurone phenotypes observed in this barley panel provides an opportunity to address these differences at the genetic level in future studies.

The contribution of sub-epidermal tissues to wholegrain traits is revealed by transverse sectioning and microscopy

One limitation of manual microscopic screens is their low throughput nature, particularly compared with high throughput automated screens of grain shape, composition and dimension used in breeding programs. However, the advantage of microscopy is that sub-epidermal features of the grain can reveal cell-type specific

contributions to wholegrain traits (Nair et al., 2011). Here, comparison of microscopy and wholegrain analyses showed clear correlations, particularly when focussing on spring 2-row barley genotypes. For example, transverse endosperm area correlated with wholegrain measurements of area, thickness and weight (Figure 4-S5).

Unexpectedly, grain hardness correlated positively with aleurone proportion and layer number (Figure 4-S5). Grain hardness has been intensively studied in the cereals. In wheat, hardness contributes to milling and baking properties and flour composition (Williams, 1967; Symes, 1969; Greffeuille et al., 2005; Pasha et al., 2010), while in barley, hardness influences pearling properties (Edney et al., 2002) in addition to the malting quality index (Psota et al., 2007). The composition of individual grain components, particularly the starchy endosperm, determines whether the grain will be hard or soft (Brennan et al., 1996; Chandra et al., 1999; Psota et al., 2007) with models suggesting that harder grains have a denser endosperm with a continuous protein matrix that prevents easy release of starch granules (Nair et al., 2011). A specific relationship between the barley aleurone and grain hardness does not appear to have been reported previously. The correlation detected here may therefore reflect an effect of starchy endosperm protein on hardness, and an indirect effect on aleurone development. Another possibility is that in the examined panel, differences in the chemical and physical properties of the aleurone cell walls may directly contribute to grain hardness. Barley aleurone cell walls are enriched in arabinoxylan polysaccharides cross-linked with phenolic acids such as ferulic acid (Wilson et al., 2012; Hassan et al., 2017), forming a robust matrix that surrounds the grain during development (Burton and Fincher, 2014). In genotypes with an increased proportion of aleurone, this reinforced cell wall matrix may provide a harder shell around the grain. This is something that might also be considered in future studies.

Variations in barley aleurone features provide opportunities for further genetic analysis, and do not appear to impact overall grain development

Despite several studies providing insight into the genetic architecture of barley aleurone development (Jestin et al., 2008; Olsen et al., 2008) the molecular basis for variation between genotypes has yet to be elucidated. Genetic data are available for a number of the genotypes investigated here, but the number was insufficient to carry out a robust genome wide association study (GWAS) to identify possible quantitative trait loci (QTL). However, our findings show that the variation between genotypes is reproducible and statistically significant; this suggests that a similar screen might be carried out on a larger panel of genotypes to support future genetic analysis.

Strangely, it has also remained unclear whether intraspecific differences in barley aleurone development are of any physiological importance. It is possible that the variation is of no major consequence, as long as the aleurone is still present and able to fulfil roles in hormone perception and enzyme release during germination. In general, mutants that show a lack of or reduced number of aleurone layers tend to show defects in seed development. For example, the barley *defective seed 5* mutant (*des5*) (Olsen et al., 2008) shows a patchy reduction in the number of aleurone cells, and severe defects in starchy endosperm fill and seed morphology. Similarly, mutations in the maize *naked endosperm 1* and *crinkly 4* genes lead to reduced aleurone phenotypes, in addition to compromised whole seed morphology (Becraft et al., 1996; Yi et al., 2015). On the other hand, mutant alleles of the maize *supernumerary aleurone 1* (*sal1*) gene, which produce two or three aleurone layers instead of the one layer detected in wild type, have relatively normal kernels (Shen et al., 2003; Tian et al., 2007). Variations in aleurone thickness, area and layer number

from two to four layers appeared to have no detrimental impact on overall grain development across the barley panel examined here.

The genotypes investigated included a combination of 2-row and 6-row varieties, malting and feed varieties; for example, Barque-73 and Mundah are Australian feed varieties, Sloop is an Australian malting variety, and YU6472 is a Chinese feed variety (Zhou et al., 2008). Based on an “average” sized grain, Barque-73 exhibited reduced aleurone area, proportion and width. At the other extreme, compared to its average grain size, YU6472 displayed increased aleurone area, proportion and width. Barque-73 also showed significantly fewer aleurone layers compared to Mundah and Sloop. Although the sample size is small, there appeared to be no clear difference in aleurone morphology to distinguish between grains from feed and malting genotypes. This observation needs to be treated with some caution, however, since there are many features that contribute to malt grade barley (Evans et al., 2008). This could be tested in a larger panel of genotypes that have been directly assessed, head-to-head, for malt quality.

Genotypes with more aleurone show increased levels of free β-amylase at grain maturity

The variation present in this barley panel provided an opportunity to assess the effect of different aleurone phenotypes on the activity of germination-related enzymes, which is one important aspect of aleurone function. During barley grain imbibition, gibberellic acid (GA) is released by the scutellum, triggering the synthesis and subsequent release of various hydrolytic enzymes from the aleurone (Jones, 1973; Fincher, 1989; Drozdowicz and Jones, 1995). Of these enzymes, β-glucanase facilitates the

hydrolysis of β-glucan polysaccharides in cell walls and allows access to starch for additional hydrolytic enzymes (Hrmova and Fincher, 2001). Enzymes involved in starch hydrolysis include α-amylase, which hydrolyses α-1,4-glycosidic bonds of starch polysaccharides and β-amylase, which is synthesised during grain development, and during germination acts to liberate the disaccharide maltose from the non-reducing end of starch molecules (Bamforth and Quain, 1989; Lauro et al., 1993; Lewis and Young, 1995; Betts et al., 2017). Function of these enzymes is critical for germination (Becraft and Gutierrez-Marcos, 2012; Han and Yang, 2015), and previous studies show that mature grain β-amylase content varies between barley genotypes (Li et al., 2002; Yin et al., 2002; Gong et al., 2013).

β-glucanase enzyme activity was barely detectable at grain maturity, but was high at 96 hpi, and the same pattern was observed for α-amylase. A relatively low level of activity was identified for both enzymes in WI4191, Steptoe and Morex, which tend to display “low” aleurone phenotypes. However, neither β-glucanase nor α-amylase levels showed a general correlation with differences in mature grain aleurone morphology. This may indicate that variation in transverse aleurone morphology at maturity has no direct impact on the amount of β-glucanase and α-amylase activity. Alternatively, the genotypes chosen for analysis did not show large enough differences in aleurone development, the panel was too small, or the 96 hpi time point was too late to identify such differences.

Two forms of β-amylase are present in the grain, a bound and free form. Bound β-amylase is located in an insoluble protein complex, mainly associated with the periphery of starch granules via disulphide bridges (Hara-Nishimura et al., 1986; Lauriere et al., 1986), while the soluble or free form is active. Both forms of β-amylase are identical in terms of mobility and molecular specific activity, indicating that once

bound β-amylase is cleaved, it is converted to free β-amylase (Hara-Nishimura et al., 1986). Total and free β-amylase were detected in mature and germinated grain samples from the nine genotypes of interest. Total β-amylase activity did not change over time, consistent with its synthesis during grain development. Free β-amylase activity increased during germination and varied between genotypes, consistent with the release of bound β-amylase and previous reports (Sopanen and Lauriere, 1989; Li et al., 2002; Yin et al., 2002; Gong et al., 2013; Betts et al., 2017). Notably, genotype-specific differences in free β-amylase activity at grain maturity correlated with aleurone area, proportion and width. Genotypes with “high” aleurone phenotypes exhibited higher free β-amylase levels. In physiological terms, we propose this may allow for an early pulse of starch hydrolysis prior to the liberation of bound β-amylase by endopeptidases. In wheat, hydrogen sulphide treatment was shown to stimulate early germination through early activation of β-amylase (Zhang et al., 2010). The authors speculate that higher levels of “active” free β-amylase can participate in starch hydrolysis, providing sugar units for seedling growth prior to the induction of α-amylases by GAs (Zhang et al., 2010). In the current study, a role for increased free β-amylase activity in germination was tested in the context of nine genotypes of interest, but this failed to identify any significant correlation. This suggests that if there is a physiological role for increased free β-amylase levels and aleurone features at maturity, it may occur prior the emergence of the barley radicle at 6 to 12 hpi.

Explaining differences in free β-amylase levels at grain maturity

There are a number of reasons why free β-amylase levels might vary at grain maturity, including variable transcriptional dynamics of different *HvBMY* genes and

polymorphisms that influence enzyme activity. Previous studies indicate that at least two β-amylase genes are expressed during grain development, and that *HvBMY1* rather than *HvBMY2* is likely to be the most important *β-amylase* gene involved in germination (Vinje et al., 2011). Our RNAseq data and analysis of 11 *HvBMY* genes from the Sloop cultivar supports this finding (Table 4-S4). Moreover, many of the cultivar-specific differences in total and free β-amylase levels can be explained by cultivar-specific differences in the *HvBMY1* gene (Panozzo et al., 2007; Evans et al., 2008; Vinje et al., 2011; Gong et al., 2013). In the Chebec and Harrington cultivars, the *HvBMY1* locus on 4HL accounts for approximately 90.5% of the variation in free β-amylase levels (Li et al., 2002). Barley genotypes can be of the Sd1-type (Harrington; lower free β-amylase levels) or Sd2-type (Chebec; higher free β-amylase levels), and this is attributed to distinct amino acid substitutions in *HvBMY1*. In addition, differences in intron 3 of the *HvBMY1* gene, a possible site of cis-regulatory-elements, may contribute to differences in total β-amylase levels (Erkkila et al., 1998). Furthermore, results from an earlier study (Hara-Nishimura et al., 1986) suggest that grain desiccation may also impact free β-amylase levels, since it contributes to the process of β-amylase being bound to starch.

Based on the well-characterised function of β-amylase post-germination, is seems unlikely that different *HvBMY* genes or alleles contribute directly to differences in aleurone morphology during early grain development. Rather, we hypothesise that differences in aleurone development may be another factor that impacts free β-amylase levels at grain maturity. This hypothesis is supported by several findings. First, early studies indirectly suggested the presence of β-amylase enzyme in the aleurone layer (Tronier and Ory, 1970) and the sub-aleurone layer (Engel, 1947; Lauriere et al., 1986). Second, genes encoding β-amylase are transcribed in the aleurone. In the

Barke cultivar, *HvBMY1* is the most abundant gene family member expressed during grain development, and was detected in the aleurone and sub-aleurone by mRNA *in situ* hybridisation (Radchuk et al., 2009). In the same study, *HvBMY2* was detected at low levels in the endosperm, but was most abundant in the pericarp where it peaked at 6 DPA (Radchuk et al., 2009). Our results in Sloop wholegrain for *HvBMY1* and *HvBMY2* show a similar temporal pattern and relative abundance during grain development, indicating that *HvBMY1* transcript is highly abundant when the aleurone is forming. Third, studies in a number of temperate grasses including barley show that the aleurone is essentially free of starch granules (Hands et al., 2012), suggesting it may provide a starch-free repository for free β-amylase storage.

In the genotypes investigated here, approximately half (on average 45 ± 14%) of the total β-amylase appears in a free form at grain maturity. Based on the relative abundance of *HvBMY1* transcript in different grain compartments, it seems unlikely that all of the free β-amylase is derived solely from the aleurone. In the Sloop cultivar, laser microdissection qPCR revealed that *HvBMY1* is detected in the aleurone, outer starchy endosperm (incorporating the sub-aleurone) and inner starchy endosperm cells. At 11 DPA, when *HvBMY1* transcript levels are increasing in the grain, approximately 13% of transcript is derived from the aleurone. If all of this transcript is translated directly into β-amylase and remains unbound (free) due to the absence of starch, then the aleurone would contribute ~30% of the free β-amylase activity detected at grain maturity. Hence, variation in the amount of aleurone between cultivars could potentially contribute to the variation observed in free β-amylase activity, but it is clearly not the main determinant.

Several points need to be considered in future studies. It is currently unclear whether *HvBMY1* transcript abundance varies along the length of the barley grain, particularly

near the embryo, which may lead to an underestimation of aleurone *HvBMY1* levels. It is also possible that the relative abundance of aleurone *HvBMY1* transcript peaks at a time point that was not investigated here (for example 13 DPA where wholegrain *HvBMY1* levels peak), before they decrease at 25 DPA. Along these lines, it is unclear exactly when the differences in aleurone development are manifested in the examined genotypes. If the differences appear early, coinciding with the stage where *HvBMY1* transcript is most abundant, then this may have an impact on downstream *HvBMY1* levels. Finally, antibodies to β-amylase have been reported (Evans et al., 1997), but current microscopic assays that distinguish the different β-amylase forms are unavailable and need to be established. These would be useful tools in determining the location of the enzymes, assessing variation between genotypes of interest and determining the dynamics of enzyme release during seed development and germination.

Acknowledgements

We wish to thank the University of Adelaide Barley Breeding program for providing grain, Ray Sindel for assistance with the SeedCount and SKCS software, Shi-Fang Khor for advice regarding enzymatic assays, Geoff Fincher, Vincent Bulone and members of the Tucker laboratory for comments and suggestions. We also acknowledge the support of Gwen Mayo at Adelaide Microscopy for assistance with laser microdissection and Anna Koltunow at CSIRO for use of a UV polymerisation chamber. MA is supported by an Australian Government Research Training Program Scholarship, a Grains Research and Development Corporation (GRDC) Grains Research Scholarship (GRS10938) and the ARC Centre of Excellence in Plant Cell Walls (CE110001007). NB is supported through an ARC Linkage Project (LP130100600) with the Carlsberg Group. MRT is supported by an ARC Future Fellowship (FT140100780).

References

Aditya J, Lewis J, Shirley NJ, Tan HT, Henderson M, Fincher GB, Burton RA, Mather DE, Tucker MR (2015) The dynamics of cereal cyst nematode infection differ between susceptible and resistant barley cultivars and lead to changes in (1,3;1,4)-β-glucan levels and *HvCslF* gene transcript abundance. New Phytologist **207:** 135-147

Bamforth CW, Quain DE (1989) Enzymes in brewing and distilling. *In* PalmerGH, ed, Cereal science and technology, Ed 1st, UK : Aberdeen Univ. Press, pp 326–366

Becraft PW, Gutierrez-Marcos J (2012) Endosperm development: Dynamic processes and cellular innovations underlying sibling altruism. Wiley Interdisciplinary Reviews-Developmental Biology **1:** 579-593

Becraft PW, Stinard PS, McCarty DR (1996) CRINKLY4: A TNFR-like receptor kinase involved in maize epidermal differentiation. Science **273:** 1406-1409

Becraft PW, Yi G (2011) Regulation of aleurone development in cereal grains. Journal of Experimental Botany **62:** 1669-1675

Behall KM, Scholfield DJ, Hallfrisch J (2004) Diets containing barley significantly reduce lipids in mildly hypercholesterolemic men and women. American Journal of Clinical Nutrition **80:** 1185-1193

Betts NS, Wilkinson LG, Khor SF, Shirley NJ, Lok F, Skadhauge B, Burton RA, Fincher GB, Collins HM (2017) Morphology, carbohydrate distribution, gene expression, and enzymatic activities related to cell wall hydrolysis in four barley varieties during simulated malting. Frontiers in Plant Science **8:** 1-15

Brennan CS, Harris N, Smith D, Shewry PR (1996) Structural differences in the mature endosperms of good and poor malting barley cultivars. Journal of Cereal Science **24:** 171-177

Brown RC, Lemmon BE (2007) The developmental biology of cereal endosperm. *In* OA Olsen, ed, Plant Cell Monographs, Vol 8, pp 1-20

Burton RA, Fincher GB (2014) Evolution and development of cell walls in cereal grains. Frontiers in Plant Science **5:** 1-15

Chandra GS, Proudlove MO, Baxter ED (1999) The structure of barley endosperm - An important determinant of malt modification. Journal of the Science of Food and Agriculture **79:** 37-46

Drozdowicz YM, Jones RL (1995) Hormonal-regulation of organic and phosphoric-acid release by barley aleurone layers and scutella. Plant Physiology **108:** 769-776

Edney MJ, Rossnagel BG, Endo Y, Ozawa S, Brophy M (2002) Pearling quality of Canadian barley varieties and their potential use as rice extenders. Journal of Cereal Science **36:** 295-305

Engel C (1947) The distribution of the enzymes in resting cereals .1. The distribution of the saccharogenic amylase in wheat, rye and barley. Biochimica Et Biophysica Acta **1:** 42-49

Erkkila MJ, Leah R, Ahokas H, Cameron-Mills V (1998) Allele-dependent barley grain beta-amylase activity. Plant Physiology **117:** 679-685

Evans DE, Li CD, Eglinton JK (2008) Improved prediction of malt fermentability by measurement of the diastatic power enzymes beta-amylase, alpha-amylase, and limit dextrinase: I. Survey of the levels of diastatic power enzymes in commercial malts. Journal of the American Society of Brewing Chemists **66:** 223-232

Evans DE, MacLeod LC, Eglinton JK, Gibson CE, Zhang X, Wallace W, Skerritt JH, Lance RCM (1997) Measurement of β-amylase in malting barley (*Hordeum vulgare* L.) .1. Development of a quantitative ELISA for β-amylase. Journal of Cereal Science **26:** 229-239

Fath A, Bethke P, Lonsdale J, Meza-Romero R, Jones R (2000) Programmed cell death in cereal aleurone. Plant Molecular Biology **44:** 255-266

Fincher GB (1989) Molecular and cellular biology associated with endosperm mobilization in germinating cereal grains. Annual Review of Plant Physiology and Plant Molecular Biology **40:** 305-346

Gamel TH, Abdel-Aal E-SM (2012) Phenolic acids and antioxidant properties of barley wholegrain and pearling fractions. Agricultural and Food Science **21:** 118-131

Gong X, Westcott S, Zhang XQ, Yan GJ, Lance R, Zhang GP, Sun DF, Li CD (2013) Discovery of novel *Bmy1* alleles increasing β-amylase activity in Chinese landraces and Tibetan wild barley for improvement of malting quality via MAS. Plos One **8:** e72875

Greffeuille V, Abecassis J, Bar L'Helgouach C, Lullien-Pellerin V (2005) Differences in the aleurone layer fate between hard and soft common wheats at grain milling. Cereal Chemistry **82:** 138-143

Han C, Yang PF (2015) Studies on the molecular mechanisms of seed germination. Proteomics **15:** 1671-1679

Hands P, Kourmpetli S, Sharples D, Harris RG, Drea S (2012) Analysis of grain characters in temperate grasses reveals distinctive patterns of endosperm organization associated with grain shape. Journal of Experimental Botany **63:** 6253-6266

Hara-Nishimura I, Nishimura M, Daussant J (1986) Conversion of free β-amylase to bound β-amylase on starch granules in the barley endosperm during desiccation phase of seed development. Protoplasma **134:** 149-153

Hassan AS, Houston K, Lahnstein J, Shirley N, Schwerdt JG, Gidley MJ, Waugh R, Little A, Burton RA (2017) A genome wide association study of arabinoxylan content in 2-row spring barley grain. Plos One **12:** 1-19

Hrmova M, Fincher GB (2001) Structure-function relationships of β-D-glucan endo- and exohydrolases from higher plants. Plant Molecular Biology **47:** 73-91

Jestin L, Ravel C, Auroy S, Laubin B, Perretant M-R, Pont C, Charmet G (2008) Inheritance of the number and thickness of cell layers in barley aleurone tissue (*Hordeum vulgare* L.): an approach using F2-F3 progeny. Theoretical and Applied Genetics **116:** 991-1002

Jones RL (1973) Gibberellins - Their physiological role. Annual Review of Plant Physiology and Plant Molecular Biology **24:** 571-598

Knauer S, Holt AL, Rubio-Somoza I, Tucker EJ, Hinze A, Pisch M, Javelle M, Timmermans MC, Tucker MR, Laux T (2013) A protodermal miR394 signal defines a region of stem cell competence in the *Arabidopsis* shoot meristem. Developmental Cell **24:** 125-132

Lauriere C, Lauriere M, Daussant J (1986) Immunohistochemical localization of β-amylase in resting barley seeds. Physiologia Plantarum **67:** 383-388

Lauro M, Suortti T, Autio K, Linko P, Poutanen K (1993) Accessibility of barley starch granules to α-amylase during different phases of gelatinization. Journal of Cereal Science **17:** 125-136

Lewis MJ, Young TW (1995) Mashing Biochemistry. *In* Brewing, Ed 1st Vol 106, UK : Chapman & Hall, p 19

Li CD, Langridge P, Zhang XQ, Eckstein PE, Rossnagel BG, Lance RCM, Lefol EB, Lu MY, Harvey BL, Scoles GJ (2002) Mapping of barley (*Hordeum vulgare*

L.) β-amylase alleles in which an amino acid substitution determines β-amylase isoenzyme type and the level of free β-amylase. Journal of Cereal Science **35:** 39-50

Lid SE, Gruis D, Jung R, Lorentzen JA, Ananiev E, Chamberlin M, Niu XM, Meeley R, Nichols S, Olsen OA (2002) The *defective kernel 1* (*dek1*) gene required for aleurone cell development in the endosperm of maize grains encodes a membrane protein of the calpain gene superfamily. Proceedings of the National Academy of Sciences of the United States of America **99:** 5460-5465

Mascher M, Gundlach H, Himmelbach A, Beier S, Twardziok SO, Wicker T, Radchuk V, Dockter C, Hedley PE, Russell J, Bayer M, Ramsay L, Liu H, Haberer G, Zhang XQ, Zhang QS, Barrero RA, Li L, Taudien S, Groth M, Felder M, Hastie A, Simkova H, Stankova H, Vrana J, Chan S, Munoz-Amatrian M, Ounit R, Wanamaker S, Bolser D, Colmsee C, Schmutzer T, Aliyeva-Schnorr L, Grasso S, Tanskanen J, Chailyan A, Sampath D, Heavens D, Clissold L, Cao SJ, Chapman B, Dai F, Han Y, Li H, Li X, Lin CY, McCooke JK, Tan C, Wang PH, Wang SB, Yin SY, Zhou GF, Poland JA, Bellgard MI, Borisjuk L, Houben A, Dolezel J, Ayling S, Lonardi S, Kersey P, Lagridge P, Muehlbauer GJ, Clark MD, Caccamo M, Schulman AH, Mayer KFX, Platzer M, Close TJ, Scholz U, Hansson M, Zhang GP, Braumann I, Spannagl M, Li CD, Waugh R, Stein N (2017) A chromosome conformation capture ordered sequence of the barley genome. Nature **544:** 426-433

Mayer KFX, Waugh R, Langridge P, Close TJ, Wise RP, Graner A, Matsumoto T, Sato K, Schulman A, Muehlbauer GJ, Stein N, Ariyadasa R, Schulte D, Poursarebani N, Zhou RN, Steuernagel B, Mascher M, Scholz U, Shi BJ, Langridge P, Madishetty K, Svensson JT, Bhat P, Moscou M, Resnik J, Close TJ, Muehlbauer GJ, Hedley P, Liu H, Morris J, Waugh R, Frenkel Z, Korol A, Berges H, Graner A, Stein N, Steuernagel B, Taudien S, Groth M, Felder M, Lonardi S, Duma D, Alpert M, Cordero F, Beccuti M, Ciardo G, Ma Y, Wanamaker S, Stein N, Close TJ, Platzer M, Brown JWS, Schulman A, Platzer M, Fincher GB, Muehlbauer GJ, Sato K, Taudien S, Sampath D, Swarbreck D, Scalabrin S, Zuccolo A, Vendramin V, Morgante M, Schulman A, Int Barley Genome Sequencing C (2012) A physical, genetic and functional sequence assembly of the barley genome. Nature **491:** 711-716

McCleary BV, Codd R (1989) Measurement of β-amylase in cereal flours and commercial enzyme preparations. Journal of Cereal Science **9:** 17-33

McCleary BV, McNally M, Monaghan D, Mugford DC, Black C, Broadbent R, Chin M, Cormack M, Fox R, Gaines C, Gothard P, Home S, Howes E, Johnson C, Keeping R, Koliatsou M, Lindhauer M, de Sa RM, Martin R, Monaghan D, Nees U, Nishwitz R, Palmer G, Panozzo J, Recabarren J, Roumeliotis S, Seddig S, Solah V, Sonnet M, Themeier H (2002) Measurement of α-amylase activity in white wheat flour, milled malt, and microbial enzyme preparations, using the ceralpha assay: Collaborative study. Journal of Aoac International **85:** 1096-1102

McCleary BV, Shameer I (1987) Assay of malt β-glucanase using azo-barley glucan: An improved precipitant. Journal of the Institute of Brewing **93:** 87-90

Nair S, Knoblauch M, Ullrich S, Baik BK (2011) Microstructure of hard and soft kernels of barley. Journal of Cereal Science **54:** 354-362

Newman CW, Newman RK (2006) A brief history of barley foods. Cereal Foods World **51:** 4-7

Nordkvist E, Salomonsson AC, Aman P (1984) Distribution of insoluble bound phenolic acids in barley grain. Journal of the Science of Food and Agriculture **35:** 657-661

Okada T, Hu YK, Tucker MR, Taylor JM, Johnson SD, Spriggs A, Tsuchiya T, Oelkers K, Rodrigues JCM, Koltunow AMG (2013) Enlarging cells initiating apomixis in *Hieracium praealtum* transition to an embryo sac program prior to entering mitosis. Plant Physiology **163:** 216-231

Olsen LT, Divon HH, Al R, Fosnes K, Lid SE, Opsahl-Sorteberg HG (2008) The *defective seed5* (*des5*) mutant: effects on barley seed development and *HvDek1*, *HvCr4*, and *HvSal1* gene regulation. Journal of Experimental Botany **59:** 3753-3765

Panozzo JF, Eckermann PJ, Mather DE, Moody DB, Black CK, Collins HM, Barr AR, Lim P, Cullis BR (2007) QTL analysis of malting quality traits in two barley populations. Australian Journal of Agricultural Research **58:** 858-866

Pasha I, Anjum FM, Morris CF (2010) Grain hardness: A major determinant of wheat quality. Food Science and Technology International **16:** 511-522

Pins JJ, Kaur H (2006) A review of the effects of barley β-glucan on cardiovascular and diabetic risk. Cereal Foods World **51:** 8-11

Pins JJ, Kaur H (2006) A review of the effects of barley β-glucan on cardiovascular and diabetic risk. Cereal Foods World **51:** 8-11

Psota V, Vejrazka K, Famera O, Hrcka M (2007) Relationship between grain hardness and malting quality of barley (*Hordeum vulgare* L.). Journal of the Institute of Brewing **113:** 80-86

Radchuk VV, Borisjuk L, Sreenivasulu N, Merx K, Mock HP, Rolletschek H, Wobus U, Weschke W (2009) Spatiotemporal profiling of starch biosynthesis and degradation in the developing barley grain. Plant Physiology **150:** 190-204

Sato K, Flavell A, Russell J, Börner A, Valkoun J (2014) Genetic diversity and germplasm management: Wild barley, landraces, breeding materials. *In* J Kumlehn, N Stein, eds, Biotechnological Approaches to Barley Improvement Vol 69. Springer Berlin Heidelberg, pp 21-36

Shapter FM, Dawes MP, Lee LS, Henry RJ (2009) Aleurone and subaleurone morphology in native Australian wild cereal relatives. Australian Journal of Botany **57:** 688-696

Shen B, Li CJ, Min Z, Meeley RB, Tarczynski MC, Olsen OA (2003) *sal1* determines the number of aleurone cell layers in maize endosperm and encodes a class E vacuolar sorting protein. Proceedings of the National Academy of Sciences of the United States of America **100:** 6552-6557

Sopanen T, Lauriere C (1989) Release and activity of bound β-amylase in a germinating barley grain. Plant Physiology **89:** 244-249

Sreenivasulu N, Radchuk V, Strickert M, Miersch O, Weschke W, Wobus U (2006) Gene expression patterns reveal tissue-specific signaling networks controlling programmed cell death and ABA-regulated maturation in developing barley seeds. Plant Journal **47:** 310-327

Symes KJ (1969) Influence of a gene causing hardness on the milling and baking quality of two wheats. Australian Journal of Agricultural Research **20:** 971-979

Thiel J, Weier D, Weschke W (2011) Laser-capture microdissection of developing barley seeds and cDNA array analysis of selected tissues. Methods Mol Biol **755:** 461-475

Tian Q, Olsen L, Sun B, Lid SE, Brown RC, Lemmon BE, Fosnes K, Gruis DF, Opsahl-Sorteberg HG, Otegui MS, Olsen OA (2007) Subcellular localization and functional domain studies of DEFECTIVE KERNEL1 in maize and

Arabidopsis suggest a model for aleurone cell fate specification involving CRINKLY4 and SUPERNUMERARY ALEURONE LAYER1. Plant Cell **19:** 3127-3145

Tronier B, Ory RL (1970) Association of bound β-amylase with protein bodies in barley. Cereal Chemistry **47:** 464-471

Tucker MR, Okada T, Hu YK, Scholefield A, Taylor JM, Koltunow AMG (2012) Somatic small RNA pathways promote the mitotic events of megagametogenesis during female reproductive development in *Arabidopsis*. Development **139:** 1399-1404

Vinje MA, Willis DK, Duke SH, Henson CA (2011) Differential expression of two beta-amylase genes (*Bmy1* and *Bmy2*) in developing and mature barley grain. Planta **233**

Vinje MA, Willis DK, Duke SH, Henson CA (2011) Differential RNA expression of *Bmy1* during barley seed development and the association with beta-amylase accumulation, activity, and total protein. Plant Physiology and Biochemistry **49:** 39-45

Wilkinson LG, Tucker MR (2017) An optimised clearing protocol for the quantitative assessment of sub-epidermal ovule tissues within whole cereal pistils. Plant Methods **13:** 67-77

Williams PC (1967) Relation of starch damage and related characteristics to kernel hardness in Australian wheat varieties. Cereal Chemistry **44:** 383-390

Wilson SM, Burton RA, Collins HM, Doblin MS, Pettolino FA, Shirley N, Fincher GB, Bacic A (2012) Pattern of deposition of cell wall polysaccharides and transcript abundance of related cell wall synthesis genes during differentiation in barley endosperm. Plant Physiology **159:** 655-670

Yan D, Duermeyer L, Leoveanu C, Nambara E (2014) The functions of the endosperm during seed germination. Plant and Cell Physiology **55:** 1521-1533

Yi G, Neelakandan AK, Gontarek BC, Vollbrecht E, Becraft PW (2015) The *naked endosperm* genes encode duplicate INDETERMINATE domain transcription factors required for maize endosperm cell patterning and differentiation. Plant physiology **167:** 443-456

Yin C, Zhang GP, Wang JM, Chen JX (2002) Variation of β-amylase activity in barley as affected by cultivar and environment and its relation to protein content and grain weight. Journal of Cereal Science **36:** 307-312

Zhang H, Dou WJ, C-X., Wei Z-J, Liu J, Jones RL (2010) Hydrogen sulfide stimulates beta-amylase activity during early stages of wheat grain germination. Plant Signal Behav **5:** 1031-1033

Zhang RX, Tucker MR, Burton RA, Shirley NJ, Little A, Morris J, Milne L, Houston K, Hedley PE, Waugh R, Fincher GB (2016) The dynamics of transcript abundance during cellularization of developing barley endosperm. Plant Physiology **170:** 1549-1565

Zhou MX, Li HB, Chen ZH, Mendham NJ (2008) Combining ability of barley flour pasting properties. Journal of Cereal Science **48:** 789-793

Zohary D, Hopf M, Weiss E (2012) Domestication of plants in the old world, Ed 4th, Oxford University Press, Oxford, UK

Figures

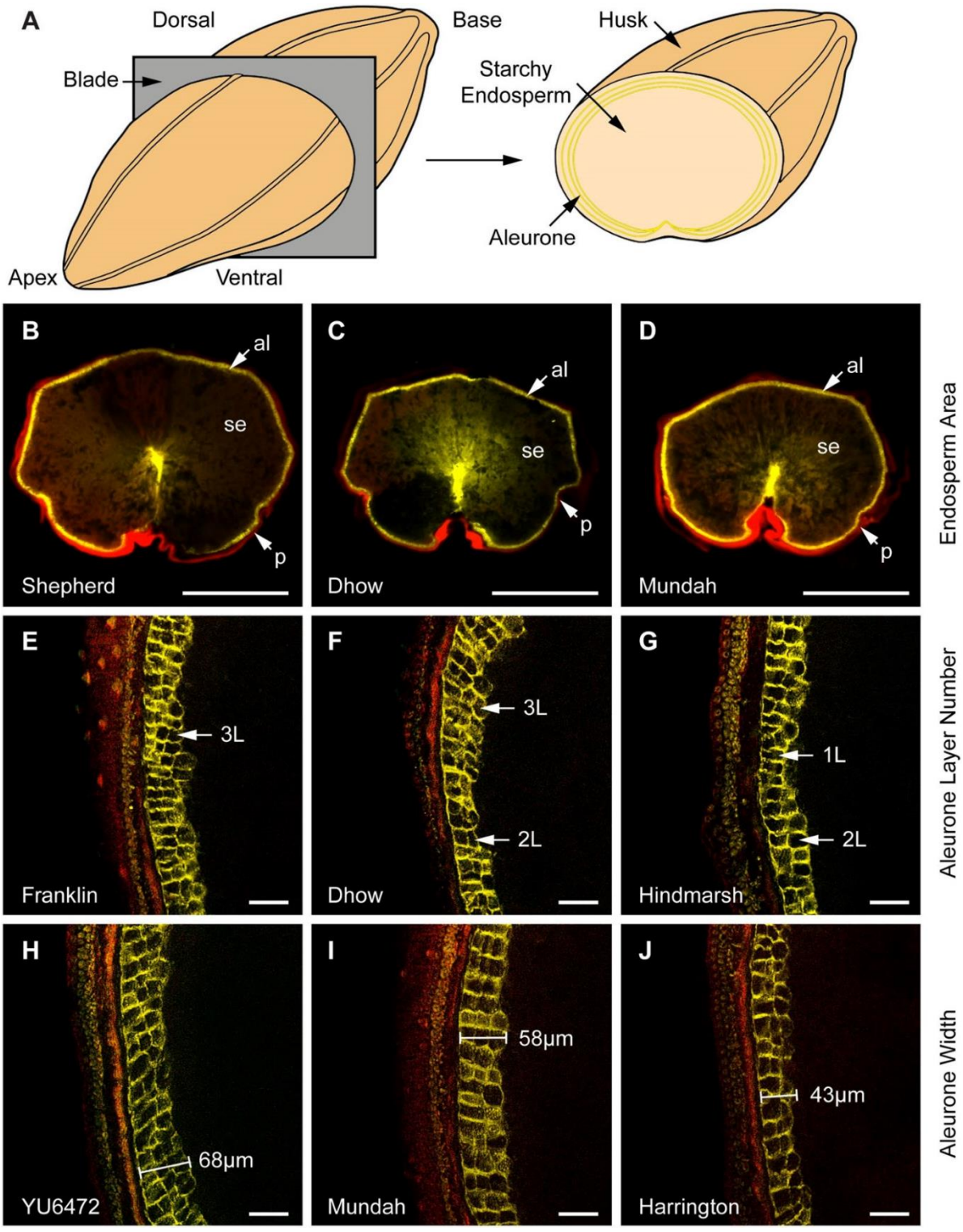

Figure 4-1. Representation of the transverse sectioning process used to image barley aleurone tissue by fluorescent microscopy. (A) Schematic representation of barley grain sectioning prior to microscopy. The different tissue layers are indicated. (B–D) Wholegrain transverse sections viewed at 1× magnification using Zeiss Filter sets 46

(false-coloured red) and 49 (DAPI; false-coloured yellow). The panels show grain exhibiting differences in transverse starchy endosperm area in decreasing order. The pericarp/husk (p), starchy endosperm (se) and aleurone (al) tissues are indicated. Scale bar = 1 mm. (E–G) Magnified views of the aleurone layers at 20× magnification using a Zeiss Apotome.2. Panels are arranged in decreasing order based on the average number of aleurone layers. Stacks of 3, 2 and 1 aleurone cell layers (L) are indicated. Scale bar = 50 µm. (H–J) Examples of grain showing differences in aleurone width at 20× magnification, arranged in decreasing order. Scale bar = 50 µm. Genotype names are indicated in each panel.

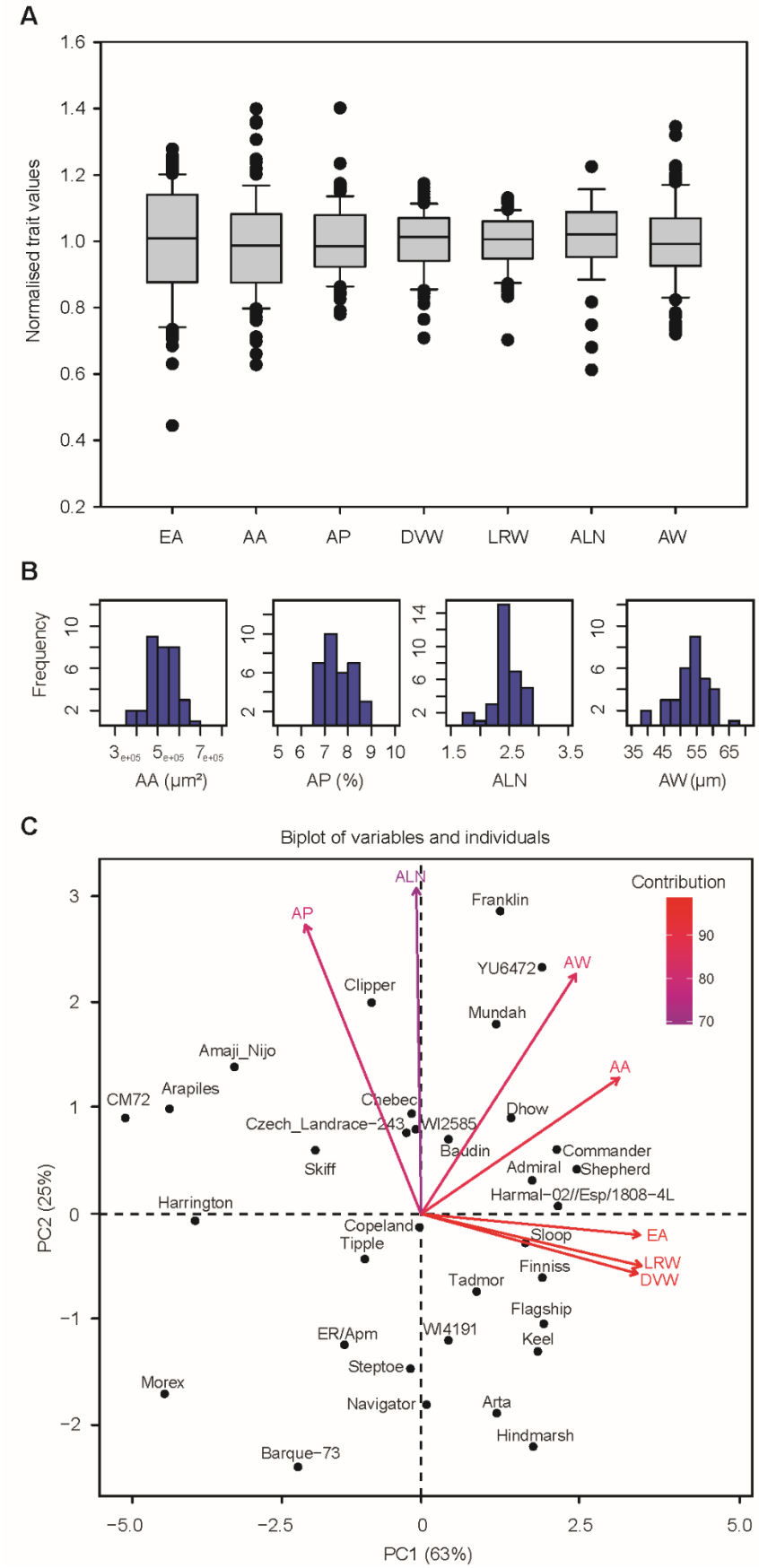
A
Normalised trait values
1.6
1.4
1.2
1.0
0.8
0.6
0.4
0.2
EA
AA
AP
DVW
LRW
ALN
AW
B
Frequency
AA (µm²)
AP (%)
ALN
AW (µm)
C
Biplot of variables and individuals
Contribution
90
80
70
ALN
AP
AW
AA
EA
LRW
DVW
Franklin
YU6472
Clipper
Mundah
Amaji_Nijo
Arapiles
CM72
Chebec
Czech_Landrace−243
WI2585
Dhow
Baudin
Commander
Admiral
Shepherd
Skiff
Harrington
Harmal−02//Esp/1808−4L
Copeland
Tipple
Sloop
Finniss
Tadmor
Flagship
ER/Apm
WI4191
Keel
Steptoe
Morex
Navigator
Arta
Hindmarsh
Barque−73
PC2 (25%)
PC1 (63%)

Figure 4-2. Variation in transverse grain measurements observed across 33 barley genotypes. (A) Box plot of normalised data showing the variation in different grain measurements. (B) Frequency distribution plots of the four aleurone measurements. (C) Principal Component Analysis separates the genotypes based on the seven transverse measurements (variables). EA, endosperm area; AA, aleurone area; AP, aleurone proportion; DVW, grain dorsal-ventral distance; LRW, transverse grain left-right width; ALN, aleurone layer number; AW, aleurone width.

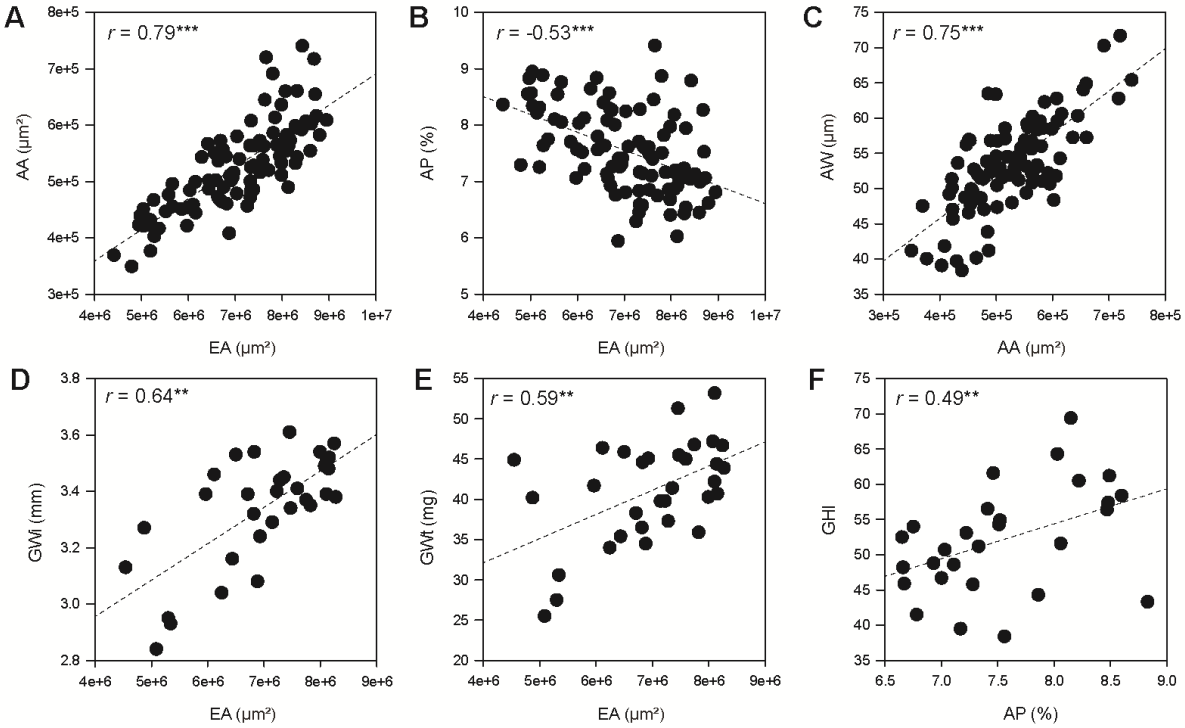

Figure 4-3. Transverse and wholegrain trait correlations across different barley genotypes. (A–C) Phenotypic measurements from all grain samples for 33 genotypes obtained using transverse grain sections. (A) Aleurone area vs endosperm area. (B) Aleurone proportion vs endosperm area. (C) Aleurone width vs aleurone area. (D–F) Correlations between grain measurements (averages) for all 2-row genotypes (n = 30) using the SeedCount, Single Kernel Characterisation System and/or transverse grain sections. (D) Grain width vs endosperm area. (E) Grain weight vs endosperm area. (F) Grain hardness index vs aleurone proportion. EA, Endosperm area; AA, aleurone area; AP, aleurone proportion; AW, aleurone width; GWi, grain width; GWt, grain weight. Significance indicators: ***p ≤ 0.001, **p ≤ 0.01, *p ≤ 0.05.

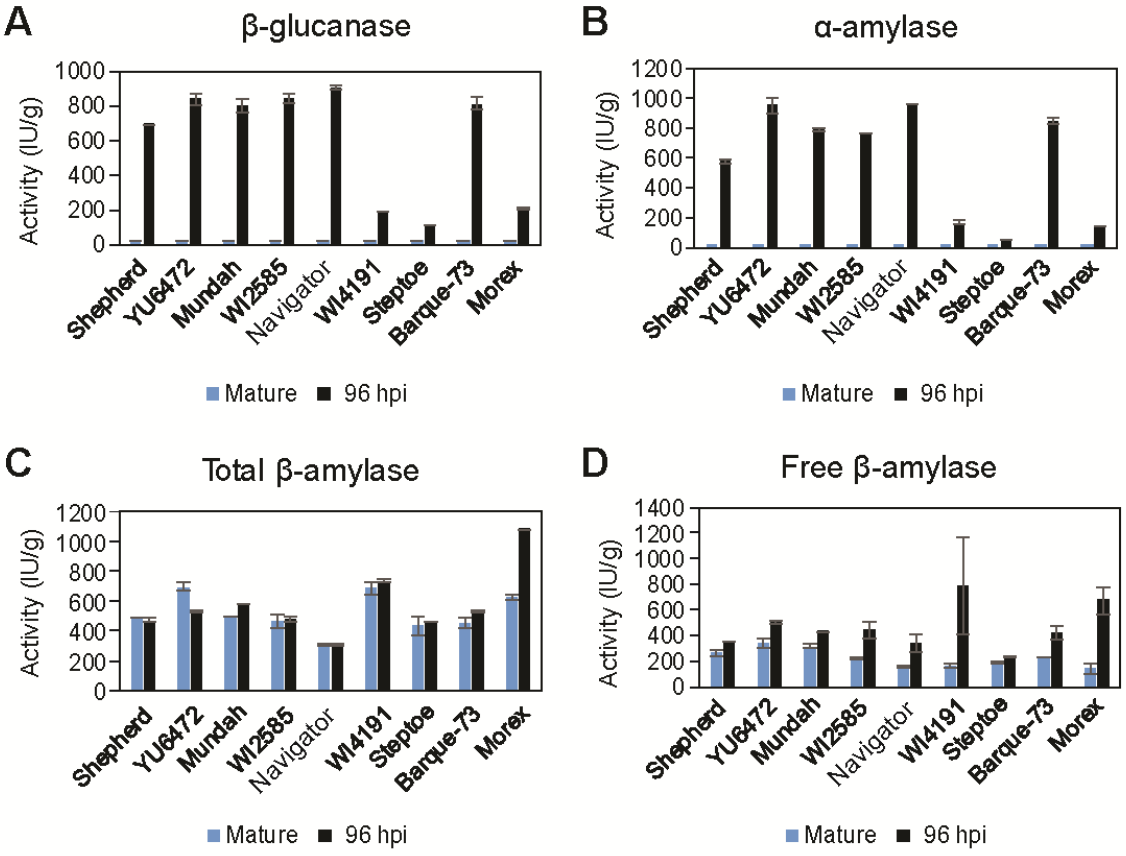

E

	EA	AA	AP	AW	ALN	β-glucanase (MG)	β-glucanase (96 hpi)	α-amylase (MG)	α-amylase (96 hpi)	Total β-amylase (MG)	Total β-amylase (96 hpi)	Free β-amylase (MG)
AA	0.90											
AP	0.45	0.80										
AW	0.80	0.85	0.68									
ALN	0.34	0.31		0.54								
β-glucanase (MG)	−0.34		0.38									
β-glucanase (96 hpi)	0.34	0.40	0.43	0.43								
α-amylase (MG)	−0.54	−0.39			0.30	0.30	−0.61					
α-amylase (96 hpi)	0.30	0.36	0.40	0.43			0.98	−0.61				
Total β-amylase (MG)							−0.38	0.66	−0.32			
Total β-amylase (96 hpi)	−0.63	−0.44		−0.41		0.56	−0.58	0.83	−0.57	0.66		
Free β-amylase (MG)	0.55	0.77	0.87	0.86	0.30		0.57		0.57		−0.32	
Free β-amylase (96 hpi)	−0.34	−0.32					−0.36	0.61	−0.31	0.78	0.76	

−1 −0.8 −0.6 −0.4 −0.2 0 0.2 0.4 0.6 0.8 1

Figure 4-4. Hydrolytic enzyme activities in grain from nine barley genotypes at grain maturity and 96 hours post imbibition (hpi). (A) 1,3;1,4-β-glucanase (β-glucanase) activity. (B) α-amylase activity. (C) Total β-amylase activity. (D) Free β-amylase activity. Error bars show standard deviation. (E) Heat map representing correlations between aleurone measurements and enzyme activities for the nine different genotypes. Note, some aleurone correlation values differ to those in Fig. S5 due to the different sample size. Blue boxes indicate positive correlations. Numbers within boxes represent correlation coefficient (r) values. All values > 0.3 or < −0.3 are shown, but only those with a p-value ≤ 0.05 are contained within shaded boxes. MG, mature grain; EA, endosperm area; AA, aleurone area; AP, aleurone proportion; AW, aleurone width; ALN, aleurone layer number.

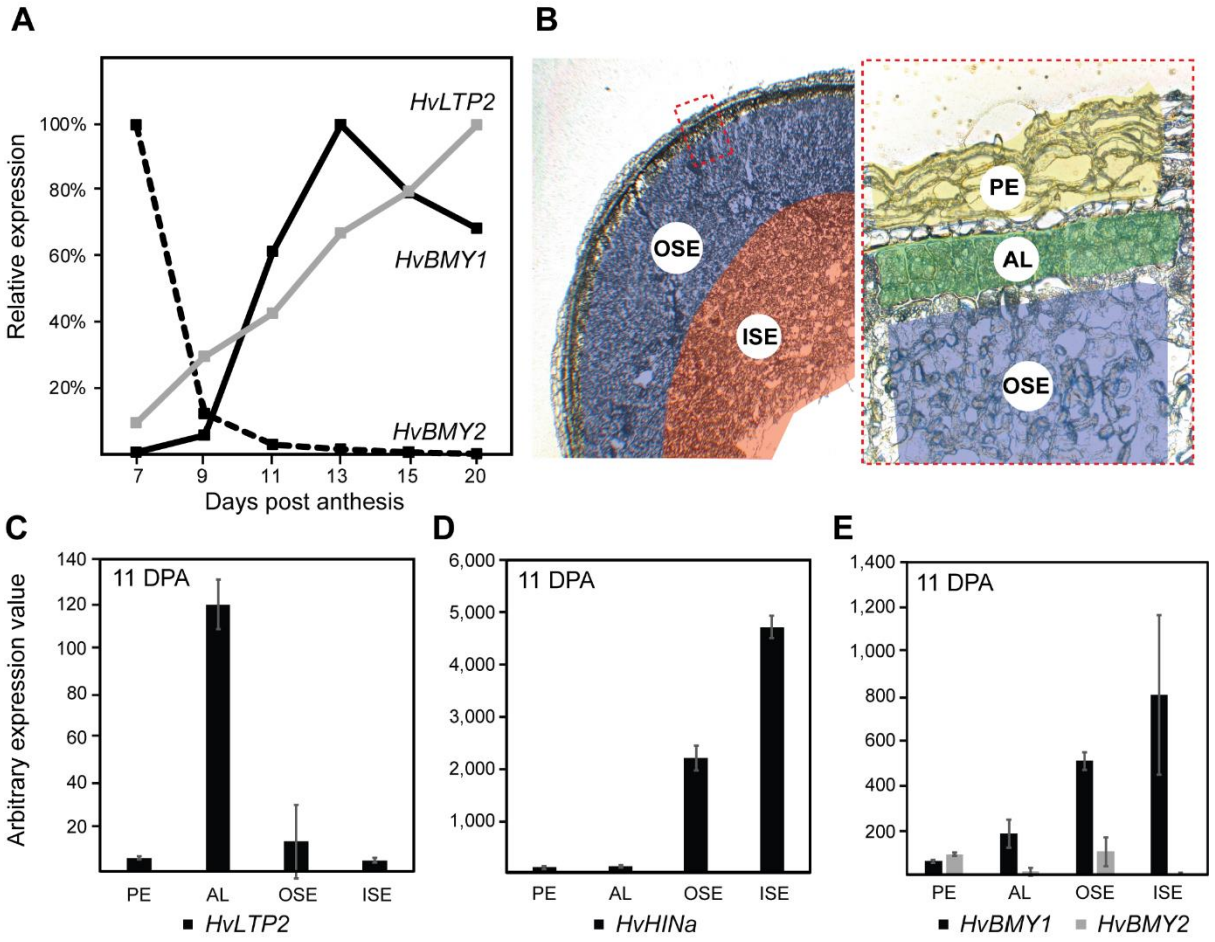

Figure 4-5. Accumulation of transcript in different barley grain tissues. (A) RNAseq analysis of transcripts from Sloop wholegrain samples, minus embryo, at 7, 9, 11, 13, 15, 20 days post anthesis (DPA). Accumulation patterns for the *HvBMY1*, *HvBMY2* and *HvLTP2* transcripts are shown, normalised to the maximum expression value for each gene. (B) Thin butyl-methyl methacrylate sections of Sloop barley grain at 11 DPA showing the regions collected by laser microdissection. PE, pericarp; AL, aleurone; OSE, outer starchy endosperm including sub-aleurone; ISE, inner starchy endosperm. The red dashed box shows a magnified view of the outer grain layers. (C–E) Quantitative PCR analysis of transcript abundance in RNA collected from laser micro dissected material. (C) *lipid transfer protein 2* (*HvLTP2*). (D) *hordoinoline a* (*HvHINa*) (E) *β-amylase 1* (*HvBMY1*) and *β-amylase 2* (*HvBMY2*).

Supplementary Figures

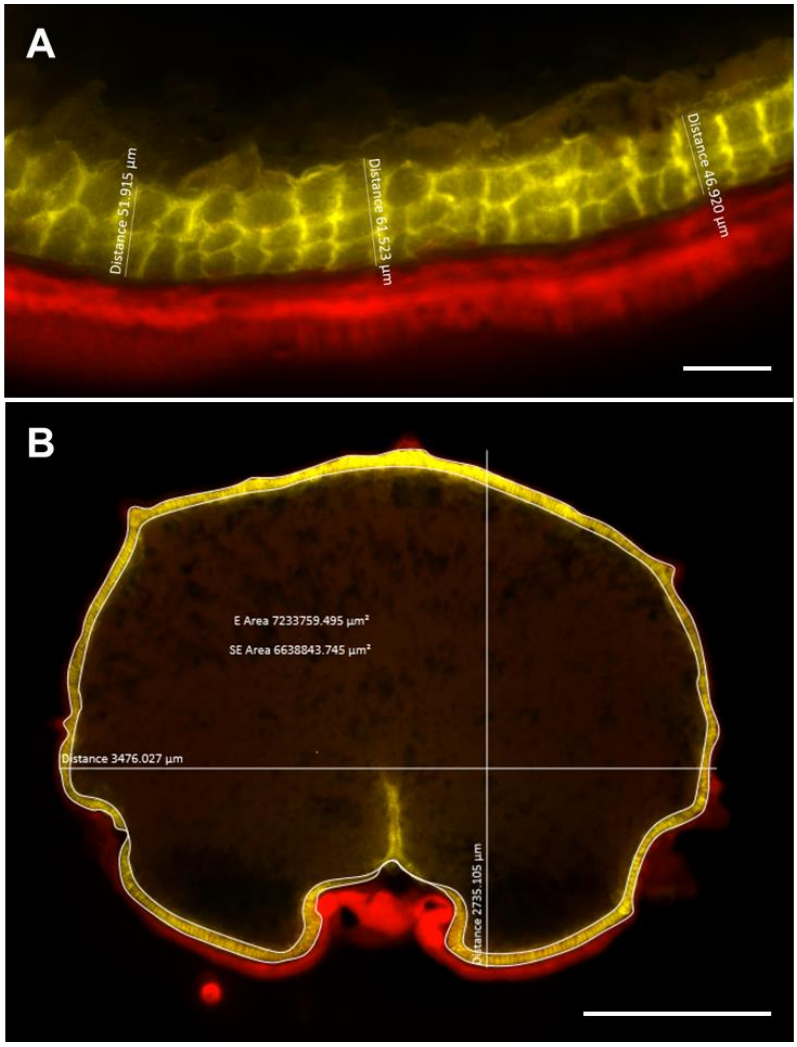

Figure 4-S1: Transverse grain measurements were recorded using ZEN 2012 software. Grain were prepared as shown in Fig. 1. (A) Image at 20× magnification showing aleurone thickness (width) measurements. (B) Image at 1× magnification showing transverse grain measurements such as endosperm (E) area, starchy endosperm (se) area, grain thickness and grain width. Scale bar = 50 µm in A and 1mm in B.

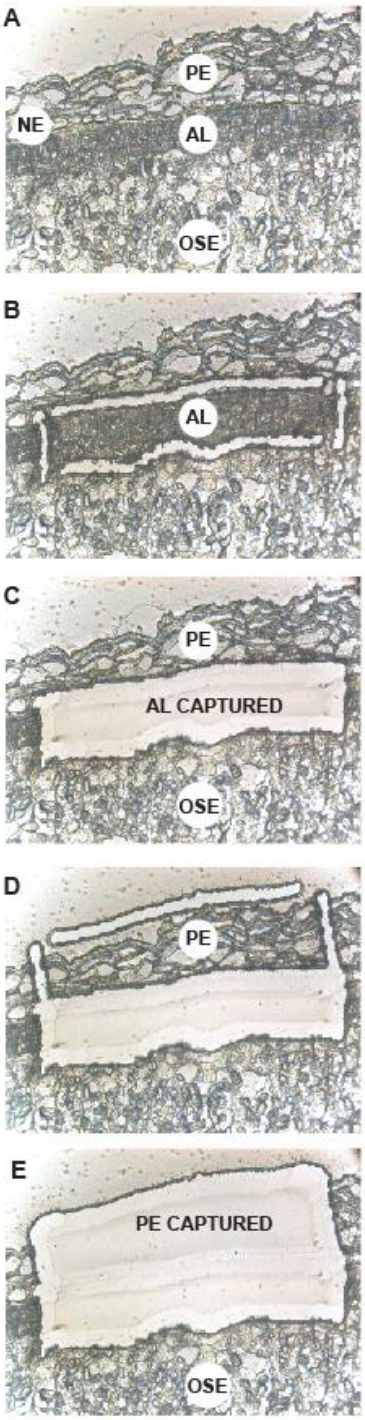

Figure 4-S2: Barley grain tissues harvested by laser microdissection. A 25 DPA grain sample is shown. (A) A butyl-methyl methacrylate (BMM) section (5 µm) showing the outer layers of the grain prior to dissection. PE, pericarp; NE, nucellar epidermis; AL, aleurone; OSE, outer starchy endosperm including the sub-aleurone. (B-C) Laser ablation of cells directly adjoining the aleurone prior to capture. (D-E) Collection of the outer maternal grain layers.

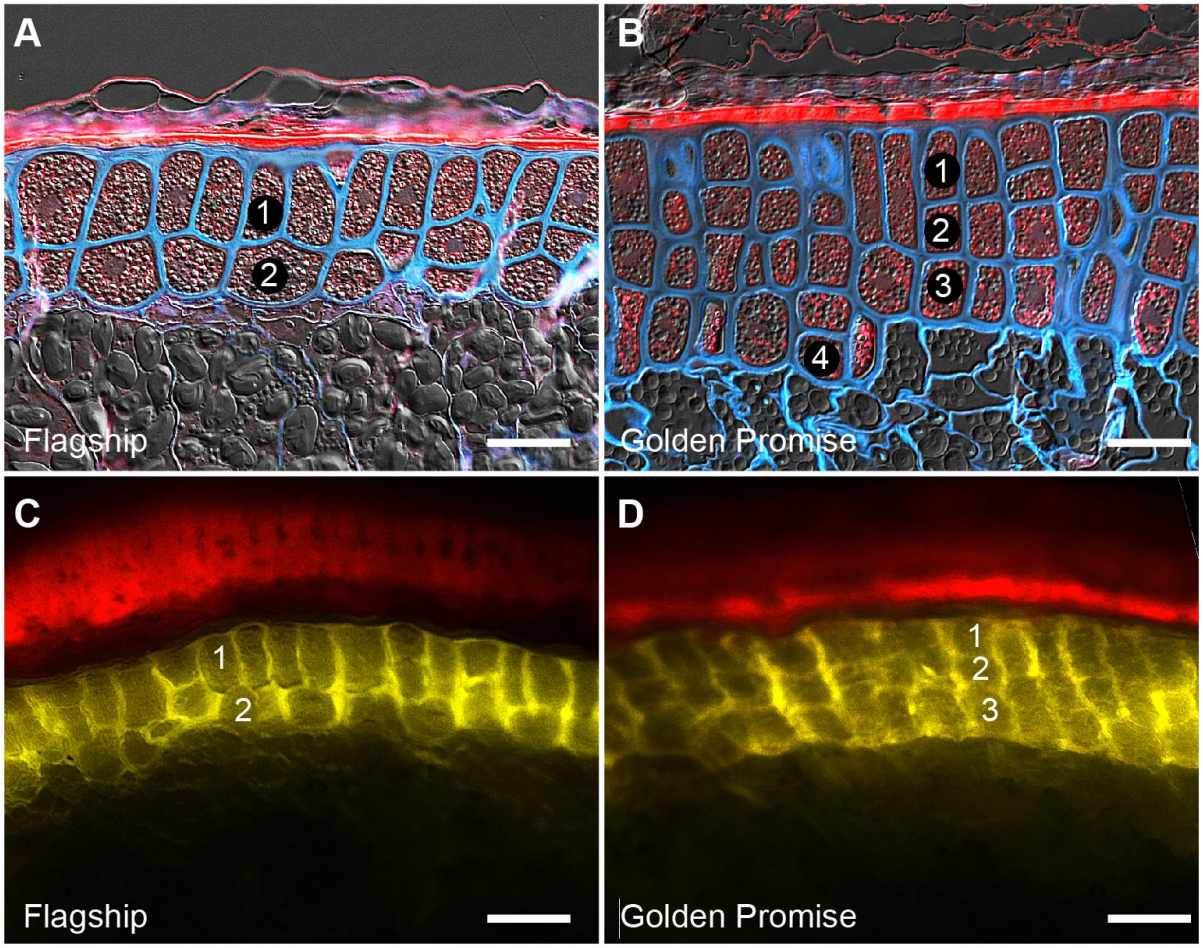

Figure 4-S3: Comparison of sectioning methods for the investigation of mature barley aleurone morphology. (A-B) Thin 1 µm sections of mature grain from Flagship and Golden Promise cultivars stained with Calcofluor White (blue). The pericarp and aleurone grains show autofluorescence using Zeiss Filter set 46 (false-coloured red). The aleurone in Flagship contains 2-3 cell layers, while the aleurone in Golden Promise contains 3-4 aleurone layers. (C-D) Hand sections of barley grain from the same cultivars shown in (A-B). The pericarp is detected using Zeiss Filter set 46 (false-coloured red) and the aleurone is detected using Filter Set 49 (DAPI; false-coloured yellow). The aleurone layer number detected by thin sectioning (shown in A and B) is the same as that detected by hand sectioning without staining. Scale bar = 50 µm in A and B, 60 µm in C and D.

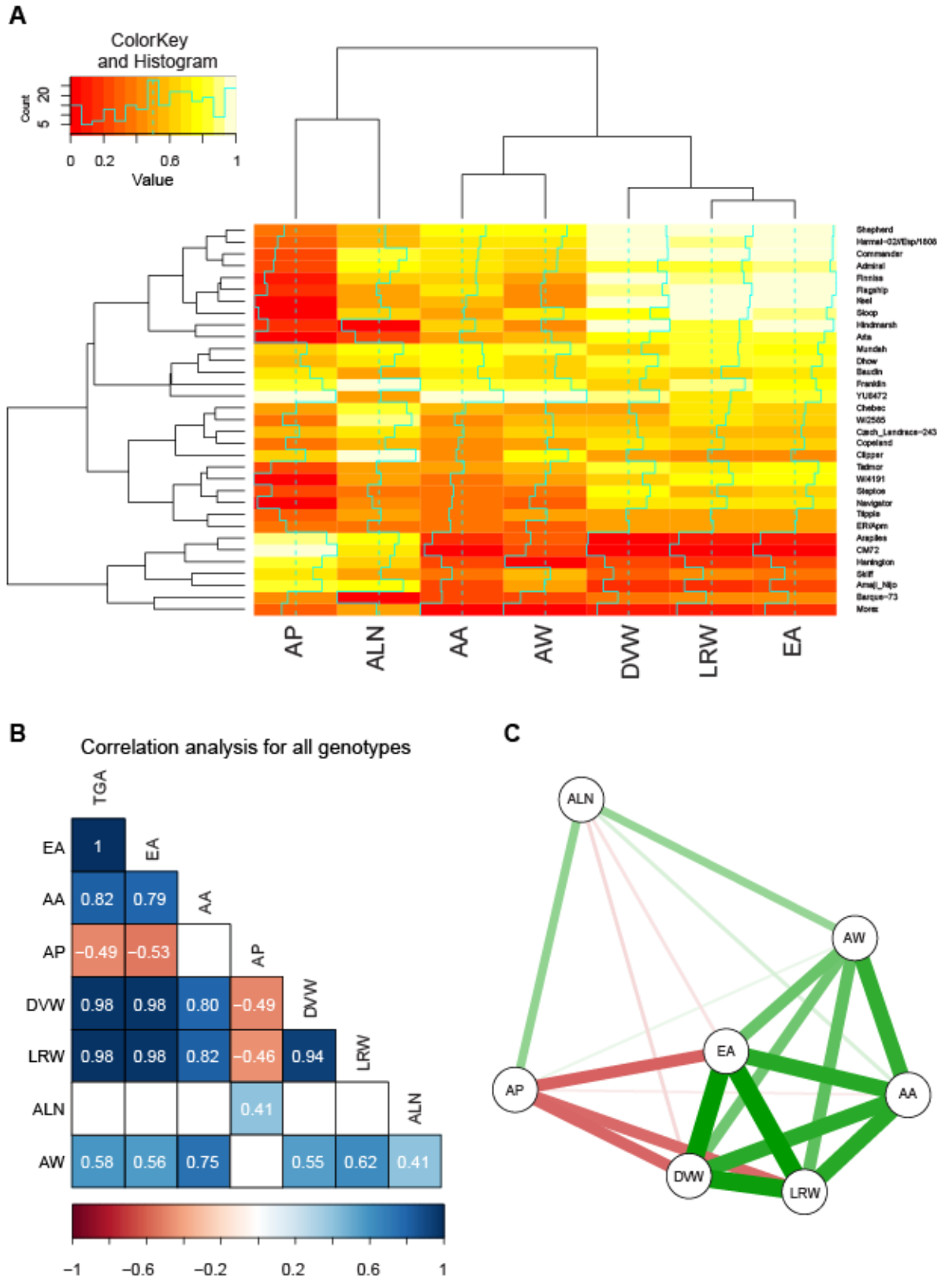

Figure 4-S4: Relationships between transverse grain measurements in a panel of 33 barley genotypes. (A) Heatmap showing clusters of different genotypes separated based on the seven different grain measurements. Trait values are normalised to a

value between 0 and 1 and the blue line indicates the ranking of each genotype for each measurement. (B) Heatmap representing correlations between transverse grain measurements for 33 barley genotypes. Blue boxes indicate positive correlations and red boxes indicate negative correlations. Numbers within boxes represent correlation coefficient (r) values and only those correlations with a p-value ≤ 0.05 are shown. TGA, transverse grain area; EA, starchy endosperm area; AA, aleurone area; AP, aleurone proportion; DVW, grain dorsal-ventral width; LRW, grain left-right width; ALN, aleurone layer number; AW, aleurone width. (C) Network analysis of the transverse grain measurements according to correlations shown in B. Line thickness provides an indication of the strength of correlation, with green indicating a positive correlation and red indicating a negative correlation.

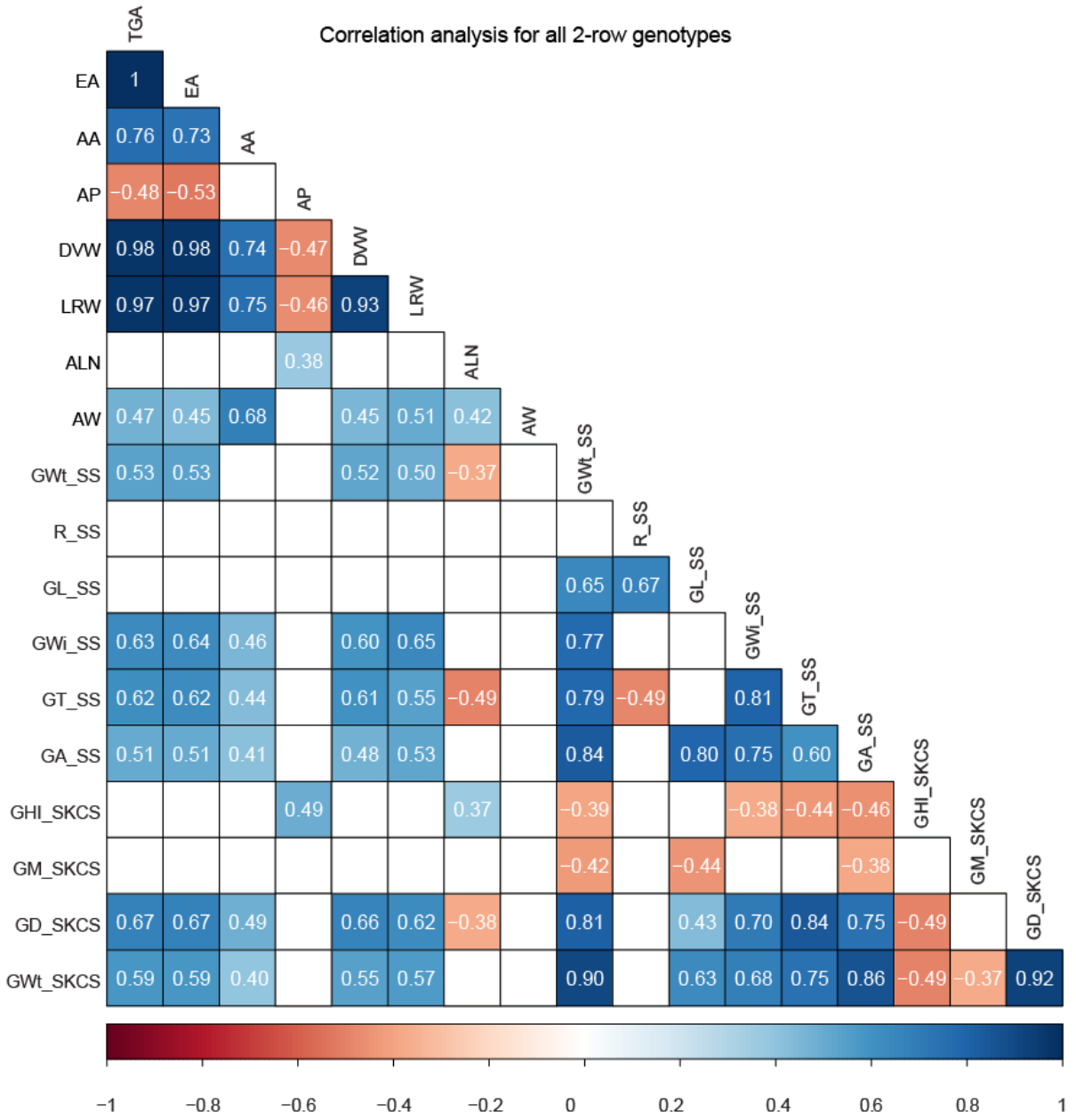

Figure 4-S5: Correlations between aleurone and wholegrain measurements for the 30 2-row barley genotypes. Blue boxes indicate positive correlations and red boxes indicate negative correlations. Numbers within boxes represent correlation coefficient (r) values and only those correlations with a p-value ≤ 0.05 are shown. TGA, transverse grain area; EA, starchy endosperm area; AA, aleurone area; AP, aleurone proportion; DVW, grain dorsal-ventral width; LRW, grain left-right width; ALN, aleurone layer number; AW, aleurone width; GWt, grain weight; R, grain roundness; GL, grain length; GWi, grain width; GT, grain thickness; GA, grain area; GHI, grain hardness index; GM,

grain moisture; GD, grain diameter; SS, seed scanner; SKCS, single kernel characterisation system.

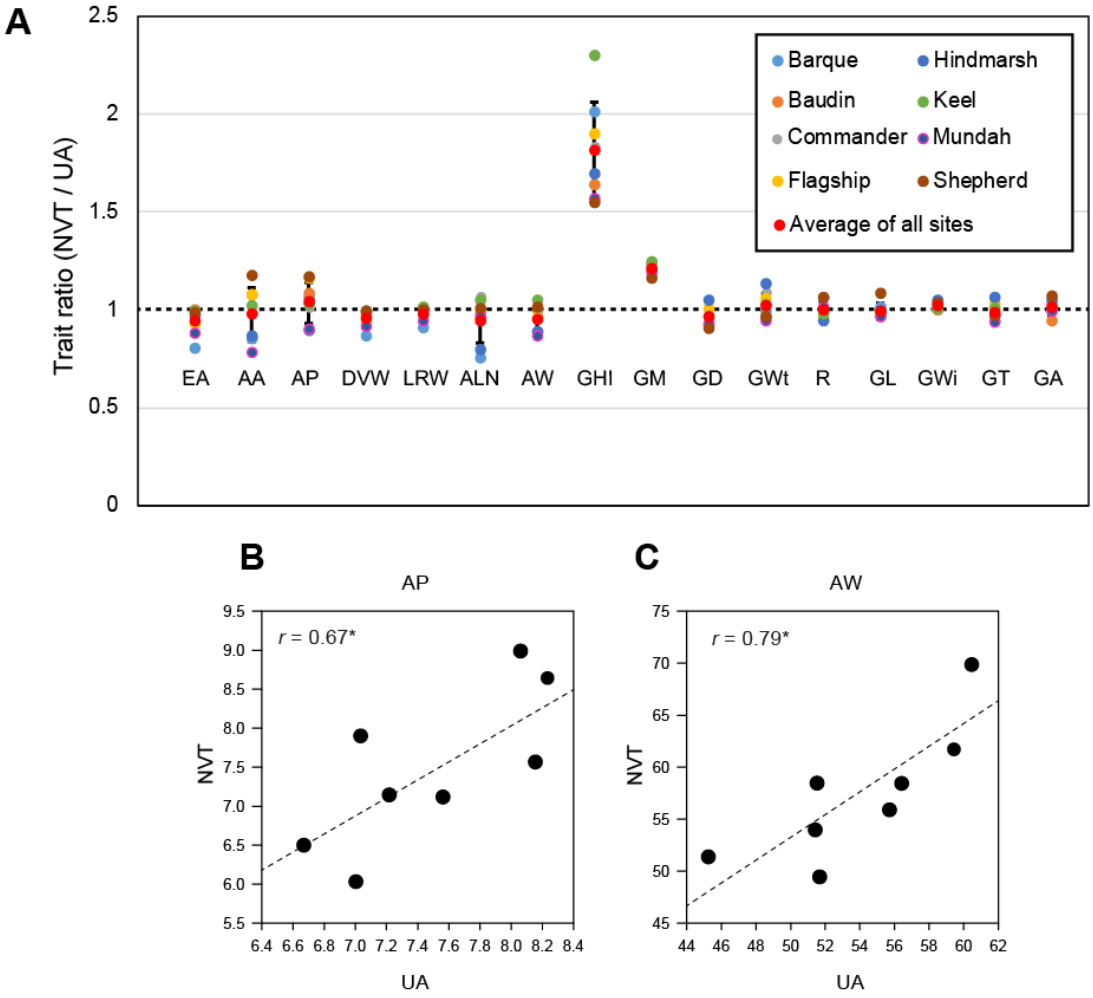

Figure 4-S6: Comparison of grain measurements for eight barley genotypes grown in field sites at Charlick SA (2013) and Goologong NSW (2015). (A) The Goologong samples formed part of the National Variety Trials (NVT) and measurements are shown as a proportion of the University of Adelaide panel (UA) value for each genotype. A value of 1 indicates the measurement was identical in the different panels. Error bars show standard deviation. (B–C) Scatterplots showing the correlations for eight genotypes from the UA and NVT panels. The correlation coefficients (r) are shown. EA, endosperm area; AA, aleurone area; AP, aleurone proportion; DVW, grain dorsal-ventral width; LRW, grain left-right width; ALN, aleurone layer number; AW, aleurone width; GHI, grain hardness index; GM, grain moisture; GD, grain diameter; GWt, grain weight; R, grain roundness; GL, grain length; GWi, grain width; GT, grain thickness; GA, grain area. Significance indicators: * = p≤0.05.

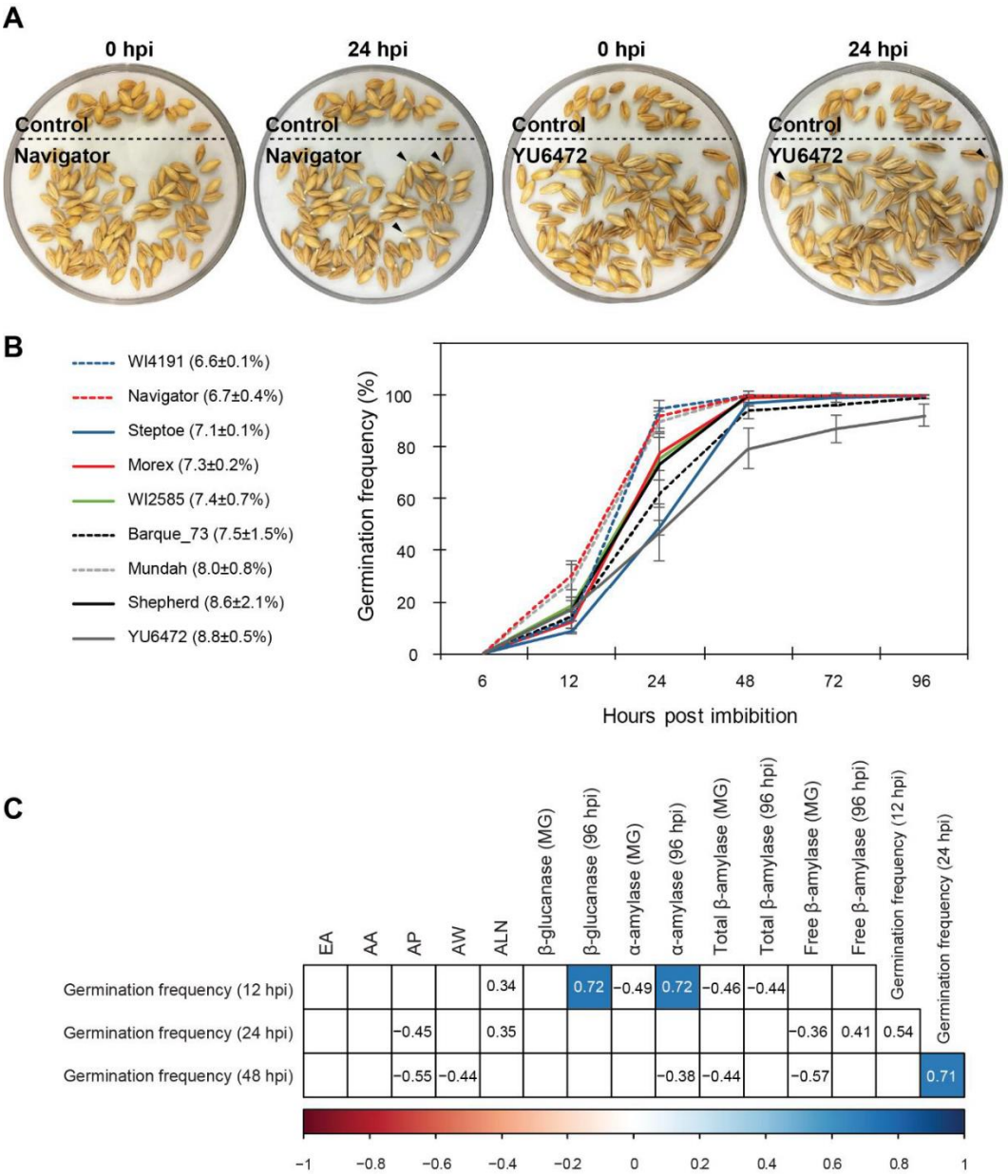

Figure 4-S7: Analysis of germination frequency in nine barley cultivars showing distinct aleurone features. (A) Petri dishes containing grains 0 hours post imbibition (hpi) and 24 hpi for the Navigator and YU6472 genotypes. Control grain are from the Flagship genotype. Arrowheads indicate the emergence of the radicle. (B) Frequency of germination at six time-points after imbibition. The legend shows the cultivars sorted from smallest to largest with regards to aleurone proportion. Error bars show standard deviation. (C) Correlation matrix for germination frequency, aleurone features and enzyme activity levels. Correlation coefficients greater than 0.3 or less than -0.3 are shown, but only coloured squares indicate a p-value ≤ 0.05.

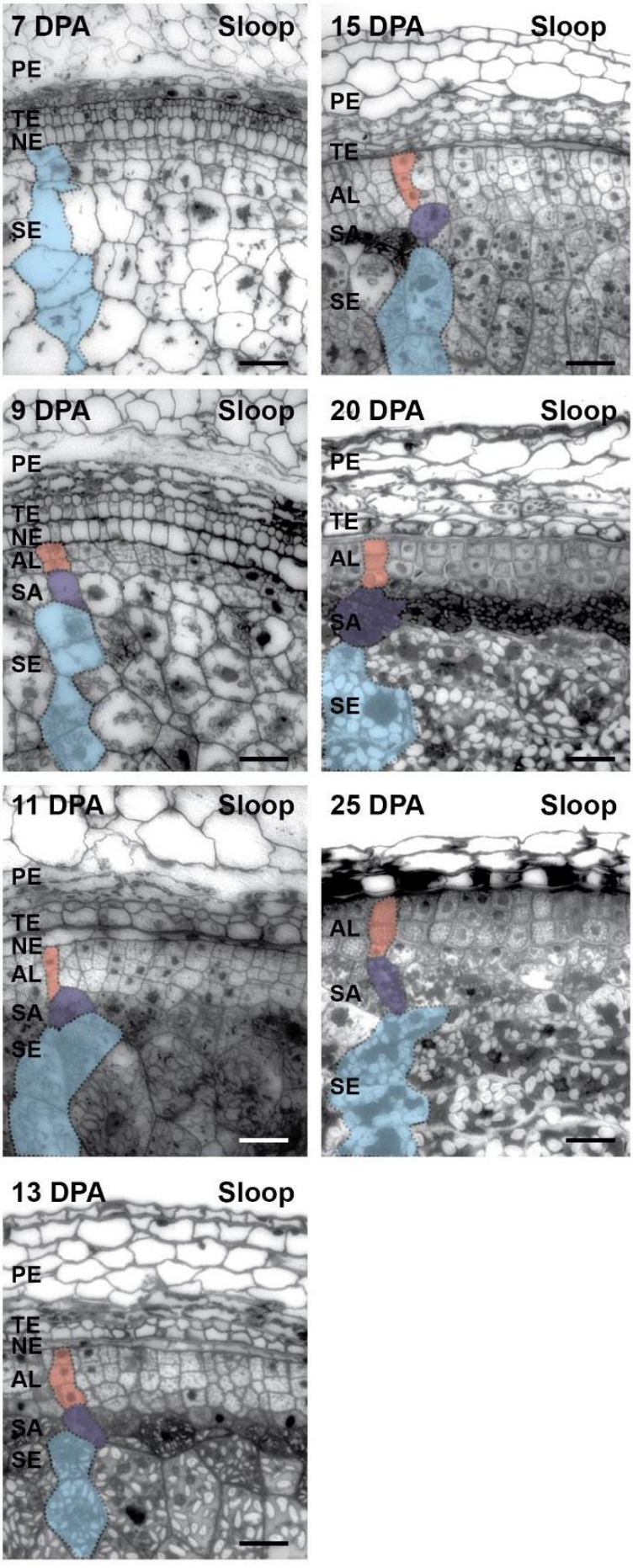
7 DPA
Sloop
PE
TE
NE
SE
15 DPA
Sloop
PE
TE
AL
SA
SE
9 DPA
Sloop
PE
TE
NE
AL
SA
SE
20 DPA
Sloop
PE
TE
AL
SA
SE
11 DPA
Sloop
PE
TE
NE
AL
SA
SE
25 DPA
Sloop
AL
SA
SE
13 DPA
Sloop
PE
TE
NE
AL
SA
SE

Figure 4-S8: Stages of grain development from Sloop, corresponding to those collected for RNAseq analysis. Developing grain were embedded in LR-white and sectioned (1µm) prior to staining with Toluidine blue. Selected aleurone cells are false coloured in orange, sub-aleurone cells in purple and starchy endosperm cells in blue. DPA, days post anthesis; AL, aleurone; NE, nucellar epidermis; PE, pericarp; SE, starchy endosperm; SA, sub-aleurone; TE, testa (integuments). Bar = 50µm.

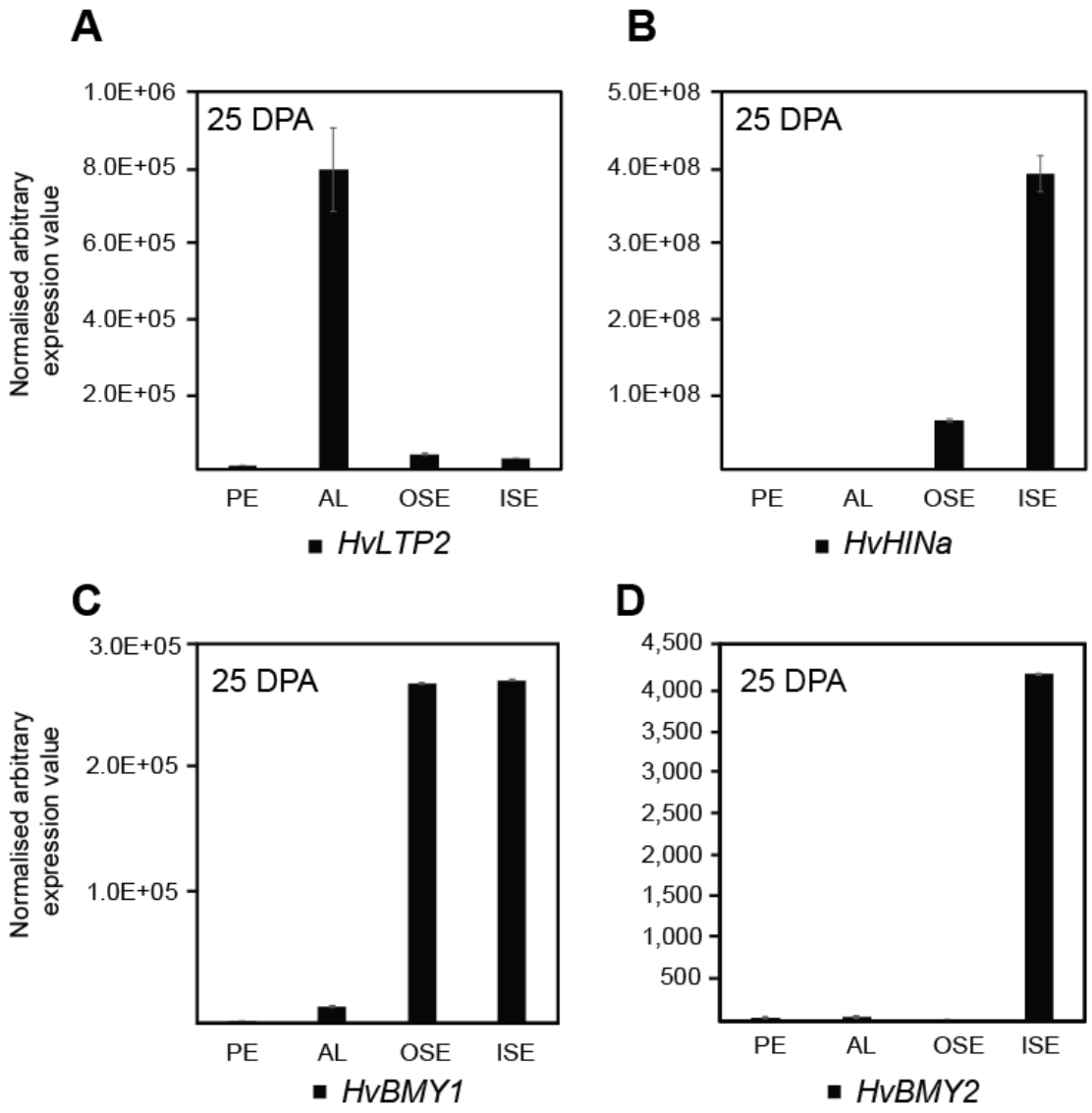

Figure 4-S9: Transcript analysis in grain tissues harvested by laser capture microdissection at 25 days post anthesis (DPA). In contrast to Fig. 5, captured RNA was amplified before conversion to cDNA. Quantitative PCR analysis of transcript abundance was undertaken for (A) lipid transfer protein 2 (HvLTP2), (B) hordoinoline_a (HvHINa), (C) β-amylase 1 (HvBMY1) and (D) β-amylase 2 (HvBMY2). PE, pericarp; AL, aleurone; OSE, outer starchy endosperm including sub-aleurone; ISE, inner starchy endosperm.

Supplementary Tables

Table 4-S1: Grain measurements for 33 barley genotypes grown in the field at Charlick, SA, in 2013

		Transverse sections								Seed Scanner (SS)				Single Kernel Characterisation System (SKCS)				
Cultivar	**Properties**	**EA (mm²)**	**SEA (mm²)**	**AA (mm²)**	**AP (%)**	**DVW (µm)**	**LRW (µm)**	**ALN**	**AW (µm)**	**R**	**GL (mm)**	**GWi (mm)**	**GT (mm)**	**GHI**	**GM**	**GD (mm)**	**GWt (mg)**	**Hardness Class**
Amaji Nijo	Malt (Japan)	5.3 ± 0.3	4.8 ± 0.2	0.450 ± 0.044	8.4 ± 0.2	2251 ± 136	3097 ± 97	2.6 ± 0.0	52.5 ± 1.1	2.47	7.83 ± 0.57	2.95 ± 0.29	2.26 ± 0.18	56.4 ± 19.3	12.5 ± 0.2	1.7 ± 0.7	31.8 ± 11.2	MIXED
Arapiles	Malt	4.8 ± 0.4	4.4 ± 0.3	0.420 ± 0.050	8.6 ± 0.2	2116 ± 123	3040 ± 86	2.6 ± 0.2	48.4 ± 3.2	2.39	8.61 ± 0.53	3.27 ± 0.32	2.63 ± 0.21	58.4 ± 14.5	12.6 ± 0.2	2.2 ± 0.5	42.3 ± 8.1	HARD
Arta	Feed (Syria)	7.7 ± 0.3	7.2 ± 0.3	0.516 ± 0.025	6.6 ± 0.5	2669 ± 96	3680 ± 81	2.0 ± 0.3	54.6 ± 2.3	2.54	9.56 ± 0.86	3.37 ± 0.36	2.65 ± 0.18	48.2 ± 18.9	12.2 ± 0.2	2.3 ± 0.3	47.1 ± 7.6	MIXED
Barque	Feed	6.1 ± 0.9	5.6 ± 0.9	0.453 ± 0.045	7.5 ± 1.5	2384 ± 133	3328 ± 244	1.8 ± 0.3	45.2 ± 2.9	2.53	9.29 ± 0.51	3.46 ± 0.34	2.64 ± 0.14	38.4 ± 13.1	12.4 ± 0.2	2.3 ± 0.5	46.4 ± 6.3	SOFT
Baudin	Malt	7.1 ± 0.6	6.5 ± 0.6	0.580 ± 0.03	8.1 ± 0.3	2641 ± 148	3482 ± 125	2.3 ± 0.2	55.7 ± 1.3	2.36	8.38 ± 0.54	3.29 ± 0.34	2.58 ± 0.11	69.4 ± 14.1	12.5 ± 0.2	2.2 ± 0.5	41.1 ± 7.2	HARD
Chebec	Malt	6.8 ± 0.3	6.3 ± 0.3	0.533 ± 0.05	7.7 ± 0.7	2490 ± 37	3568 ± 99	2.7 ± 0.1	53.0 ± 4.9	2.50	8.25 ± 0.52	3.08 ± 0.32	2.36 ± 0.18	52.2 ± 21.8	12.7 ± 0.3	1.9 ± 0.7	37.9 ± 11.4	MIXED
Clipper	Malt	6.2 ± 0.4	5.7 ± 0.3	0.503 ± 0.05	8.0 ± 0.2	2463 ± 58	3346 ± 93	2.8 ± 0.0	59.6 ± 3.3	2.46	8.02 ± 0.62	3.04 ± 0.32	2.33 ± 0.16	64.3 ± 23.3	12.3 ± 0.3	1.9 ± 0.8	36.3 ± 14.2	MIXED
CM 72	Feed (Nth Africa, 6r)	4.5 ± 1.2	4.1 ± 1.1	0.390 ± 0.051	8.8 ± 1.5	2104 ± 239	2945 ± 417	2.5 ± 0.1	46.8 ± 2.4	2.86	10.9 ± 0.66	3.13 ± 0.31	2.74 ± 0.23	47.1 ± 17.7	12.4 ± 0.2	2.3 ± 0.5	44.4 ± 7.3	MIXED
Commander	Malt	8.1 ± 0.9	7.5 ± 0.9	0.583 ± 0.037	7.2 ± 0.4	2834 ± 250	3779 ± 195	2.7 ± 0.3	56.4 ± 4.5	2.44	8.84 ± 0.64	3.51 ± 0.33	2.56 ± 0.13	53.1 ± 13.2	12.6 ± 0.2	2.4 ± 0.3	44.3 ± 6.1	HARD
Copeland	Malt (Canada)	6.8 ± 0.6	6.3 ± 0.6	0.513 ± 0.050	7.5 ± 0.1	2611 ± 143	3512 ± 134	2.4 ± 0.1	53.3 ± 4.6	2.28	8.61 ± 0.57	3.54 ± 0.32	2.74 ± 0.16	54.3 ± 17.4	12.4 ± 0.2	2.1 ± 0.6	39.3 ± 6.7	HARD
Czech Landrace-243	Landrace	6.7 ± 0.5	6.1 ± 0.5	0.530 ± 0.085	7.8 ± 0.5	2562 ± 125	3438 ± 112	2.5 ± 0.1	55.3 ± 7.0	2.34	8.34 ± 0.54	3.39 ± 0.28	2.55 ± 0.13	44.3 ± 16.9	12.4 ± 0.2	2.1 ± 0.5	38.9 ± 7.3	MIXED
Dhow	Malt	7.6 ± 0.7	7.0 ± 0.6	0.600 ± 0.087	7.8 ± 0.5	2749 ± 150	3669 ± 165	2.5 ± 0.3	56.0 ± 5.0	2.33	8.11 ± 0.48	3.27 ± 0.32	2.53 ± 0.37	n.d.	n.d.	n.d.	n.d.	n.d.
ER-Apm	Feed (ICARDA)	6.4 ± 0.4	5.9 ± 0.4	0.483 ± 0.030	7.5 ± 0.0	2482 ± 110	3397 ± 80	2.2 ± 0.3	46.8 ± 5.2	2.85	9.95 ± 0.87	3.16 ± 0.31	2.41 ± 0.15	54.9 ± 16.1	12.4 ± 0.2	2 ± 0.7	40.3 ± 11.7	HARD
Finniss	Hulless	8.2 ± 0.1	7.7 ± 0.1	0.570 ± 0.026	6.9 ± 0.3	2827 ± 69	3721 ± 43	2.5 ± 0.0	52.3 ± 1.4	2.33	8.81 ± 1.06	3.38 ± 0.41	2.74 ± 0.24	48.8 ± 13.6	12.4 ± 0.2	2.3 ± 0.4	43.2 ± 7.3	MIXED
Flagship	Malt	8.2 ± 0.2	7.6 ± 0.2	0.576 ± 0.030	7.0 ± 0.1	2785 ± 78	3808 ± 49	2.3 ± 0.2	51.4 ± 1.8	2.30	8.72 ± 0.51	3.57 ± 0.38	2.73 ± 0.12	46.7 ± 10.1	12.4 ± 0.2	2.5 ± 0.3	48.6 ± 5.7	HARD
Franklin	Malt	7.3 ± 0.9	6.7 ± 0.8	0.623 ± 0.076	8.4 ± 0.4	2585 ± 227	3732 ± 207	2.8 ± 0.1	60.6 ± 8.4	2.41	8.43 ± 0.41	3.45 ± 0.33	2.48 ± 0.17	61.2 ± 16.3	12.6 ± 0.2	2.1 ± 0.4	41.7 ± 6.1	HARD
Harmal-02//Esp/1808/4L	Feed (ICARDA)	8.1 ± 0.6	7.5 ± 0.5	0.590 ± 0.026	7.2 ± 0.2	2829 ± 94	3735 ± 71	2.4 ± 0.1	57.8 ± 3.9	2.57	9.97 ± 0.93	3.39 ± 0.41	2.75 ± 0.21	45.8 ± 12.5	12.1 ± 0.3	2.6 ± 0.3	52.5 ± 7.8	MIXED
Harrington	Malt (Canada)	5.3 ± 0.6	4.8 ± 0.5	0.450 ± 0.026	8.4 ± 0.4	2266 ± 141	3098 ± 181	2.5 ± 0.2	40.6 ± 2.8	2.62	8.12 ± 0.87	2.93 ± 0.37	2.27 ± 0.35	57.4 ± 21.3	12.4 ± 0.3	1.8 ± 0.7	32.3 ± 10.5	MIXED
Hindmarsh	Feed	8.1 ± 0.5	7.5 ± 0.5	0.570 ± 0.026	7.0 ± 0.5	2854 ± 157	3679 ± 106	1.8 ± 0.5	51.5 ± 1.3	2.15	8.01 ± 0.48	3.48 ± 0.52	2.79 ± 0.12	50.7 ± 12.8	12.2 ± 0.2	2.4 ± 0.3	44.1 ± 5.3	HARD
Keel	Feed	8.0 ± 0.6	7.5 ± 0.6	0.536 ± 0.060	6.6 ± 0.2	2844 ± 128	3785 ± 70	2.3 ± 0.2	51.6 ± 2.9	2.46	9.21 ± 0.77	3.49 ± 0.36	2.64 ± 0.11	45.9 ± 12.4	12.3 ± 0.2	2.4 ± 0.3	47.1 ± 5.4	MIXED
Morex	Malt (USA, 6r)	5.0 ± 0.2	4.7 ± 0.2	0.376 ± 0.025	7.3 ± 0.2	2196 ± 41	3015 ± 77	2.3 ± 0.2	40.1 ± 1.0	2.70	8.24 ± 1.02	2.84 ± 0.36	2.15 ± 0.31	75.2 ± 18.8	12.5 ± 0.2	1.7 ± 0.7	30.3 ± 11.4	HARD

Mundah	Feed	7.4 ± 0.9	6.8 ± 0.8	0.596 ± 0.055	8.0 ± 0.8	2599 ± 97	3660 ± 268	2.7 ± 0.0	60.4 ± 4.2	2.56	9.69 ± 0.61	3.61 ± 0.33	2.66 ± 0.12	51.6 ± 12.4	12.3 ± 0.2	2.4 ± 0.3	48.8 ± 5.9	HARD
Shepherd	Feed	8.7 ± 1.1	7.9 ± 0.9	0.770 ± 0.289	8.6 ± 2.1	2896 ± 145	3919 ± 226	2.4 ± 0.1	59.4 ± 4.0	2.42	9.35 ± 0.76	3.52 ± 0.41	2.73 ± 0.24	61.6 ± 14.5	12.4 ± 0.3	2.3 ± 0.5	42.5 ± 10.1	HARD
Skiff	Malt	5.9 ± 0.7	5.4 ± 0.6	0.490 ± 0.045	8.2 ± 0.2	2343 ± 171	3295 ± 188	2.3 ± 0.1	54.4 ± 2.6	2.35	8.47 ± 0.47	3.39 ± 0.32	2.58 ± 0.13	60.5 ± 12.5	12.3 ± 0.2	2.1 ± 0.5	41.6 ± 6.9	HARD
Sloop	Malt	7.8 ± 0.3	7.2 ± 0.3	0.533 ± 0.037	6.7 ± 0.1	2679 ± 102	3766 ± 54	2.5 ± 0.0	58.3 ± 4.4	2.16	7.53 ± 1.91	3.35 ± 0.94	2.68 ± 0.21	41.5 ± 12.4	12.5 ± 0.2	2.5 ± 0.4	45.6 ± 5.3	SOFT
Steptoe	Feed (USA, 6r)	6.9 ± 0.3	6.4 ± 0.3	0.493 ± 0.035	7.1 ± 0.1	2672 ± 66	3442 ± 208	2.2 ± 0.5	49.6 ± 8.5	2.59	9.65 ± 1.79	3.24 ± 0.56	2.69 ± 0.13	63.6 ± 14.1	12.3 ± 0.2	2.4 ± 0.5	44.3 ± 6.5	HARD
Tadmor	Feed (Syria)	7.4 ± 0.7	6.9 ± 0.6	0.530 ± 0.060	7.1 ± 0.4	2721 ± 153	3564 ± 174	2.3 ± 0.3	54.3 ± 7.0	2.53	9.26 ± 0.69	3.34 ± 0.38	2.65 ± 0.21	48.6 ± 14.5	11.9 ± 0.3	2.4 ± 0.4	46.2 ± 6.7	MIXED
Tipple	Malt (Europe)	6.4 ± 0.4	6.0 ± 0.4	0.476 ± 0.049	7.3 ± 0.2	2460 ± 116	3369 ± 90	2.3 ± 0.2	53.2 ± 3.3	2.52	8.96 ± 0.51	3.53 ± 0.41	2.68 ± 0.41	51.2 ± 18.4	12.5 ± 0.2	2.3 ± 0.4	45.5 ± 7.3	MIXED
WI2585	Breeding line	6.8 ± 1.7	6.3 ± 1.6	0.496 ± 0.072	7.4 ± 0.7	2552 ± 352	3535 ± 365	2.7 ± 0.3	55.1 ± 4.5	2.66	8.91 ± 0.65	3.32 ± 0.25	2.32 ± 0.17	56.5 ± 15.1	12.2 ± 0.3	2.1 ± 0.7	38.8 ± 12.5	HARD
WI4191	Malt breeding line	7.2 ± 0.4	6.7 ± 0.4	0.483 ± 0.032	6.6 ± 0.1	2604 ± 46	3604 ± 127	2.3 ± 0.2	52.9 ± 1.5	2.16	7.68 ± 0.44	3.44 ± 0.26	2.61 ± 0.21	52.5 ± 12.6	12.5 ± 0.2	2.1 ± 0.5	37.5 ± 7.5	HARD
WI4259 (Admiral)	Malt	7.9 ± 0.6	7.4 ± 0.5	0.576 ± 0.124	7.1 ± 0.9	2745 ± 83	3700 ± 207	2.6 ± 0.2	56.3 ± 5.7	2.43	8.69 ± 0.44	3.54 ± 0.36	2.65 ± 0.38	39.5 ± 14.1	12.2 ± 0.2	2.1 ± 0.4	41.1 ± 7.2	SOFT
WI4262 (Navigator)	Malt	7.2 ± 0.1	6.7 ± 0.1	0.490 ± 0.036	6.7 ± 0.4	2644 ± 39	3541 ± 57	2.2 ± 0.2	48.0 ± 1.0	2.25	8.11 ± 0.36	3.41 ± 0.36	2.64 ± 0.12	54.1 ± 14.5	12.5 ± 0.2	2.2 ± 0.5	39.1 ± 7.1	HARD
YU6472	Feed (China)	7.5 ± 0.8	6.9 ± 0.7	0.673 ± 0.098	8.8 ± 0.5	2760 ± 112	3587 ± 237	2.3 ± 0.1	65.4 ± 6.2	2.43	9.22 ± 0.64	3.41 ± 0.31	2.74 ± 0.15	43.3 ± 12.1	12.3 ± 0.2	2.6 ± 0.5	46.6 ± 7.1	SOFT
AVERAGE		**6.9±1.2**	**6.4±1.1**	**0.529±0.099**	**7.6±0.8**	**2582±247**	**3510±288**	**2.4±0.2**	**53.2±6.5**	**2.45 ± 0.17**	**8.8 ± 0.7**	**3.3 ± 0.4**	**2.6 ± 0.2**	**53.0 ± 15.3**	**12.4 ± 0.2**	**2.2 ± 0.5**	**42.1 ± 7.9**	

EA, endosperm area; AA, aleurone area; AP, aleurone proportion; DVH, grain dorsal-ventral height; LRW, grain left-right width; AL_LN, aleurone layer number; AW, aleurone width; GHI, grain hardness index; GM, grain moisture; GD, grain diameter; GWt, grain weight; R, grain roundness; GL, grain length; GWi, grain width; GT, grain thickness; GA, grain area

Table 4-S2: Grain measurements for eight barley genotypes grown in the field at Gooloogong, NSW, in 2015.

Variety	EA (mm²)	AA (mm²)	AP (%)	DVW (µm)	LRW (µm)	ALN	AW (µm)	GHI	GM	GD (mm)	GWt (mg)	Hardness Class	R	GL (mm)	GWi (mm)	GT (mm)
Barque	7.64 ± 1.02	0.54 ± 0.02	7.12 ± 1.16	2758 ± 147	3685 ± 243	2.4 ± 0.8	51.37 ± 7.70	19 ± 17	10.1 ± 0.3	2.5 ± 0.6	47.0 ± 9.5	SOFT	2.39	9.21 ± 0.78	3.48 ± 0.30	2.81 ± 0.22
Baudin	7.17 ± 0.27	0.54 ± 0.02	7.57 ± 0.11	2702 ± 105	3508 ± 81	2.4 ± 0.6	55.89 ± 5.79	43 ± 18	10.2 ± 0.3	2.4 ± 0.6	42.7 ± 10	MIXED	2.37	8.74 ± 0.71	3.31 ± 0.35	2.67 ± 0.22
Commander	8.30 ± 0.44	0.59 ± 0.00	7.14 ± 0.34	2874 ± 120	3760 ± 98	2.6 ± 0.5	58.43 ± 6.32	29 ± 18	10.4 ± 0.4	2.4 ± 0.6	40.6 ± 9.8	SOFT	2.32	8.76 ± 0.59	3.41 ± 0.36	2.84 ± 0.33
Flagship	8.93 ± 0.35	0.54 ± 0.02	6.03 ± 0.25	2976 ± 135	3911 ± 100	2.4 ± 0.5	53.96 ± 8.53	25 ± 20	10.3 ± 0.4	2.5 ± 0.5	46.3 ± 8.6	SOFT	2.41	8.88 ± 0.79	3.46 ± 0.39	2.67 ± 0.26
Hindmarsh	8.40 ± 0.53	0.66 ± 0.07	7.90 ± 0.46	2893 ± 156	3760 ± 158	2.4 ± 0.6	58.46 ± 6.82	30 ± 21	10.3 ± 0.3	2.3 ± 0.6	39.0 ± 9	SOFT	2.29	8.11 ± 0.55	3.32 ± 0.39	2.64 ± 0.28
Keel	8.14 ± 0.17	0.53 ± 0.01	6.50 ± 0.27	2871 ± 41	3746 ± 61	2.3 ± 0.7	49.44 ± 7.15	20 ± 17	9.9 ± 0.4	2.5 ± 0.5	45.8 ± 8.4	SOFT	2.52	9.45 ± 0.85	3.49 ± 0.32	2.64 ± 0.26
Mundah	8.52 ± 0.55	0.77 ± 0.09	8.99 ± 0.52	2859 ± 51	3886 ± 88	2.8 ± 0.8	69.87 ± 10.41	33 ± 17	10.3 ± 0.3	2.6 ± 0.5	51.9 ± 9.7	SOFT	2.54	10.11 ± 0.69	3.52 ± 0.40	2.85 ± 0.29
Shepherd	8.90 ± 0.73	0.66 ± 0.04	7.43 ± 0.21	2931 ± 100	3926 ± 166	2.4 ± 0.5	58.81 ± 6.91	40 ± 19	10.7 ± 0.3	2.5 ± 0.5	44.3 ± 10.1	MIXED	2.28	8.63 ± 0.69	3.42 ± 0.40	2.81 ± 0.22

EA, endosperm area; AA, aleurone area; AP, aleurone proportion; DVH, grain dorsal-ventral height; LRW, grain left-right width; AL_LN, aleurone layer number; AW, aleurone width; GHI, grain hardness index; GM, grain moisture; GD, grain diameter; GWt, grain weight; R, grain roundness; GL, grain length; GWi, grain width; GT, grain thickness; GA, grain area

Table 4-S3: One-way analysis of variance (ANOVA) for barley grain features and flour enzymatic assays for nine genotypes of interest.

	Grain features					Free β-amylase		Total β-amylase		α-amylase		β-glucanase	
Comparison	**SEA**	**AA**	**AP**	**ALN**	**AW**	**Mature**	**96hpg**	**Mature**	**96hpg**	**Mature**	**96hpg**	**Mature**	**96hpg**
Barque-Shepherd	**	**	-	**	**	-	-	-	**	**	**	-	**
Barque-YU6472	-	**	**	**	**	**	-	-	-	**	**	**	-
Barque-Mundah	-	**	-	**	**	**	-	-	**	**	**	-	-
Barque-WI2585	-	-	-	**	**	-	-	-	**	**	**	-	-
Barque-Flagship	-	-	-	-	-	**	-	**	**	**	**	**	**
Barque-WI4191	-	-	-	**	-	**	**	**	**	**	**	**	**
Barque-Steptoe	-	-	-	-	-	-	-	-	**	**	**	**	**
Barque-Morex	-	-	-	**	-	**	-	**	**	**	**	**	**
Shepherd-YU6472	-	**	**	-	-	**	-	-	**	**	**	**	**
Shepherd-Mundah	-	-	-	-	-	**	-	-	**	**	**	-	**
Shepherd-WI2585	-	**	-	-	-	**	-	-	-	**	**	-	**
Shepherd-Flagship	-	**	**	-	**	**	-	**	**	**	**	**	**
Shepherd-WI4191	-	**	**	-	-	**	**	**	**	**	**	**	**
Shepherd-Steptoe	-	**	-	-	**	**	-	-	-	**	**	**	**
Shepherd-Morex	**	**	-	-	**	**	**	**	**	**	**	**	**
YU6472-Mundah	-	**	-	-	-	-	-	-	**	**	**	**	-
YU6472-WI2585	-	**	**	-	**	**	-	-	**	-	**	-	**
YU6472-Flagship	-	**	**	-	**	**	-	**	**	-	-	-	**
YU6472-WI4191	-	**	**	-	**	**	**	**	**	-	**	-	**
YU6472-Steptoe	-	**	**	-	**	**	-	-	**	-	**	-	**
YU6472-Morex	**	**	**	-	**	**	-	**	**	**	**	**	**
Mundah-WI2585	-	**	-	-	-	**	-	-	**	**	-	**	-
Mundah-Flagship	-	**	-	-	**	**	-	**	**	**	**	**	**
Mundah-WI4191	-	**	**	-	-	**	**	**	**	**	**	**	**
Mundah-Steptoe	-	**	-	-	**	**	-	-	**	**	**	**	**
Mundah-Morex	**	**	-	-	**	**	-	**	**	**	**	-	**
WI2585-Flagship	-	-	-	**	-	**	-	**	**	-	**	-	**
WI2585-WI4191	-	-	-	-	-	**	**	**	**	-	**	-	**
WI2585-Steptoe	-	-	-	**	-	-	-	-	**	-	**	-	**
WI2585-Morex	**	**	-	-	**	**	-	**	**	**	**	**	**
Flagship-WI4191	-	-	-	-	-	-	**	**	**	-	**	-	**
Flagship-Steptoe	-	-	-	-	-	-	-	**	**	-	**	-	**
Flagship-Morex	**	**	-	-	-	-	**	**	**	**	**	**	**
WI4191-Steptoe	-	-	-	-	-	-	**	**	**	-	**	-	**
WI4191-Morex	**	**	-	-	**	-	-	-	**	**	-	**	-
Steptoe-Morex	**	**	-	-	**	**	**	**	**	**	**	**	**

SEA, transverse starchy endosperm area; AA, transverse aleurone area; AP, transverse aleurone proportion; ALN, aleurone layer number; AW, aleurone width. ** indicates a significant difference.

Table 4-S4: *β-amylase* transcript abundance in developing barley ovaries and grain.

		Pistils (Golden Promise)				Wholegrain (minus embryo; Sloop)					
Name	**Gene ID**	**FG4**	**FG8**	**FGmat**	**FGanth**	**7DPA**	**9DPA**	**11DPA**	**13DPA**	**15DPA**	**20DPA**
BMY1	HORVU4Hr1G089510	0.0	0.1	0.1	0.0	29.9	420.0	4735.9	7706.7	6088.4	5283.7
BMY2	HORVU2Hr1G043930	113.7	130.2	152.7	3032.9	893.4	110.3	26.8	11.1	5.0	1.8
BMY3	HORVU4Hr1G084390	3.8	3.2	2.5	85.8	6.1	6.6	6.1	2.5	5.8	4.7
BMY4	HORVU1Hr1G038950	1.4	1.7	2.6	1.3	1.4	0.5	0.4	0.6	0.6	1.0
BMY5	HORVU1Hr1G055140	175.8	101.6	402.2	221.0	9.2	4.1	9.3	4.5	7.2	2.5
BMY6	HORVU4Hr1G000520	6.8	8.0	4.9	6.7	3.6	2.7	1.4	1.6	0.7	0.7
BMY7	HORVU6Hr1G015670	18.8	14.4	16.4	12.9	9.7	6.4	4.4	4.6	5.0	3.5
BMY8	HORVU3Hr1G032160	81.3	72.7	80.6	58.0	16.5	13.5	9.4	10.5	13.0	9.4
BMY9	HORVU2Hr1G020970	0.0	0.0	0.1	0.0	0.0	0.0	0.0	0.0	0.1	0.0
BMY10	HORVU1Hr1G038920	0.0	0.1	0.0	125.4	0.0	0.0	0.0	0.0	0.0	0.0
BMY11	HORVU2Hr1G043920	1.2	3.6	2.4	10.6	1.6	2.1	1.4	1.7	2.7	1.8

Numbers represent TPM values. DPA, days post anthesis; FG, female gametophyte; FGmat, mature female gametophyte; FGanth, female gametophyte at anthesis.

Table 4-S5: Oligonucleotides used for quantitative PCR analysis

Annotations	Horvul	Fwd Primer	Rev Primer	Size Bp	T Acq (C)	Sequence ID	Sequence
Hv Glyceraldehyde-3-phosphate dehydrogenase C2	HORVU7Hr1G074690	GTGAGGCTGGTGCTGATTACG	TGGTGCAGCTAGCATTTGAGAC	198	82		TGGTGCAGCTAGCATTTGAGACAATGTTAACATCCGAGGTGTA CTTGTCCTCATTGACACCAACCACAAACATAGGGGCATCTTTG CTTGGGGCAGAGATGACCACCTTCTTGGCACCACCCTTCAAG TGAGCAGCGGCCTTGTCCTTGTCAGTGAAGACACCGGTGGAC TCCACAACGTAATCAGCACCAGCCTCAC
Hv Peptidyl-prolyl cis-trans isomerase (cyclophilin)	HORVU6Hr1G012570	CCTGTCGTGTCGTCGGTCTAAA	ACGCAGATCCAGCAGCCTAAAG	122	81		CCTGTCGTGTCGTCGGTCTAAATAAGGAGTCGTGTCGTGTCTT GCCCCTGTCCGTCCGATGAGATCTCCGTGGTTGGTTTAGGAG GGTTTTAGGTGGACTCTTTAGGCTGCTGGATCTGCGT
Hv Tubulin alpha-4 chain	HORVU1Hr1G081280	AGTGTCCTGTCCACCCACTC	AGCATGAAGTGGATCCTTGG	248	82		AGTGTCCTGTCCACCCACTCCCTCCTTGAGCACACCGATGTCT CTATCCTGCTTGACAATGAGGCCATCTATGACATCTGCCGCCG CTCCCTTGACATTGAGCGCCCAACATACACCAACCTCAACAGG CTTGTTTCTCAGGTCATATCATCACTGACTGCTTCCCTGAGGTT TGACGGTGCTCTGAATGTTGATGTGAATGAGTTCCAAACCAAC CTGGTGCCCTACCCAAGGATCCACTTCATGCT
Hv Heat shock 70 kDa protein 3	HORVU5Hr1G113180	CGACCAGGGCAACCGCACCAC	ACGGTGTTGATGGGGTTCATG	108	85		CGACCAGGGCAACCGCACCACGCCCTCGTACGTCGCCTTCAC CGACTCGGAGCGCCTCATCGGCGATGCCGCCAAGAACCAGG TCGCCATGAACCCCATCAACACCGT
Hv Elongation factor 1-alpha	HORVU5Hr1G100700	GGTACCTCCCAGGCTGACTGT	GTGGTGGCGTCCATCTTGTTA	164	81		GGTACCTCCCAGGCTGACTGTGCTGTGCTCATCATTGACTCC ACCACTGGTGGTTTTGAGGCTGGTATCTCCAAGGATGGCCAG ACACGTGAGCATGCCCTCCTTGCTTTCACTCTTGGAGTGAAGC AGATGATCTGCTGCTGTAACAAGATGGACGCCACCAC
Hv Actin 7	HORVU1Hr1G002840	TGGCATCACACTTTCTACAAT	GCTGACACCATCACCAGAGTC	225	82		TGGCATCACACTTTCTACAATGAGCTCCGTGTGGCACCCGAGG AGCACCCTGTGTTGCTCACTGAGGCCCCTTTGAACCCAAAAGC CAACAGAGAGAAGATGACCCAGATTATGTTTGAGACTTTCAATG TTCCTGCCATGTACGTCGCTATTCAGGCCGTGCTTTCCCTCTAT GCAAGTGGTCGTACTACTGGTATCGTTCTCGACTCTGGTGATG GTGTCAGC
Hv Beta-amylase 5 (*HvBMYI*)	HORVU4Hr1G089510	CCTCGTGACCCATATGTTGAT	CCAGTAGGGCCTTTAACTTGC	212	82	KF302675.1	CCTCGTGACCCATATGTTGATCCAATGGCGCCTTTGCCAAGAT CAGGGCCAGAAATATCGATTGAGATGATCCTACAAGCAGCACA GCCAAAACTGCAGCCATTCCCCTTCCAGGAGCACACCGACCTG CCAGTAGGCCCTACTGGTGGCATGGGTGGGCAGGCTGAAGGC CCCACCTGTGGCATGGGTGGGCAAGTTAAAGGCCCTACTGG
undescribed protein (*HvBMY2*)	HORVU2Hr1G043930	AACTGGAGCCATTCCCTTTT	AGCACCTCTTGACCCTCTCA	167	80	FJ936156.1	AACTGGAGCCATTCCCTTTTGATAAGAACACCGACCTGCCAGT TAAAGATCACACTGATGTCGTGGATGAGGCGCTCCTTGCCCCT GTGGCTGTGTAGAAATCTTTCTCTGCCTTCGTAAAATAATGTGC ATCACTGATGCAGTCTATGAGAGGGTCAAGAGGTGCT
Non-specific lipid-transfer protein 2G (*HvLTP2*)	HORVU4Hr1G089500	TGTGCCAGTACGTCAAGGAC	GCTAGCCAGGAAGCAAGCTA	185	83	X69793.1	TGTGCCAGTACGTCAAGGACCCCAACTACGGGCACTACGTGA GCAGCCCACACGCGCGCGACACCCTCAACTTGTGCGGCATAC CCGTACCGCACTGCTAGCCGCCTAGCCGATCGAGGGCTCCAG GCACGCATGCATGTTCCTGTTATGTGGATGTTGGAATAAAATG CTGGTGATCTATGGCGGCTAGCTTGCTTCCTGGCTAGC
Puroindoline-A (*HvHINa*)	HORVU5Hr1G000680	TCATCCAGGGATCAATCCAAC	TAGCCAGTAGTGCTGGGGATG	145	82	JN636829.1	TTCATCCAGGGATCAATCCAACGTGATCTCGGTGGTTTCTTCG GATTTCAGCGTGATCGGACAGTCAAAGTGATACAAGCAGCCAA GAACCTGCCCCCCAGGTGCAACCAGGGCCCTGCCTGCAACAT CCCCAGCACTACTGGCTA

Chapter 5

Identification of candidate genes involved in barley (*Hordeum vulgare* L.) aleurone development by laser capture microdissection and genome wide association studies

Statement of Authorship

Title of Paper	Identification of candidate genes involved in barley (*Hordeum vulgare* L.) aleurone development by laser capture microdissection and genome wide association studies
Publication Status	☐ Published ☐ Accepted for Publication ☐ Submitted for Publication ☑ Unpublished and Unsubmitted work written in manuscript style
Publication Details	Matthew K. Aubert[1,2], Kelly Houston[3], Rachel A. Burton[2], Ali S. Hassan[1,2], Tobias Würschum[4], Neil J. Shirley[2] and Matthew R. Tucker[1]*.

Principal Author

Name of Principal Author (Candidate)	Matthew K. Aubert		
Contribution to the Paper	Performed experiments, analysed all samples, interpreted data and wrote manuscript.		
Overall percentage (%)	80%		
Certification:	This paper reports on original research I conducted during the period of my Higher Degree by Research candidature and is not subject to any obligations or contractual agreements with a third party that would constrain its inclusion in this thesis. I am the primary author of this paper.		
Signature		Date	21/11/2018

Co-Author Contributions

By signing the Statement of Authorship, each author certifies that:

i. the candidate's stated contribution to the publication is accurate (as detailed above);

ii. permission is granted for the candidate in include the publication in the thesis; and

iii. the sum of all co-author contributions is equal to 100% less the candidate's stated contribution.

Name of Co-Author	Kelly Houston		
Contribution to the Paper	Assisted with GWAS analysis, program function and statistical analysis. I hereby certify that the statement of authorship is accurate.		
Signature		Date	06/11/2018

Name of Co-Author	Rachel A. Burton		
Contribution to the Paper	Helped to design experiments. Contributed to the preparation of the manuscript. I hereby certify that the statement of authorship is accurate.		
Signature		Date	22/11/2018

Name of Co-Author	Ali S. Hassan		
Contribution to the Paper	Completed grain compositional analyses and provided data. I hereby certify that the statement of authorship is accurate.		
Signature		Date	21/11/2018

Name of Co-Author	Tobias Würschum		
Contribution to the Paper	Assisted with statistical analysis and preparation. I hereby certify that the statement of authorship is accurate.		
Signature		Date	20. Nov. 2018

Name of Co-Author	Neil J. Shirley		
Contribution to the Paper	Performed quantitative PCR, assembled RNA sequencing library and helped with sample analysis. Contributed to the preparation of the manuscript. I hereby certify that the statement of authorship is accurate.		
Signature		Date	21/11/18

Name of Co-Author	Matthew R. Tucker		
Contribution to the Paper	Conceived project and designed experiments. Contributed to the preparation of the manuscript. I hereby certify that the statement of authorship is accurate.		
Signature		Date	20/11/18

Title Identification of candidate genes involved in barley (*Hordeum vulgare* L.) aleurone development by laser capture microdissection and genome wide association studies

Authors Matthew K. Aubert[1,2], Kelly Houston[3], Rachel A. Burton[2], Ali S. Hassan[1,2], Tobias Würschum[4], Neil J. Shirley[2] and Matthew R. Tucker[1]

[1]School of Agriculture, Food and Wine, Waite Research Institute, the University of Adelaide, Glen Osmond, SA, Australia

[2]Australian Research Council Centre of Excellence in Plant Cell Walls, the University of Adelaide, Adelaide, Australia.

[3]Cell and Molecular Sciences, the James Hutton Institute, Dundee, UK.

[4]State Plant Breeding Institute, University of Hohenheim, Stuttgart, Germany.

Keywords Barley, aleurone, endosperm, development, grain, GWAS, association, gene

Abbreviations

AX	Arabinoxylan
BMM	Butyl methyl methacrylate
Chr	Chromosome
CKDs	Cyclin-dependent kinases
CR4	CRINKLY 4
CYC	Cyclins
DAP	Days after pollination
DEK1	DEFECTIVE KERNEL 1
DES5	DEFECTIVE SEED 5
DPA	Days post anthesis
DTT	1,4-Dithiothreitol
EU	European 2-row spring barley
FC	Fold change
GA	Gibberellic acid
GO	Gene ontology
GWAS	Genome Wide Association Studies
HorB1	HORDEIN B1
IDD	INDETERMINATE1 domain
LCM	Laser capture microdissection
LOD	High logarithm of the odds
LTP2	LIPID TRANSFER PROTEIN 2
µCT	micro computed tomography
NF-Y	NUCLEAR FACTOR Y
NKD1	NAKED ENDOSPERM 1

PBS	Phosphate-buffered saline
PCA	Principle component analysis
qPCR	quantitative Polymerase chain reaction
QTL	Quantitative trait loci
RBRs	Retinoblastoma-related proteins
RBs	Retinoblastoma proteins
ROS1	REPRESSOR OF SILENCING 1
RNAseq	RNA sequencing
SAL1	SUPERNUMERARY ALEURONE LAYER 1
SNP	Single nucleotide polymorphism
TA2	THICK ALEURONE 2
TPM	Transcripts per million
UA	University of Adelaide
UTR	Untranslated region
VP1	VIVIPAROUS 1

Abstract

The aleurone is a critical part of the cereal grain since it contains many key components including protein and lipid bodies and produces enzymes crucial for germination. The aleurone is located at the periphery of the starchy endosperm and has previously been shown to be multilayered with variable morphology in different barley (*Hordeum vulgare* L.) genotypes. The cause of this variation in barley and the genes involved remain unclear. In this study, natural variation in mature aleurone morphology was examined in 150 European two-row spring barley lines. Variation was assessed in the number of aleurone cell layers, the transverse thickness and area of the aleurone and the proportion of aleurone relative to the starchy endosperm. Genome Wide Association Studies (GWAS) revealed twenty-one dispersed genomic regions significantly associated with aleurone morphological traits. From these, four quantitative trait loci (QTL) with a high logarithm of the odds (LOD) score were investigated. To examine genomic details of the QTL, transcriptome datasets were developed using techniques including laser capture microdissection and differential transcript profiling, via RNAseq. Candidate genes likely to be involved in aleurone development were identified by differential transcript abundance patterns across grain development between high and low aleurone genotypes (varying for aleurone area, proportion and thickness), from tissue-specific enrichment and/or selected from QTL genomic regions. The results reveal apparently novel QTL along with several associated candidate genes that may influence aleurone development in barley or be used as aleurone marker genes for further analysis.

Introduction

Cereal grains represent a crucial human food source that also underpin a wide range of industrial processes such as beverage, animal feed and biofuel production. One cereal used as a malting grain for whisky and beer production is barley (*Hordeum vulgare* L.; Newman and Newman (2006)). Apart from containing many nutrients, antioxidants and dietary fibres that benefit the human diet (Behall et al., 2004; Pins and Kaur, 2006; Gamel and Abdel-Aal, 2012), barley enjoys advantages over other cereal grains that makes it ideal as a raw material for brewing. For example, barley plants tend to grow well under a range of environmental conditions (Finlay and Wilkinson, 1963), the grain is surrounded by a husk that provides protection during manual handling and helps to filter wort during the brewing process, and the endosperm exhibits an enzyme:starch ratio that facilitates optimal utilisation of sugars for malt production (Burger and La-Berge, 1985). Most of the beneficial nutrients, enzymes and sugars found in barley grain accumulate in a tissue known as the endosperm. Thus, further investigations into endosperm development may lead to improved grain traits for both malt production and human health.

Barley endosperm development initiates after fusion of two maternal polar nuclei with one male sperm nucleus during fertilisation of the central cell within the embryo sac (Olsen, 2004; Wilkinson and Tucker, 2017). Successive nuclear divisions of the primary endosperm nucleus without cytokinesis leads to the formation of a nuclear syncytium, which begins to cellularise at approximately five days post anthesis (DPA; Wilson et al. (2006)). During cellularisation, the endosperm begins to differentiate and consists of three main cell types that contribute different biological functions: the endosperm transfer cells, starchy endosperm and aleurone layer (Gillies et al., 2012).

The aleurone is located at the periphery of the grain and separates the inner starchy endosperm from the outer maternal husk. Mature aleurone cells are characterised by thick cell walls enriched in autofluorescent phenolic acids and polysaccharides such as arabinoxylan (Nordkvist et al., 1984; Wilson et al., 2012; Hassan et al., 2017a; Aubert et al., 2018), and by aleurone granules that form in protein storing vacuoles (Brown and Lemmon, 2007). At grain maturity, the aleurone layer is crucial for metabolite mobilisation and the initiation of germination, and contains living cells compared to the starchy endosperm in which metabolism has essentially ceased. During germination, the embryo releases gibberellic acid (GA), which translocates to the aleurone where it induces the transcription of genes encoding hydrolytic enzymes (Fath et al., 2000). These enzymes catalyse the breakdown of cell wall polysaccharides and starchy energy reserves that are essential for germination and the production of malt for brewing (Betts et al., 2017).

In other cereal species, differences are observed in the number of aleurone cell layers. Most cereal grains such as maize (*Zea mays* L.) and wheat (*Triticum aestivum* L.) have a single layer of aleurone cells, while barley and occasionally rice (*Oryza sativa* L.) have a multilayered aleurone (Shapter et al., 2009). The significance of having more (or fewer) aleurone layers during germination and seed development remains uncertain, while the molecular mechanisms that define aleurone cell identity are poorly understood outside of maize. In maize, the *defective kernel 1* (*dek1*), *crinkly 4* (*cr4*), *naked endosperm 1* (*nkd1*) and *supernumerary aleurone layer 1* (*sal1*) mutants show defects in aleurone development (Becraft et al., 1996; Shen et al., 2003; Tian et al., 2007; Olsen et al., 2008; Yi et al., 2015). Additionally, in rice, the *thick aleurone 2* (*TA2*) mutant produces more aleurone cell layers (Liu et al., 2018). *DEK1* encodes a putative cell-wall integrity sensor (Amanda et al., 2016), *CR4* encodes a receptor-like kinase

that accumulates near plasmodesmata (Jin et al., 2000), *NKD1* encodes an IDD-type transcription factor (Gontarek et al., 2016), *SAL1* encodes a putative vacuolar sorting protein (Shen et al., 2003) and *TA2* encodes a DNA demethylase, REPRESSOR OF SILENCING 1 (ROS1) (Liu et al., 2018). While DEK1 and CR4 are positive regulators of aleurone development, *SAL1* encodes a putative negative regulator that is implicated in recycling of the positive regulatory proteins (Becraft et al., 2002; Shen et al., 2003). Importantly, previous results from this thesis (Chapter 3) suggest that the NKD1 and SAL1 components of this regulatory loop are likely to be conserved in barley.

In general, the identification of genes controlling aleurone development has been challenged by the intimate developmental relationship between the starchy endosperm and aleurone, and the difficulty in accurately harvesting pure aleurone tissue from immature seeds for molecular analysis. For example, the barley *defective seed 5* (*des5*) mutant shows defects in aleurone development but the mutation has pleiotropic effects on seed fill and the causative lesion in a gene has not been determined (Olsen et al., 2008). In addition to this, the formation of the aleurone in barley appears to be under the control of multiple genes. A previous study identified several quantitative trait loci (QTL) that influence the number of aleurone layers in an Erhard Frederichen × Criolla Negra population (Jestin et al., 2008). One of the QTL identified on chromosome 7H was located close to the *SAL1* gene, but genetic analysis suggested allelic variation in *SAL1* was not the basis of the phenotype. At the molecular level, few resources are available for the developing barley aleurone tissues that might help to complement mutant and QTL analysis. Betts et al. (2017) harvested aleurone tissues from mature barley grain to identify genes expressed during germination, but these are unlikely to relate directly to genes involved in aleurone formation. By comparison, laser

microdissection was used in maize to generate cell type specific profiles of different grain compartments, thereby identifying genes expressed in the aleurone during kernel development (Zhan et al., 2015).

To date, a broad survey of the intra-species variation in aleurone development coupled to genetic analysis has not been applied to barley. In Chapter 4, variation in mature aleurone morphology was reported in a small population of 33 barley genotypes (Aubert et al., 2018), suggesting that a genome wide scan for genetic variation might be possible in a larger panel of genotypes. Genome Wide Association Studies (GWAS) are a useful tool to investigate the genetic architecture of diverse traits, since the barley cultivation process has led to the development and identification of over 460,000 barley accessions, including cultivars, landraces, breeding lines and wild *Hordeum* relatives (Sato et al., 2014). By utilising numerous barley genotypes together with the sequenced genome (Mayer et al., 2012; Mascher et al., 2017), it is possible to narrow down candidate loci and potentially genes that contribute to the trait of interest (Houston et al., 2014; Hassan et al., 2017a).

In this study, 150 European 2-row spring barley genotypes were surveyed to measure natural variation in mature aleurone morphology using the autofluorescence method developed in Chapter 4. Differences were confirmed by histological analysis of grain development in a subset of divergent cultivars, which also revealed the stages of grain development when differences appear. The measurements on mature aleurone were coupled with genotypic data and utilised for GWAS to identify regions of the barley genome associated with variation in aleurone morphology. The expression of candidate genes located in these regions was assessed by RNAseq of laser-capture microdissected grain tissues and wholegrain samples from divergent cultivars. Analysis of these transcriptomes identified potential candidate genes that may

influence aleurone development in barley or be used as aleurone marker genes for future analysis, and identified potentially important allelic differences in candidate genes in different cultivars.

Methods and materials

Plant material and growth conditions

A population of 2-row spring-type barley was provided by the James Hutton Institute (Comadran et al., 2012). This population comprised 150 lines grown in The Plant Accelerator, Adelaide, Australia, at day and night temperatures of 22°C and 15°C, respectively. The genotyped population was selected to contain minimum population structure while maintaining as much diversity as possible (Comadran et al., 2012; Hassan et al., 2017a). Mature grains were stored at room temperature until selected for morphological analysis.

Genotyping of SNP markers

All lines were genotyped using the 9K iSelect SNP genotyping platform described previously (Comadran et al., 2012). Prior to GWAS analysis, all monomorphic markers with an allele frequency of > 95% and markers with missing data > 5% were excluded from the analysis.

Transverse grain and aleurone morphological trait analysis

To observe the aleurone in mature grain, three to five grain were collected from the middle of a representative spike for each line in one generation, sectioned by hand and used to measure transverse grain features as described in Aubert et al. (2018). Grain morphology traits were recorded using the ZEN 2012 software (Zeiss, Germany) as described in Chapter 4 (Aubert et al., 2018). Endosperm area was measured by tracing

the outline of the whole endosperm, whist aleurone area was measured by tracing around the starchy endosperm and subtracting from the total endosperm area. Aleurone proportion was measured by taking the aleurone area as a percentage of the endosperm area. Aleurone layer number was recorded as an average where, in each section of barley grain, a maximum and minimum layer number was recorded at the dorsal and two lateral positions. Similarly, aleurone width was measured as the distance from the most peripheral autofluorescent aleurone wall to the starchy endosperm, where the endpoint was marked by the innermost autofluorescent aleurone cell wall. Interesting genotypes identified were analysed across three generations.

Whole grain phenotypic analysis

Barley grain weight, dimensions and screenings (a measure of seed size), were determined using a SeedCount™ SC4 (Seed Count Australasia, Condell Park, Australia), following manufacturer's instructions.

Correlation analysis and figure preparation

All correlation and PCA analyses were carried out in RStudio using the 'corrplot' package. (RStudio®, Boston, USA; https://cran.r-project.org/web/packages/corrplot/corrplot.pdf). Selected graphs were prepared in GraphPad Prism or Microsoft Excel. Statistical differences were determined using one-way ANOVA followed by the Tukey-Kramer test. Molecular phylogenetic analysis was determined by using the Maximum Likelihood method based on the Tamura-Nei model

(Tamura and Nei, 1993; Kumar et al., 2018). Phylogenetic analysis involved 150 nucleotide sequences generated from the 9K iSelect SNP genotyping dataset from each cultivar, where a total of 7842 SNP positions were present in the final dataset. The phylogenetic tree was assembled and drawn to scale using MEGA-X (Kumar et al., 2018) with branch lengths measured in the number of substitutions per site. Initial tree(s) for the heuristic search were obtained automatically by applying Neighbor-Join and BioNJ algorithms to a matrix of pairwise distances estimated using the Maximum Composite Likelihood (MCL) approach and the topology with the superior log likelihood value was selected. Figures were assembled in Adobe Photoshop CS6 and Adobe Illustrator CS6.

Grain germination and sample preparation for enzyme assays

Grain from selected barley cultivars were germinated for enzyme analysis as following the method described in Chapter 4 (Aubert et al., 2018).

Hydrolytic enzyme assays

Enzyme assays were performed on both mature grain and dried germinated grain flour, respectively, using downscaled methods (approximately four-fold) from Megazyme (Ireland) (Betts et al., 2017). The β-Glucanase Assay Kit (K-MBGL) (McCleary and Shameer, 1987), the α-Amylase Assay Kit (K-CERA) (McCleary et al., 2002) and the Betamyl-3; β-Amylase Kit (K-BETA3) (McCleary and Codd, 1989) were all used following manufacturer's instructions.

Tissue collection

Developing grains were staged by opening florets and squashing anthers on a fingernail to determine when the anthers were ready to rupture and had pollen present. If pollen was present, this was marked as 0 days post anthesis (DPA). Various developmental stages were collected for microscopy analysis, these included 7, 9, 11, 13, 15, 20 and 25 DPA. To observe aleurone morphology, staged samples were fixed in 0.25% glutaraldehyde, 4% paraformaldehyde and 4% sucrose in phosphate-buffered saline (PBS; pH 7.2), embedded in LR-White resin and sectioned to 1.0 µm. Sections were stained with toluidine blue (ProSciTech, Australia).

RNA extraction and cDNA synthesis

Developing barley grains were collected at stages mentioned above (7 – 25 DPA) with embryo tissue removed using a razor blade. Fresh tissue was placed into liquid nitrogen and stored at –80°C until required. Total RNA was extracted using the SpectrumTM Plant Total RNA kit (Sigma-Aldrich, Darmstadt, Germany). Post DNase treatment with the Ambion® TURBO DNA-*free*™ kit was completed according to the manufacturer's instructions (Life Technologies Corporation, USA). The Superscript®III Reverse Transcriptase kit (Invitrogen, USA) was used to synthesise cDNA according to Burton et al. (2008).

Primer Design

Primers for *HvNKD1* (HORVU2Hr1G095730), *HvCR4* (HORVU7Hr1G071390) and *HvSAL1* (HORVU7Hr1G115800) were designed to encompass some coding

sequence, the stop codon and the 3' untranslated region (UTR) using Primer3 (v.0.4.0) (Untergasser et al., 2012), as shown in Table 5-S11. Primers were used in a blastn search against the barley nucleotide sequences available on the NCBI database (http://blast.ncbi.nlm.nih.gov/Blast.cgi) to obtain full length gene sequences and to determine primer pair specificity in Geneious version 8.1.3. (Kearse et al., 2012).

Quantitative polymerase chain reaction

qPCR was conducted based on Burton et al. (2008); primers and PCR products are described in Table 5-S11. Two biological replicates of cDNAs from developing grains, 7 – 25 DPA, were used. Normalisation factors from control genes (see Table 5-S11) were determined according to Vandesompele et al. (2002) and Burton et al. (2004). Normalisation factors were generated from the geometric means of control genes (Vandesompele et al., 2002; Burton et al., 2004).

RNAseq Analysis

Developing grain were collected from six barley cultivars including Alabama, Class, Extract, Hopper, Sloop and Taphouse at 7, 9, 11, 13, 15 and 20 DPA. The embryo was discarded and all remaining (wholegrain) tissues were frozen in liquid nitrogen. At least six grains from three independent plants were collected and pooled to form a single composite sample at each time point. RNA for all samples was extracted as described above. Samples were submitted for sequencing using the Illumina Hiseq Platform (AGRF, Australia), and reads were assembled against the most recent barley reference sequence using CLC Genomics (Mascher et al., 2013; Mascher et al., 2017).

Normalised read counts (transcripts per million; TPM) were determined for each HORVU sequence and used to determine the abundance of each transcript in each sample.

Laser Capture Microdissection

Laser capture microdissection was carried out as described by Tucker et al. (2012) with minor modifications. Developing barley grains were collected at stages mentioned above (7 – 25 DPA), cut in half and immediately fixed with an ice-cold mixture of 3:1 ethanol: acetic acid and 1mM 1,4-Dithiothreitol (DTT). Samples were stored at 4°C overnight then placed in 70% ethanol and kept at -20°C until required. Samples were dehydrated in an ethanol series from 10%, 30%, 50%, 70 %, 80%, 90%, 95% and 100% ethanol (all with + 1mM DTT) and embedded in BMM resin containing 40mL n-butyl methacrylate, 10mL methyl methacrylate, 250mg benzoin methyl ether (ProSciTech, Australia) and 1mM DTT in BEEM capsules (ProSciTech, Australia). Samples were polymerised in a Cryo Chamber located in the Koltunow lab at CSIRO Agriculture and Food set at -20°C under UV light for 5 days. Transverse sections (5µm thick) were cut from the middle of the grain using a glass knife and ultramicrotome (Leica microsystems, Germany) and placed onto water droplets on a PEN-Membrane slide (Leica microsystems, Germany) on a 42°C slide warmer. Pericarp, aleurone, outer starchy endosperm (containing the sub-aleurone zone of the starchy endosperm) and inner starchy endosperm tissue were dissected using a Leica LMD Laser Dissection Microscope (Leica microsystems, Germany).

LCM RNA Extraction, Amplification and cDNA Synthesis

Total RNA from laser dissected tissues was extracted with a Picopure RNA isolation kit (Molecular Devices, USA) using DNase I. RNA integrity and concentration was determined using a NanoDrop One (Thermo Fisher Scientific, USA). Total RNA was used in two rounds of amplification using a MessageAmp II aRNA Amplification kit (Thermo Fisher Scientific, USA). cDNA synthesis was performed using the Superscript®III Reverse Transcriptase kit (Invitrogen, USA) according to Burton et al. (2008), however, random hexamer primers from Roche Transcriptor First Strand cDNA Synthesis Kit (Roche Molecular Systems, Australia) were used instead of the Oligo dT Primer.

GWAS Analysis

As part of the GWAS process, marker-trait association analysis was carried out in GenStat 15th Edition using the Eigen analysis relationship model. The mean values for wholegrain and aleurone measurements were used as trait values. To identify genes within intervals associated with the trait of interest, the Barleymap website (http://floresta.eead.csic.es/barleymap/) was used. SNPs significantly associated with the trait of interest (highest LOD score) were examined with the intervals being extended by 2.5 cM either side of the SNP(s) to account for marker order uncertainty. Other SNPs within 5 cM of the significantly associated SNP were considered to be linked to that SNP. To obtain more consistent map locations, marker positions were compared across three maps described in Comadran et al. (2012), IBGS (2012), and Mascher et al. (2013). QTL nomenclature is as described by Szűcs et al. (2009) and available at (http://wheat.pw.usda.gov/ggpages/maps/OWB/).

Bioinformatics and gene identification

Genes of interest within expression datasets and QTL intervals were selected using a number of methods. Makers with the highest LOD score and surrounding markers with LOD ≥ 3 were taken as QTL regions and analysed further. HORVUs were extracted from these regions using the Barleymap website (http://floresta.eead.csic.es/barleymap/). Concurrently, several lists of genes were developed using results from both wholegrain RNAseq and LCM tissue-specific RNAseq. In the wholegrain dataset, transcripts from two high aleurone varieties, cv Extract and Taphouse, were pooled to create a “high” expression pattern and transcripts from three low aleurone lines, cv Alabama, Hopper and Pewter, were pooled to create the “low” expression pattern. A similar genotype pooling approach was used to identify candidate natural modifiers of shoot meristem development in Arabidopsis (Tucker et al., 2013). Genes showing differential expression (logFC difference ≥ 2) between pooled “high” and “low” aleurone cultivars from at least one developmental stage were identified. Similarly, genes were required to show a normalised TPM expression value of at least 10 at a minimum of one developmental stage. The LCM data was analysed to identify genes that were expressed in the aleurone and/or outer starchy endosperm samples with a TPM value greater than 10 at 13 and/or 25 DPA. Furthermore, genes showing differential expression (difference logFC ≥ 2) between the “aleurone” and “outer starchy endosperm” were noted. The overlaps between these individual lists were visualised using VennPainter (Lin et al., 2016). This process was repeated for various QTL regions. Gene ontology (GO) analysis was performed using agriGO, using the corresponding rice LOC identifier for each barley HORVU gene (Tian et al., 2017).

Results

Sub-epidermal grain features vary in different European genotypes of 2-row spring barley

A population of 150 glasshouse-grown European 2-row spring barley (EU) cultivars was used in this study. This population was selected to incorporate broad genetic variability and limited population structure (Hassan et al., 2017a). From this population, a subpanel of 101 cultivars with normal grain filling was selected to avoid potentially confounding effects of a poor-quality seed set. Transverse grain sections were generated for all cultivars to assess features of the barley aleurone and grain at maturity (Figure 5-1) and significant statistical differences were identified (Figure 5-1, Figure 5-S1, Figure 5-S2, Table 5-S1). Aleurone layer number was not evenly distributed around the entire grain periphery. Hence, the number of layers from three regions (dorsal, left and right) was averaged to provide a representative measurement for comparisons between cultivars. The average number of aleurone cell layers for all cultivars was 2.7 ± 0.7 layers, which was similar to the average observed in Chapter 4 (2.4 ± 0.2), but this varied significantly depending on the genotype. For example, cv Host (3.4 ± 1.0; Table 5-S1) and cv Minstrel (3.4 ± 1.1; Figure 5-1D, Table 5-S1) typically possessed more aleurone cell layers, cv Cellar showed an intermediate number of layers (2.7 ± 0.7; Figure 5-1E, Table 5-S1) and cv Alabama possessed significantly fewer layers (2.1 ± 0.9; Figure 5-1F, Table 5-S1). Additionally, genotypes differed in regards to aleurone width, with an average of 66.7 ± 11.6 µm, which was significantly larger than the average observed for material in Chapter 4 (53.2 ± 6.5 µm). The cv Pitcher showed a thick aleurone (89.9 ± 18.7 µm; Figure 5-1G, Table 5-S1), cv Franklin (67.1 ± 7.9 µm; Figure 5-1H, Table 5-S1) was intermediate and cv Pewter (47.9 ± 8.6 µm; Figure 5-1I, Table 5-S1) possessed a thinner aleurone. With respect

to aleurone-specific measurements, the values appear to display normal distributions (Figure 5-2A). Principle component analysis (PCA) separated the genotypes based on seven transverse grain measurements (Figure 5-2B and 5-S1). Genotypes such as cv Extract, Taphouse, Class, Pewter, Alabama, Fairytale, Vankkuri and Celebra showed distinct differences. Phylogenetic analysis revealed a number of the high and low cultivars appeared to show some overall genetic similarity in the context of the European cultivar subpanel (Figure 5-2C).

Some mature aleurone features are related to wholegrain measurements

Wholegrain traits were recorded using a SeedCount™ system or seed scanner and correlations with aleurone traits were examined. Two correlation plots were generated, one with 150 genotypes and the other with the 101 genotypes selected to avoid potentially confounding effects of a poor-quality seed set (Figure 5-3, Table 5-S1). While many traits appeared unrelated to each other, some showed strong correlations. Similar to that reported in Chapter 4 for the University of Adelaide (UA) panel, aleurone area correlated with endosperm area (0.57*** and 0.52***, representing the correlation coefficient and level of significance, Figure 5-3A-B), while aleurone proportion negatively correlated with endosperm area (-0.76*** and -0.54***, Figure 5-3A-B). This is consistent with our previous observations that bigger grains contain more aleurone, but the proportion of aleurone in grain decreases relative to the amount of starchy endosperm. Increased aleurone area appeared to be driven by aleurone width (0.82*** and 0.76***, Figure 5-3A-B), while layer number had little impact in the 150 genotypes (0.23*, Figure 5-3A) and no impact in the smaller panel of 101 genotypes. Curiously,

layer number contributed to aleurone width in the full panel (0.3**, Figure 5-3A) but not the smaller panel.

Some wholegrain traits also appeared to correlate with the aleurone measurements. For example, grain weight, width and thickness all correlated with aleurone area (0.25**, 0.22**, 0.24**, respectively, Figure 5-3A) and the correlations improved in the set of well-filled genotypes (0.29**, 0.30**, 0.31**, respectively, Figure 5-3B). Grain thickness also correlated with aleurone width, but only in the smaller panel (0.20*, Figure 5-3B). These correlations, albeit weak, are likely to reflect an effect of endosperm area on seed size rather than a direct effect of the aleurone. Interestingly, no wholegrain trait appeared to significantly correlate with aleurone layer number, confirming that layer number at the midpoint of the grain is independent of grain size. This held true for both the complete 150 genotype and 101 genotype panels (Figure 5-3A and 5-3B, respectively). In the larger panel, aleurone proportion showed weak correlations with grain weight (-0.22*), roundness (0.26*), width (-0.25*) and thickness (-0.19*), while no correlation was observed in the 101 genotype panel. These correlations may reflect the issues with grain fill (i.e. abnormal starchy endosperm area), since almost one third of the genotypes in the 150 panel were biased towards having increased aleurone proportion due to the relationship between endosperm area and aleurone proportion (see Chapter 4). Taken together, these results appear to be consistent with those reported in Chapter 4 for the UA panel. Increased transverse aleurone measurements in mature barley grain are mainly determined by expansion of aleurone cells and starchy endosperm area, with a limited effect from aleurone layer number that appears to vary independently of other grain measurements in a genotype-dependent manner.

To examine some compositional aspects of the aleurone, cell wall components such as (1,3;1,4)-β-glucan, arabinoxylan, ferulic acid and p-coumaric acid were also examined for aleurone trait correlations (data collected from Houston et al. (2014), Hassan et al. (2017a) and Hassan et al. (2017b); Figure 5-S3). When examining the non-cellulosic polysaccharides, (1,3;1,4)-β-glucan and arabinoxylans, only arabinoxylan correlated with aleurone proportion (0.23*) and negatively correlated with aleurone layer number (-0.26*). This suggested that more arabinoxylan was present in genotypes with more aleurone proportion but did not increase with more aleurone layers. Similarly, when examining aleurone phenolic content, specifically ferulic acid and p-coumaric acid, only p-coumaric acid weakly correlated with aleurone area (0.25*), suggesting that genotypes with more aleurone area had more p-coumaric acid. Further analysis of other aleurone compositional components would be of interest in the future.

Morphological differences in the aleurone appear during early stages of grain development in high and low genotypes

Based on the PCA analysis (Figure 5-2B) and correlation plots (Figure 5-3A and 5-3B), interesting genotypes were identified that possess distinct aleurone traits (Figure 5-S4, Table 5-S2, Table 5-S3). Since grain fill and endosperm area appear to have some impact on transverse aleurone features, we focussed on six genotypes that show “average” endosperm area but differences in aleurone traits such as aleurone area, proportion and width. Genotypes were selected based on possessing large or small aleurone traits, i.e. large aleurone area, proportion and width, becoming the “high” group and vice versa. Three “high” genotypes (cv Extract, Class and Pitcher), two “low”

genotypes (cv Alabama and Pewter) and one average genotype (cv Franklin) were selected for further analysis. Two further lines were also selected that showed small (cv Taphouse) and large (cv Hopper) grain size, in addition to larger or smaller aleurone traits than expected compared to genotypes of a similar grain size. All eight genotypes were re-sown and grains were harvested at selected time-points to track the development of aleurone tissue. Analysis of mature grains across three generations showed some variability in aleurone morphology. However, some trends remained stable in that high aleurone genotypes were likely to remain high when compared to the other genotypes (Figure 5-S5). To assess when differences appeared in the aleurone during grain development, samples were sectioned and stained with Toluidine Blue (Figure 5-4, Figure 5-S6, Figure 5-S7). Two genotypes, cv Extract and Alabama, were selected to represent high and low aleurone genotypes. As seen in Figure 5-4, aleurone cells were apparent at the periphery of both genotypes at 11 DPA, as defined by the darker Toluidine Blue stain and possessing a small cubical cell structure. Prior to this at 9 DPA, the cells at the periphery of the starchy endosperm in cv Extract (Figure 5-4G) already exhibited some aleurone characteristics and appeared more cuboid in shape. At the same stage in cv Alabama (Figure 5-4B), fewer cells appeared to have adopted a cubical shape. Similarly, at 11 DPA (Figure 5-4C and 5-4H), cv Extract appeared to have thicker aleurone with more aleurone cell layers on average when compared to cv Alabama (26 µm and 2-3 layers compared to 18 µm and 1-2, respectively). This also appeared to be consistent when comparing other high (cv Class) and low (cv Pewter) lines (Figure 5-S6). Similarly, in later developmental stages, aleurone cell size and layer number appeared larger in cv Extract compared to cv Alabama (Figure 5-4) and was consistent throughout the other genotypes (Figure 5-S6; Figure 5-S7). Extract, Alabama and the remaining six genotypes of interest are

the focus in this study for further experiments to determine if altered aleurone traits are due to genetic differences between these lines.

Markers of aleurone cellular identity and candidate regulators of aleurone development are differentially expressed in high and low aleurone genotypes

Genes contributing to aleurone development have been identified in maize, and include *DEFECTIVE KERNEL 1* (*DEK1*), *CRINKLY 4* (*CR4*), *NAKED ENDOSPERM 1* (*NKD1*) and *SUPERNUMERARY ALEURONE LAYER 1* (*SAL1*) (Becraft et al., 1996; Shen et al., 2003; Tian et al., 2007; Olsen et al., 2008; Yi et al., 2015). Other genes that act as specific markers for the aleurone include *LIPID TRANSFER PROTEIN 2* (*LTP2*), which has been described in a number of studies (Kalla et al., 1994; Morino et al., 2004; Wisniewski and Rogowsky, 2004; Gruis et al., 2006). We considered the possibility that the barley orthologues of these genes might show differential expression in genotypes showing differences in aleurone development. To assess this, RNA was extracted across the key stages of aleurone development (7-25 DPA), converted into cDNA and relative transcript abundance for genes of interest was measured by quantitative PCR (qPCR; Figure 5-5; Table 5-S4; Table 5-S5). The aleurone marker gene *HvLTP2* (Kalla et al., 1994; Opsahl-Sorteberg et al., 2004) was first detected between 7 and 11 DPA, and in general showed an increase in transcript abundance across grain development. However, the stage at which expression was first detected differed between the genotypes. Transcript was detected in all of the high genotypes (i.e. cv Extract, Class and Taphouse) at 9DPA, but was not detected in the low genotypes (i.e. cv Alabama, Hopper and Pewter) until 11 DPA. Transcript was also detected at 9 DPA for cv Pitcher, Sloop and Franklin, which tend to be high to intermediate genotypes. By contrast, at 25 DPA transcript levels for *HvLTP2* tended to be higher in the low genotypes (cv Alabama, Hopper and Pewter) than that detected

in the high to intermediate genotypes. Thus, earlier expression of *HvLTP2* (7-9 DPA) corresponds to the early appearance of aleurone shown by cytology and eventually to more aleurone at maturity. The later appearance of *HvLTP2* expression (10-12 DPA) and higher expression at 25 DPA appears to correspond to the later appearance of aleurone cells and smaller aleurone measurements at maturity.

The putative regulator of aleurone proliferation and identify, *HvNKD1* was also detected at 7 DPA and in general showed an increase in transcript abundance until mid-aleurone development before decreasing during aleurone maturation (Figure 5-5B). However, transcript significantly differed between the high and low genotypes at 9 DPA. This earlier abundance of *HvNKD1* expression may correspond to the advanced/faster aleurone differentiation observed in high aleurone genotypes compared to low aleurone genotypes at 9 DPA. As observed in *HvLTP2* abundance, *HvNKD1* transcript levels tended to be higher in the high genotypes than that detected in the low to intermediate genotypes, which may also correspond to the later appearance of aleurone cells. For the remaining two genes, *HvSAL1* and *HvCR4*, transcripts showed no significant differences between high and low genotypes (Figure 5-5C and 5-5D). *HvSAL1* showed a steady transcript abundance throughout grain development before dropping at 25 DPA. Higher abundance of transcript was observed in high aleurone genotypes compared to the low class, however, since large variations were observed it is impossible to assign any significance. *HvCR4* showed a decrease in transcript abundance across grain development before becoming significantly different at 25 DPA. However, transcript abundance was much lower compared to the other genes and was generally similar for both high and low aleurone genotypes.

GWAS analysis and SNP identification

The expression patterns of *HvNKD1* and *HvLTP2* in the different genotypes are consistent with morphological differences in aleurone development, but it is unclear whether the effects are causative or consequential. Combined with the results of Chapter 3, where *HvNKD1* was identified as a putative positive regulator of aleurone layer number, area and proportion, we considered that *HvNKD1* may play a broader role influencing natural variation in aleurone development. To assess this, a GWAS was performed using the 101 well-filled genotypes to identify regions significantly associated with variation in aleurone morphology, i.e. aleurone area, layer number, proportion and width. A total of 4559 SNP markers with a minimum allele frequency of 5% and less than 5% missing data were used to conduct the GWAS. An Eigenstrat model was used to account for any population structure and to reduce the risk of false positive associations. Twenty-one significant marker associations with a $-\log_{10}(P) \geq 3$ were identified across the four aleurone measurements (Figure 5-6; Table 5-1). Significant associations were found on all barley chromosomes and the strongest QTL, QALN2.S-5H1, was located on chromosome 5H (~89 cM) with a $-\log_{10}(P)$ value of 4.88. Two of the aleurone traits, layer number and width, appeared to have similar associations on chromosome 2H (QALN2.S-2H2 and QAT2.S-2H1) at 89.5 cM and 93.86 cM, respectively, and on chromosome 5H (QALN2.S-5H2 and QAT2.S-5H1) at positions 156.5 cM and 156.82 cM, respectively (Table 5-1). This was curious since, in our data, aleurone layer number and aleurone thickness traits didn't significantly correlate with each other (Figure 5-3B). While these QTL are relatively close together, the most significantly associated markers are still different between them, suggesting that these are not the same QTL.

The position of the QTL was compared to the approximate location of candidate regulators of aleurone development including *HvNKD1* (Chr 2H, 86 cM), *HvSAL1* (Chr 7H, 129 cM), *HvCR4* (Chr 5H, 42 cM; MLOC) (Chr 7H, HORVU) *HvDEK1* (Chr 6H, 65 cM) and *HvROS1* (Chr 5H, 48 cM). Although these positions did not lie directly within any QTL positions, the close proximity of *HvNKD1* to QALN2.S-2H2 and QAT2.S-2H1 was of interest. Despite this, when examining SNP markers located directly within *HvNKD1* and *HvSAL1*, no correlations were identified with aleurone traits (Table 5-S6A and 5-S6B). This suggests that barley orthologues of maize genes involved in aleurone development are unlikely to directly explain the natural variation observed in this panel.

RNA expression profiles of specific grain stages and tissues reveal genes showing differential transcript patterns in high and low aleurone lines

To narrow the number of genes that are co-located with QTL and also potentially contribute to natural variation in aleurone development, several different RNAseq datasets were generated. The first dataset comprised a developmental time course of wholegrain (minus embryo) samples at 7, 9, 11, 13, 15 and 20 days post anthesis (DPA). Tissues were collected from high genotypes including cv Extract and Taphouse, and low genotypes including cv Alabama, Hopper and Pewter. RNA from cv Sloop was also examined as a reference (see Chapter 4). To assess the quality of these datasets, we again examined the expression of *HvLTP2*, *HvNKD1*, *HvSAL1* and *HvCR4*. The results show that qPCR and RNAseq transcript analysis produced similar patterns. The most notable similarities were the early differences between high and low genotypes at 9 DPA for *HvLTP2*, *HvNKD1* and *HvCR4* (Figure 5-S8).

Next, genes were identified that show differential expression between cultivars at one or more stages of grain development. In the most stringent approach, transcripts from two high aleurone varieties, cv Extract and Taphouse, were pooled to create a “high” expression pattern and transcripts from three low aleurone lines, cv Alabama, Hopper and Pewter, were pooled to create the “low” expression pattern. A similar genotype pooling approach was previously used to identify candidate natural modifiers of shoot meristem development in Arabidopsis (Tucker et al., 2013). As a minimum threshold for gene abundance, only HORVUs with a TPM value of 10 or greater in at least one developmental stage (DPA) were analysed. There are estimated to be 81683 genes in barley, and of these, 14014 genes (17%) were expressed during at least one stage of grain development. Of these, 1316 genes were significantly differentially expressed between the high and low genotypes based on a fold change (FC) ≥ 2 or ≤ 0.5 and p-value ≤ 0.05. *HvLTP2* and *HvNKD1* were the only genes previously mentioned to be included within this list. Gene ontology (GO) analysis revealed 47 significantly unique GO identifiers and confirmed that these genes are predicted to be involved in diverse biological processes associated with grain development (Figure 5-S9, Table 5-S7).

The second dataset was generated using laser microdissection (LCM) to collect specific grain tissues from developing barley caryopses (cv. Sloop), as described in Chapter 4. RNA from microdissected pericarp, aleurone, outer starchy endosperm and inner starchy endosperm tissues at 13 DPA and 25 DPA was amplified and sequenced to generate tissue specific profiles. Analysis of the sequencing data suggested that 12087 genes (15%) are expressed in at least one of the tissues at the two stages. Of these, 8354 genes were detected in at least one of the aleurone samples. Examination of *HvLTP2*, *HvHorB1*, *HvNKD1*, *HvSAL1*, *HvCR4* and *HvDEK1* expression in the LCM data revealed distinct patterns (Figure 5-7). In terms of *HvLTP2* and *HvHorB1* (*B1*

HORDEIN), the patterns were consistent with the expected location of expression (i.e. aleurone and starchy endosperm, respectively) and matched those reported in Chapters 3 and 4. The other genes showed patterns that varied in terms of absolute abundance and the preferred location of expression. Notably, analysis of *HvNKD1* suggested that it was predominately expressed in the aleurone and outer starchy endosperm with some expression in the pericarp. Additionally, *HvSAL1* expression was observed in the aleurone and outer starchy endosperm, however, it was predominately expressed in the pericarp. Genes such as *HvCR4* and *HvDEK1* were also predominately expressed in the aleurone but transcript abundance was substantially lower than that of *HvNKD1* and *HvSAL1*.

The LCM data was examined to identify genes that were enriched in the aleurone or outer-starchy endosperm relative to other grain tissues. Using a cut-off of log2FC ≥ 2, 709 genes were enriched in the aleurone relative to the outer starchy endosperm, inner starchy endosperm and pericarp at 13 DPA, while 51 genes were enriched in the outer starchy endosperm relative to other tissues. At 25 DPA, 2507 genes were enriched in the aleurone relative to the outer starchy endosperm and inner starchy endosperm, and 111 genes were enriched in the outer starchy endosperm. These datasets were compared, revealing that 238 genes were aleurone-enriched and two genes were enriched in the outer-endosperm at two the distinct stages (Table 5-S8). LCM and wholegrain datasets were also compared, revealing that 10 aleurone-enriched genes were also differentially expressed between high and low aleurone lines, while no outer-endosperm enriched genes showed differential expression (Figure 5-8). From the aleurone-enriched genes, GO analysis revealed 90 significantly unique GO identifiers where genes are predicted to be involved in protein metabolic processes and gene expression and regulation (Figure 5-S10, Table 5-S10).

Collectively, these different RNAseq sets provide a significant resource to analyse genes involved in barley aleurone development as well as to narrow down candidate genes underlying QTL that influence aleurone morphology.

Candidate genes involved in aleurone development co-locate with aleurone QTL

To test the robustness of the expression datasets, genes predicted to be located within the four QTL intervals of interest were examined. To generate these gene lists, the most significant marker association for each of the four aleurone traits was selected for analysis, including QAA2.S-6H1 ($-\log_{10}(P) = 4.00$), QAP2.S-2H1 ($-\log_{10}(P) = 4.82$), QAT2.S-7H1 ($-\log_{10}(P) = 4.22$), and QALN2.S-5H1 ($-\log_{10}(P) = 4.88$) (Table 5-1). Gene lists were extracted from a 5cM window flanking these markers, resulting in candidate lists of 251 genes, 99 genes, 140 genes and 358 genes for each QTL respectively. All ATL and expression lists were compared and the outputs are shown as a Venn diagram (Figure 5-8)

To be considered as an interesting gene, the basic selection criteria was a minimum expression value of TPM > 10 in at least one developmental stage (DPA) and at least one tissue. Additional criteria were considered including (1) the gene was expressed in the aleurone at 13 and/or 25 DPA, (2) the gene was differentially expressed between high and low aleurone lines and (3) the gene was differentially expressed in the aleurone or outer starchy endosperm at 13 and/or 25 DPA. Using the Venn Diagram (Figure 5-8), only one gene fulfilled all of the most stringent selection criteria. This gene encoded a Katanin p60 ATPase-containing subunit (KATNAL2) (HORVU3Hr1G072910). In addition, eleven genes were identified within the QTL

intervals that were enriched in the 13 DPA or 13+25 DPA aleurone samples, but were not differentially expressed between the high and low cultivar groups (Table 5-S8; Figure 5-8; Table 5-S9). These consisted of multiple undescribed proteins and histone superfamily proteins, as well as an oleosin, receptor-like kinase and transcription factor (Table 5-S8; Figure 5-8; Table 5-S9). An additional 31 genes were identified within the QTL intervals that were enriched in the 25 DPA aleurone sample; these are indicated in Table 5-S8 but were not considered in further detail here since the morphological differences between cultivars appeared much earlier. Finally, ten genes were also identified that showed differential expression and were aleurone enriched but were not located within the QTL intervals (Table 5-S8; Figure 5-8; Table 5-S9). Wholegrain and LCM RNAseq transcript patterns for selected genes located in the QTL regions and enriched in the 13 DPA (and possibly 25DPA) aleurone are shown in Figure 5-S11 and Figure 5-S12, where dynamic transcript patterns can be observed.

Discussion

Sub-epidermal grain features show natural variation across a diverse panel of barley genotypes

The aleurone is a crucial tissue that performs important roles in grain development and germination, and affects applications in the health and brewing industries (Burton and Fincher, 2014). In this study, we focus on the multilayered aleurone of barley and used autofluorescence microscopy to assess morphology at grain maturity. A panel of diverse European barley genotypes (EU) showing minimal or no population structure was analysed by GWAS and coupled with molecular studies to identify candidate genes that may be involved in aleurone development.

Within the barley grain, the aleurone and starchy endosperm are both derived from the fertilised central cell and only begin to differentiate around 7-10 days after pollination (Bosnes et al., 1992; Kalla et al., 1994; Burton and Fincher, 2014; Aubert et al., 2018). A previous study (Chapter 4) examined the relationship between aleurone and other grain traits in a panel of 33 barley genotypes (UA), showing that in most cultivars, the development of the starchy endosperm and aleurone are intimately linked. Here, we confirmed this observation in a larger panel of 150 barley genotypes from Europe. Cultivars producing grain with more aleurone layers also tended to have a wider aleurone, and this aleurone width contributed directly to aleurone area. However, this observation didn't hold true for the subpanel of 101 cultivars (with well-filled grain) since no significant correlation between aleurone width and the number of aleurone layers was identified. A weak correlation was observed between these traits, but it failed to make significance thresholds (Figure 5-S2). Similar to the UA panel in Chapter 4, aleurone layer number was only weakly correlated with aleurone area, suggesting that

aleurone cell expansion is likely to be the main determinant of aleurone thickness. In some geneotyes, the relative amount of aleurone may also be influenced by grain fill independent of aleurone layer number or cell size, since a reduction in aleurone proportion correlated with an increase in starchy endosperm area. This could be due to due to physical constraints imparted by the pericarp and starchy endosperm (Aubert et al., 2018). Alternatively, it is possible that the aleurone itself contributes directly to grain fill. Xu et al. (2016) identified an aleurone layer specific NUCLEAR FACTOR Y (NF-Y) transcription factor (OsNF-YB1) in rice that regulates grain fill and endosperm development. This role is achieved through direct regulation of genes involved in the transport of nutrients such as sugars and amino acids.

In our current analysis of 150 genotypes, it was observed that almost one third exhibited sub-optimal grain fill and therefore it was unclear how inclusion of these may skew results (Table 5-S1). Correlation analysis was repeated with the 101 genotypes showing correct/healthy grain fill (Table 5-S1). Remarkably, in the absence of the 49 poor filling genotypes, similar but slightly weaker aleurone:grain correlations were observed (Figure 5-3B), although aleurone layer number appeared to be completely independent of all other grain and aleurone traits. These data suggest that the overall relationships between tissues are relatively stable across the panel and argues against grain fill having a severe impact on aleurone measurements. In spite of this, because the precise interaction between the aleurone and starchy endosperm remains unknown and this study was focussed on four main aleurone traits, subsequent analysis focussed on the 101 genotypes where altered grain fill could be disregarded as a potentially confounding factor.

Differences in the amount of aleurone at maturity correlate with specific changes in grain composition

Chemical components of the barley grain, some of which are known to accumulate in the aleurone , were previously investigated in an overlapping set of cultivars (Houston et al., 2014; Hassan et al., 2017a; Hassan et al., 2017b). Hence, cell wall components such as (1,3;1,4)-β-glucan, arabinoxylan, ferulic acid and p-coumaric acid were also examined for aleurone trait correlations (Figure 5-S3). The non-cellulosic polysaccharide, (1,3;1,4)-β-glucan, is an important component of the cell walls of barley endosperm as it affects the production of alcoholic beverages and has significant human health benefits (Li et al., 2005; Houston et al., 2014). Arabinoxylans (AX) are the second most abundant non-cellulosic polysaccharides in cell walls of barley endosperm and are the most common polysaccharides found in the aleurone walls and outer layers of barley grain (Bacic and Stone, 1981; Fincher and Stone, 1986). Together, (1,3;1,4)-β-glucan constitutes around 75% of the barley starchy endosperm cell walls whilst AX contributes the majority of the remaining 25% of the cell wall matrix (Lee et al., 2001). When examining (1,3;1,4)-β-glucan and AX, only AX weakly correlated with aleurone proportion and negatively correlated with aleurone layer number. This suggested that overall AX content was more abundant in genotypes with more aleurone but was not necessarily due to more aleurone layers. This could also suggest that similar levels of cell wall components are present within the genotypes but dispersed across varying numbers of aleurone layers. Additionally, ferulic acid and p-coumaric acid, both phenolic acids present within the aleurone, were also examined since they can be linked via ester bonds to AX present in the cell walls of cereal grains (Nordkvist et al., 1984). However, only p-coumaric acid weakly correlated with aleurone area. Therefore, results suggest the size of the aleurone is a

contributing factor to the abundance of specific cell wall components. However, since only weak correlations were observed, other factors, such as polysaccharide biosynthesis enzymes and genetic components may potentially be stronger influencers. Collectively, some endosperm cell wall components correlate with mature aleurone traits, however further analysis examining aleurone composition in high and low cultivars is required.

Early aleurone development may lead to larger aleurone traits at grain maturity

The formation of the aleurone has been characterised in a variety of cereal species. In maize, the aleurone typically appears at 6-10 days after pollination (DAP) depending on genetic and environmental factors (Sabelli and Larkins, 2009; Chen et al., 2014; Doll et al., 2017). In rice, the aleurone can appear as early as 4-5 DPA in wild-type grains (Ishimaru et al., 2015; Xu et al., 2016), while the barley and wheat aleurone appears around 6-10 DPA (Bosnes et al., 1992; Kalla et al., 1994; Gillies et al., 2012; Burton and Fincher, 2014; Aubert et al., 2018). Here, in barley, aleurone development in five genotypes with similar transverse endosperm areas, but different aleurone morphology at grain maturity, was compared to determine when differences appear. Consistent with previous reports (Burton and Fincher, 2014), aleurone differentiation was observed between 9 and 11 DPA. From there, the aleurone appeared to undergo cell divisions between 11 and 15 DPA, whilst cell expansion occurred thereafter. Key differences were observed between genotypes. The genotypes with more aleurone area, proportion and width at maturity appeared to differentiate and develop and aleurone faster than genotypes with less aleurone. This is similar to that observed after exogenous application of auxin (see Chapter 3), suggesting that hormone signalling or

response may vary between these cultivars. This could also involve cell division and/or differentiation factors such as cyclins, cyclin-dependent kinases (CDKs) and retinoblastoma-related proteins (RBRs) may be influencing the differences observed. For example, cyclins displayed unique tissue and subcellular localisation patterns during endosperm development; in maize, CYCD5 was detected only in the aleurone and sub-aleurone layers (Dante et al., 2014). Another possibility is that the genotypes themselves may have different overall rates of development; genotypes possessing more aleurone mature faster and provided the aleurone with greater access to competitive resources. One way to measure the relative age of the grain in future studies may be to assess nucellar epidermis morphology. This maternal layer, located between the integuments and the aleurone, becomes compressed through cereal development and acts as an indicator of developmental progress (Opanowicz et al., 2011; Hands et al., 2012).

In parallel with the temporal differences in aleurone development, transcripts from *HvLTP2* and *HvNKD1* were more abundant in genotypes with more aleurone at 9 DPA. Both of these genes are expressed in the developing aleurone according to LCM qPCR and RNAseq. This suggests that at both the molecular and morphological level, the aleurone develops/differentiates earlier in the genotypes that produce more aleurone at grain maturity. Whether early *HvNKD1* expression is contributing to this earlier aleurone differentiation remains unclear. The results from Chapter 3 suggest that *HvNKD1* contributes to aleurone development without significantly contributing to grain size but disentangling the effects of the gene on initiation versus division would be best undertaken via mutant analysis.

There are several reasons why earlier aleurone development might lead to increased aleurone traits at maturity in genotypes with more aleurone. One possibility is that

earlier aleurone differentiation allows the tissue to divide and/or expand further before grain fill applies a restrictive pressure. Another possibility (not mutually exclusive from the first) is that earlier aleurone development may occur prior to the appearance of aleurone inhibitory signals in the starchy endosperm, pericarp or nucellar epidermis. Further studies will be required to determine the precise timing of aleurone initiation relative to other grain tissues, ideally using non-destructive techniques such as X-ray micro computed tomography (µCT) (Hughes et al., 2017). Moreover, the genotypes showing significant differences in aleurone traits identified here may be promising candidates for future bi-parental population studies to determine the genetic basis for differences.

A genome-wide association study reveals several QTL for aleurone traits

A popular approach to explore the genetic architecture of complex traits is the use of Genome Wide Association Studies (GWAS), whereby genomic regions can be identified as associating with particular traits. In recent years, GWAS has been utilised to identify regions associated with complex traits in barley including salt tolerance (Long et al., 2013), frost tolerance (Visioni et al., 2013), agronomic performance (Pauli et al., 2014) and (1,3;1,4)-β-glucan content of barley grain (Houston et al., 2014). Other tools can be employed in parallel, such as genetic linkage mapping with a bi-parental cross. Jestin et al. (2008) examined the inheritance of aleurone thickness and layer number using a bi-parental cross between Erhard Frederichen x Criolla Negra, a three-layer and two-layer aleurone barley, respectively. They identified various quantitative trait loci (QTL) on chromosomes 2H, 5H and 7H that associated with these aleurone traits. Here we employed GWAS to identify genomic regions associating with various

aleurone traits from a panel of 101 genotypes. QTL were identified for the four aleurone traits examined; aleurone width, layer number, area and proportion relative to the endosperm. Twenty-one QTL markers were found to associate with variation across the four aleurone traits, which did not overlap with previously identified QTL (Jestin et al., 2008). The large number of marker associations was not surprising given the number of genes that appear to influence aleurone development in other systems. Mutations in genes such as *DEFECTIVE SEED 5* (*DES5*), *TA2*, DEK1, *CR4*, *NKD1*, *SAL1* have all been found to affect aleurone development in some way (Becraft et al., 1996; Shen et al., 2003; Tian et al., 2007; Olsen et al., 2008; Yi et al., 2015). Therefore, it might be expected that these genes could be found within QTL regions or markers within these genes may show an association with aleurone traits in the GWAS output. However, when examining these candidate genes, they do not appear directly within QTL regions identified (Figure 5-6). Similarly, when examining markers within these genes, no correlations with aleurone traits could be found (Table 5-S6A and 5-S6B). This was intriguing since the twenty-one QTL identified in the GWAS may reflect novel genes contributing to aleurone development.

Candidate genes potentially involved in aleurone development are identified within genomic regions associating with aleurone traits

As described above, several genes involved in aleurone development have previously been identified (Becraft et al., 1996; Shen et al., 2003; Tian et al., 2007; Olsen et al., 2008; Yi et al., 2015). However, comprehensive cell-type specific datasets covering the stages and tissues involved in barley aleurone development have yet to be reported, making it difficult to predict molecular basis for QTL. Proir to this study,

relevant datasets were available from different cereal species, late stages of aleurone development or from the endosperm as a whole. For example, proteomes of barley grains at various later stages of seed development and germination were reported (Finnie and Svensson, 2009). Using these proteomes, factors involved in enzyme metabolism (Finnie and Svensson, 2003; Bønsager et al., 2007), hormonal response (Jacobsen and Knox, 1973; Ritchie et al., 1999; Hirano et al., 2008) and plasma membrane protein coordination (Hynek et al., 2006) were identified. Several studies have also examined aleurone gene expression in response to hormonal changes using micro-arrays in rice and barley (Bethke et al., 2006; Chen and An, 2006; Yano et al., 2015). Similarly, to identify molecular determinants of early endosperm development, custom microarray data was generated using RNA isolated from young developing barley grain endosperm (3 – 8 days after pollination) (Zhang et al., 2016). Transcriptomes for developing wheat aleurone and starchy endosperm tissue (6, 9 and 14 DPA) were also developed, and their analysis identified highly differentially expressed transcripts (Gillies et al., 2012). To improve the barley resources and address the broader molecular network involved in barley aleurone development, we generated multiple RNAseq datasets and aligned them with the GWAS data. Interesting genes identified could then be analysed within proteome, microarray and transcriptome databases to allude possible molecular functions. The transcriptome presented in this study captures large variation across grain and aleurone development since it encapsulates early, mid and late stages of barley grain development, as well as providing two stages of tissue-specific transcriptomic data. This dataset therefore provides an important resource for the barley grain community and a broader understanding of dynamic expression patterns of candidate genes identified in the GWAS output.

Of the twenty-one QTL that were identified, four were analysed in greater detail in this study (Table 5-1). These QTL produced the highest LOD for each aleurone trait and included QAA2.S-6H1 ($-\log_{10}(P) = 4.00$), QAP2.S-2H1 ($-\log_{10}(P) = 4.82$), QAT2.S-7H1 ($-\log_{10}(P) = 4.22$), and QALN2.S-5H1 ($-\log_{10}(P) = 4.88$) (Table 5-1). To narrow candidate genes of interest underlying these QTL, wholegrain and laser capture microdissection (LCM) RNAseq datasets were examined. These datasets revealed genes showing differential expression between high and low aleurone cultivars, along with tissue-specific expression in the aleurone or outer starchy endosperm tissue. Further analysis revealed genes that were aleurone-enriched, located within QTL intervals but not differentially expressed between the high and low cultivar groups. These genes are of interest given that not all causative polymorphisms between cultivars will lead to differences in mRNA levels. Finally, genes were identified as being aleurone-enriched and differentially expressed but not located within QTL intervals. Collectively, a total of twenty-two genes were identified as being promising candidates; these included several undescribed proteins, an oleosin, a receptor-like kinase and a transcription factor, all of which may be interesting for further analysis (Figure 5-S11; Figure 5-S12).

From the dataset comparisons, only one gene was identified as being aleurone enriched, differentially expressed and located within a QTL interval. This was a Katanin p60 ATPase-containing subunit (KATNAL2; HORVU7Hr1G087190; QAT2.S-7H1). *KATNAL2* encodes an ATP-dependent microtubule-severing enzyme, which promotes rapid reorganisation of cellular microtubule arrays (Roll-Mecak and McNally, 2010). KATNAL proteins normally localise within the cytoplasm, partially overlapping with microtubules and to the mitotic spindle and spindle poles during mitosis (Cheung et al., 2016). In Arabidopsis, Katanin 1 is involved in embryo sac and seed development,

whereby mutant seeds are misshapen and sometimes larger than wild type (Luptovčiak et al., 2017). The identification of this gene at the late stages of barley aleurone development (25 DPA compared to 13 DPA) might indicate a role in cell polarity or cell division (Figure 5-S12), although aleurone cell divisions appear to have ceased by this stage. Further studies will be required to determine whether this gene might play a regulatory role in aleurone development.

The identification of only one candidate QTL gene based on the selection criteria might indicate that the stringency of comparisons was too high. It is possible that QTL genes influencing aleurone development in these lines are not differentially expressed, but rather show differences in protein function. Hence we also considered genes that were ocated within QTL regions, enriched in the aleurone but not differentially expressed between cultivars, such as the undescribed protein and oleosin.

Little is known about the undescribed protein; HORVU2Hr1G098150 at this stage. Analysis of public datasets and other species suggest that it might be an oleosin. When performing a BLAST through the James Hutton Institute website, morexGenes (https://ics.hutton.ac.uk/morexGenes/), the only match for the undescribed protein sequence is the neighbouring gene, an oleosin. This may suggest another poor gene model has been identified. Micro-array data available showed that this gene is highly abundant in caryopsis tissue at 15 DPA, with some expression at 5 DPA but little to no expression is present in the remaining tissues. Additionally, using the Rice PP6 and the Arabidopsis P10 databases, the sequence matches a LOC_Os04g46200.1 and AT4G25140.1, respectively, with both possessing an oleosin annotation. When using the NCBI BLAST function (https://blast.ncbi.nlm.nih.gov/Blast.cgi), no matches were found in maize or wheat. Since the protein appears to lack defined motifs characteristic of regulatory proteins, one possibility is that the associated gene may serve as an

aleurone marker gene similar to *LTP2* (Kalla et al., 1994; Opsahl-Sorteberg et al., 2004). LTP2 is a lipid transfer protein found to be aleurone-specific, and possesses aleurone regulatory cis elements (Simmonds et al., 1998). This gene has been used in many transgenic assays targeting the development of the aleurone in a variety of species (Lid et al., 2002; Morino et al., 2004; Gruis et al., 2006). Using the datasets reported in this study, LTP2 could be used in a co-expression analysis in future studies to identify other aleurone-enriched genes that may be controlled by the same regulatory elements.

The oleosin gene, HORVU2Hr1G098160, accumulates in the aleurone but presents a different pattern to LTP2, and the specific role it contributes to aleurone development is unclear. Oleosins are structural proteins that form lipid and oil bodies within cells. Protein bodies within aleurone cells are also are surrounded by numerous oleosomes (Fernandez and Staehelin, 1985) and are mobilised upon germination, providing energy for protein synthesis via the breakdown of triacylglycerols to free fatty acids (Fernandez and Staehelin, 1987). The aleurone has been found to accumulate many oil and lipid bodies compared to other grain tissues (Chen et al., 2012; Gillies et al., 2012; Wu et al., 2016). It is possible that the oleosin protein accumulates in the aleurone but may not actually contribute mechanistically to the development of the aleurone. If this is the case, then this oleosin gene would be another candidate gene marker for the aleurone. Some additional evidence supporting this comes from maize, where oleosin genes are found to be induced by Viviparous1 (VP1). Maize Viviparous1 (VP1) and Arabidopsis ABI3 are orthologous transcription factors that regulate key aspects of plant seed development, ABA signalling and the anthocyanin biosynthesis pathway (Crowe et al., 2000; Suzuki et al., 2003; Cao et al., 2007). VP1 transcription is directly activated by NKD1 (Gontarek et al., 2016), which is required for correct

aleurone development in maize as previously mentioned (Yi et al., 2015). In barley, *HvVP1* is also predominately transcribed in the aleurone and follows a similar transcript abundance pattern as NKD1 across grain development (Figure 5-S13). Therefore, NKD1 could be indirectly affecting the expression of oleosin, possibly via VP1, within the aleurone. This might place the gene well downstream of aleurone differentiation pathways. Thw *NKD1* locus was located close to two QTL, QALN2.S-2H2 and QT2.S-2H1, but markers within and surrounding *NKD1* in the eight cultiavrs examined here showed no clear correlation with aleurone traits (Table 5-S6). Thus, other unknown genes that contribute to aleurone development may also be directly or indirectly affecting NKD1 and therefore oleosin content. Further analysis is required to examine other genes of interest within the QTL regions uncovered in the GWAS through transgenic or CRISPR/Cas9 knockout and over expression lines. For now, it appears the oleosin gene may be a good candidate as an aleurone marker.

Other genes that were located in QTL regions, showed aleurone-enriched expression via LCM but did not show differential expression between cultivars included a receptor-like kinase (HORVU2Hr1G098040; QAP2.S-2H1) and putative transcription factor (HORVU5Hr1G073410; QALN2.S-5H1). These two genes are of particular interest since they might be expected to fulfil regulatory functions. When analysing the receptor-like kinase (HORVU2Hr1G098040), it was found to be aleurone-enriched and matched a rice transmembrane kinase-like 1 (TMKL1; LOC_Os04g46320) that showed expression in the developing rice endosperm (Ouyang et al., 2007). Receptor kinases are important components of regulatory loops in many systems whereby they respond to various signals, cue signalling cascades and alter development (Knaap et al., 1999). An important kinase previously reported to be involved in aleurone development in maize is *CR4*, which encodes a receptor-like kinase that accumulates near

plasmodesmata (Jin et al., 2000). CR4 protein has greater affinity for the plasma membrane adjoining aleurone-associated plasmodesmata than any other plasma membrane site (Jin et al., 2000; Tian et al., 2007), and may be critical for allowing aleurone specific signals to pass between cells. Further analysis into the receptor-like kinase (HORVU2Hr1G098040) may reveal its role in aleurone development.

Another gene of interest that showed aleurone-enriched expression and was located within a QTL interval was the transcription factor HORVU5Hr1G073410. Further analysis of this gene revealed it was a putative TGA transcription factor, which is part of the bZIP transcription factor family, and shows homology with a rice gene (LOC_Os09g31390) that is also expressed during early stages of rice grain development (Ouyang et al., 2007). TGA transcription factors are required for development of anther tissue in Arabidopsis, and are involved in hormone signalling during various stages of development (Murmu et al., 2010). How this uncharacterised transcription factor might contribute to aleurone development remains unknown, but will be a key focus in future studies.

In summary, it is important to note that this study utilised a stringent FC cut-off between grouped high and low cultivars, and/or required genes to be enriched in the aleurone or outer starchy endosperm in order to be considered as a candidate gene underlying the QTL. This approach appears to have successfully identified several candidate regulatory genes as well as several marker genes that may be involved in aleurone development. Future research will focus on their role via functional studies. The overarching power of this study is that comprehensive GWAS and RNAseq datasets are now available that may be used to determine the contribution of specific genes to barley aleurone development.

References

Amanda D, Doblin MS, Galletti R, Bacic A, Ingram GC, Johnson KL (2016) DEFECTIVE KERNEL1 (DEK1) regulates cell walls in the leaf epidermis. Plant Physiology **172:** 2204-2218

Aubert MK, Coventry S, Shirley NJ, Betts NS, Wurschum T, Burton RA, Tucker MR (2018) Differences in hydrolytic enzyme activity accompany natural variation in mature aleurone morphology in barley (*Hordeum vulgare* L.). Scientific Reports **8:** 1-14

Bacic A, Stone BA (1981) Chemistry and organization of aleurone cell-wall components from wheat and barley. Australian Journal of Plant Physiology **8:** 475-495

Becraft PW, Li KJ, Dey N, Asuncion-Crabb Y (2002) The maize *dek1* gene functions in embryonic pattern formation and cell fate specification. Development **129:** 5217-5225

Becraft PW, Stinard PS, McCarty DR (1996) CRINKLY4: A TNFR-like receptor kinase involved in maize epidermal differentiation. Science **273:** 1406-1409

Behall KM, Scholfield DJ, Hallfrisch J (2004) Diets containing barley significantly reduce lipids in mildly hypercholesterolemic men and women. American Journal of Clinical Nutrition **80:** 1185-1193

Bethke PC, Hwang YS, Zhu T, Jones RL (2006) Global patterns of gene expression in the aleurone of wild-type and dwarf1 mutant rice. Plant Physiology **140:** 484-498

Betts NS, Wilkinson LG, Khor SF, Shirley NJ, Lok F, Skadhauge B, Burton RA, Fincher GB, Collins HM (2017) Morphology, carbohydrate distribution, gene expression, and enzymatic activities related to cell wall hydrolysis in four barley varieties during simulated malting. Frontiers in Plant Science **8:** 1-15

Bønsager BC, Finnie C, Roepstorff P, Svensson B (2007) Germination and radicle elongation in barley tracked using proteome analysis of dissected embryo, aleurone layer and endosperm tissues. Proteomics **7:** 4538-4540

Bosnes M, Weideman F, Olsen OA (1992) Endosperm differentiation in barley wild-type and sex mutants. Plant Journal **2:** 661-674

Brown RC, Lemmon BE (2007) The developmental biology of cereal endosperm. *In* OA Olsen, ed, Plant cell monographs. Endosperm, Vol 8. Springer-Verlag, Berlin, Germany, pp 1–20

Burger WC, La-Berge DE (1985) Malting and Brewing quality. *In* DC Rasmusson, ed, Barley, Madison, WI, USA

Burton RA, Fincher GB (2014) Evolution and development of cell walls in cereal grains. Frontiers in Plant Science **5:** 1-15

Burton RA, Jobling SA, Harvey AJ, Shirley NJ, Mather DE, Bacic A, Fincher GB (2008) The genetics and transcriptional profiles of the cellulose synthase-like *HvCslF* gene family in barley. Plant Physiology **146:** 1821-1833

Burton RA, Shirley NJ, King BJ, Harvey AJ, Fincher GB (2004) The *CesA* gene family of barley. Quantitative analysis of transcripts reveals two groups of co-expressed genes. Plant Physiology **134:** 224-236

Cao XY, Costa LM, Biderre-Petit C, Kbhaya B, Dey N, Perez P, McCarty DR, Gutierrez-Marcos JF, Becraft PW (2007) Abscisic acid and stress signals induce *Viviparous1* expression in seed and vegetative tissues of maize. Plant Physiology **143:** 720-731

Chen DH, Chyan CL, Jiang PL, Chen CS, Tzen JTC (2012) The same oleosin isoforms are present in oil bodies of rice embryo and aleurone layer while caleosin exists only in those of the embryo. Plant Physiology and Biochemistry **60:** 18-24

Chen J, Lausser A, Dresselhaus T (2014) Hormonal responses during early embryogenesis in maize. Biochem. Soc. Trans **42**: 325-331

Chen KG, An YQC (2006) Transcriptional responses to gibberellin and abscisic acid in barley aleurone. Journal of Integrative Plant Biology **48:** 591-612

Cheung K, Senese S, Kuang J, Bui N, Ongpipattanakul C, Gholkar A, Cohn W, Capri J, Whitelegge JP, Torres JZ (2016) Proteomic analysis of the mammalian Katanin family of microtubule-severing enzymes defines Katanin p80 subunit B-like 1 (KATNBL1) as a regulator of mammalian Katanin microtubule-severing. Mol. Cell. Proteomics **15:**1658-1669

Comadran J, Kilian B, Russell J, Ramsay L, Stein N, Ganal M, Shaw P, Bayer M, Thomas W, Marshall D, Hedley P, Tondelli A, Pecchioni N, Francia E, Korzun V, Walther A, Waugh R (2012) Natural variation in a homolog of *Antirrhinum CENTRORADIALIS* contributed to spring growth habit and environmental adaptation in cultivated barley. Nature Genetics **44:** 1388-1392

Crowe AJ, Abenes M, Plant A, Moloney MM (2000) The seed-specific transactivator, ABI3, induces oleosin gene expression. Plant Science **151:** 171-181

Dante RA, Sabelli PA, Nguyen HN, Leiva-Neto JT, Tao YM, Lowe KS, Hoerster GJ, Gordon-Kamm WJ, Jung R, Larkins BA (2014) Cyclin-dependent kinase complexes in developing maize endosperm: evidence for differential expression and functional specialization. Planta **239:** 493-509

Doll NM, Depége-Fargeix N, Rogowsky PM, Widiez T (2017) Signaling in early maize kernel development. Molecular Plant **10**: 375-388

Fath A, Bethke P, Lonsdale J, Meza-Romero R, Jones R (2000) Programmed cell death in cereal aleurone. Plant Molecular Biology **44:** 255-266

Fernandez DE, Staehelin LA (1985) Structural organization of ultrarapidly frozen barley aleurone cells actively involved in protein secretion. Planta **165:** 455-468

Fernandez DE, Staehelin LA (1987) Does gibberellic-acid induce the transfer of lipase from protein bodies to lipid bodies in barley aleurone cells. Plant Physiology **85:** 487-496

Fincher GB, Stone BA (1986) Cell walls and their components in cereal grain technology. Advances in Cereal Science and Technology **8:** 207-295

Finlay KW, Wilkinson GN (1963) The analysis of adaptation in a plant-breeding programme. Australian Journal of Agricultural Research **14:** 742-754

Finnie C, Svensson B (2003) Feasibility study of a tissue-specific approach to barley proteome analysis: aleurone layer, endosperm, embryo and single seeds. Journal of Cereal Science **38:** 217-227

Finnie C, Svensson B (2009) Barley seed proteomics from spots to structures. Journal of Proteomics **72:** 315-324

Gamel TH, Abdel-Aal EM (2012) Phenolic acids and antioxidant properties of barley wholegrain and pearling fractions. Agricultural and Food Science **21:** 118-131

Gillies SA, Futardo A, Henry RJ (2012) Gene expression in the developing aleurone and starchy endosperm of wheat. Plant Biotechnology Journal **10:** 668-679

Gontarek BC, Neelakandan AK, Wu H, Becraft PW (2016) NKD transcription factors are central regulators of maize endosperm development. Plant Cell **28:** 2916-2936

Gruis D, Guo HN, Selinger D, Tian Q, Olsen OA (2006) Surface position, not signaling from surrounding maternal tissues, specifies aleurone epidermal cell fate in maize. Plant Physiology **141:** 898-909

Hands P, Kourmpetli S, Sharples D, Harris RG, Drea S (2012) Analysis of grain characters in temperate grasses reveals distinctive patterns of endosperm organization associated with grain shape. Journal of Experimental Botany **63:** 6253-6266

Hassan AS, Houston K, Lahnstein J, Shirley N, Schwerdt JG, Gidley MJ, Waugh R, Little A, Burton RA (2017a) A genome wide association study of arabinoxylan content in 2-row spring barley grain. Plos One **12:** e0182537

Hassan AS, Houston K, Learmonth A, Oakey H, Bayer M, Macaulay M, Lahnstein J, Shirley NJ, Waugh R, Halpin C, Little A, Burton RA (2017b) Application of genome wide association mapping for identification of genes involved in the biosynthesis of cell wall bound phenolic acids in 2-row spring barley. *In* PhD Thesis. The University of Adelaide, pp 92-135

Hirano K, Ueguchi-Tanaka M, Matsuoka M (2008) GID1-mediated gibberellin signalling in plant cells. Trends in Plant Science **13:** 192-199

Houston K, Russell J, Schreiber M, Halpin C, Oakey H, Washington JM, Booth A, Shirley N, Burton RA, Fincher GB, Waugh R (2014) A genome wide association scan for (1,3;1,4)-beta-glucan content in the grain of contemporary 2-row Spring and Winter barleys. Bmc Genomics **15:** 1-15

Hughes N, Askew K, Scotson CP, Williams K, Sauze C, Corke F, Doonan JH, Nibau C (2017) Non-destructive, high-content analysis of wheat grain traits using X-ray micro computed tomography. Plant Methods **13:** 1-16

Hynek R, Svensson B, Jensen ON, Barkholt V, Finnie C (2006) Enrichment and identification of integral membrane proteins from barley aleurone layers by reversed-phase chromatography, SDS-PAGE, and LC-MS/MS. Journal of Proteome Research **5:** 3105-3113

IBGS (2012) A physical, genetic and functional sequence assembly of the barley genome. Nature **491:** 711-716

Ishimaru T, Ida M, Hirose S, Shimamura S, Masumura T, Nishizawa NK, Nakazono M, Kondo M (2015) Laser microdissection-based gene expression analysis in the aleurone layer and starchy endosperm of developing rice caryopses in the early storage phase. Rice **8:** 1-15

Jacobsen JV, Knox RB (1973) Cytochemical localization and antigenicity of alpha-amylase in barley aleurone tissue. Planta **112:** 213-224

Jestin L, Ravel C, Auroy S, Laubin B, Perretant MR, Pont C, Charmet G (2008) Inheritance of the number and thickness of cell layers in barley aleurone tissue (*Hordeum vulgare* L.): an approach using F2-F3 progeny. Theoretical and Applied Genetics **116:** 991-1002

Jin P, Guo T, Becraft PW (2000) The maize CR4 receptor-like kinase mediates a growth factor-like differentiation response. Genesis **27:** 104-116

Kalla R, Shimamoto K, Potter R, Nielsen PS, Linnestad C, Olsen OA (1994) The promoter of the barley aleurone-specific gene encoding a putative 7-kDa lipid transfer protein confers aleurone cell-specific expression in transgenic rice. Plant Journal **6:** 849-860

Kearse M, Moir R, Wilson A, Stones-Havas S, Cheung M, Sturrock S, Buxton S, Cooper A, Markowitz S, Duran C, Thierer T, Ashton B, Meintjes P, Drummond A (2012) Geneious Basic: An integrated and extendable desktop software platform for the organization and analysis of sequence data. Bioinformatics **28:** 1647-1649

Knaap E, Song W, Ruan D, Sauter M, Ronald PC, Kende H (1999) Expression of a gibberellin-induced leucine-rich repeat receptor-like protein kinase in deepwater rice and its interaction with kinase-associated protein phosphatase. Growth and Development **120:** 559-569

Kumar S, Stecher G, Li M, Knyaz C, Tamura K (2018) MEGA X: Molecular evolutionary genetics analysis across computing platforms. Molecular Biology and Evolution **35:** 1547-1549

Lee RC, Burton RA, Hrmova M, Fincher GB (2001) Barley arabinoxylan arabinofuranohydrolases: purification, characterization and determination of primary structures from cDNA clones. Biochemical Journal **356:** 181-189

Li Y, Lu H, Gu GX, Shi ZP, Mao ZG (2005) Studies on water-extractable arabinoxylans during malting and brewing. Food Chemistry **93:** 33-38

Lid SE, Gruis D, Jung R, Lorentzen JA, Ananiev E, Chamberlin M, Niu XM, Meeley R, Nichols S, Olsen OA (2002) The *defective kernel 1* (*dek1*) gene required for aleurone cell development in the endosperm of maize grains encodes a membrane protein of the calpain gene superfamily. Proceedings of the National Academy of Sciences of the United States of America **99:** 5460-5465

Lin GL, Chai J, Yuan S, Mai C, Cai L, Murphy RW, Zhou W, Luo J (2016) VennPainter: A tool for the comparison and identification of candidate genes based on venn diagrams. Plos One **11:** e0154315

Liu J, Wu X, Yao X, Yu R, Larkin PJ, Liu C-M (2018) Mutations in the DNA demethylase *OsROS1* result in a thickened aleurone and improved nutritional value in rice grains. Proc Natl Acad Sci USA**:** 1-6

Long NV, Dolstra O, Malosetti M, Kilian B, Graner A, Visser RGF, van der Linden CG (2013) Association mapping of salt tolerance in barley (*Hordeum vulgare* L.). Theoretical and Applied Genetics **126:** 2335-2351

Luptovčiak I, Samakovli D, Komis G, Šamaj J (2017) KATANIN 1 is essential for embryogenesis and seed formation in Arabidopsis. Front Plant Sci. **8:**1-12

Mascher M, Gundlach H, Himmelbach A, Beier S, Twardziok SO, Wicker T, Radchuk V, Dockter C, Hedley PE, Russell J, Bayer M, Ramsay L, Liu H, Haberer G, Zhang XQ, Zhang QS, Barrero RA, Li L, Taudien S, Groth M, Felder M, Hastie A, Simkova H, Stankova H, Vrana J, Chan S, Munoz-Amatrian M, Ounit R, Wanamaker S, Bolser D, Colmsee C, Schmutzer T, Aliyeva-Schnorr L, Grasso S, Tanskanen J, Chailyan A, Sampath D, Heavens D, Clissold L, Cao SJ, Chapman B, Dai F, Han Y, Li H, Li X, Lin CY, McCooke JK, Tan C, Wang PH, Wang SB, Yin SY, Zhou GF, Poland JA, Bellgard MI, Borisjuk L, Houben A, Dolezel J, Ayling S, Lonardi S, Kersey P, Lagridge P, Muehlbauer GJ, Clark MD, Caccamo M, Schulman AH, Mayer KFX, Platzer M, Close TJ, Scholz U, Hansson M, Zhang GP, Braumann I, Spannagl M, Li CD, Waugh R, Stein N (2017) A chromosome conformation capture ordered sequence of the barley genome. Nature **544:** 426-433

Mascher M, Muehlbauer GJ, Rokhsar DS, Chapman J, Schmutz J, Barry K, Munoz-Amatriain M, Close TJ, Wise RP, Schulman AH, Himmelbach A, Mayer KFX, Scholz U, Poland JA, Stein N, Waugh R (2013) Anchoring and ordering NGS contig assemblies by population sequencing (POPSEQ). Plant Journal **76:** 718-727

Mayer KFX, Waugh R, Langridge P, Close TJ, Wise RP, Graner A, Matsumoto T, Sato K, Schulman A, Muehlbauer GJ, Stein N, Ariyadasa R, Schulte D, Poursarebani N, Zhou RN, Steuernagel B, Mascher M, Scholz U, Shi BJ, Langridge P, Madishetty K, Svensson JT, Bhat P, Moscou M, Resnik J,

Close TJ, Muehlbauer GJ, Hedley P, Liu H, Morris J, Waugh R, Frenkel Z, Korol A, Berges H, Graner A, Stein N, Steuernagel B, Taudien S, Groth M, Felder M, Lonardi S, Duma D, Alpert M, Cordero F, Beccuti M, Ciardo G, Ma Y, Wanamaker S, Stein N, Close TJ, Platzer M, Brown JWS, Schulman A, Platzer M, Fincher GB, Muehlbauer GJ, Sato K, Taudien S, Sampath D, Swarbreck D, Scalabrin S, Zuccolo A, Vendramin V, Morgante M, Schulman A, Int Barley Genome Sequencing C (2012) A physical, genetic and functional sequence assembly of the barley genome. Nature **491:** 711-716

McCleary BV, Codd R (1989) Measurement of β-amylase in cereal flours and commercial enzyme preparations. Journal of Cereal Science **9:** 17-33

McCleary BV, McNally M, Monaghan D, Mugford DC, Black C, Broadbent R, Chin M, Cormack M, Fox R, Gaines C, Gothard P, Home S, Howes E, Johnson C, Keeping R, Koliatsou M, Lindhauer M, de Sa RM, Martin R, Monaghan D, Nees U, Nishwitz R, Palmer G, Panozzo J, Recabarren J, Roumeliotis S, Seddig S, Solah V, Sonnet M, Themeier H (2002) Measurement of alpha-amylase activity in white wheat flour, milled malt, and microbial enzyme preparations, using the ceralpha assay: Collaborative study. Journal of Aoac International **85:** 1096-1102

McCleary BV, Shameer I (1987) Assay of malt β-glucanase using azo-barley glucan: An improved precipitant. Journal of the Institute of Brewing **93:** 87-90

Morino K, Olsen OA, Shimamoto K (2004) Silencing of the aleurone-specific *Ltp2-gus* gene in transgenic rice is reversed by transgene rearrangements and loss of aberrant transcripts. Plant and Cell Physiology **45:** 1500-1508

Murmu J, Bush MJ, DeLong C, Li S, Xu M, Khan M, Malcolmson C, Fobert PR, Zachgo S, Hepworth SR (2010) Arabidopsis basic leucine-zipper transcription factors TGA9 and TGA10 interact with floral glutaredoxins ROXY1 and ROXY2 and are redundantly required for anther development. Plant Physiology Nov **154**:1492-1504

Newman CW, Newman RK (2006) A brief history of barley foods. Cereal Foods World **51:** 4-7

Nordkvist E, Salomonsson AC, Aman P (1984) Distribution of insoluble bound phenolic acids in barley grain. Journal of the Science of Food and Agriculture **35:** 657-661

Olsen LT, Divon HH, Al R, Fosnes K, Lid SE, Opsahl-Sorteberg HG (2008) The *defective seed5* (*des5*) mutant: effects on barley seed development and *HvDek1*, *HvCr4*, and *HvSal1* gene regulation. Journal of Experimental Botany **59:** 3753-3765

Olsen OA (2004) Nuclear endosperm development in cereals and *Arabidopsis thaliana*. Plant Cell **16:** S214-S227

Opanowicz M, Hands P, Betts D, Parker ML, Toole GA, Mills ENC, Doonan JH, Drea S (2011) Endosperm development in *Brachypodium distachyon*. Journal of Experimental Botany **62:** 735-748

Opsahl-Sorteberg HG, Divon HH, Nielsen PS, Kalla R, Hammond-Kosack B, Shimamoto K, Kohli A (2004) Identification of a 49-bp fragment of the *HvLTP2* promoter directing aleurone cell specific expression. Gene **341:** 49-58

Ouyang S, Zhu W, Hamilton J, Lin H, Campbell M, Childs K, Thibaud-Nissen F, Malek RL, Lee Y, Zheng L, Orvis J, Haas B, Wortman J, Buell CR (2007) The TIGR Rice Genome Annotation Resource: improvements and new features. NAR 35 Database Issue: D846-851.

Pauli D, Muehlbauer GJ, Smith KP, Cooper B, Hole D, Obert DE, Ullrich SE, Blake TK (2014) Association mapping of agronomic QTLs in US spring barley breeding germplasm. Plant Genome **7:** 1-15

Pins JJ, Kaur H (2006) A review of the effects of barley β-glucan on cardiovascular and diabetic risk. Cereal Foods World **51:** 8-11

Ritchie S, McCubbin A, Ambrose G, Kao TH, Gilroy S (1999) The sensitivity of barley aleurone tissue to gibberellin is heterogeneous and may be spatially determined. Plant Physiology **120:** 361-370

Roll-Mecak A, McNally FJ (2010) Microtubule-severing enzymes. Current Opinion in Cell Biology **22**:96-103

Sabelli PA, Larkins BA (2009) The development of endosperm in grasses. Plant Physiology **149**: 14-26

Sato K, Flavell A, Russell J, Börner A, Valkoun J (2014) Genetic diversity and germplasm management - wild barley, landraces, breeding materials. *In* J Kumlehn, N Stein, eds, Biotechnological approaches to barley improvement. Springer-Verlag, Berlin Heidelberg, Germany, pp 21-36

Shapter FM, Dawes MP, Lee LS, Henry RJ (2009) Aleurone and subaleurone morphology in native Australian wild cereal relatives. Australian Journal of Botany **57:** 688-696

Shen B, Li CJ, Min Z, Meeley RB, Tarczynski MC, Olsen OA (2003) *sal1* determines the number of aleurone cell layers in maize endosperm and encodes a class E vacuolar sorting protein. Proceedings of the National Academy of Sciences of the United States of America **100:** 6552-6557

Simmonds J, Cass L, Harris L, Allard S (1998) Wheat aleurone regulatory elements. *In*. Agriculture and Agri-Food Canada USA

Suzuki M, Ketterling MG, Li QB, McCarty DR (2003) Viviparous1 alters global gene expression patterns through regulation of abscisic acid signaling. Plant Physiology **132:** 1664-1677

Szűcs P, Blake VC, Bhat PR, Chao SAM, Close TJ, Cuesta-Marcos A, Muehlbauer GJ, Ramsay L, Waugh R, Hayes PM (2009) An integrated resource for barley linkage map and malting quality QTL alignment. Plant Genome **2:** 134-140

Tamura K, Nei M (1993) Estimation of the number of nucleotide substitutions in the control region of mitochondrial-DNA in humans and chimpanzees. Molecular Biology and Evolution **10:** 512-526

Tian Q, Olsen L, Sun B, Lid SE, Brown RC, Lemmon BE, Fosnes K, Gruis DF, Opsahl-Sorteberg HG, Otegui MS, Olsen OA (2007) Subcellular localization and functional domain studies of DEFECTIVE KERNEL1 in maize and *Arabidopsis* suggest a model for aleurone cell fate specification involving CRINKLY4 and SUPERNUMERARY ALEURONE LAYER1. Plant Cell **19:** 3127-3145

Tian T, Liu Y, Yan HY, You Q, Yi X, Du Z, Xu WY, Su Z (2017) agriGO v2.0: a GO analysis toolkit for the agricultural community, 2017 update. Nucleic Acids Research **45:** W122-W129

Tucker MR, Okada T, Hu YK, Scholefield A, Taylor JM, Koltunow AMG (2012) Somatic small RNA pathways promote the mitotic events of megagametogenesis during female reproductive development in *Arabidopsis*. Development **139:** 1399-1404

Tucker MR, Roodbarkelari F, Truernit E, Adamski NM, Hinze A, Lohmuller B, Wurschum T, Laux T (2013) Accession-specific modifiers act with ZWILLE/ARGONAUTE10 to maintain shoot meristem stem cells during embryogenesis in *Arabidopsis*. Bmc Genomics **14:** 1-15

Untergasser A, Cutcutache I, Koressaar T, Ye J, Faircloth BC, Remm M, Rozen SG (2012) Primer3-new capabilities and interfaces. Nucleic Acids Research **40:** e115

Vandesompele J, De Preter K, Pattyn F, Poppe B, Van Roy N, De Paepe A, Speleman F (2002) Accurate normalization of real-time quantitative RT-PCR data by geometric averaging of multiple internal control genes. Genome Biology **3:** 1-12

Visioni A, Tondelli A, Francia E, Pswarayi A, Malosetti M, Russell J, Thomas W, Waugh R, Pecchioni N, Romagosa I, Comadran J (2013) Genome-wide association mapping of frost tolerance in barley (*Hordeum vulgare* L.). Bmc Genomics **14:** 1-13

Wilkinson LG, Tucker MR (2017) An optimised clearing protocol for the quantitative assessment of sub-epidermal ovule tissues within whole cereal pistils. Plant Methods **13:** 67-77

Wilson SM, Burton RA, Collins HM, Doblin MS, Pettolino FA, Shirley N, Fincher GB, Bacic A (2012) Pattern of deposition of cell wall polysaccharides and transcript abundance of related cell wall synthesis genes during differentiation in barley endosperm. Plant Physiology **159:** 655-670

Wilson SM, Burton RA, Doblin MS, Stone BA, Newbigin EJ, Fincher GB, Bacic A (2006) Temporal and spatial appearance of wall polysaccharides during cellularization of barley (*Hordeum vulgare*) endosperm. Planta **224:** 655-667

Wisniewski JP, Rogowsky PM (2004) Vacuolar H+-translocating inorganic pyrophosphatase (Vpp1) marks partial aleurone cell fate in cereal endosperm development. Plant Molecular Biology **56:** 325-337

Wu XB, Liu JX, Li DQ, Liu CM (2016) Rice caryopsis development I: Dynamic changes in different cell layers. Journal of Integrative Plant Biology **58:** 772-785

Xu JJ, Zhang XF, Xue HW (2016) Rice aleurone layer specific OsNF-YB1 regulates grain filling and endosperm development by interacting with an ERF transcription factor. Journal of Experimental Botany **67:** 6399-6411

Yano K, Aya K, Hirano K, Ordonio RL, Ueguchi-Tanaka M, Matsuoka M (2015) Comprehensive gene expression analysis of rice aleurone cells: Probing the existence of an alternative gibberellin receptor. Plant Physiology **167:** 531-544

Yi G, Neelakandan AK, Gontarek BC, Vollbrecht E, Becraft PW (2015) The *naked endosperm* genes encode duplicate indeterminate domain transcription factors required for maize endosperm cell patterning and differentiation. Plant Physiology **167:** 443-456

Zhan JP, Thakare D, Ma C, Lloyd A, Nixon NM, Arakaki AM, Burnett WJ, Logan KO, Wang DF, Wang XF, Drews GN, Yadegaria R (2015) RNA sequencing of laser-capture microdissected compartments of the maize kernel identifies regulatory modules associated with endosperm cell differentiation. Plant Cell **27:** 513-531

Zhang RX, Tucker MR, Burton RA, Shirley NJ, Little A, Morris J, Milne L, Houston K, Hedley PE, Waugh R, Fincher GB (2016) The dynamics of transcript abundance during cellularization of developing barley endosperm. Plant Physiology **170:** 1549-1565

Figures

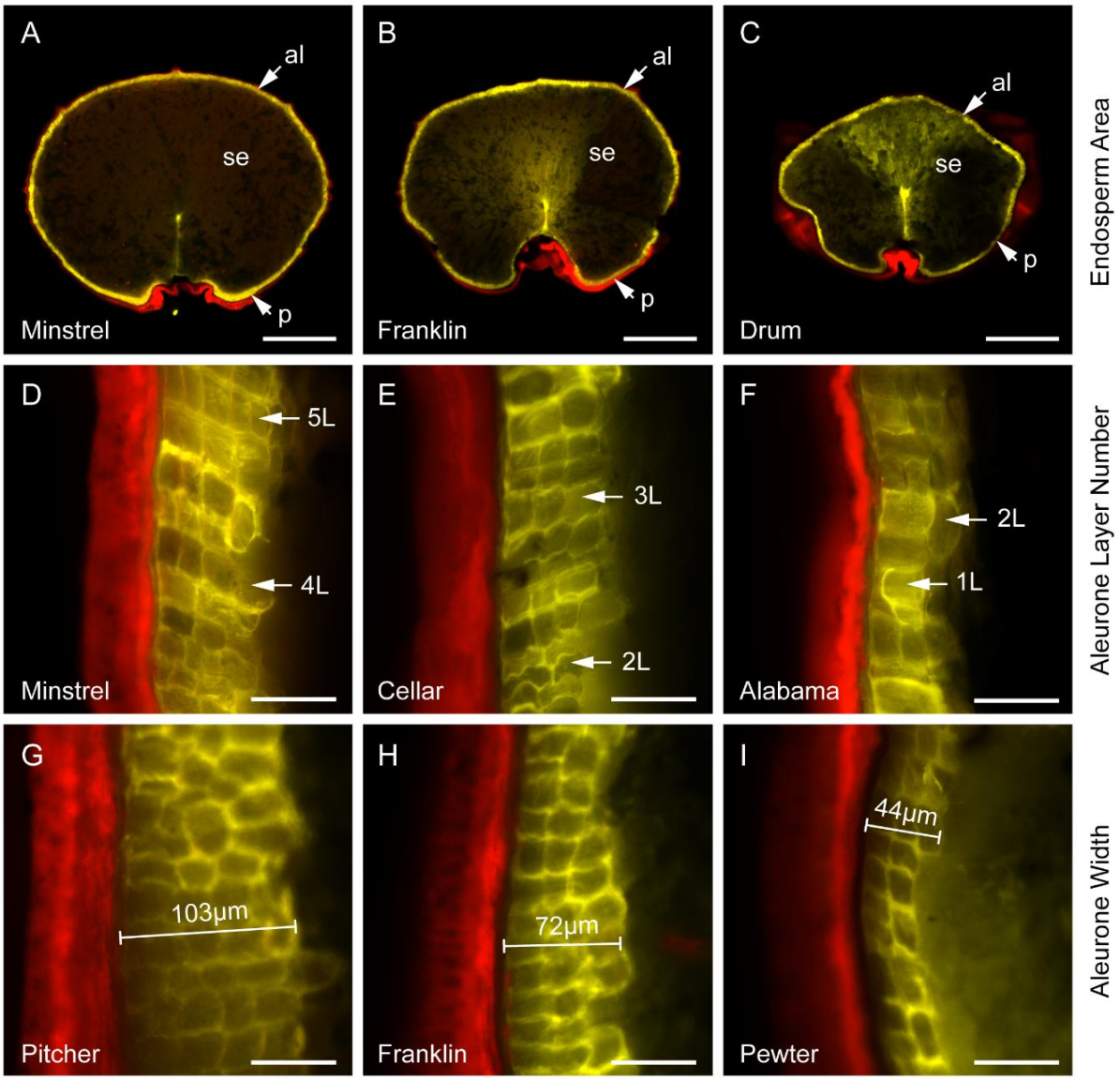

Figure 5-1: Representation of the transverse sectioning process used to image barley aleurone tissue by fluorescent microscopy. (A–C) Wholegrain transverse sections viewed using Zeiss Filter sets 46 (false-coloured red) and 49 (DAPI; false-coloured yellow). The panels show grain exhibiting differences in transverse starchy endosperm area in decreasing order. The pericarp (p), starchy endosperm (se) and aleurone (al) tissues are indicated. Scale bar = 1 mm. (D–F) Magnified views of the aleurone layers. Panels are arranged in decreasing order based on the average number of aleurone layers. Stacks of multiple aleurone cell layers (L) are indicated. Scale bar = 50 µm. (G–

I) Examples of grain showing differences in aleurone width, arranged in decreasing order. Scale bar = 50 μm. Genotype names are indicated in each panel.

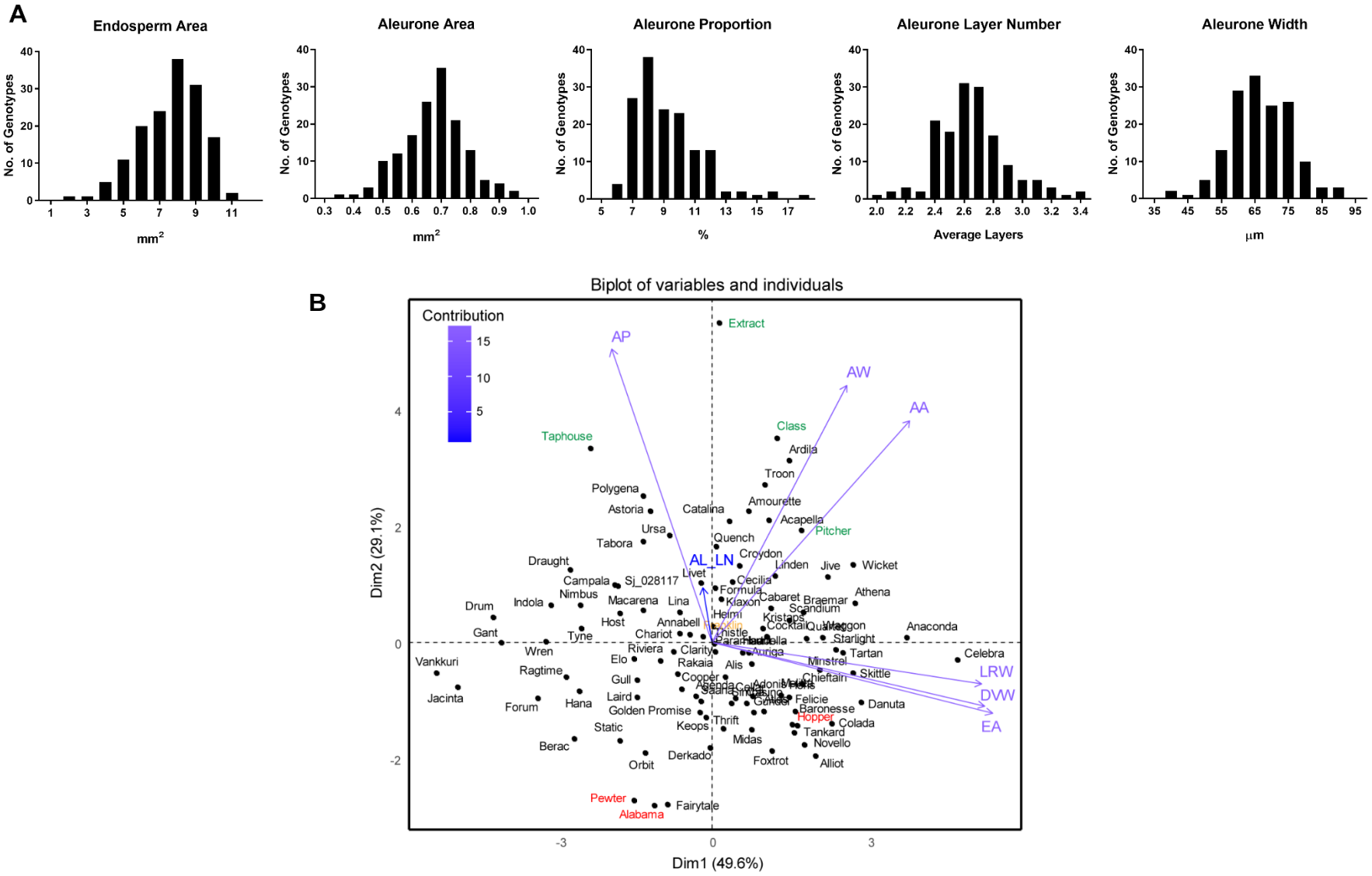
A
Endosperm Area
No. of Genotypes
mm²
Aleurone Area
No. of Genotypes
mm²
Aleurone Proportion
No. of Genotypes
%
Aleurone Layer Number
No. of Genotypes
Average Layers
Aleurone Width
No. of Genotypes
µm
B
Biplot of variables and individuals
Contribution
Dim2 (29.1%)
Dim1 (49.6%)
AP
AW
AA
AL
LN
LRW
DWW
EA
Extract
Taphouse
Class
Ardila
Troon
Polygena
Astoria
Catalina
Amourette
Acapella
Pitcher
Ursa
Tabora
Quench
Croydon
Linden
Jive
Wicket
Draught
Campala
Sj_028117
Livet
Cecilia
Formula
Athena
Nimbus
Klaxon
Cabaret
Braemar
Scandium
Drum
Indola
Macarena
Lina
Heimi
Kristaps
Host
Annabell
Cocktail
Anaconda
Gant
Tyne
Chariot
Starlight
Wren
Riviera
Clarity
Auriga
Tartan
Celebra
Vankkuri
Elo
Rakaia
Alis
Minstrel
Ragtime
Cooper
Chieftain
Skittle
Gull
Jacinta
Laird
Felicie
Forum
Hana
Golden Promise
Danuta
Baronesse
Hopper
Thrift
Colada
Keops
Tankard
Static
Midas
Novello
Berac
Derkado
Foxtrot
Alliot
Orbit
Pewter
Alabama
Fairytale

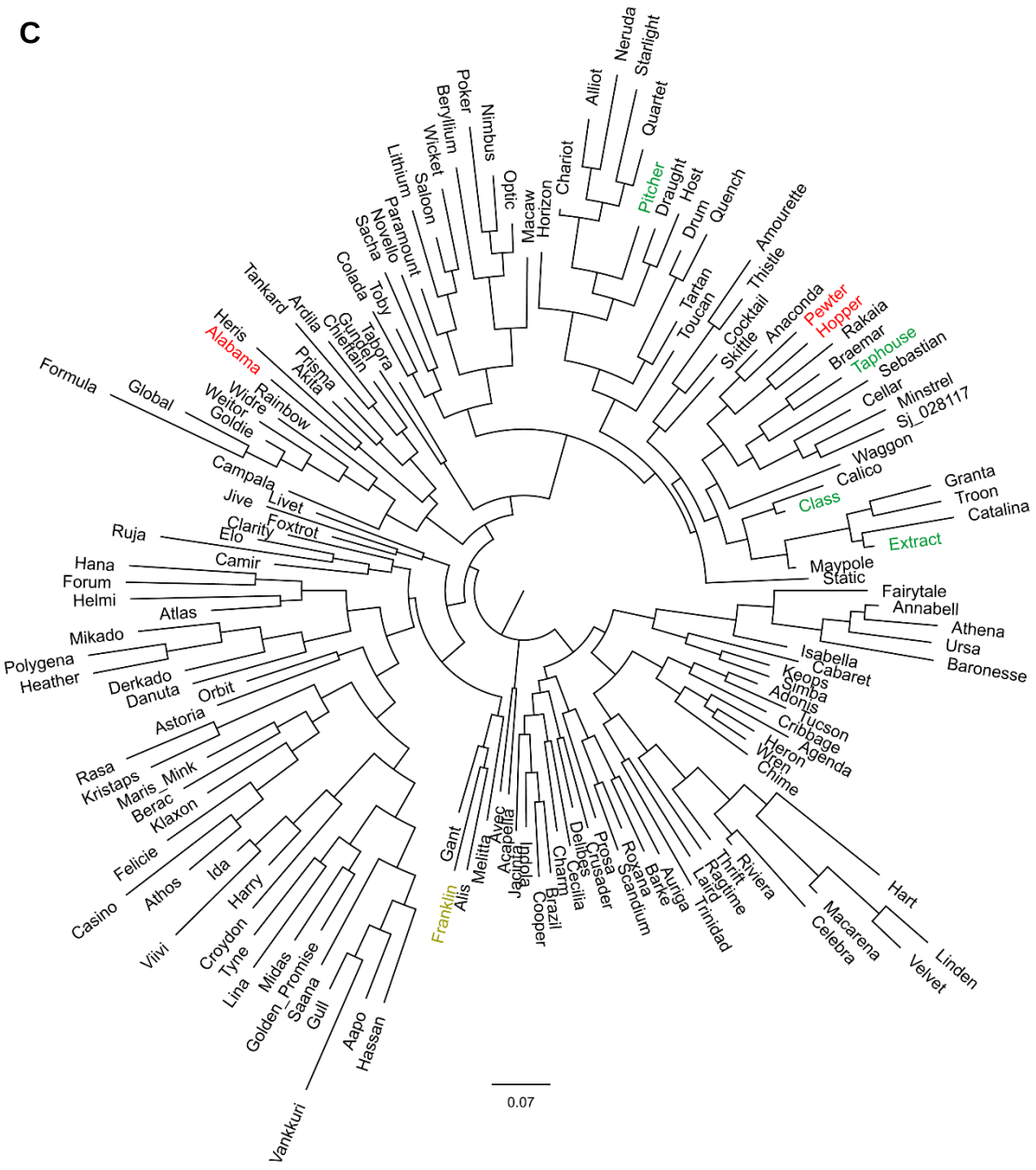

Figure 5-2: Variation in transverse grain measurements observed across 101 barley genotypes. (A) Frequency distribution plots of endosperm area and the four aleurone measurements. (B) Principal Component Analysis separates the genotypes based on the seven transverse measurements. EA, endosperm area; AA, aleurone area; AP, aleurone proportion; DVW, grain dorsal-ventral distance; LRW, transverse grain left-right width; AL_LN, aleurone layer number; AW, aleurone width. (C) Molecular phylogenetic analysis inferred by using the Maximum Likelihood method based on the Tamura-Nei model. High aleurone genoypes (green), intermediate aleurone genotype (yellow), low aleurone genotypes (red).

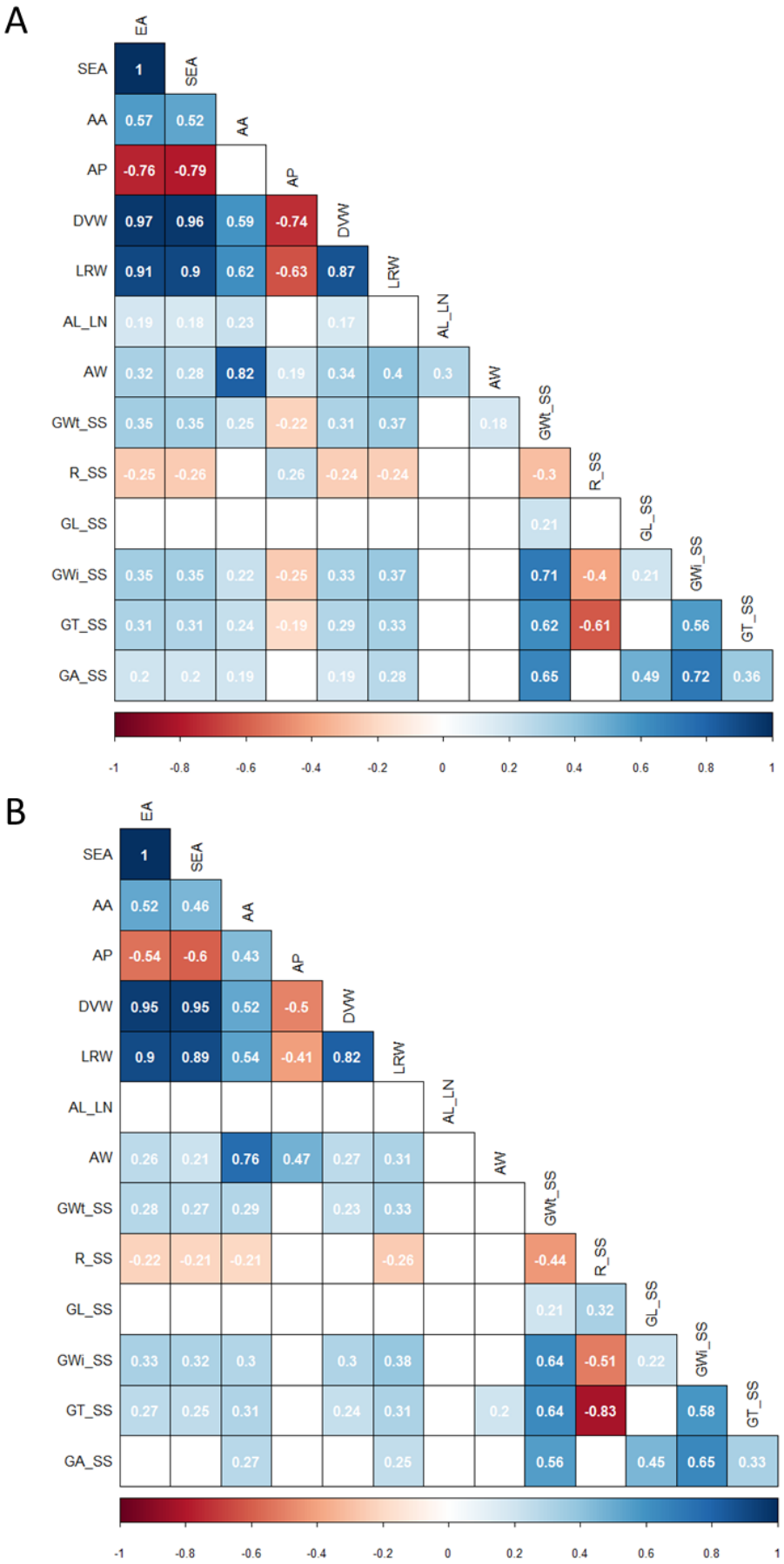
A
EA
SEA
AA
AP
DVW
LRW
AL_LN
AW
GWt_SS
R_SS
GL_SS
GWi_SS
GT_SS
GA_SS
1
0.57 0.52
-0.76 -0.79
0.97 0.96 0.59 -0.74
0.91 0.9 0.62 -0.63 0.87
0.19 0.18 0.23 0.17
0.32 0.28 0.82 0.19 0.34 0.4 0.3
0.35 0.35 0.25 -0.22 0.31 0.37 0.18
-0.25 -0.26 0.26 -0.24 -0.24 -0.3
0.21
0.35 0.35 0.22 -0.25 0.33 0.37 0.71 -0.4 0.21
0.31 0.31 0.24 -0.19 0.29 0.33 0.62 -0.61 0.56
0.2 0.2 0.19 0.19 0.28 0.65 0.49 0.72 0.36
-1 -0.8 -0.6 -0.4 -0.2 0 0.2 0.4 0.6 0.8 1
B
EA
SEA
AA
AP
DVW
LRW
AL_LN
AW
GWt_SS
R_SS
GL_SS
GWi_SS
GT_SS
GA_SS
1
0.52 0.46
-0.54 -0.6 0.43
0.95 0.95 0.52 -0.5
0.9 0.89 0.54 -0.41 0.82
0.26 0.21 0.76 0.47 0.27 0.31
0.28 0.27 0.29 0.23 0.33
-0.22 -0.21 -0.21 -0.26 -0.44
0.21 0.32
0.33 0.32 0.3 0.3 0.38 0.64 -0.51 0.22
0.27 0.25 0.31 0.24 0.31 0.2 0.64 -0.83 0.58
0.27 0.25 0.56 0.45 0.65 0.33
-1 -0.8 -0.6 -0.4 -0.2 0 0.2 0.4 0.6 0.8 1

Figure 5-3: Heat maps representing correlations across grain traits from (A) 150 genotypes and (B) 101 genotypes. Blue boxes indicate positive correlations and red boxes indicate negative correlations. Numbers within boxes represent correlation coefficient (r) values and only those with a p-value ≤ 0.05 are shown. EA, endosperm area; SEA, starchy endosperm area; AA, aleurone area; AP, aleurone proportion; DVW, grain dorsal-ventral distance; LRW, transverse grain left-right width; ALN, aleurone layer number; AW, aleurone width; GWt_SS, grain weight; R_SS, grain roundness; GL_SS, grain length; GWi_SS, grain width; GT_SS, grain thickness; SS, seed scanner.

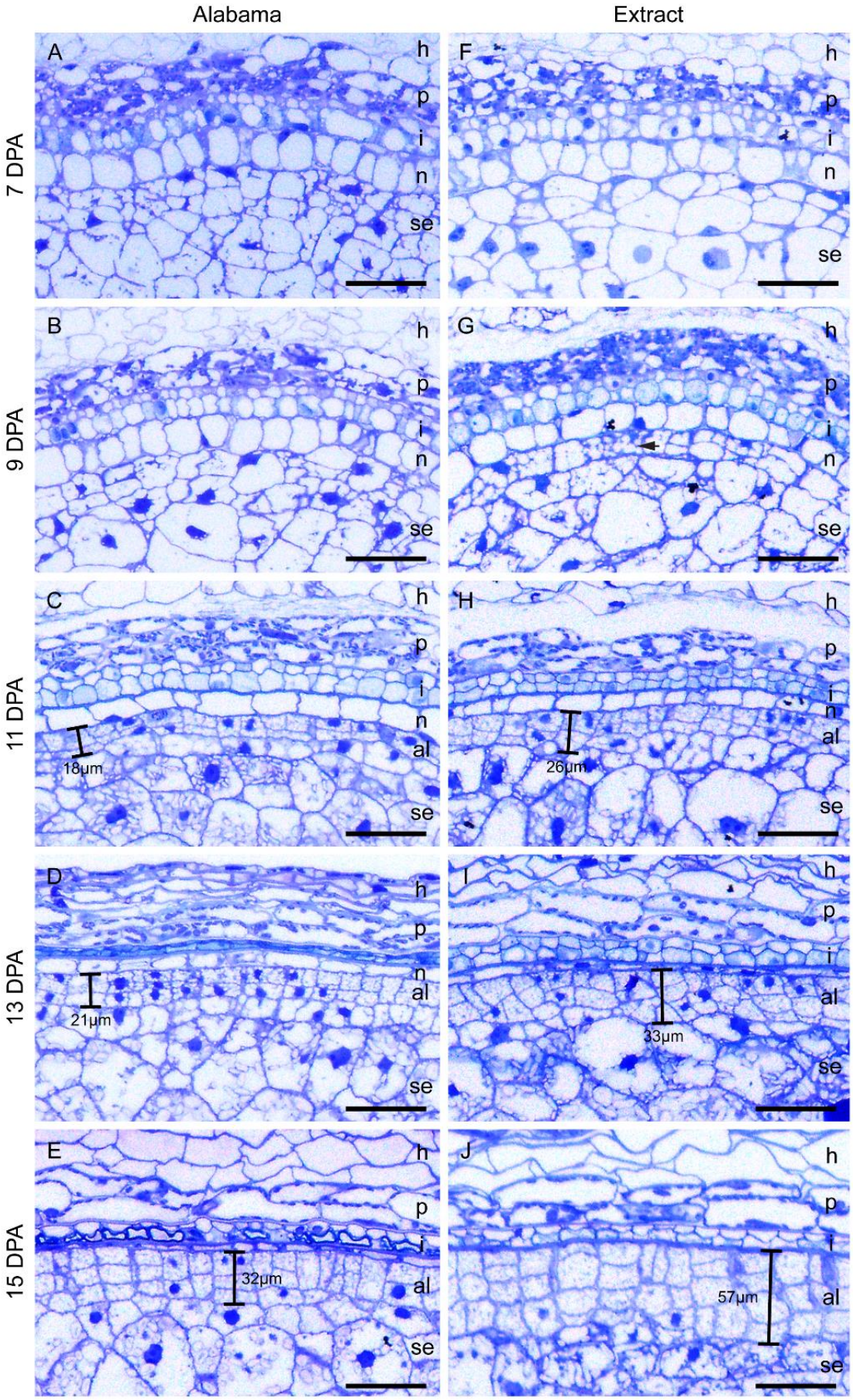
Alabama
Extract
7 DPA
9 DPA
11 DPA
13 DPA
15 DPA
A
B
C
D
E
F
G
H
I
J
h
p
i
n
al
se
18µm
21µm
32µm
26µm
33µm
57µm

Figure 5-4: Developing barley grain sections stained with Toluidine Blue to demonstrate changes in aleurone morphology between a low aleurone line (cv Alabama) and a high aleurone line (cv Extract). (A–E) Alabama developing sections from 7 DPA to 15 DPA. (F–J) Extract developing sections from 7 DPA to 15 DPA. h, hull; p, pericarp; i, integuments; n, nucellus; al, aleurone; se, starchy endosperm. Scale bar = 50 μm

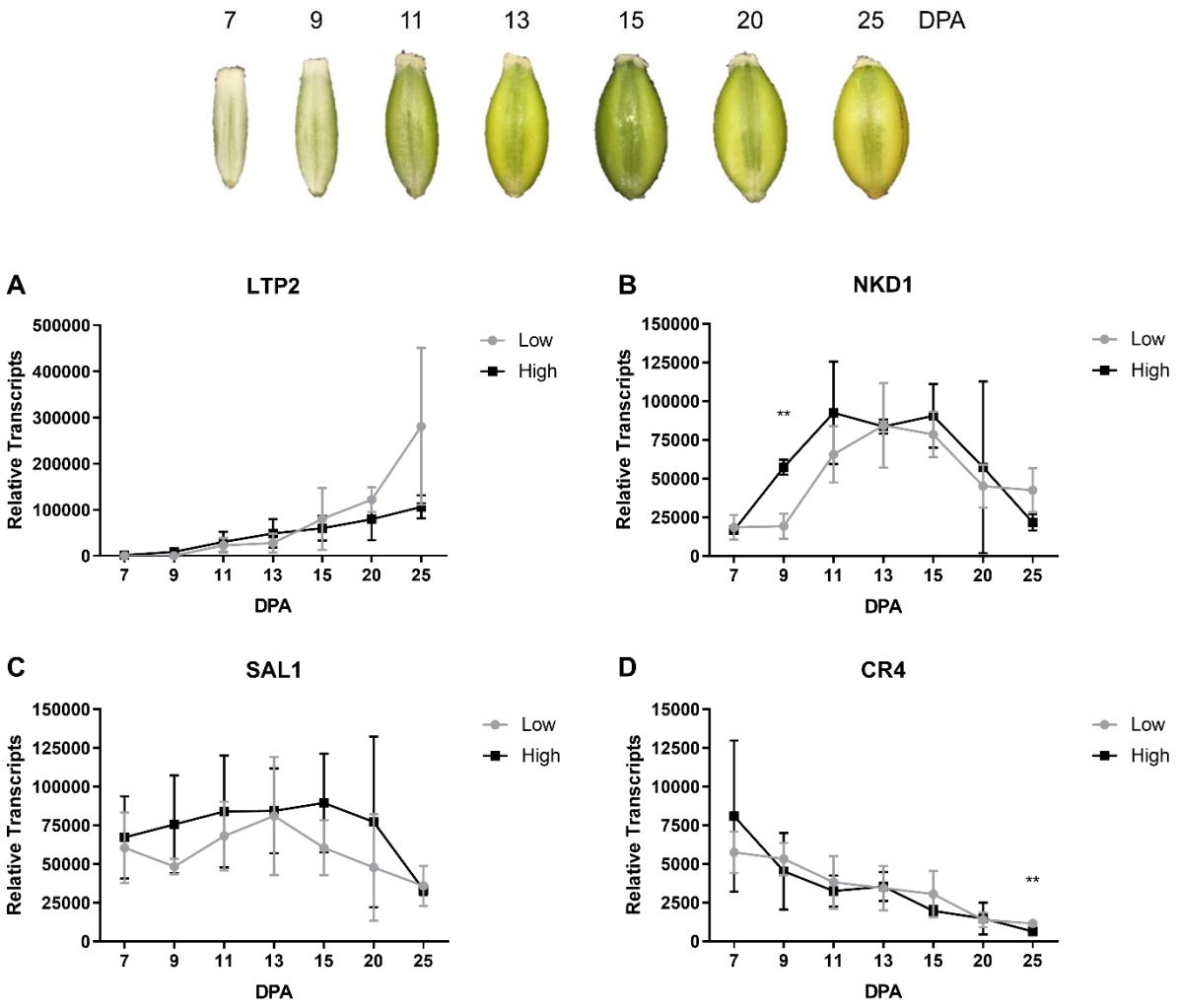

Figure 5-5: Transcript abundance of genes predicted to contribute to aleurone formation across grain development using quantitative PCR (qPCR). Arbitrary transcript units from high aleurone genotypes (cv Extract, Class and Taphouse) were averaged to become the "high" group (in black) and low aleurone genotypes (cv Alabama, Pewter and Hopper) were averaged to become the "low" group (in grey). Transcriptional differences were observed between high and low groups across grain development for aleurone associated genes (*LTP2*, *NKD1*, *SAL1* and *CR4*). However, the only significant difference between the high and low groups was *NKD1* at 9 DPA and *CR4* at 25 DPA, respectively. Significance ** = p≤0.0021.

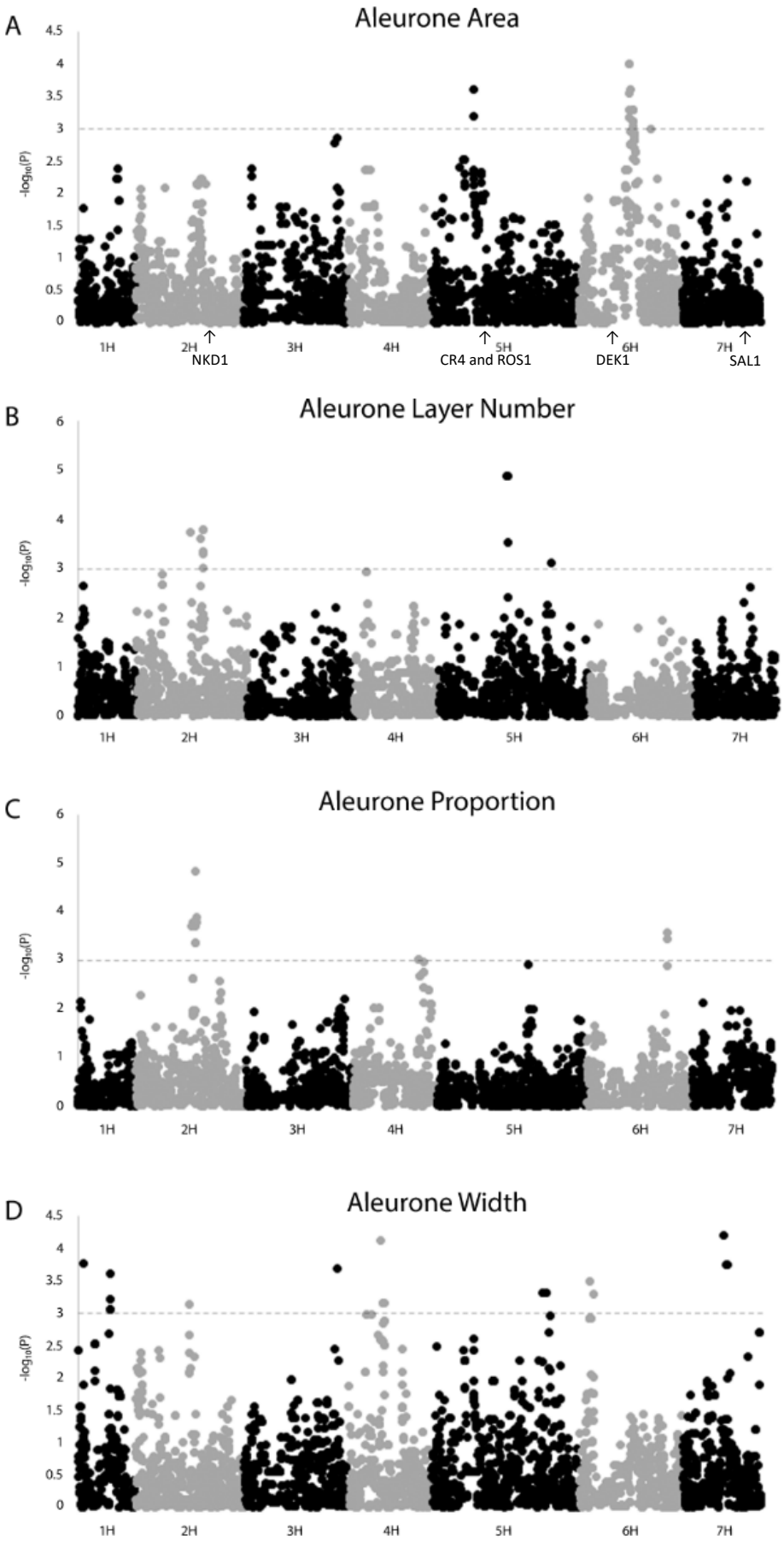
A
Aleurone Area
-log10(P)
1H
2H
3H
4H
5H
6H
7H
NKD1
CR4 and ROS1
DEK1
SAL1
B
Aleurone Layer Number
C
Aleurone Proportion
D
Aleurone Width

Figure 5-6: Manhattan plots of the GWAS of various aleurone traits from the European 2-row spring barley using the Eigenstrat model. The $-\log_{10}(P)$ (P-value) is shown on the Y axis. The X axis shows the seven barley chromosomes. (A) Aleurone area used for marker-trait association analysis. (B) Aleurone layer number used for marker-trait association analysis. (C) Aleurone proportion of the endosperm used for marker-trait association analysis. (D) Average aleurone width used for marker-trait association analysis. Dashed line represents the cut off for significant marker associations ($-\log_{10}(P) \geq 3$). The Location of candidate aleurone genes relative to the marker associations is shown in Panel A.

Table 5-1: Marker associations with aleurone traits identified in this study and the subsequent QTL contribution with related trait effect.

								Alternative Allele			
Trait	**QTL Name**	**Marker**	**Chr**	**cM**	**Eigen LOD**	**Allele**	**Frequency (%)**	**Allele**	**Frequency (%)**	**Effect (%)**	**Effect**
Aleurone Area	QAA2.S-6H1	11_10513	6H	60.96	4	A	57.4	G	42.6	-0.4 ± 0.11	-0.03 ± 0.01 (mm²)
	QAA2.S-6H2	SCRI_RS_170672	6H	63.77	3.62	C	57.4	T	42.6	-0.4 ± 0.11	-0.03 ± 0.01 (mm²)
	QAA2.S-5H1	SCRI_RS_237877	5H	49.06	3.6	G	54.5	A	45.5	0.4 ± 0.12	0.03 ± 0.01 (mm²)
Aleurone Layer Number	QALN2.S-5H1	SCRI_RS_170151	5H	89.5	4.88	C	81.2	T	18.8	4.7 ± 1.08	0.12 ± 0.03 (layers)
	QALN2.S-2H1	SCRI_RS_156045	2H	110.62	3.8	C	65.3	A	34.7	-3.5 ± 0.93	-0.09 ± 0.02 (layers)
	QALN2.S-2H2	SCRI_RS_196316	2H	89.5	3.76	C	78.8	A	21.2	4.1 ± 1.08	0.11 ± 0.03 (layers)
	QALN2.S-5H2	11_10080	5H	156.5	3.13	A	94.1	G	5.9	6.3 ± 1.86	0.17 ± 0.05 (layers)
Aleurone Proportion	QAP2.S-2H1	11_20923	2H	101.54	4.82	C	87.1	A	12.9	8.0 ± 1.83	0.66 ± 0.15 (%)
	QAP2.S-2H2	SCRI_RS_221763	2H	99.77	3.79	A	52.5	G	47.5	4.7 ± 1.25	0.39 ± 0.10 (%)
	QAP2.S-6H1	11_10815	6H	85.06	3.57	A	86.1	G	13.9	6.6 ± 1.82	0.55 ± 0.15 (%)
	QAP2.S-4H1	SCRI_RS_122057	4H	88.18	3.01	T	86.1	C	13.9	6.1 ± 1.83	0.50 ± 0.15 (%)
Aleurone Thickness	QAT2.S-7H1	SCRI_RS_175164	7H	70.81	4.22	T	52.5	C	47.5	4.6 ± 1.15	3.07 ± 0.77 (µm)
	QAT2.S-4H1	12_30839	4H	52.95	4.14	A	74.3	C	25.7	5.0 ± 1.26	3.35 ± 0.84 (µm)
	QAT2.S-1H1	SCRI_RS_169369	1H	13.24	3.77	T	59.4	C	40.6	4.3 ± 1.15	2.90 ± 0.77 (µm)
	QAT2.S-7H2	SCRI_RS_2914	7H	76.6	3.75	T	53.5	G	46.5	4.3 ± 1.15	2.87 ± 0.77 (µm)
	QAT2.S-3H1	12_11208	3H	146.6	3.69	G	88.1	A	11.9	-6.5 ± 1.74	-4.32 ± 1.16 (µm)
	QAT2.S-1H2	11_21126	1H	74.73	3.62	G	71.3	C	28.7	-4.6 ± 1.26	-3.09 ± 0.84 (µm)
	QAT2.S-6H1	SCRI_RS_7397	6H	51.93	3.49	C	87.1	T	12.9	-6.0 ± 1.68	-4.05 ± 1.13 (µm)
	QAT2.S-5H1	SCRI_RS_138029	5H	156.82	3.33	T	66.3	C	33.7	-4.3 ± 1.23	-2.89 ± 0.83 (µm)
	QAT2.S-2H1	SCRI_RS_237763	2H	93.86	3.15	A	66.3	G	33.7	-4.1 ± 1.22	-2.76 ± 0.81 (µm)
	QAT2.S-1H3	SCRI_RS_138527	1H	74.73	3.07	C	70.3	T	29.7	-4.2 ± 1.27	-2.82 ± 0.85 (µm)

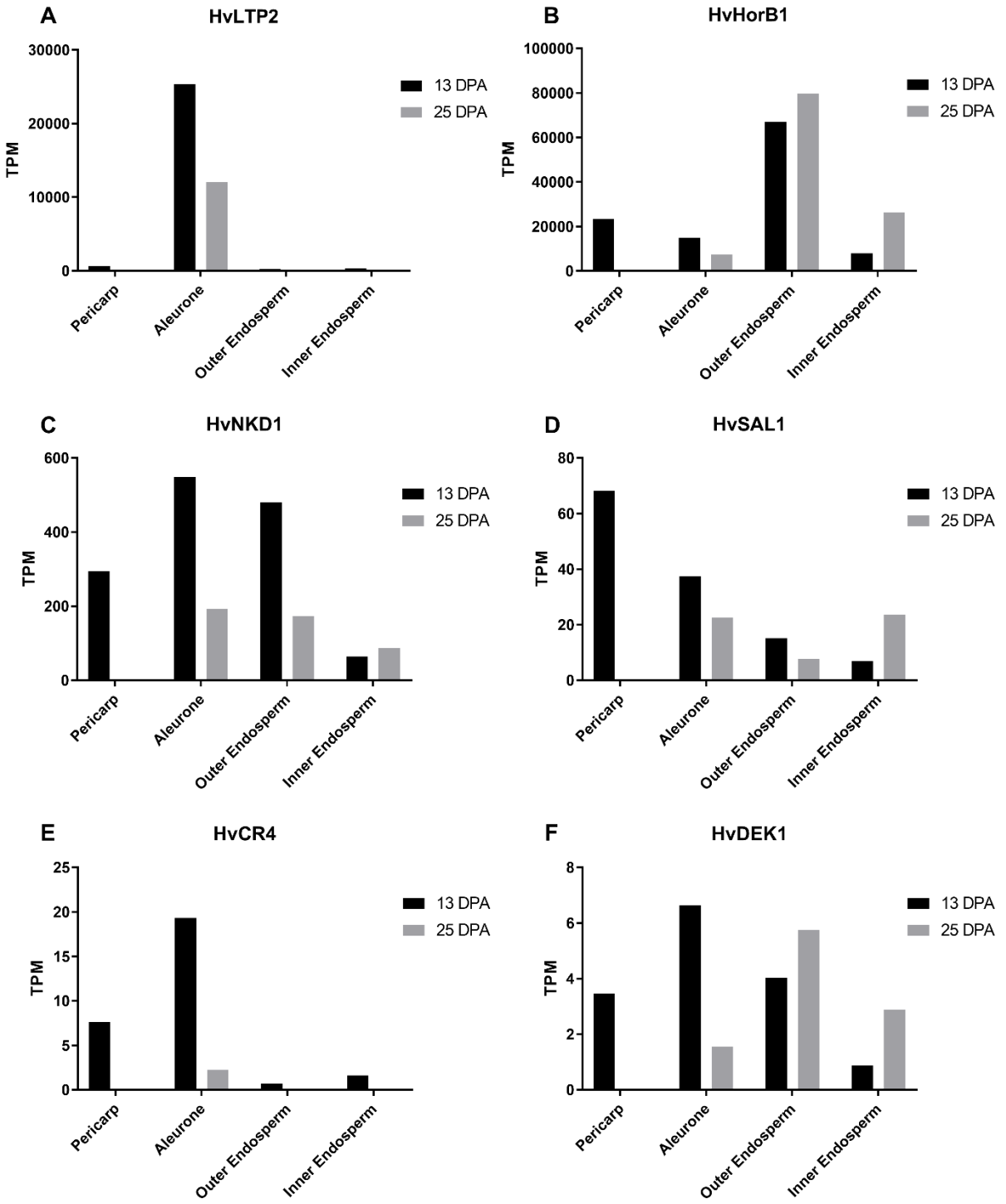

Figure 5-7: Tissue-specific transcript levels of genes from developing grain at 13 and 25 days post anthesis (DPA) using LCM and RNAseq. Tissues collected were the pericarp, aleurone, outer starchy endosperm and inner starchy endosperm from developing cv Sloop grain. TPM; transcripts per million.

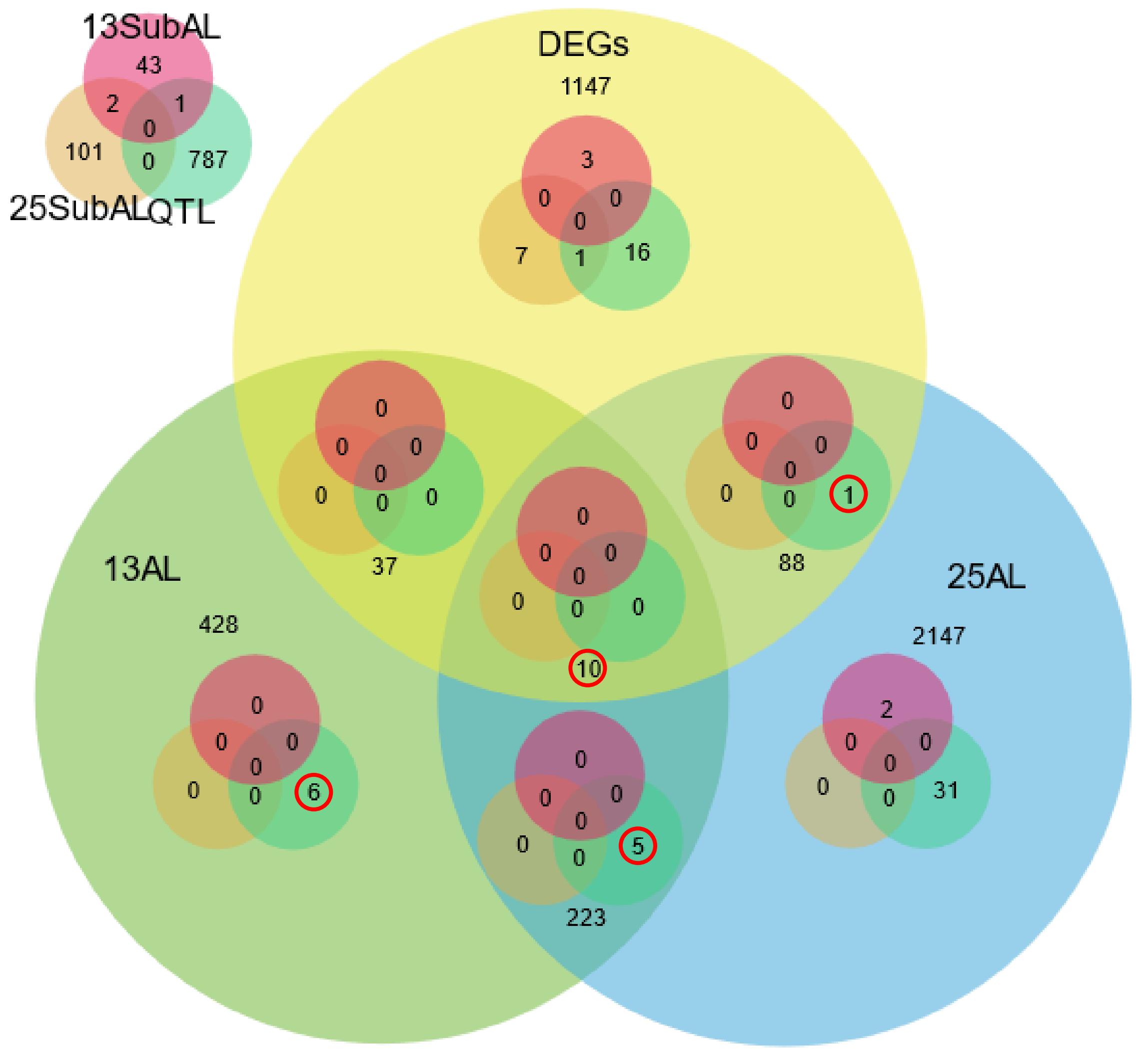

Figure 5-8: A Venn diagram used to narrow down candidate aleurone genes within QTL regions. Red circles indicate HORVUs of interest. Wholegrain differential expression (DEGs), HORVUs with TPM > 10 in at least one developmental stage (DPA) from wholegrain RNAseq with a FC ≥2 and ≤0.5; Aleurone 13 DPA (13Al), HORVUs with TPM > 10 in aleurone tissue at 13 DPA; Aleurone 25 DPA (25AL), HORVUs with TPM > 10 in aleurone tissue at 25 DPA; Outer starchy endosperm 13 DPA (13SubAl), HORVUs with TPM > 10 in outer starchy endosperm tissue at 13 DPA; Outer starchy endosperm 25 DPA (25SubAL), HORVUs with TPM > 10 in outer starchy endosperm tissue at 25 DPA; QTL, HORVUs within the four QTL of interest.

Supplementary Figures

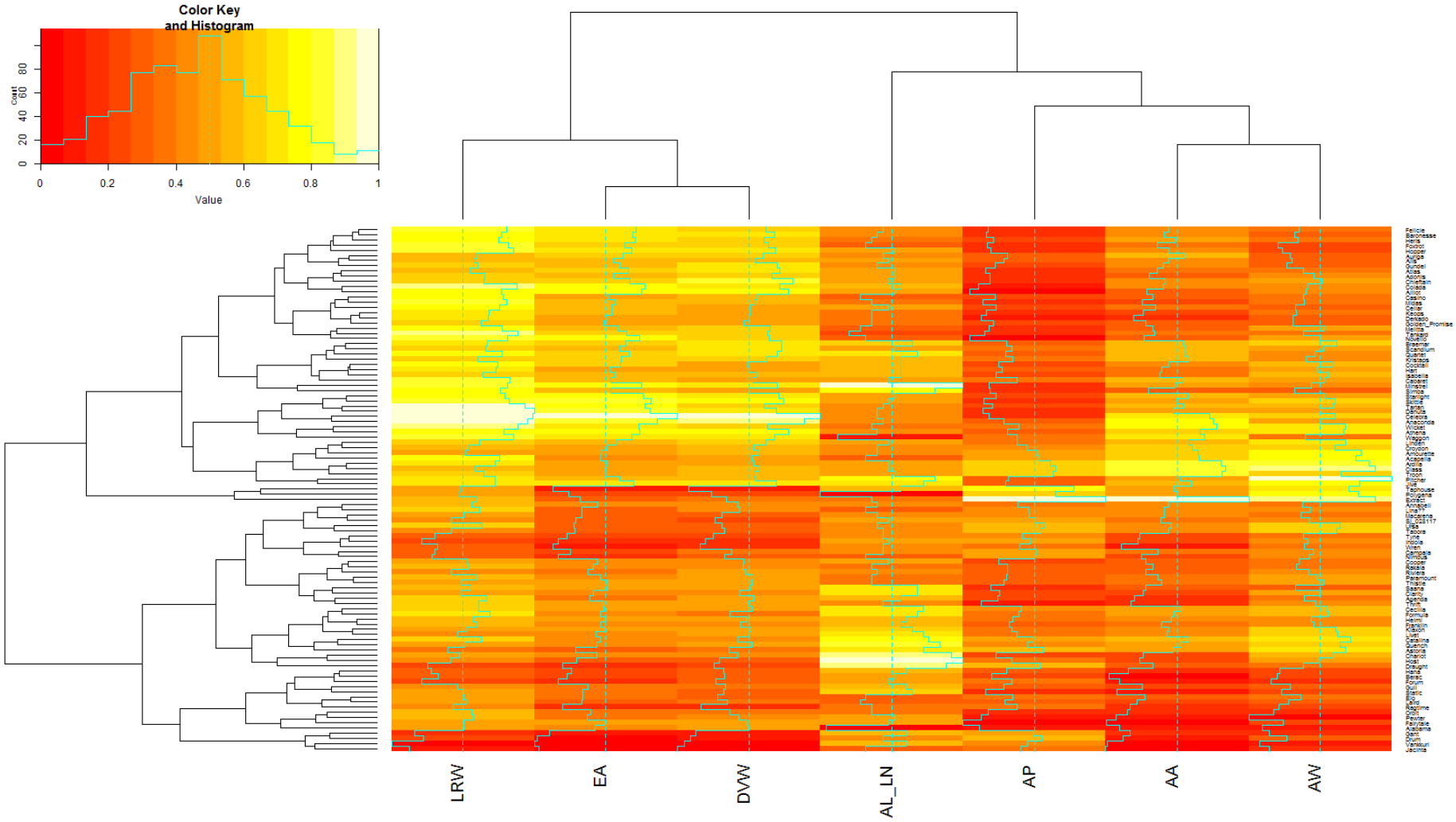

Figure 5-S1: Relationships between transverse grain measurements in a panel of 150 barley genotypes. A heatmap showing clusters of different genotypes separated based on the seven different grain measurements. Trait values are normalised to a value between 0 and 1 and the blue line indicates the position of each genotype for each trait measurement. LRW, transverse grain left-right width; EA, endosperm area; DVW, grain dorsal-ventral distance; AL_LN, aleurone layer number; AP, aleurone proportion; AA, aleurone area; AW, aleurone width.

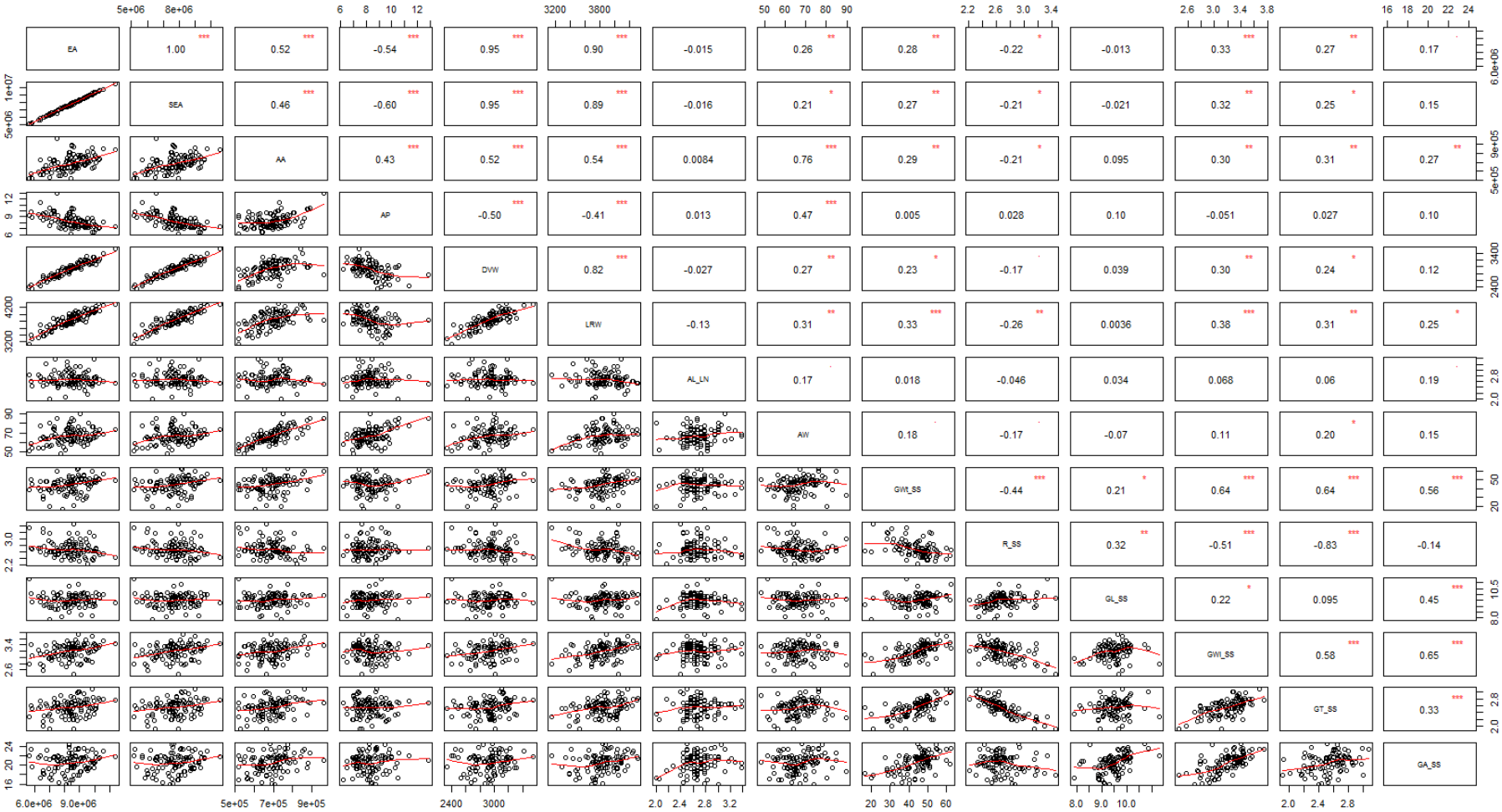
EA
SEA
AA
AP
DVW
LRW
AL_LN
AW
GWI_SS
R_SS
GL_SS
GWI_SS
GT_SS
GA_SS

Figure 5-S2: Correlation plot representing the relatedness of the aleurone and grain traits across 101 genotypes. Significance: *** = p≤0.001, ** = p≤0.01, * = p≤0.05 and · = p≤0.1. EA, endosperm area; SEA, starchy endosperm area; AA, aleurone area; AP, aleurone proportion; DVW, grain dorsal-ventral distance; LRW, transverse grain left-right width; ALN, aleurone layer number; AW, aleurone width; GWt_SS, grain weight; R_SS, grain roundness; GL_SS, grain length; GWi_SS, grain width; GT_SS, grain thickness; GA_SS, grain area; SS, seed scanner.

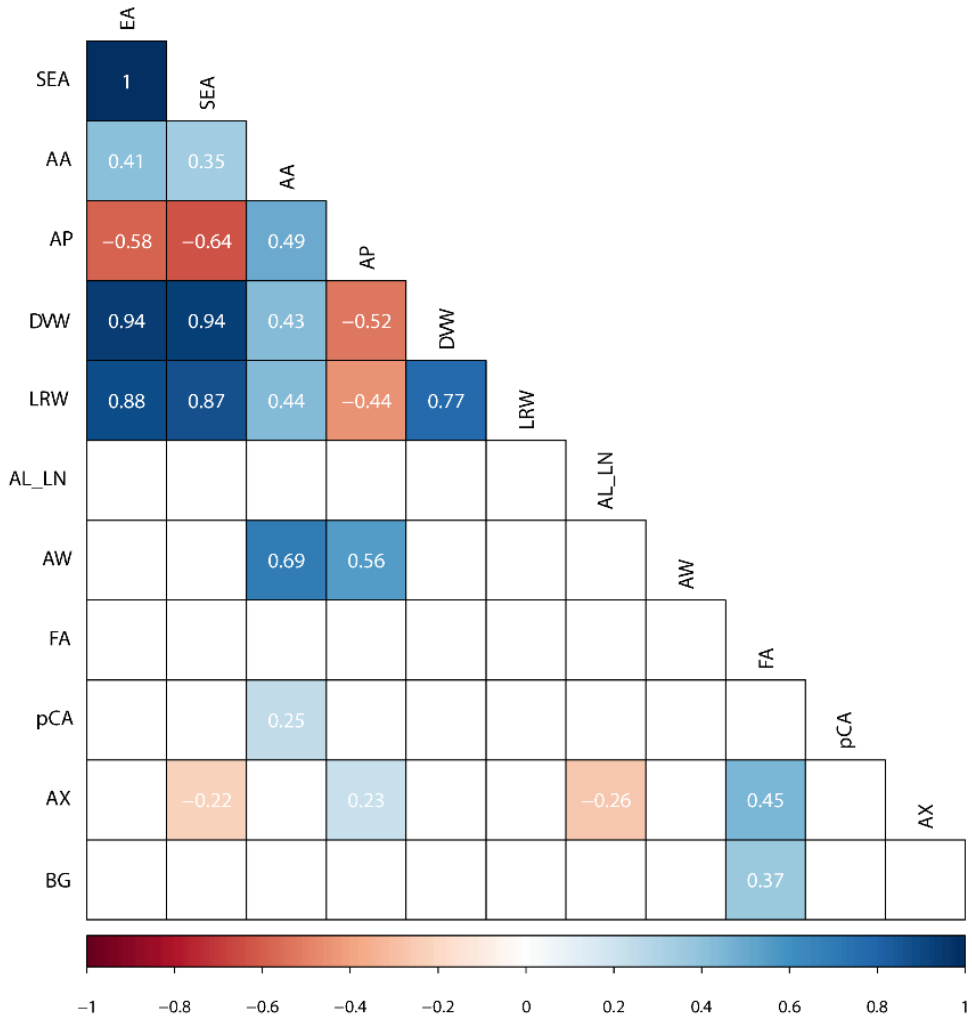

Figure 5-S3: Heat map representing correlations across grain traits between aleurone features and grain composition. Blue boxes indicate positive correlations and red boxes indicate negative correlations. Numbers within boxes represent correlation coefficient (r) values and only those with a p-value ≤ 0.05 are shown. EA, endosperm area; SEA, starchy endosperm area; AA, aleurone area; AP, aleurone proportion; DVW, grain dorsal-ventral distance; LRW, transverse grain left-right width; ALN, aleurone layer number; AW, aleurone width; FA, ferulic acid; pCA, p-Coumaric acid; AX, arabinoxylan; BG; (1,3)(1,4)-β-glucan.

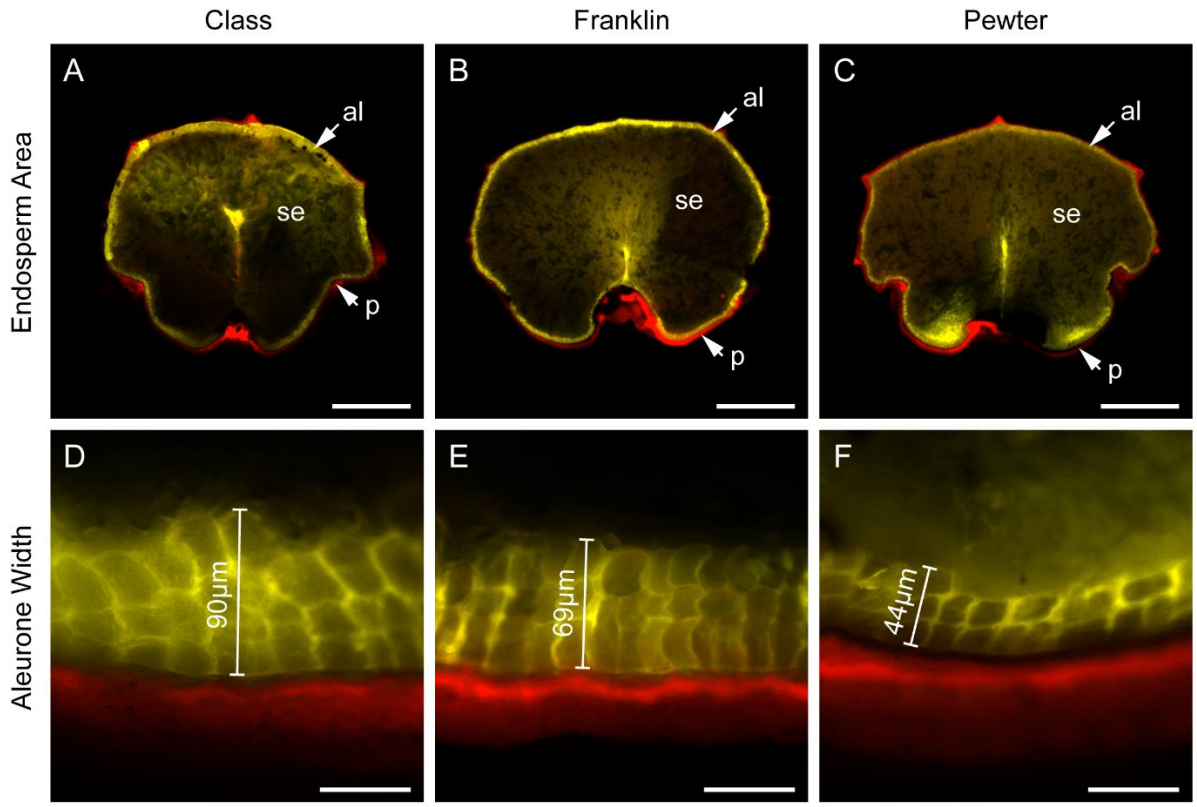

Figure 5-S4: Representation of the transverse sections from interesting genotypes. (A–C) Wholegrain transverse sections viewed using Zeiss Filter sets 46 (false-coloured red) and 49 (DAPI; false-coloured yellow). The panels depict three genotypes, cv Class, Franklin and Pewter, exhibiting similar transverse starchy endosperm area. The pericarp (p), starchy endosperm (se) and aleurone (al) tissues are indicated. Scale bar = 1 mm. (D–F) Differences in aleurone width from the corresponding genotypes, arranged in decreasing order. Scale bar = 50 µm.

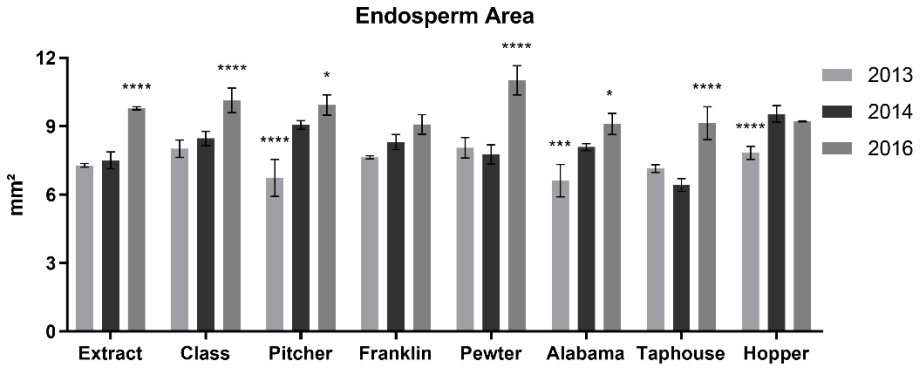
Endosperm Area
mm²
2013
2014
2016
Extract
Class
Pitcher
Franklin
Pewter
Alabama
Taphouse
Hopper

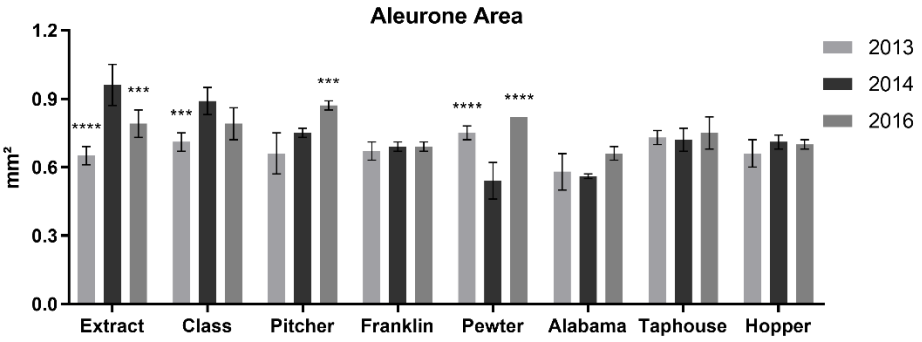
Aleurone Area
mm²
2013
2014
2016
Extract
Class
Pitcher
Franklin
Pewter
Alabama
Taphouse
Hopper

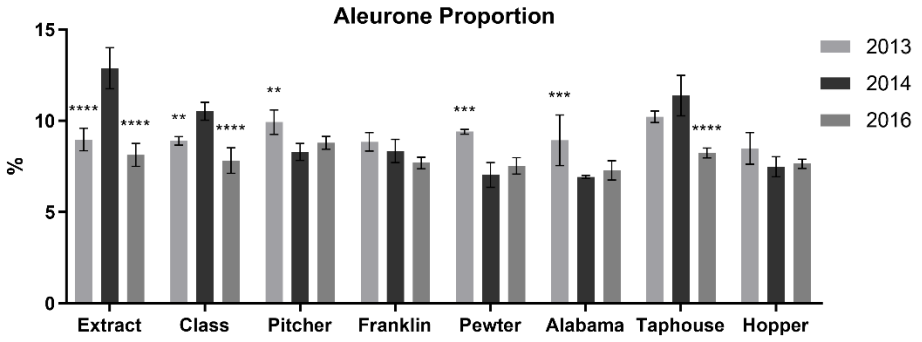
Aleurone Proportion
%
2013
2014
2016
Extract
Class
Pitcher
Franklin
Pewter
Alabama
Taphouse
Hopper

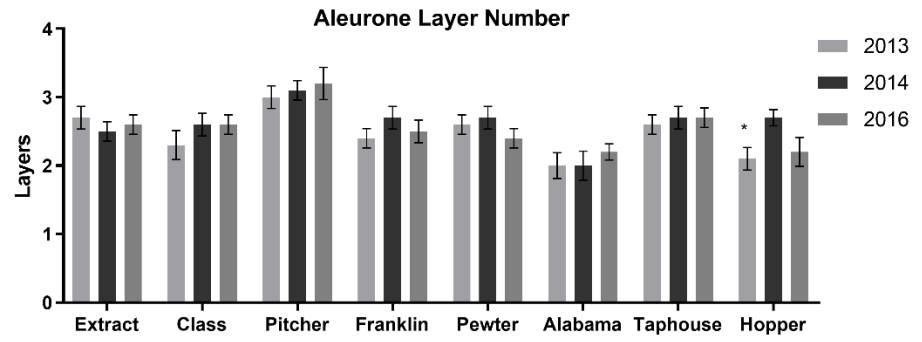
Aleurone Layer Number
Layers
2013
2014
2016
Extract
Class
Pitcher
Franklin
Pewter
Alabama
Taphouse
Hopper

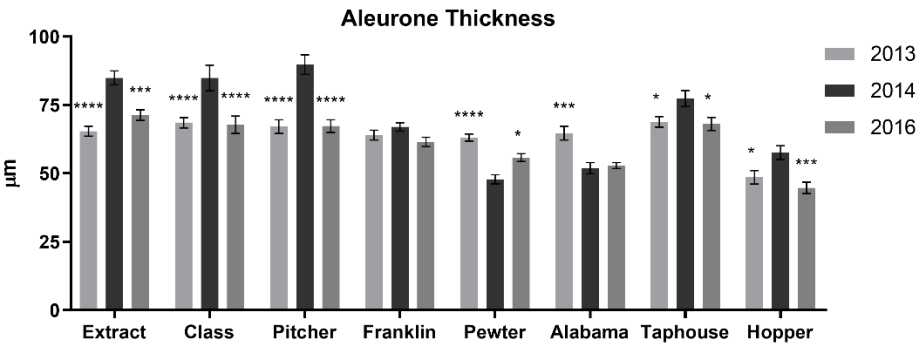
Aleurone Thickness
µm
2013
2014
2016
Extract
Class
Pitcher
Franklin
Pewter
Alabama
Taphouse
Hopper

Figure 5-S5: Mature grain measurements across three generations. Error bars represent standard deviation for endosperm area, aleurone area and aleurone proportion, while error bars represent standard error of the mean for aleurone layer number and aleurone thickness. Two-way analysis of variance (ANOVA) was performed between 2013-2014 and 2014-2016. Significance indicates difference from 2014 trait measurements. Significance: * = $p \leq 0.0332$, ** = $p \leq 0.0021$, *** = $p \leq 0.0002$, **** = $p < 0.0001$.

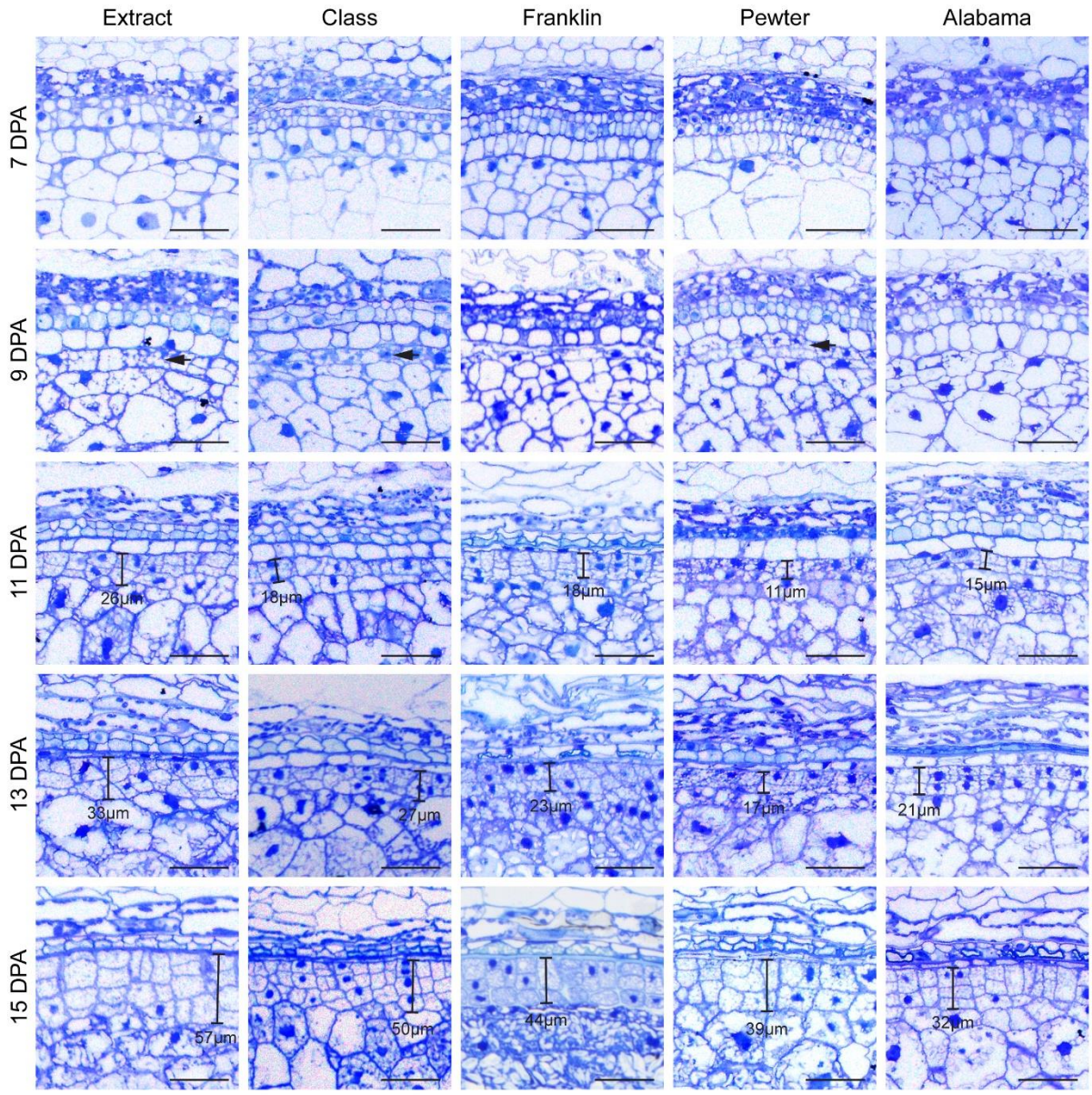

Figure 5-S6: Developing barley grain sections stained with Toluidine Blue to depict changes in aleurone morphology across development. High aleurone lines are cv Extract and Class, intermediate aleurone line is cv Franklin, while low aleurone lines are cv Pewter and Alabama. Scale bar = 50 µm

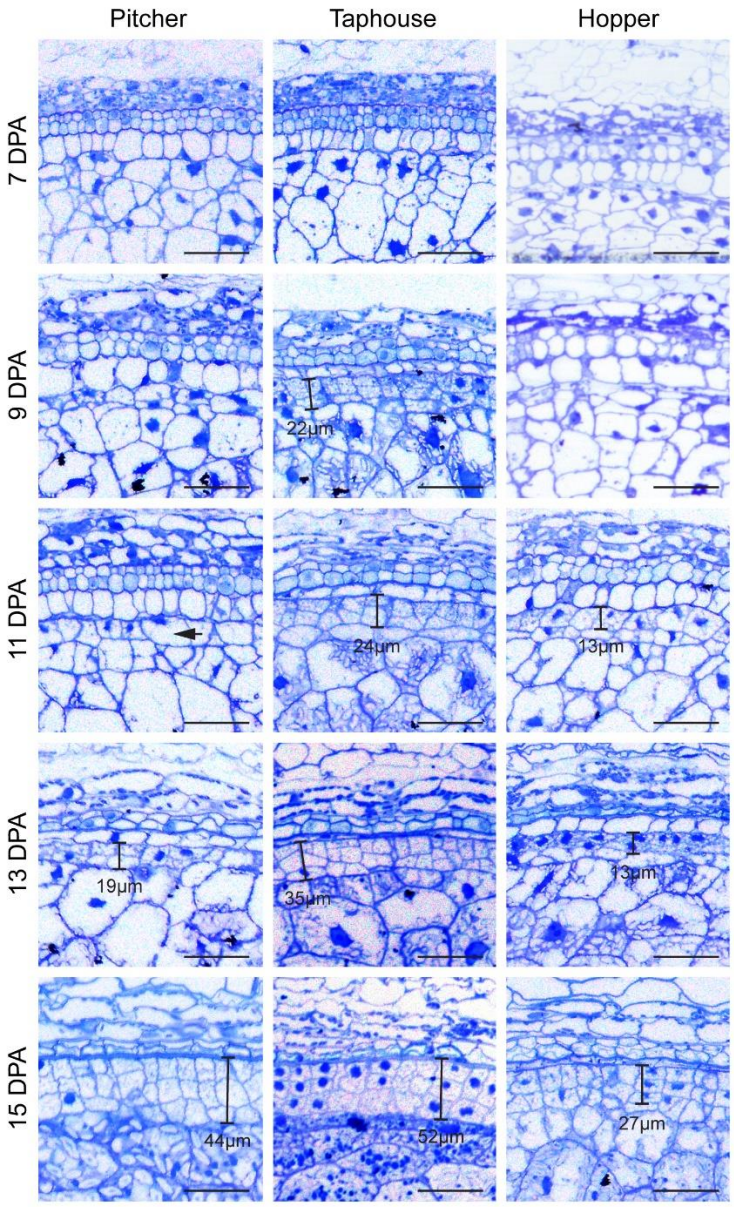

Figure 5-S7: Developing barley grain sections stained with Toluidine Blue to depict changes in aleurone morphology across development. High, intermediate and low aleurone lines are cv Pitcher (high), Taphouse (high/intermediate) and Hopper (low). Scale bar = 50 µm

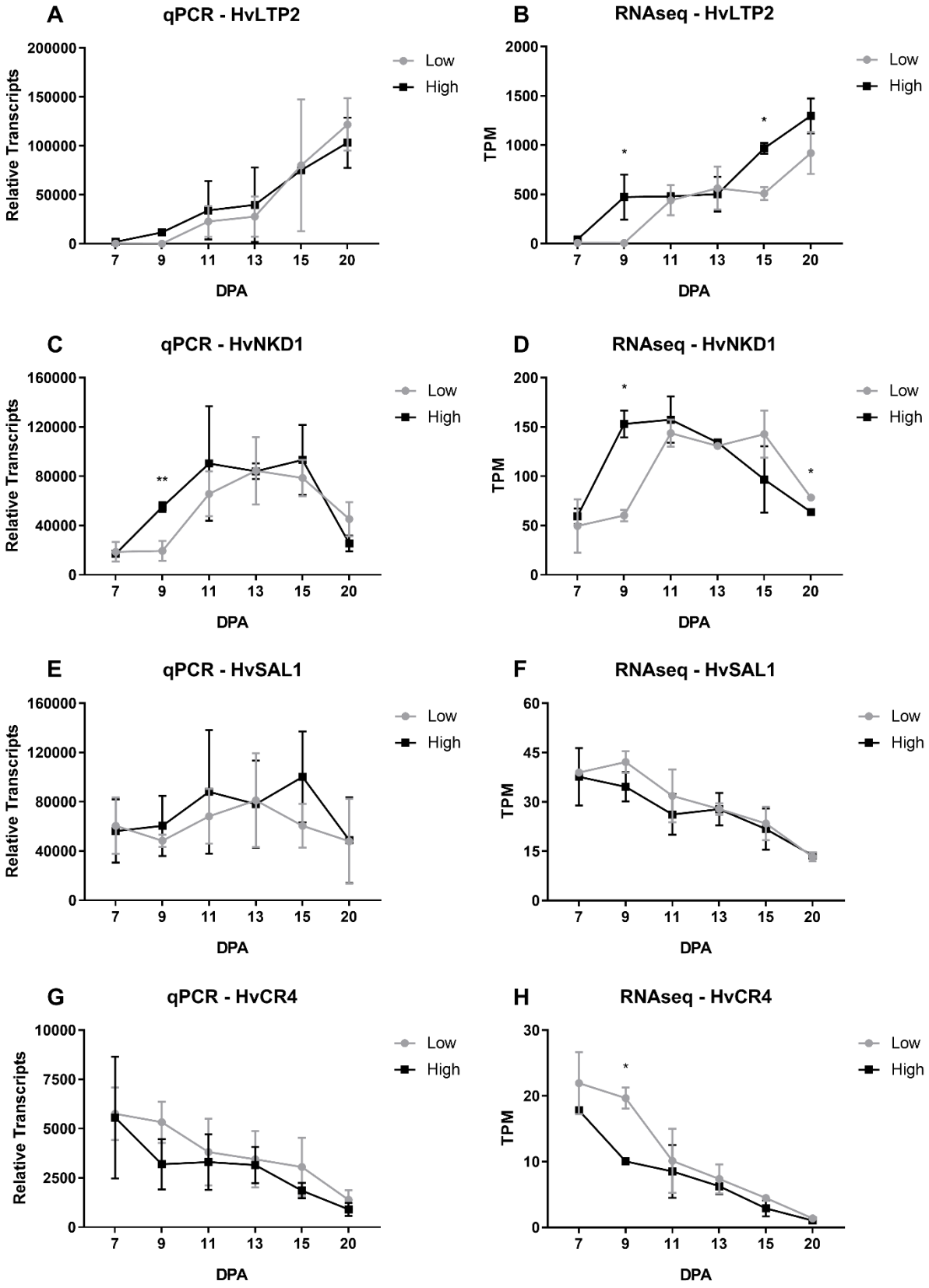
A
qPCR - HvLTP2
Relative Transcripts
200000
150000
100000
50000
0
7
9
11
13
15
20
DPA
Low
High
B
RNAseq - HvLTP2
TPM
2000
1500
1000
500
0
*
*
C
qPCR - HvNKD1
160000
120000
80000
40000
**
D
RNAseq - HvNKD1
200
150
100
50
E
qPCR - HvSAL1
F
RNAseq - HvSAL1
60
45
30
15
G
qPCR - HvCR4
10000
7500
5000
2500
H
RNAseq - HvCR4
30
20
10

Figure 5-S8: Comparison of transcript levels of candidate aleurone genes by quantitative PCR (qPCR) and RNA sequencing (RNAseq). Relative transcript abundance from high aleurone genotypes (cv Extract and Taphouse averaged; black) and low aleurone genotypes (cv Alabama, Pewter and Hopper averaged; grey) were compared to validate quality of both datasets. Transcript level differences were observed between high and low genotypes across grain development for known aleurone genes (*HvLTP2*, *HvNKD1*, *HvSAL1* and *HvCR4*). Significance * = $p \leq 0.05$, ** = $p \leq 0.0021$.

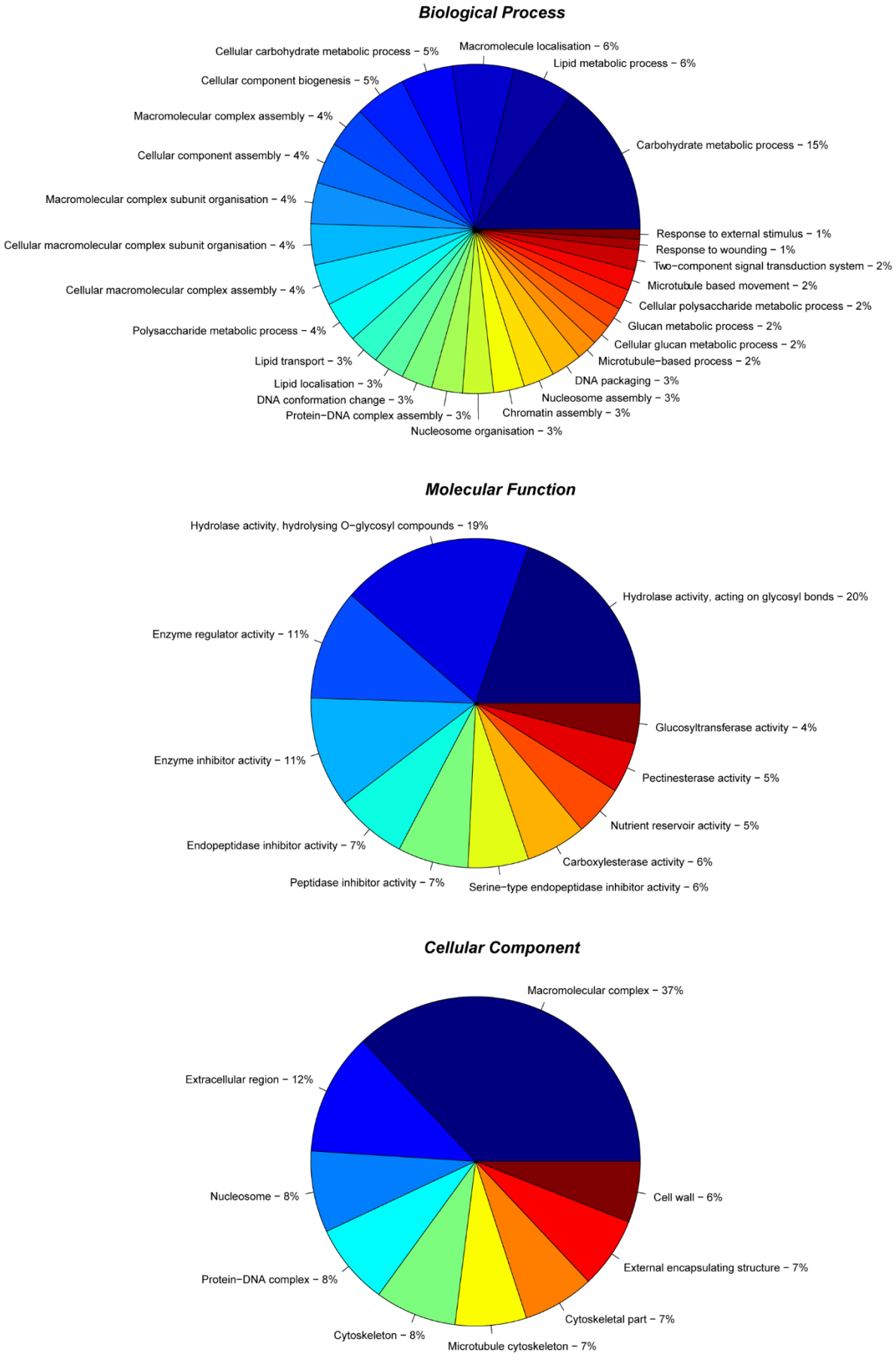
Biological Process
Macromolecule localisation − 6%
Lipid metabolic process − 6%
Carbohydrate metabolic process − 15%
Response to external stimulus − 1%
Response to wounding − 1%
Two−component signal transduction system − 2%
Microtubule based movement − 2%
Cellular polysaccharide metabolic process − 2%
Glucan metabolic process − 2%
Cellular glucan metabolic process − 2%
Microtubule−based process − 2%
DNA packaging − 3%
Nucleosome assembly − 3%
Chromatin assembly − 3%
Nucleosome organisation − 3%
Protein−DNA complex assembly − 3%
DNA conformation change − 3%
Lipid localisation − 3%
Lipid transport − 3%
Polysaccharide metabolic process − 4%
Cellular macromolecular complex assembly − 4%
Cellular macromolecular complex subunit organisation − 4%
Macromolecular complex subunit organisation − 4%
Cellular component assembly − 4%
Macromolecular complex assembly − 4%
Cellular component biogenesis − 5%
Cellular carbohydrate metabolic process − 5%
Molecular Function
Hydrolase activity, hydrolysing O−glycosyl compounds − 19%
Hydrolase activity, acting on glycosyl bonds − 20%
Glucosyltransferase activity − 4%
Pectinesterase activity − 5%
Nutrient reservoir activity − 5%
Carboxylesterase activity − 6%
Serine−type endopeptidase inhibitor activity − 6%
Peptidase inhibitor activity − 7%
Endopeptidase inhibitor activity − 7%
Enzyme inhibitor activity − 11%
Enzyme regulator activity − 11%
Cellular Component
Macromolecular complex − 37%
Cell wall − 6%
External encapsulating structure − 7%
Cytoskeletal part − 7%
Microtubule cytoskeleton − 7%
Cytoskeleton − 8%
Protein−DNA complex − 8%
Nucleosome − 8%
Extracellular region − 12%

Figure 5-S9: Distribution of the 47 significantly unique gene ontology (GO) identifiers from the wholegrain differentially expressed genes. Categories are biological process, molecular function and cellular component. The segments represent the number of genes as a percentage within each identifier.

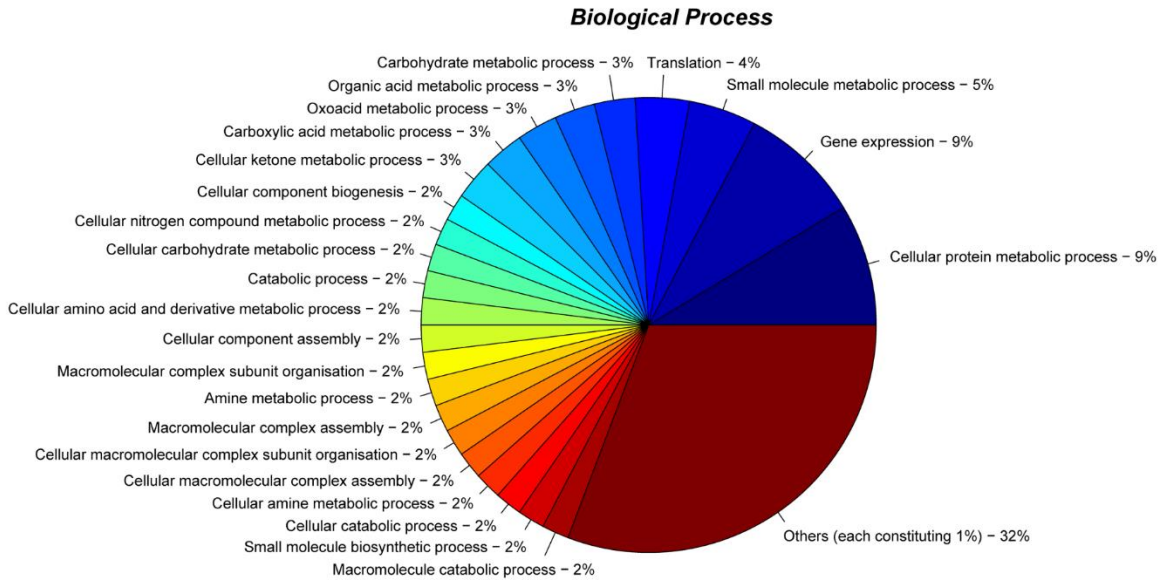
Biological Process
Carbohydrate metabolic process − 3%
Translation − 4%
Organic acid metabolic process − 3%
Small molecule metabolic process − 5%
Oxoacid metabolic process − 3%
Carboxylic acid metabolic process − 3%
Gene expression − 9%
Cellular ketone metabolic process − 3%
Cellular component biogenesis − 2%
Cellular nitrogen compound metabolic process − 2%
Cellular carbohydrate metabolic process − 2%
Cellular protein metabolic process − 9%
Catabolic process − 2%
Cellular amino acid and derivative metabolic process − 2%
Cellular component assembly − 2%
Macromolecular complex subunit organisation − 2%
Amine metabolic process − 2%
Macromolecular complex assembly − 2%
Cellular macromolecular complex subunit organisation − 2%
Cellular macromolecular complex assembly − 2%
Cellular amine metabolic process − 2%
Cellular catabolic process − 2%
Small molecule biosynthetic process − 2%
Macromolecule catabolic process − 2%
Others (each constituting 1%) − 32%

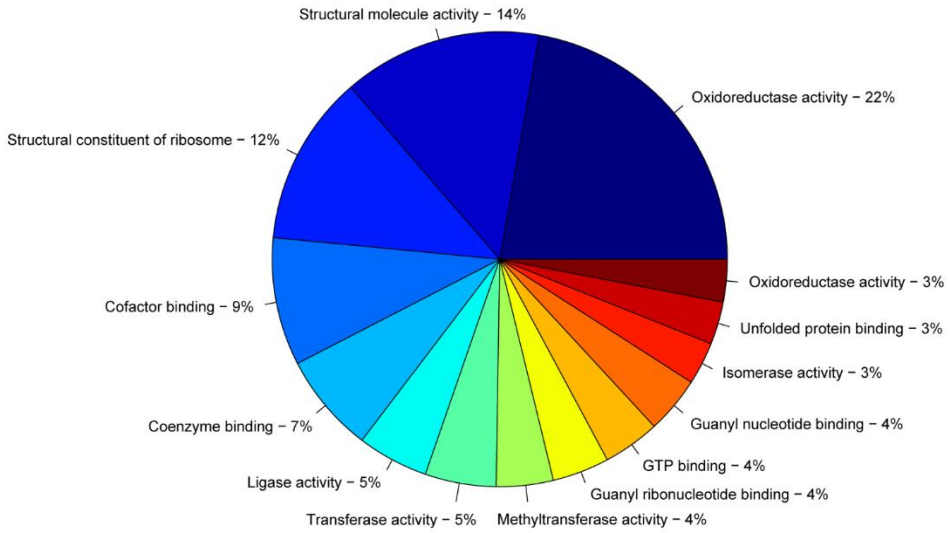
Molecular Function
Structural molecule activity − 14%
Oxidoreductase activity − 22%
Structural constituent of ribosome − 12%
Oxidoreductase activity − 3%
Cofactor binding − 9%
Unfolded protein binding − 3%
Isomerase activity − 3%
Guanyl nucleotide binding − 4%
Coenzyme binding − 7%
GTP binding − 4%
Ligase activity − 5%
Guanyl ribonucleotide binding − 4%
Transferase activity − 5%
Methyltransferase activity − 4%

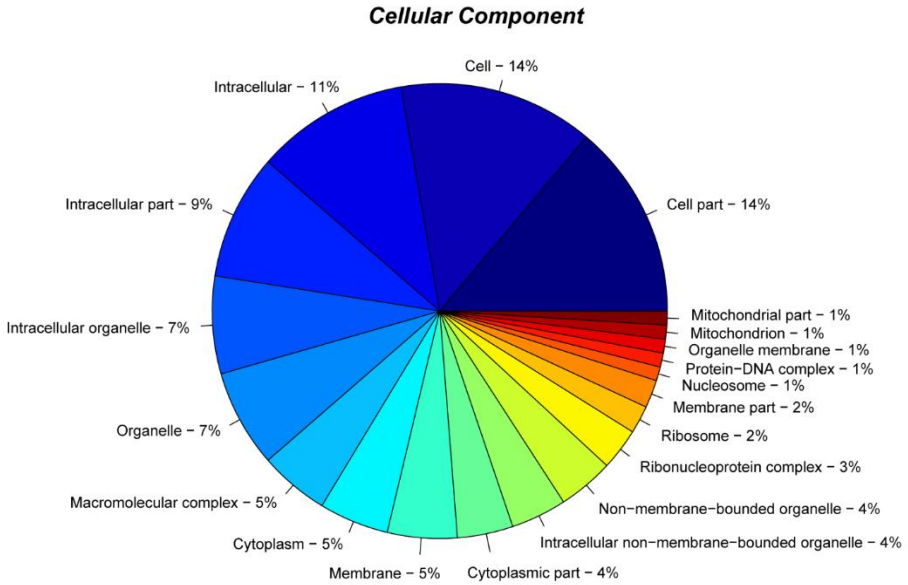
Cellular Component
Cell − 14%
Intracellular − 11%
Intracellular part − 9%
Cell part − 14%
Mitochondrial part − 1%
Intracellular organelle − 7%
Mitochondrion − 1%
Organelle membrane − 1%
Protein−DNA complex − 1%
Nucleosome − 1%
Membrane part − 2%
Organelle − 7%
Ribosome − 2%
Ribonucleoprotein complex − 3%
Macromolecular complex − 5%
Non−membrane−bounded organelle − 4%
Cytoplasm − 5%
Intracellular non−membrane−bounded organelle − 4%
Membrane − 5%
Cytoplasmic part − 4%

Figure 5-S10: Distribution of the 90 significantly unique gene ontology (GO) identifiers from LCM RNAseq for genes enriched in the aleurone. Categories are biological process, molecular function and cellular component. The segments represent the number of genes as a percentage within each identifier.

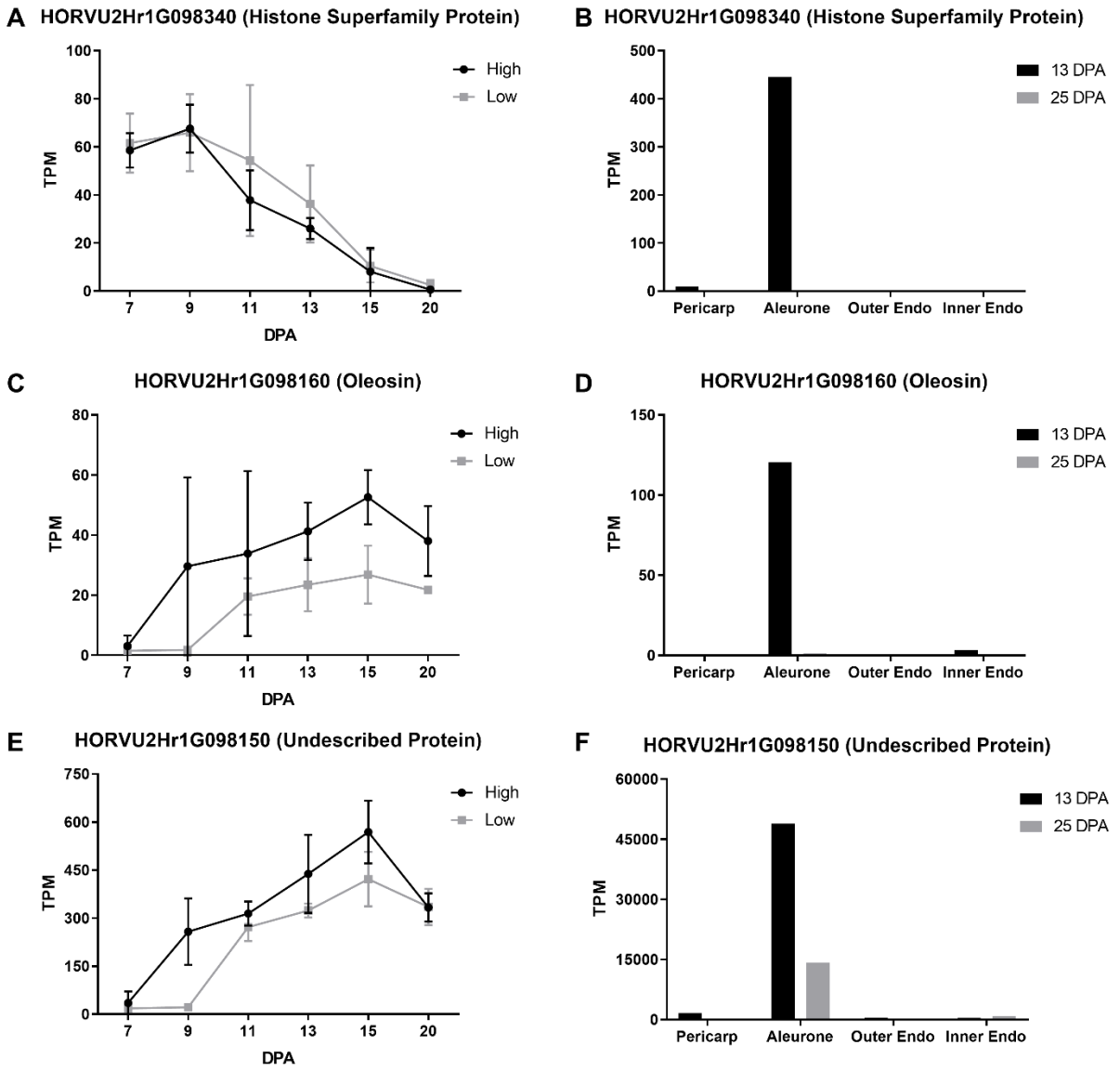

Figure 5-S11: Transcript abundance (TPM) of interesting HORVUs identified under aleurone QTL. Graphs A, C and E indicate relative transcript abundance from high aleurone genotypes (cv Extract and Taphouse averaged; black) and low aleurone genotypes (cv Alabama, Pewter and Hopper averaged; grey) across grain development. Graphs B, D and F indicate differential transcript abundance between developing tissues (13 and 25 DPA) from LCM samples.

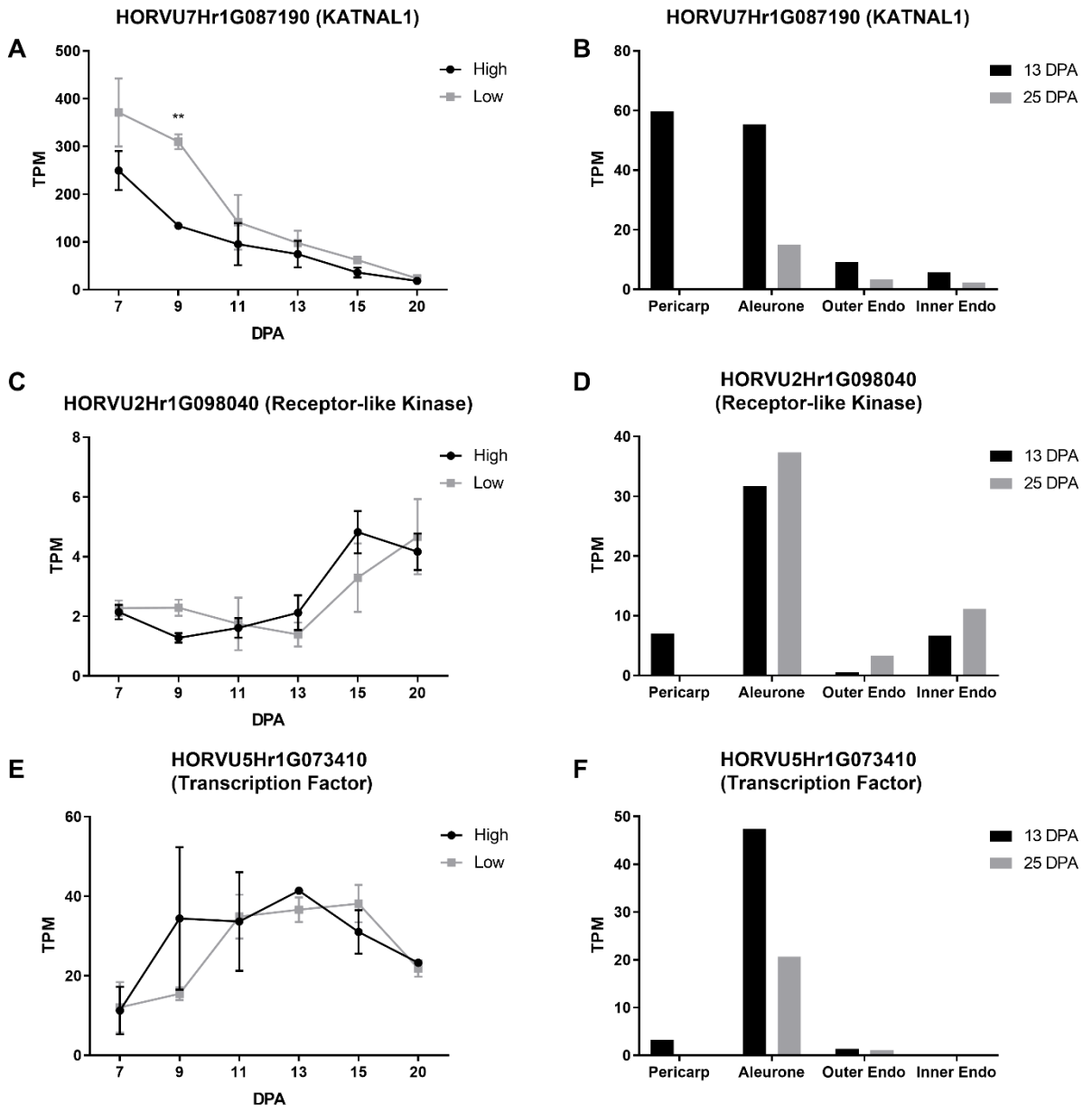

Figure 5-S12: Transcript abundance (TPM) of interesting HORVUs identified under aleurone QTL. Graphs A, C and E indicate relative transcript abundance from high aleurone genotypes (cv Extract and Taphouse averaged; black) and low aleurone genotypes (cv Alabama, Pewter and Hopper averaged; grey) across grain development. Graphs B, D and F indicate differential transcript abundance between developing tissues (13 and 25 DPA) from LCM samples. Significance; ** = $p \leq 0.01$.

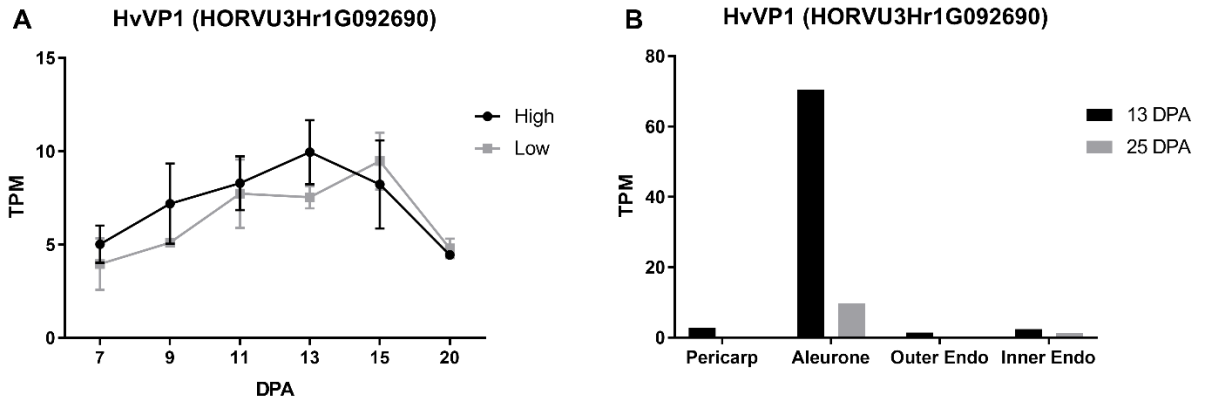

Figure 5-S13: Transcript abundance (TPM) of *HvVP1*. A) Relative transcript abundance from high aleurone genotypes (cv Extract and Taphouse averaged; black) and low aleurone genotypes (cv Alabama, Pewter and Hopper averaged; grey) across grain development. B) Differential transcript levels between developing tissues (13 and 25 DPA) from LCM samples.

Supplementary Tables

Table 5-S1: Grain measurements for 150 European 2-row spring barley genotypes

		Transverse sections								Seed Scanner (SS)			
Cultivar	**Genetic cluster**	**EA (mm²)**	**SEA (mm²)**	**AA (mm²)**	**AP (%)**	**DVW (µm)**	**LRW (µm)**	**ALN**	**AW (µm)**	**R**	**GL (mm)**	**GWi (mm)**	**GT (mm)**
Aapo	old spring 2r	3.76 ± 0.16	3.17 ± 0.16	0.59 ± 0.02	15.60 ± 0.86	1923 ± 71	2982 ± 123	2.8 ± 0.6	62.5 ± 5.8	2.61	9.63 ± 0.57	3.06 ± 0.38	2.76 ± 0.11
Acapella *	elite spring 2r	8.30 ± 0.24	7.49 ± 0.19	0.81 ± 0.10	9.74 ± 1.01	2967 ± 54	4026 ± 126	2.4 ± 0.5	79.4 ± 15.4	3.17	9.90 ± 0.73	3.43 ± 0.53	2.21 ± 1.18
Adonis *	elite spring 2r	8.83 ± 0.47	8.18 ± 0.55	0.65 ± 0.10	7.43 ± 1.53	3136 ± 90	3904 ± 87	2.7 ± 0.8	67.1 ± 17.8	2.49	9.50 ± 0.58	3.47 ± 0.40	2.98 ± 0.17
Agenda *	elite spring 2r	7.88 ± 0.77	7.27 ± 0.83	0.61 ± 0.07	7.79 ± 1.67	2982 ± 146	3918 ± 94	2.8 ± 0.8	64.2 ± 12.1	2.61	9.15 ± 0.68	3.08 ± 0.50	2.55 ± 1.00
Akita	elite spring 2r	7.64 ± 0.33	6.83 ± 0.33	0.81 ± 0.02	10.60 ± 0.47	2831 ± 224	3945 ± 67	2.7 ± 0.8	74.6 ± 10.1	2.42	9.60 ± 3.35	3.27 ± 1.09	2.95 ± 0.01
Alabama *	admixted	8.09 ± 0.16	7.52 ± 0.15	0.56 ± 0.01	6.93 ± 0.09	2934 ± 50	3730 ± 38	2.1 ± 0.9	52.0 ± 10.8	2.81	8.87 ± 0.44	3.07 ± 0.42	2.21 ± 1.18
Alis *	elite spring 2r	8.84 ± 0.17	8.12 ± 0.15	0.71 ± 0.03	8.07 ± 0.23	3000 ± 59	3820 ± 28	2.7 ± 0.8	60.6 ± 10.1	3.16	9.55 ± 0.81	2.80 ± 0.44	2.16 ± 0.42
Alliot *	elite spring 2r	9.96 ± 0.43	9.32 ± 0.37	0.65 ± 0.05	6.48 ± 0.27	3280 ± 69	4044 ± 77	2.7 ± 0.8	64.8 ± 10.6	3.07	9.41 ± 0.55	3.21 ± 0.43	2.35 ± 0.87
Amourette *	elite spring 2r	8.34 ± 0.45	7.53 ± 0.39	0.81 ± 0.08	9.66 ± 0.60	3029 ± 38	3749 ± 176	2.6 ± 0.6	80.8 ± 15.2	2.73	9.77 ± 0.53	3.21 ± 0.54	2.50 ± 0.24
Anaconda *	elite spring 2r	10.58 ± 0.61	9.72 ± 0.62	0.85 ± 0.03	8.10 ± 0.64	3412 ± 40	4256 ± 30	2.6 ± 0.6	68.8 ± 10.9	2.54	9.98 ± 0.71	3.53 ± 0.37	2.80 ± 0.12
Annabell *	elite spring 2r	8.20 ± 0.32	7.48 ± 0.36	0.71 ± 0.05	8.74 ± 0.93	2848 ± 82	3800 ± 47	2.6 ± 0.9	63.6 ± 8.4	2.60	9.14 ± 0.67	3.54 ± 0.39	2.66 ± 0.71
Ardila *	elite spring 2r	8.60 ± 0.69	7.72 ± 0.70	0.88 ± 0.04	10.26 ± 0.96	2981 ± 235	3988 ± 80	2.7 ± 0.8	83.1 ± 13.1	2.75	9.10 ± 0.53	3.09 ± 0.50	2.32 ± 0.59
Astoria *	elite spring 2r	7.31 ± 0.31	6.59 ± 0.24	0.73 ± 0.09	9.94 ± 0.94	2774 ± 215	3608 ± 46	3.0 ± 0.8	76.3 ± 15.3	2.62	9.68 ± 0.71	3.31 ± 0.39	2.56 ± 0.13
Athena *	admixted	9.88 ± 0.81	9.07 ± 0.81	0.81 ± 0.002	8.26 ± 0.68	3280 ± 64	4063 ± 183	2.6 ± 0.8	75.9 ± 12.1	2.34	9.00 ± 1.34	3.38 ± 0.56	2.85 ± 0.18
Athos	admixted	6.31 ± 0.98	5.71 ± 1.01	0.60 ± 0.09	9.73 ± 2.52	2518 ± 234	3442 ± 108	2.4 ± 0.8	63.0 ± 11.5	2.62	9.80 ± 0.92	3.22 ± 0.43	2.67 ± 0.04
Atlas *	admixted	9.43 ± 0.76	8.75 ± 0.77	0.68 ± 0.03	7.23 ± 0.70	3204 ± 130	3782 ± 169	2.7 ± 0.8	64.0 ± 10.7	2.98	9.66 ± 0.58	2.95 ± 0.33	2.22 ± 0.27
Auriga *	elite spring 2r	9.21 ± 0.07	8.45 ± 0.06	0.76 ± 0.02	8.27 ± 0.13	3064 ± 43	3839 ± 22	2.6 ± 1.0	60.2 ± 8.0	2.66	10.08 ± 0.56	3.28 ± 0.51	2.66 ± 0.07
Avec	elite spring 2r	5.98 ± 0.11	5.44 ± 0.12	0.55 ± 0.004	9.15 ± 0.24	2527 ± 46	3399 ± 41	2.7 ± 0.7	52.5 ± 7.8	2.92	9.65 ± 0.53	3.26 ± 0.37	2.24 ± 0.64
Barke	elite spring 2r	4.16 ± 0.07	3.73 ± 0.08	0.43 ± 0.02	10.4 ± 0.66	2062 ± 28	3071 ± 72	2.5 ± 0.9	43.1 ± 5.5	2.34	9.14 ± 0.35	3.13 ± 0.54	2.85 ± 1.00
Baronesse *	admixted	9.60 ± 0.58	8.91 ± 0.51	0.70 ± 0.12	7.26 ± 1.05	3156 ± 99	4043 ± 130	2.6 ± 0.8	61.4 ± 15.2	2.79	9.65 ± 0.78	2.92 ± 0.49	2.43 ± 0.43
Berac *	admixted	6.98 ± 0.13	6.46 ± 0.12	0.53 ± 0.02	7.53 ± 0.23	2736 ± 35	3524 ± 49	2.7 ± 0.8	56.4 ± 8.2	3.15	8.92 ± 3.25	3.11 ± 1.03	1.93 ± 0.96
Beryllium	TBD	7.06 ± 0.25	6.37 ± 0.13	0.69 ± 0.11	9.74 ± 1.30	2635 ± 30	3745 ± 79	2.6 ± 0.7	74.4 ± 12.2	3.64	9.78 ± 0.62	3.49 ± 0.47	2.02 ± 1.27
Braemar *	elite spring 2r	9.32 ± 0.59	8.56 ± 0.63	0.76 ± 0.06	8.20 ± 1.01	3220 ± 98	3928 ± 6	2.9 ± 0.8	73.6 ± 14.6	2.64	9.88 ± 1.40	3.43 ± 0.55	2.67 ± 0.39

Brazil	elite spring 2r	4.61 ± 0.10	4.10 ± 0.10	0.51 ± 0.02	11.10 ± 0.59	2300 ± 156	3040 ± 68	2.4 ± 0.7	68.4 ± 11.5	2.88	9.45 ± 0.63	2.79 ± 0.39	2.33 ± 0.29
Cabaret *	elite spring 2r	8.72 ± 0.36	7.97 ± 0.37	0.76 ± 0.05	8.69 ± 0.66	2972 ± 213	4113 ± 51	2.7 ± 0.7	70.0 ± 13.4	2.65	9.90 ± 0.42	3.44 ± 0.52	2.65 ± 0.05
Calico	elite spring 2r	8.27 ± 0.27	7.72 ± 0.22	0.55 ± 0.05	6.67 ± 0.39	2981 ± 60	3793 ± 64	2.6 ± 0.5	62.5 ± 14.4	2.76	10.19 ± 0.67	3.42 ± 0.58	2.59 ± 0.57
Cambrinus	TBD	4.30 ± 0.20	3.78 ± 0.18	0.51 ± 0.02	11.94 ± 0.16	2103 ± 158	3125 ± 107	3.1 ± 1.0	62.3 ± 8.6	2.51	8.30 ± 2.69	2.96 ± 0.91	2.45 ± 0.12
Camir	admixted	5.85 ± 0.44	5.14 ± 0.46	0.71 ± 0.03	12.25 ± 1.26	2342 ± 108	3439 ± 51	2.6 ± 0.6	70.6 ± 10.4	2.45	8.34 ± 0.38	2.96 ± 0.39	2.47 ± 0.11
Campala *	elite spring 2r	7.11 ± 0.36	6.43 ± 0.38	0.68 ± 0.04	9.59 ± 0.86	2801 ± 67	3500 ± 32	2.6 ± 0.6	66.7 ± 11.1	2.89	8.87 ± 1.70	2.92 ± 0.53	2.18 ± 0.58
Casino *	TBD	8.61 ± 0.62	7.94 ± 0.52	0.66 ± 0.14	7.67 ± 1.25	3015 ± 148	4052 ± 137	2.4 ± 0.6	64.1 ± 10.1	3.45	9.66 ± 0.27	2.46 ± 0.78	1.92 ± 0.17
Catalina *	elite spring 2r	8.29 ± 0.58	7.51 ± 0.65	0.78 ± 0.08	9.44 ± 1.61	2846 ± 239	3879 ± 80	3.1 ± 0.6	77.9 ± 12.5	2.43	8.51 ± 4.10	2.97 ± 1.25	2.66 ± 0.08
Cecilia *	admixted	8.45 ± 0.75	7.69 ± 0.71	0.75 ± 0.09	8.92 ± 0.90	2966 ± 128	3856 ± 87	3.0 ± 0.6	70.7 ± 8.3	2.73	9.32 ± 1.55	3.21 ± 0.55	2.35 ± 0.54
Celebra *	admixted	11.38 ± 0.21	10.54 ± 0.2	0.84 ± 0.03	7.41 ± 0.16	3545 ± 54	4300 ± 62	2.6 ± 0.5	73.1 ± 11.4	2.43	9.30 ± 0.67	3.45 ± 0.37	2.76 ± 0.52
Cellar *	elite spring 2r	8.74 ± 0.21	8.07 ± 0.23	0.67 ± 0.03	7.71 ± 0.45	2949 ± 40	4023 ± 35	2.7 ± 0.7	61.8 ± 8.2	2.89	10.10 ± 0.79	3.21 ± 0.31	2.32 ± 0.54
Chariot *	elite spring 2r	8.17 ± 0.26	7.53 ± 0.21	0.63 ± 0.07	7.74 ± 0.65	2850 ± 137	3694 ± 68	3.3 ± 0.7	72.5 ± 9.6	2.73	9.55 ± 0.73	3.30 ± 0.66	2.51 ± 1.00
Charm	elite spring 2r	4.73 ± 0.36	4.17 ± 0.35	0.56 ± 0.03	11.96 ± 0.97	2223 ± 55	2987 ± 99	2.6 ± 0.6	59.7 ± 9.0	2.73	9.23 ± 0.67	3.05 ± 0.38	2.40 ± 0.12
Chieftain *	elite spring 2r	9.47 ± 0.42	8.77 ± 0.45	0.70 ± 0.07	7.42 ± 0.88	3316 ± 86	3895 ± 57	2.7 ± 0.8	69.4 ± 19.4	2.87	9.31 ± 1.04	2.90 ± 0.56	2.32 ± 0.40
Chime	elite spring 2r	4.96 ± 0.33	4.37 ± 0.33	0.60 ± 0.02	12.11 ± 0.85	2244 ± 143	3179 ± 238	2.6 ± 0.9	58.0 ± 12.0	3.00	9.54 ± 0.82	3.14 ± 0.37	2.48 ± 0.57
Clarity *	admixted	8.02 ± 0.25	7.38 ± 0.24	0.63 ± 0.02	7.90 ± 0.23	2864 ± 39	3711 ± 91	2.9 ± 1.1	68.9 ± 8.7	2.45	9.28 ± 0.64	3.36 ± 0.31	2.73 ± 0.16
Class *	elite spring 2r	8.47 ± 0.31	7.58 ± 0.25	0.89 ± 0.07	10.52 ± 0.50	3026 ± 88	3828 ± 169	2.7 ± 0.8	84.9 ± 24.3	2.61	9.89 ± 0.69	3.44 ± 0.40	2.68 ± 0.19
Cocktail *	TBD	9.12 ± 0.15	8.41 ± 0.16	0.71 ± 0.02	7.84 ± 0.30	2929 ± 36	4015 ± 66	2.8 ± 0.7	72.4 ± 9.6	2.80	8.26 ± 4.06	2.78 ± 1.33	2.43 ± 0.23
Colada *	elite spring 2r	10.09 ± 0.38	9.40 ± 0.33	0.70 ± 0.08	6.90 ± 0.60	3207 ± 123	4166 ± 49	2.8 ± 1.0	65.3 ± 14.4	2.69	9.87 ± 0.66	3.26 ± 0.60	2.52 ± 0.48
Cooper *	elite spring 2r	8.21 ± 0.39	7.57 ± 0.37	0.64 ± 0.02	7.83 ± 0.14	2898 ± 61	3759 ± 60	2.7 ± 0.8	62.6 ± 9.7	2.55	9.50 ± 0.86	3.10 ± 0.53	2.70 ± 0.06
Cribbage	admixted	7.81 ± 0.33	7.34 ± 0.31	0.46 ± 0.07	5.93 ± 0.87	2823 ± 91	3752 ± 99	2.4 ± 0.7	61.2 ± 9.2	2.52	9.56 ± 0.60	3.26 ± 0.44	2.77 ± 1.00
Croydon *	admixted	8.59 ± 0.11	7.81 ± 0.10	0.79 ± 0.05	9.16 ± 0.53	2983 ± 15	3774 ± 10	2.6 ± 0.6	73.2 ± 10.0	2.38	9.15 ± 0.59	3.36 ± 0.34	2.85 ± 0.11
Crusader	elite spring 2r	5.85 ± 0.09	5.16 ± 0.13	0.69 ± 0.08	11.8 ± 1.41	2474 ± 113	3695 ± 81	2.6 ± 0.7	72.6 ± 14.4	4.62	10.19 ± 1.02	3.08 ± 0.59	1.81 ± 1.07
Danuta *	elite spring 2r	10.28 ± 0.25	9.55 ± 0.22	0.73 ± 0.03	7.08 ± 0.15	3175 ± 91	4311 ± 32	2.6 ± 0.6	69.0 ± 9.5	2.57	10.02 ± 0.86	3.33 ± 0.42	2.82 ± 0.18
Delibes	elite spring 2r	1.87 ± 0.05	1.54 ± 0.04	0.33 ± 0.01	17.67 ± 0.36	1415 ± 103	2592 ± 64	2.4 ± 0.8	41.8 ± 4.4	2.78	9.43 ± 1.43	3.03 ± 0.49	2.49 ± 0.30
Derkado *	elite spring 2r	8.56 ± 0.17	7.96 ± 0.13	0.60 ± 0.04	7.03 ± 0.37	2944 ± 77	3930 ± 22	2.5 ± 0.6	60.9 ± 9.2	2.81	9.91 ± 0.84	3.43 ± 0.52	2.20 ± 1.10
Draught *	elite spring 2r	6.79 ± 0.10	6.13 ± 0.11	0.66 ± 0.02	9.77 ± 0.36	2649 ± 54	3439 ± 113	3.2 ± 0.8	63.9 ± 9.0	2.50	9.15 ± 1.58	3.38 ± 0.62	2.65 ± 0.19
Drum *	elite spring 2r	5.76 ± 0.26	5.19 ± 0.19	0.57 ± 0.07	9.86 ± 0.72	2452 ± 56	3407 ± 53	2.6 ± 0.7	59.2 ± 14.7	2.71	10.04 ± 0.85	3.40 ± 0.46	2.61 ± 0.32
Elo *	admixted	7.60 ± 0.70	6.96 ± 0.71	0.64 ± 0.01	8.48 ± 0.95	2679 ± 200	3735 ± 50	2.4 ± 0.6	63.1 ± 16.3	2.54	9.10 ± 0.64	2.93 ± 0.35	2.53 ± 0.07

Extract *	elite spring 2r	7.50 ± 0.37	6.54 ± 0.34	0.97 ± 0.09	12.88 ± 1.13	2755 ± 71	3831 ± 207	2.5 ± 0.6	85.0 ± 13.2	2.71	9.90 ± 0.68	3.37 ± 0.45	2.69 ± 0.13
Fairytale *	elite spring 2r	8.46 ± 0.53	7.94 ± 0.56	0.52 ± 0.06	6.17 ± 0.91	2925 ± 6	3733 ± 250	2.7 ± 0.8	58.0 ± 12.0	2.47	8.89 ± 0.68	3.01 ± 0.48	2.67 ± 0.06
Felicie *	admixted	9.72 ± 0.12	9.01 ± 0.09	0.71 ± 0.03	7.33 ± 0.22	3084 ± 39	4085 ± 24	2.6 ± 0.7	62.6 ± 8.4	2.66	9.45 ± 1.20	3.17 ± 0.52	2.54 ± 0.35
Formula *	admixted	8.30 ± 0.59	7.57 ± 0.52	0.73 ± 0.07	8.78 ± 0.28	2784 ± 172	3946 ± 79	2.9 ± 0.7	71.2 ± 12.8	2.94	10.06 ± 0.71	3.30 ± 0.50	2.30 ± 0.63
Forum *	admixted	6.60 ± 0.11	6.05 ± 0.15	0.56 ± 0.06	8.47 ± 1.02	2665 ± 51	3388 ± 64	2.7 ± 0.6	54.4 ± 10.2	3.30	9.83 ± 0.37	2.58 ± 0.50	2.01 ± 0.23
Foxtrot *	elite spring 2r	9.28 ± 0.16	8.61 ± 0.22	0.68 ± 0.06	7.29 ± 0.73	3110 ± 151	4095 ± 77	2.4 ± 0.8	56.5 ± 8.7	2.58	10.15 ± 0.73	3.37 ± 0.39	2.96 ± 0.19
Franklin *	admixted	8.31 ± 0.33	7.62 ± 0.36	0.69 ± 0.03	8.34 ± 0.65	2869 ± 19	3843 ± 103	2.8 ± 0.7	67.1 ± 7.9	2.83	9.12 ± 0.57	2.82 ± 0.43	2.44 ± 0.27
Gant *	admixted	6.28 ± 0.20	5.69 ± 0.20	0.59 ± 0.03	9.44 ± 0.52	2495 ± 86	3330 ± 89	2.8 ± 0.9	54.0 ± 7.2	2.71	9.86 ± 0.74	3.22 ± 0.46	2.51 ± 0.18
Global	elite spring 2r	9.61 ± 0.72	8.80 ± 0.90	0.80 ± 0.20	8.50 ± 2.78	3058 ± 67	4138 ± 112	3.1 ± 1.0	80.7 ± 22.9	2.61	8.85 ± 0.70	3.41 ± 0.38	2.57 ± 0.65
Golden Promise *	TBD	8.42 ± 0.67	7.78 ± 0.58	0.64 ± 0.09	7.60 ± 0.49	2903 ± 67	3877 ± 88	2.5 ± 0.7	61.0 ± 9.0	2.55	8.88 ± 0.63	3.31 ± 0.41	2.45 ± 0.27
Goldie	admixted	7.36 ± 0.46	6.54 ± 0.46	0.82 ± 0.05	11.15 ± 0.99	2987 ± 64	4136 ± 75	2.7 ± 0.8	79.6 ± 16	2.48	8.98 ± 0.69	3.36 ± 0.73	2.55 ± 0.20
Granta	elite spring 2r	7.88 ± 0.14	7.17 ± 0.12	0.70 ± 0.03	8.92 ± 0.26	2752 ± 181	4025 ± 65	2.7 ± 0.7	74.4 ± 11	2.69	10.63 ± 0.71	3.42 ± 0.47	2.78 ± 0.14
Gull *	old spring 2r	7.82 ± 0.17	7.19 ± 0.20	0.63 ± 0.03	8.07 ± 0.58	2744 ± 40	3686 ± 39	2.8 ± 0.9	60.1 ± 6.3	2.35	8.12 ± 3.66	2.79 ± 1.05	2.61 ± 0.01
Gundel *	admixted	9.08 ± 0.18	8.38 ± 0.18	0.70 ± 0.04	7.68 ± 0.41	3182 ± 34	3851 ± 52	2.6 ± 0.6	59.2 ± 11.3	2.84	10.10 ± 0.76	3.30 ± 0.31	2.60 ± 0.77
Hana *	admixted	7.16 ± 0.49	6.57 ± 0.46	0.59 ± 0.03	8.21 ± 0.18	2730 ± 115	3471 ± 99	2.8 ± 0.9	57.0 ± 9.2	2.59	9.02 ± 0.67	2.99 ± 0.32	2.52 ± 0.13
Harry	old spring 2r	6.40 ± 0.33	5.71 ± 0.29	0.69 ± 0.05	10.79 ± 0.46	2486 ± 160	3912 ± 17	2.5 ± 0.6	73.6 ± 11.2	2.62	10.18 ± 0.65	3.24 ± 0.54	2.68 ± 0.14
Hart *	admixted	8.67 ± 0.06	7.98 ± 0.05	0.69 ± 0.03	7.99 ± 0.29	2944 ± 43	3997 ± 79	2.8 ± 0.7	68.1 ± 12.3	2.46	9.26 ± 0.56	3.30 ± 0.48	2.74 ± 0.20
Hassan	old spring 2r	7.66 ± 0.37	6.92 ± 0.35	0.74 ± 0.02	9.68 ± 0.17	2818 ± 157	3933 ± 54	2.6 ± 0.7	72.1 ± 13.9	2.47	9.31 ± 1.45	3.45 ± 0.54	2.64 ± 0.19
Heather	admixted	6.00 ± 0.12	5.36 ± 0.14	0.64 ± 0.02	10.72 ± 0.55	2579 ± 82	3381 ± 16	2.7 ± 0.8	57.4 ± 7.2	2.45	8.69 ± 0.22	3.05 ± 0.45	2.70 ± 1.00
Helmi *	admixted	8.49 ± 0.27	7.77 ± 0.27	0.72 ± 0.02	8.50 ± 0.35	2921 ± 86	3811 ± 64	2.8 ± 0.9	66.3 ± 12.3	3.00	9.86 ± 0.84	3.01 ± 0.38	2.30 ± 0.47
Heris *	admixted	9.69 ± 0.44	8.96 ± 0.40	0.74 ± 0.04	7.59 ± 0.11	3071 ± 84	4022 ± 62	2.5 ± 0.5	62.4 ± 10.1	3.18	9.04 ± 0.63	3.26 ± 0.36	2.27 ± 1.00
Heron	admixted	6.56 ± 0.34	5.81 ± 0.34	0.76 ± 0.02	11.55 ± 0.75	2656 ± 147	3439 ± 80	2.9 ± 0.8	74.1 ± 11.2	2.58	9.25 ± 0.70	3.43 ± 0.43	2.49 ± 0.56
Hopper *	elite spring 2r	9.54 ± 0.37	8.83 ± 0.39	0.71 ± 0.03	7.49 ± 0.56	3168 ± 108	4143 ± 103	2.7 ± 0.6	57.7 ± 13.3	2.70	10.1 ± 0.76	3.43 ± 0.42	2.60 ± 0.15
Horizon	elite spring 2r	6.05 ± 0.18	5.38 ± 0.18	0.67 ± 0.002	11.07 ± 0.36	2537 ± 32	3555 ± 56	2.8 ± 0.9	66.0 ± 7.8	2.53	9.41 ± 1.27	3.40 ± 0.57	2.64 ± 0.18
Host *	elite spring 2r	7.36 ± 0.34	6.74 ± 0.32	0.62 ± 0.04	8.45 ± 0.30	2693 ± 122	3628 ± 72	3.4 ± 1.0	68.6 ± 7.9	2.50	8.72 ± 1.97	3.12 ± 0.67	2.58 ± 0.13
Ida	old spring 2r	5.95 ± 0.22	5.07 ± 0.38	0.88 ± 0.16	14.94 ± 3.22	2438 ± 151	3360 ± 74	3.0 ± 0.8	90.2 ± 19.8	2.94	10.46 ± 0.59	3.42 ± 0.57	2.31 ± 0.69
Indola *	elite spring 2r	6.63 ± 0.97	6.02 ± 0.89	0.62 ± 0.09	9.31 ± 0.22	2575 ± 236	3387 ± 225	2.7 ± 0.6	65.2 ± 7.8	2.76	9.03 ± 0.69	3.08 ± 0.36	2.30 ± 0.83
Isabella *	elite spring 2r	8.89 ± 0.33	8.21 ± 0.38	0.69 ± 0.05	7.72 ± 0.85	3007 ± 84	3890 ± 27	2.8 ± 0.8	71.3 ± 14.2	2.48	9.65 ± 0.59	3.75 ± 0.41	2.75 ± 0.41
Jacinta *	TBD	5.84 ± 0.24	5.32 ± 0.23	0.52 ± 0.01	8.85 ± 0.25	2339 ± 86	3287 ± 45	2.4 ± 0.8	54.0 ± 10.6	2.68	9.33 ± 1.73	3.05 ± 0.61	2.53 ± 0.30

Jive *	admixted	9.62 ± 0.14	8.83 ± 0.14	0.78 ± 0.02	8.16 ± 0.22	3174 ± 78	3987 ± 52	3.0 ± 0.9	80.3 ± 18.1	2.61	9.46 ± 1.43	3.14 ± 0.50	2.66 ± 0.17
Keops *	elite spring 2r	8.74 ± 0.08	8.11 ± 0.07	0.63 ± 0.02	7.25 ± 0.12	2953 ± 54	3941 ± 23	2.5 ± 0.5	61.9 ± 6.8	2.81	9.50 ± 1.43	3.07 ± 0.52	2.33 ± 0.42
Klaxon *	admixted	8.46 ± 0.08	7.75 ± 0.11	0.71 ± 0.04	8.44 ± 0.49	2956 ± 24	3756 ± 47	2.9 ± 0.8	73.5 ± 8.6	2.61	9.62 ± 0.81	3.08 ± 0.34	2.68 ± 0.29
Kristaps *	admixted	9.13 ± 0.11	8.36 ± 0.06	0.78 ± 0.05	8.50 ± 0.43	3096 ± 38	3850 ± 16	2.8 ± 0.7	64.8 ± 8.3	2.68	9.47 ± 0.43	3.05 ± 0.41	2.49 ± 0.22
Laird *	TBD	7.57 ± 0.68	6.95 ± 0.64	0.62 ± 0.04	8.14 ± 0.19	2763 ± 166	3752 ± 49	2.4 ± 0.9	59.7 ± 9.2	2.52	8.73 ± 0.41	3.19 ± 0.58	2.45 ± 0.18
Lina *	admixted	7.55 ± 0.30	6.85 ± 0.27	0.70 ± 0.07	9.26 ± 0.86	2864 ± 54	3862 ± 106	2.4 ± 0.6	65.9 ± 14.7	2.66	10.03 ± 0.49	3.04 ± 0.66	2.68 ± 0.14
Linden *	elite spring 2r	8.92 ± 0.08	8.14 ± 0.05	0.78 ± 0.03	8.70 ± 0.31	3082 ± 25	3861 ± 23	2.7 ± 0.7	76.3 ± 12.2	2.65	10.85 ± 0.77	3.29 ± 0.43	2.99 ± 0.09
Lithium	elite spring 2r	6.38 ± 0.45	5.66 ± 0.46	0.72 ± 0.02	11.28 ± 0.92	2494 ± 68	3512 ± 110	2.7 ± 0.6	76.2 ± 17.0	2.68	9.80 ± 0.73	3.36 ± 0.44	2.53 ± 0.28
Livet *	elite spring 2r	8.13 ± 0.17	7.42 ± 0.14	0.71 ± 0.03	8.71 ± 0.26	2948 ± 21	3682 ± 32	3.0 ± 0.7	73.9 ± 13.2	2.87	9.31 ± 0.61	2.70 ± 0.46	2.40 ± 0.34
Macarena *	elite spring 2r	7.56 ± 0.40	6.86 ± 0.42	0.70 ± 0.04	9.30 ± 0.92	2718 ± 94	3733 ± 213	2.6 ± 0.8	63.3 ± 13.3	2.61	9.92 ± 0.62	3.21 ± 0.46	2.69 ± 0.18
Macaw	elite spring 2r	9.25 ± 1.44	8.60 ± 1.48	0.65 ± 0.10	7.18 ± 1.66	3172 ± 415	4159 ± 160	2.8 ± 0.6	62.5 ± 11.4	2.43	10.15 ± 0.44	3.54 ± 0.45	3.02 ± 0.04
Maris Mink	TBD	4.62 ± 0.22	4.13 ± 0.20	0.48 ± 0.02	10.50 ± 0.18	2094 ± 29	3051 ± 113	2.4 ± 0.5	58.5 ± 7.2	2.68	9.56 ± 0.80	3.41 ± 0.37	2.51 ± 0.58
Maypole	elite spring 2r	5.93 ± 0.24	5.23 ± 0.24	0.70 ± 0.06	11.79 ± 1.1	2582 ± 184	3468 ± 191	2.7 ± 0.7	79.9 ± 21.6	2.78	10.38 ± 0.84	3.37 ± 0.42	2.58 ± 0.50
Melitta *	elite spring 2r	9.01 ± 0.14	8.34 ± 0.09	0.67 ± 0.09	7.38 ± 0.93	3122 ± 74	4048 ± 37	2.4 ± 0.7	70.0 ± 20.7	2.31	8.92 ± 0.90	3.27 ± 0.51	3.01 ± 0.08
Midas *	admixted	8.90 ± 0.58	8.26 ± 0.56	0.63 ± 0.02	7.11 ± 0.27	2987 ± 68	4083 ± 33	2.5 ± 0.5	64.3 ± 9.2	2.54	9.13 ± 0.54	3.36 ± 0.48	2.59 ± 0.32
Mikado	admixted	6.08 ± 0.08	5.46 ± 0.06	0.62 ± 0.11	10.21 ± 1.7	2334 ± 89	3627 ± 26	2.4 ± 0.6	65.8 ± 12.0	2.73	9.53 ± 0.70	2.90 ± 0.42	2.52 ± 0.20
Minstrel *	elite spring 2r	9.94 ± 0.29	9.21 ± 0.30	0.73 ± 0.01	7.39 ± 0.28	3180 ± 58	4091 ± 49	3.4 ± 1.1	66.4 ± 12.1	2.42	9.22 ± 0.74	3.43 ± 0.37	2.73 ± 0.24
Neruda	elite spring 2r	4.88 ± 0.21	4.38 ± 0.21	0.50 ± 0.01	10.26 ± 0.5	2294 ± 37	3187 ± 89	2.6 ± 1.0	54.4 ± 13.1	2.66	9.99 ± 0.78	3.39 ± 0.36	2.62 ± 0.44
Nimbus *	elite spring 2r	6.60 ± 0.38	5.97 ± 0.37	0.63 ± 0.01	9.53 ± 0.37	2734 ± 19	3476 ± 234	2.4 ± 0.6	65.7 ± 9.4	3.19	10.13 ± 0.8	2.74 ± 0.45	2.14 ± 0.31
Novello *	elite spring 2r	9.86 ± 0.56	9.22 ± 0.54	0.64 ± 0.02	6.47 ± 0.29	3118 ± 70	4089 ± 151	2.4 ± 0.6	68.8 ± 15.1	2.62	8.20 ± 3.50	2.85 ± 1.15	2.51 ± 0.37
Optic	elite spring 2r	4.57 ± 0.16	3.95 ± 0.15	0.62 ± 0.02	13.59 ± 0.41	2138 ± 28	3069 ± 43	2.4 ± 0.5	62.3 ± 8.3	7.96	9.12 ± 3.42	2.51 ± 0.88	1.81 ± 1.15
Orbit *	admixted	7.92 ± 0.27	7.34 ± 0.23	0.58 ± 0.06	7.36 ± 0.57	2783 ± 37	3797 ± 7	2.5 ± 0.6	55.1 ± 8.2	2.74	9.52 ± 0.51	3.38 ± 0.43	2.41 ± 0.33
Paramount *	elite spring 2r	8.31 ± 0.42	7.63 ± 0.42	0.68 ± 0.01	8.21 ± 0.49	2973 ± 96	3831 ± 58	2.5 ± 0.5	68.0 ± 8.9	2.92	10.7 ± 0.64	3.40 ± 0.41	2.52 ± 0.20
Pewter *	elite spring 2r	7.76 ± 0.43	7.21 ± 0.35	0.55 ± 0.08	7.03 ± 0.68	2858 ± 60	3811 ± 97	2.7 ± 0.8	47.9 ± 8.6	2.63	10.14 ± 0.73	3.34 ± 0.37	2.90 ± 0.16
Pitcher *	elite spring 2r	9.05 ± 0.20	8.30 ± 0.22	0.75 ± 0.03	8.29 ± 0.47	2994 ± 41	3992 ± 16	3.1 ± 0.7	89.9 ± 18.7	3.00	9.61 ± 0.69	2.76 ± 0.45	2.26 ± 0.22
Poker	elite spring 2r	4.33 ± 0.09	3.82 ± 0.13	0.51 ± 0.04	11.73 ± 1.18	2103 ± 107	3203 ± 239	2.5 ± 0.5	53.8 ± 8.0	2.62	9.79 ± 0.63	3.29 ± 0.35	2.68 ± 0.11
Polygena *	elite spring 2r	7.03 ± 0.87	6.29 ± 0.77	0.74 ± 0.10	10.51 ± 0.35	2624 ± 135	3695 ± 104	2.0 ± 0.8	80.2 ± 11.8	2.58	7.89 ± 1.00	2.97 ± 0.38	2.35 ± 1.00
Prisma	elite spring 2r	6.14 ± 0.21	5.31 ± 0.24	0.83 ± 0.07	13.51 ± 1.31	2618 ± 213	3481 ± 131	2.6 ± 0.9	79.3 ± 15.9	3.17	10.76 ± 0.65	2.66 ± 0.32	2.39 ± 0.30
Prosa	admixted	6.66 ± 0.32	5.87 ± 0.30	0.79 ± 0.04	11.86 ± 0.49	2696 ± 339	3926 ± 98	2.4 ± 0.6	71.2 ± 14.5	3.17	10.76 ± 0.65	2.66 ± 0.32	2.39 ± 0.30

Quartet *	elite spring 2r	9.44 ± 0.57	8.68 ± 0.68	0.77 ± 0.13	8.18 ± 1.83	3184 ± 29	4046 ± 187	2.9 ± 0.9	67.2 ± 18.4	2.38	9.31 ± 0.76	3.56 ± 0.47	2.80 ± 0.30
Quench *	elite spring 2r	8.17 ± 0.18	7.42 ± 0.18	0.75 ± 0.01	9.20 ± 0.30	2967 ± 47	3737 ± 21	3.2 ± 0.8	74.8 ± 10.5	2.57	9.35 ± 1.24	3.24 ± 0.52	2.66 ± 0.48
Ragtime *	admixted	6.80 ± 0.29	6.21 ± 0.26	0.59 ± 0.06	8.70 ± 0.62	2536 ± 133	3645 ± 30	2.5 ± 1.0	56.9 ± 12.5	2.61	9.69 ± 1.90	3.18 ± 0.81	2.60 ± 0.17
Rainbow	elite spring 2r	2.81 ± 0.05	2.43 ± 0.05	0.38 ± 0.03	13.41 ± 1.06	1882 ± 86	2959 ± 149	2.3 ± 0.6	51.0 ± 7.5	3.32	9.56 ± 1.41	2.71 ± 0.49	1.33 ± 1.08
Rakaia *	elite spring 2r	8.02 ± 0.28	7.35 ± 0.26	0.66 ± 0.04	8.27 ± 0.36	2896 ± 19	3767 ± 105	2.5 ± 0.5	61.9 ± 9.4	2.64	8.86 ± 0.75	3.03 ± 0.52	2.48 ± 0.44
Rasa	admixted	5.90 ± 0.80	5.34 ± 0.74	0.56 ± 0.05	9.58 ± 0.38	2579 ± 109	3356 ± 159	2.2 ± 0.8	55.4 ± 7.7	2.65	9.38 ± 0.62	3.31 ± 0.47	2.53 ± 0.40
Riviera *	admixted	7.79 ± 0.24	7.15 ± 0.22	0.64 ± 0.03	8.24 ± 0.34	2915 ± 42	3631 ± 38	2.6 ± 0.6	65.6 ± 8.3	2.80	9.61 ± 0.85	3.17 ± 0.34	2.29 ± 0.51
Roxana	elite spring 2r	5.47 ± 0.24	5.04 ± 0.25	0.43 ± 0.03	7.95 ± 0.72	2408 ± 232	3463 ± 139	2.2 ± 0.8	39.5 ± 8.5	2.85	8.89 ± 2.05	2.83 ± 0.61	2.24 ± 0.30
Ruja	admixted	5.30 ± 0.41	4.71 ± 0.37	0.60 ± 0.04	11.24 ± 0.47	2166 ± 71	3564 ± 163	2.4 ± 0.6	60.3 ± 8.2	2.88	9.08 ± 0.50	2.68 ± 0.35	2.40 ± 0.52
Saana *	admixted	8.58 ± 0.34	7.94 ± 0.32	0.64 ± 0.03	7.49 ± 0.21	2955 ± 44	3789 ± 125	2.9 ± 0.9	61.7 ± 8.1	2.83	9.37 ± 0.65	3.27 ± 0.39	2.20 ± 0.79
Sacha	elite spring 2r	7.34 ± 0.74	6.59 ± 0.76	0.76 ± 0.04	10.37 ± 1.36	2774 ± 186	4019 ± 20	2.6 ± 0.6	69.6 ± 12.4	2.79	10.89 ± 0.59	3.38 ± 0.57	2.72 ± 0.19
Saloon	elite spring 2r	5.23 ± 0.24	4.73 ± 0.23	0.50 ± 0.02	9.54 ± 0.21	2305 ± 68	3311 ± 81	2.5 ± 0.7	54.3 ± 5.3	2.86	9.00 ± 3.15	2.85 ± 0.90	2.35 ± 0.20
Scandium *	elite spring 2r	9.06 ± 0.15	8.29 ± 0.17	0.76 ± 0.05	8.45 ± 0.62	3219 ± 35	3915 ± 91	2.7 ± 0.7	69.9 ± 15.6	2.55	9.91 ± 0.66	3.27 ± 0.38	2.73 ± 0.17
Sebastian	elite spring 2r	6.69 ± 0.51	5.98 ± 0.54	0.71 ± 0.08	10.69 ± 1.72	2693 ± 264	3781 ± 97	2.5 ± 0.5	81.3 ± 16.7	2.54	9.26 ± 1.32	3.40 ± 0.51	2.70 ± 0.47
Simba *	admixted	8.72 ± 0.15	8.07 ± 0.11	0.65 ± 0.06	7.44 ± 0.58	2948 ± 10	4033 ± 51	3.1 ± 0.8	61.5 ± 9.7	2.62	9.84 ± 0.67	3.57 ± 0.47	2.63 ± 0.58
Sj Christina *	TBD	7.31 ± 0.67	6.62 ± 0.73	0.69 ± 0.10	9.54 ± 2.12	2655 ± 242	3636 ± 103	2.7 ± 0.6	65.8 ± 14.7	2.42	9.42 ± 0.68	3.46 ± 0.48	2.82 ± 0.24
Skittle *	elite spring 2r	10.33 ± 0.73	9.59 ± 0.67	0.74 ± 0.07	7.15 ± 0.26	3230 ± 103	4105 ± 156	2.7 ± 0.8	73.3 ± 9.4	2.52	9.68 ± 0.83	3.39 ± 0.37	2.75 ± 0.53
Starlight *	elite spring 2r	10.02 ± 0.30	9.25 ± 0.25	0.77 ± 0.08	7.73 ± 0.63	3197 ± 52	4069 ± 48	2.7 ± 0.6	70.3 ± 10.9	2.61	9.07 ± 1.60	3.41 ± 0.59	2.49 ± 0.71
Static *	elite spring 2r	7.60 ± 0.06	7.05 ± 0.07	0.55 ± 0.05	7.23 ± 0.69	2731 ± 88	3727 ± 45	2.9 ± 0.9	57.6 ± 11.3	2.62	9.69 ± 0.90	3.34 ± 0.40	2.55 ± 0.33
Tabora *	elite spring 2r	7.30 ± 0.55	6.58 ± 0.56	0.71 ± 0.04	9.81 ± 1.00	2739 ± 123	3632 ± 62	2.6 ± 0.6	73.8 ± 11.6	2.58	9.45 ± 0.50	3.01 ± 0.42	2.69 ± 0.14
Tankard *	elite spring 2r	9.34 ± 0.61	8.67 ± 0.63	0.67 ± 0.03	7.19 ± 0.72	3102 ± 141	4179 ± 197	2.3 ± 0.8	64.1 ± 17.1	2.43	8.9 ± 0.63	3.42 ± 0.36	2.66 ± 0.28
Taphouse *	elite spring 2r	6.42 ± 0.29	5.69 ± 0.30	0.73 ± 0.06	11.38 ± 1.11	2432 ± 130	3708 ± 175	2.8 ± 0.7	77.4 ± 15.2	2.59	9.35 ± 2.79	3.10 ± 0.80	2.74 ± 0.34
Tartan *	elite spring 2r	10.07 ± 0.15	9.31 ± 0.16	0.76 ± 0.02	7.55 ± 0.27	3067 ± 23	4235 ± 33	2.6 ± 0.7	72.7 ± 8.5	2.70	10.16 ± 0.77	3.29 ± 0.41	2.59 ± 0.26
Thistle *	elite spring 2r	8.58 ± 0.11	7.88 ± 0.13	0.69 ± 0.07	8.08 ± 0.82	2969 ± 110	3713 ± 82	2.5 ± 0.5	70.0 ± 10.4	2.67	9.65 ± 0.97	2.90 ± 0.35	2.52 ± 0.17
Thrift *	admixted	8.41 ± 0.54	7.82 ± 0.39	0.59 ± 0.14	7.02 ± 1.25	2936 ± 90	3857 ± 207	2.6 ± 0.7	67.5 ± 12.6	2.33	9.48 ± 0.41	3.34 ± 0.47	2.87 ± 0.01
Toby	elite spring 2r	7.03 ± 0.74	6.53 ± 0.81	0.50 ± 0.07	7.27 ± 1.63	2471 ± 275	4000 ± 68	2.4 ± 0.7	60.0 ± 9.2	2.80	10.65 ± 0.71	3.56 ± 0.50	2.72 ± 0.19
Toucan *	elite spring 2r	5.47 ± 0.10	4.93 ± 0.10	0.54 ± 0.02	9.92 ± 0.41	2564 ± 42	3285 ± 65	2.5 ± 0.9	57.7 ± 9.0	2.58	9.76 ± 1.37	3.37 ± 0.62	2.68 ± 0.41
Trinidad	elite spring 2r	5.53 ± 0.21	4.88 ± 0.21	0.65 ± 0.04	11.84 ± 0.83	2393 ± 54	3271 ± 46	2.9 ± 0.5	70.0 ± 7.7	2.69	9.09 ± 0.56	2.90 ± 0.38	2.32 ± 0.76
Troon *	elite spring 2r	8.51 ± 0.29	7.62 ± 0.27	0.88 ± 0.03	10.38 ± 0.21	2990 ± 60	3900 ± 149	2.7 ± 0.7	75.1 ± 13.6	2.64	9.82 ± 0.83	3.30 ± 0.32	2.70 ± 0.19

Tucson	elite spring 2r	7.46 ± 0.86	6.74 ± 0.82	0.72 ± 0.04	9.75 ± 0.71	2706 ± 185	3816 ± 164	2.7 ± 0.8	68.4 ± 14.6	2.92	9.76 ± 1.37	2.99 ± 0.52	2.36 ± 0.31
Tyne *	admixted	6.96 ± 0.15	6.34 ± 0.12	0.62 ± 0.04	8.96 ± 0.37	2642 ± 26	3498 ± 61	2.6 ± 0.6	63.9 ± 9.6	2.93	9.48 ± 0.54	2.98 ± 0.34	2.31 ± 0.27
Ursa *	elite spring 2r	7.24 ± 0.29	6.52 ± 0.29	0.72 ± 0.03	9.97 ± 0.61	2718 ± 108	3886 ± 32	2.6 ± 0.6	74.7 ± 9.9	2.81	10.12 ± 0.86	3.16 ± 0.40	2.54 ± 0.30
Vankkuri *	old spring 2r	5.67 ± 0.15	5.15 ± 0.15	0.52 ± 0.02	9.18 ± 0.45	2399 ± 34	3145 ± 35	2.8 ± 0.9	51.2 ± 7.8	3.34	11.33 ± 0.60	2.80 ± 0.38	2.28 ± 0.28
Velvet	elite spring 2r	4.21 ± 0.28	3.53 ± 0.26	0.69 ± 0.06	16.31 ± 1.56	1898 ± 134	3524 ± 176	2.8 ± 0.8	76.5 ± 14.7	3.15	10.09 ± 0.65	2.79 ± 0.62	2.34 ± 0.24
Viivi	admixted	7.86 ± 0.22	6.89 ± 0.17	0.97 ± 0.05	12.33 ± 0.27	3051 ± 76	3931 ± 18	3.2 ± 0.9	90.4 ± 26.5	2.85	9.83 ± 0.90	2.93 ± 0.48	2.49 ± 0.09
Waggon *	elite spring 2r	9.55 ± 0.76	8.72 ± 0.82	0.83 ± 0.08	8.71 ± 1.38	3156 ± 194	4144 ± 113	2.2 ± 0.8	64.4 ± 11.7	2.22	9.55 ± 0.56	3.19 ± 0.33	2.78 ± 0.14
Weitor	admixted	6.75 ± 0.07	5.94 ± 0.06	0.81 ± 0.02	12.04 ± 0.17	2772 ± 85	3733 ± 17	2.1 ± 0.7	75.5 ± 16.2	2.68	9.52 ± 0.82	3.11 ± 0.50	2.57 ± 0.39
Wicket *	elite spring 2r	9.83 ± 0.33	8.96 ± 0.28	0.86 ± 0.06	8.79 ± 0.37	3104 ± 62	4173 ± 94	2.5 ± 0.6	76.3 ± 13.0	2.36	9.83 ± 0.41	3.67 ± 0.44	3.08 ± 0.14
Widre	admixted	5.23 ± 0.47	4.58 ± 0.44	0.65 ± 0.03	12.39 ± 0.53	2472 ± 54	3280 ± 53	2.4 ± 0.8	70.6 ± 16.7	2.95	9.72 ± 0.61	2.64 ± 0.38	2.43 ± 0.09
Wren *	admixted	6.40 ± 0.11	5.83 ± 0.10	0.57 ± 0.01	8.85 ± 0.07	2530 ± 48	3521 ± 50	2.6 ± 0.7	64.1 ± 9.3	2.72	9.67 ± 0.39	2.78 ± 0.43	2.56 ± 0.05
AVERAGE		**7.61 ± 0.35**	**6.94 ± 0.34**	**0.67 ± 0.05**	**9.22 ± 0.70**	**2784 ± 97**	**3732 ± 85**	**2.7 ± 0.7**	**66.7 ± 11.6**	**2.75**	**9.54 ± 0.95**	**3.17 ± 0.50**	**2.53 ± 0.29**

EA, endosperm area; AA, aleurone area; AP, aleurone proportion; DVH, grain dorsal-ventral height; LRW, grain left-right width; AL_LN, aleurone layer number; AW, aleurone width; R, grain roundness; GL, grain length; GWi, grain width; GT, grain thickness. *; indicates cultivar included in the 101 subpanel.

Table 5-S2: Interesting barley genotypes identified that possess varying aleurone traits

Variety	Endosperm Area (mm²)	Aleurone Area (mm²)	Aleurone Proportion (%)	Aleurone Width (µm)
Extract	7.50 ± 0.37	0.97 ± 0.09	12.88 ± 1.13	85.00 ± 13.20
Class	8.47 ± 0.31	0.89 ± 0.07	10.52 ± 0.50	84.92 ± 24.30
Pitcher	9.05 ± 0.20	0.75 ± 0.03	8.29 ± 0.47	89.90 ± 18.70
Franklin	8.31 ± 0.33	0.69 ± 0.03	8.34 ± 0.65	67.10 ± 7.90
Pewter	7.76 ± 0.43	0.55 ± 0.08	7.03 ± 0.68	47.95 ± 8.60
Alabama	8.09 ± 0.16	0.56 ± 0.01	6.93 ± 0.09	52.00 ± 10.80
Taphouse	6.42 ± 0.29	0.73 ± 0.06	11.38 ± 1.11	77.42 ± 15.20
Hopper	9.54 ± 0.37	0.71 ± 0.03	7.49 ± 0.56	57.67 ± 13.3

Interesting genotypes identified based on four aleurone-related traits. Red represents low trait value, yellow represents average trait value and green represents high trait value as observed in the population.

Table 5-S3: Transverse grain and aleurone traits measurements across three generations for interesting barley genoytpes.

A	2013							
Genotype	**EA (mm²)**	**SEA (mm²)**	**AA (mm²)**	**AP (%)**	**DVW (µm)**	**LRW (µm)**	**ALN**	**AW (µm)**
Extract	7.28 ± 0.08	6.63 ± 0.09	0.65 ± 0.04	8.97 ± 0.62	2719 ± 58	3643 ± 62	2.7 ± 0.7	65.4 ± 9.3
Class	8.01 ± 0.38	7.30 ± 0.34	0.71 ± 0.04	8.90 ± 0.23	3012 ± 44	3732 ± 158	2.3 ± 0.9	68.5 ± 9.8
Pitcher	6.73 ± 0.81	6.06 ± 0.73	0.66 ± 0.09	9.93 ± 0.67	2564 ± 144	3641 ± 288	3.0 ± 0.7	67.1 ± 13.0
Franklin	7.63 ± 0.07	6.95 ± 0.05	0.67 ± 0.04	8.85 ± 0.51	2720 ± 27	3574 ± 46	2.4 ± 0.6	64.0 ± 9.3
Pewter	8.05 ± 0.45	7.29 ± 0.41	0.75 ± 0.03	9.40 ± 0.13	2950 ± 96	3767 ± 95	2.6 ± 0.6	63.1 ± 6.8
Alabama	6.61 ± 0.71	6.02 ± 0.71	0.58 ± 0.08	8.93 ± 1.39	2607 ± 106	3463 ± 59	2.0 ± 0.8	64.7 ± 13.0
Taphouse	7.14 ± 0.17	6.41 ± 0.14	0.73 ± 0.03	10.22 ± 0.31	2774 ± 107	3659 ± 95	2.6 ± 0.6	68.8 ± 10.2
Hopper	7.83 ± 0.29	7.17 ± 0.30	0.66 ± 0.06	8.49 ± 0.87	2639 ± 97	3916 ± 31	2.1 ± 0.7	48.6 ± 12.7

B	2014							
Genotype	**EA (mm²)**	**SEA (mm²)**	**AA (mm²)**	**AP (%)**	**DVW (µm)**	**LRW (µm)**	**ALN**	**AW (µm)**
Extract	7.50 ± 0.37	6.53 ± 0.34	0.96 ± 0.09	12.88 ± 1.13	2755 ± 71	3831 ± 206	2.5 ± 0.6	84.9 ± 13.2
Class	8.46 ± 0.31	7.57 ± 0.24	0.89 ± 0.06	10.52 ± 0.49	3025 ± 87	3827 ± 168	2.6 ± 0.7	84.9 ± 24.3
Pitcher	9.05 ± 0.19	8.30 ± 0.22	0.75 ± 0.02	8.29 ± 0.46	2994 ± 41	3992 ± 15	3.1 ± 0.6	89.8 ± 18.6
Franklin	8.30 ± 0.33	7.61 ± 0.35	0.69 ± 0.02	8.34 ± 0.64	2868 ± 18	3842 ± 103	2.7 ± 0.7	67.0 ± 7.9
Pewter	7.76 ± 0.43	7.21 ± 0.35	0.54 ± 0.08	7.03 ± 0.67	2858 ± 59	3811 ± 97	2.7 ± 0.7	47.9 ± 8.6
Alabama	8.08 ± 0.15	7.52 ± 0.14	0.56 ± 0.01	6.92 ± 0.08	2934 ± 50	3729 ± 37	2.0 ± 0.9	51.9 ± 10.7
Taphouse	6.42 ± 0.28	5.69 ± 0.30	0.72 ± 0.05	11.38 ± 1.11	2431 ± 129	3707 ± 175	2.7 ± 0.7	77.4 ± 15.2
Hopper	9.54 ± 0.37	8.82 ± 0.39	0.71 ± 0.03	7.48 ± 0.55	3167 ± 108	4143 ± 103	2.7 ± 0.5	57.6 ± 13.3

C	2016							
Genotype	**EA (mm²)**	**SEA (mm²)**	**AA (mm²)**	**AP (%)**	**DVW (µm)**	**LRW (µm)**	**ALN**	**AW (µm)**
Extract	9.79 ± 0.07	9.00 ± 0.07	0.79 ± 0.06	8.13 ± 0.62	3255 ± 68	3974 ± 18	2.6 ± 0.6	71.3 ± 10.2
Class	10.13 ± 0.54	9.34 ± 0.52	0.79 ± 0.07	7.82 ± 0.70	3238 ± 196	4105 ± 28	2.6 ± 0.6	67.8 ± 16.4
Pitcher	9.93 ± 0.45	9.06 ± 0.44	0.87 ± 0.02	8.79 ± 0.35	3119 ± 36	4045 ± 177	3.2 ± 1.0	67.3 ± 12.2
Franklin	9.07 ± 0.43	8.38 ± 0.42	0.69 ± 0.02	7.69 ± 0.32	2967 ± 79	4022 ± 134	2.5 ± 0.7	61.5 ± 8.7
Pewter	11.01 ± 0.64	10.18 ± 0.64	0.82 ± 0.00	7.53 ± 0.45	3395 ± 110	4214 ± 165	2.4 ± 0.6	55.8 ± 7.5
Alabama	9.10 ± 0.46	8.43 ± 0.47	0.66 ± 0.03	7.28 ± 0.53	3073 ± 54	3735 ± 106	2.2 ± 0.5	52.9 ± 5.6
Taphouse	9.13 ± 0.72	8.37 ± 0.65	0.75 ± 0.07	8.24 ± 0.27	3105 ± 82	3909 ± 287	2.7 ± 0.6	68.1 ± 12.3
Hopper	9.21 ± 0.02	8.51 ± 0.04	0.70 ± 0.02	7.64 ± 0.25	3123 ± 77	4088 ± 65	2.2 ± 0.9	44.7 ± 10.7

Table 5-S4: qPCR results for aleurone genes across interesting barley varieties showing variation in aleurone development.

A	HvLTP2								
DPA	**HvLTP2 Sloop**	**HvLTP2 Alabama**	**HvLTP2 Taphouse**	**HvLTP2 Hopper**	**HvLTP2 Class**	**HvLTP2 Extract**	**HvLTP2 Pitcher**	**HvLTP2 Franklin**	**HvLTP2 Pewter**
7	3098 ± 141	355 ± 29	655 ± 23	27 ± 6	57 ± 16	3161 ± 207	29 ± 11	140 ± 16	124 ± 13
9	10985 ± 445	68 ± 15	10559 ± 523	188 ± 17	2686 ± 94	12681 ± 875	894 ± 111	11656 ± 782	132 ± 34
11	25101 ± 935	20677 ± 1289	13057 ± 1319	7999 ± 403	22448 ± 1512	55136 ± 1110	7033 ± 1462	41460 ± 1482	39441 ± 2415
13	38795 ± 256	13793 ± 512	12978 ± 362	18069 ± 1226	66415 ± 2578	66601 ± 1337	7940 ± 669	101415 ± 3172	51551 ± 3231
15	64371 ± 2900	44061 ± 2958	75995 ± 6108	38568 ± 2353	29148 ± 1132	74183 ± 5705	24661 ± 1857	157705 ± 16159	157726 ± 11186
20	64755 ± 2923	93982 ± 2542	85097 ± 4242	124238 ± 8100	31133 ± 3915	121345 ± 4901	152028 ± 8102	190946 ± 17999	147240 ± 9521
25	91654 ± 3881	186185 ± 7971	82059 ± 9752	178473 ± 8151	132318 ± 5156	104197 ± 4870	131266 ± 13419	156567 ± 11243	476844 ± 16060

B	HvNKD1								
DPA	**HvNKD1 Sloop**	**HvNKD1 Alabama**	**HvNKD1 Taphouse**	**HvNKD1 Hopper**	**HvNKD1 Class**	**HvNKD1 Extract**	**HvNKD1 Pitcher**	**HvNKD1 Franklin**	**HvNKD1 Pewter**
7	46403 ± 2369	26038 ± 2217	16758 ± 572	10245 ± 352	16044 ± 1565	17429 ± 1615	13735 ± 1076	16632 ± 1608	19590 ± 514
9	75708 ± 1680	17720 ± 1250	52331 ± 2202	28213 ± 2315	62112 ± 3642	57870 ± 1303	35441 ± 1955	71716 ± 2740	12182 ± 778
11	63659 ± 2587	85679 ± 1851	57385 ± 5116	50116 ± 3036	96957 ± 11339	123225 ± 3204	84000 ± 4315	168602 ± 9512	61344 ± 5515
13	59006 ± 2577	70088 ± 4548	79606 ± 9102	67164 ± 5976	82713 ± 1000	88619 ± 3556	72286 ± 2792	66682 ± 3561	115965 ± 2855
15	45655 ± 2641	90920 ± 5353	73188 ± 1368	82516 ± 7478	85188 ± 2433	113310 ± 13775	161758 ± 5460	50305 ± 3620	62335 ± 2397
20	26270 ± 615	33044 ± 1086	21043 ± 2057	60263 ± 7174	121355 ± 11254	30024 ± 1073	50235 ± 1093	32814 ± 4842	42303 ± 4295
25	89519 ± 1938	34182 ± 4160	24221 ± 1722	34533 ± 133	25254 ± 663	15681 ± 888	29261 ± 2171	79057 ± 2989	59016 ± 574

C	HvSAL1								
DPA	**HvSAL1 Sloop**	**HvSAL1 Alabama**	**HvSAL1 Taphouse**	**HvSAL1 Hopper**	**HvSAL1 Class**	**HvSAL1 Extract**	**HvSAL1 Pitcher**	**HvSAL1 Franklin**	**HvSAL1 Pewter**
7	49515 ± 3048	45471 ± 3525	37995 ± 3457	49348 ± 2065	89625 ± 8780	74400 ± 1718	86156 ± 9940	75935 ± 6116	86780 ± 5697
9	52687 ± 2930	48927 ± 4229	43096 ± 2272	53171 ± 2328	106331 ± 11302	77749 ± 1260	87360 ± 881	89876 ± 756	43100 ± 3463
11	53754 ± 5019	62420 ± 2026	52652 ± 2904	49369 ± 1862	75988 ± 3148	123548 ± 11875	109479 ± 2562	155117 ± 3325	92833 ± 12227
13	65103 ± 4881	56808 ± 2415	52960 ± 3272	61672 ± 6468	97326 ± 286	103181 ± 6312	99208 ± 1899	73646 ± 1399	125073 ± 9757
15	92108 ± 7368	65268 ± 3943	74192 ± 3924	75470 ± 4231	68146 ± 2020	126208 ± 13515	117462 ± 6171	55830 ± 2842	40847 ± 1834
20	36806 ± 2360	27335 ± 1117	24196 ± 1011	87702 ± 7029	134310 ± 11047	73571 ± 9610	86229 ± 3477	39671 ± 2010	28901 ± 1244
25	125459 ± 16593	30469 ± 665	31062 ± 987	50664 ± 2583	31945 ± 2186	37597 ± 2930	39465 ± 2648	87404 ± 5436	26566 ± 1021

D	HvCR4								
DPA	**HvCR4 Sloop**	**HvCR4 Alabama**	**HvCR4 Taphouse**	**HvCR4 Hopper**	**HvCR4 Class**	**HvCR4 Extract**	**HvCR4 Pitcher**	**HvCR4 Franklin**	**HvCR4 Pewter**
7	3397 ± 281	4240 ± 226	3382 ± 99	6252 ± 306	13149 ± 680	7749 ± 662	10541 ± 1497	5846 ± 503	6767 ± 523
9	2138 ± 93	4394 ± 279	2293 ± 101	6461 ± 569	7193 ± 276	4092 ± 98	6757 ± 340	3872 ± 46	5122 ± 382
11	1962 ± 144	2337 ± 110	2311 ± 88	3436 ± 129	3144 ± 266	4306 ± 232	4244 ± 68	5475 ± 822	5672 ± 616
13	2149 ± 19	2287 ± 64	2506 ± 143	3019 ± 71	4323 ± 366	3802 ± 269	4055 ± 254	2247 ± 202	5034 ± 143
15	2138 ± 86	1984 ± 114	1579 ± 74	2431 ± 154	2183 ± 53	2130 ± 335	4265 ± 106	1933 ± 254	4751 ± 293
20	2088 ± 164	964 ± 82	672 ± 35	1910 ± 325	2639 ± 280	1137 ± 114	1475 ± 99	2638 ± 2598	1296 ± 39
25	1793 ± 225	1087 ± 68	606 ± 62	1068 ± 6	757 ± 45	584 ± 107	865 ± 163	2738 ± 487	1303 ± 331

Table 5-S5: qPCR results for aleurone genes between pooled high (cv Extract and Taphouse) and low (cv Alabama, Hopper and Pewter) barley expression patterns.

A	HvLTP2	
DPA	**HvLTP2 Low**	**HvLTP2 High**
7	169 ± 169	1291 ± 1647
9	129 ± 60	8642 ± 5266
11	22706 ± 15819	30214 ± 22088
13	27804 ± 20676	48665 ± 30906
15	80118 ± 67266	59775 ± 26540
20	121820 ± 26711	79192 ± 45395
25	280501 ± 170082	106191 ± 25189

B	HvNKD1	
DPA	**HvNKD1 Low**	**HvNKD1 High**
7	18624 ± 7941	16744 ± 693
9	19372 ± 8142	57438 ± 4905
11	65713 ± 18179	92522 ± 33143
13	84406 ± 27370	83646 ± 4579
15	78590 ± 14692	90562 ± 20594
20	45203 ± 13839	57474 ± 55504
25	42577 ± 14238	21719 ± 5254

C	HvSAL1	
DPA	**HvSAL1 Low**	**HvSAL1 High**
7	60533 ± 22813	67340 ± 26529
9	48399 ± 5056	75726 ± 31666
11	68207 ± 22303	84063 ± 36131
13	81184 ± 38086	84489 ± 27461
15	60528 ± 17791	89515 ± 31920
20	47980 ± 34410	77359 ± 55155
25	35900 ± 12934	33535 ± 3546

D	HvCR4	
DPA	**HvCR4 Low**	**HvCR4 High**
7	5753 ± 1336	8093 ± 4893
9	5326 ± 1048	4526 ± 2479
11	3815 ± 1699	3254 ± 1002
13	3447 ± 1423	3544 ± 936
15	3055 ± 1486	1964 ± 334
20	1390 ± 480	1483 ± 1028
25	1152 ± 131	649 ± 94

Table 5-S6: Correlation analysis between aleurone traits and markers within and surrounding *NKD1* and *SAL1* genomic regions.

A	**Within *NKD1***								
	12_10689	*SCRI_RS_186847*	***SCRI_RS_116694***	*11_10214*	*SCRI_RS_237763*	*Aleurone Area*	*Aleurone Proportion*	*Aleurone Layer Number*	*Aleurone Thickness*
12_10689	1								
SCRI_RS_186847	-0.088	1							
SCRI_RS_116694	-0.088	0.283	1						
11_10214	-0.317	-0.106	-0.106	1					
SCRI_RS_237763	-0.080	0.173	0.760	0.253	1				
Aleurone Area	-0.033	0.134	-0.144	-0.103	-0.185	1			
Aleurone Proportion	-0.062	-0.071	-0.025	-0.059	-0.082	0.392	1		
Aleurone Layer Number	-0.130	-0.052	0.103	0.131	0.210	0.030	-0.040	1	
Aleurone Thickness	-0.032	0.043	-0.224	-0.056	-0.287	0.787	0.471	0.058	1

B	**Within *SAL1***									
	12_31166	*SCRI_RS_140282*	*11_21363*	***SCRI_RS_179575***	*SCRI_RS_223076*	*11_11440*	*Aleurone Area*	*Aleurone Proportion*	*Aleurone Layer Number*	*Aleurone Thickness*
12_31166	1									
SCRI_RS_140282	-0.960	1								
11_21363	-0.980	0.980	1							
SCRI_RS_179575	0.960	-0.959	-0.980	1						
SCRI_RS_223076	-0.939	0.899	0.919	-0.939	1					
11_11440	-0.939	0.899	0.919	-0.939	1	1				
Aleurone Area	0.074	-0.052	-0.052	0.039	-0.065	-0.065	1			
Aleurone Proportion	0.139	-0.160	-0.160	0.152	-0.132	-0.132	0.455	1		
Aleurone Layer Number	-0.004	-0.016	-0.008	0.030	-0.022	-0.022	0.008	0.010	1	
Aleurone Thickness	0.144	-0.112	-0.111	0.116	-0.182	-0.182	0.776	0.484	0.160	1

Table 5-S7: Distribution of the 47 significantly unique gene ontology (GO) identifiers from the wholegrain differentially expressed genes

GO term	Ontology	Description	HORVUs in input list	Percentage	p-value	FDR
GO:0005975	Biological Process	carbohydrate metabolic process	50	15	3.90E-12	2.60E-09
GO:0006629	Biological Process	lipid metabolic process	21	6	0.00049	0.015
GO:0033036	Biological Process	macromolecule localization	19	6	0.00033	0.011
GO:0044262	Biological Process	cellular carbohydrate metabolic process	17	5	0.00098	0.026
GO:0044085	Biological Process	cellular component biogenesis	16	5	5.30E-05	0.0022
GO:0065003	Biological Process	macromolecular complex assembly	14	4	2.40E-05	0.0013
GO:0022607	Biological Process	cellular component assembly	14	4	2.70E-05	0.0013
GO:0043933	Biological Process	macromolecular complex subunit organization	14	4	4.80E-05	0.0022
GO:0034621	Biological Process	cellular macromolecular complex subunit organization	13	4	1.10E-05	0.00088
GO:0034622	Biological Process	cellular macromolecular complex assembly	13	4	4.60E-06	0.00088
GO:0005976	Biological Process	polysaccharide metabolic process	13	4	4.60E-06	0.00088
GO:0006869	Biological Process	lipid transport	11	3	8.00E-06	0.00088
GO:0010876	Biological Process	lipid localization	11	3	8.00E-06	0.00088
GO:0071103	Biological Process	DNA conformation change	10	3	1.70E-05	0.00093
GO:0065004	Biological Process	protein-DNA complex assembly	9	3	1.30E-05	0.00088
GO:0034728	Biological Process	nucleosome organization	9	3	1.30E-05	0.00088
GO:0031497	Biological Process	chromatin assembly	9	3	1.30E-05	0.00088
GO:0006334	Biological Process	nucleosome assembly	9	3	1.30E-05	0.00088
GO:0006323	Biological Process	DNA packaging	9	3	1.40E-05	0.00088
GO:0007017	Biological Process	microtubule-based process	8	2	0.00023	0.0082
GO:0006073	Biological Process	cellular glucan metabolic process	8	2	0.00058	0.016
GO:0044042	Biological Process	glucan metabolic process	8	2	0.00058	0.016
GO:0044264	Biological Process	cellular polysaccharide metabolic process	8	2	0.00079	0.021
GO:0007018	Biological Process	microtubule-based movement	7	2	0.00014	0.0053
GO:0000160	Biological Process	two-component signal transduction system (phosphorelay)	6	2	0.0012	0.031
GO:0009611	Biological Process	response to wounding	5	1	9.10E-05	0.0036
GO:0009605	Biological Process	response to external stimulus	5	1	0.00045	0.015
GO:0016798	Molecular Function	hydrolase activity, acting on glycosyl bonds	36	20	2.10E-11	7.20E-09
GO:0004553	Molecular Function	hydrolase activity, hydrolyzing O-glycosyl compounds	34	19	2.50E-11	7.20E-09
GO:0030234	Molecular Function	enzyme regulator activity	20	11	2.70E-07	2.60E-05
GO:0004857	Molecular Function	enzyme inhibitor activity	19	11	1.90E-09	3.60E-07
GO:0004866	Molecular Function	endopeptidase inhibitor activity	12	7	2.70E-07	2.60E-05
GO:0030414	Molecular Function	peptidase inhibitor activity	12	7	3.30E-07	2.80E-05
GO:0004867	Molecular Function	serine-type endopeptidase inhibitor activity	11	6	2.10E-07	2.60E-05
GO:0004091	Molecular Function	carboxylesterase activity	11	6	0.00079	0.042
GO:0045735	Molecular Function	nutrient reservoir activity	9	5	2.60E-05	0.0019
GO:0030599	Molecular Function	pectinesterase activity	9	5	0.00014	0.0094
GO:0046527	Molecular Function	glucosyltransferase activity	7	4	0.00045	0.027
GO:0032991	Cellular Component	macromolecular complex	42	37	0.0011	0.026
GO:0005576	Cellular Component	extracellular region	13	12	0.002	0.04
GO:0000786	Cellular Component	nucleosome	9	8	1.00E-05	0.001

GO:0032993	Cellular Component	protein-DNA complex	9	8	1.20E-05	0.001
GO:0005856	Cellular Component	cytoskeleton	9	8	0.00095	0.026
GO:0015630	Cellular Component	microtubule cytoskeleton	8	7	0.00029	0.017
GO:0044430	Cellular Component	cytoskeletal part	8	7	0.00084	0.026
GO:0030312	Cellular Component	external encapsulating structure	8	7	0.00094	0.026
GO:0005618	Cellular Component	cell wall	7	6	0.0012	0.026

Table 5-S8: LCM data of aleurone-enriched and outer-endosperm-enriched genes at two stages of grain development. TPM values are shown.

			13 DPA				25 DPA			
HORVUs	Tissue Enrichment	Annotation	P	AL	OE	IE	P	AL	OE	IE
HORVU5Hr1G116590	OE	calreticulin 1a	31.47	37.66	181.20	0.00	0.00	0.10	10.21	1.05
HORVU6Hr1G070450	OE	Protein NRT1/ PTR FAMILY 7.3	2.54	1.26	10.97	0.00	0.00	0.75	10.13	1.17
HORVU0Hr1G005250	AL	Aquaporin-like superfamily protein	0.09	57.02	0.64	0.40	0.00	233.41	1.09	3.40
HORVU0Hr1G012940	AL	Alcohol dehydrogenase	2.55	41.91	0.25	0.28	0.00	59.58	0.22	4.05
HORVU0Hr1G015390	AL	Formin-like protein 10	8.53	34.91	1.68	0.44	0.00	29.63	0.09	0.27
HORVU0Hr1G017760	AL	Remorin family protein	0.53	18.65	0.07	0.00	0.00	185.87	0.23	2.56
HORVU0Hr1G021200	AL	7SK snRNA methylphosphate capping enzyme	5.25	21.58	2.46	3.56	0.00	25.64	5.05	2.78
HORVU0Hr1G025850	AL	Non-specific lipid-transfer protein-like protein	43.12	215.27	3.08	0.44	0.00	101.50	0.00	4.08
HORVU0Hr1G038050	AL	-	173.64	1328.39	16.85	8.20	0.00	51.30	0.42	9.01
HORVU0Hr1G038780	AL	Chromosome 3B genomic scaffold cultivar Chinese Spring	4.02	22.80	5.06	0.00	0.00	12.29	0.41	0.00
HORVU1Hr1G002150	AL	methionine S-methyltransferase	5.67	25.20	4.64	0.73	0.00	21.52	0.40	2.70
HORVU1Hr1G004210	AL	undescribed protein	3.80	108.35	12.63	2.40	0.00	11.33	0.00	0.29
HORVU1Hr1G012710	AL	Low temperature-induced protein lt101.2	1.26	45.38	0.12	0.00	0.00	851.17	2.87	2.91
HORVU1Hr1G018140	AL	Dehydrogenase/reductase SDR family member 4	171.33	3308.94	35.75	95.62	0.00	25959.20	110.78	398.37
HORVU1Hr1G020590	AL	unknown function	3.80	45.36	0.45	0.10	0.00	20.35	0.34	1.41
HORVU1Hr1G023260	AL	Adenine nucleotide alpha hydrolases-like superfamily protein	102.71	461.93	28.98	28.69	0.00	320.96	28.89	44.97
HORVU1Hr1G024640	AL	Kinase interacting (KIP1-like) family protein	7.83	40.09	7.04	1.06	0.00	33.24	2.36	0.32
HORVU1Hr1G042820	AL	Metal-dependent phosphohydrolase	6.46	59.81	9.42	7.06	0.00	12.74	2.79	0.79
HORVU1Hr1G043890	AL	Aquaporin-like superfamily protein	46.69	551.29	39.19	38.18	0.00	6418.39	11.41	113.73
HORVU1Hr1G044780	AL	LanC-like protein 2	0.89	12.14	0.04	0.00	0.00	43.88	0.41	1.09
HORVU1Hr1G046010	AL	Tetraspanin-10	10.02	44.58	2.09	1.32	0.00	42.48	2.74	2.26
HORVU1Hr1G046580	AL	undescribed protein	5.24	24.30	0.44	0.00	0.00	222.31	0.96	42.53
HORVU1Hr1G049280	AL	Glutathione S-transferase family protein	30.90	145.71	8.58	0.00	0.00	99.46	0.00	0.81
HORVU1Hr1G057460	AL	Aldolase-type TIM barrel family protein	8.20	53.84	0.72	0.68	0.00	26.97	0.10	0.09
HORVU1Hr1G058040	AL	hydroxyproline-rich glycoprotein family protein	10.75	106.26	3.36	3.68	0.00	77.80	2.12	5.54
HORVU1Hr1G058400	AL	Late embryogenesis abundant (LEA) hydroxyproline-rich glycoprotein family	1.92	29.64	1.10	0.00	0.00	41.02	0.19	0.68
HORVU1Hr1G059900	AL	Late embryogenesis abundant protein D-19	0.46	33.39	0.12	0.00	0.00	11945.36	15.83	15.26
HORVU1Hr1G061160	AL	Pyruvate phosphate dikinase 2	41.15	494.48	14.32	3.40	0.00	85.94	3.03	0.06
HORVU1Hr1G063100	AL	Ethylene-responsive transcription factor 1	8.73	211.46	2.00	2.60	0.00	1869.93	4.81	23.47
HORVU1Hr1G068460	AL	Histone-lysine N-methyltransferase 2A	2.26	19.10	2.29	1.00	0.00	12.69	0.55	0.76
HORVU1Hr1G068830	AL	Non-specific lipid-transfer protein-like protein	3.16	55.13	1.67	1.70	0.00	13.94	0.00	0.85
HORVU1Hr1G072600	AL	undescribed protein	77.34	311.29	4.76	3.32	0.00	411.54	3.91	5.13
HORVU1Hr1G073670	AL	Histone superfamily protein	120.84	1273.11	32.54	214.25	0.00	46.76	1.69	2.17
HORVU1Hr1G076880	AL	GTP-binding RHO-like protein	4.89	37.60	0.64	0.30	0.00	11.97	0.06	0.05
HORVU1Hr1G077820	AL	Poly [ADP-ribose] polymerase 3	4.10	38.50	0.62	5.18	0.00	55.51	1.90	2.73
HORVU1Hr1G080480	AL	6-phosphogluconate dehydrogenase decarboxylating 1	28.42	126.07	11.96	1.43	0.00	239.69	4.18	6.58
HORVU1Hr1G082690	AL	AFG1-like ATPase family protein	3.46	14.99	0.06	0.53	0.00	10.31	0.15	0.00
HORVU1Hr1G082820	AL	unknown function	2.91	40.48	0.11	2.61	0.00	878.19	1.26	35.42

HORVU1Hr1G083380	AL	12-dihydroxy-3-keto-5-methylthiopentene dioxygenase 4	0.42	13.48	0.33	0.23	0.00	18.32	0.00	0.04
HORVU1Hr1G085920	AL	undescribed protein	0.00	13.15	0.00	0.00	0.00	11.97	0.00	0.00
HORVU1Hr1G086580	AL	BEST Arabidopsis thaliana protein match is: transcription factor-related .	38.16	1084.03	16.17	5.57	0.00	1483.24	4.49	6.40
HORVU1Hr1G091010	AL	Oleosin family protein	3.02	53.69	0.91	0.00	0.00	785.72	2.54	32.09
HORVU1Hr1G093170	AL	unknown function	32.42	509.92	8.71	1.98	0.00	867.79	1.75	6.67
HORVU1Hr1G094660	AL	Retrotransposon protein, putative, unclassified,	22.17	140.70	29.62	0.64	0.00	47.49	3.90	4.83
HORVU2Hr1G005470	AL	Major facilitator superfamily protein	4.10	16.58	0.29	0.53	0.00	37.88	0.21	0.03
HORVU2Hr1G012710	AL	amine oxidase 1	17.48	85.50	1.72	0.12	0.00	71.56	0.07	1.63
HORVU2Hr1G012790	AL	Transketolase	1.04	21.86	0.11	0.15	0.00	235.45	0.57	4.17
HORVU2Hr1G015140	AL	Short-chain dehydrogenase reductase 2a	0.65	25.33	2.23	0.00	0.00	72.26	0.81	13.60
HORVU2Hr1G015150	AL	Short-chain dehydrogenase reductase 2a	0.16	10.02	0.19	0.36	0.00	67.85	0.57	0.07
HORVU2Hr1G020310	AL	ankyrin repeat family protein	15.11	68.69	1.00	0.26	0.00	60.45	5.73	2.48
HORVU2Hr1G020350	AL	undescribed protein	7.68	34.44	4.60	0.00	0.00	109.73	7.21	1.00
HORVU2Hr1G025810	AL	GDSL esterase/lipase	3.02	50.25	1.02	0.00	0.00	28.43	0.13	0.00
HORVU2Hr1G026760	AL	undescribed protein	838.61	20290.71	268.52	307.37	0.00	70311.67	193.21	1600.68
HORVU2Hr1G026810	AL	Peroxiredoxin-6	0.83	52.65	0.22	0.00	0.00	46.84	0.36	1.33
HORVU2Hr1G027750	AL	SNARE associated Golgi protein family	1.35	24.03	0.23	0.00	0.00	28.49	0.00	0.00
HORVU2Hr1G028490	AL	undescribed protein	65.74	418.11	6.55	7.53	0.00	130.27	2.43	6.54
HORVU2Hr1G033520	AL	dihydroflavonol 4-reductase	0.08	18.81	0.35	0.18	0.00	175.11	0.38	0.00
HORVU2Hr1G034500	AL	undescribed protein	3.25	17.97	0.88	0.45	0.00	12.38	2.73	0.16
HORVU2Hr1G036930	AL	Cathepsin B-like cysteine proteinase	2.85	30.22	1.10	0.00	0.00	84.83	0.30	0.00
HORVU2Hr1G040380	AL	undescribed protein	6.30	266.37	2.49	1.16	0.00	528.39	3.42	0.21
HORVU2Hr1G045200	AL	Glutathione S-transferase family protein	8.71	87.90	0.50	0.46	0.00	19.93	0.00	0.76
HORVU2Hr1G047510	AL	undescribed protein	3.36	31.92	0.55	0.62	0.00	16.65	0.24	0.00
HORVU2Hr1G048220	AL	Transmembrane protein 184A	1.61	13.28	0.98	0.63	0.00	14.38	1.63	0.39
HORVU2Hr1G054050	AL	undescribed protein	161.28	784.75	76.40	4.82	0.00	107.54	9.46	10.94
HORVU2Hr1G070360	AL	hydroxysteroid dehydrogenase 1	16.81	433.42	5.40	5.17	0.00	929.99	2.76	11.31
HORVU2Hr1G074690	AL	FAD/NAD(P)-binding oxidoreductase family protein	8.00	32.52	4.56	0.44	0.00	37.67	0.99	0.04
HORVU2Hr1G075370	AL	undescribed protein	3.33	146.59	2.27	3.43	0.00	429.42	2.02	5.11
HORVU2Hr1G075840	AL	Protein of unknown function (DUF668)	3.91	34.79	1.27	0.37	0.00	19.72	0.46	0.00
HORVU2Hr1G075930	AL	Late embryogenesis abundant protein (LEA) family protein	1.16	21.91	0.11	0.12	0.00	53.66	0.56	2.45
HORVU2Hr1G080590	AL	Transmembrane amino acid transporter family protein	7.80	112.10	1.42	2.64	0.00	79.18	0.09	0.00
HORVU2Hr1G080870	AL	vacuolar iron transporter 1	4.85	44.04	0.89	0.65	0.00	59.96	0.30	0.04
HORVU2Hr1G081670	AL	ATP-dependent 6-phosphofructokinase 2	23.32	93.56	2.34	1.45	0.00	128.27	1.82	5.00
HORVU2Hr1G081740	AL	Small nuclear ribonucleoprotein family protein	4.45	21.87	2.13	2.45	0.00	56.17	0.78	1.29
HORVU2Hr1G083550	AL	Retrotransposon protein, putative, unclassified,	17.62	71.31	10.35	4.14	0.00	49.20	2.75	2.93
HORVU2Hr1G086560	AL	MatR	7.87	55.32	5.39	2.40	0.00	10.58	0.16	1.72
HORVU2Hr1G088560	AL	Caleosin-related family protein	25.47	791.90	7.16	21.81	0.00	2494.04	15.21	88.27
HORVU2Hr1G090210	AL	Histone superfamily protein	8.86	128.35	4.08	18.13	0.00	17.03	0.00	0.32
HORVU2Hr1G096290	AL	Thioredoxin superfamily protein	2.87	13.24	0.65	0.45	0.00	40.14	3.69	0.04
HORVU2Hr1G097980	AL	unknown function	0.65	16.30	0.00	0.00	0.00	130.32	0.62	0.00
HORVU2Hr1G097990	AL	Histone superfamily protein	67.18	1307.97	22.96	193.78	0.00	21.58	0.43	0.79
HORVU2Hr1G098150	AL	undescribed protein	1607.50	48836.49	506.45	409.89	0.00	14163.08	52.26	917.21
HORVU2Hr1G099330	AL	Polyglutamine-binding protein 1	3.52	16.99	3.21	0.74	0.00	13.62	1.71	1.50
HORVU2Hr1G099870	AL	Late embryogenesis abundant protein (LEA) family protein	7.50	158.68	1.56	9.88	0.00	944.70	1.78	16.21

HORVU2Hr1G103180	AL	L-lactate dehydrogenase	5.91	92.52	3.28	1.93	0.00	31.06	1.92	0.17
HORVU2Hr1G104960	AL	Protein of unknown function (DUF581)	12.88	56.75	2.10	0.00	0.00	34.11	0.25	0.23
HORVU2Hr1G105740	AL	undescribed protein	2.43	44.76	2.25	0.00	0.00	1160.22	8.45	51.95
HORVU2Hr1G106440	AL	undescribed protein	26.81	200.36	8.02	8.79	0.00	57.44	0.00	3.19
HORVU2Hr1G107660	AL	Sugar transport protein 5	1.67	10.28	0.29	0.00	0.00	11.68	0.85	0.35
HORVU2Hr1G107740	AL	Glycosyltransferase	15.97	265.46	2.73	45.72	0.00	609.62	1.09	44.52
HORVU2Hr1G110810	AL	inositol-pentakisphosphate 2-kinase 1	13.18	69.27	7.54	3.36	0.00	24.01	3.30	0.81
HORVU2Hr1G113180	AL	D-3-phosphoglycerate dehydrogenase	57.12	287.14	19.80	38.96	0.00	212.23	6.23	21.34
HORVU2Hr1G113830	AL	Filament-like plant protein 7	8.16	43.43	1.98	2.12	0.00	14.75	1.93	0.63
HORVU2Hr1G114840	AL	undescribed protein	7.77	54.65	4.62	11.46	0.00	43.90	0.00	0.00
HORVU2Hr1G116200	AL	undescribed protein	18.18	109.75	0.73	0.31	0.00	18.09	0.37	1.20
HORVU2Hr1G126720	AL	Chitinase 12	3.45	98.90	1.17	0.00	0.00	41.18	0.12	2.77
HORVU3Hr1G001000	AL	Phosphatidylethanolamine-binding protein 1	0.00	10.78	0.03	1.10	0.00	21.31	0.32	0.00
HORVU3Hr1G003950	AL	Mannose-6-phosphate isomerase 2	8.45	64.41	3.18	0.21	0.00	29.44	0.58	0.27
HORVU3Hr1G007100	AL	Protein of unknown function (DUF1639)	9.19	43.98	0.13	0.00	0.00	33.90	0.56	0.00
HORVU3Hr1G013840	AL	Metallothioneine type2	700.33	3481.54	719.97	42.52	0.00	2063.39	74.59	124.88
HORVU3Hr1G013910	AL	Asparagine synthetase [glutamine-hydrolyzing]	0.85	13.38	0.25	0.12	0.00	217.70	0.49	0.82
HORVU3Hr1G017910	AL	undescribed protein	1.90	10.67	0.16	0.00	0.00	13.19	0.00	0.00
HORVU3Hr1G018550	AL	pyruvate decarboxylase-3	46.83	752.29	15.08	5.25	0.00	26.20	0.15	0.92
HORVU3Hr1G019510	AL	Zinc finger CCCH domain-containing protein 2	3.20	31.81	0.32	3.86	0.00	188.44	1.62	12.25
HORVU3Hr1G030620	AL	3-methyl-2-oxobutanoate hydroxymethyltransferase	7.51	30.04	0.97	1.51	0.00	18.69	0.38	0.41
HORVU3Hr1G031620	AL	Aquaporin-like superfamily protein	1.49	42.89	0.92	0.00	0.00	369.99	1.15	0.60
HORVU3Hr1G032820	AL	Glutaredoxin family protein	10.12	540.23	7.86	1.79	0.00	41.34	0.88	0.16
HORVU3Hr1G059030	AL	unknown protein	0.83	75.56	0.77	0.61	0.00	2554.07	5.17	18.33
HORVU3Hr1G063660	AL	UDP-Glycosyltransferase superfamily protein	1.12	23.46	1.44	0.31	0.00	36.47	0.06	0.11
HORVU3Hr1G064990	AL	Phosphoethanolamine N-methyltransferase 1	32.56	245.27	15.69	5.84	0.00	331.61	9.33	0.52
HORVU3Hr1G065860	AL	unknown function	0.95	12.54	1.05	2.23	0.00	407.11	1.09	13.88
HORVU3Hr1G066340	AL	Late embryogenesis abundant protein 76	8.75	106.82	1.53	0.50	0.00	48.43	0.99	12.04
HORVU3Hr1G070770	AL	undescribed protein	6.70	120.29	0.00	0.00	0.00	990.74	2.05	0.00
HORVU3Hr1G070850	AL	NAD-dependent malic enzyme 2	1.56	37.85	0.59	0.00	0.00	315.50	1.75	6.78
HORVU3Hr1G071490	AL	Protein of unknown function (DUF1264)	35.26	559.82	5.64	28.93	0.00	2121.35	4.36	40.23
HORVU3Hr1G072910	AL	Katanin p60 ATPase-containing subunit A-like 2	12.45	75.09	2.96	15.74	0.00	31.02	0.99	0.75
HORVU3Hr1G073730	AL	50S ribosomal protein L33	39.71	282.51	23.14	4.48	0.00	60.78	3.51	2.54
HORVU3Hr1G078840	AL	UDP-Glycosyltransferase superfamily protein	3.35	14.10	0.43	0.00	0.00	94.02	0.63	0.00
HORVU3Hr1G084360	AL	ABSCISIC ACID-INSENSITIVE 5-like protein 2	9.58	67.89	7.27	4.12	0.00	74.60	7.61	5.22
HORVU3Hr1G087170	AL	Histone superfamily protein	368.75	1783.20	130.15	95.77	0.00	34.51	1.67	4.88
HORVU3Hr1G091230	AL	Bidirectional sugar transporter N3	1.75	61.72	1.12	1.14	0.00	69.66	0.22	0.69
HORVU3Hr1G093350	AL	selenium-binding protein 1	119.88	547.80	94.34	12.50	0.00	259.17	25.97	8.66
HORVU3Hr1G097180	AL	tropinone reductase	0.20	47.28	0.57	0.00	0.00	359.57	1.60	0.16
HORVU3Hr1G099770	AL	hydroxyethylthiazole kinase family protein	8.26	82.55	3.63	0.54	0.00	129.46	15.78	5.50
HORVU3Hr1G100350	AL	Xylanase inhibitor	7.62	82.77	5.85	4.97	0.00	427.30	18.75	47.19
HORVU3Hr1G105850	AL	unknown protein	7.52	63.64	5.74	7.15	0.00	150.84	23.08	20.19
HORVU3Hr1G107240	AL	Early-responsive to dehydration stress protein (ERD4)	0.46	13.54	0.10	1.64	0.00	24.73	0.32	0.12
HORVU3Hr1G112350	AL	Peroxidase superfamily protein	0.53	34.04	0.17	0.47	0.00	61.71	0.18	1.11
HORVU3Hr1G116300	AL	undescribed protein	8.14	36.50	3.82	0.67	0.00	11.93	0.00	0.12
HORVU4Hr1G002800	AL	Globulin-2	119.19	2780.20	33.62	28.32	0.00	6219.06	26.81	117.33
HORVU4Hr1G005740	AL	Polyketide cyclase/dehydrase and lipid	5.14	143.16	2.83	30.68	0.00	169.03	1.41	5.34

		transport superfamily protein .								
HORVU4Hr1G008990	AL	Late embryogenesis abundant protein	2.01	51.47	0.27	0.00	0.00	1044.22	2.53	25.61
HORVU4Hr1G009040	AL	Histone H2B.1	266.80	4565.40	133.81	164.17	0.00	500.54	11.25	59.86
HORVU4Hr1G010750	AL	Dehydrin 6	3.43	54.34	0.61	0.62	0.00	127.10	0.49	7.86
HORVU4Hr1G013210	AL	Gibberellin-regulated family protein	18.81	291.72	1.77	8.55	0.00	607.53	2.12	3.19
HORVU4Hr1G018650	AL	Disease resistance-responsive (dirigent-like protein) family protein	170.47	882.26	153.76	5.50	0.00	136.38	0.22	0.50
HORVU4Hr1G022280	AL	Peroxidase superfamily protein	16.54	315.53	4.93	1.51	0.00	57.88	0.15	1.01
HORVU4Hr1G023910	AL	undescribed protein	271.92	1245.45	142.71	5.67	0.00	197.13	15.94	14.06
HORVU4Hr1G025360	AL	Putative adipose-regulatory protein (Seipin)	2.70	11.01	0.39	0.00	0.00	31.93	1.11	0.58
HORVU4Hr1G050210	AL	Vicilin-like antimicrobial peptides 2-3	3.55	17.07	3.07	1.90	0.00	2708.16	15.84	117.63
HORVU4Hr1G051780	AL	Late embryogenesis abundant protein 1	3.79	30.70	0.14	0.00	0.00	438.89	2.04	4.27
HORVU4Hr1G052780	AL	undescribed protein	19.15	93.14	3.71	0.00	0.00	77.57	0.17	0.00
HORVU4Hr1G053950	AL	TenA family transcriptional regulator	0.15	42.03	4.50	0.33	0.00	16.34	0.84	0.99
HORVU4Hr1G054080	AL	Mitochondrial import inner membrane translocase	0.17	14.60	0.47	0.00	0.00	15.03	0.00	0.47
HORVU4Hr1G054240	AL	cAMP-regulated phosphoprotein 19-related protein	5.86	151.94	2.12	2.96	0.00	34.33	0.04	0.00
HORVU4Hr1G058950	AL	undescribed protein	52.45	232.40	30.01	25.78	0.00	24.15	0.63	0.00
HORVU4Hr1G059270	AL	Glyoxalase family protein expressed	34.36	1146.06	12.33	20.16	0.00	6397.73	17.97	105.97
HORVU4Hr1G059280	AL	Seed maturation protein PM41	1.00	181.11	1.19	0.00	0.00	739.72	3.05	21.77
HORVU4Hr1G070780	AL	ORF48	128.70	674.13	10.79	10.59	0.00	52.15	0.64	0.00
HORVU4Hr1G070970	AL	Vicilin-like antimicrobial peptides 2-2	7.37	111.09	0.53	4.52	0.00	686.92	6.02	85.61
HORVU4Hr1G073500	AL	Protein of unknown function (DUF 3339)	45.54	1122.85	28.95	5.08	0.00	359.79	1.58	0.54
HORVU4Hr1G074750	AL	Late embryogenesis abundant protein expressed	1.49	10.10	0.00	0.16	0.00	233.33	1.01	17.03
HORVU4Hr1G076600	AL	Protein LURP-one-related 6	4.83	69.21	1.19	0.00	0.00	26.01	0.28	0.00
HORVU4Hr1G076970	AL	Cyanate hydratase	4.13	207.15	2.25	0.41	0.00	10.10	0.48	0.29
HORVU4Hr1G078460	AL	alcohol dehydrogenase 1	1.95	54.72	0.92	0.47	0.00	241.31	0.64	1.86
HORVU4Hr1G083310	AL	DET1- and DDB1-associated protein 1	8.43	53.21	3.37	1.09	0.00	22.41	2.29	3.33
HORVU4Hr1G089500	AL	Non-specific lipid-transfer protein 2G	619.31	25323.38	226.76	292.24	0.00	12019.69	69.07	64.90
HORVU5Hr1G000400	AL	undescribed protein	8.60	43.80	1.12	0.00	0.00	2130.13	4.48	26.00
HORVU5Hr1G005930	AL	Late embryogenesis abundant protein D-34	0.82	23.58	0.39	0.00	0.00	481.39	0.71	3.03
HORVU5Hr1G010330	AL	Outer envelope pore protein 16-2 chloroplastic	0.61	50.01	0.48	0.45	0.00	196.14	0.88	0.16
HORVU5Hr1G026330	AL	undescribed protein	0.82	24.89	0.33	1.58	0.00	282.92	1.31	0.63
HORVU5Hr1G034700	AL	undescribed protein	3.72	35.02	0.00	0.00	0.00	10.82	0.00	0.43
HORVU5Hr1G040310	AL	Ovate protein	7.73	82.39	1.16	0.87	0.00	25.94	0.00	0.16
HORVU5Hr1G042660	AL	undescribed protein	85.46	375.58	7.35	0.00	0.00	94.32	0.38	4.26
HORVU5Hr1G044630	AL	undescribed protein	7.86	36.23	2.49	0.99	0.00	27.91	2.15	0.72
HORVU5Hr1G044640	AL	zinc induced facilitator-like 1	0.31	20.20	0.04	0.00	0.00	24.95	0.20	0.27
HORVU5Hr1G047920	AL	Two-component response regulator ORR21	7.33	75.21	2.73	0.20	0.00	71.42	1.55	1.79
HORVU5Hr1G050950	AL	unknown protein	6.16	277.39	6.63	0.97	0.00	1115.03	4.21	29.87
HORVU5Hr1G053030	AL	undescribed protein	15.68	146.48	25.77	0.00	0.00	681.73	4.77	8.81
HORVU5Hr1G056030	AL	oleosin 1	84.65	3057.83	41.62	19.30	0.00	5561.10	33.80	78.78
HORVU5Hr1G059540	AL	unknown function	5.34	141.72	17.21	0.00	0.00	61.03	0.16	1.33
HORVU5Hr1G060370	AL	vacuolar iron transporter 1	4.72	77.53	1.81	1.05	0.00	293.42	0.91	0.08
HORVU5Hr1G060620	AL	Centromere protein V	2.01	21.83	0.66	1.17	0.00	23.96	0.58	0.10
HORVU5Hr1G062990	AL	alanine aminotransferase 2	0.10	10.18	0.24	0.00	0.00	115.76	1.25	1.42
HORVU5Hr1G065740	AL	Zinc-finger homeodomain protein 9	2.80	22.75	0.17	1.11	0.00	28.65	0.09	0.87
HORVU5Hr1G069360	AL	Protein of unknown function (DUF1264)	28.65	413.69	15.57	12.53	0.00	1093.13	3.75	13.98
HORVU5Hr1G069730	AL	Zinc-finger homeodomain protein 1	4.56	36.63	0.84	2.21	0.00	13.89	0.05	0.85

HORVU5Hr1G073410	AL	transcription factor-related	3.29	47.36	1.31	0.19	0.00	20.64	1.10	0.27
HORVU5Hr1G073960	AL	dihydroflavonol 4-reductase-like1	14.43	146.43	13.61	1.52	0.00	23.81	2.95	1.02
HORVU5Hr1G082620	AL	Protein of unknown function (DUF1442)	4.18	49.70	0.53	1.19	0.00	147.14	0.23	2.06
HORVU5Hr1G082690	AL	Protein of unknown function (DUF1442)	0.77	26.36	0.84	0.43	0.00	51.03	0.33	0.70
HORVU5Hr1G087780	AL	Glutamyl-tRNA(Gln) amidotransferase subunit A	7.89	184.08	3.33	1.27	0.00	29.94	0.15	0.00
HORVU5Hr1G088410	AL	unknown function	63.75	272.70	42.49	2.19	0.00	103.44	17.65	0.64
HORVU5Hr1G093120	AL	BTB/POZ domain-containing protein	2.94	25.97	0.27	0.34	0.00	10.07	0.35	0.70
HORVU5Hr1G095160	AL	Adenine nucleotide alpha hydrolases-like superfamily protein	4.33	40.83	0.54	0.00	0.00	120.62	0.35	0.05
HORVU5Hr1G095180	AL	Adenine nucleotide alpha hydrolases-like superfamily protein	2.46	23.71	1.37	0.00	0.00	141.71	1.10	1.50
HORVU5Hr1G105840	AL	Aluminium induced protein with YGL and LRDR motifs	3.68	95.99	1.28	0.25	0.00	776.80	12.70	27.93
HORVU5Hr1G106550	AL	histone H1-3	188.77	1072.36	104.04	152.25	0.00	58.24	14.28	12.84
HORVU5Hr1G109290	AL	Calcium-binding EF-hand family protein	3.63	21.79	0.00	0.00	0.00	633.93	2.13	61.76
HORVU5Hr1G112350	AL	Multiple inositol polyphosphate phosphatase 1	11.20	50.52	6.18	1.21	0.00	21.84	2.05	0.82
HORVU5Hr1G120110	AL	Dehydrogenase/reductase SDR family protein 7-like	2.24	44.56	1.06	0.00	0.00	145.73	0.16	0.29
HORVU5Hr1G125320	AL	2-oxoglutarate (2OG) and Fe(II)-dependent oxygenase superfamily protein	21.65	273.90	4.88	0.80	0.00	14.05	0.08	0.00
HORVU5Hr1G125480	AL	undescribed protein	36.21	264.57	5.39	0.89	0.00	496.43	0.70	0.32
HORVU6Hr1G006010	AL	2-oxoglutarate (2OG) and Fe(II)-dependent oxygenase superfamily protein	5.67	156.53	2.67	6.28	0.00	20.84	0.31	0.00
HORVU6Hr1G012570	AL	Peptidyl-prolyl cis-trans isomerase	83.28	402.97	22.65	21.35	0.00	130.94	3.75	11.41
HORVU6Hr1G013000	AL	Pentatricopeptide repeat-containing protein	1.84	12.55	3.03	0.33	0.00	15.79	3.26	0.41
HORVU6Hr1G020080	AL	unknown protein	6.92	48.79	0.69	0.00	0.00	830.29	2.48	1.32
HORVU6Hr1G024920	AL	HXXXD-type acyl-transferase family protein	15.93	184.52	20.74	5.53	0.00	216.54	11.13	4.32
HORVU6Hr1G026300	AL	LYR motif-containing protein	19.66	89.27	1.49	3.03	0.00	34.77	0.00	0.14
HORVU6Hr1G033210	AL	unknown function	138.86	605.37	76.81	18.86	0.00	740.62	19.00	17.27
HORVU6Hr1G060990	AL	Vacuolar-processing enzyme	13.13	126.38	1.08	1.26	0.00	549.35	1.58	7.28
HORVU6Hr1G062070	AL	Sugar phosphate exchanger 2	0.39	13.25	0.09	0.00	0.00	76.70	0.88	0.00
HORVU6Hr1G064980	AL	undescribed protein	15.07	82.87	13.19	19.88	0.00	133.44	0.23	0.64
HORVU6Hr1G065820	AL	undescribed protein	0.00	33.69	0.14	0.00	0.00	65.26	0.32	0.00
HORVU6Hr1G072140	AL	Nuclear transcription factor Y subunit B-1	19.34	461.00	5.76	1.69	0.00	228.20	0.50	3.84
HORVU6Hr1G072150	AL	undescribed protein	25.64	762.31	7.61	2.93	0.00	508.57	4.09	4.90
HORVU6Hr1G080500	AL	Peptide methionine sulfoxide reductase MsrB	68.00	483.34	51.92	35.16	0.00	195.75	34.69	33.55
HORVU6Hr1G085760	AL	Transmembrane protein 184C	0.75	10.44	0.88	1.27	0.00	35.96	0.63	1.21
HORVU6Hr1G092530	AL	unknown function	18.01	155.76	2.85	0.00	0.00	637.39	3.78	6.39
HORVU6Hr1G093260	AL	M-1	299.99	7228.08	53.38	81.16	0.00	7952.31	14.02	244.87
HORVU7Hr1G002450	AL	Fiber protein Fb34	9.40	62.92	14.44	2.09	0.00	43.72	0.76	0.16
HORVU7Hr1G017640	AL	Enolase	6.83	158.89	1.37	0.34	0.00	402.24	1.54	0.40
HORVU7Hr1G021120	AL	Sec14p-like phosphatidylinositol transfer family protein	2.95	16.93	0.18	0.08	0.00	15.48	0.08	0.00
HORVU7Hr1G021770	AL	undescribed protein	10.71	68.20	4.27	0.32	0.00	12.57	0.63	0.53
HORVU7Hr1G024570	AL	Succinate dehydrogenase assembly factor 4 mitochondrial	3.07	21.46	3.23	0.17	0.00	60.39	1.14	0.67
HORVU7Hr1G030660	AL	Dehydrogenase/reductase SDR family member 4	2.90	117.29	0.66	0.00	0.00	56.50	0.09	0.00
HORVU7Hr1G036970	AL	undescribed protein	1.66	10.33	0.00	0.00	0.00	1944.58	4.91	10.95
HORVU7Hr1G038330	AL	amino acid permease 1	2.43	10.64	0.44	0.00	0.00	24.84	2.15	5.14
HORVU7Hr1G040460	AL	Pyruvate dehydrogenase E1 component subunit alpha	14.58	128.07	1.68	0.00	0.00	114.41	10.38	11.18
HORVU7Hr1G041380	AL	Caleosin-related family protein	1.18	31.84	0.14	0.52	0.00	16.49	0.20	0.00
HORVU7Hr1G041710	AL	Ribonucleoside-diphosphate reductase small chain	24.00	199.62	3.35	12.69	0.00	10.80	0.07	0.36

HORVU7Hr1G045630	AL	HVA22 homologue E	0.20	27.69	2.16	6.25	0.00	664.50	35.91	42.12
HORVU7Hr1G046030	AL	Na+/H+ (sodium hydrogen) exchanger 3	3.86	47.95	0.54	0.32	0.00	309.65	1.05	0.03
HORVU7Hr1G046340	AL	Protein LE25	2.93	69.74	0.61	0.00	0.00	244.99	1.61	5.21
HORVU7Hr1G046970	AL	diacylglycerol acyltransferase family	20.39	284.09	15.10	5.89	0.00	96.58	15.96	16.72
HORVU7Hr1G048100	AL	undescribed protein	3.07	107.38	1.41	1.43	0.00	346.23	0.56	0.91
HORVU7Hr1G054090	AL	purple acid phosphatase 27	7.55	97.71	4.24	1.71	0.00	110.99	1.04	0.31
HORVU7Hr1G057470	AL	acyl carrier protein 3	575.14	2307.51	51.20	40.94	0.00	1077.87	14.75	21.55
HORVU7Hr1G059290	AL	F1F0-ATPase inhibitor protein putative	31.39	137.98	34.47	5.81	0.00	16.72	3.04	2.93
HORVU7Hr1G066990	AL	undescribed protein	9.18	50.26	0.58	0.64	0.00	11.52	0.00	0.00
HORVU7Hr1G073770	AL	ATP-dependent RNA helicase eIF4A	5.07	24.19	5.20	3.99	0.00	16.17	2.31	2.17
HORVU7Hr1G074760	AL	receptor kinase 2	4.50	23.60	5.14	0.72	0.00	21.40	0.47	0.02
HORVU7Hr1G086170	AL	Protein NRT1/ PTR FAMILY 4.6	2.36	35.96	0.37	0.22	0.00	24.40	0.16	1.99
HORVU7Hr1G088510	AL	amino acid permease 1	2.12	35.42	0.88	0.36	0.00	14.83	1.93	1.70
HORVU7Hr1G090420	AL	undescribed protein	67.58	283.09	35.69	0.00	0.00	32.24	1.96	0.00
HORVU7Hr1G091380	AL	Myb/SANT-like DNA-binding domain protein	2.03	14.13	0.80	0.00	0.00	93.90	0.66	0.00
HORVU7Hr1G091440	AL	CASP-like protein 1	1.28	13.62	0.13	0.00	0.00	72.03	0.18	0.30
HORVU7Hr1G093020	AL	Peroxiredoxin-2B	50.36	491.03	21.44	4.62	0.00	648.98	4.90	6.88
HORVU7Hr1G110060	AL	undescribed protein	0.00	11.55	0.67	0.00	0.00	158.22	0.73	1.86
HORVU7Hr1G110360	AL	ubiquitin-conjugating enzyme 22	4.61	22.71	4.64	3.95	0.00	26.36	4.63	0.20
HORVU7Hr1G113400	AL	Magnesium transporter MRS2-B	11.24	222.52	6.22	1.73	0.00	260.57	7.65	6.05

Legend: Yellow; candidate genes with differential expression and aleurone enriched.

Green; candidate genes within QTL intervals and aleurone enriched.

Table 5-S9: LCM data of aleurone-enriched and outer-endosperm-enriched genes at two stages of grain development as identified in the Venn diagram. TPM values are shown.

		13 DPA				25 DPA			
HORVU	Annotation	P	AL	OE	IE	P	AL	OE	IE
HORVU7Hr1G090420	undescribed protein	67.58	283.09	35.69	0.00	0.00	32.24	1.96	0.00
HORVU3Hr1G072910	Katanin p60 ATPase-containing subunit A-like 2	12.45	75.09	2.96	15.74	0.00	31.02	0.99	0.75
HORVU0Hr1G017760	Remorin family protein	0.53	18.65	0.07	0.00	0.00	185.87	0.23	2.56
HORVU4Hr1G078460	alcohol dehydrogenase 1	1.95	54.72	0.92	0.47	0.00	241.31	0.64	1.86
HORVU2Hr1G026810	Peroxiredoxin-6	0.83	52.65	0.22	0.00	0.00	46.84	0.36	1.33
HORVU6Hr1G020080	unknown protein	6.92	48.79	0.69	0.00	0.00	830.29	2.48	1.32
HORVU3Hr1G100350	Xylanase inhibitor	7.62	82.77	5.85	4.97	0.00	427.30	18.75	47.19
HORVU1Hr1G082820	unknown function	2.91	40.48	0.11	2.61	0.00	878.19	1.26	35.42
HORVU3Hr1G013840	Metallothioneine type2	700.33	3481.54	719.97	42.52	0.00	2063.39	74.59	124.88
HORVU4Hr1G089500	Non-specific lipid-transfer protein 2G	619.31	25323.38	226.76	292.24	0.00	12019.69	69.07	64.90
HORVU2Hr1G098360	undescribed protein	1.50	36.06	0.00	0.95	0.00	39.32	1.12	238.42
HORVU2Hr1G098340	Histone superfamily protein	9.82	445.05	1.85	1.66	0.00	0.00	0.00	0.37
HORVU2Hr1G098040	receptor-like kinase 1	7.06	31.69	0.53	6.69	0.00	37.33	3.36	11.17
HORVU5Hr1G072070	caffeoyl-CoA 3-O-methyltransferase	9.42	93.75	4.01	0.00	0.00	1.47	1.47	0.93
HORVU2Hr1G098160	Oleosin	0.22	120.66	0.41	3.25	0.00	1.19	0.29	0.18
HORVU7Hr1G078760	High mobility group B protein 7	20.71	375.95	7.77	44.13	0.00	0.19	0.15	0.61
HORVU5Hr1G073960	dihydroflavonol 4-reductase-like1	14.43	146.43	13.61	1.52	0.00	23.81	2.95	1.02
HORVU2Hr1G097990	Histone superfamily protein	67.18	1307.97	22.96	193.78	0.00	21.58	0.43	0.79
HORVU2Hr1G097980	unknown function	0.65	16.30	0.00	0.00	0.00	130.32	0.62	0.00
HORVU5Hr1G073410	transcription factor-related	3.29	47.36	1.31	0.19	0.00	20.64	1.10	0.27
HORVU2Hr1G098150	undescribed protein	1607.50	48836.49	506.45	409.89	0.00	14163.08	52.26	917.21
HORVU5Hr1G072800	undescribed protein	0.54	0.00	0.00	0.00	0.00	34.74	0.00	0.43
HORVU5Hr1G074340	Chitinase family protein	196.55	10.48	0.98	2.82	0.00	43.61	3.10	1.13
HORVU6Hr1G057320	undescribed protein	0.04	3.47	0.58	0.00	0.00	107.93	0.60	1.79
HORVU6Hr1G056960	undescribed protein	84.90	28.85	24.01	36.48	0.00	89.28	5.14	1.78
HORVU5Hr1G073930	Calcineurin subunit B	17.54	24.34	11.63	1.45	0.00	13.18	2.30	0.53
HORVU5Hr1G073620	undescribed protein	8.04	2.05	2.55	2.67	0.00	16.20	0.87	1.94
HORVU6Hr1G056610	40S ribosomal protein S11	16.53	32.54	9.52	1.24	0.00	12.15	0.28	0.03
HORVU5Hr1G074770	ER membrane protein complex subunit 3	17.92	14.82	3.75	3.45	0.00	12.73	2.33	2.37
HORVU2Hr1G098920	Dehydrogenase/reductase SDR family member 4	46.76	107.30	3.63	12.10	0.00	44.68	8.97	4.27
HORVU6Hr1G058100	E3 ubiquitin-protein ligase PRT1	30.40	33.02	12.24	9.81	0.00	39.02	7.50	4.76
HORVU2Hr1G098660	Calcium-binding EF-hand family protein	1.12	10.22	4.20	0.86	0.00	166.25	10.31	15.25
HORVU7Hr1G077580	unknown protein	79.53	20.18	8.33	2.18	0.00	30.56	2.51	6.27
HORVU5Hr1G072660	undescribed protein	5.39	0.45	1.79	0.36	0.00	16.43	2.31	3.30
HORVU7Hr1G075700	Reticulon family protein	14.33	21.43	11.48	32.82	0.00	42.41	7.60	5.67
HORVU7Hr1G078670	Cleavage and polyadenylation specificity factor subunit 5	3.55	0.00	0.00	0.00	0.00	34.02	0.48	0.25
HORVU6Hr1G058560	60S ribosomal protein L14-1	308.94	716.38	576.84	63.77	0.00	570.65	75.94	14.31
HORVU5Hr1G075270	undescribed protein	24.48	12.09	3.12	0.00	0.00	39.22	1.71	4.44

HORVU5Hr1G073450	NAD(P)-binding Rossmann-fold superfamily protein	6.36	11.87	3.30	0.45	0.00	11.06	1.62	0.39
HORVU5Hr1G075200	unknown protein	25.56	10.56	9.20	3.02	0.00	24.91	4.80	5.07
HORVU5Hr1G072490	lipid-binding serum glycoprotein family protein	16.25	5.92	0.37	0.00	0.00	11.24	2.01	0.05
HORVU7Hr1G087210	Transmembrane 9 superfamily member 7	44.26	8.85	0.99	5.19	0.00	18.35	0.52	0.74
HORVU2Hr1G098140	Ethylene-responsive transcription factor 5	0.00	0.00	0.00	0.00	0.00	37.08	0.07	0.60
HORVU5Hr1G072420	HEAT SHOCK PROTEIN 81.4	284.34	675.99	113.54	99.32	0.00	292.13	19.00	40.18
HORVU6Hr1G056520	undescribed protein	0.49	0.00	0.00	0.00	0.00	16.95	0.98	0.00
HORVU2Hr1G098880	Succinylornithine transaminase/acetylornithine aminotransferase	27.63	35.97	1.94	1.62	0.00	13.68	0.85	0.10
HORVU5Hr1G075060	O-fucosyltransferase family protein	36.35	73.97	5.43	1.46	0.00	15.16	0.94	0.14
HORVU5Hr1G074920	30S ribosomal protein S16	16.54	38.46	12.11	2.24	0.00	28.58	2.39	2.84
HORVU7Hr1G077790	RING/U-box superfamily protein	12.00	7.79	0.17	0.55	0.00	10.03	0.22	0.45
HORVU6Hr1G058010	undescribed protein	27.37	60.40	8.23	0.00	0.00	118.04	0.00	6.06
HORVU6Hr1G057640	H/ACA ribonucleoprotein complex subunit 3-like protein	106.53	214.71	78.87	27.01	0.00	142.42	19.69	7.97
HORVU6Hr1G057630	Two-component response regulator-like PRR1	24.38	31.95	9.60	1.58	0.00	29.59	6.02	2.30

Legend: Yellow; candidate genes with differential expression and aleurone enriched. Orange; candidate genes within QTL intervals and aleurone enriched at 13 DPA. Green; candidate genes within QTL intervals and aleurone enriched at both 13 and 25 DPA. Blue; candidate genes within QTL intervals and aleurone enriched at 25 DPA.

Table 5-S10: Distribution of the 90 significantly unique gene ontology (GO) identifiers from LCM RNAseq for genes enriched in the aleurone

GO term	Ontology	Description	HORVUs in input list	Percentage	p-value	FDR
GO:0044267	Biological Process	cellular protein metabolic process	186	9	2.00E-05	1.10E-03
GO:0010467	Biological Process	gene expression	176	9	2.00E-07	1.40E-05
GO:0044281	Biological Process	small molecule metabolic process	109	5	2.40E-13	4.70E-11
GO:0006412	Biological Process	translation	84	4	1.30E-14	9.00E-12
GO:0005975	Biological Process	carbohydrate metabolic process	61	3	1.10E-03	2.70E-02
GO:0006082	Biological Process	organic acid metabolic process	53	3	6.00E-08	5.20E-06
GO:0043436	Biological Process	oxoacid metabolic process	52	3	1.30E-07	1.00E-05
GO:0019752	Biological Process	carboxylic acid metabolic process	52	3	1.30E-07	1.00E-05
GO:0042180	Biological Process	cellular ketone metabolic process	52	3	1.80E-07	1.40E-05
GO:0044085	Biological Process	cellular component biogenesis	50	2	2.10E-15	2.90E-12
GO:0034641	Biological Process	cellular nitrogen compound metabolic process	41	2	1.90E-04	6.40E-03
GO:0044262	Biological Process	cellular carbohydrate metabolic process	40	2	4.00E-06	2.40E-04
GO:0009056	Biological Process	catabolic process	39	2	1.60E-04	5.80E-03
GO:0006519	Biological Process	cellular amino acid and derivative metabolic process	38	2	8.50E-05	3.60E-03
GO:0022607	Biological Process	cellular component assembly	37	2	8.20E-12	9.60E-10
GO:0043933	Biological Process	macromolecular complex subunit organization	37	2	3.40E-11	3.40E-09
GO:0009308	Biological Process	amine metabolic process	37	2	2.20E-04	6.80E-03
GO:0065003	Biological Process	macromolecular complex assembly	36	2	2.40E-11	2.60E-09
GO:0034621	Biological Process	cellular macromolecular complex subunit organization	34	2	1.70E-12	2.20E-10
GO:0034622	Biological Process	cellular macromolecular complex assembly	33	2	9.00E-13	1.40E-10
GO:0044106	Biological Process	cellular amine metabolic process	33	2	4.10E-04	1.20E-02
GO:0044248	Biological Process	cellular catabolic process	32	2	1.30E-04	5.00E-03
GO:0044283	Biological Process	small molecule biosynthetic process	31	2	5.70E-05	2.80E-03
GO:0009057	Biological Process	macromolecule catabolic process	31	2	1.30E-04	0.005
Others (each constituting 1%)						
GO:0006520	Biological Process	cellular amino acid metabolic process	30	1	7.20E-04	0.019
GO:0006091	Biological Process	generation of precursor metabolites and energy	28	1	9.70E-04	0.024
GO:0071103	Biological Process	DNA conformation change	27	1	1.40E-12	2E-10
GO:0006066	Biological Process	alcohol metabolic process	27	1	2.60E-06	1.60E-04
GO:0006323	Biological Process	DNA packaging	26	1	5.60E-14	2.6E-11
GO:0006396	Biological Process	RNA processing	26	1	5.70E-06	3.20E-04
GO:0044265	Biological Process	cellular macromolecule catabolic process	26	1	2.10E-04	0.0067
GO:0034728	Biological Process	nucleosome organization	25	1	2.70E-13	4.7E-11
GO:0065004	Biological Process	protein-DNA complex assembly	25	1	2.70E-13	4.7E-11
GO:0031497	Biological Process	chromatin assembly	25	1	2.70E-13	4.7E-11
GO:0006334	Biological Process	nucleosome assembly	25	1	2.70E-13	4.7E-11
GO:0006457	Biological Process	protein folding	24	1	3.80E-06	2.30E-04
GO:0016053	Biological Process	organic acid biosynthetic process	21	1	9.40E-04	0.024
GO:0046394	Biological Process	carboxylic acid biosynthetic process	21	1	9.40E-04	0.024
GO:0034660	Biological Process	ncRNA metabolic process	20	1	8.00E-08	0.021
GO:0019318	Biological Process	hexose metabolic process	19	1	4.40E-05	0.0023

GO:0016052	Biological Process	carbohydrate catabolic process	19	1	4.90E-05	0.0024
GO:0005996	Biological Process	monosaccharide metabolic process	19	1	1.80E-04	0.0063
GO:0051186	Biological Process	cofactor metabolic process	18	1	2.50E-04	0.0073
GO:0044282	Biological Process	small molecule catabolic process	17	1	7.10E-04	0.019
GO:0022613	Biological Process	ribonucleoprotein complex biogenesis	16	1	5.70E-08	5.20E-06
GO:0006006	Biological Process	glucose metabolic process	16	1	1.60E-04	0.0058
GO:0044275	Biological Process	cellular carbohydrate catabolic process	15	1	1.30E-04	0.005
GO:0046164	Biological Process	alcohol catabolic process	15	1	1.30E-04	0.005
GO:0042254	Biological Process	ribosome biogenesis	14	1	1.00E-06	6.90E-05
GO:0019320	Biological Process	hexose catabolic process	14	1	2.30E-04	0.0068
GO:0046365	Biological Process	monosaccharide catabolic process	14	1	2.30E-04	0.0068
GO:0006007	Biological Process	glucose catabolic process	14	1	2.30E-04	0.0068
GO:0006732	Biological Process	coenzyme metabolic process	14	1	4.80E-04	0.013
GO:0032787	Biological Process	monocarboxylic acid metabolic process	14	1	1.60E-03	0.039
GO:0034470	Biological Process	ncRNA processing	13	1	4.80E-04	0.013
GO:0006096	Biological Process	glycolysis	11	1	1.20E-03	0.029
GO:0016491	Molecular Function	oxidoreductase activity	126	22	3.10E-04	0.027
GO:0005198	Molecular Function	structural molecule activity	79	14	6.7E-18	6.3E-15
GO:0003735	Molecular Function	structural constituent of ribosome	70	12	1.2E-16	5.6E-14
GO:0048037	Molecular Function	cofactor binding	55	9	2.80E-07	8.80E-05
GO:0050662	Molecular Function	coenzyme binding	40	7	4.30E-06	0.001
GO:0016874	Molecular Function	ligase activity	31	5	5.60E-04	0.041
GO:0016741	Molecular Function	transferase activity, transferring one-carbon groups	27	5	2.00E-04	2.10E-02
GO:0008168	Molecular Function	methyltransferase activity	26	4	3.40E-04	2.70E-02
GO:0032561	Molecular Function	guanyl ribonucleotide binding	25	4	4.70E-05	6.40E-03
GO:0005525	Molecular Function	GTP binding	25	4	4.70E-05	0.0064
GO:0019001	Molecular Function	guanyl nucleotide binding	25	4	6.20E-05	0.0073
GO:0016853	Molecular Function	isomerase activity	20	3	2.80E-04	0.027
GO:0051082	Molecular Function	unfolded protein binding	18	3	3.30E-05	0.0062
GO:0016614	Molecular Function	oxidoreductase activity, acting on CH-OH group of donors	15	3	6.60E-04	0.044
GO:0044464	Cellular Component	cell part	421	14	1.3E-16	5.1E-15
GO:0005623	Cellular Component	cell	421	14	1.3E-16	5.1E-15
GO:0005622	Cellular Component	intracellular	314	11	6.1E-15	2.1E-13
GO:0044424	Cellular Component	intracellular part	271	9	6.1E-13	1.9E-11
GO:0043229	Cellular Component	intracellular organelle	217	7	3.3E-09	6.90E-08
GO:0043226	Cellular Component	organelle	217	7	3.3E-09	6.90E-08
GO:0032991	Cellular Component	macromolecular complex	155	5	3.30E-23	5.70E-21
GO:0005737	Cellular Component	cytoplasm	148	5	4.10E-23	5.70E-21
GO:0016020	Cellular Component	membrane	136	5	3.20E-04	5.50E-03
GO:0044444	Cellular Component	cytoplasmic part	116	4	2.60E-19	2.40E-17
GO:0043232	Cellular Component	intracellular non-membrane-bounded organelle	116	4	1.70E-06	3.20E-05
GO:0043228	Cellular Component	non-membrane-bounded organelle	116	4	1.70E-06	3.20E-05
GO:0030529	Cellular Component	ribonucleoprotein complex	78	3	1.30E-18	9.10E-17
GO:0005840	Cellular Component	ribosome	70	2	1.30E-16	5.10E-15
GO:0044425	Cellular Component	membrane part	68	2	1.70E-03	2.40E-02
GO:0000786	Cellular Component	nucleosome	23	1	6.00E-12	1.70E-10

GO:0032993	Cellular Component	protein-DNA complex	23	1	7.70E-12	1.90E-10
GO:0031090	Cellular Component	organelle membrane	19	1	3.30E-03	4.10E-02
GO:0005739	Cellular Component	mitochondrion	16	1	7.70E-04	1.20E-02
GO:0044429	Cellular Component	mitochondrial part	15	1	9.70E-04	1.50E-02

Table 5-S11: Table of primer sequences for qPCR.

Gene	HORVU	Forward	Reverse	Product Size (bp)
LTP2	HORVU4Hr1G089500	TGTGCCAGTACGTCAAGGAC	GCTAGCCAGGAAGCAAGCTA	207
NKD1	HORVU2Hr1G095730	GATGTTTGATCCGAGGATGTG	TACGGCTTGTGTAAGCTCGAT	297
SAL1	HORVU7Hr1G115800	CAGTTCGTCAACATGGAGGTC	GATCTGAAGCGTAAGCGTTTG	268
CR4	HORVU7Hr1G071390	AGCAGCATAGGAGATGGTCTG	TTTCAGCTGATCTTGGCATTT	113
HvGAP	HORVU7Hr1G074690	GTGAGGCTGGTGCTGATTACG	TGGTGCAGCTAGCATTTGAGAC	198
HvCyclophilin	HORVU6Hr1G012570	CCTGTCGTGTCGTCGGTCTAAA	ACGCAGATCCAGCAGCCTAAAG	122
HvTubulin	HORVU1Hr1G081280	AGTGTCCTGTCCACCCACTC	AGCATGAAGTGGATCCTTGG	248
HvHSP70	HORVU5Hr1G113180	CGACCAGGGCAACCGCACCAC	ACGGTGTTGATGGGGTTCATG	108

Chapter 6

Summary and Future Directions

ꕥ • ꕥ

Thesis Summary

Understanding the development of the cereal endosperm is important to further our knowledge of seed developmental biology and to contribute new information to the food, feed and malting industries. The outer layer of the endosperm, known as the aleurone, is an intriguing tissue as it fulfils key functions in the cereal grain, yet large differences in development and layer number are observed across species. It is currently unclear why aleurone morphology differs so significantly between species such as wheat, barley and maize. Research presented in this thesis has addressed this question in the context of barley. The findings reveal multiple components of barley aleurone development that complement studies in other cereal systems.

Currently, understanding of pathways involved in aleurone development in the cereals arises primarily from studies in maize, while relatively little is known in other cereal species. In Chapter 3, investigations into barley homologues of several maize genes, *NKD1* and *SAL1*, provided insight regarding the role of these genes in barley and potential cross-species conservation. The spatial distribution of *HvNKD1* and *HvSAL1* transcript appearance was determined by laser capture microdissection (LCM), showing that both genes are abundant in the aleurone but also detected in adjoining grain tissues. Function was assessed by utilising transgenic cell-type specific knockdown and overexpression lines. Based on consistent phenotypes observed in multiple lines, *HvNKD1* and *HvSAL1* appear to be required for normal development of the multi-layered aleurone in barley. Although amiRNA and over-expression lines showed altered aleurone development, in neither case did modification prevent the formation of an aleurone. Hence, *HvNKD1* and *HvSAL1* appear to regulate aleurone proliferation in barley, suggesting that other factors are likely to contribute to aleurone differentiation. Additionally, both *HvNKD1* and *HvSAL1* appear to respond to altered auxin levels and/or regulation, which suggests they may act downstream of the primary

aleurone differentiation signal. Exogenous auxin application and inhibition induced morphological changes in either the aleurone or sub-aleurone, suggesting that these tissues may accumulate auxin or respond to auxin and thereby influence cell fate determination.

In Chapter 4, aleurone morphology was examined across a range of Australian barley cultivars and breeding materials to document the degree of natural variation, and to assess whether further quantitative genetic studies might be utilised for aleurone related gene discovery. A method was developed to measure features of the aleurone in mature grain based on UV-autofluorescence of the thick aleurone walls. Unsurprisingly, analysis confirmed that development of the starchy endosperm and aleurone are intimately linked. Relationships between aleurone traits, such as aleurone area, thickness and the number of cell layers were also observed, where genotypes producing more aleurone layers tended to show a thicker aleurone, and aleurone width contributed directly to aleurone area. However, the number of aleurone layers shared no direct relationship with aleurone area, suggesting that factors determining aleurone cell expansion are influencing this trait. Based on the findings from Chapter 3, it would seem that *HvNKD1* and *HvSAL1* could be candidate factors involved in this regulation. Although aleurone layer number varied from approximately two to four layers in the panel, this appeared to have no detrimental impact on overall grain development. To assess whether this variation impacted aleurone function, physiologically relevant traits such as the activity of germination related enzymes were examined. Notably, genotype-specific differences in free β-amylase activity at grain maturity correlated with aleurone area, proportion and width. In physiological terms, we propose this may allow for an early pulse of starch hydrolysis prior to the liberation of bound β-amylase by endopeptidases. When examining β-amylase genes in the LCM data, transcript analysis suggested that the aleurone contributed a significant amount of *HvBMY1*

transcript, and possibly up to ~30% of the free β-amylase levels at grain maturity. It was concluded that different *HvBMY* genes or alleles were unlikely to contribute directly to differences in aleurone morphology, but rather, differences in aleurone development may contribute to free β-amylase levels at grain maturity.

The results presented in Chapter 4 revealed considerable diversity in aleurone morphology across barley genotypes, which suggested that the genetic basis for these differences might be examined at the population level. In Chapter 5, a population of 150 European two-row spring barley lines, for which genotypic information was available, were examined for aleurone traits similar with those reported in Chapter 4. Similar levels of variation were identified in the Australian and European panels. The number of genotypes in the European two-row spring barley panel was sufficient to carry out a Genome Wide Association Study (GWAS). When performing the GWAS on this panel, twenty-one dispersed genomic regions or quantitative trait loci (QTL) were identified, significantly associated with aleurone morphological traits. This suggests that aleurone development is almost certainly under the control of multiple loci in the elite germplasm examined. Analysis of the top four significantly associated loci, utilising a wholegrain developmental time course and tissue-specific RNA sequencing data, revealed a single candidate gene that was aleurone-enriched, differentially expressed between cultivars and was located in a QTL region (QAT2.S-7H1). This gene was Katanin p60 ATPase-containing subunit A-like (KATNAL), which may be involved in the regulation of cell division based on homology with genes from other species. Additional genes that were aleurone-enriched, located in QTL regions but were not differentially expressed between cultivars included several undescribed proteins, an oleosin, a receptor-like kinase and a bZIP transcription factor. The lack of differential expression for these genes needs to be considered carefully, since protein level or sequence polymorphisms may be the driver for variation. All of these genes

will need to be considered in future studies to assess their role in the aleurone. In regards to known regulators of aleurone development, insignificant association peaks were observed near the predicted genomic location of *HvNKD1* and *HvSAL1*, but it appears unlikely that either gene is the underlying cause of most variation in the panel. Moreover, no clear association was identified between homologues of other characterised cereal aleurone regulators in barley such as *HvDEK1*, *HvCR4* and *HvROS1*. This does not rule out the possibility that that upstream regulators or downstream targets of these pathways are involved. Based on the large number of significantly associated genomic regions, further studies of the different genotypes and transcriptional resources generated here may yet reveal genes potentially contributing to aleurone development.

The results presented in this thesis were obtained via a range of genetic, molecular and physiological analyses, all aimed at investigating components of the aleurone developmental pathway in barley. This has uncovered a range of components including regulatory genes, phytohormone signals, wholegrain features and enzyme levels. How each component may be interacting with each other in barley is summarised in Figure 6-1. In summary, we have shown that: (1) Genes involved in maize aleurone development appear to play a role in barley aleurone development. (2) Auxin distribution and/or regulation appears to influence barley aleurone and sub-aleurone morphology during early grain development. (3) Natural variation across barley genotypes correlates with mature grain traits such as the activity of germination-related enzyme β-amylase, and hence may have some industrial relevance in the malt industry. (4) Natural variation between barley genotypes can be exploited using GWAS to identify genomic loci involved in aleurone development. (5) Although the molecular basis for this variation remains unknown, the diverse genetic, transgenic, molecular and transcriptomic datasets generated in this study will form the basis of future

investigations of barley grain development. In conclusion, the work presented in this thesis adds to the body of knowledge regarding the molecular genetics of aleurone development in barley, and therefore supports a broad aim of improving barley for food and malting applications.

Future Directions

Results from this study show that it is possible to manipulate the multilayered barley aleurone using transgenic methods to make it resemble the single aleurone layer of wheat. Despite this, it remains unclear why barley naturally produces a multilayered aleurone and wheat does not. The work presented here has demonstrated the potential for investigating known and novel genes contributing to aleurone development. As a product of this study, key questions remain to be answered which could form the basis for future work.

Further characterisation and development of transgenic lines

Transgenic lines targeting *HvNKD1* and *HvSAL1* expression in the outer starchy endosperm induced morphological changes in the aleurone and/or sub-aleurone tissues. Although phenotypes were robustly detected in multiple independent transgenic lines, further work is required to validate these results since only T1 grains were examined for consistency between experiments. T2 and T3 grains will need to be analysed to confirm heritable changes in aleurone morphology. It will also be important to extract RNA from the T2 developing grains to confirm knockdown and overexpression of the transgenes. Additionally, developing T2 grains could be collected for sectioning to identify stages where aleurone development is most affected, and to examine changes in gene expression by *in situ* hybridisation. Furthermore, the development of CRISPR/Cas9 plants targeting *HvNKD1* and *HvSAL1* may lead to more extreme aleurone alterations since transgenic knockdowns may allow for some residual gene function.

How and why do HvNKD1 and HvSAL1 respond to auxin?

Preliminary analysis suggests that *HvNKD1* and *HvSAL1* respond to altered levels of auxin, but the mechanism is unknown. Also, the morphological effects of auxin treatments on aleurone development were relatively subtle compared to the severe alterations observed in transgenic lines. First, it would be interesting to analyse the levels and location of auxin in the developing barley caryopsis, similar to that reported for wheat and maize (reviewed in Shirley et al., 2018; See Appendix I). Moreover, the DR5 marker has been utilised in other species to map auxin accumulation. We have generated barley lines containing *DR5:3xnlsYFP* and these should be analysed throughout grain development to complement the results of this study. Auxin treatments reported here could also be repeated with different concentrations of NAA and TIBA, and developing grains could be directly treated rather than exposing the whole plant to altered auxin. Secondly, transgenic lines generated in this study, as well as potential future CRISPR/Cas9 lines, could also be used to determine how plants deficient for *HvNKD1* and *HvSAL1* respond to altered auxin levels. For example, transgenic lines overexpressing *HvSAL1* or *amiRNA-HvNKD1*, which produce less aleurone, could be treated with exogenous auxin to assess for rescue, whether that be through an increase in aleurone cell layers or cell expansion. These studies might suggest whether *HvNKD1* and/or *HvSAL1* are absolutely required for aleurone proliferation, responding to altered levels of auxin that ultimately affects the aleurone development pathway. Candidate genes involved in auxin signalling (Appendix III) might then be examined to further elucidate a molecular mechanism.

Where do HvNKD1 and HvSAL1 actually function?

The basis for *HvNKD1* and *HvSAL1* expression versus function during aleurone development is currently unclear. These genes were shown to be expressed in maize

aleurone, and since mutants produced aleurone defects, the aleurone was suggested as the main tissue for eventual expression. However, in barley, LCM data suggest that *HvNKD1* and *HvSAL1* are transcribed in the aleurone and the neighbouring tissues, the outer starchy endosperm and pericarp. Similarly, transgenics targeting *HvNKD1* and *HvSAL1* expression in the outer starchy endosperm induced altered aleurone morphology, while transgenics targeting their expression in the aleurone showed no obvious changes in development. This may suggest a possible signalling mechanism whereby *HvNKD1* and *HvSAL1* are transcribed within the outer starchy endosperm / sub-aleurone tissue, and thereby control a signal that functions in the aleurone. Answering this question is likely to be challenging since it would normally require creation of a null mutant for each gene, followed by cell-type specific rescue experiments. Additionally, transgenic reporter lines could also be developed which employ the *HvNKD1* and *HvSAL1* promoters controlling the expression of YFP. In the meantime, control experiments will require application of *in situ* hybridisation to confirm the effectiveness of aleurone-specific over-expression and down-regulation constructs.

Physiological relationships between the aleurone, free-β-amylase and germination efficiency

In this study, increased free β-amylase activity correlated with an increased amount of aleurone, however how this affects germination remains unclear. This would need to be analysed in a larger panel of cultivars than that examined for enzyme levels in Chapter 4. *HvBMY1* transcripts were analysed within aleurone tissue during grain development, in which it was shown that transcripts peaked around 13 DPA before decreasing late in development. It is currently unclear whether *HvBMY1* transcript abundance varies along the length of the barley grain, particularly near the embryo,

which may have led to an underestimation of aleurone *HvBMY1* levels. It is also possible that the relative abundance of aleurone-specific *HvBMY1* transcript peaks at a time point that was not investigated here. Furthermore, current microscopic assays that distinguish the free and bound β-amylase forms are currently unavailable and need to be established. These would be useful tools in confirming the location of the enzymes, assessing variation between genotypes of interest and determining the dynamics of enzyme release during seed development and germination. Another important point regarding germination assays relates to the transgenic plants with modified *HvNKD1* and *HvSAL1* expression. These may prove to be a useful resource to investigate the effect of modified aleurone development on enzyme levels and germination efficiency, mainly because they show specific alterations in the aleurone and are all in a common cultivar background.

Compositional analysis of lines containing more aleurone tissue

One way to improve the nutritional quality of wholegrain products would be to increase the ratio of aleurone to starchy endosperm. The aleurone from cereal grains possesses key nutrients that contribute to human health by decreasing cholesterol and reducing diabetes symptoms. For industrial purposes such as food production, the aleurone, along with the pericarp and testa, is considered part of the cereal bran. Bread and breakfast cereals that contain a large proportion of bran act to increase dietary fibre content for human consumption. Work presented here shows that aleurone traits correlated with levels of several nutritional components. For example, when examining aleurone phenolic antioxidants and cell wall contents, increased *p*-coumaric acid and arabinoxylan levels correlated with increased aleurone traits. This suggests that genotypes with increase aleurone content possessed higher levels of beneficial

factors. However, detailed aleurone composition was not examined in this study and hence further analysis of other aleurone components would be of interest in the future.

Could a bi-parental population be used to map genes underlying altered aleurone development?

To determine the genetic basis of aleurone development, tools other than GWAS can be employed, such as genetic linkage mapping with a bi-parental cross. Prior to this study, Jestin et al. (2008) examined the inheritance of aleurone thickness and layer number using a bi-parental cross between Erhard Frederichen x Criolla Negra, a three-layer and two-layer aleurone barley, respectively. The authors identified various quantitative trait loci (QTL) on chromosomes 2H, 5H and 7H that associated with these aleurone traits, however, genes contributing to aleurone development underlying these QTL are still unknown. In our study, assessing natural variation in aleurone traits across many barley genotypes may be beneficial for identifying candidates, showing significant differences in aleurone traits, for a bi-parental population. Examples of crosses that might be made: from the UA panel (Chapter 4); High (cv Shepherd or YU6472 or Mundah) x Low (cv W14191 or Barque-73 or Morex) aleurone lines. From the European panel (Chapter 5); High (cv Class or Extract) x Low (cv Pewter or Alabama) aleurone lines. Populations already available at the University of Adelaide (Coventry S., per communication) include: YU6472 (high) x WI3788 double haploid population, where WI3788 is 75% similar to WI4262 (low; cv Navigator). Commander (high) x WI4191 (low), where this population is already mapped by genome by sequencing (GBS), and SNP variation in interesting genes could be examined. A Mundah (high) x WI4262 (cv Navigator) (low) population has also recently been generated. Finally, an existing Mundah (high) x Keel (average/low) population could also be examined since it segregates for grain size (Coventry S., per communication).

Further candidate gene identification and characterisation

The main focus of this study to was to utilise natural variation in aleurone traits across barley to employ GWAS to identify candidate genomic regions significantly associated with particular aleurone traits. To identify candidate genes within these regions and determine spatial and temporal location, LCM and RNAseq was used. Analysis of these transcriptomes identified candidate genes that may influence aleurone development in barley or be used as aleurone marker genes for future analysis. Future research should focus on characterising these genes of interest within the QTL regions by generating transgenic/CRISPR plants, or by sourcing mutants from TILLING populations, to elucidate possible functions. Similarly, co-expression analysis should be used to build a network of regulatory pathways involved in barley grain development, taking into consideration both temporal and spatial data. This could potentially lead to the identification of candidate regulatory genes outside of the QTL regions, but whose targets or partners lie within it. At a basic level, this could initially involve examining the expression patterns of known aleurone genes and identifying other genes with similar expression patterns across wholegrain and tissue-specific development.

The generation of resources from this study could also be used to identify regulatory genes not only within the aleurone, but within the surrounding pericarp and endosperm tissues. The relationship between the aleurone and surrounding tissues appears to be crucial for correct aleurone development, as shown here using transgenic lines altering the expression of genes in the outer starchy endosperm. Using the developing grain tissue-specific LCM and wholegrain RNAseq datasets, genes contributing to pericarp and/or endosperm development could be identified. Additionally, LCM could be repeated to gather endosperm tissues from additional stages (i.e. 7 and 9 DPA) from

the transgenic overexpression or amiRNA lines, to reveal changes as a result of modified *HvNKD1* and *HvSAL1* expression. Continued refinement of the expression datasets currently available should contribute to the discovery of a wide range of genes involved in tissue development in the barley grain.

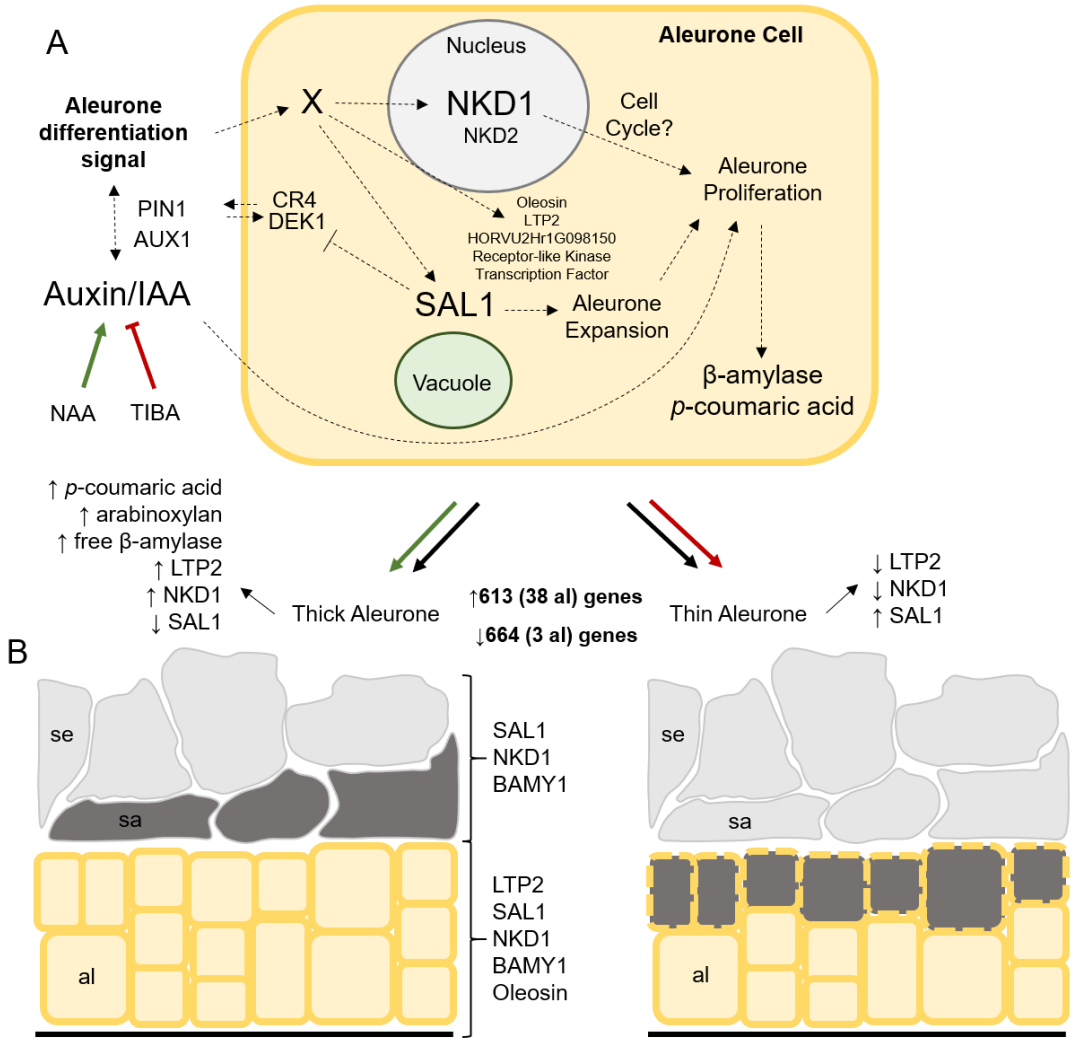

Figure 6-1: Proposed molecular model involving genes in the aleurone signal and auxin pathways. (A) Molecular pathway of key factors affecting aleurone development within the aleurone cell. X represents a possible unknown intermediate factor. Dashed arrows represent possible interactions that are less defined in barley. Green arrows represent effect of NAA treatment while red arrows represent effect of TIBA treatment. (B) Possible aleurone morphological outcomes of either a thick or thin aleurone. Dark grey cells represent morphological change in that layer due to NAA or TIBA treatment. Genes overlapping tissues represent location of protein expression. Pooled transcripts from high and low developing aleurone lines (Chapter 5), 613 genes were up-regulated, where 38 gene were enriched in the aleurone (al). Similarly, 664 genes were down-regulated, where 3 genes were enriched in the aleurone.

Appendix I

Exploring the Role of Cell Wall-Related Genes and Polysaccharides during Plant Development

Published and Accepted Manuscript

Statement of Authorship

Title of Paper	Exploring the Role of Cell Wall-Related Genes and Polysaccharides during Plant Development
Publication Status	☑ Published ☐ Accepted for Publication ☐ Submitted for Publication ☐ Unpublished and Unsubmitted work written in manuscript style
Publication Details	Matthew R. Tucker[1,*], Haoyu Lou[1,2], Matthew K. Aubert[1,2], Laura G. Wilkinson[1,2], Alan Little[1], Kelly Houston[3], Sara C. Pinto[4] and Neil J. Shirley[1,2]

Principal Author

Name of Principal Author (Candidate)	Matthew R. Tucker		
Contribution to the Paper	Compiled information and wrote manuscript. I hereby certify that the statement of authorship is accurate.		
Overall percentage (%)	60%		
Certification:	This paper reports on original research I conducted during the period of my Higher Degree by Research candidature and is not subject to any obligations or contractual agreements with a third party that would constrain its inclusion in this thesis. I am the primary author of this paper.		
Signature		Date	22/11/2018

Co-Author Contributions

By signing the Statement of Authorship, each author certifies that:

i. the candidate's stated contribution to the publication is accurate (as detailed above);

ii. permission is granted for the candidate in include the publication in the thesis; and

iii. the sum of all co-author contributions is equal to 100% less the candidate's stated contribution.

Name of Co-Author	Haoyu Lou		
Contribution to the Paper	Compiled information and contributed to the preparation of the manuscript. I hereby certify that the statement of authorship is accurate.		
Signature		Date	23/11/2018

Name of Co-Author	Matthew K. Aubert		
Contribution to the Paper	Compiled information and contributed to the preparation of the manuscript. I hereby certify that the statement of authorship is accurate.		
Signature		Date	21/11/2018

Please cut and paste additional co-author panels here as required.

Name of Co-Author	Laura G. Wilkinson		
Contribution to the Paper	Compiled information and contributed to the preparation of the manuscript. I hereby certify that the statement of authorship is accurate.		
Signature		Date	22/11/2018

Name of Co-Author	Alan Little		
Contribution to the Paper	Compiled information and contributed to the preparation of the manuscript. I hereby certify that the statement of authorship is accurate.		
Signature		Date	21/11/18

Name of Co-Author	Kelly Houston		
Contribution to the Paper	Compiled information and contributed to the preparation of the manuscript. I hereby certify that the statement of authorship is accurate.		
Signature		Date	22/11/2018

Name of Co-Author	Sara C. Pinto		
Contribution to the Paper	Compiled information and contributed to the preparation of the manuscript. I hereby certify that the statement of authorship is accurate.		
Signature		Date	23/11/2018

Name of Co-Author	Neil J. Shirley		
Contribution to the Paper	Compiled information and contributed to the preparation of the manuscript. I hereby certify that the statement of authorship is accurate.		
Signature		Date	21/11/18

plants

MDPI

Review

Exploring the Role of Cell Wall-Related Genes and Polysaccharides during Plant Development

Matthew R. Tucker [1,*], Haoyu Lou [1,2], Matthew K. Aubert [1,2], Laura G. Wilkinson [1,2], Alan Little [1], Kelly Houston [3], Sara C. Pinto [4] and Neil J. Shirley [1,2]

1 School of Agriculture, Food and Wine, Waite Research Institute, The University of Adelaide, Glen Osmond, SA 5062, Australia; haoyu.lou@adelaide.edu.au (H.L.); matthew.aubert@adelaide.edu.au (M.K.A.); laura.g.wilkinson@adelaide.edu.au (L.G.W.); alan.little@adelaide.edu.au (A.L.); neil.shirley@adelaide.edu.au (N.J.S.)

2 Australian Research Council Centre of Excellence in Plant Cell Walls, The University of Adelaide, Glen Osmond, SA 5062, Australia

3 Cell and Molecular Sciences, The James Hutton Institute, Dundee DD2 5DA,UK; Kelly.Houston@hutton.ac.uk

4 Departamento de Biologia, Faculdade de Ciências da Universidade do Porto, 4169-007 Porto,Portugal; sarapintomendes94@gmail.com

* Correspondence: matthew.tucker@adelaide.edu.au; Tel.: +61-8313-9241

Received: 29 April 2018; Accepted: 29 May 2018; Published: 31 May 2018

Abstract: The majority of organs in plants are not established until after germination, when pluripotent stem cells in the growing apices give rise to daughter cells that proliferate and subsequently differentiate into new tissues and organ primordia. This remarkable capacity is not only restricted to the meristem, since maturing cells in many organs can also rapidly alter their identity depending on the cues they receive. One general feature of plant cell differentiation is a change in cell wall composition at the cell surface. Historically, this has been viewed as a downstream response to primary cues controlling differentiation, but a closer inspection of the wall suggests that it may play a much more active role. Specific polymers within the wall can act as substrates for modifications that impact receptor binding, signal mobility, and cell flexibility. Therefore, far from being a static barrier, the cell wall and its constituent polysaccharides can dictate signal transmission and perception, and directly contribute to a cell's capacity to differentiate. In this review, we re-visit the role of plant cell wall-related genes and polysaccharides during various stages of development, with a particular focus on how changes in cell wall machinery accompany the exit of cells from the stem cell niche.

Keywords: cell wall; polysaccharide; development; glycosyltransferase; glycosyl hydrolase; differentiation; shoot meristem; root meristem

1. Introduction

As plant cells divide away from apical meristems, their molecular and biochemical profiles change. At the molecular level, cells adopt identities through changes in their nuclear morphology, genomic landscape, and transcriptional signatures. Changes also occur at the periphery of the cell, most notably in the abundance and organization of cell wall components such as cellulose, non-cellulosic polysaccharides, phenolic acids, lipids, and proteins [1]. Sometimes this results in terminal differentiation, for example in vascular tissues such as lignified mature fibers [2]. Changes in wall composition influence the downstream function of cells as storage units, structural networks, and solute transporters [3]. In many cases, differentiation also influences the capacity of cells to respond to stresses imparted through pathogens and the environment [4].

Despite its importance for growth and reproduction, plant cell differentiation is infrequently irreversible [5]. Many plant cells, not only those located in the meristems, possess the remarkable ability to adopt new identities. This can be a simple switch in identity between adjoining cells; for example, in the developing maize seed (kernel), where aberrant inward (periclinal) divisions of aleurone cells at the periphery result in one daughter cell retaining aleurone identity and the other adopting inner starchy endosperm identity [6]. The same thing can occur in more complex systems such as apomictic (asexual) plants, where ovule cells that adjoin normal sexual cells can spontaneously adopt germline-like identity and initiate a form of gametophyte development [7,8]. However, the plant meristem remains the epitome of differentiation capacity; meristematic stem cells can give rise to many different cell types, often referred to as pluripotency (the ability to either give rise to all cells and tissues in an organ) or totipotency (the ability to give rise to the entire organism) [9]. At a fundamental level, this indicates that fate is not fixed, and plant cells must maintain flexible cellular properties compatible with differentiation.

Much of our knowledge regarding cell differentiation has come from in vitro studies involving tissue culture, during which plant cells can be induced to de-differentiate (essentially reverse differentiation and lose specialized characteristics [10]), forming protoplasts or callus [11]. Somewhat similar to pluripotent stem cells, these totipotent undifferentiated cells can be stimulated to give rise to entire new tissues and eventually whole plants, depending on the correct exogenous application of growth hormones and vitamin supplements. Importantly, one component of in vitro de-differentiation appears to be modification or removal of the cell wall from the progenitor cell [12,13]. Moreover, in some cell types, the over-accumulation of specific cell wall components even appears to prevent de-differentiation or regeneration [14,15]. Therefore, variation in cell wall composition may contribute to the maintenance of cellular identity in some cases, while promoting the capacity for differentiation in others. How this is determined has yet to be addressed in sufficient detail, since it requires a thorough qualitative and quantitative assessment of cell wall composition at the single cell level.

Prevailing models suggest that there are two types of walls in plants; primary cell walls are relatively thin and flexible and are synthesized during cell growth and division, while secondary cell walls provide strength and rigidity in tissues that are no longer growing [16,17]. In general, the plant cell wall comprises a framework of cellulose microfibrils coated in diverse non-cellulosic polysaccharides. Xyloglucan (XyG) is proposed to cross-link cellulosic microfibrils, while pectins such as homogalacturonan (HG) and rhamnogalacturonan (RG) form a structurally diverse glue that provides flexibility or stiffness depending on chemical modifications [18,19]. Other classes of polymers include 1,3-β-glucan, 1,3;1,4-β-glucan, mannan, arabinan, xylan, and phenolic compounds such as lignin, which vary depending on the cell type, species, and developmental age, and appear to fulfil diverse roles [20–23]. Figure 1 shows thin sections from a number of dicot and monocot tissues labelled with cell wall-related antibodies and/or viewed under UV light, highlighting the diversity of polysaccharides present in growing tissues, as well as specific differences between organs, tissues, and individual cell types. How the different polymers interact within the cell wall matrix is constantly being revisited; direct covalent connections have been reported between pectin and xylan [24], xylan and lignin [25], and xyloglucan and cellulose [26]. However, the nature of the cross-linkages and hydrophobic interactions within the wall are not fully understood, and present significant challenges for the prediction and modelling of cell wall physicochemical properties [27]. Additional complexity is conveyed through glycoproteins such as arabinogalactan proteins (Figure 1), and other cell wall proteins such as proline-rich proteins, extensins, and expansins [28].

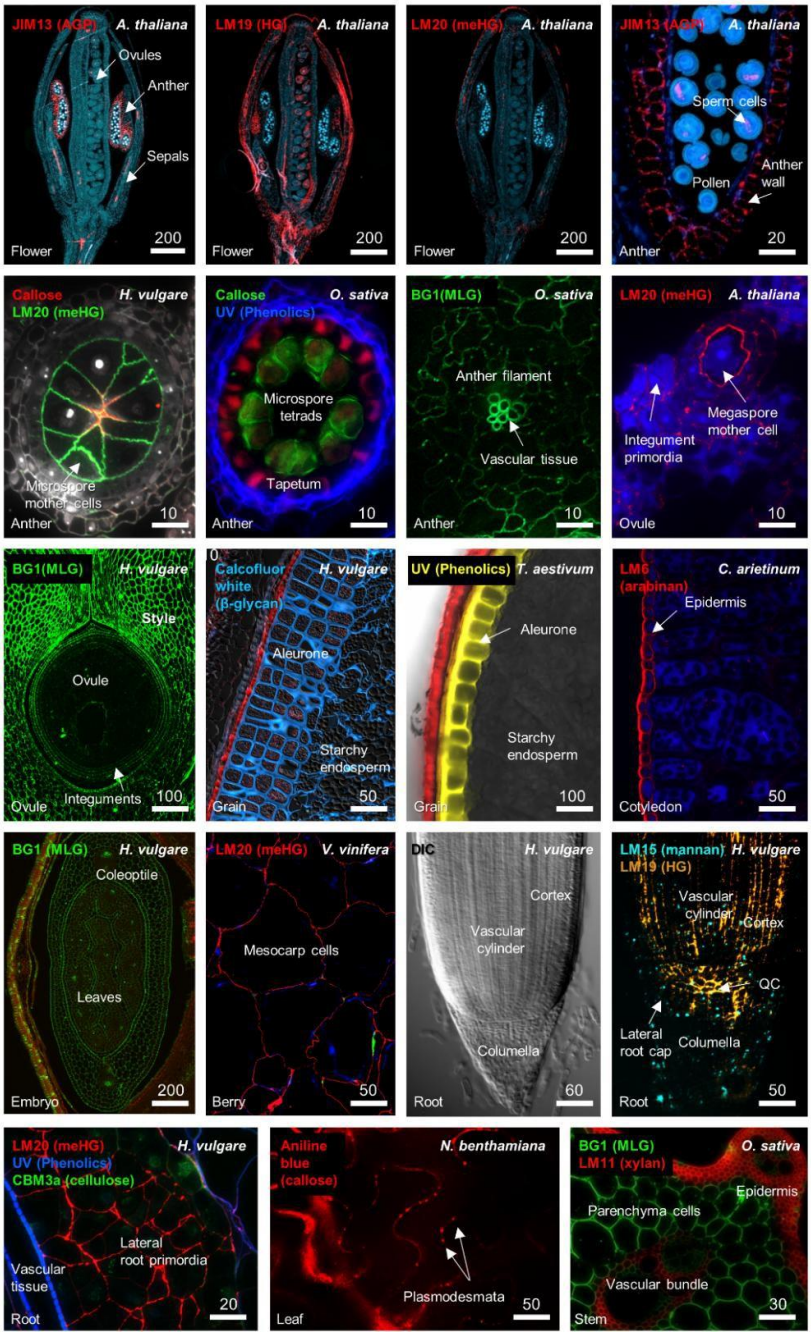

Figure 1. Detection of different cell wall components in distinct tissues of *Arabidopsis thaliana*, *Hordeum vulgare* (barley), *Oryza sativa* (rice), *Cicer arietinum* (chickpea), *Vitis vinifera* (grape), *Nicotiana benthamiana* (tobacco), and *Triticum aestivum* (bread wheat). The tissue origin of each section is indicated at the bottom left of each panel. The antibody or stain is indicated at the top left of each panel. Labelling of polymers was achieved through the use of diverse antibodies including BG1 (1,3;1,4-β-glucan), JIM13 (arabinogalactan proteins, AGP), LM19 (homogalacturonan, HG), LM20 (methylesterified homogalacturonan, meHG), callose (1,3-β-glucan), LM15 (mannan), LM6 (arabinan), LM11 (arabinoxylan), and CBM3a (cellulose), or stains such as aniline blue (1,3-β-glucan) and Calcofluor White (β-glycan), or UV autofluorescence. Differential contrast (DIC) microscopy was used to image the barley root tip and is shown as a reference for the adjoining immunolabelled sample. Images were generated for this review, but further details can be found in previous studies [23,29–32]. Scale bar dimensions are shown in μm.

Classical studies in two-celled embryos of the alga *Fucus* [33] showed that there is a direct role of the cell wall in maintaining cellular fate. Extending this hypothesis to examine the role of the cell wall during differentiation of specialized cells and tissues of higher plants has proved challenging, partially due to compositional complexity and the sub-epidermal location of cells [34]. Moreover, it remains technically challenging to view the cell wall in a high throughput manner, and with enough resolution, to identify specific quantitative and qualitative changes in composition that directly accompany or precede changes in cellular identity. Dogma suggests that as cells divide into new microenvironments they are exposed to new combinations of hormones and signals, which subsequently activate receptors at the plasma membrane to cue signal cascades and downstream transcriptional changes [35,36]. As a result of this feedback, the cell wall is remodeled to introduce new or modified polymers that exhibit different properties and contribute to new cellular identity. This almost certainly involves changes in biomechanical properties, which have been extensively reviewed in recent times [37–39]. However, in order to receive and process a particular differentiation signal, what basic structural or biochemical features are required? Do specific polysaccharides or cell wall proteins enable the preferential accumulation of receptors, transmission of signals or the synthesis of signaling molecules that potentiate differentiation? Is there an ideal wall composition required for cell differentiation? Studies in recent years provide some answers, hinting that the cell wall plays a dynamic role in development, and that cues to initiate remodeling may arise from and depend on the composition of the wall itself. As mentioned above, recent reviews have considered in detail the role of cell wall integrity and sensors in controlling plant growth [40,41]. In this review, we consider molecular and genetic evidence supporting a role for distinct cell wall polysaccharides during plant development, particularly in light of recent studies and technological advances in cell-type specific transcriptional profiling.

2. Cell Wall Modification during Growth, Differentiation, and Development

The molecular determinants of cell wall composition incorporate large families of enzymes including glycosyltransferases (GT), glycosylhydrolases (GH), methyltransferases, and acetylesterases (see the Carbohydrate Active enZyme database; CAZy [42]). The location and presumed site of activity of these enzymes can vary between the Golgi, the plasma membrane or a combination of both [43]. The addition of new polymers to a wall through the action of glycosyltransferases can immediately lead to changes in the pH, providing substrates for de-acetylation [44], de-esterification [19], and transglycosylation [45], and even new binding sites for receptors [46,47]. Specific differences in cell wall composition can be observed at different stages of development, between adjoining cells and tissues, and between monocots and dicots (See Figure 1). Several polymers that are labeled in Figure 1, pectin and callose, have been implicated in key stages of plant development. In the following sections we consider these polysaccharides, in addition to several "structural" polymers, with a view to addressing how their synthesis and/or modification can influence differentiation and development.

2.1. Pectin

Pectin is an important polymer during development since it can undergo considerable modification once it is deposited in the cell wall [48]. Multiple types of pectin are detected in the primary walls of dicots and monocots, including homogalacturonan (HG), rhamnogalacturonan-I (RG-I), rhamnogalacturonan-II (RG-II), and xylogalacturonan (XGA) [48,49]. Immunolabelling shows that pectic polymers are particularly enriched in young flowers, ovules, fruits, and roots (Figure 1). RG-I is detected in a number of tissues and is particularly prominent in the *Arabidopsis* seed coat [50] and the transition zone of developing roots [51]. The tight developmental regulation of RG-I deposition in seedling roots suggests it may play a role in cell expansion [51], but its exact role and the details of its biosynthesis remain unclear [52]. HG is methylesterified (meHG) during synthesis in the Golgi, and this forms a substrate for pectin methylesterase (PME, CE8), which depending on the cellular context can lead to loosening or strengthening of cell walls [19]. Clear roles for PME have been demonstrated in meristem development, seed mucilage biosynthesis, and pollen tube growth [53–55]. In the shoot

meristem, organ primordia initiation requires demethylesterification of HG in sub-epidermal layers through the action of PME [56], which reduces stiffness and promotes outgrowth (Figure 2). Negative regulation of *PME5* in the meristem dome by the BELLRINGER transcription factor ensures that the meHG substrate is only targeted by PME5 at the flanks of the meristem, leading to correct positioning of organ primordial [37]. Similarly, in the root, alterations in PME activity and increased demethylesterification are associated with expansion of cell types in the root tip [57,58].

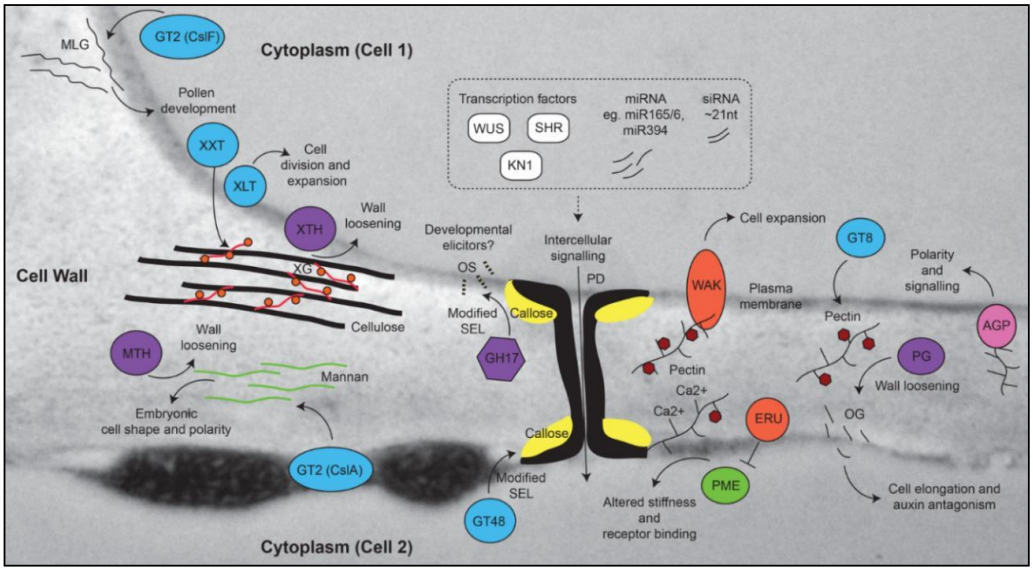

Figure 2. Cell wall components that contribute to growth, development, and differentiation. The model shows polymers superimposed on a TEM image of a leaf cell wall, including 1,3;1,4-β-glucan (MLG), cellulose, xyloglucan (XG), mannan, callose, and pectin. Enzymes that contribute to the biosynthesis or modification of these components are shown. The spatial separation of polymers is only shown for schematic purposes. Biosynthetic enzymes are shown in blue, hydrolytic enzymes are shown in purple, receptors are shown in orange, mobile transcription factors are shown in white, pectin methylesterase (PME) is shown in green, and arabinogalactan protein (AGPs) in pink. Deposition and hydrolysis of callose at the neck of plasmodesmata (PD) can alter the size exclusion limit (SEL) of the PD, hence limiting the mobility of intercellular signaling molecules such as transcription factors (e.g., WUSCHEL [59], SHORT ROOT [60], and KNOTTED [61]), microRNAs (miRNAs [60,62]), and short interfering RNAs (siRNAs [63,64]). Hydrolysis of callose by GH17 enzymes leads to the release of stimulatory oligosaccharides (OS) from the glucan backbone in fungi, but it remains unclear if similar OS contribute to growth and development in plants. By contrast, release of oligogalacturonides (OG) from pectin by polygalacturonase (PG) has been implicated in plant development through antagonistic effects on auxin pathways. The small circles on XG indicate galactosyl residues present due to the activity of XLT2 (xyloglucan galactosyltransferase). GT8 family enzymes contribute to the biosynthesis of pectin, which is usually synthesized in a methylesterified form (e.g., methylesterified homogalacturonan; meHG). Removal of methylesters (red hexagons) through the activity of PME can lead to calcium binding and subsequent cross-linking of pectin polysaccharides, which influences wall stiffness. GT, glycosyltransferase, XXT, xylosyltransferase, MTH, mannan transglycosylase/hydrolase, XTH, xyloglucan transglycosylase/hydrolase, CslF, cellulose synthase-like F, CslA, cellulose synthase-like A, GH, glycosyl hydrolase, WAK, wall-associated kinase, ERU, ERULUS receptor-like kinase.

Other factors that influence cell expansion are the Wall-Associated Kinases (WAKs), which directly bind pectin polymers in the cell wall in a way that is at least partially dependent upon the degree of methylesterification [65,66] (Figure 2). Mutations in several WAK genes suggest they play a role in mediating resistance against various pathogens [67,68], as well as in cell expansion during development [69]. Another putative receptor involved in the pectin pathway is the *Arabidopsis*

Catharanthus roseus receptor-like kinase 1-like (CrRLK1) ERULUS (ERU) protein, which is required for correct root hair formation, and regulates cell wall composition through negative control of PME activity [70] (Figure 2). Interestingly, ERU transcription is downregulated in several mutants showing changes in cell wall composition related to pectin, suggesting a possible feedback mechanism from the wall to regulate pectin composition and root hair development. ERU is part of the FERONIA (FER) family of kinases [41,71] that are implicated in fertilization, cell wall sensing, and root growth. Defects in the FER signaling pathway lead to pronounced defects in pectin composition of pollen tubes and root hairs, and a recent report indicates that FER directly interacts with pectin *in vivo* and in vitro [72]. Curiously, the ability of cell walls to sense change may be restricted to components of the primary wall, since limited signaling and transcriptomic responses were observed in mutants showing altered secondary cell wall biosynthesis in *Arabidopsis* [73].

Finally, modification of pectin by hydrolytic enzymes can lead to the release of small fragments called oligogalacturonides, which are reported to effect plant growth and development [74]. These pectin fragments impact diverse physiological processes, including fruit ripening in tomato [48] and stem elongation in pea [75] via a mechanism that appears to involve antagonism with the plant hormone auxin [76]. In summary, these studies indicate that specific pectic polymers within the wall may predispose cells to respond to stimuli that influence growth and differentiation.

2.2. Callose and Plasmodesmata

Another polymer that influences cellular differentiation is callose. Comprised of a water-insoluble linear form of (1,3)-β-glucan, callose is an atypical cell wall polysaccharide in that it is not often co-extensive throughout cell walls with pectin and cellulose but has specific restricted occurrences and functions in locations such as the cell plate, reproductive tissues, and plasmodesmata (PD). Genes involved in callose biosynthesis and hydrolysis are well characterized and include the 1,3-β-glucan synthases (GT48 family) and 1,3-β-glucan hydrolases (GH17 family), respectively. These enzymes have historically been associated with roles in pathogen response, dormancy, cell division, and plant reproduction [21,77,78], but recent studies emphasize their general importance in controlling intercellular transport of developmental regulators through PD (Figures 1 and 2). PD are intercellular channels embedded in the cell wall that provide a cytoplasmic continuum between cells [79]. Different types of PD can be detected in the cell wall, which vary in terms of their structure and their arrangement within and between cell layers [80,81]. The formation of lateral roots in *Arabidopsis* depends upon restrictive callose deposits in the cell wall adjoining the PD [82], often referred to as the "neck" region. PD also regulate intercellular movement of transcription factors and microRNAs between the stele and endodermis to control xylem development [60]. Although the cues that drive PD formation are unknown, PD are present in many cell types and are accompanied by increased pectin and decreased cellulose deposits in flanking cell wall regions [83]. Enzymes regulating callose biosynthesis and turnover are enriched in the general PD proteome [84] in addition to several PMEs, polygalacturonases and diverse receptor kinases that likely influence PD function [85,86]. The biochemical analysis of PD highlights a potential relationship between pectin and callose that has yet to be explored in significant detail.

The removal of callose from PD and specialized cell walls in the anthers and ovule is mediated by GH17 enzymes, which form a large family found in archaea, bacteria, and eukaryotes [87]. In general, GH17 activity is likely to influence growth and development in several ways by (1) decreasing the size exclusion limit (SEL) of PD and allowing increased symplastic intercellular transport [88]; (2) removing apoplastic barriers that are proposed to insulate cells such as the megaspores or microspores against mobile signals [89,90] and (3) removing a transient matrix for deposition of secondary polymers during cytokinesis and cell division [91]. Consistent with a role in regulating the SEL of PD, studies in the shoot meristem have shown that mobile tracers are free to move between distinct "symplastic fields", which incorporate different zones and layers [92,93]. This indicates that differential regulation of PD conductance is likely to be required for meristem cell identity and function. One key transcription factor involved in meristem maintenance, WUSCHEL, moves from the organizing centre (OC) of the

meristem into above-lying stem cells through PD [59]. Therefore, the presence of PD and associated cell wall polymers is another example by which cells may be predisposed to be responsive to non-cell autonomous stimuli; in essence, the PD and adjoining regions of cell wall provide a substrate for receptor binding as well as for cell wall remodeling activities that can influence intercellular signaling and differentiation (Figure 2).

In addition to these developmental functions, GH17 enzymes also form a defensive barrier during pathogen attack that targets 1,3-β-glucan polymers in the fungal cell wall. A recent study showed that non-branched fungal 1,3-β-glucan oligosaccharides are able to trigger immune responses in *Arabidopsis* via CERK1 (chitin elicitor receptor kinase 1) [94]. It is tempting to speculate that similar to oligogalacturonides, cleavage of endogenous 1,3-β-glucan polymers might release backbone oligosaccharides that elicit responses during growth and development (Figure 2).

2.3. Roles for Other "Structural" Polymers in Growth and Development

1,3;1,4-β-glucan is predominantly found in monocots, particularly the *Poaceae*, where it accumulates in the primary and secondary walls of diverse tissues [95,96] (Figure 1). Evidence suggests that accumulation of 1,3;1,4-β-glucan is required for correct grain fill in barley and wheat [97,98]. However, genetic studies also reveal specific developmental abnormalities, such as male infertility, in rice plants lacking the primary biosynthetic enzyme controlling 1,3;1,4-β-glucan biosynthesis [99] (Cellulose synthase-like F6; CslF6). In barley, tissue-specific over-accumulation of 1,3;1,4-β-glucan appears to inhibit signal and/or solute transmission [29,97] while barley *cslf6* mutants are shorter and show defects in leaf growth [100]. This is perhaps unsurprising given that *CslF6* is expressed in a range of tissues [101], however, the specific role of 1,3;1,4-β-glucan and the *CslF* gene family in plant development requires further investigation.

Unlike 1,3;1,4-β-glucan, xyloglucan (XyG) is a highly branched polysaccharide found in the primary cell wall of many plant tissues and is characterized as a structural cell wall component that binds to cellulose [102] (Figure 2). Remarkably, mutants lacking activity of three xylosyltransferase (*XXT*) genes (*XXT1*, *2* and *5*) contain no detectable xyloglucan in their cell walls, yet develop relatively normally apart from defects in root hairs [103]. By contrast, *murus3* mutants that are deficient for a XyG-specific galactosyltransferase contain normal levels of xyloglucan, but in a form that is depleted of galactosyl substituents, and this results in extreme developmental defects including dwarfism [104]. Hence, while XyG is not required per se for *Arabidopsis* development, incorrect substitution of XyG may compromise interactions between different wall polymers, resulting in a cell wall composition that is incompatible with cell growth.

Similar to xyloglucan, several types of structurally diverse mannans are also linked to the cellulose network providing mechanical support [105], while others are involved in carbohydrate storage. Loss-of-function mutations in the *Cellulose synthase-like A* (*CslA*) 2, 3, and 9 genes, encoding putative glucomannan synthases, result in no detectable glucomannan in stems but plants appear phenotypically normal [106]. However, mutants lacking function of the *CslA7* gene show embryo lethality, suggesting that in some tissues glucomannan is a critical component for growth and differentiation [107]. Although the mechanistic basis for this lethality is unclear, the *csla7* mutant embryos appear remarkably similar to those showing defects in developmental patterning and organ differentiation, such as double mutants of the *WUSCHEL-HOMEOBOX* 8/9 transcription factors [108] and *ARGONAUTE* 1/10 genes involved in post-transcriptional gene silencing [109,110]. This may indicate that targets of these transcriptional and post-transcriptional regulators converge at the cell wall, or that a distinct cell wall composition contributes to downstream function of these regulatory pathways. Interestingly, both mannan and xyloglucan are targets of transglycosylase enzymes activities, which essentially cleave the polysaccharide chain and attach it to a new chain to retain strength in the cell wall (Figure 2). Both mannan endotransglycosylases/hydrolases (MTH) and xyloglucan endotransglycosylases/hydrolases (XET/XTH) have been implicated in fruit development. LeMAN4a, an MTH from tomato, exhibits transglycosylase activity and is expressed in young floral buds where it

is hypothesized to function in tissue softening [111]. Similarly, *XTH* genes are associated with fruit development in persimmon, apple, and tomato [112,113]. Therefore, even in the case of polysaccharides that have historically been associated with structural functions, there is evidence to suggest their presence in the wall may provide a substrate for remodeling enzymes that impact growth and differentiation during diverse stages of plant development.

3. Specific Cell Wall-Related Genes Accompany Differentiation in Meristematic Zones

Antibodies and glyco-arrays are an outstanding resource [114,115] to localize and identify specific cell wall-related epitopes, and this is highlighted by the distinct labelling patterns shown in Figure 1. The limitation of antibodies is that they only provide a limited view of the chemical complexity present in a cell wall at a particular time point. Technologies that enable local qualitative and quantitative assessments of wall complexity, particularly in the case of the shoot and root meristem and reproductive tissues, would provide a significant advantage in understanding cell wall changes during differentiation. Methods such as coherent anti-Stokes Raman scattering (CARS [1]) and FTIR microspectroscopy [116] may enable specific compositional changes to be identified, although they are yet to deliver the required precision for cell-type specific analysis during development. By contrast, at the molecular level, definition of the transcriptional programs underlying cell wall formation has recently become much more accessible. The analysis and identification of cell wall-related genes that define specific cell types and/or show altered expression during development remains a viable approach to assess the role of different cell wall components in facilitating differentiation.

In *Arabidopsis*, studies have utilized the elegant method of fluorescence-assisted cell sorting (FACS) to collect specific populations of cells from developing tissues [117–119]. This approach was used successfully in *Arabidopsis* roots [117,118] to profile RNA from, among others, cell types located in the meristematic zone including the quiescent centre (QC), the adjoining columella, and the lateral root cap (LRC). The QC is marked by the expression of *AGL42* and *WOX5* genes and contains slowly dividing, "undifferentiated" cells that stimulate the formation of adjoining stem cells [120] (Figure 1). Underlying the QC are the columella initials; stem cells that divide periclinally to give rise to one daughter that adopts columella fate and another that retains stem cell identity. Similarly, the LRC initial cells adjoin the QC and give rise to all cells in the lateral root cap. These cell types are in close proximity but assume different identities as soon as they divide away from the QC. Therefore, the cell-type specific transcriptional datasets provide an excellent resource to assess changes in the cell wall machinery during differentiation.

Houston et al. [4] examined transcriptional datasets from *Arabidopsis* and other species to highlight cell wall gene families associated with cell wall remodeling during abiotic stress and pathogen attack. A similar survey of the *Arabidopsis* root cell-type specific RNA profiles [118] reveals a comprehensive set of cell wall genes potentially contributing to growth and differentiation (Figure 3). Relative to the QC (as an undifferentiated reference), cells that adopt LRC or columella fate express different gene families involved in polysaccharide biosynthesis and modification. Examples include the arabinogalactan proteins (AGPs), pectin methylesterases (CE8), glucoronyl/galacturonosyltransferases (GT8), and xylan 1,4-β-xylosyltransferases (GT43). Arabinogalactan proteins are cell wall proteins that have been implicated in many aspects of growth and development [30,31,121,122], while the other families are implicated in pectin and xylan biosynthesis and modification. The majority of these gene families are upregulated as cells adopt columella or LRC identity, consistent with the formation of new wall types compared to the relatively naïve wall in the undifferentiated QC. Notably, within the QC itself, representatives from the pectate lyase (PL1), expansin, 1,3-β-glucanase (GH17), and 1,3-β-glucan synthase (GT48) families are up-regulated, hinting at a key requirement for intercellular signaling and wall flexibility. This analysis exemplifies how transcriptomic studies can enable identification of cell wall-related genes and families that accompany changes in cell identity during differentiation. In many cases, these transcriptional changes directly relate to alterations in root cell wall composition [123] indicating a close link between transcript abundance and putative enzyme activity.

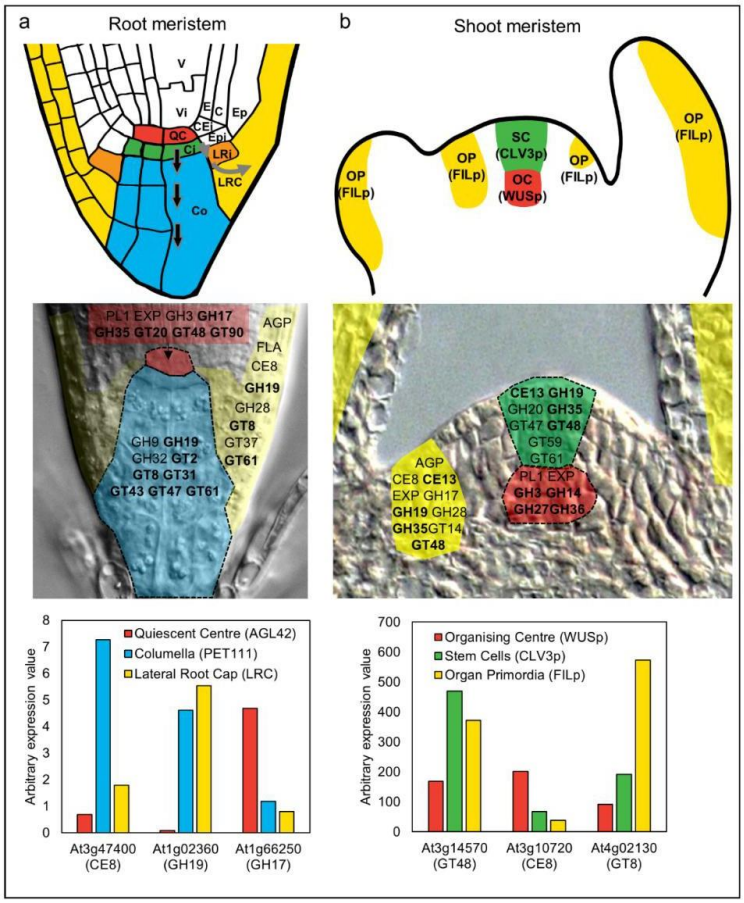

Figure 3. Analysis of cell wall-related gene expression during differentiation of stem cells in the root and shoot meristem of *Arabidopsis thaliana*. The upper panels in (**a**,**b**) show schematic representations of the root and shoot apical meristem [120]. (**a**) In the root meristem, initial cells (stem cells) directly adjoining the QC enter differentiation pathways as they divide away from the niche (shown by arrows for columella and lateral root cap). V, vasculature, Vi, vascular initial, QC, quiescent centre, E, endodermis, C, cortex, CEi, cortex/endodermis initials, Epi, epidermal initials, Ep, epidermis, LRi, lateral root cap initial, LRC, lateral root cap, Ci, columella initial, Co, columella. (**b**) In the shoot meristem, the organizing center (OC) functions via WUSCHEL (WUS) to maintain the stem cells (SC) in an undifferentiated state. The stem cells express the signal peptide CLAVATA3 (CLV3). Divisions of the stem cells provide daughters that enter differentiation pathways at the flanks of the meristem and become organ primordia (OP), which is marked by expression of genes such as *FILAMENTOUS FLOWER* (*FIL*). The second row of panels highlights gene families encoding CAZy carbohydrate-related enzymes [42] that are enriched in each meristem cell type according to FACS-mediated sorting and transcriptional profiling [118,119]. The genes are superimposed on sections of root and shoot meristem tissues. Family names in bold indicate that multiple members from the same family were up-regulated in the QC or OC (depending on the meristem) relative to both of the other cell types. GH, glycosyl hydrolase, GT, glycosyltransferase, PL, pectate lyase, AGP, arabinogalactan protein, EXP, expansin, CE, carbohydrate esterase, FLA, fasciclin-like arabinogalactan protein. See Table 1 for putative functions of enzyme families. The third row of panels shows expression patterns of selected CAZy family members in the different meristem cell types. Several of the individual genes reflect the behavior of the entire family. For example, At1g02360 is up-regulated in the columella and LRC relative to the OC, and this is a pattern shown for many GH19 family members. However, other genes such as At3g47400, At3g10720, and At4g02130 show unique patterns compared to other members of their families. The reason why multiple family members are recruited into some cell-type preferential expression pathways, while in others only individual members are expressed, remains to be elucidated.

In the shoot apical meristem (SAM), Yang et al. (2016) characterized changes in cell wall composition by immunolabelling, in addition to profiling cell wall-related gene expression in different meristematic regions [124]. Their results indicate that as cells divide through the meristem, different enzymes build new walls compared to those that build maturing walls. Complementing this, studies have examined transcriptional changes at the level of individual meristematic cell types (Figure 3). The organizing centre (OC) of the SAM is marked by expression of the *WUSCHEL* gene and is somewhat similar to the root QC, in that it is undifferentiated, slow to divide, and specifies adjoining cells as stem cells [120]. The shoot stem cells express the *CLAVATA3* gene, and as they divide anticlinally, they exit the control of the OC and enter organ differentiation pathways where expression of transcription factors such as *FILAMENTOUS FLOWER* are detected (Figure 3). Yadav et al. (2009) used these cell-type specific markers to isolate and transcriptionally profile shoot stem cell types [119]. Around half of the *Arabidopsis* CAZy cell wall families are up-regulated in organ primordia but downregulated in the stem cells relative to the OC; gene families include the expansins (EXP), fasciclin-like arabinogalactan proteins (FLAs), pectate lyases (PL1), pectin methylesterases (CE8), polygalacturonases (GH28), and endo-arabinanases (GH43). The lack of glycosyltransferases and abundance of cell wall modifying enzymes suggests that, similar to the root meristem, cell wall remodeling is the predominant feature of cell and organ differentiation in the shoot. Interestingly, gene families that are up-regulated in the stem cells relative to the OC and organ primordia include a number of key polysaccharide synthases and hydrolases such as 1,3-β-glucan synthase (GT48), arabinosyl/xylosyltransferase (GT61), and xylanase (GH10). As discussed above, the GT48 genes contribute to callose biosynthesis, and their up-regulation may relate to the formation of symplastic zones through altered PD conductance. Although a direct role for GT61 and GH10 genes during development has not been explicitly reported, GT61 enzymes have been implicated in substitution of polysaccharides to potentially influence wall polymer viscosity in seed-coat epidermal cells [125,126], and some GH10 xylanases are expressed during secondary wall synthesis in poplar [127].

In summary, these studies show that as cells exit the stem cell niche and start differentiating, clear trends are seen in the transcriptional behavior of CAZy families. The CAZy signatures of distinct cell-types within the shoot and root meristem are summarized in Figure 3. It is important to note that despite their grouping via functional domains and proposed carbohydrate-related activities, the vast majority of the CAZy genes remain uncharacterized. The transcriptional profiles of the meristematic cells are remarkably dynamic yet similar between the shoot and root meristems, identifying key activities whose role in differentiation might be addressed in more detail through further mutant and cell-type specific analyses.

4. Perspectives

The basis for this review was to consider the role of the plant cell wall in growth and development, and to assess how cell wall polysaccharides might predispose cells to undergo differentiation. We have focused our attention on polysaccharides including pectin, callose, xyloglucan, and mannan, which fulfil roles during different stages of growth and development. The presence and modification of these polymers correlates with changes in cell identity and function, and their depletion through mutagenesis or transgenic modification results in altered plant development. Callose and pectin in particular provide multiple avenues to influence differentiation, initially through deposition and subsequently through hydrolysis, chemical modification, and receptor binding. Consistent with the chemical complexity of the cell wall, the transcriptional machinery underlying cell wall polysaccharide deposition and modification is intricate. However, common activities are identified in cell types that exit from apical (shoot and root) stem cell niches and initiate differentiation. This overlap suggests that while the cellular context (i.e., roots vs. shoots) and specific gene family members might differ, early stages of differentiation likely depend on a similar wall composition that is compatible with remodeling. In this context, it seems prudent to consider the cell wall in the same light as other

key factors, such as genomic and epigenetic modifications, that facilitate important steps of the cell differentiation process.

Table 1. Protein families potentially involved in polysaccharide biosynthesis and modification in *Arabidopsis*.

CAZy Family	Putative Polysaccharide Target	Gene ID	Enzyme Description
AGP			arabinogalactan protein *
CE13	Pectin		pectin acetylesterase
CE8	Pectin	PME	pectin methylesterase
EXP			expansin
FLA			fasciclin-like arabinogalactan protein
GH3	Glucan/Xylan/Xyloglucan		β-D-glucosidase, α-L-arabinofuranosidase, β-D-xylopyranosidase
GH5	Mannan	MTH	endo-β-mannanase
GH9	Cellulose		cellulase
GH10	Xylan		endo-β-xylanase
GH14	Starch		β-amylase
GH16	Xyloglucan	XTH/XET	xyloglucan:xyloglucosyltransferases
GH17	Callose	GLUC	glucan endo-1,3-β-glucosidase
GH19	Chitin		chitinase; lysozyme
GH20			beta-hexosaminidase
GH27			α-galactosidase
GH28	Pectin	PG	polygalacturonase
GH32			invertase
GH35	Pectin/Xyloglucan		β-galactosidase
GH36			α-galactosidase
GT2	Cellulose/Mannan/1,3;1,4-β-glucan	CslA/CslF	cellulose synthase/cellulose synthase-like
GT8	Pectin/Xylan		homogalacturonan 1,4-α galacturonosyltransferase
GT14	AGP		UDP-GlcA: xylan α-glucuronyltransferase UDP-GlcA: [arabinogalactan] 1,3-β-/1,6-β-galactan 1,6-β-glucuronosyltransferase
GT20			alpha,alpha-trehalose-phosphate synthase [UDP-forming]
GT31	AGP/Pectin		1,3-β-glucuronyltransferase
GT34	Xyloglucan	XXT	xyloglucan 1,6-α-xylosyltransferases
GT37	Xyloglucan		xyloglucan 1,2-α-α-fucosyltransferase
GT43	Xylan		glucuronoxylan glycosyltransferase
GT47	Xylan/Xyloglucan	MUR3	xylosyltransferase/xyloglucan galactosyltransferase
GT48	Callose	GSL	1,3-β-glucan synthase
GT59			1,2-α-glucosyltransferase
GT61	Xylan/Xyloglucan		xylosyltransferase/arabinosyltransferase
GT90	Mannan		UDP-Xyl: (mannosyl) glucuronoxylomannan galactoxylomannan 1,2-β-xylosyltransferase
PL1	Pectin		pectate lyase

Note: * AGPs are not reported to exhibit enzymatic activity. Only families relevant to Figure 2 or the main text are included while genes that are referred to in the text are listed in the Gene ID column.

Author Contributions: All authors contributed to the Investigation, Visualization and Writing-Review & Editing of this review article.

Funding: This work was supported by the Australian Research Council grant numbers FT140100780 and CE110001007, the Grains Research and Development Corporation (GRDC) grant number GRS10938, the H2020-MSCA-RISE-2015 initiative "SEXSEED" and the Scottish Government via Rural Affairs Food and Environment Strategic Research (RESAS).

Acknowledgments: We wish to thank members of the Tucker lab for and four anonymous reviewers for helpful comments.

Conflicts of Interest: The authors declare no conflict of interest.

References

1. Zeng, Y.; Himmel, M.E.; Ding, S.Y. Visualizing chemical functionality in plant cell walls. *Biotechnol. Biofuels* **2017**, *10*, 1–16. [CrossRef] [PubMed]
2. Heo, J.O.; Blob, B.; Helariutta, Y. Differentiation of conductive cells: A matter of life and death. *Curr. Opin. Plant Biol.* **2017**, *35*, 23–29. [CrossRef] [PubMed]
3. Burton, R.A.; Gidley, M.J.; Fincher, G.B. Heterogeneity in the chemistry, structure and function of plant cell walls. *Nat. Chem. Biol.* **2010**, *6*, 724–732. [CrossRef] [PubMed]
4. Houston, K.; Tucker, M.R.; Chowdhury, J.; Shirley, N.; Little, A. The plant cell wall: A complex and dynamic structure as revealed by the responses of genes under stress conditions. *Front. Plant Sci.* **2016**, *7*, 984. [CrossRef] [PubMed]

5. Grafi, G.; Florentin, A.; Ransbotyn, V.; Morgenstern, Y. The stem cell state in plant development and in response to stress. *Front. Plant Sci.* **2011**, *2*, 53. [CrossRef] [PubMed]
6. Becraft, P.W.; Asuncion-Crabb, Y. Positional cues specify and maintain aleurone cell fate in maize endosperm development. *Development* **2000**, *127*, 4039–4048. [PubMed]
7. Tucker, M.R.; Araujo, A.C.; Paech, N.A.; Hecht, V.; Schmidt, E.D.; Rossell, J.B.; De Vries, S.C.; Koltunow, A.M. Sexual and apomictic reproduction in *Hieracium* subgenus *Pilosella* are closely interrelated developmental pathways. *Plant Cell* **2003**, *15*, 1524–1537. [CrossRef] [PubMed]
8. Tucker, M.R.; Okada, T.; Johnson, S.D.; Takaiwa, F.; Koltunow, A.M. Sporophytic ovule tissues modulate the initiation and progression of apomixis in *Hieracium*. *J. Exp. Bot.* **2012**, *63*, 3229–3241. [CrossRef] [PubMed]
9. Gaillochet, C.; Lohmann, J.U. The never-ending story: From pluripotency to plant developmental plasticity. *Development* **2015**, *142*, 2237–2249. [CrossRef] [PubMed]
10. Verdeil, J.L.; Alemanno, L.; Niemenak, N.; Tranbarger, T.J. Pluripotent versus totipotent plant stem cells: Dependence versus autonomy? *Trends Plant Sci.* **2007**, *12*, 245–252. [CrossRef] [PubMed]
11. Fukuda, H.; Ito, M.; Sugiyama, M.; Komamine, A. Mechanisms of the proliferation and differentiation of plant cells in cell culture systems. *Int. J. Dev. Biol.* **1994**, *38*, 287–299. [PubMed]
12. Ikeuchi, M.; Ogawa, Y.; Iwase, A.; Sugimoto, K. Plant regeneration: Cellular origins and molecular mechanisms. *Development* **2016**, *143*, 1442–1451. [CrossRef] [PubMed]
13. Ikeuchi, M.; Sugimoto, K.; Iwase, A. Plant callus: Mechanisms of induction and repression. *Plant Cell* **2013**, *25*, 3159–3173. [CrossRef] [PubMed]
14. Lozovaya, V.; Gorshkova, T.; Yablokova, E.; Zabotina, O.; Ageeva, M.; Rumyantseva, N.; Kolesnichenk, E.; Waranyuwat, A.; Widholm, J. Callus cell wall phenolics and plant regeneration ability. *J. Plant Physiol.* **1996**, *148*, 711–717. [CrossRef]
15. Chen, C.C.; Fu, S.F.; Lee, Y.I.; Lin, C.Y.; Lin, W.C.; Huang, H.J. Transcriptome analysis of age-related gain of callus-forming capacity in *Arabidopsis* hypocotyls. *Plant Cell Physiol.* **2012**, *53*, 1457–1469. [CrossRef] [PubMed]
16. Cosgrove, D.J.; Jarvis, M.C. Comparative structure and biomechanics of plant primary and secondary cell walls. *Front. Plant Sci.* **2012**, *3*, 204. [CrossRef] [PubMed]
17. Hofte, H.; Voxeur, A. Plant cell walls. *Curr. Biol.* **2017**, *27*, R865–R870. [CrossRef] [PubMed]
18. Park, Y.B.; Cosgrove, D.J. Xyloglucan and its interactions with other components of the growing cell wall. *Plant Cell Physiol.* **2015**, *56*, 180–194. [CrossRef] [PubMed]
19. Levesque-Tremblay, G.; Pelloux, J.; Braybrook, S.A.; Muller, K. Tuning of pectin methylesterification: Consequences for cell wall biomechanics and development. *Planta* **2015**, *242*, 791–811. [CrossRef] [PubMed]
20. Rancour, D.M.; Marita, J.M.; Hatfield, R.D. Cell wall composition throughout development for the model grass *Brachypodium distachyon*. *Front. Plant Sci.* **2012**, *3*, 266. [CrossRef] [PubMed]
21. Gibeaut, D.M.; Pauly, M.; Bacic, A.; Fincher, G.B. Changes in cell wall polysaccharides in developing barley (*Hordeum vulgare*) coleoptiles. *Planta* **2005**, *221*, 729–738. [CrossRef] [PubMed]
22. Nunan, K.J.; Sims, I.M.; Bacic, A.; Robinson, S.P.; Fincher, G.B. Changes in cell wall composition during ripening of grape berries. *Plant Physiol.* **1998**, *118*, 783–792. [CrossRef] [PubMed]
23. Wood, J.A.; Tan, H.T.; Collins, H.M.; Yap, K.; Khor, S.; Lim, W.L.; Xing, X.; Bulone, V.; Burton, R.A.; Fincher, G.B.; et al. Genetic and environmental factors contribute to variation in cell wall composition in mature desi chickpea (*Cicer arietinum* L.) cotyledons. *Plant Cell Environ.* **2018**. [CrossRef] [PubMed]
24. Tan, L.; Eberhard, S.; Pattathil, S.; Warder, C.; Glushka, J.; Yuan, C.; Hao, Z.; Zhu, X.; Avci, U.; Miller, J.S.; et al. An *Arabidopsis* cell wall proteoglycan consists of pectin and arabinoxylan covalently linked to an arabinogalactan protein. *Plant Cell* **2013**, *25*, 270–287. [CrossRef] [PubMed]
25. Grabber, J.H.; Ralph, J.; Hatfield, R.D. Cross-linking of maize walls by ferulate dimerization and incorporation into lignin. *J. Agric. Food Chem.* **2000**, *48*, 6106–6113. [CrossRef] [PubMed]
26. Hrmova, M.; Farkas, V.; Lahnstein, J.; Fincher, G.B. A barley xyloglucan xyloglucosyl transferase covalently links xyloglucan, cellulosic substrates, and (1,3;1,4)-β-D-glucans. *J. Biol. Chem.* **2007**, *282*, 12951–12962. [CrossRef] [PubMed]
27. Cosgrove, D.J. Re-constructing our models of cellulose and primary cell wall assembly. *Curr. Opin. Plant Biol.* **2014**, *22*, 122–131. [CrossRef] [PubMed]
28. Jamet, E.; Canut, H.; Boudart, G.; Pont-Lezica, R.F. Cell wall proteins: A new insight through proteomics. *Trends Plant Sci.* **2006**, *11*, 33–39. [CrossRef] [PubMed]

29. Aditya, J.; Lewis, J.; Shirley, N.J.; Tan, H.T.; Henderson, M.; Fincher, G.B.; Burton, R.A.; Mather, D.E.; Tucker, M.R. The dynamics of cereal cyst nematode infection differ between susceptible and resistant barley cultivars and lead to changes in (1,3;1,4)-β-glucan levels and *HvCslF* gene transcript abundance. *New Phytol.* **2015**, *207*, 135–147. [CrossRef] [PubMed]
30. Lora, J.; Herrero, M.; Tucker, M.R.; Hormaza, J.I. The transition from somatic to germline identity shows conserved and specialized features during angiosperm evolution. *New Phytol.* **2017**, *216*, 495–509. [CrossRef] [PubMed]
31. Coimbra, S.; Almeida, J.; Junqueira, V.; Costa, M.L.; Pereira, L.G. Arabinogalactan proteins as molecular markers in *Arabidopsis* thaliana sexual reproduction. *J. Exp. Bot.* **2007**, *58*, 4027–4035. [CrossRef] [PubMed]
32. Yu, J.; Meng, Z.; Liang, W.; Behera, S.; Kudla, J.; Tucker, M.R.; Luo, Z.; Chen, M.; Xu, D.; Zhao, G.; et al. A rice Ca^{2+} binding protein is required for tapetum function and pollen formation. *Plant Physiol.* **2016**, *172*, 1772–1786. [CrossRef] [PubMed]
33. Berger, F.; Taylor, A.; Brownlee, C. Cell fate determination by the cell wall in early *Fucus* development. *Science* **1994**, *263*, 1421–1423. [CrossRef] [PubMed]
34. Fleming, A.J. The co-ordination of cell division, differentiation and morphogenesis in the shoot apical meristem: A perspective. *J. Exp. Bot.* **2006**, *57*, 25–32. [CrossRef] [PubMed]
35. Torii, K.U. Stomatal differentiation: The beginning and the end. *Curr. Opin. Plant Biol.* **2015**, *28*, 16–22. [CrossRef] [PubMed]
36. Benfey, P.N. Defining the path from stem cells to differentiated tissue. *Essays Dev. Biol. Part A* **2016**, *116*, 35–43.
37. Vogler, H.; Felekis, D.; Nelson, B.J.; Grossniklaus, U. Measuring the mechanical properties of plant cell walls. *Plants* **2015**, *4*, 167–182. [CrossRef] [PubMed]
38. Braybrook, S.A.; Jonsson, H. Shifting foundations: The mechanical cell wall and development. *Curr. Opin. Plant Biol.* **2016**, *29*, 115–120. [CrossRef] [PubMed]
39. Cosgrove, D.J. Diffuse growth of plant cell walls. *Plant Physiol.* **2018**, *176*, 16–27. [CrossRef] [PubMed]
40. Wolf, S.; Hematy, K.; Hofte, H. Growth control and cell wall signaling in plants. *Annu. Rev. Plant Biol.* **2012**, *63*, 381–407. [CrossRef] [PubMed]
41. Franck, C.M.; Westermann, J.; Boisson-Dernier, A. Plant malectin-like receptor kinases: From cell wall integrity to immunity and beyond. *Annu. Rev. Plant Biol.* **2018**, *69*, 301–328. [CrossRef] [PubMed]
42. Lombard, V.; Golaconda Ramulu, H.; Drula, E.; Coutinho, P.M.; Henrissat, B. The carbohydrate-active enzymes database (CAZy) in 2013. *Nucleic Acids Res.* **2014**, *42*, D490–D495. [CrossRef] [PubMed]
43. Oikawa, A.; Lund, C.H.; Sakuragi, Y.; Scheller, H.V. Golgi-localized enzyme complexes for plant cell wall biosynthesis. *Trends Plant Sci.* **2013**, *18*, 49–58. [CrossRef] [PubMed]
44. Gou, J.Y.; Miller, L.M.; Hou, G.C.; Yu, X.H.; Chen, X.Y.; Liu, C.J. Acetylesterase-mediated deacetylation of pectin impairs cell elongation, pollen germination, and plant reproduction. *Plant Cell* **2012**, *24*, 50–65. [CrossRef] [PubMed]
45. Bourquin, V.; Nishikubo, N.; Abe, H.; Brumer, H.; Denman, S.; Eklund, M.; Christiernin, M.; Teeri, T.T.; Sundberg, B.; Mellerowicz, E.J. Xyloglucan endotransglycosylases have a function during the formation of secondary cell walls of vascular tissues. *Plant Cell* **2002**, *14*, 3073–3088. [CrossRef] [PubMed]
46. Kohorn, B.D.; Kobayashi, M.; Johansen, S.; Friedman, H.P.; Fischer, A.; Byers, N. Wall-associated kinase 1 (WAK1) is crosslinked in endomembranes, and transport to the cell surface requires correct cell-wall synthesis. *J. Cell Sci.* **2006**, *119*, 2282–2290. [CrossRef] [PubMed]
47. Decreux, A.; Messiaen, J. Wall-associated kinase WAK1 interacts with cell wall pectins in a calcium-induced conformation. *Plant Cell Physiol.* **2005**, *46*, 268–278. [CrossRef] [PubMed]
48. Wolf, S.; Greiner, S. Growth control by cell wall pectins. *Protoplasma* **2012**, *249* (Suppl. 2), S169–S175. [CrossRef] [PubMed]
49. Sorieul, M.; Dickson, A.; Hill, S.J.; Pearson, H. Plant fibre: Molecular structure and biomechanical properties, of a complex living material, influencing its deconstruction towards a biobased composite. *Materials* **2016**, *9*, 618. [CrossRef] [PubMed]
50. Griffiths, J.S.; Tsai, A.Y.; Xue, H.; Voiniciuc, C.; Sola, K.; Seifert, G.J.; Mansfield, S.D.; Haughn, G.W. SALT-OVERLY SENSITIVE5 mediates *Arabidopsis* seed coat mucilage adherence and organization through pectins. *Plant Physiol.* **2014**, *165*, 991–1004. [CrossRef] [PubMed]

51. McCartney, L.; Steele-King, C.G.; Jordan, E.; Knox, J.P. Cell wall pectic (1→4)-β-D-galactan marks the acceleration of cell elongation in the *Arabidopsis* seedling root meristem. *Plant J.* **2003**, *33*, 447–454. [CrossRef] [PubMed]
52. Harholt, J.; Suttangkakul, A.; Vibe Scheller, H. Biosynthesis of pectin. *Plant Physiol.* **2010**, *153*, 384–395. [CrossRef] [PubMed]
53. Turbant, A.; Fournet, F.; Lequart, M.; Zabijak, L.; Pageau, K.; Bouton, S.; Van Wuytswinkel, O. Pme58 plays a role in pectin distribution during seed coat mucilage extrusion through homogalacturonan modification. *J. Exp. Bot.* **2016**, *67*, 2177–2190. [CrossRef] [PubMed]
54. Jiang, L.; Yang, S.L.; Xie, L.F.; Puah, C.S.; Zhang, X.Q.; Yang, W.C.; Sundaresan, V.; Ye, D. Vanguard1 encodes a pectin methylesterase that enhances pollen tube growth in the *Arabidopsis* style and transmitting tract. *Plant Cell* **2005**, *17*, 584–596. [CrossRef] [PubMed]
55. Etchells, J.P.; Moore, L.; Jiang, W.Z.; Prescott, H.; Capper, R.; Saunders, N.J.; Bhatt, A.M.; Dickinson, H.G. A role for *BELLRINGER* in cell wall development is supported by loss-of-function phenotypes. *BMC Plant Biol.* **2012**, *12*, 212. [CrossRef] [PubMed]
56. Peaucelle, A.; Braybrook, S.A.; Le Guillou, L.; Bron, E.; Kuhlemeier, C.; Hofte, H. Pectin-induced changes in cell wall mechanics underlie organ initiation in *Arabidopsis*. *Curr. Biol.* **2011**, *21*, 1720–1726. [CrossRef] [PubMed]
57. Xiong, J.; Yang, Y.; Fu, G.; Tao, L. Novel roles of hydrogen peroxide (H_2O_2) in regulating pectin synthesis and demethylesterification in the cell wall of rice (*Oryza sativa*) root tips. *New Phytol.* **2015**, *206*, 118–126. [CrossRef] [PubMed]
58. Lionetti, V.; Raiola, A.; Camardella, L.; Giovane, A.; Obel, N.; Pauly, M.; Favaron, F.; Cervone, F.; Bellincampi, D. Overexpression of pectin methylesterase inhibitors in *Arabidopsis* restricts fungal infection by *Botrytis cinerea*. *Plant Physiol.* **2007**, *143*, 1871–1880. [CrossRef] [PubMed]
59. Daum, G.; Medzihradszky, A.; Suzaki, T.; Lohmann, J.U. A mechanistic framework for noncell autonomous stem cell induction in *Arabidopsis*. *Proc. Natl. Acad. Sci. USA* **2014**, *111*, 14619–14624. [CrossRef] [PubMed]
60. Vaten, A.; Dettmer, J.; Wu, S.; Stierhof, Y.D.; Miyashima, S.; Yadav, S.R.; Roberts, C.J.; Campilho, A.; Bulone, V.; Lichtenberger, R.; et al. Callose biosynthesis regulates symplastic trafficking during root development. *Dev. Cell* **2011**, *21*, 1144–1155. [CrossRef] [PubMed]
61. Lucas, W.J.; Bouché-Pillon, S.; Jackson, D.P.; Nguyen, L.; Baker, L.; Ding, B.; Hake, S. Selective trafficking of KNOTTED1 homeodomain protein and its mRNA through plasmodesmata. *Science* **1995**, *270*, 1980–1983. [CrossRef] [PubMed]
62. Knauer, S.; Holt, A.L.; Rubio-Somoza, I.; Tucker, E.J.; Hinze, A.; Pisch, M.; Javelle, M.; Timmermans, M.C.; Tucker, M.R.; Laux, T. A protodermal miR394 signal defines a region of stem cell competence in the *Arabidopsis* shoot meristem. *Dev. Cell* **2013**, *24*, 125–132. [CrossRef] [PubMed]
63. Molnar, A.; Melnyk, C.; Baulcombe, D.C. Silencing signals in plants: A long journey for small rnas. *Genome Biol.* **2011**, *12*, 215. [CrossRef] [PubMed]
64. Taochy, C.; Gursanscky, N.R.; Cao, J.; Fletcher, S.J.; Dressel, U.; Mitter, N.; Tucker, M.R.; Koltunow, A.M.G.; Bowman, J.L.; Vaucheret, H.; Carroll, B.J. A genetic screen for impaired systemic RNAi highlights the crucial role of *Dicer-like 2*. *Plant Physiol.* **2017**, *175*, 1424–1437. [CrossRef] [PubMed]
65. Kohorn, B.D.; Johansen, S.; Shishido, A.; Todorova, T.; Martinez, R.; Defeo, E.; Obregon, P. Pectin activation of MAP kinase and gene expression is WAK2 dependent. *Plant J.* **2009**, *60*, 974–982. [CrossRef] [PubMed]
66. Kohorn, B.D.; Kohorn, S.L.; Saba, N.J.; Martinez, V.M. Requirement for pectin methyl esterase and preference for fragmented over native pectins for wall-associated kinase-activated, EDS1/PAD4-dependent stress response in *Arabidopsis*. *J. Biol. Chem.* **2014**, *289*, 18978–18986. [CrossRef] [PubMed]
67. Saintenac, C.; Lee, W.S.; Cambon, F.; Rudd, J.J.; King, R.C.; Marande, W.; Powers, S.J.; Berges, H.; Phillips, A.L.; Uauy, C.; et al. Wheat receptor-kinase-like protein STB6 controls gene-for-gene resistance to fungal pathogen *Zymoseptoria tritici*. *Nat. Genet.* **2018**, *50*, 368–374. [CrossRef] [PubMed]
68. Zhang, N.; Zhang, B.; Zuo, W.; Xing, Y.; Konlasuk, S.; Tan, G.; Zhang, Q.; Ye, J.; Xu, M. Cytological and molecular characterization of *ZmWAK*-mediated head-smut resistance in maize. *Mol. Plant Microbe Interact.* **2017**, *30*, 455–465. [CrossRef] [PubMed]
69. Wagner, T.A.; Kohorn, B.D. Wall-associated kinases are expressed throughout plant development and are required for cell expansion. *Plant Cell* **2001**, *13*, 303–318. [CrossRef] [PubMed]

70. Schoenaers, S.; Balcerowicz, D.; Breen, G.; Hill, K.; Zdanio, M.; Mouille, G.; Holman, T.J.; Oh, J.; Wilson, M.H.; Nikonorova, N.; et al. The auxin-regulated CrRLK1L kinase *ERULUS* controls cell wall composition during root hair tip growth. *Curr. Biol.* **2018**, *28*, 722–732. [CrossRef] [PubMed]
71. Kessler, S.A.; Shimosato-Asano, H.; Keinath, N.F.; Wuest, S.E.; Ingram, G.; Panstruga, R.; Grossniklaus, U. Conserved molecular components for pollen tube reception and fungal invasion. *Science* **2010**, *330*, 968–971. [CrossRef] [PubMed]
72. Lin, W.; Tang, W.; Anderson, C.; Yang, Z. FERONIA's sensing of cell wall pectin activates ROP GTPase signaling in *Arabidopsis*. *bioRxiv* **2018**. [CrossRef]
73. Faria-Blanc, N.; Mortimer, J.C.; Dupree, P. A transcriptomic analysis of xylan mutants does not support the existence of a secondary cell wall integrity system in *Arabidopsis*. *Front. Plant Sci.* **2018**, *9*, 384. [CrossRef] [PubMed]
74. Ferrari, S.; Savatin, D.V.; Sicilia, F.; Gramegna, G.; Cervone, F.; Lorenzo, G.D. Oligogalacturonides: Plant damage-associated molecular patterns and regulators of growth and development. *Front. Plant Sci.* **2013**, *4*, 49. [CrossRef] [PubMed]
75. Branca, C.; Lorenzo, G.D.; Cervone, F. Competitive inhibition of the auxin-induced elongation by α-D-oligogalacturonides in pea stem segments. *Physiol. Plant.* **1988**, *72*, 499–504. [CrossRef]
76. Gramegna, G.; Modesti, V.; Savatin, D.V.; Sicilia, F.; Cervone, F.; De Lorenzo, G. GRP-3 and KAPP, encoding interactors of WAK1, negatively affect defense responses induced by oligogalacturonides and local response to wounding. *J. Exp. Bot.* **2016**, *67*, 1715–1729. [CrossRef] [PubMed]
77. Balasubramanian, V.; Vashisht, D.; Cletus, J.; Sakthivel, N. Plant β-1,3-glucanases: Their biological functions and transgenic expression against phytopathogenic fungi. *Biotechnol. Lett.* **2012**, *34*, 1983–1990. [CrossRef] [PubMed]
78. van der Schoot, C.; Rinne, P.L.H. Dormancy cycling at the shoot apical meristem: Transitioning between self-organization and self-arrest. *Plant Sci.* **2011**, *180*, 120–131. [CrossRef] [PubMed]
79. Sevilem, I.; Miyashima, S.; Helariutta, Y. Cell-to-cell communication via plasmodesmata in vascular plants. *Cell Adhes. Migr.* **2013**, *7*, 27–32. [CrossRef] [PubMed]
80. Kitagawa, M.; Jackson, D. Plasmodesmata-mediated cell-to-cell communication in the shoot apical meristem: How stem cells talk. *Plants* **2017**, *6*, 12. [CrossRef] [PubMed]
81. Amsbury, S.; Kirk, P.; Benitez-Alfonso, Y. Emerging models on the regulation of intercellular transport by plasmodesmata-associated callose. *J. Exp. Bot.* **2017**, *69*, 105–115. [CrossRef] [PubMed]
82. Benitez-Alfonso, Y.; Faulkner, C.; Pendle, A.; Miyashima, S.; Helariutta, Y.; Maule, A. Symplastic intercellular connectivity regulates lateral root patterning. *Dev. Cell* **2013**, *26*, 136–147. [CrossRef] [PubMed]
83. Faulkner, C.; Akman, O.E.; Bell, K.; Jeffree, C.; Oparka, K. Peeking into pit fields: A multiple twinning model of secondary plasmodesmata formation in tobacco. *Plant Cell* **2008**, *20*, 1504–1518. [CrossRef] [PubMed]
84. Fernandez-Calvino, L.; Faulkner, C.; Walshaw, J.; Saalbach, G.; Bayer, E.; Benitez-Alfonso, Y.; Maule, A. *Arabidopsis* plasmodesmal proteome. *PLoS ONE* **2011**, *6*, e18880. [CrossRef] [PubMed]
85. Knox, J.P.; Benitez-Alfonso, Y. Roles and regulation of plant cell walls surrounding plasmodesmata. *Curr. Opin. Plant Biol.* **2014**, *22*, 93–100. [CrossRef] [PubMed]
86. Stavolone, L.; Lionetti, V. Extracellular matrix in plants and animals: Hooks and locks for viruses. *Front. Microbiol* **2017**, *8*, 1760. [CrossRef] [PubMed]
87. Doxey, A.C.; Yaish, M.W.; Moffatt, B.A.; Griffith, M.; McConkey, B.J. Functional divergence in the *Arabidopsis* β-1,3-glucanase gene family inferred by phylogenetic reconstruction of expression states. *Mol. Biol. Evol.* **2007**, *24*, 1045–1055. [CrossRef] [PubMed]
88. Maule, A.; Faulkner, C.; Benitez-Alfonso, Y. Plasmodesmata "in communicado". *Front. Plant Sci.* **2012**, *3*, 30. [CrossRef] [PubMed]
89. Bell, P.R. Megaspore abortion: A consequence of selective apoptosis. *Int. J. Plant Sci.* **1996**, *157*, 1–7. [CrossRef]
90. Bucciaglia, P.A.; Zimmermann, E.; Smith, A.G. Functional analysis of a β-1,3-glucanase gene (*Tag1*) with anther-specific RNA and protein accumulation using antisense RNA inhibition. *J. Plant Physiol.* **2003**, *160*, 1367–1373. [CrossRef] [PubMed]
91. Tucker, M.R.; Koltunow, A.M. Traffic monitors at the cell periphery: The role of cell walls during early female reproductive cell differentiation in plants. *Curr. Opin. Plant Biol.* **2014**, *17*, 137–145. [CrossRef] [PubMed]

92. Gisel, A.; Barella, S.; Hempel, F.D.; Zambryski, P.C. Temporal and spatial regulation of symplastic trafficking during development in *Arabidopsis thaliana* apices. *Development* **1999**, *126*, 1879–1889. [PubMed]
93. Kim, I.; Kobayashi, K.; Cho, E.; Zambryski, P.C. Subdomains for transport via plasmodesmata corresponding to the apical-basal axis are established during *Arabidopsis* embryogenesis. *Proc. Natl. Acad. Sci. USA* **2005**, *102*, 11945–11950. [CrossRef] [PubMed]
94. Melida, H.; Sopena-Torres, S.; Bacete, L.; Garrido-Arandia, M.; Jorda, L.; Lopez, G.; Munoz-Barrios, A.; Pacios, L.F.; Molina, A. Non-branched β-1,3-glucan oligosaccharides trigger immune responses in *Arabidopsis*. *Plant J.* **2018**, *93*, 34–49. [CrossRef] [PubMed]
95. Burton, R.A.; Fincher, G.B. (1, 3;1, 4)-β-D-glucans in cell walls of the *Poaceae*, lower plants, and fungi: A tale of two linkages. *Mol. Plant* **2009**, *2*, 873–882. [CrossRef] [PubMed]
96. Little, A.; Schwerdt, J.G.; Shirley, N.J.; Khor, S.-F.; Neumann, K.; O'Donovan, L.A.; Lahnstein, J.; Collins, H.C.; Henderson, M.; Fincher, G.B.; et al. Revised phylogeny of the cellulose synthase gene superfamily: New insights into cell wall evolution. *Plant Physiol.* **2018**. [CrossRef] [PubMed]
97. Burton, R.A.; Collins, H.M.; Kibble, N.A.; Smith, J.A.; Shirley, N.J.; Jobling, S.A.; Henderson, M.; Singh, R.R.; Pettolino, F.; Wilson, S.M.; et al. Over-expression of specific *HvCslF* cellulose synthase-like genes in transgenic barley increases the levels of cell wall (1, 3;1, 4)-β-D-glucans and alters their fine structure. *Plant Biotechnol. J.* **2011**, *9*, 117–135. [CrossRef] [PubMed]
98. Nemeth, C.; Freeman, J.; Jones, H.D.; Sparks, C.; Pellny, T.K.; Wilkinson, M.D.; Dunwell, J.; Andersson, A.A.M.; Aman, P.; Guillon, F.; et al. Down-regulation of the *CslF6* gene results in decreased (1,3;1,4)-β-D-glucan in endosperm of wheat. *Plant Physiol.* **2010**, *152*, 1209–1218. [CrossRef] [PubMed]
99. Vega-Sanchez, M.E.; Verhertbruggen, Y.; Christensen, U.; Chen, X.W.; Sharma, V.; Varanasi, P.; Jobling, S.A.; Talbot, M.; White, R.G.; Joo, M.; et al. Loss of cellulose synthase-like f6 function affects mixed-linkage glucan deposition, cell wall mechanical properties, and defense responses in vegetative tissues of rice. *Plant Physiol.* **2012**, *159*, 56–69. [CrossRef] [PubMed]
100. Taketa, S.; Yuo, T.; Tonooka, T.; Tsumuraya, Y.; Inagaki, Y.; Haruyama, N.; Larroque, O.; Jobling, S.A. Functional characterization of barley betaglucanless mutants demonstrates a unique role for *CslF6* in (1,3;1,4)-β-D-glucan biosynthesis. *J. Exp. Bot.* **2012**, *63*, 381–392. [CrossRef] [PubMed]
101. Burton, R.A.; Jobling, S.A.; Harvey, A.J.; Shirley, N.J.; Mather, D.E.; Bacic, A.; Fincher, G.B. The genetics and transcriptional profiles of the cellulose synthase-like *HvCslF* gene family in barley. *Plant Physiol.* **2008**, *146*, 1821–1833. [CrossRef] [PubMed]
102. Zabotina, O. Xyloglucan and its biosynthesis. *Front. Plant Sci.* **2012**, *3*, 134. [CrossRef] [PubMed]
103. Zabotina, O.A.; Avci, U.; Cavalier, D.; Pattathil, S.; Chou, Y.H.; Eberhard, S.; Danhof, L.; Keegstra, K.; Hahn, M.G. Mutations in multiple *XXT* genes of *Arabidopsis* reveal the complexity of xyloglucan biosynthesis. *Plant Physiol.* **2012**, *159*, 1367–1384. [CrossRef] [PubMed]
104. Kong, Y.; Pena, M.J.; Renna, L.; Avci, U.; Pattathil, S.; Tuomivaara, S.T.; Li, X.; Reiter, W.D.; Brandizzi, F.; Hahn, M.G.; et al. Galactose-depleted xyloglucan is dysfunctional and leads to dwarfism in *Arabidopsis*. *Plant Physiol.* **2015**, *167*, 1296–1306. [CrossRef] [PubMed]
105. Schröder, R.; Atkinson, R.G.; Redgwell, R.J. Re-interpreting the role of endo-β-mannanases as mannan endotransglycosylase/hydrolases in the plant cell wall. *Ann. Bot.* **2009**, *104*, 197–204. [CrossRef] [PubMed]
106. Goubet, F.; Barton, C.J.; Mortimer, J.C.; Yu, X.; Zhang, Z.; Miles, G.P.; Richens, J.; Liepman, A.H.; Seffen, K.; Dupree, P. Cell wall glucomannan in *Arabidopsis* is synthesised by *CslA* glycosyltransferases, and influences the progression of embryogenesis. *Plant J.* **2009**, *60*, 527–538. [CrossRef] [PubMed]
107. Rodriguez-Gacio Mdel, C.; Iglesias-Fernandez, R.; Carbonero, P.; Matilla, A.J. Softening-up mannan-rich cell walls. *J. Exp. Bot.* **2012**, *63*, 3976–3988. [CrossRef] [PubMed]
108. Ueda, M.; Zhang, Z.; Laux, T. Transcriptional activation of *Arabidopsis* axis patterning genes *WOX8/9* links zygote polarity to embryo development. *Dev. Cell* **2011**, *20*, 264–270. [CrossRef] [PubMed]
109. Mallory, A.C.; Hinze, A.; Tucker, M.R.; Bouche, N.; Gasciolli, V.; Elmayan, T.; Lauressergues, D.; Jauvion, V.; Vaucheret, H.; Laux, T. Redundant and specific roles of the ARGONAUTEe proteins AGO1 and ZLL in development and small RNA-directed gene silencing. *PLoS Genet.* **2009**, *5*, e1000646. [CrossRef] [PubMed]
110. Bohmert, K.; Camus, I.; Bellini, C.; Bouchez, D.; Caboche, M.; Benning, C. *AGO1* defines a novel locus of *Arabidopsis* controlling leaf development. *EMBO J.* **1998**, *17*, 170–180. [CrossRef] [PubMed]
111. Schröder, R.; Wegrzyn, T.F.; Sharma, N.N.; Atkinson, R.G. LeMAN4 endo-β-mannanase from ripe tomato fruit can act as a mannan transglycosylase or hydrolase. *Planta* **2006**, *224*, 1091–1102. [CrossRef] [PubMed]

112. Han, Y.; Ban, Q.; Hou, Y.; Meng, K.; Suo, J.; Rao, J. Isolation and characterization of two persimmon xyloglucan endotransglycosylase/hydrolase (*XTH*) genes that have divergent functions in cell wall modification and fruit postharvest softening. *Front. Plant Sci.* **2016**, *7*, 624. [CrossRef] [PubMed]
113. Muñoz-Bertomeu, J.; Miedes, E.; Lorences, E.P. Expression of xyloglucan endotransglucosylase/hydrolase (*XTH*) genes and XET activity in ethylene treated apple and tomato fruits. *J. Plant Physiol.* **2013**, *170*, 1194–1201. [CrossRef] [PubMed]
114. Knox, J.P. The use of antibodies to study the architecture and developmental regulation of plant cell walls. *Int. Rev. Cytol.* **1997**, *171*, 79–120. [PubMed]
115. Pedersen, H.L.; Fangel, J.U.; McCleary, B.; Ruzanski, C.; Rydahl, M.G.; Ralet, M.C.; Farkas, V.; von Schantz, L.; Marcus, S.E.; Andersen, M.C.; et al. Versatile high resolution oligosaccharide microarrays for plant glycobiology and cell wall research. *J. Biol. Chem.* **2012**, *287*, 39429–39438. [CrossRef] [PubMed]
116. Gierlinger, N. New insights into plant cell walls by vibrational microspectroscopy. *Appl. Spectrosc. Rev.* **2017**. [CrossRef]
117. Birnbaum, K.; Shasha, D.E.; Wang, J.Y.; Jung, J.W.; Lambert, G.M.; Galbraith, D.W.; Benfey, P.N. A gene expression map of the *Arabidopsis* root. *Science* **2003**, *302*, 1956–1960. [CrossRef] [PubMed]
118. Brady, S.M.; Orlando, D.A.; Lee, J.-Y.; Wang, J.Y.; Koch, J.; Dinneny, J.R.; Mace, D.; Ohler, U.; Benfey, P.N. A high-resolution root spatiotemporal map reveals dominant expression patterns. *Science* **2007**, *318*, 801–806. [CrossRef] [PubMed]
119. Yadav, R.K.; Girke, T.; Pasala, S.; Xie, M.; Reddy, G.V. Gene expression map of the *Arabidopsis* shoot apical meristem stem cell niche. *Proc. Natl. Acad. Sci. USA* **2009**, *106*, 4941–4946. [CrossRef] [PubMed]
120. Tucker, M.R.; Laux, T. Connecting the paths in plant stem cell regulation. *Trends Cell Biol.* **2007**, *17*, 403–410. [CrossRef] [PubMed]
121. Nguema-Ona, E.; Coimbra, S.; Vicre-Gibouin, M.; Mollet, J.C.; Driouich, A. Arabinogalactan proteins in root and pollen-tube cells: Distribution and functional aspects. *Ann. Bot.* **2012**, *110*, 383–404. [CrossRef] [PubMed]
122. Lee, K.J.; Sakata, Y.; Mau, S.L.; Pettolino, F.; Bacic, A.; Quatrano, R.S.; Knight, C.D.; Knox, J.P. Arabinogalactan proteins are required for apical cell extension in the moss physcomitrella patens. *Plant Cell* **2005**, *17*, 3051–3065. [CrossRef] [PubMed]
123. Somssich, M.; Khan, G.A.; Persson, S. Cell wall heterogeneity in root development of *Arabidopsis*. *Front. Plant Sci.* **2016**, *7*, 1242. [CrossRef] [PubMed]
124. Yang, W.; Schuster, C.; Beahan, C.T.; Charoensawan, V.; Peaucelle, A.; Bacic, A.; Doblin, M.S.; Wightman, R.; Meyerowitz, E.M. Regulation of meristem morphogenesis by cell wall synthases in *Arabidopsis*. *Curr. Biol.* **2016**, *26*, 1404–1415. [CrossRef] [PubMed]
125. Tucker, M.R.; Ma, C.; Phan, J.; Neumann, K.; Shirley, N.J.; Hahn, M.G.; Cozzolino, D.; Burton, R.A. Dissecting the genetic basis for seed coat mucilage heteroxylan biosynthesis in *Plantago ovata* using gamma irradiation and infrared spectroscopy. *Front. Plant Sci.* **2017**, *8*, 326. [CrossRef] [PubMed]
126. Phan, J.L.; Tucker, M.R.; Khor, S.F.; Shirley, N.; Lahnstein, J.; Beahan, C.; Bacic, A.; Burton, R.A. Differences in glycosyltransferase family 61 accompany variation in seed coat mucilage composition in *Plantago* spp. *J. Exp. Bot.* **2016**, *67*, 6481–6495. [CrossRef] [PubMed]
127. Derba-Maceluch, M.; Awano, T.; Takahashi, J.; Lucenius, J.; Ratke, C.; Kontro, I.; Busse-Wicher, M.; Kosik, O.; Tanaka, R.; Winzéll, A.; et al. Suppression of xylan endotransglycosylase *PtxtXyn10A* affects cellulose microfibril angle in secondary wall in aspen wood. *New Phytol.* **2015**, *205*, 666–681. [CrossRef] [PubMed]

Appendix II

Differences in hydrolytic enzyme activity accompany natural variation in mature aleurone morphology in barley (Hordeum vulgare L.)

www.nature.com/scientificreports

SCIENTIFIC REPORTS

Differences in hydrolytic enzyme activity accompany natural variation in mature aleurone morphology in barley (*Hordeum vulgare* L.)

Matthew K. Aubert [1,2], Stewart Coventry[1], Neil J. Shirley[1,2], Natalie S. Betts[1], Tobias Würschum [3], Rachel A. Burton[2] & Matthew R. Tucker [1]

The aleurone is a critical component of the cereal seed and is located at the periphery of the starchy endosperm. During germination, the aleurone is responsible for releasing hydrolytic enzymes that degrade cell wall polysaccharides and starch granules, which is a key requirement for barley malt production. Inter- and intra-species differences in aleurone layer number have been identified in the cereals but the significance of this variation during seed development and germination remains unclear. In this study, natural variation in mature aleurone features was examined in a panel of 33 *Hordeum vulgare* (barley) genotypes. Differences were identified in the number of aleurone cell layers, the transverse thickness of the aleurone and the proportion of aleurone relative to starchy endosperm.

In addition, variation was identified in the activity of hydrolytic enzymes that are associated with germination. Notably, activity of the free fraction of β-amylase (BMY), but not the bound fraction, was increased at grain maturity in barley varieties possessing more aleurone. Laser capture microdissection (LCM) and transcriptional profiling confirmed that *HvBMY1* is the most abundant *BMY* gene in developing grain and accumulates in the aleurone during early stages of grain fill. The results reveal a link between molecular pathways influencing early aleurone development and increased levels of free β-amylase enzyme, potentially highlighting the aleurone as a repository of free β-amylase at grain maturity.

Barley (*Hordeum vulgare* L.) is recorded as one of the first agricultural crops to be domesticated[1] and is a major food source in both Asia and northern Africa. The highest economic value for the crop is in its use as a malting grain for whisky and beer production[2]. Extensive worldwide cultivation has led to the development and identification of over 460,000 barley accessions, including cultivars, landraces, breeding lines and wild *Hordeum* relatives[3]. Coupled with a diploid sequenced genome[4,5], these genetic resources provide excellent opportunities to study the fundamental details of barley growth and development, with potential to tailor barley varieties for specific end uses.

Barley grain contains many key nutrients, antioxidants and dietary fibres that benefit the human diet[6–8]. Most of these nutrients accumulate in the endosperm, a filial tissue that supports embryonic growth in addition to providing physical protection during seed development[9]. The endosperm consists of three main cell types - the endosperm transfer cells, starchy endosperm and aleurone layer - each of which confer different biological functions during grain maturation and seed germination. Endosperm development begins after fertilisation of the central cell within the embryo sac[10], when successive nuclear divisions without cytokinesis lead to the formation of a nuclear syncytium. This mass of nuclei begins to cellularise at the embryo sac periphery at approximately 5 days post anthesis (DPA). The aleurone first appears as a single layer at approximately 6–9 DPA and divides to

[1]School of Agriculture, Food and Wine, Waite Research Institute, The University of Adelaide, Glen Osmond, SA, Australia. [2]Australian Research Council Centre of Excellence in Plant Cell Walls, the University of Adelaide, Adelaide, Australia. [3]State Plant Breeding Institute, University of Hohenheim, Stuttgart, Germany. Correspondence and requests for materials should be addressed to M.R.T. (email: matthew.tucker@adelaide.edu.au)

form multiple layers by around 12–15 DPA. At maturity, the aleurone layers separate the mass of inner starchy endosperm from outer maternal layers, which include the nucellar epidermis, integuments and pericarp. The aleurone cells display a cuboid shape with reinforced cell walls[11] that are enriched in phenolic acids and polysaccharides such as arabinoxylan[12–14]. During germination, the embryo releases gibberellic acid (GA), which translocates to the aleurone where it induces the transcription of genes encoding hydrolytic enzymes[15]. Enzymes, such as 1,3;1,4-β-glucanase (β-glucanase), α-amylase and β-amylase, are released to catalyse the breakdown of cell wall polysaccharides and starchy energy reserves that are essential for germination and the production of malt for brewing[16]. β-glucanase hydrolyses 1,3;1,4-β-glucan, which is the predominant cell wall polysaccharide present in barley endosperm, α-amylase cleaves internal amylose and amylopectin residues, and the β-amylase exo-hydrolase liberates maltose from the non-reducing end of starch molecules[16]. While α-amylase appears to be transcribed and translated *de novo* during germination, β-amylase is transcribed and translated during grain development[17]. Some of the β-amylase enzyme is present in a free form, while most is present in an inactive bound form, purportedly linked through protein bridges to starch molecules[18–20].

Seeds from mutants showing defects in aleurone development are often shrunken or misshapen[21]. However, natural differences in aleurone layer number and structure have been observed between cereal species. Cereal grains from species such as maize (*Zea mays* L.) and wheat (*Triticum aestivum* L.) have a single layer of aleurone cells while the barley aleurone is multilayered[22]. Intra-species variation has been found between barley cultivars, and several QTL were identified in an Erhard Frederichen×Criolla Negra population that influence the number of aleurone layers[23]. Genes such as *naked endosperm1*, *supernumerary aleurone layer1*, *defective kernel1* and *crinkly4* influence aleurone development in maize[24–27], but whether similar genes influence variation in barley aleurone development has yet to be reported. Moreover, the significance of having more or fewer aleurone layers on seed development or germination, particularly in the context of barley, remains unclear.

In this study, 33 barley genotypes were surveyed to identify natural variation in aleurone phenotypes. A method was developed to measure features of the aleurone in mature grain based on UV-autofluoresence of the thick aleurone walls, and to assess correlations with wholegrain traits. Selected genotypes were examined in greater detail to assess the relationship between the aleurone and hydrolytic enzyme activities. Finally, transcriptional profiling of fresh and laser micro-dissected grain tissues was used to ascertain when and where key germination-related genes are transcribed during grain development.

Materials and Methods

Plant material. A University of Adelaide (UA) barley diversity panel of 33 genotypes was grown in the field at Charlick, SA, in 2013. A partially overlapping set of genotypes was grown at Gooloogong, NSW, in 2015 and grain was obtained from the National Variety Trials (NVT; www.nvtonline.com.au). The UA panel was chosen to reflect a diverse array of genetic stocks and row-types (Table S1), and consists of both 2-row (n=30) and 6-row (n=3) spring genotypes and breeding lines. Grain samples were sieved using a 2.5 mm screen to remove broken grain, long awns and foreign material prior to analysis. The majority of intact grain are retained using this method, allowing analyses to be performed on grains of varying sizes and shapes.

Grain sectioning and imaging. Mature grain were cut into quarters and fixed overnight in TEM fix (0.25% glutaraldehyde, 4% paraformaldehyde, 4% sucrose in phosphate buffered saline). Samples were rinsed with phosphate buffered saline (3 ×4 hour washes) and then dehydrated in an ethanol series (3 ×8 hours in 70%, 80%, 90%, 95% and 100%). This was followed by an overnight infiltration in a 50:50 mix of 100% ethanol/LR White resin, and 3 changes of pure LR White resin for 8 hours each. Infiltrated specimens were transferred to gelatin capsules in fresh LR White resin, covered with lids and polymerized in a 60 °C oven for at least 48 hours. Sections were prepared at a thickness of 1 μm using a Reichert Ultracut ultramicrotome (Leica, Wetzlar, Germany). For the anatomical study of aleurone cells, sections were stained with 0.01% (w/v) Toluidine Blue and viewed using brightfield microscopy, or 0.001% (w/v) Calcofluor White and viewed using Zeiss Filter set 47 (BP 436/20, FT 455, BP 480/40; blue staining in Fig. S3) and Filter set 46 (BP 500/20, FT 515, BP 535/30; false coloured red in Fig. S3) on a Zeiss M2 AxioImager equipped with DIC optics and an Apotome.2 (Zeiss, Germany).

To observe the aleurone in fresh samples, mature grain were bisected by hand (transversely) using a reinforced single-edge razor blade (ProSciTech, Australia) and adhered to a microscopy slide using Blu-Tack® (Bostick, Australia) with the flat midpoint of the grain facing upwards. Between 3 and 10 grain from each cultivar were imaged using a Zeiss M2 AxioImager with an attached AxioCam MrM camera (Zeiss, Germany). Zeiss Filter set 46 (BP 500/20, FT 515, BP 535/30) was used to view pericarp and husk autofluorescence (false coloured red in Fig. 1) and Filter set 49 (G365, FT395, BP445/50) was used to view aleurone wall autofluoresence (false coloured yellow in Fig. 1). Images were processed using ZEN 2012 software (Zeiss, Germany).

Grain measurements were also recorded using ZEN 2012 software (Zeiss, Germany; Fig. S1). Transverse endosperm area was measured by tracing the outline of whole endosperm, while aleurone area was calculated by subtracting the starchy endosperm area from the total endosperm area. Aleurone proportion was measured by calculating the aleurone area as a percentage of the total transverse endosperm area. Aleurone layer number was recorded as an average where, in each section of barley grain, a maximum and minimum layer number was recorded at dorsal, left and right positions. Similarly, aleurone width was measured as the distance from the edge of the endosperm to the innermost autofluorescent aleurone cell wall.

Wholegrain phenotypic analysis. Barley grain weight and dimensions were determined using a SeedCount™ SC4 (Seed Count Australasia, Condell Park, Australia), following manufacturer's instructions. Single grain hardness, moisture content and diameter of 300 grain were analysed using a Single Kernel Characterisation System, SKCS 4100 (SKCS; Perten Instruments, Springfield, IL), following the manufacturer's instructions.

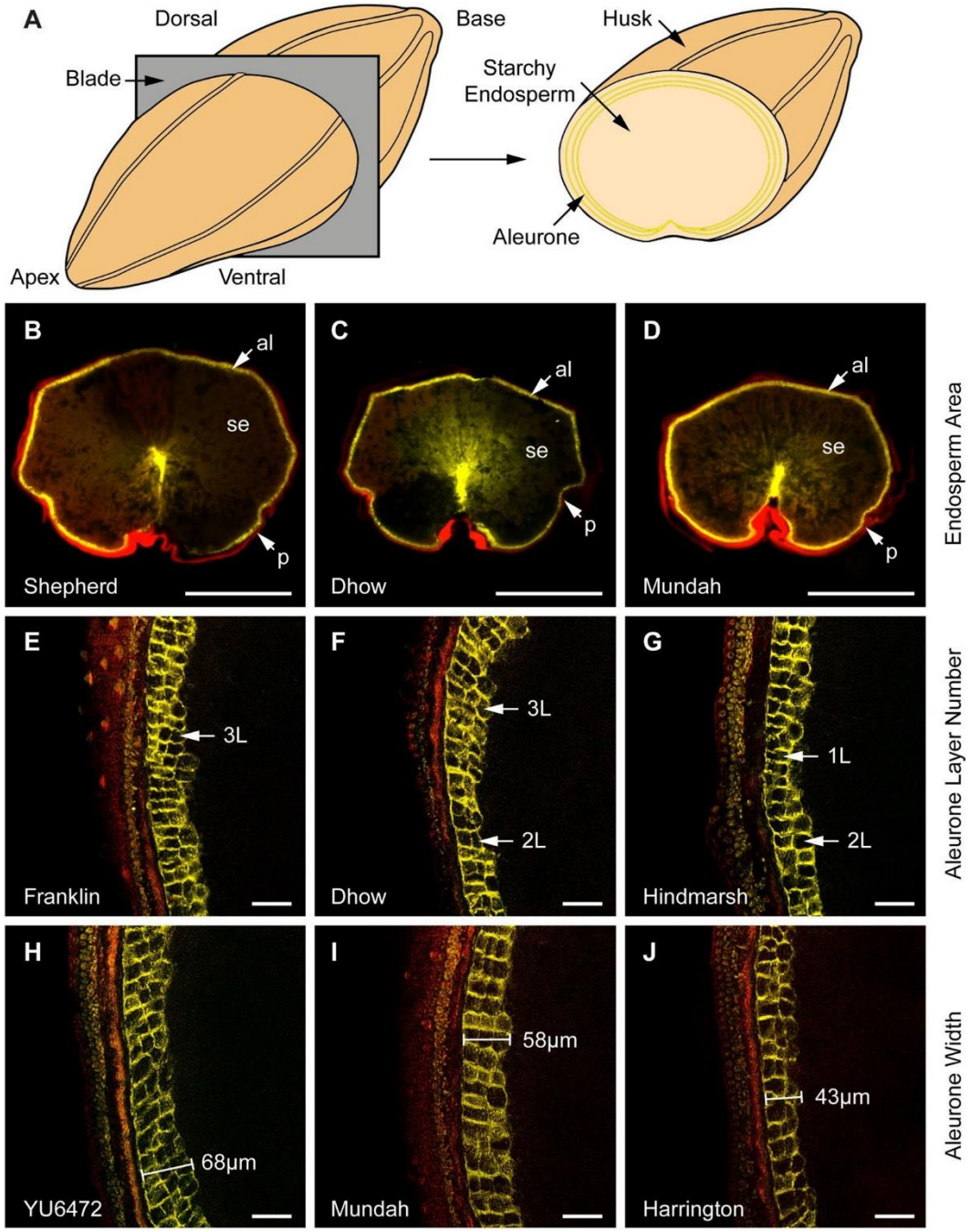

Figure 1. Representation of the transverse sectioning process used to image barley aleurone tissue by fluorescent microscopy. (**A**) Schematic representation of barley grain sectioning prior to microscopy. The different tissue layers are indicated. (**B–D**) Whole grain transverse sections viewed at 1× magnification using Zeiss Filter sets 46 (false-coloured red) and 49 (DAPI; false-coloured yellow). The panels show grain exhibiting differences in transverse starchy endosperm area in decreasing order. The pericarp/husk (p), starchy endosperm (se) and aleurone (al) tissues are indicated. Scale bar=1 mm. (**E–G**) Magnified views of the aleurone layers at 20× magnification using a Zeiss Apotome.2. Panels are arranged in decreasing order based on the average number of aleurone layers. Stacks of 3, 2 and 1 aleurone cell layers (L) are indicated. Scale bar=50 µm. (**H–J**) Examples of grain showing differences in aleurone width at 20× magnification, arranged in decreasing order. Scale bar=50 µm. Genotypes names are indicated in each panel.

Grain germination and sample preparation for enzyme assays. Grain from selected barley genotypes was placed at 37 °C for two days to remove residual moisture. Dry grains were subsequently sprinkled onto 10 cm diameter No 1. Whatman® filter paper disks (×2), placed in a 10 cm diameter Petri dish and soaked with 4 mL sterilised water. For the germination assay, 70 sample grains were plated alongside 30 control Navigator

grain. For the enzyme assays, 30 sample grains were used alongside 70 sacrificial Sloop and Navigator grains for standards and water saturation balances. The Petri dishes were sealed with Parafilm® (Bemis, USA) then placed in an incubator at 20 °C in the dark for 6, 12, 24, 48 or 96 hours. For the germination assay, plates were removed and scored visually to determine the frequency of grain germination at each time point. For the enzyme assays, grain were removed from the incubator and all 30 germinating grains placed into 10 mL tubes (for each variety) and freeze dried for 96 hours to remove residual moisture. Mature grain and dried germinated grains were ground to flour with a Retsch MM400 Mixer Mill (Retsch GmbH, Haan, Germany).

Hydrolytic enzyme assays. Enzyme assays were performed on both mature grain and dried germinated grain flour, respectively, using downscaled methods (approximately four-fold) from Megazyme (Ireland). The β-Glucanase Assay Kit (K-MBGL)[28], the α-Amylase Assay Kit (K-CERA)[29] and the Betamyl-3; β-Amylase Kit (K-BETA3)[30] were all used following manufacturer's instructions.

Correlation analysis and figure preparation. All correlation and PCA analyses were carried out in RStudio using the 'corrplot' package. (RStudio® , Boston, USA; https://cran.r-project.org/web/packages/corrplot/corrplot.pdf). Selected graphs were prepared in SigmaPlot or Microsoft Excel. Statistical differences were determined using one-way ANOVA followed by the Tukey-Kramer test. Figures were assembled in Adobe Photoshop CS6 and Adobe Illustrator CS6.

RNAseq analysis. Developing grain were collected from *H. vulgare* cv. Sloop plants at 7, 9, 11, 13, 15 and 20 days post anthesis (DPA). The embryo was discarded and all remaining (wholegrain) tissues were snap frozen in liquid nitrogen. At least six grain from three independent plants were collected and pooled to form a single composite sample at each time point. RNA for all samples was extracted using the Spectrum™ Plant Total RNA kit (Sigma-Aldrich, Darmstadt, Germany). Samples were submitted for sequencing using the Illumina Hiseq Platform (AGRF, Australia), and reads were assembled against the most recent barley reference sequence using CLC Genomics[4]. Normalised read counts (transcripts per million; TPM) were determined for each HORVU sequence and used to determine the abundance of each transcript in each sample. For RNAseq analysis of pre-fertilisation stages, developing ovaries (pistils) were harvested from *H. vulgare* cv. Golden Promise at female gametophyte stage 4 (FG4), FG8, FG mature and FG anthesis and processed in a similar manner to that described above. The two different genotypes (Sloop and Golden Promise) were used for historical reasons; we have previously used Golden Promise as a resource for studies of floral organ fertility while Sloop has been used for studies of grain development and seedling growth.

Laser Capture Microdissection and Quantitative PCR. Grain samples from *H. vulgare* cv. Sloop were collected at 11 and 25 DPA, bisected transversely and fixed in ethanol:acetic acid as described previously[31]. Tissues were embedded in butyl methyl methacrylate (BMM) and polymerised at −20 °C under UV light[31,32]. Samples were sectioned to 5 µm using a Leica Ultracut microtome, adhered to Leica PEN membrane slides and dissected using a Leica LMD microscope (Leica, Wetzlar, Germany; Adelaide Microscopy, Adelaide; Fig. S2). Approximately 6–10 sections from three grain were collected from the outer grain layers (predominantly pericarp), aleurone, outer-starchy endosperm (incorporating sub-aleurone and some adjoining starchy cells) and inner starchy endosperm (incorporating starchy endosperm cells and the grain cavity) and stored at −80 °C. Total RNA was isolated using the PicoPure kit (ThermoFisher, Australia) and converted to cDNA using Superscript™ III reverse transcriptase (ThermoFisher, Australia) and oligodT primer with a 2 hour synthesis step at 37 °C. For the 25 DPA samples, RNA was amplified twice using the MessageAmp™ II kit (ThermoFisher, Australia) before converting to cDNA using Superscript III and random hexamers[27]. Multiple control genes were used to normalise samples[33] and primer sequences are included in Table S5.

Results

Sub-epidermal grain features are revealed by autofluorescence microscopy. The aleurone layers and cell structure present at the periphery of the barley endosperm were examined by hand-sectioning (Fig. 1A) and autofluorescence microscopy (Fig. 1B–J). UV-light revealed different types of autofluorescence depending on the filter set and clearly distinguished the pericarp (false coloured red) and aleurone cells (false-coloured yel- low). Hand sections provided sufficient detail to measure transverse features of the aleurone, starchy endosperm and pericarp/husk using a 1× objective (Figs 1B–D and S1), while the number of aleurone layers and aleurone thickness could be determined using a 20×objective (Figs 1E–J and S1). To assess whether these measurements were consistent with those generated by thin sections, mature grain samples from two genotypes showing differences (Golden Promise and Flagship) were embedded in resin and sectioned prior to staining with Calcofluor White. Staining revealed differences between the genotypes, with Flagship tending to show fewer aleurone layers (Fig. S3A) than Golden Promise (Fig. S3B). A similar result was obtained by hand-sectioning (Fig. S3C,D), suggesting that the hand-sectioning method is appropriate to measure differences in aleurone phenotypes

Transverse grain sections were generated for 33 different barley genotypes and significant differences in aleurone phenotypes were identified (Figs 1 and 2, Table S1). Aleurone layer number was not identical around the entire grain periphery, but the average number of layers from three regions (dorsal, left and right) in each grain provided a representative measurement for comparisons between genotypes. The average number of aleurone layers for all genotypes was 2.4±0.2, but showed genotype-dependent variation. Clipper (2.8±0.01; Table S1) and Franklin (2.8±0.01; Fig. 1E, Table S1) typically possessed more aleurone layers, Dhow showed an intermediate number of layers (2.5±0.02; Fig. 1F) and Hindmarsh possessed significantly fewer layers (1.8±0.05; Fig. 1G). Additionally, genotypes differed in regards to aleurone width, which was on average 53.2±6.5 µm. The YU6472 genotype showed a thick aleurone (65.4±6.2 µm; Fig. 1H), Mundah was intermediate (60.4±4.2 µm; Fig. 1I) and Harrington possessed a thinner aleurone (40.6±2.8 µm; Fig. 1J). The variation in each measurement across the

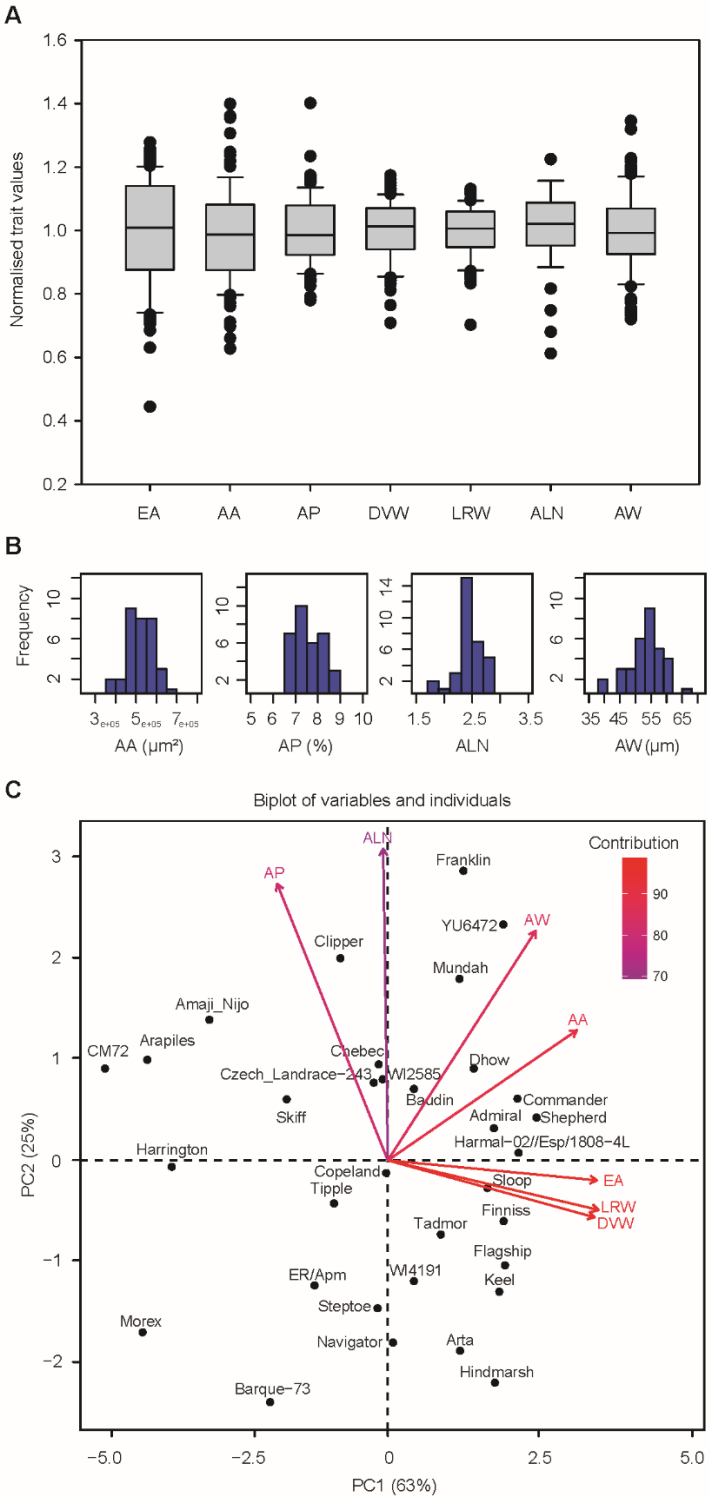

Figure 2. Variation in transverse grain measurements observed across 33 barley genotypes. (**A**) Box plot of normalised data showing the variation in different grain measurements. (**B**) Frequency distribution plots of the four aleurone measurements. (**C**) Principal Component Analysis separates the genotypes based on the seven transverse measurements (variables). EA, endosperm area; AA, aleurone area; AP, aleurone proportion; DVW, grain dorsal-ventral distance; LRW, transverse grain left-right width; ALN, aleurone layer number; AW, aleurone width.

panel was normalised to the average trait value, which was assigned a value of 1 (Fig. 2A). The largest variation was observed in transverse endosperm area, followed by aleurone area, aleurone layer number and aleurone width, whilst aleurone proportion and transverse grain width were less variable (Fig. 2A). The lack of variation

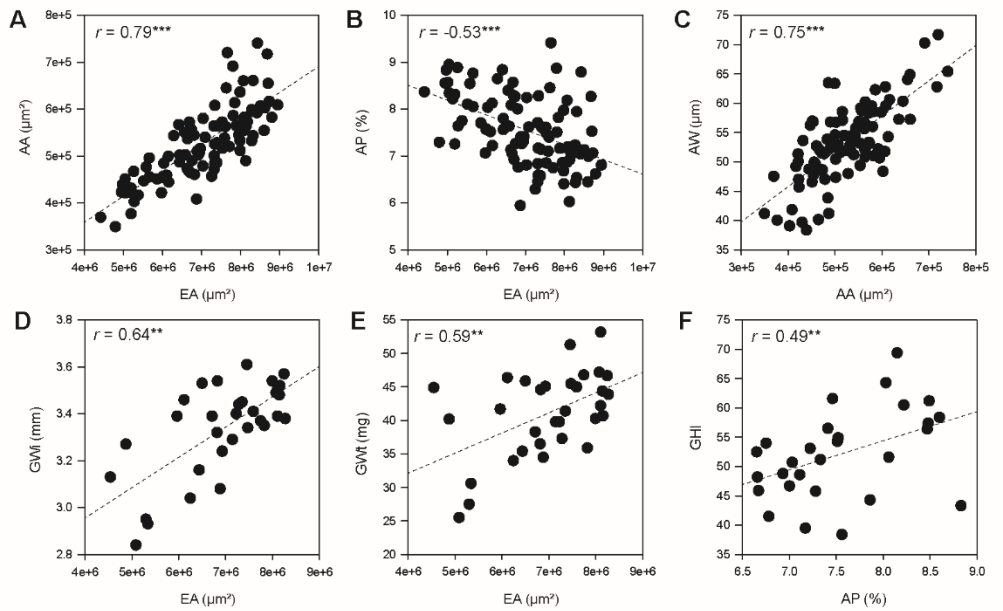

Figure 3. Transverse and wholegrain trait correlations across different barley genotypes. (**A–C**) Phenotypic measurements from all grain samples for 33 genotypes obtained using transverse grain sections. (**A**) Aleurone area vs endosperm area. (**B**) Aleurone proportion vs endosperm area. (**C**) Aleurone width vs aleurone area. (**D–F**) Correlations between grain measurements (averages) for all 2-row genotypes (n = 30) using the SeedCount, Single Kernel Characterisation System and/or transverse grain sections. (**D**) Grain width vs endosperm area. (**E**) Grain weight vs endosperm area. (**F**) Grain hardness index vs aleurone proportion. EA, Endosperm area; AA, aleurone area; AP, aleurone proportion; AW, aleurone width; GWi, grain width; GWt, grain weight. Significance indicators: ***p≤0.001, **p≤0.01, *p≤0.05.

in grain width is likely to be a result of grain screening. When focussing on aleurone-specific measurements, the values appeared to display normal distributions (Fig. 2B).

Principal component analysis (PCA) separated the genotypes based on the seven transverse grain measurements (Figs 2C and S4A). Genotypes such as CM72, Morex, Barque-73, Hindmarsh, Franklin, Harrington and YU6472 showed distinct differences.

Differences in aleurone measurements at grain maturity correlate with other grain features. The relationship between mature grain and aleurone measurements was examined across the 33 different genotypes by correlation analysis (Figs 3, S4 and S5). While some traits appeared unrelated across the panel, others showed strong correlations, and in the following sections significance indicators are included as follows: ***p ≤0.001, **p ≤0.01 and *p≤0.05. For example, aleurone area was positively correlated with endosperm area (0.79***; Figs 3A and S4B), while aleurone proportion negatively correlated with endosperm area (−0.53***; Figs 3B and S4B). These results suggest that although bigger grains contain more aleurone, the increase in grain size is driven by the starchy endosperm, and aleurone proliferation/expansion is compromised proportionally. Increased aleurone area was driven by increased aleurone width (0.75***; Figs 3C and S4B) but was independent of layer number, while an increased proportion of aleurone was partly due to more aleurone layers (0.41***; Fig. S4B). Aleurone width only showed a weak correlation with aleurone layer number (0.41**; Fig. S4B). Thus, larger grains contain more aleurone, mainly as a result of increased aleurone width (i.e., thickness), but smaller grains contain more aleurone layers with a higher proportion of aleurone relative to starchy endosperm. Together, these results indicate that mature aleurone morphology in barley is determined by the number and size of aleurone cells, which are in turn influenced by starchy endosperm development, and the contribution of each feature can vary depending on genotype.

Comparisons between wholegrain and transverse section measurements were examined in greater detail for the 2-row genotypes (n=30; Figs 3D–F and S5, Table S1). Increased transverse endosperm area was positively correlated with wholegrain measurements including grain width (0.64**; Figs 3D and S5) and grain weight (0.59**; Figs 3E and S5), confirming that some of the transverse measurements relate directly to overall grain features. Several aleurone measurements showed similar correlations to grain size; for example, aleurone area was positively correlated with grain width, thickness, area, diameter and weight (Fig. S5). Interestingly, the only transverse grain measurements to show a correlation with grain hardness were aleurone proportion (0.49**; Figs 3F and S5) and aleurone layer number (0.37*; Fig. S5). This indicates that in this panel, some 2-row genotypes producing harder grains tend to contain more aleurone layers and a higher proportion of aleurone relative to starchy endosperm.

Differences in aleurone development are maintained across different field sites. To determine how consistent the transverse grain measurements were across different environments and years, grain from eight genotypes including Barque, Baudin, Commander, Flagship, Hindmarsh, Keel, Mundah and Shepherd were compared from Charlick, UA, in 2013 (UA), and Gooloogong, NSW, in 2015 (NVT). The aleurone and wholegrain measurements were recorded and compared as a ratio between the different environments and years, i.e., NVT value / UA value (Table S2; Fig. S6). The majority of genotypes showed less than 10% variation for all transverse measurements between environments; for example, the least variable transverse measurement was grain width (Fig. S6A) while the most variable measurements were aleurone layer number and proportion (Fig. S6A). The variation in aleurone layer number was most obvious in Barque and Hindmarsh, which tend to have more layers in the NVT samples (1.83 UA vs 2.44 NVT and 1.88 UA vs 2.38 NVT, respectively), while the variation in aleurone proportion was most obvious in Flagship, which showed more endosperm overall but less aleurone in the NVT samples. Although this reveals an effect of environment on transverse grain features, particularly with regard to the aleurone, correlation analysis indicated that the aleurone measurements generally show a similar trend between environments. For example, measurements of aleurone proportion (0.67*; Fig. S6B) and width (0.79*; Fig. S6C) were significantly correlated despite the different environments. Although this analysis is limited to a small number of genotypes, it suggests there is some degree of stability in aleurone measurements between distinct environments.

Identification of barley genotypes for downstream analysis. Genotypes showing distinct grain phenotypes were selected for more detailed analysis based on transverse grain measurements and PCA (Figs 2C and S4A). Shepherd tended to be at the high extreme for most measurements, while Morex and Barque-73 tended to be at the low extreme (Table S1). Other genotypes were chosen to specifically examine differences in aleurone development, with the aim of avoiding confounding factors such as starchy endosperm area and grain size. For example, endosperm area in Mundah, YU6472, WI2585, WI4262 (Navigator), WI4191 and Steptoe was similar, but aleurone features such as area, proportion and width were distinct. The Mundah and YU6472 genotypes appeared to be "high" genotypes for these characteristics, WI2585 was "average", while Flagship, WI4191 and Steptoe were "low" (Fig. 2C and Table S1). It is important to note that unlike most of the barley genotypes examined here, Morex and Steptoe are 6-row barleys. Based on the small number of 6-row genotypes in the panel, it is currently unclear whether the 6-row phenotype contributes directly to differences in aleurone development.

Hydrolytic enzyme activities differ between genotypes with different aleurone phenotypes. The distinct genotypes were examined to determine whether grain with more aleurone might display increased enzyme activity during germination. The results of β-glucanase, α-amylase, total and free β-amylase activity assays for the nine genotypes of interest are shown for two time points in Fig. 4, with some genotypes showing significant differences (Table S3). One of the two time points was grain maturity, allowing detection of enzymes that had been synthesised and stored during grain development, and the other was 96 hours post imbibition (hpi), which detects enzymes that have been synthesised during germination. The total β-amylase assay used a reducing agent to liberate bound enzyme before activity analysis, while the free β-amylase assay measured activity of unbound enzyme.

Consistent with previous studies, β-glucanase (Fig. 4A) and α-amylase (Fig. 4B) activity was barely detectable in mature grain, while total (Fig. 4C) and free β-amylase (Fig. 4D) activity was detectable at grain maturity. By 96 hpi, activity could be detected for all enzymes in the selected genotypes and clear differences were observed. For example, at 96 hpi, WI4191 (2-row), Steptoe (6-row) and Morex (6-row) showed relatively low β-glucanase and α-amylase activity compared to the other varieties (Fig. 4A,B). Conversely, WI4191 and Morex showed relatively high total and free β-amylase activity compared to the other varieties (Fig. 4C,D). Average total β-amylase activity was similar at grain maturity and germination for most of the varieties (Fig. 4C), although free β-amylase levels tended to be lower at grain maturity compared to the 96 hpi samples, presumably as more enzyme is released through proteolytic cleavage from starch bodies.

Correlation analysis was used to assess the relationships between aleurone morphology and enzyme activ- ity (Fig. 4E). Significant correlations ($p \leq 0.05$) were identified between (1) β-glucanase and α-amylase activity after germination (0.98*), (2) total β-amylase activity at grain maturity and free β-amylase after germination (0.78*) and (3) total β-amylase and free β-amylase after germination (0.76*). By contrast, none of the transverse endosperm or aleurone measurements showed a significant correlation with β-glucanase or α-amylase activity at maturity or 96 hpi (Fig. 4E). Also, differences in total β-amylase activity did not correlate with differences in any of the transverse grain measurements (Fig. 4E).

Conversely, free β-amylase activity showed a significant correlation ($p \leq 0.05$) with transverse aleurone area (0.77*), aleurone proportion (0.87*) and aleurone width (0.86*) at grain maturity (Fig. 4E). Furthermore, although aleurone area and endosperm area were correlated (0.90*), endosperm area itself did not directly correlate with free β-amylase activity. This suggests that direct variation in aleurone cell size or area, or perhaps indirect features of the starchy endosperm that influence aleurone development, may contribute to differential abundance of free β-amylase in different barley genotypes.

To assess if variation in enzyme levels, particularly free β-amylase, might contribute to the rate of grain germination we utilised an *in vitro* germination assay (Fig. S7). Differences were observed between genotypes, particularly in the case of WI4262 (Navigator) and YU6472 (Fig. S7). Comparisons between grain features, germination frequency and enzyme levels revealed significant correlations between the number of germinated seedlings at 12 hours post imbibition (hpi) and β-glucanase and α-amylase levels at 96 hpi (0.72*), and the frequency of germinated seedlings at 24 hpi and 48 hpi (0.71*). However, no significant correlation was detected between any transverse mature grain features or β-amylase activity compared to the frequency of germination at the time

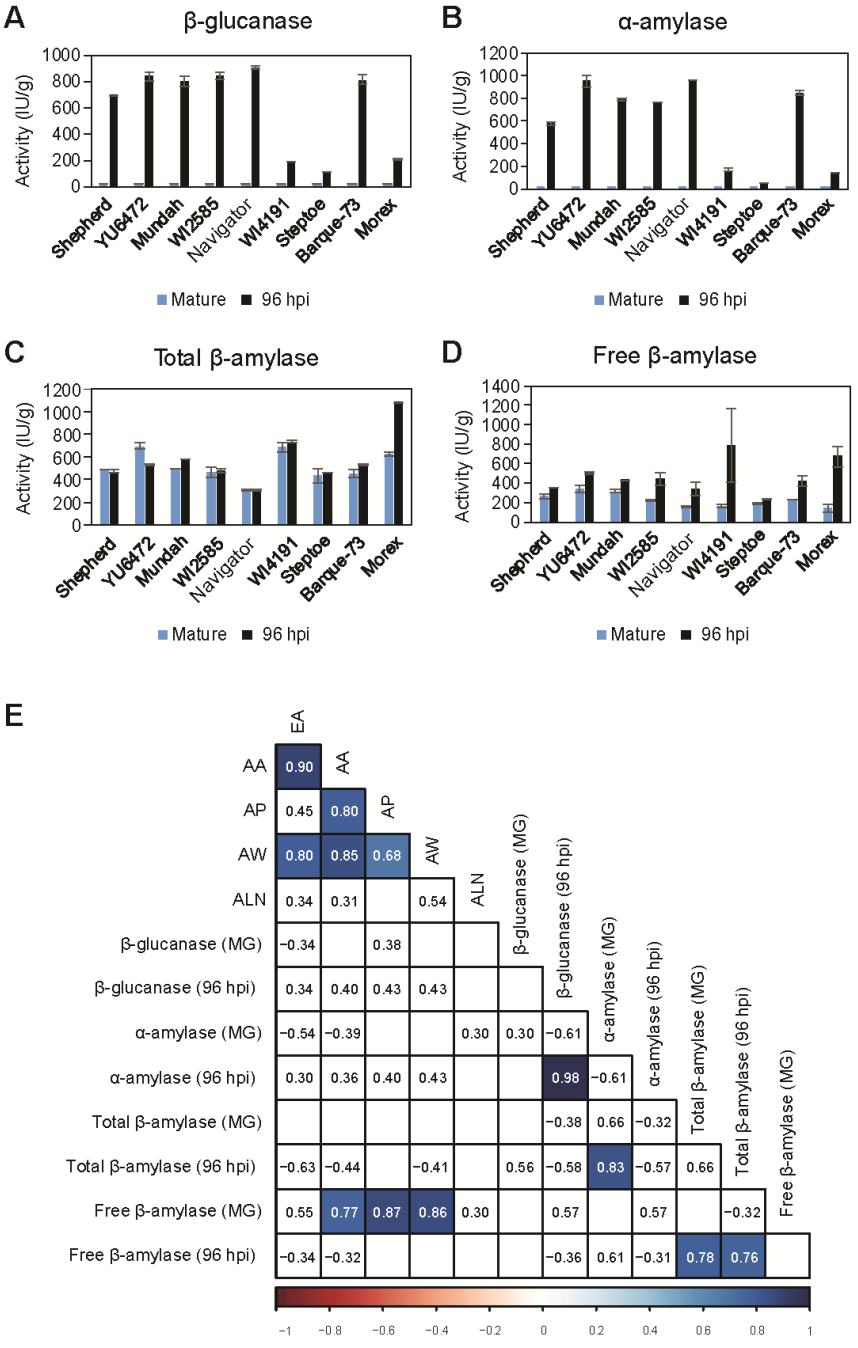

Figure 4. Hydrolytic enzyme activities in grain from nine barley genotypes at grain maturity and 96 hours post imbibition (hpi). (**A**) 1,3;1,4-β-glucanase (β-glucanase) activity. (**B**) α-amylase activity. (**C**) Total β-amylase activity. (**D**) Free β-amylase activity. Error bars show standard deviation. (**E**) Heat map representing correlations between aleurone measurements and enzyme activities for the nine different genotypes. Note, some aleurone correlation values differ to those in Fig. S5 due to the different sample size. Blue boxes indicate positive correlations. Numbers within boxes represent correlation coefficient (*r*) values. All values>0.3 or<−0.3 are shown, but only those with a p-value≤0.05 are contained within shaded boxes. MG, mature grain; EA, endosperm area; AA, aleurone area; AP, aleurone proportion; AW, aleurone width; ALN, aleurone layer number.

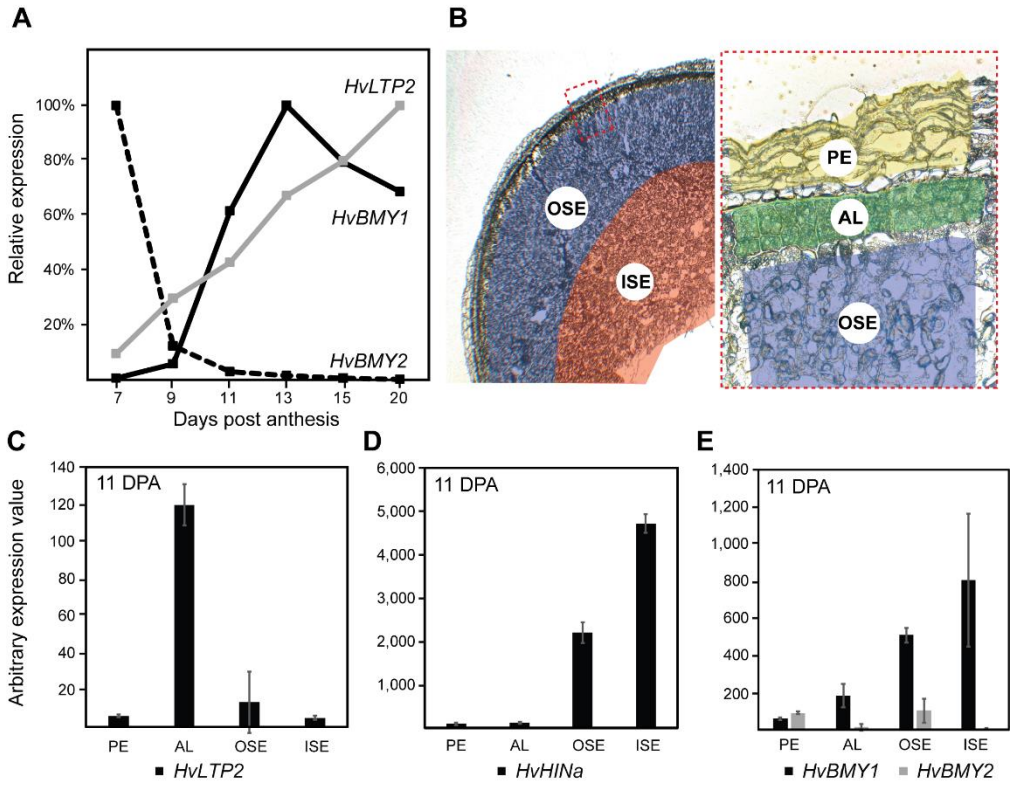

Figure 5. Accumulation of transcript in different barley grain tissues. (**A**) RNAseq analysis of transcripts from Sloop wholegrain samples, minus embryo, at 7, 9, 11, 13, 15, 20 days post anthesis (DPA). Accumulation patterns for the *HvBMY1*, *HvBMY2* and *HvLTP2* transcripts are shown, normalised to the maximum expression value for each gene. (**B**) Thin butyl-methyl methacrylate sections of Sloop barley grain at 11 DPA showing the regions collected by laser microdissection. PE, pericarp; AL, aleurone; OSE, outer starchy endosperm including sub-aleurone; ISE, inner starchy endosperm. The red dashed box shows a magnified view of the outer grain layers. (**C–E**) Quantitative PCR analysis of transcript abundance in RNA collected from laser micro dissected material. (**C**) *lipid transfer protein 2* (*HvLTP2*). (**D**) *hordoinoline a* (*HvHINa*) (**E**) *β-amylase 1* (*HvBMY1*) and *β-amylase 2* (*HvBMY2*).

points analysed. Therefore, it seems unlikely that the varying aleurone features, and their association with free β-amylase activity, relate directly to the rate of germination from 12 hpi onwards.

***β-amylase* transcript abundance varies in specific grain cell-types.** To address how variation in aleurone features might directly contribute to increased wholegrain free β-amylase levels at grain maturity, we considered the spatial and temporal dynamics of *β-amylase* transcript abundance. Previous studies have shown that *β-amylase* genes are transcribed and translated during barley grain development[16,17], with some enrichment in sub-aleurone or aleurone tissues. In this study, several datasets were generated to examine the abundance of 11 putative barley *β-amylase*-encoding genes identified in the latest release of the barley genome (Table S4). First, a developmental series of early grain development was generated from Sloop wholegrain samples (minus embryo) at 7, 9, 11, 13, 15 and 20 days post anthesis (DPA), which covers the main stages of aleurone differentiation and development (Fig. S8). This overlaps with datasets from several studies[17,34–36]. Analysis confirmed that *HvBMY1* was the most abundant *β-amylase* gene in the developing grain, increasing in abundance from 9 DPA onwards (Table S4; Fig. 5A). This pattern was distinct from that of the *lipid transfer protein 2* (*HvLTP2*) gene, a specific marker for aleurone tissue, although transcripts for both genes accumulated over time (Fig. 5A). *HvBMY2* was the second most abundant *β-amylase* transcript in the developing grain, but showed a significant decrease in abundance from 7 DPA onwards (Table S4; Fig. 5A). The expression at 7 DPA may correspond to residual expression from vegetative tissues, since in a separate dataset generated from pre-fertilisation pistil tissues (from the Golden Promise cultivar), *HvBMY2* was most abundant *β-amylase* gene (Table S4).

Next, we utilised laser microdissection to precisely separate the pericarp, aleurone, outer starchy endosperm (including sub-aleurone) and inner starchy endosperm tissues from transverse mid-point grain sections at 11 DPA (Fig. 5B) and 25 DPA (Fig. S9). RNA from these specific regions was analysed by quantitative PCR (qPCR) using known markers of grain development. At 11 DPA, transcript from the *HvLTP2* aleurone marker was barely detected in the pericarp, outer starchy endosperm and inner starchy endosperm cells, but was abundant in the aleurone (Fig. 5C). In contrast, transcript from the barley *hordoinoline* (*HvHINa*) gene that influences grain hardness and accumulates in the endosperm was predominantly detected in the outer starchy endosperm

and inner starchy endosperm tissues (Fig. 5D). Unlike *HvLTP2* and *HvHINa*, *HvBMY2* transcript was predominantly detected in the pericarp and outer starchy endosperm samples, and not in the aleurone or inner starchy endosperm (Fig. 5E). *HvBMY1* transcript was detected in the aleurone, outer starchy endosperm and inner starchy endosperm samples. On average, expression was ~4 fold higher in the inner starchy endosperm tissues compared to the aleurone (Fig. 5E) and the ratio of aleurone: outer starchy endosperm: inner starchy endosperm was approximately 1:3:4. Transcript patterns were similar at 25 DPA (Fig. S9A–D), although the aleurone appeared to contribute only 3% of the total detected *HvBMY1* transcript. Taken together, these data suggest that the inner and outer starchy endosperm are the major sites of *HvBMY1* expression. However, an increase in *HvBMY1* transcript during grain development is driven by expression in multiple tissues, with the aleurone contributing up to 13% of the overall grain transcript levels depending on the developmental stage. Therefore, the increase in free β-amylase levels at grain maturity in genotypes exhibiting a larger aleurone may be partly due to expression of *HvBMY1* in aleurone tissues.

Discussion

The cereal aleurone is a multifunctional tissue with important roles in grain development and germination, and applications in the health and brewing industries[37]. In this study, we utilised autofluorescence microscopy to identify differences in aleurone morphology within a panel of diverse barley genotypes, and considered how these differences relate to grain biology and the amount of germination-related enzyme activity.

Within the cereal grain, the aleurone and starchy endosperm are both derived from the fertilised central cell and only begin to differentiate around 7–10 days after pollination[37]. Unsurprisingly, analysis of 33 barley genotypes confirmed that development of the starchy endosperm and aleurone are intimately linked; as radial starchy endosperm area increased, so too did the radial area of aleurone. Genotypes producing grain with more aleurone layers also tended to show a thicker aleurone, and aleurone width contributed directly to aleurone area. However, the number of aleurone layers shared no direct relationship with aleurone area, suggesting that factors determining aleurone cell expansion have a greater impact on this trait. A reduced proportion of aleurone was typically linked to an increase in starchy endosperm area, while an increased proportion correlated with increased aleurone layer number. These data indicate that pathways promoting increased grain fill (i.e., starchy endosperm cell division and/or cell expansion) are (1) unlikely to be perceived by aleurone cells, (2) may inhibit the formation/maintenance of additional inner aleurone layers and (3) may indirectly impact the size of aleurone cells, possibly due to physical constraints imparted by the pericarp.

Of all the aleurone and grain features measured in this study, aleurone layer number appeared to be the most independent (see Fig. S4B). This may be due to difficulty in collecting precise measurements or perhaps a unique mechanism underlying layer formation. In maize, specific pathways appear to prevent an increase in aleurone layer number, since aberrant periclinal divisions of aleurone cells result in them adopting starchy endosperm fate[21]. A similar mechanism may contribute to subtle variations in aleurone layer number in barley. Genotypes such as Barque-73 and Hindmarsh, which produce fewer aleurone layers (~1.8 on average), may be more sensitive to differentiation signals that promote starchy endosperm identity compared to genotypes such as Clipper and Franklin, which produce more aleurone layers (~2.8 on average). The source and temporal activity of the fate-determining signals is unclear[21]; one possibility is that aleurone cells perceive a stimulatory cue at the periphery of the grain that only reaches a certain radial depth. Similar basic mechanisms have been identified in Arabidopsis, where diffusible epidermal signals control sub-epidermal cell identity during shoot meristem development[31,38]. Alternatively, the starchy endosperm generates signals that do not reach or are not perceived by the aleurone. The diversity of aleurone phenotypes observed in this barley panel provides an opportunity to address these differences at the genetic level in future studies.

The contribution of sub-epidermal tissues to wholegrain traits is revealed by transverse sectioning and microscopy. One limitation of manual microscopic screens is their low throughput nature, particularly compared with high throughput automated screens of grain shape, composition and dimension used in breeding programs. However, the advantage of microscopy is that sub-epidermal features of the grain can reveal cell-type specific contributions to wholegrain traits[39]. Here, comparison of microscopy and wholegrain analyses showed clear correlations, particularly when focussing on spring 2-row barley genotypes. For example, transverse endosperm area correlated with wholegrain measurements of area, thickness and weight (Fig. S5).

Unexpectedly, grain hardness correlated positively with aleurone proportion and layer number (Fig. S5). Grain hardness has been intensively studied in the cereals. In wheat, hardness contributes to milling and baking properties and flour composition[40–43], while in barley, hardness influences pearling properties[44] in addition to the malting quality index[45]. The composition of individual grain components, particularly the starchy endosperm, determines whether the grain will be hard or soft[45–47] with models suggesting that harder grains have a denser endosperm with a continuous protein matrix that prevents easy release of starch granules[39]. A specific relationship between the barley aleurone and grain hardness does not appear to have been reported previously. The correlation detected here may therefore reflect an effect of starchy endosperm protein on hardness, and an indirect effect on aleurone development. Another possibility is that in the examined panel, differences in the chemical and physical properties of the aleurone cell walls may directly contribute to grain hardness. Barley aleurone cell walls are enriched in arabinoxylan polysaccharides cross-linked with phenolic acids such as ferulic acid[12,14], forming a robust matrix that surrounds the grain during development[37]. In genotypes with an increased proportion of aleurone, this reinforced cell wall matrix may provide a harder shell around the grain. This is something that might also be considered in future studies.

Variations in barley aleurone features provide opportunities for further genetic analysis, and do not appear to impact overall grain development. Despite several studies providing insight into the

genetic architecture of barley aleurone development[23,48] the molecular basis for variation between genotypes has yet to be elucidated. Genetic data is available for a number of the genotypes investigated here, but the number was insufficient to carry out a robust genome wide association study (GWAS) to identify possible quantitative trait loci (QTL). However, our findings show that the variation between genotypes is reproducible and statistically significant; this suggests that a similar screen might be carried out on a larger panel of genotypes to support future genetic analysis.

Strangely, it has also remained unclear whether intraspecific differences in barley aleurone development are of any physiological importance. It is possible that the variation is of no major consequence, as long as the aleurone is still present and able to fulfil roles in hormone perception and enzyme release during germination. In general, mutants that show a lack of or reduced number of aleurone layers tend to show defects in seed development. For example, the *barley defective seed 5* mutant (*des5*)[48] shows a patchy reduction in the number of aleurone cells, and severe defects in starchy endosperm fill and seed morphology. Similarly, mutations in the maize *naked endosperm1* and *crinkly4* genes lead to reduced aleurone phenotypes, in addition to compromised whole seed morphology[24,27]. On the other hand, mutant alleles of the maize *supernumerary aleurone 1* (*sal1*) gene, which produce two or three aleurone layers instead of the one layer detected in wild type, have relatively normal kernels[26,49]. Variations in aleurone thickness, area and layer number from two to four layers appeared to have no detrimental impact on overall grain development across the barley panel examined here.

The genotypes investigated included a combination of 2-row and 6-row varieties, malting and feed varieties; for example, Barque-73 and Mundah are Australian feed varieties, Sloop is an Australian malting variety, and YU6472 is a Chinese feed variety[50]. Based on an "average" sized grain, Barque-73 exhibited reduced aleurone area, proportion and width. At the other extreme, compared to its average grain size, YU6472 displayed increased aleurone area, proportion and width. Barque-73 also showed significantly fewer aleurone layers compared to Mundah and Sloop. Although the sample size is small, there appeared to be no clear difference in aleurone morphology to distinguish between grains from feed and malting genotypes. This observation needs to be treated with some caution, however, since there are many features that contribute to malt grade barley[51]. This could be tested in a larger panel of genotypes that have been directly assessed, head-to-head, for malt quality.

Genotypes with more aleurone show increased levels of free β-amylase at grain maturity. The variation present in this barley panel provided an opportunity to assess the effect of different aleurone phenotypes on the activity of germination-related enzymes, which is one important aspect of aleurone function. During barley grain imbibition, gibberellic acid (GA) is released by the scutellum, triggering the synthesis and subsequent release of various hydrolytic enzymes from the aleurone[52–54]. Of these enzymes, β-glucanase facilitates the hydrolysis of β-glucan polysaccharides in cell walls and allows access to starch for additional hydrolytic enzymes[55]. Enzymes involved in starch hydrolysis include α-amylase, which hydrolyses α-1,4-glycosidic bonds of starch polysaccharides and β-amylase, which is synthesised during grain development, and during germination acts to liberate the disaccharide maltose from the non-reducing end of starch molecules[16,56–58]. Function of these enzymes is critical for germination[59,60], and previous studies show that mature grain β-amylase content varies between barley genotypes[61–63].

β-glucanase enzyme activity was barely detectable at grain maturity, but was high at 96 hpi, and the same pattern was observed for α-amylase. A relatively low level of activity was identified for both enzymes in WI4191, Steptoe and Morex, which tend to display "low" aleurone phenotypes. However, neither β-glucanase nor α-amylase levels showed a general correlation with differences in mature grain aleurone morphology. This may indicate that variation in transverse aleurone morphology at maturity has no direct impact on the amount of β-glucanase and α-amylase activity. Alternatively, the genotypes chosen for analysis did not show large enough differences in aleurone development, the panel was too small, or the 96 hpi time point was too late to identify such differences.

Two forms of β-amylase are present in the grain, a bound and free form. Bound β-amylase is located in an insoluble protein complex, mainly associated with the periphery of starch granules via disulphide bridges[18,64], while the soluble or free form is active. Both forms of β-amylase are identical in terms of mobility and molecular specific activity, indicating that once bound β-amylase is cleaved, it is converted to free β-amylase[18]. Total and free β-amylase were detected in mature and germinated grain samples from the nine genotypes of interest. Total β-amylase activity did not change over time, consistent with its synthesis during grain development. Free β-amylase activity increased during germination and varied between genotypes, consistent with the release of bound β-amylase and previous reports[16,19,61–63]. Notably, genotype-specific differences in free β-amylase activity at grain maturity correlated with aleurone area, proportion and width. Genotypes with "high" aleurone phenotypes exhibited higher free β-amylase levels. In physiological terms, we propose this may allow for an early pulse of starch hydrolysis prior to the liberation of bound β-amylase by endopeptidases. In wheat, hydrogen sulphide treatment was shown to stimulate early germination through early activation of β-amylase[65]. The authors speculate that higher levels of "active" free β-amylase can participate in starch hydrolysis, providing sugar units for seedling growth prior to the induction of α-amylases by GAs[65]. In the current study, a role for increased free β-amylase activity in germination was tested in the context of nine genotypes of interest, but this failed to identify any significant correlation. This suggests that if there is a physiological role for increased free β-amylase levels and aleurone features at maturity, it may occur prior the emergence of the barley radicle at 6 to 12 hpi.

Explaining differences in free β-amylase levels at grain maturity. There are a number of reasons why free β-amylase levels might vary at grain maturity, including variable transcriptional dynamics of different *HvBMY* genes and polymorphisms that influence enzyme activity. Previous studies indicate that at least two β-amylase genes are expressed during grain development, and that *HvBMY1* rather than *HvBMY2* is likely to be the most important *β-amylase* gene involved in germination[66]. Our RNAseq data and analysis of 11 *HvBMY* genes

from the Sloop cultivar supports this finding (Table S4). Moreover, many of the cultivar-specific differences in total and free β-amylase levels can be explained by cultivar-specific differences in the *HvBMY1* gene[51,61,67,68]. In the Chebec and Harrington cultivars, the *HvBMY1* locus on 4HL accounts for approximately 90.5% of the variation in free β-amylase levels[62]. Barley genotypes can be of the Sd1-type (Harrington; lower free β-amylase levels) or Sd2-type (Chebec; higher free β-amylase levels), and this is attributed to distinct amino acid substitutions in *Hv*BMY1. In addition, differences in intron 3 of the *HvBMY1* gene, a possible site of *cis*-regulatory-elements, may contribute to differences in total β-amylase levels[69]. Furthermore, results from an earlier study[18] suggest that grain desiccation may also impact free β-amylase levels, since it contributes to the process of β-amylase being bound to starch.

Based on the well-characterised function of β-amylase post-germination, is seems unlikely that different *HvBMY* genes or alleles contribute directly to differences in aleurone morphology during early grain development. Rather, we hypothesise that differences in aleurone development may be another factor that impact free β-amylase levels at grain maturity. This hypothesis is supported by several findings. First, early studies indirectly suggested the presence of β-amylase enzyme in the aleurone layer[20] and the sub-aleurone layer[64,70]. Second, genes encoding β-amylase are transcribed in the aleurone. In the Barke cultivar, *HvBMY1* is the most abundant gene family member expressed during grain development, and was detected in the aleurone and sub-aleurone by mRNA *in situ* hybridisation[17]. In the same study, *HvBMY2* was detected at low levels in the endosperm, but was most abundant in the pericarp where it peaked at 6 DPA[17]. Our results in Sloop wholegrain for *HvBMY1* and *HvBMY2* show a similar temporal pattern and relative abundance during grain development, indicating that *HvBMY1* transcript is highly abundant when the aleurone is forming. Third, studies in a number of temperate grasses including barley show that the aleurone is essentially free of starch granules[71], suggesting it may provide a starch-free repository for free β-amylase storage.

In the genotypes investigated here, approximately half (on average 45±14%) of the total β-amylase appears in a free form at grain maturity. Based on the relative abundance of *HvBMY1* transcript in different grain compartments, it seems unlikely that all of the free β-amylase is derived solely from the aleurone. In the Sloop cultivar, laser microdissection qPCR revealed that *HvBMY1* is detected in the aleurone, outer starchy endosperm (incorporating the sub-aleurone) and inner starchy endosperm cells. At 11 DPA, when *HvBMY1* transcript levels are increasing in the grain, approximately 13% of transcript is derived from the aleurone. If all of this transcript is translated directly into β-amylase and remains unbound (free) due to the absence of starch, then the aleurone would contribute ~30% of the free β-amylase activity detected at grain maturity. Hence, variation in the amount of aleurone between cultivars could potentially contribute to the variation observed in free β-amylase activity, but it is clearly not the main determinant.

Several points need to be considered in future studies. It is currently unclear whether *HvBMY1* transcript abundance varies along the length of the barley grain, particularly near the embryo, which may lead to an underestimation of aleurone *HvBMY1* levels. It is also possible that the relative abundance of aleurone *HvBMY1* transcript peaks at a time point that was not investigated here (for example 13 DPA where wholegrain *HvBMY1* levels peak), before they decrease at 25 DPA. Along these lines, it is unclear exactly when the differences in aleurone development are manifested in the examined genotypes. If the differences appear early, coinciding with the stage where *HvBMY1* transcript is most abundant, then this may have an impact on downstream *Hv*BMY1 levels. Finally, antibodies to β-amylase have been reported[72], but current microscopic assays that distinguish the different β-amylase forms are unavailable and need to be established. These would be useful tools in determining the location of the enzymes, assessing variation between genotypes of interest and determining the dynamics of enzyme release during seed development and germination.

References

1. Zohary, D., Hopf, M. & Weiss, E. Domestication of plants in the old world. 4th edn, p1-237 (2012).
2. Newman, C. W. & Newman, R. K. A brief history of barley foods. Cereal Foods World **51**, 4–7 (2006).
3. Sato, K., Flavell, A., Russell, J., Börner, A. & Valkoun, J. In Biotechnological Approaches to Barley Improvement Vol. 69 Biotechnology in Agriculture and Forestry (eds Jochen Kumlehn & Nils Stein) p 21–36 (Springer Berlin Heidelberg, 2014).
4. Mascher, M. et al. A chromosome conformation capture ordered sequence of the barley genome. Nature **544**, 426–433 (2017).
5. Mayer, K. F. X. et al. A physical, genetic and functional sequence assembly of the barley genome. Nature **491**, 711–716 (2012).
6. Behall, K. M., Scholfield, D. J. & Hallfrisch, J. Diets containing barley significantly reduce lipids in mildly hypercholesterolemic men and women. American Journal of Clinical Nutrition **80**, 1185–1193 (2004).
7. Gamel, T. H. & Abdel-Aal, E.-S. M. Phenolic acids and antioxidant properties of barley wholegrain and pearling fractions. Agricultural and Food Science **21**, 118–131 (2012).
8. Pins, J. J. & Kaur, H. A review of the effects of barley β-glucan on cardiovascular and diabetic risk. Cereal Foods World **51**, 8–11 (2006).
9. Yan, D., Duermeyer, L., Leoveanu, C. & Nambara, E. The functions of the endosperm during seed germination. Plant and Cell Physiology **55**, 1521–1533 (2014).
10. Wilkinson, L. G. & Tucker, M. R. An optimised clearing protocol for the quantitative assessment of sub-epidermal ovule tissues within whole cereal pistils. Plant Methods **13**, 67–77 (2017).
11. Brown, R. C. & Lemmon, B. E. In Plant Cell Monographs Vol. 8 Plant Cell Monographs (ed Olsen, O. A.), p 1–20 (2007).
12. Hassan, A. S. et al. A genome wide association study of arabinoxylan content in 2-row spring barley grain. Plos One **12**, 1–19 (2017).
13. Nordkvist, E., Salomonsson, A. C. & Aman, P. Distribution of insoluble bound phenolic acids in barley grain. Journal of the Science of Food and Agriculture **35**, 657–661 (1984).
14. Wilson, S. M. et al. Pattern of deposition of cell wall polysaccharides and transcript abundance of related cell wall synthesis genes during differentiation in barley endosperm. Plant Physiology **159**, 655–670 (2012).
15. Fath, A., Bethke, P., Lonsdale, J., Meza-Romero, R. & Jones, R. Programmed cell death in cereal aleurone. Plant Molecular Biology **44**, 255–266 (2000).
16. Betts, N. S. et al. Morphology, carbohydrate distribution, gene expression, and enzymatic activities related to cell wall hydrolysis in four barley varieties during simulated malting. Frontiers in Plant Science **8**, 1–15 (2017).

17. Radchuk, V. V. et al. Spatiotemporal profiling of starch biosynthesis and degradation in the developing barley grain. Plant Physiology **150**, 190–204 (2009).
18. Hara-Nishimura, I., Nishimura, M. & Daussant, J. Conversion of free β-amylase to bound β-amylase on starch granules in the barley endosperm during desiccation phase of seed development. Protoplasma **134**, 149–153 (1986)
19. Sopanen, T. & Lauriere, C. Release and activity of bound β-amylase in a germinating barley grain. Plant Physiology **89**, 244–249 (1989).
20. Tronier, B. & Ory, R. L. Association of bound β-amylase with protein bodies in barley. Cereal Chemistry **47**, 464–471 (1970).
21. Becraft, P. W. & Yi, G. Regulation of aleurone development in cereal grains. Journal of Experimental Botany **62**, 1669–1675 (2011).
22. Shapter, F. M., Dawes, M. P., Lee, L. S. & Henry, R. J. Aleurone and subaleurone morphology in native Australian wild cereal relatives. Australian Journal of Botany **57**, 688–696 (2009).
23. Jestin, L. et al. Inheritance of the number and thickness of cell layers in barley aleurone tissue (Hordeum vulgare L.): an approach using F2-F3 progeny. Theoretical and Applied Genetics **116**, 991–1002 (2008).
24. Becraft, P. W., Stinard, P. S. & McCarty, D. R. CRINKLY4: A TNFR-like receptor kinase involved in maize epidermal differentiation.
Science **273**, 1406–1409 (1996).
25. Lid, S. E. et al. The defective kernel 1 (dek1) gene required for aleurone cell development in the endosperm of maize grains encodes a membrane protein of the calpain gene superfamily. Proceedings of the National Academy of Sciences of the United States of America 99, 5460–5465 (2002).
26. Shen, B. et al. sal1 determines the number of aleurone cell layers in maize endosperm and encodes a class E vacuolar sorting protein. Proceedings of the National Academy of Sciences of the United States of America 100, 6552–6557, https://doi.org/10.1073/ pnas.0732023100 (2003).
27. Yi, G., Neelakandan, A. K., Gontarek, B. C., Vollbrecht, E. & Becraft, P. W. The naked endosperm genes encode duplicate INDETERMINATE domain transcription factors required for maize endosperm cell patterning and differentiation. Plant physiology 167, (2015).
28. Lid, S. E. et al. The defective kernel 1 (dek1) gene required for aleurone cell development in the endosperm of maize grains encodes a membrane protein of the calpain gene superfamily. Proceedings of the National Academy of Sciences of the United States of America **99**, 5460–5465 (2002).
29. McCleary, B. V. & Shameer, I. Assay of malt β-glucanase using azo-barley glucan: An improved precipitant. Journal of the Institute of Brewing **93**, 87–90 (1987).
30. McCleary, B. V. et al. Measurement of α-amylase activity in white wheat flour, milled malt, and microbial enzyme preparations, using the ceralpha assay: Collaborative study. Journal of Aoac International **85**, 1096–1102 (2002).
31. McCleary, B. V. & Codd, R. Measurement of β-amylase in cereal flours and commercial enzyme preparations. Journal of Cereal Science **9**, 17–33 (1989).
32. Tucker, M. R. et al. Somatic small RNA pathways promote the mitotic events of megagametogenesis during female reproductive development in Arabidopsis. Development **139**, (2012).
33. Okada, T. et al. Enlarging cells initiating apomixis in Hieracium praealtum transition to an embryo sac program prior to entering mitosis. *Plant Physiology* **163**, 216–231 (2013).
34. Aditya, J. *et al*. The dynamics of cereal cyst nematode infection differ between susceptible and resistant barley cultivars and lead to changes in (1,3;1,4)-β-glucan levels and *HvCslF* gene transcript abundance. *New Phytologist* **207**, 135–147 (2015).
35. Zhang, R. *et al*. The Dynamics of Transcript Abundance during Cellularization of Developing Barley Endosperm. *Plant Physiol* **170**, 1549–1565 (2016).
36. Sreenivasulu, N. *et al*. Gene expression patterns reveal tissue-specific signaling networks controlling programmed cell death and ABA-regulated maturation in developing barley seeds. *The Plant Journal* **47**, 310–327 (2006).
37. Thiel, J., Weier, D. & Weschke, W. Laser-capture microdissection of developing barley seeds and cDNA array analysis of selected tissues. *Methods Mol Biol* **755**, 461–475 (2011).
38. Burton, R. A. & Fincher, G. B. Evolution and development of cell walls in cereal grains. *Frontiers in Plant Science* **5**, 1–15 (2014).
39. Knauer, S. *et al*. A protodermal miR394 signal defines a region of stem cell competence in the *Arabidopsis* shoot meristem. *Developmental Cell* **24**, 125–132 (2013).
40. Nair, S., Knoblauch, M., Ullrich, S. & Baik, B. K. Microstructure of hard and soft kernels of barley. *Journal of Cereal Science* **54**, 354–362 (2011).
41. Greffeuille, V., Abecassis, J., Bar L'Helgouach, C. & Lullien-Pellerin, V. Differences in the aleurone layer fate between hard and soft common wheats at grain milling. *Cereal Chemistry* **82**, 138–143 (2005).
42. Pasha, I., Anjum, F. M. & Morris, C. F. Grain hardness: A major determinant of wheat quality. *Food Science and Technology International* **16**, 511–522 (2010).
43. Symes, K. J. Influence of a gene causing hardness on the milling and baking quality of two wheats. *Australian Journal of Agricultural Research* **20**, 971–979 (1969).
44. Williams, P. C. Relation of starch damage and related characteristics to kernel hardness in Australian wheat varieties. *Cereal Chemistry* **44**, 383–390 (1967).
45. Edney, M. J., Rossnagel, B. G., Endo, Y., Ozawa, S. & Brophy, M. Pearling quality of Canadian barley varieties and their potential use as rice extenders. *Journal of Cereal Science* **36**, 295–305 (2002).
46. Psota, V., Vejrazka, K., Famera, O. & Hrcka, M. Relationship between grain hardness and malting quality of barley (*Hordeum vulgare* L.). *Journal of the Institute of Brewing* **113**, 80–86 (2007).
47. Brennan, C. S., Harris, N., Smith, D. & Shewry, P. R. Structural differences in the mature endosperms of good and poor malting barley cultivars. *Journal of Cereal Science* **24**, 171–177 (1996).
48. Chandra, G. S., Proudlove, M. O. & Baxter, E. D. The structure of barley endosperm - An important determinant of malt modification. *Journal of the Science of Food and Agriculture* **79**, 37–46 (1999).
49. Olsen, L. T. *et al*. The defectiveseed5 (des5) mutant: effects on barley seed development and HvDek1, HvCr4, and HvSal1 gene regulation. *J Exp Bot* **59**, 3753–3765 (2008).
50. Tian, Q. *et al*. Subcellular localization and functional domain studies of DEFECTIVE KERNEL1 in maize and Arabidopsis suggest a model for aleurone cell fate specification involving CRINKLY4 and SUPERNUMERARY ALEURONE LAYER1. *Plant Cell* **19**, 3127–

3145 (2007).
51. Zhou, M. X., Li, H. B., Chen, Z. H. & Mendham, N. J. Combining ability of barley flour pasting properties. *Journal of Cereal Science* **48**, 789–793 (2008).
52. Evans, D. E., Li, C. D. & Eglinton, J. K. Improved Prediction of Malt Fermentability by Measurement of the Diastatic Power Enzymes beta-Amylase, alpha-Amylase, and Limit Dextrinase: I. Survey of the Levels of Diastatic Power Enzymes in Commercial Malts. *J Am Soc Brew Chem* **66**, 223–232 (2008).
53. Drozdowicz, Y. M. & Jones, R. L. Hormonal-regulation of organic and phosphoric-acid release by barley aleurone layers and scutella. *Plant Physiology* **108**, 769–776 (1995).
54. Fincher, G. B. Molecular and cellular biology associated with endosperm mobilization in germinating cereal grains. *Annual Review of Plant Physiology and Plant Molecular Biology* **40**, 305–346 (1989).
55. Jones, R. L. Gibberellins - Their physiological role. *Annual Review of Plant Physiology and Plant Molecular Biology* **24**, 571–598 (1973).
56. Hrmova, M. & Fincher, G. B. Structure-function relationships of β-D-glucan endo- and exohydrolases from higher plants. *Plant Molecular Biology* **47**, 73–91 (2001).
57. Bamforth, C. W. & Quain, D. E. In *Cereal science and technology* (ed PalmerGH) p 326–366 (1989).
58. Lauro, M., Suortti, T., Autio, K., Linko, P. & Poutanen, K. Accessibility of barley starch granules to α-amylase during different phases of gelatinization. *Journal of Cereal Science* **17**, 125–136 (1993).
59. Lewis, M. J. & Young, T. W. In *Brewing* Vol. 106, p 19 (1995).
60. Han, C. & Yang, P. F. Studies on the molecular mechanisms of seed germination. *Proteomics* **15**, 1671–1679 (2015).
61. Becraft, P. W. & Gutierrez-Marcos, J. Endosperm development: dynamic processes and cellular innovations underlying sibling altruism. *Wiley Interdisciplinary Reviews: Developmental Biology* **1**, 579–593 (2012).
62. Gong, X. *et al*. Discovery of novel *Bmy1* alleles increasing β-amylase activity in Chinese landraces and Tibetan wild barley for improvement of malting quality via MAS. *Plos One* **8**, e72875 (2013).
63. Li, C. D. *et al*. Mapping of barley (*Hordeum vulgare* L.) β-amylase alleles in which an amino acid substitution determines β-amylase isoenzyme type and the level of free β-amylase. *Journal of Cereal Science* **35** (2002).
64. Yin, C., Zhang, G. P., Wang, J. M. & Chen, J. X. Variation of β-amylase activity in barley as affected by cultivar and environment and its relation to protein content and grain weight. *Journal of Cereal Science* **36**, 307–312 (2002).
65. Lauriere, C., Lauriere, M. & Daussant, J. Immunohistochemical localization of β-amylase in resting barley seeds. *Physiologia Plantarum* **67**, 383–388 (1986).
66. Zhang, H. *et al*. Hydrogen sulfide stimulates beta-amylase activity during early stages of wheat grain germination. *Plant Signal Behav* **5**, 1031–1033 (2010).
67. Vinje, M. A., Willis, D. K., Duke, S. H. & Henson, C. A. Differential expression of two beta-amylase genes (Bmy1 and Bmy2) in developing and mature barley grain. *Planta* **233**, 1001–1010 (2011).
68. Panozzo, J. F. *et al*. QTL analysis of malting quality traits in two barley populations. *Aust J Agr Res* **58**, 858–866 (2007).
69. Vinje, M. A., Willis, D. K., Duke, S. H. & Henson, C. A. Differential RNA expression of Bmy1 during barley seed development and the association with beta-amylase accumulation, activity, and total protein. *Plant Physiol Biochem* **49**, 39–45 (2011).
70. Erkkila, M. J., Leah, R., Ahokas, H. & Cameron-Mills, V. Allele-dependent barley grain beta-amylase activity. *Plant Physiol* **117**, 679–685 (1998).
71. Engel, C. The distribution of the enzymes in resting cereals .1. The distribution of the saccharogenic amylase in wheat, rye and barley. *Biochimica Et Biophysica Acta* **1**, 42–49 (1947).
72. Hands, P., Kourmpetli, S., Sharples, D., Harris, R. G. & Drea, S. Analysis of grain characters in temperate grasses reveals distinctive patterns of endosperm organization associated with grain shape. *J Exp Bot* **63**, 6253–6266 (2012).
73. Evans, D. E. *et al*. Measurement of β-amylase in malting barley (*Hordeum vulgare* L.) .1. Development of a quantitative ELISA for β-amylase. *Journal of Cereal Science* **26**, 229–239 (1997).

Acknowledgements

We wish to thank the University of Adelaide Barley Breeding program for providing grain, Ray Sindel for assistance with the SeedCount and SKCS software, Shi-Fang Khor for advice regarding enzymatic assays, Geoff Fincher, Vincent Bulone and members of the Tucker laboratory for comments and suggestions. We also acknowledge the support of Gwen Mayo at Adelaide Microscopy for assistance with laser microdissection and Anna Koltunow at CSIRO for use of a UV polymerisation chamber. MA is supported by an Australian Government Research Training Program Scholarship, a Grains Research and Development Corporation (GRDC) Grains Research Scholarship (GRS10938) and the ARC Centre of Excellence in Plant Cell Walls (CE110001007). NB is supported through an ARC Linkage Project (LP130100600) with the Carlsberg Group. MRT is supported by an ARC Future Fellowship (FT140100780).

Author Contributions

M.A. carried out the majority of data collection and analysis. N.S. carried out qPCR and data analysis. N.B. analysed the *BMY* family in barley. T.W. provided scripts and support for correlation analysis. S.C. provided grain samples and wholegrain phenotyping data. M.T., R.B. and M.A. conceived the study. All authors contributed to the writing and editing of the manuscript.

Additional Information

Supplementary information accompanies this paper at https://doi.org/10.1038/s41598-018-29068-4.

Competing Interests: The authors declare no competing interests.

Publisher's note: Springer Nature remains neutral with regard to jurisdictional claims in published maps and institutional affiliations.

Appendix III

Translating auxin responses into ovules, seeds and yield: insight from Arabidopsis and the cereals

Journal of Integrative Plant Biology

Translating auxin responses into ovules, seeds and yield: insight from Arabidopsis and the cereals

Journal:	*Journal of Integrative Plant Biology*
Manuscript ID	JIPB-2018-0192.R1
Manuscript Type:	Invited Expert Review
Date Submitted by the Author:	22-Oct-2018
Complete List of Authors:	Shirley, Neil; University of Adelaide Aubert, Matthew; University of Adelaide Wilkinson, Laura; University of Adelaide Bird, Dayton; University of Adelaide Lora, Jorge; Instituto de Hortofruticultura Subtropical y Mediterranea 'La Mayora' (IHSM-UMA-CSIC) Yang, Xiujuan; University of Adelaide Tucker, Matthew; University of Adelaide,
Keywords:	Ovule, Seed, Auxin, Barley, Arabidopsis, Development, Plant, Yield, Grain, Phytohormone
TOC Category:	Plant Reproduction Biology, Cell and Developmental Biology

Statement of Authorship

Title of Paper	Translating auxin responses into ovules, seeds and yield: insight from Arabidopsis and the cereals
Publication Status	☐ Published ☑ Accepted for Publication ☐ Submitted for Publication ☐ Unpublished and Unsubmitted work written in manuscript style
Publication Details	Neil. J Shirley, Matthew K. Aubert, Laura G. Wilkinson, Dayton C. Bird, Jorge Lora, Xiujuan Yang and Matthew R. Tucker*

Principal Author

Name of Principal Author (Candidate)	Neil. J Shirley		
Contribution to the Paper	Compiled information and wrote manuscript. I hereby certify that the statement of authorship is accurate.		
Overall percentage (%)	60%		
Certification:	This paper reports on original research I conducted during the period of my Higher Degree by Research candidature and is not subject to any obligations or contractual agreements with a third party that would constrain its inclusion in this thesis. I am the primary author of this paper.		
Signature		Date	21/11/18

Co-Author Contributions

By signing the Statement of Authorship, each author certifies that:

i. the candidate's stated contribution to the publication is accurate (as detailed above);

ii. permission is granted for the candidate in include the publication in the thesis; and

iii. the sum of all co-author contributions is equal to 100% less the candidate's stated contribution.

Name of Co-Author	Matthew K. Aubert		
Contribution to the Paper	Compiled information and contributed to the preparation of the manuscript. I hereby certify that the statement of authorship is accurate.		
Signature		Date	21/11/2018

Name of Co-Author	Laura G. Wilkinson		
Contribution to the Paper	Compiled information and contributed to the preparation of the manuscript. I hereby certify that the statement of authorship is accurate.		
Signature		Date	22/11/2018

Please cut and paste additional co-author panels here as required.

Name of Co-Author	Dayton C. Bird		
Contribution to the Paper	Compiled information and contributed to the preparation of the manuscript. I hereby certify that the statement of authorship is accurate.		
Signature		Date	22/11/2018

Name of Co-Author	Jorge Lora		
Contribution to the Paper	Compiled information and contributed to the preparation of the manuscript. I hereby certify that the statement of authorship is accurate.		
Signature		Date	22/11/2018

Name of Co-Author	Xiujuan Yang		
Contribution to the Paper	Compiled information and contributed to the preparation of the manuscript. I hereby certify that the statement of authorship is accurate.		
Signature		Date	22/11/2018

Name of Co-Author	Matthew R. Tucker		
Contribution to the Paper	Compiled information and contributed to the preparation of the manuscript. I hereby certify that the statement of authorship is accurate.		
Signature		Date	22/11/2018

Translating auxin responses into ovules, seeds and yield: insight from Arabidopsis and the cereals

Neil. J Shirley, Matthew K. Aubert, Laura G. Wilkinson, Dayton C. Bird, Jorge Lora, Xiujuan Yang and Matthew R. Tucker*

School of Agriculture, Food and Wine, Waite Research Institute, The University of Adelaide, Glen Osmond, SA, Australia

*Correspondence: matthew.tucker@adelaide.edu.au; Tel.: +61-8313-9241

Running Title: Auxin signalling during ovule and seed development

Abstract

Grain production in cereal crops depends upon the stable formation of male and female germ cells in the flower. In most angiosperms, the female germ cells are located deep within the ovary, protected by several layers of maternal tissue including the ovary wall, ovule integuments and nucellus. In the field, germline formation and floret fertility are major determinants of yield potential, contributing to traits such as seed number, weight and size. Despite this, viable gametes are not the sole determinants of yield. Stimuli affecting the timing and duration of reproductive phases as well as the viability, size and number of cells within reproductive organs also play a role. One key stimulant is the phytohormone auxin, which influences growth and morphogenesis of female tissues during gynoecium development, gametophyte formation, and endosperm cellularisation. In this review we consider the role of the auxin signalling pathway during ovule and seed development, first in the context of Arabidopsis and then in the cereals. We summarise the gene families involved and highlight distinct expression patterns in barley that suggest a range of roles in reproductive cell specification and fate. This is discussed in terms of seed production and how targeted modification of different tissues might facilitate improvements.

Keywords: grain, seed, barley, ovule, auxin, phytohormone, yield, development, plant, Arabidopsis

Introduction

Plant cells possess an innate developmental plasticity that allows them to adopt different fates dependent on their environment and the signals they perceive (Wolters and Jurgens 2009; Vanstraelen and Benkova 2012; Tucker et al. 2018). Given the vast array of signalling molecules that exist in nature, the architectural limitations of the plant cell wall and the difficulty in accessing sub-epidermal plant cells for molecular analysis, piecing together how a cell actually adopts identity in a complex organ is a remarkably challenging process. This is particularly so in the plant ovule, which develops deep within the flower, but is an essential component of seed formation and therefore plant yield. Since the green revolution, annual yield improvements in cereal crops have plateaued and based on current predictions will not meet global food demands at some point near the middle of this century (Ray et al. 2013). Hence, there is pressing need to develop new strategies that might lead to improvements in grain size, number and/or quality. One area that still holds considerable promise is the detailed study of reproductive organ development at the individual tissue and cellular level, directly in the crops that underlie most of our food, feed and beverage industries. Although many regulators of plant growth and development have already been utilised in the context of germplasm improvement (Sasaki et al. 2002; Mathan et al. 2016; Wurschum et al. 2017), greater understanding of cell and tissue formation in the reproductive organs will provide novel targets for refined genetic improvements and increased yield. For example, the pathways controlling female gamete formation, which depend on interactions between a small subset of epidermal and sub-epidermal cell types in the ovule, are targets for the synthetic control of hybrid production and

heterosis (Sailer et al. 2016). Moreover, the capacity to induce additional germline cells at different stages of ovule development and in different cell types is a target of research into asexual seed formation (apomixis; Hand and Koltunow 2014). Both of these approaches hold potential to significantly increase yields through modification of specific reproductive events.

The central role of the ovule in seed development

The plant ovule hosts processes essential for sexual plant reproduction (Fig. 1A), including the transition from somatic to germline development (megasporogenesis), the formation of a female gametophyte (megagametogenesis), fertilization, embryogenesis, and finally, the generation of the persistent propagule, the seed. In eudicots such as Arabidopsis thaliana (Arabidopsis), the diploid sporophytic tissues of the ovule consists primarily of the proximal funiculus, which connects the ovule to the placenta, the central chalaza and the distal nucellus surrounded by the integuments (Fig. 1B; Reiser and Fischer 1993). The nucellus facilitates the production of a single haploid female gametophyte from a single somatic precursor, which in turn hosts embryo and endosperm development during seed development (reviewed in Wilkinson et al. 2018). After fertilisation in Arabidopsis, division of the central cell within the gametophyte gives rise to a nuclear syncytium that eventually cellularises to form a non-persistent starchy endosperm and persistent peripheral aleurone, while the egg cell is fertilised to give rise to the zygote which divides to form the embryo. At seed maturity, as in most eudicot angiosperms, the embryo consumes most of the endosperm and finally comprises the majority of the seed, leaving only a single layer

of endosperm cells (Brown et al. 1999). At maturity, the embryo makes up over 90% of the seed (Dumas and Rogowsky 2008; Kondou et al. 2008).

In monocots from the grass family such as barley and wheat (i.e. the Poales), the process of ovule initiation and development is similar to Arabidopsis, except that the funiculus is essentially absent, the nucellus is expanded to form the bulk (~65%; Wilkinson and Tucker 2017) of the sporophytic ovule tissue and the female gametophyte accumulates a large number of antipodal cells at the chalazal (proximal) end of the gametophyte (Fig. 1A; Wilkinson et al. 2018). The main difference between eudicots such as Arabidopsis and cereal monocots is observed after fertilisation, during the later stages of endosperm development. Cereal species such as rice (*Oryza sativa*), maize (*Zea mays*) and barley (*Hordeum vulgare*), produce a persistent endosperm that is only consumed during germination by the developing seedling (Yan et al. 2014). The outer layer of the endosperm forms the aleurone, which plays a critical role during germination (Becraft and Yi 2011), while the mature embryo makes up only a fraction (e.g. approximately 10% in barley) of the mature seed.

Variation in reproductive development and possible roles for hormones

Ovule and seed development are under the control of multiple cues that carefully coordinate the reproductive process in space and time (Bencivenga et al. 2011; Tucker and Koltunow 2014). Although all angiosperms produce seed, considerable natural variation is present in the timing of reproductive development and size of constituent organs, which impacts the size and number of seeds both among and within related species (Guo et al. 2015; Guo et al. 2016; Li and Yang 2017). For example, increased ovary size, which is largely due to increased cell number has been positively linked to

the size of mature grains in both wheat and sorghum (Yang et al. 2009; Xie et al. 2015; Reale et al. 2017). In wheat and barley, the greatest potential to establish increased seed number from an individual inflorescence is during the period of the reproductive phase in which spikelet initiation has ended, floret differentiation has begun, and floret death is yet to occur (Alqudah et al. 2014). Therefore, factors that influence the duration of the reproductive phase are likely to have a significant impact on both the size and number of seed (Gonzalez-Navarro et al. 2016). The timing of these phases is undoubtedly due to the interplay of many regulatory factors, of which phytohormones are prime candidates as organisers.

Auxin as a regulator of yield

In Arabidopsis, it is difficult to disentangle the key events of ovule and seed development from auxin, which contributes to growth, morphogenesis and progression through different reproductive stages (Weijers et al. 2006; Pagnussat et al. 2009; Sehra and Franks 2015). Although there are comparatively fewer details known about the relationship between auxin, ovule and seed development in agriculturally important cereal species, evidence points to an important role. In rice, mutants in the auxin pathway have pleiotropic effects on reproductive development, ranging from decreased fertility and seed abortion to increased seed size and increased grain weight (Jun et al. 2011; Ishimaru et al. 2013; Zhang et al. 2015; Hu et al. 2018). In maize, the relative timing of silking and pollen shed, required to coincide for fertilisation to occur, can be altered by overexpression of *PLASTOCHRON1* (*PLA1*), a cytochrome P450 gene in the same group as AtCYP78A5/KLUH (Anastasiou et al. 2007), which disrupts auxin metabolism and causes substantially increased leaf growth (Sun et al. 2017).

Hybrid maize progeny resulting from a cross between ox-KLUH and wild type yield cobs with 7-15% more kernel rows, and kernels that are 6-16% larger than WT (Sun et al. 2017). In contrast, overexpression of the wheat orthologue of *AtCYP78A5*/*KLUH*, *TaCYP78A5*, has been linked to a reduction in cell number in the wheat ovary and developing seed coat, ultimately reducing the size of the mature grain (Ma et al. 2016).

To address the current status of research in this area, in the following sections we summarise the events of auxin biosynthesis, transport and signalling with a primary focus on key stages of ovule and seed development, highlighting the detailed knowledge available for Arabidopsis. We also summarise recent findings from barley, maize and rice, which suggest the tools to investigate and capitalise on the role of auxin in cereal ovule and seed development are rapidly becoming available.

Components of auxin signalling pathways

Auxin can accumulate in a tissue by two methods, through local biosynthesis or transport from a distant source. Studies suggest that the most abundant form of auxin in plants, indole-3-acetic acid auxin (IAA), is synthesised in a number of young tissues via two different pathways, the tryptophan-dependent pathway and the tryptophan-independent pathway (Mano and Nemoto 2012). In Arabidopsis, biosynthesis of auxin requires activity of the *TRYPTOPHAN AMINOTRANSFERASE OF ARABIDOPSIS* (*TAA1*) gene together with *TRYPTOPHAN AMINOTRANSFERASE RELATED* genes (*TAR1* and *TAR2*), to produce indole-3-pyruvic acid (IPA), followed by activity of YUCCA flavin monooxygenase-like enzymes to convert IPA to IAA (Fig. 2; Stepanova et al. 2008; Mashiguchi et al. 2011; Robert et al. 2015). Models suggest that movement

of IAA into cells (influx) can occur passively, or can be bolstered by the AUXIN1/LIKE AUX1 (AUX1/LAX) plasma membrane transporter proteins (Marchant et al. 1999; Enders and Strader 2015), while movement of IAA out of cells (efflux) is mediated by multiple proteins from the PIN-FORMED family (for example, PIN1; Vernoux et al. 2000, Moller et al. 2009, Ganguly et al. 2010) and ATP-BINDING CASSETTE SUBFAMILY B (ABCB) proteins (Noh et al. 2001, Cho et al. 2013). The PIN1 auxin transporter localises to the plasma membrane and shows an asymmetric distribution in cells, which is consistent with its role in polar auxin efflux (reviewed by Remy and Duque 2014).

Within the cell, auxin is initially perceived by the TRANSPORT INHIBITOR RESPONSE 1 / AUXIN SIGNALING F-BOX (TIR1/AFB) proteins, leading to a series of events that activate auxin responsive genes (Fig. 2A,B). There are several models that explain auxin responses (Salehin et al. 2015). In the first model, INDOLE-3-ACETIC ACID INDUCIBLE (Aux/IAA) proteins bind to and repress AUXIN RESPONSE FACTOR (ARF) activator proteins that in turn bind the promoters of auxin-responsive genes; in the absence of auxin, the auxin responsive genes remain untranscribed (Farcot et al. 2015). This repression is partly mediated through recruitment of various co-repressor proteins by the Aux/IAAs, such as TOPLESS/TOPLESS-RELATED (TPL/TPR; Long et al. 2002). The Aux/IAA proteins can also bind TIR1/AFB proteins. When the TIR1/AFBs perceive and bind auxin via their leucine rich repeat repeats, this strengthens their interaction with Aux/IAA proteins and leads to Aux/IAA polyubiquitination and degradation via the proteasome (Worley et al. 2000; Ramos et al. 2001; Mockaitis and Estelle 2008). Hence, when auxin is perceived, the repression of ARFs by Aux/IAA is lifted, and the ARF proteins are able to regulate transcription of

auxin responsive target genes in a positive or negative manner depending on the ARF, the promoter sequence of the target gene and the interaction with additional coactivators or corepressors (Fig. 2; Lee et al. 2009; Farcot et al. 2015).

In the second model, ARF-Aux/IAA dimers are able to sequester ARF activators away from promoters, and upon the perception of auxin this repressive function is lifted, allowing the ARFs to be active on the auxin-responsive promoters (Farcot et al. 2015). In essence, Aux/IAA proteins are the primary responders to auxin and mediate downstream transcriptional responses through interactions with the ARF proteins. In Arabidopsis, 29 Aux/IAA proteins and 23 ARF proteins have been identified, in addition to six TIR1/AFBs (Ulmasov et al. 1997; Guilfoyle et al. 1998b; Parry et al. 2009).

Locating auxin in the reproductive organs and interactions between signalling components

As auxin cannot be directly quantified *in planta* by immunolabelling, various reporter genes have been employed to track its transport and accumulation in plant tissues. A number of these reporters are summarised in Table 1, highlighting cross-species functionality and in some cases, accumulation in specific reproductive tissues. In the Arabidopsis ovule, DR5rev::GFP is reproducibly detected in the young ovule primordia, subsequently in the tip of the nucellus and weakly in the funiculus, and after fertilisation in the integuments adjoining the micropyle and near the chalazal end of the fertilised female gametophyte (Fig. 1B,C; Benkova et al. 2003; Pagnussat et al. 2009). A similar pattern was observed for DR5:nlsGFP in young ovules from the daisy *Hieracium piloselloides* (Fig. 1D,E; Tucker et al. 2012), in early divergent angiosperms (Lora et

al. 2017) and in maize (Forestan and Varotto 2012; Lituiev et al. 2013). In maize, DR5rev::mRFPer shows abundant expression in antipodal cells at the chalazal pole of the female gametophyte (Chettoor and Evans 2015). A recent study in rice indicated that the DR5v2 marker accumulates in meristems and roots, but the pattern in ovule primordia and seeds was not reported (Yang et al. 2017). Moreover, another recent report indicates that in barley, the DR5v2 marker does not respond to auxin (Kirschner et al. 2018), although we have previously observed DR5v2:3xnlsYFP signal in proximal ovule tissues adjoining the female gametophyte in maturing ovules (Fig 1F,G).

In Arabidopsis, regions of the placenta about to give rise to the ovule primordium are marked by PIN3 expression (Larsson et al. 2014), while Pagnussat et al., (2009), showed that PIN1:GFP accumulates in the epidermal cells surrounding the germline until early gametophyte development (FG1 stage). This was later investigated by Bencivenga et al., (2012) in regards to the interactions between auxin signalling and genes involved in ovule patterning, which showed PIN1 is localised towards the apical pole of nucellar epidermal cells. *PIN1* orthologues have been identified in many angiosperm species (Kirschner et al., 2018; Bennett et al., 2014), and the location of expression in ovules has been reported for Arabidopsis, maize (Forestan et al., 2012; Lituiev et al., 2013) and theearly-divergent angiosperms Annona cherimola (custard apple) and *Persea americana* (avocado; Lora et al., 2017a). In all species where ovules have been examined, *PIN1* expression is observed in distal regions of the nucellus, showing polar localisation in epidermal cells, which likely coincides with the accumulation of auxin in the ovule tip prior to megasporogenesis (Forestan et al., 2012; Lituiev et al., 2013; Lora et al., 2017).

The role of auxin in ovule formation

In most angiosperms, the ovule primordium develops through protrusion of the placenta, quickly giving rise to distinct proximal and distal regions. Several studies in Arabidopsis have shown the essential role of auxin in placental protrusion and ovule number. Mutations in the auxin polar transport system, specifically *PIN1* (Vernoux et al. 2000), or inhibition of polar transport by chemical compounds (for example 9-hydroxyfluorene-9-carboxylic acid (HFCA) and 1-N-Naphthylphthalamic acid (NPA)) lead to a reduced number of ovule primordia (Okada et al., 1991). The actual role of auxin accumulation in the distal region of the ovule is not precisely defined, although it clearly accompanies outgrowth from the placenta and thereby mimics the growth of other tissues such as root tips (Friml et al., 2002; Benková et al., 2003).

The action of auxin is dependent upon another phytohormone, cytokinin, which accumulates in the proximal region of the ovule primordium in Arabidopsis (Bartrina et al., 2011). Similar to inhibition of the auxin transport pathway, mutants of the cytokinin receptor genes, *cre1-12 ahk2-2 ahk3-3*, produce fewer ovules (Riefler et al., 2006; Kinoshita-Tsujimura et Kakimoto, 2011), while mutations in the cytokinin oxidase/dehydrogenase (CKK) deactivating enzyme result in a larger number of ovule primordia. Bencivenga et al., (2012) suggest that in Arabidopsis, this relationship is achieved through the cytokinin-dependent regulation of *PIN1* expression; *PIN1* levels are reduced in *cre1-12 ahk2-2 ahk3-3* triple mutants while treatment with exogenous cytokinin increases *PIN1* expression (Bencivenga et al., 2012). Consistent with this, triple mutants of the *cytokinin reponse factor 2* (*crf2*) *crf3 crf6* (Cucinotta et al., 2016) show a reduced number of ovules and lower *PIN1* expression. In roots, the CRFs

modulate *PIN1* expression by binding to a specific *PIN CYTOKININ RESPONSE ELEMENT* (*PCRE*) in the *PIN1* promoter (Šimášková et al., 2015).

Auxin function during germline formation and female gametophyte growth

Apart from its role in ovule formation, auxin also fulfils an important role during subsequent stages of ovule growth. Upon establishment of the primary germline cell (megaspore mother cell; MMC), expression of *TAA1* is detected in the chalazal nucellus and inner integument primordia (Ceccato et al. 2013; Robert et al. 2015), which is complemented by expression of *PIN1* and DR5 markers in the distal nucellar tissue (Pagnussat et al. 2009, Bencivenga et al. 2012). A similar pattern of PIN1 expression has been observed in custard apple, avocado (Lora et al. 2017) and maize (Forestan et al. 2012). This pattern suggests that as ovule development proceeds, auxin is synthesised in the base and transported into the nucellar tissue surrounding the MMC, where it affects a response as the ovule progresses through meiosis and early (FG1 and FG2) stages of gametophyte development.

Genetic and molecular studies indicate that PIN1 expression is organised by the transcription factors *WUSCHEL* (*WUS*), *SPOROCYTLESS* (*SPL*) and *BELL1* (*BEL1*), whereby *WUS* responds to cytokinin, inducing nucellar expression of *SPL* and chalazal expression of *BEL1*. SPL and BEL1 activate and repress PIN1 expression, respectively (Bencivenga et al. 2012). Other studies suggest that genes involved in auxin response may restrict MMC formation to one cell (Su et al. 2017). Mutations in components of the THO/TREX (TRanscription Export) complex, which contributes to the biogenesis of specific inhibitory small RNA molecules (ta-siRNAs; (Jauvion et al. 2010; Yelina et

al. 2010), result in the formation of supernumerary MMC-like cells. Some ta-siRNAs target *ARF* family members for repression, such as *ARF3* and *ARF4*, through tasiR-ARF (Fei et al. 2013). Consistent with incorrect regulation of *ARF3* in THO/TREX mutants, ectopic expression of *ARF3* in wild-type ovules results in supernumerary MMC-like cells (Su et al. 2017).

Auxin also functions during integument formation. *ABERRANT TESTA SHAPE* (*ATS*) is a *KANADI* (*KAN*) transcription factor that maintains tissue boundaries during ovule development (McAbee et al., 2006). Studies have shown that ATS physically interacts with ARF3, otherwise known as *ETTIN* (*ETT*), and both genes are co-expressed within the inner integument. Single or double mutants in *ETT* or *ATS* result in congenital fusion of the integuments, highlighting an auxin-dependent regulatory pathway involved in integument differentiation (Kelley et al., 2012). Further work conducted by Lora et al., (2015) suggests that *ETT* orthologues in *Prunus* species are also required for bitegmic ovule formation. This is consistent with a conserved function of *ATS* and *ETT* during integument growth.

As megagametogenesis proceeds (Figure 1), expression of TAA1 is detected at the micropylar end of the developing female gametophyte in addition to the pre-existing expression in the chalaza and inner integument (Ceccato et al. 2013; Panoli et al. 2015). Concurrently, expression of the *YUCCA* family genes *YUC1*, *YUC2* and *YUC8* begins in the micropylar end of the FG, suggesting that auxin is synthesised in a polar manner (Pagnussat et al. 2009; Panoli et al. 2015; Larsson et al. 2017). Expression of *YUC1*, *YUC2* and *YUC8* is maintained until the FG6 stage of female gametophyte development, whereas *TAA1* expression is maintained until gametogenesis is complete. In contrast, expression of PIN1 in Arabidopsis has not been observed from

the FG3 stage onwards, indicating that auxin required for female gametophyte development may arise in the gametophyte itself, and if transport into the nucellus is required, it may follow a different mechanism. Consistent with these observations, mutations in *YUC8* lead to mitotic arrest during megagametogenesis (Panoli et al. 2015). Moreover, when auxin responses are specifically dampened in the female gametophyte by downregulation of *ARF* genes such as *ARF1* to *8* and *ARF19*, ovules produce defective female gametophytes that cannot be fertilized despite developing to maturity (Pagnussat et al. 2009).

The sustained expression of both *TAA1* and *YUC* throughout Arabidopsis female gametophyte development, and the apparent block of auxin transport from FG3 suggests that the female gametophyte may be enriched for auxin. Contrasting this, recent reports have only described expression of the DR5 auxin marker within the egg cell and synergids, reducing in expression before turning off at FG6 (Panoli et al. 2015), and in the micropylar nucellus from FG6 onward (Lituiev et al. 2013). This is different from that observed in maize, where from FG6 onwards, PIN1 and DR5 are expressed in the nucellar cells flanking the female gametophyte and in the chalazal cluster of antipodals (Chettoor et al. 2015). PIN1 is additionally expressed in the nucellar cells at the chalazal end of the female gametophyte. Hence, it is unclear whether auxin synthesised in the maize gametophyte acts locally, or is transported out of the chalazal end of the female gametophyte and into the surrounding nucellus to elicit auxin-dependent responses.

A role for auxin after fertilisation

Angiosperm seed development initiates when the paternal and maternal gametes fuse to create the diploid embryo and the triploid endosperm (Olsen 2004; Becraft and Yi 2011; Yan et al. 2014). In general, the mature seed consists of three main structures: the seed coat (originating from the integuments), endosperm and embryo (both originating from the gametophyte). Each of these structures comprise multiple tissues derived through synchronised patterns of proliferation and differentiation (Chaudhury et al. 2001). Although the three structures exhibit different morphology and functions, they must coordinate their growth in order to achieve seed viability (Ingram 2010; Figueiredo and Kohler 2018). Two recent studies provide insight regarding the role of auxin during these events. Figueiredo et al. (2018) show that Arabidopsis seeds containing an excess dosage of paternal genomes over-accumulate auxin in the endosperm, and this leads to an inhibition of endosperm cellularisation. Increased activity of DR5v2::VENUS in these seeds was most prominent in the seed coat, consistent with a previous study that showed auxin generated by the fertilization products may be rapidly transported to the seed coat to support sporophytic development (Figueiredo et al. 2016). However, in another study Robert et al. (2018) suggest that auxin biosynthesis in the integuments co-ordinates early development of the embryo, ensuring correct establishment of an apical/basal axis. The authors conclude that the source of auxin in this case is not the endosperm, since only maternal loss of auxin biosynthesis via mutations in *TAA1* (*wei8*) and *TAA-RELATED 1* (*tar1*) induces early defects in embryo development similar to those in which auxin-dependent establishment of apical identity in the proembryo is compromised. Hence, a complex interplay between auxin synthesis and transport in both maternal and filial

tissues coordinates early development of the seed. This is an interesting riddle, particularly in the context of the cereals where the endosperm is a much more prominent component of the seed, grain quality and yield.

Translating knowledge of auxin from Arabidopsis to the cereals

In a recent publication, Locascio et al. (2014) provide a review of auxin function during maize seed development in comparison to Arabidopsis. From this report and others, it is clear that some aspects of the auxin pathway differ across different plant species, especially between monocots and eudicots (McSteen 2010; Poulet and Kriechbaumer 2017). For example, in Arabidopsis, extremely weak or no developmental defects are observed in single auxin biosynthetic gene knockouts due to genetic redundancy (Cheng et al. 2006, 2007; Stepanova et al. 2008; Tao et al. 2008). However in monocot species such as maize, *Brachypodium* and rice, mutations in auxin biosynthetic genes such as *TAA1* lead to dramatic developmental defects (Abu-Zaitoon et al. 2012; Pacheco-Villalobos et al. 2013; Yoshikawa et al. 2014; Pacheco-Villalobos et al. 2016). Conversely in monocots, auxin transporter genes such as PIN1 appear to have more redundant copies than Arabidopsis; for example, two copies of *PIN1* exist in barley, *HvPIN1a* and *HvPIN1b* (O'Connor et al. 2014), versus one for Arabidopsis. Single *pin1* mutants in Arabidopsis fail to develop flowers, while no complete *pin1* knockout phenotypes in the cereals have been reported to date (Galweiler et al. 1998; Xu et al. 2005).

To explore additional aspects of auxin function during cereal grain development, the following sections focus on the role of auxin in somatic tissue (pericarp) at the grain periphery, and in the endosperm tissues located within.

Auxin and the cereal pericarp

The seed coat and hull are derived from the integuments and ovary wall, and protect the endosperm and embryo tissues throughout seed development and after dehiscence. Cell division in the pericarp of barley ceases as early as 2 days after fertilisation and further growth depends on cell expansion (Radchuk et al. 2011), which influences the final shape and size of the caryopsis (Ugarte et al. 2007). Auxin is one of the key drivers of cell expansion (Perrot-Rechenmann 2010; Kutschera and Wang 2016) and induces H+-ATPases, K+ channels, expansins and cell wall remodelling enzymes (Ringli 2010). Expression of various auxin transport and metabolic genes have been detected in barley pericarp tissues, including the biosynthetic *YUCCA* enzymes, the auxin repressor indole-3-acetic acid-amido synthetases, efflux (*PIN*/*ABCB*) and influx (*AUX1*/*LAX*) transporters (Pielot et al. 2015). Array-based transcript profiling during pericarp development showed auxin transporter genes are predominantly expressed during early stages, while auxin biosynthetic enzymes are only expressed during later stages of development (Pielot et al. 2015). This suggests that during early stages of seed growth, auxin is not synthesised in the pericarp but is imported, and PIN- and ABCB-type efflux transporters possibly generate and maintain required auxin levels.

Auxin and the cereal endosperm

The inner parts of the seed adjoining the seed coat and pericarp include the starchy endosperm and aleurone. The aleurone constitutes the epidermal cell layer of the endosperm and separates hull tissues from the inner starchy endosperm. Aleurone cell differentiation occurs in response to surface position but the effect of maternal versus filial signals has been debated (Gruis et al. 2006; Reyes et al. 2010). Several studies suggest that phytohormones fulfil a prominent role in this process (Geisler-Lee and Gallie 2005; Bethke et al. 2006; Forestan et al. 2010). In maize, application of the auxin inhibitor NPA, which inhibits polar auxin transport and disrupts IAA distribution, results in the development of up to four aleurone cell layers instead of the usual one (Forestan et al. 2010). This phenotype may be due to auxin being trapped in the kernel, similar to that seen for NPA-treated ovules in *Hieracium* (Tucker et al. 2012). Each aleurone layer showed ectopic expression of *PIN1* genes and uniform PIN1 distribution, along with auxin accumulation (Forestan et al. 2010). This indicates that auxin accumulation in the aleurone layer in not solely controlled by PIN1 expression and other auxin transporters expressed in the aleurone or pericarp may have a more prominent role in aleurone cell fate.

Adjoining the aleurone, the starchy endosperm is the largest tissue within the cereal seed and accumulates starch and storage proteins to be metabolised by the embryo during germination. Starchy endosperm cells are generated from the first periclinal cell division of the endosperm during cellularisation, while the external cells will differentiate into aleurone (Becraft and Asuncion-Crabb, 2000; Geisler-Lee and Gallie, 2005). Starchy endosperm cells undergo rapid growth, accumulate starch and storage proteins, and initiate endoreduplication (Sabelli 2012), and as such are major

contributors to grain size and grain weight (Li and Yang 2017). In maize and rice, auxin activity is detected during early endosperm development using the *DR5* auxin reporter (Chen et al. 2014; Yang et al. 2017), which correlates with accumulation of IAA in the endosperm (Chourey et al. 2010; Abu-Zaitoon et al. 2012). After fertilisation in maize, PIN1 is up-regulated in the endosperm and localises to the plasma membrane during cellularisation (Forestan et al. 2010). Once the endosperm is fully cellularised, PIN1 becomes confined to the chalazal endosperm region where auxin accumulates, coinciding with the stage when endosperm transfer cells begin to differentiate (Forestan et al. 2010). In the maize mutant *defective endosperm-B18* (*de18*), endosperm IAA levels are severely reduced and the endosperm shows lower total cell number, smaller cell volume and a reduced level of endoreduplication, but defects can be restored by exogenous application of auxin (Torti et al. 1986; Bernardi et al. 2012). Some of the observed defects may be due to abnormal function of the endosperm transfer cells (ETC), which facilitate transport of substances between the maternal tissues and the endosperm (Thiel 2014). The *de18* mutant also shows reduced accumulation of auxin in the transfer cells, and defects in their polarisation and differentiation (Forestan and Varotto 2012). This implicates auxin in maintaining endosperm development in maize by establishing communication pathways between the maternal and filial tissues.

Studies also show an important role for auxin during grain fill in rice. The rice *THOUSAND GRAIN WIGHT 6* (*TGW6*) gene encodes a novel protein with indole-3-acetic acid (IAA)-glucose hydrolase activity. TGW6 controls IAA supply to sink organs, thereby influencing the timing of the syncytial to cellular transition in the endosperm, cell number and grain length (Ishimaru et al. 2013). Also, in rice, mutations in *OsARF4*

lead to an increase in grain size, possibly as a result of de-repression of auxin-responsive genes (Hu et al. 2018). In addition, Liu et al. (2015) isolated a dominant mutant *big grain1-D* (*Bg1-D*) that produces extra-large grains caused by overexpression of the *BG1* gene. *BG1* encodes a novel membrane-localised protein and may physically interact with auxin transporters (Liu et al. 2015; Mishra et al. 2017), and *Bg1-D* mutants exhibit increased basipetal auxin transport and altered auxin distribution suggesting a role in regulating auxin transport.

Taken together, these studies provide compelling evidence for a role of auxin during cereal endosperm development. In light of the recent advances regarding auxin supply during Arabidopsis seed development (discussed above), future studies in the cereals might consider the maternal or filial origin of the auxin in greater detail, while also assessing the tissue-specific nature of auxin responses in different grain tissues.

Expression dynamics of the auxin signalling pathway in barley

The extensive molecular characterisation of the auxin signalling pathway in Arabidopsis provides an opportunity to assess the broader molecular conservation of auxin-related pathways in agriculturally relevant cereal crops. As described in the preceding sections, some insight has already been provided through studies in maize, rice and barley. These confirm that auxin fulfils key functions during reproductive development in a window spanning ovule initiation through to fertilisation, which has a major impact on grain yield (Alqudah et al. 2014; Wurschum et al. 2018). Because auxin plays such a prominent role in cell growth and tissue formation, it is a promising candidate for the regulation of inter cultivar differences in organ size, floret fertility and

the differentiation of tissues in the seed. In the final section of this review, we summarise molecular and phylogenetic details of the auxin signalling pathway (Fig 2). We focus in particular on barley a diploid cereal that has not been extensively studied in terms of auxin responses, but for which considerable transcriptomic, mutant and yield-data resources might be used to highlight key auxin-related genes for further study (Fig. 3).

Auxin perception and the *TIR1*/*AFB* genes

In Arabidopsis, the six TIR1/AFB genes are expressed throughout the plant, particularly in areas of cell division and expansion (Dharmasiri et al. 2005a; Dharmasiri et al. 2005b; Parry et al. 2009). Of these genes, *AtTIR1*, *AtAFB1*, *2*, *3* and *5* have been shown to function as auxin receptors (Dharmasiri et al. 2005a; Dharmasiri et al. 2005b; Kepinski and Leyser 2005; Parry et al. 2009; Calderon Villalobos et al. 2012). Five *TIR1*/*AFB* genes are present in rice, barley and sorghum, while six are present in *Brachypodium* (Fig. 4). Phylogenetic analysis indicates that the cereal genes cluster in five main groups, showing broad homology to the *AtTIR1*/*AtAFB1*, *AtAFB2*/*3* and *AtAFB4*/*5* genes from Arabidopsis. Based on publically available RNAseq data from 8 different barley tissues (IBGS 2012), *HvTIR1*, *HvAFB2* and *HvAFB4* are the most abundant members of this family. Along with *HvAFB3* and *HvAFB5*, they show highest expression in the 5 to 15mm inflorescence samples (Table 2). RNAseq data from developing pistils and seeds (minus embryos; Aubert et al. 2018) indicates that all five *HvTIR*/*AFB* genes are most abundant in the female tissues prior to fertilisation, although *HvTIR1* and *HvAFB2* maintain expression during the early stages of seed development (Fig 3A,D).

Auxin signalling and the Aux/IAA genes

The Aux/IAA proteins contain four key domains (Paul et al. 2016; Wu et al. 2017; Luo et al. 2018); domain I recruits TPL/TPR co-repressors to enhance repression of ARF target genes, domain II facilitates interaction with the TIR1/AFB proteins (Worley et al. 2000; Ramos et al. 2001; Lee et al. 2009), and domains III and IV facilitate interaction with ARF activator proteins and dimerisation between Aux/IAA proteins (Ulmasov et al. 1997; Guilfoyle et al. 1998a). These domains are sometimes absent, depending on the gene and species (Luo et al. 2018). According to current estimates, 32 Aux/IAA proteins are present in rice (although 31 are reported in some studies; (Jain et al. 2006), 28 in sorghum, 27 in Brachypodium and 27 in barley (excluding a likely pseudogene HORVU2Hr1G027570), compared with the 29 present in Arabidopsis. Despite generally low support values for a number of clades, many of the cereal Aux/IAA sequences show closer homology to each other than to the Arabidopsis genes and mixed Arabidopsis/Poales clades were only found in a few cases; *AtIAA33* - *OsIAA33*, *AtIAA18*/*26*/*28* - *OsIAA7*, *AtIAA10/11/12/13/29/32/34* - *OsIAA10*, and *AtIAA20/30/31* - *OsIAA4/8/9/20* (Fig. 5). Some gene duplication/diversification appears to have occurred in the grasses; for example, *OsIAA22*/*25*, *OsIAA4*/*8* and *OsIAA28*/*29* duplications appear to be restricted to rice, while barley appears to lack *OsIAA17*, *18* and *24* orthologues. In addition, two genes showing high homology to *OsIAA5* are present in

barley but only one is found in Brachypodium, sorghum and rice. Based on tissue RNAseq data (Table 2), multiple *HvIAA* genes are highly expressed in the internodes of barley, but *HvIAA3*, *21*, *28* and *30* are highly abundant during inflorescence and/or caryopsis development. *HvIAA1*, *2*, *10*, *16*, *19* and *31* expression is also detected in

the reproductive tissues (Table 2). In the developmental series of pistil and seed samples, expression of *HvIAA3*, *11*, *21*, *28* and *31* is prominent (Fig. 3B). *HvIAA28* and *HvIAA5* show unique patterns that may suggest a role during the early stages of seed development (Fig. 3D).

Auxin response and the *ARF* genes

The ARF transcription factors (Hagen 2015; Li et al. 2016) contain a conserved B3 DNA-binding domain (DBD) at their N-terminus that binds auxin responsive elements (AuxRE; Quint and Gray 2006). A dimerisation domain (DD) is also present within the DBD that facilitates interactions between two ARF proteins (Boer et al. 2014). The middle region of the ARF proteins determines whether they act as an activator or repressor of auxin signalling (Quint and Gray, 2006) and the C-terminus of the ARF proteins contains a protein-protein interaction domain that shares homology with domains III and IV in Aux/IAA proteins. This allows ARF proteins to interact with Aux/IAA proteins in homodimers, heterodimers or large oligomers. ARF proteins are thought to act in several ways as previously summarised (Finet and Jaillais 2012; Finet et al. 2013). ARF activators mediate auxin-dependent transcriptional regulation as shown in Fig. 1, while ARF repressors have limited interactions with other ARF and Aux/IAA proteins (Vernoux et al. 2011). Compared to Arabidopsis where 23 ARF genes are present, 25 are present in rice (Wang et al. 2007), 25 in sorghum, 24 in Brachypodium and 23 in barley. Phylogenetic analysis highlights a range of clades containing genes from both Arabidopsis and the grasses, while some clades are expanded in the cereals such as *OsARF6*/*17* and *OsARF5*/*19*/*21* in Clade A, *OsARF3*/*14* and *OsARF23*/*24* in Clade B and *OsARF8*/*10* in Clade C (Fig. 6). Although

the naming of the proteins is not always consistent between the species based on the clade names (Finet et al., 2012), the clade structure that generally separates activators (Clade A) from repressors (Clades B and C) is maintained in the Arabidopsis/Poales tree. Several notable genomic differences are apparent for the HvARF genes compared to the other grasses; two Clade C *HvARF10* genes appear to be present along with three Clade B *HvARF4* genes, while an *OsARF23* and *OsARF24* homologue appear to be lacking. Most of the *HvARF* genes show maximum expression in the inflorescence and caryopsis tissues (Table 2), and the pistil/seed datasets suggest that most of these are expressed during pre-fertilisation stages (Fig. 3C). The Clade B *ARF* genes *HvARF4c*, *HvARF4*, *HvARF9* and *HvARF17* are the most prominent during pistil development. In contrast to the majority of ARF genes, only a few show patterns of expression that peak after fertilisation (e.g. *HvARF1*, *3*, *10b* and *13*). However, expression of these genes is generally low in the whole organ datasets, suggesting they may fulfil more specific roles in isolated regions of the seed.

Transcriptional signatures of the auxin-signalling pathway during caryopsis development

Based on these published datasets and other studies (Thiel et al. 2011; Pielot et al. 2015), most genes in the auxin signalling pathway are expressed during early stages of barley pistil development, while the number dramatically decreases during the middle stages of grain development. High expression appears to coincide with stages where maternal tissues are actively proliferating to establish an environment suitable for seed development, and/or when early divisions of the endosperm are taking place. The low abundance of most transcripts after fertilisation is intriguing; although

comparisons with pre-fertilisation measurements are lacking, auxin (IAA) levels clearly increase during maize endosperm and rice grain development (Lur and Setter, 1993; Abu-Zaitoon et al. 2012), which is consistent with an important role during these stages. One possibility is that there is considerable specialisation of ARF and AuxIAA genes, with multiple family members fulfilling key roles during the diverse processes associated with pre-fertilisation ovule and gametophyte development, and only specific members during the less complex events of endosperm differentiation. Clustering of barley genes based on relative expression (normalised to the maximum expression value for each gene) in the tissue series highlights a number of interesting patterns for specific ARF and Aux/IAA genes (Fig. 3D). For example, the patterns of *HvIAA16*/*19* and *HvARF41*/*b*/*c* genes in young pistils, *HvIAA5b/6/9/12* and *HvARF19*/*21* genes in late pistils, and *HvIAA5a/HvIAA11/HvIAA28* and *HvARF10b*/*13* in young seeds might justify further investigation. One important point to note is that the resolution of the RNA-seq datasets currently available for barley is limited to a few stages of pistil and grain development without separation of tissues. This makes it difficult to propose hypotheses on tissue- and development-specific regulatory processes and is something that might be addressed in future research.

Perspectives

The aim of this review was to consider the role of auxin signalling during ovule and seed development in Arabidopsis and cereal species. The literature provides compelling evidence for key roles in ovule initiation, germline formation and progression, integument growth, endosperm and embryo development. Many aspects

of these roles appear to be conserved across the eudicot / monocot (Poales) divide, although the location of auxin synthesis and transport appears to differ due to morphological constraints in ovule and seed development. How these findings might be applied in the context of agriculture is yet to be explored in detail, but there is enough evidence to suggest that new strategies for yield improvement might be achieved through modification of cell-type or tissue-specific pathways during reproduction. Analysis of the auxin signalling pathway provides a number of candidate targets to implement this. Auxin synthesis, transport and response is dynamic during ovule and seed development, with localised pulses occurring in different tissues and stages as development proceeds. If this information can be combined with modern techniques that provide refined cell-type specific gene expression analysis, methylation and chromatin status, it should be possible to tailor specific auxin responses through modification of specific genes and regulatory motifs. In principal, this could allow pleiotropic effects of mutations to be dampened, while the desired effect can be achieved in the cell, tissue or stage of choice.

Acknowledgements

We thank members of the Tucker laboratory, Tobias Würschum and Christopher Davies for fruitful discussions. We apologise to authors whose work we did not cite due to space constraints. We acknowledge funding from the Australian Research Council (FT140100780 & DP180104092), the Grains Research Development Corporation (GRS10938) and the University of Adelaide.

Author contributions

All authors contributed to the writing and editing of the manuscript.

References

Abu-Zaitoon YM, Bennett K, Normanly J, Nonhebel HM (2012) A large increase in IAA during development of rice grains correlates with the expression of tryptophan aminotransferase *OsTAR1* and a grain-specific *YUCCA*. ***Physiologia Plantarum*** 146, 487-499.

Alqudah AM, Sharma R, Pasam RK, Graner A, Kilian B, Schnurbusch T (2014) Genetic dissection of photoperiod response based on GWAS of pre-anthesis phase duration in spring barley. ***PLoS One*** 9, e113120.

Anastasiou E, Kenz S, Gerstung M, MacLean D, Timmer J, Fleck C, Lenhard M (2007) Control of plant organ size by KLUH/CYP78A5-dependent intercellular signaling. ***Dev Cell*** 13, 843-856.

Aubert, MK, Coventry, S, Shirley, NJ, Betts NS, Wurschum, T, Burton RA, Tucker MR (2018). Differences in hydrolytic enzyme activity accompany natural variation in mature aleurone morphology in barley (*Hordeum vulgare* L.). ***Sci Rep*** 8(1): 11025.

Becraft PW, Yi G (2011) Regulation of aleurone development in cereal grains. ***J Exp Bot*** 62, 1669-1675.

Bencivenga S, Colombo L, Masiero S (2011) Cross talk between the sporophyte and the megagametophyte during ovule development. ***Sex Plant Reprod*** 24, 113-121.

Bencivenga S, Simonini S, Benková E, Colombo L (2012) The transcription factors *BEL1* and *SPL* are required for cytokinin and auxin signaling during ovule development in *Arabidopsis*. ***Plant Cell*** 24, 2886-2897.

Bender RL, Fekete ML, Klinkenberg PM, Hampton M, Bauer B, Malecha M, Lindgren K, J AM, Perera MA, Nikolau BJ, Carter CJ (2013) PIN6 is required for nectary auxin response and short stamen development. ***Plant J*** 74, 893-904.

Benkova E, Michniewicz M, Sauer M, Teichmann T, Seifertova D, Jurgens G, Friml J (2003) Local, Efflux-Dependent Auxin Gradients as a Common Module for Plant Organ Formation. ***Cell*** 115, 591-602.

Bernardi J, Lanubile A, Li QB, Kumar D, Kladnik A, Cook SD, Ross JJ, Marocco A, Chourey PS (2012) Impaired auxin biosynthesis in the *defective endosperm18* mutant is due to mutational loss of expression in the *ZmYUC1* gene encoding endosperm-specific YUCCA1 protein in maize. ***Plant Phys*** 160, 1318-1328.

Bethke PC, Hwang YS, Zhu T, Jones RL (2006) Global patterns of gene expression in the aleurone of wild-type and *dwarf1* mutant rice. ***Plant Phys*** 140, 484-498.

Blilou I, Frugier F, Folmer S, Serralbo O, Willemsen V, Wolkenfelt H, Eloy NB, Ferreira PC, Weisbeek P, Scheres B (2002) The *Arabidopsis HOBBIT* gene encodes a *CDC27* homolog that links the plant cell cycle to progression of cell differentiation. ***Genes Dev*** 16, 2566-2575.

Blilou I, Xu J, Wildwater M, Willemsen V, Paponov I, Friml J, Heidstra R, Aida M, Palme K, Scheres B (2005) The PIN auxin efflux facilitator network controls growth and patterning in *Arabidopsis* roots. ***Nature*** 433, 39-44.

Boer DR, Freire-Rios A, van den Berg WA, Saaki T, Manfield IW, Kepinski S, Lopez-Vidrieo I, Franco-Zorrilla JM, de Vries SC, Solano R, Weijers D, Coll M (2014) Structural basis for DNA binding specificity by the auxin-dependent ARF transcription factors. ***Cell*** 156, 577-589.

Brown RC, Lemmon BE, Nguyen H, Olsen OA (1999) Development of endosperm in *Arabidopsis thaliana*. ***Sex Plant Reprod*** 12, 32-42.

Brunoud G, Wells DM, Oliva M, Larrieu A, Mirabet V, Burrow AH, Beeckman T, Kepinski S, Traas J, Bennett MJ, Vernoux T (2012) A novel sensor to map auxin response and distribution at high spatio-temporal resolution. ***Nature*** 482, 103-106.

Calderon Villalobos LI, Lee S, De Oliveira C, Ivetac A, Brandt W, Armitage L, Sheard LB, Tan X, Parry G, Mao H, Zheng N, Napier R, Kepinski S, Estelle M (2012) A combinatorial TIR1/AFB- Aux/IAA co-receptor system for differential sensing of auxin. ***Nat Chem Biol*** 8, 477-485.

Ceccato L, Masiero S, Sinha Roy D, Bencivenga S, Roig-Villanova I, Ditengou FA, Palme K, Simon R, Colombo L (2013) Maternal control of PIN1 is required for female gametophyte development in Arabidopsis. ***PLoS One*** 8, e66148.

Chaudhury AM, Koltunow A, Payne T, Luo M, Tucker MR, Dennis ES, Peacock WJ (2001) Control of early seed development. ***Annu Rev Cell Dev Biol*** 17, 677-699.

Chen JY, Lausser A, Dresselhaus T (2014) Hormonal responses during early embryogenesis in maize. ***Biochemical Society Transactions*** 42, 325-331.

Chen Y, Yordanov YS, Ma C, Strauss S, Busov VB (2013) DR5 as a reporter system to study auxin response in Populus. ***Plant Cell Rep*** 32, 453-463.

Cheng YF, Dai XH, Zhao YD (2006) Auxin biosynthesis by the YUCCA flavin monooxygenases controls the formation of floral organs and vascular tissues in *Arabidopsis*. **Genes Dev** 20, 1790- 678 1799.

Cheng YF, Dai XH, Zhao YD (2007) Auxin synthesized by the YUCCA flavin monooxygenases is essential for embryogenesis and leaf formation in *Arabidopsis*. ***Plant Cell*** 19, 2430-2439.

Chettoor AM, Evans MM (2015) Correlation between a loss of auxin signaling and a loss of proliferation in maize antipodal cells. ***Front Plant Sci*** 6, 187.

Cho, M, Cho H (2013) The function of ABCB transporters in auxin transport. Plant ***Signaling & Behavior*** 8(2): e22990.

Chourey PS, Li QB, Kumar D (2010) Sugar-hormone cross-talk in seed development: Two redundant pathways of IAA biosynthesis are regulated differentially in the *Invertase-deficient miniature1* (*mn1*) seed mutant in maize. ***Mol Plant*** 3, 1026-1036.

Dal Bosco C, Dovzhenko A, Liu X, Woerner N, Rensch T, Eismann M, Eimer S, Hegermann J, Paponov IA, Ruperti B, Heberle-Bors E, Touraev A, Cohen JD, Palme K (2012) The endoplasmic reticulum localized PIN8 is a pollen-specific auxin carrier involved in intracellular auxin homeostasis. ***Plant J*** 71, 860-870.

Dharmasiri N, Dharmasiri S, Estelle M (2005a) The F-box protein TIR1 is an auxin receptor. ***Nature*** 435, 441-445.

Dharmasiri N, Dharmasiri S, Weijers D, Lechner E, Yamada M, Hobbie L, Ehrismann JS, Jurgens G, Estelle M (2005b) Plant development is regulated by a family of auxin receptor F box proteins. ***Dev Cell*** 9, 109-119.

Dumas C, Rogowsky P (2008) Fertilization and early seed formation. ***Comptes Rendus Biologies*** 331, 715-725.

Enders TA, Strader LC (2015) Auxin activity: Past, present, and future. ***Am J Bot*** 102, 180-196.

Farcot E, Lavedrine C, Vernoux T (2015) A modular analysis of the auxin signalling network. ***PLoS One*** 10, e0122231.

Fei Q, Xia R, Meyers BC (2013) Phased, secondary, small interfering RNAs in post transcriptional regulatory networks. ***Plant Cell*** 25, 2400-2415.

Figueiredo DD, Batista RA, Kohler C (2018) Auxin regulates endosperm cellularization in *Arabidopsis*. ***bioRxiv***.

Figueiredo DD, Batista RA, Roszak PJ, Hennig L, Kohler C (2016) Auxin production in the endosperm drives seed coat development in *Arabidopsis*. ***Elife*** 5.

Figueiredo DD, Kohler C (2018) Auxin: a molecular trigger of seed development. ***Genes & Development*** 32, 479-490.

Finet C, Berne-Dedieu A, Scutt CP, Marletaz F (2013) Evolution of the *ARF* gene family in land plants: old domains, new tricks. ***Mol Biol Evol*** 30, 45-56.

Finet C, Jaillais Y (2012) Auxology: when auxin meets plant evo-devo. ***Dev Biol*** 369, 19-31.

Forestan C, Meda S, Varotto S (2010) ZmPIN1-mediated auxin transport is related to cellular differentiation during maize embryogenesis and endosperm development. ***Plant Physiol*** 152, 1373-1390.

Forestan C, Varotto S (2012) The role of PIN auxin efflux carriers in polar auxin transport and accumulation and their effect on shaping maize development. ***Mol Plant*** 5, 787-798.

Friml J, Benkova E, Blilou I, Wisniewska J, Hamann T, Ljung K, Woody S, Sandberg G, Scheres B, Jurgens G, Palme K (2002) *AtPIN4* mediates sink-driven auxin gradients and root patterning in Arabidopsis. ***Cell*** 108, 661-673.

Gallavotti A, Yang Y, Schmidt RJ, Jackson D (2008) The Relationship between auxin transport and maize branching. ***Plant Physiol*** 147, 1913-1923.

Galweiler L, Guan CH, Muller A, Wisman E, Mendgen K, Yephremov A, Palme K (1998) Regulation of polar auxin transport by *AtPIN1* in *Arabidopsis* vascular tissue. ***Science*** 282, 2226-2230.

Ganguly A, Lee SH, Cho M, Lee OR, Yoo H, Cho H (2010) Differential Auxin-Transporting Activities of PIN-FORMED Proteins in Arabidopsis Root Hair Cells. ***Plant Physiol*** 153, 1046-1061.

Geisler-Lee J, Gallie DR (2005) Aleurone cell identity is suppressed following connation in maize kernels. ***Plant Physiol*** 139, 204-212.

Gonzalez-Navarro OE, Griffiths S, Molero G, Reynolds MP, Slafer GA (2016) Variation in developmental patterns among elite wheat lines and relationships with yield, yield components and spike fertility. ***Field Crops Res*** 196, 294-304.

Gruis D, Guo HN, Selinger D, Tian Q, Olsen OA (2006) Surface position, not signaling from surrounding maternal tissues, specifies aleurone epidermal cell fate in maize. ***Plant Physiol*** 141, 737 898-909.

Guilfoyle T, Hagen G, Ulmasov T, Murfett J (1998a) How does auxin turn on genes? ***Plant Physiol*** 118, 341-347.

Guilfoyle TJ, Ulmasov T, Hagen G (1998b) The ARF family of transcription factors and their role in plant hormone- responsive transcription. ***Cell. Mol. Life. Sci***. 54, 619-627.

Guo Z, Chen D, Schnurbusch T (2015) Variance components, heritability and correlation analysis of anther and ovary size during the floral development of bread wheat. ***J Exp Bot*** 66, 3099-3111.

Guo Z, Slafer GA, Schnurbusch T (2016) Genotypic variation in spike fertility traits and ovary size as determinants of floret and grain survival rate in wheat. ***J Exp Bot*** 67, 4221-4230.

Hagen G (2015) Auxin signal transduction. ***Essays Biochem*** 58, 1-12.

Hand ML, Koltunow AM (2014) The genetic control of apomixis: asexual seed formation. ***GENETICS*** 197, 441-450.

Heisler MG, Ohno C, Das P, Sieber P, Reddy GV, Long JA, Meyerowitz EM (2005) Patterns of auxin transport and gene expression during primordium development revealed by live imaging of the *Arabidopsis* inflorescence meristem. ***Curr Biol*** 15, 1899-1911.

Hu Z, Lu SJ, Wang MJ, He H, Sun L, Wang H, Liu XH, Jiang L, Sun JL, Xin X, Kong W, Chu C, Xue HW, Yang J, Luo X, Liu JX (2018) A Novel QTL *qTGW3* Encodes the GSK3/SHAGGY-Like Kinase *OsGSK5*/*OsSK41* that Interacts with *OsARF4* to Negatively Regulate Grain Size and Weight in Rice. ***Mol Plant*** 11, 736-749.

IBGS (2012) A physical, genetic and functional sequence assembly of the barley genome. ***Nature*** 491, 711-716.

Ingram GC (2010) Family life at close quarters: communication and constraint in angiosperm seed development. ***Protoplasma*** 247, 195-214.

Ishimaru K, Hirotsu N, Madoka Y, Murakami N, Hara N, Onodera H, Kashiwagi T, Ujiie K, Shimizu B, Onishi A, Miyagawa H, Katoh E (2013) Loss of function of the IAA-glucose hydrolase gene *TGW6* enhances rice grain weight and increases yield. ***Nat Genet*** 45, 707-711.

Jain M, Kaur N, Garg R, Thakur JK, Tyagi AK, Khurana JP (2006) Structure and expression analysis of early auxin-responsive *Aux*/*IAA* gene family in rice (Oryza sativa). ***Funct Integr Genomics*** 6, 47-59.

Jauvion V, Elmayan T, Vaucheret H (2010) The conserved RNA trafficking proteins HPR1 and TEX1 are involved in the production of endogenous and exogenous small interfering RNA in Arabidopsis. ***Plant Cell*** 22, 2697-2709.

Jun N, Gaohang W, Zhenxing Z, Huanhuan Z, Yunrong W, Ping W (2011) *OsIAA23*-mediated auxin signaling defines postembryonic maintenance of QC in rice. ***Plant J*** 68, 433-442.

Kepinski S, Leyser O (2005) The Arabidopsis F-box protein TIR1 is an auxin receptor. ***Nature*** 435, 446-451.

Kirschner GK, Stahl Y, Imani J, von Korff M, Simon R (2018) Fluorescent reporter lines for auxin and cytokinin signalling in barley (Hordeum vulgare). ***PLoS One*** 13, e0196086.

Kondou Y, Nakazawa M, Kawashima M, Ichikawa T, Yoshizumi T, Suzuki K, Ishikawa A, Koshi T, Matsui R, Muto S, Matsui M (2008) RETARDED GROWTH OF EMBRYO1, a new basic helix-loop-helix protein, expresses in endosperm to control embryo growth. ***Plant Physiol*** 147, 1924-1935.

Kutschera U, Wang ZY (2016) Growth-limiting proteins in maize coleoptiles and the auxin-brassinosteroid hypothesis of mesocotyl elongation. ***Protoplasma*** 253, 3-14.

Larsson E, Roberts CJ, Claes AR, Franks RG, Sundberg E (2014) Polar auxin transport is essential for medial versus lateral tissue specification and vascular-mediated valve outgrowth in Arabidopsis gynoecia. ***Plant Physiol*** 166, 1998-2012.

Larsson E, Vivian-Smith A, Offringa R, Sundberg E (2017) Auxin Homeostasis in Arabidopsis Ovules Is Anther-Dependent at Maturation and Changes Dynamically upon Fertilization. ***Front Plant Sci*** 8, 1735.

Lee DJ, Park JW, Lee HW, Kim J (2009) Genome-wide analysis of the auxin-responsive transcriptome downstream of *IAA1* and its expression analysis reveal the diversity and complexity of auxin-regulated gene expression. ***J Exp Bot*** 60, 3935-3957.

Li SB, Xie ZZ, Hu CG, Zhang JZ (2016) A Review of Auxin Response Factors (ARFs) in Plants. ***Front Plant Sci*** 7, 47.

Li W, Yang B (2017) Translational genomics of grain size regulation in wheat. ***Theor Appl Genet*** 130, 1765-1771.

Liao CY, Smet W, Brunoud G, Yoshida S, Vernoux T, Weijers D (2015) Reporters for sensitive and quantitative measurement of auxin response. ***Nat Methods*** 12, 207-210

Lituiev DS, Krohn NG, Muller B, Jackson D, Hellriegel B, Dresselhaus T, Grossniklaus U (2013) Theoretical and experimental evidence indicates that there is no detectable auxin gradient in the angiosperm female gametophyte. ***Development*** 140, 4544-4553.

Liu LC, Tong HN, Xiao YH, Che RH, Xu F, Hu B, Liang CZ, Chu JF, Li JY, Chu CC (2015) Activation of *Big Grain1* significantly improves grain size by regulating auxin transport in rice. ***Proc Natl Acad Sci U S A*** 112, 11102-11107.

Locascio A, Roig-Villanova I, Bernardi J, Varotto S (2014) Current perspectives on the hormonal control of seed development in *Arabidopsis* and maize: a focus on auxin. ***Front Plant Sci*** 5, 412.

Long JA, Woody S, Poethig S, Meyerowitz EM, Barton MK (2002) Transformation of shoots into roots in *Arabidopsis* embryos mutant at the *TOPLESS* locus. Development 129, 2797-2806.

Lora J, Herrero M, Tucker MR, Hormaza JI (2017) The transition from somatic to germline identity shows conserved and specialized features during angiosperm evolution. ***New Phytol*** 216, 495-509.

Luo J, Zhou JJ, Zhang JZ (2018) *Aux*/*IAA* Gene Family in Plants: Molecular Structure, Regulation, and Function. ***Int J Mol Sci*** 19.

Ma M, Zhao H, Li Z, Hu S, Song W, Liu X (2016) *TaCYP78A5* regulates seed size in wheat (*Triticum aestivum*). ***J Exp Bot*** 67, 1397-1410.

Ma W, Li J, Qu B, He X, Zhao X, Li B, Fu X, and Tong, Y (2014) Auxin biosynthetic gene *TAR2* is involved in low nitrogen-mediated reprogramming of root architecture in *Arabidopsis*. ***The Plant Journal***, 78(1), pp.70-79.

Mano Y, Nemoto K (2012) The pathway of auxin biosynthesis in plants. ***J Exp Bot*** 63, 2853-2872.

Marchant A, Kargul J, May ST, Muller P, Delbarre A, Perrot-Rechenmann C, Bennett MJ (1999) AUX1 regulates root gravitropism in *Arabidopsis* by facilitating auxin uptake within root apical tissues. ***EMBO J*** 18, 2066-2073.

Marin E, Jouannet V, Herz A, Lokerse AS, Weijers D, Vaucheret H, Nussaume L, Crespi MD, Maizel A (2010) miR390, *Arabidopsis* TAS3 tasiRNAs, and their *AUXIN RESPONSE FACTOR* targets define an autoregulatory network quantitatively regulating lateral root growth. ***Plant Cell*** 22, 1104-1117.

Mashiguchi K, Tanaka K, Sakai T, Sugawara S, Kawaide H, Natsume M, Hanada A, Yaeno T, Shirasu K, Yao H, McSteen P, Zhao Y, Hayashi K, Kamiya Y, Kasahara H (2011) The main auxin biosynthesis pathway in *Arabidopsis*. ***Proc Natl Acad Sci U S A*** 108, 18512-18517.

Mathan J, Bhattacharya J, Ranjan A (2016) Enhancing crop yield by optimizing plant developmental features. ***Development*** 143, 3283-3294.

McSteen P (2010) Auxin and monocot development. ***Cold Spring Harbor Perspectives in Biology*** 2.

Mishra BS, Jamsheer KM, Singh D, Sharma M, Laxmi A (2017) Genome-wide identification and expression, protein-protein interaction and evolutionary analysis of the seed plant-specific *BIG GRAIN* and *BIG GRAIN LIKE* gene family. ***Front Plant Sci*** 8.

Mockaitis K, Estelle M (2008) Auxin receptors and plant development: a new signaling paradigm. ***Annu Rev Cell Dev Biol*** 24, 55-80.

Moller, B, Weijers D (2009) Auxin Control of Embryo Patterning. ***Cold Spring Harbor Perspectives in Biology*** 1(5).

Mravec J, Skupa P, Bailly A, Hoyerova K, Krecek P, Bielach A, Petrasek J, Zhang J, Gaykova V, Stierhof YD, Dobrev PI, Schwarzerova K, Rolcik J, Seifertova D, Luschnig C, Benkova E, Zazimalova E, Geisler M, Friml J (2009) Subcellular homeostasis of phytohormone auxin is mediated by the ER-localized PIN5 transporter. ***Nature*** 459, 1136-1140.

Noh B, Murphy AS, Spalding EP (2001) Multidrug resistance-like genes of *Arabidopsis* required for auxin transport and auxin-mediated development. ***Plant Cell*** 13, 2441-2454.

O'Connor DL, Runions A, Sluis A, Bragg J, Vogel JP, Prusinkiewicz P, Hake S (2014) A division in PIN-mediated auxin patterning during organ initiation in grasses. ***PLoS Comput Biol*** 10, e1003447.

Olsen OA (2004) Nuclear endosperm development in cereals and *Arabidopsis thaliana*. ***Plant Cell*** 16, S214-S227.

Ottenschlager I, Wolff P, Wolverton C, Bhalerao RP, Sandberg G, Ishikawa H, Evans M, Palme K (2003) Gravity-regulated differential auxin transport from columella to lateral root cap cells. ***Proc Natl Acad Sci U S A*** 100, 2987-2991.

Pacheco-Villalobos D, Diaz-Moreno SM, van der Schuren A, Tamaki T, Kang YH, Gujas B, Novak O, Jaspert N, Li ZN, Wolf S, Oecking C, Ljung K, Bulone V, Hardtke CS (2016) The effects of high steady state auxin levels on root cell elongation in *Brachypodium*. Plant Cell 28, 1009-1024.

Pacheco-Villalobos D, Sankar M, Ljung K, Hardtke CS (2013) Disturbed local auxin homeostasis enhances cellular anisotropy and reveals alternative wiring of auxin-ethylene crosstalk in *Brachypodium distachyon* seminal roots. ***Plos Genetics*** 9.

Pagnussat GC, Alandete-Saez M, Bowman JL, Sundaresan V (2009) Auxin-dependent patterning and gamete specification in the *Arabidopsis* female gametophyte. ***Science*** 324, 1684-1689.

Panoli A, Martin MV, Alandete-Saez M, Simon M, Neff C, Swarup R, Bellido A, Yuan L, Pagnussat GC, Sundaresan V (2015) Auxin Import and Local Auxin Biosynthesis Are Required for Mitotic Divisions, Cell Expansion and Cell Specification during Female Gametophyte Development in *Arabidopsis thaliana*. ***PLoS One*** 10, e0126164.

Parry G, Calderon-Villalobos LI, Prigge M, Peret B, Dharmasiri S, Itoh H, Lechner E, Gray WM, Bennett M, Estelle M (2009) Complex regulation of the TIR1/AFB family of auxin receptors. ***Proc Natl Acad Sci U S A*** 106, 22540-22545.

Paul P, Dhandapani V, Rameneni JJ, Li X, Sivanandhan G, Choi SR, Pang W, Im S, Lim YP (2016) Genome-Wide Analysis and Characterization of *Aux*/*IAA* Family Genes in *Brassica rapa*. ***PLoS One*** 11, e0151522.

Perrot-Rechenmann C (2010) Cellular responses to auxin: Division versus expansion. ***Cold Spring Harbor Perspectives in Biology*** 2.

Pielot R, Kohl S, Manz B, Rutten T, Weier D, Tarkowska D, Rolcik J, Strnad M, Volke F, Weber H, Weschke W (2015) Hormone-mediated growth dynamics of the barley pericarp as revealed by magnetic resonance imaging and transcript profiling. ***J Exp Bot*** 66, 6927-6943.

Poulet A, Kriechbaumer V (2017) Bioinformatics analysis of phylogeny and transcription of *TAA*/*YUC* auxin biosynthetic genes. ***Int J Mol Sci*** 18.

Quint M, Gray WM (2006) Auxin signaling. ***Curr Opin Plant Biol*** 9, 448-453.

Radchuk V, Weier D, Radchuk R, Weschke W, Weber H (2011) Development of maternal seed tissue in barley is mediated by regulated cell expansion and cell disintegration and coordinated with endosperm growth. ***J Exp Bot*** 62, 1217-1227.

Ramos JA, Zenser N, Leyser O, Callis J (2001) Rapid degradation of auxin/indoleacetic acid proteins requires conserved amino acids of domain II and is proteasome dependent. ***Plant Cell*** 13, 2349-2360.

Ray DK, Mueller ND, West PC, Foley JA (2013) Yield Trends Are Insufficient to Double Global Crop Production by 2050. ***PLoS One*** 8, e66428.

Reale L, Rosati A, Tedeschini E, Ferri V, Cerri M, Ghitarrini S, Timorato V, Ayano BE, Porfiri O, Frenguelli G, Ferranti F, Benincasa P (2017) Ovary Size in Wheat (*Triticum aestivum* L.) is Related to Cell Number. ***Crop Sci*** 57, 914-925.

Reiser L, Fischer RL (1993) The ovule and the embryo sac. ***Plant Cell*** 5, 1291-1301.

Remy E, Duque P (2014) Beyond cellular detoxification: a plethora of physiological roles for MDR transporter homologs in plants. ***Front Physiol*** 5, 201.

Reyes FC, Sun BM, Guo HN, Gruis D, Otegui MS (2010) *Agrobacterium tumefaciens*-mediated transformation of maize endosperm as a tool to study endosperm cell biology. ***Plant Physiol*** 153, 624-631.

Ringli C (2010) Monitoring the outside: Cell wall-sensing mechanisms. ***Plant Physiol*** 153, 1445-1452.

Robert HS, Grones P, Stepanova AN, Robles LM, Lokerse AS, Alonso JM, Weijers D, Friml J (2013) Local auxin sources orient the apical-basal axis in *Arabidopsis* embryos. ***Curr Biol***, 23(24), pp.2506-2512.

Robert HS, Crhak Khaitova L, Mroue S, Benkova E (2015) The importance of localized auxin production for morphogenesis of reproductive organs and embryos in *Arabidopsis*. ***J Exp Bot*** 66, 5029-5042.

Robert HS, Park C, Gutierrez CL, Wojcikowska B, Pencik A, Novak O, Chen J, Grunewald W, Dresselhaus T, Friml J, Laux T (2018) Maternal auxin supply contributes to early embryo patterning in *Arabidopsis*. ***Nat Plants***.

Sabatini S, Beis D, Wolkenfelt H, Murfett J, Guilfoyle T, Malamy J, Benfey P, Leyser O, Bechtold N, Weisbeek P, Scheres B (1999) An auxin-dependent distal organizer of pattern and polarity in the *Arabidopsis* root. ***Cell*** 99, 463-472.

Sabelli PA (2012) Replicate and die for your own good: Endoreduplication and cell death in the cereal endosperm. ***J Cereal Sci*** 56, 9-20.

Sailer C, Schmid B, Grossniklaus U (2016) Apomixis Allows the Transgenerational Fixation of Phenotypes in Hybrid Plants. ***Curr Biol*** 26, 331-337.

Salehin M, Bagchi R, Estelle M (2015) *SCFTIR1/AFB*-based auxin perception: mechanism and role in plant growth and development. ***Plant Cell*** 27, 9-19.

Sasaki A, Ashikari M, Ueguchi-Tanaka M, Itoh H, Nishimura A, Swapan D, Ishiyama K, Saito T, Kobayashi M, Khush GS, Kitano H, Matsuoka M (2002) Green revolution: a mutant gibberellin-synthesis gene in rice. ***Nature*** 416, 701-702.

Sehra B, Franks RG (2015) Auxin and cytokinin act during gynoecial patterning and the development of ovules from the meristematic medial domain. ***Wiley Interdiscip Rev Dev Biol*** 4, 555-571.

Spiegelman Z, Ham BK, Zhang Z, Toal TW, Brady SM, Zheng Y, Fei Z, Lucas WJ, Wolf S (2015) A tomato phloem-mobile protein regulates the shoot-to-root ratio by mediating the auxin response in distant organs. ***Plant J*** 83, 853-863.

Stepanova AN, Robertson-Hoyt J, Yun J, Benavente LM, Xie DY, Dolezal K, Schlereth A, Jurgens G, Alonso JM (2008) *TAA1*-mediated auxin biosynthesis is essential for hormone crosstalk and plant development. ***Cell*** 133, 177-191.

Su Z, Zhao L, Zhao Y, Li S, Won S, Cai H, Wang L, Li Z, Chen P, Qin Y (2017) The THO Complex Non-Cell-Autonomously Represses Female Germline Specification through the TAS3-ARF3 Module. ***Curr Biol***.

Sun X, Cahill J, Van Hautegem T, Feys K, Whipple C, Novak O, Delbare S, Versteele C, Demuynck K, De Block J, Storme V, Claeys H, Van Lijsebettens M, Coussens G, Ljung K, De Vliegher A, Muszynski M, Inze D, Nelissen H (2017) Altered expression of maize *PLASTOCHRON1* enhances biomass and seed yield by extending cell division duration. ***Nat Commun*** 8, 14752.

Tao Y, Ferrer JL, Ljung K, Pojer F, Hong FX, Long JA, Li L, Moreno JE, Bowman ME, Ivans LJ, Cheng YF, Lim J, Zhao YD, Ballare CL, Sandberg G, Noel JP, Chory J (2008) Rapid synthesis of auxin via a new tryptophan-dependent pathway is required for shade avoidance in plants. ***Cell*** 133, 164-176.

Thiel J (2014) Development of endosperm transfer cells in barley. ***Front Plant Sci*** 5.

Thiel J, Weier D, Weschke W (2011) Laser-capture microdissection of developing barley seeds and cDNA array analysis of selected tissues. ***Methods Mol Biol*** 755, 461-475.

Torti G, Manzocchi L, Salamini F (1986) Free and bound indole-acetic acid is low in the endosperm of the maize mutant *defective-endosperm-b18*. ***Theor Appl Genet*** 72, 602-605.

Tucker MR, Koltunow AM (2014) Traffic monitors at the cell periphery: the role of cell walls during early female reproductive cell differentiation in plants. ***Curr Opin Plant Biol*** 17, 137-145.

Tucker MR, Lou H, Aubert MK, Wilkinson LG, Little A, Houston K, Pinto SC, Shirley NJ (2018) Exploring the Role of Cell Wall-Related Genes and Polysaccharides during Plant Development. ***Plants*** (Basel) 7.

Tucker MR, Okada T, Johnson SD, Takaiwa F, Koltunow AMG (2012) Sporophytic ovule tissues modulate the initiation and progression of apomixis in *Hieracium*. ***J Exp Bot*** 63, 3229-3241.

Ugarte C, Calderini DF, Slafer GA (2007) Grain weight and grain number responsiveness to pre-anthesis temperature in wheat, barley and triticale. ***Field Crops Res*** 100, 240-248.

Ulmasov T, Murfett J, Hagen G, Guilfoyle TJ (1997) Aux / IAA proteins repress expression of reporter genes containing natural and highly active synthetic auxin response elements. ***Plant Cell*** 9, 1963-1971.

Vanstraelen M, Benkova E (2012) Hormonal interactions in the regulation of plant development. ***Annu Rev Cell Dev Biol*** 28, 463-487.

Vernoux T, Brunoud G, Farcot E, Morin V, Van den Daele H, Legrand J, Oliva M, Das P, Larrieu A, Wells D, Guedon Y, Armitage L, Picard F, Guyomarc'h S, Cellier C, Parry G, Koumproglou R, Doonan JH, Estelle M, Godin C, Kepinski S, Bennett M, De Veylder L, Traas J (2011) The auxin signalling network translates dynamic input into robust patterning at the shoot apex. ***Mol Syst Biol*** 7, 508.

Vernoux T, Kronenberger J, Grandjean O, Laufs P, Traas J (2000) *PIN-FORMED 1* regulates cell fate at the periphery of the shoot apical meristem. ***Development*** 127, 5157-5165.

Wang D, Pei K, Fu Y, Sun Z, Li S, Liu H, Tang K, Han B, Tao Y (2007) Genome-wide analysis of the *auxin response factors* (*ARF*) gene family in rice (*Oryza sativa*). ***Gene*** 394, 13-24.

Weijers D, Schlereth A, Ehrismann JS, Schwank G, Kientz M, Jurgens G (2006) Auxin triggers transient local signaling for cell specification in *Arabidopsis* embryogenesis. ***Dev Cell*** 10, 265-270.

Wilkinson LG, Bird DC, Tucker MR (2018) Exploring the Role of the Ovule in Cereal Grain Development and Reproductive Stress Tolerance. ***Annual Plant Reviews***.

Wilkinson LG, Tucker MR (2017) An optimised clearing protocol for the quantitative assessment of sub-epidermal ovule tissues within whole cereal pistils. ***Plant Methods*** 13, 67.

Wolters H, Jurgens G (2009) Survival of the flexible: hormonal growth control and adaptation in plant development. ***Nat Rev Genet*** 10, 305-317.

Worley CK, Zenser N, Ramos J, Rouse D, Leyser O, Theologis A, Callis J (2000) Degradation of Aux / IAA proteins is essential for normal auxin signalling. ***Plant J***. 21, 553-562.

Wu W, Liu Y, Wang Y, Li H, Liu J, Tan J, He J, Bai J, Ma H (2017) Evolution Analysis of the *Aux*/*IAA* Gene Family in Plants Shows Dual Origins and Variable Nuclear Localization Signals. ***Int J Mol Sci*** 18.

Wurschum T, Langer SM, Longin CFH, Tucker MR, Leiser WL (2017) A modern Green Revolution gene for reduced height in wheat. ***Plant J*** 92, 892-903.

Wurschum T, Leiser WL, Langer SM, Tucker MR, Longin CFH (2018) Phenotypic and genetic analysis of spike and kernel characteristics in wheat reveals long-term genetic trends of grain yield components. ***Theor Appl Genet***.

Xie Q, Mayes S, Sparkes DL (2015) Carpel size, grain filling, and morphology determine individual grain weight in wheat. ***J Exp Bot*** 66, 6715-6730.

Xu M, Zhu L, Shou HX, Wu P (2005) A *PIN1* family gene, *OsPIN1*, involved in auxin-dependent adventitious root emergence and tillering in rice. ***Plant Cell Physiol*** 46, 1674-1681.

Yan DW, Duermeyer L, Leoveanu C, Nambara E (2014) The Functions of the Endosperm During Seed Germination. ***Plant Cell Physiol*** 55, 1521-1533.

Yang J, Yuan Z, Meng Q, Huang G, Périn C, Bureau C, Meunier A-C, Ingouff M, Bennett MJ, Liang W (2017a) Dynamic regulation of auxin response during rice development revealed by newly established hormone biosensor markers. ***Front Plant Sci*** 8.

Yang Z, van Oosterom EJ, Jordan DR, Hammer GL (2009) Pre-anthesis ovary development determines genotypic differences in potential kernel weight in sorghum. ***J Exp Bot*** 60, 1399-1408.

Yelina NE, Smith LM, Jones AM, Patel K, Kelly KA, Baulcombe DC (2010) Putative *Arabidopsis* THO/TREX mRNA export complex is involved in transgene and endogenous siRNA biosynthesis. ***Proc Natl Acad Sci U S A*** 107, 13948-13953.

Yoshikawa T, Ito M, Sumikura T, Nakayama A, Nishimura T, Kitano H, Yamaguchi I, Koshiba T, Hibara KI, Nagato Y, Itoh JI (2014) The rice *FISH BONE* gene encodes a tryptophan aminotransferase, which affects pleiotropic auxin-related processes. ***Plant J*** 78, 927-936.

Zhang S, Wang S, Xu Y, Yu C, Shen C, Qian Q, Geisler M, Jiang de A, Qi Y (2015) The auxin response factor, *OsARF19*, controls rice leaf angles through positively regulating *OsGH3-5* and *OsBRI1*. ***Plant Cell Environ*** 38, 638-654.

Zhao FY, Hu F, Zhang SY, Wang K, Zhang CR, Liu T (2013) MAPKs regulate root growth by influencing auxin signaling and cell cycle-related gene expression in cadmium-stressed rice. ***Environ Sci Pollut Res Int*** 20, 5449-5460.

Table 1: Reporter genes for auxin synthesis, distribution and transport available in plants.

					Expression		
Marker type/name	Usage	Mechanism	Reporter	Species	Vegetative Tissues	Reproductive Tissues	Reference
Auxin synthesis							
pTAA1::TAA1-GFP	Indicates the IPA pathway of auxin synthesis	TAA1 is an tryptophan aminotransferase	GFP	Arabidopsis	QC area in root, vasculature of hypocotyls and apical hooks	Young flowers, embryo attachment region, chalaza and funiculus	Stepanova et al., 2008; Robert et al., 2018
pTAR2::GUS	Indicates the IPA pathway of auxin synthesis	TAR2 is a close homolog of TAA1	GUS	Arabidopsis	Nascent leaves, root pericycle and vasculature	The micropylar end of the embryo sac	Ma et al., 2014; Panoli et al., 2015
YUC1::GUS	Indicates the YUC pathway of auxin synthesis	YUCs are flavin monooxygenase-like enzymes	GUS	Arabidopsis	Leaves	Floral meristem, base of floral organs, discrete groups of cells in both stamens and carpels, female gametophyte and neighbouring cells, embryo	Cheng et al., 2006; Cheng et al., 2007; Pagnussat et al., 2009
YUC1::GFP			nuclear targeted 3 X GFP	Arabidopsis		Suspensor cells at 16-cell stage of embryogenesis	Robert et al., 2013
YUC2::GUS			GUS	Arabidopsis		Young flower buds, petals, stamens, and gynoecium of young flowers, nucellus, micropylar end of the embryo sac	Cheng et al., 2006; Pagnussat et al., 2009
YUC4::GFP			nuclear targeted 3 X GFP	Arabidopsis		Protodermal cells from globular and transition stages of embryogenesis, suspensor cells at 16-cell stage of embryogenesis	Robert et al., 2013
YUC4::GUS			GUS	Arabidopsis		Apical meristems and young floral primordia, apical regions of the carpels, stamens, and sepals, inner integument cells close to the micropyle	Cheng et al., 2006; Ceccato et al., 2013
YUC6::GUS			GUS	Arabidopsis		Stamens and pollen	Cheng et al., 2006

YUC8::GFP			GFP	Arabidopsis		Micropylar pole of the female gametophyte, integuments	Panoli et al., 2015
YUC8::GUS			GUS	Arabidopsis		Provascular cells at a late globular stage of embryogenesis	Robert et al., 2013
YUC9::GFP			Cytosolic GFP	Arabidopsis		Suspensor cells at 16-cell stage of embryogenesis	Robert et al., 2013
YUC10::GFP			nuclear targeted 3 X GFP	Arabidopsis		Endosperm	Robert et al., 2013
YUC11::GFP			Cytosolic GFP	Arabidopsis		Endosperm	Robert et al., 2013
Auxin distribution and response							
DR5::GUS	Monitors auxin distribution	7X TGTCTC AuxRE	GUS	Arabidopsis	Seedlings, roots		Ulmasov et al., 1997; Sabatini et al., 1999
				Populus	Leaves, roots, stems		Chen et al., 2013
				Rice		Base of the anther and the mature spikelet	Zhao et al., 2013
DR5::GFP		9X CCTTTTGTCTC AuxRE	GFP	Arabidopsis	Root	Nucellus and embryo sac of the ovule	Ottenschläger et al., 2002; Pagnussat et al., 2009
DR5rev::PEH A		9X TGTCTC AuxRE	Phosphonate monoester hydrolase	Arabidopsis		Embryo	Friml et al., 2002
DR5rev::GFP		9X TGTCTC AuxRE	GFP	Arabidopsis	Whole plant	Floral primordia, floral organs, ovule primordia, mature ovules, integuments	Benková et al., 2003
DR5rev::mRFPer		9X TGTCTC AuxRE	ER targeted monomeric RFP	Arabidopsis	Root		Marin et al., 2010

				Maize		Spikelet-pair meristem, glume primordia, floral meristem. L2 micropylar nucellus of ovule	Gallavotti et al., 2008; Lituiev et al., 2013
DR5v2:ntdTomato/3nGFP	Monitors auxin distribution, enhanced sensitivity via the higher affinity of AuxRE	9X TGTCGG AuxRE	Nuclear tandem Tomato or nuclear 3×eGFP	Arabidopsis	Root		Liao et al., 2015
DR5::3XVENUSnls		NA	Nuclear 3XVENUS	Tomato	Root		Spiegelman et al., 2015
DR5rev::3XVENUS-N7		9X TGTCTC AuxRE	Nuclear 3XVENUS (a rapidly folding YFP)	Arabidopsis		Inflorescence meristem, primordial areas	Heisler et al., 2005
				Rice	Root	Inflorescence meristem, spikelet meristems, glume/lemma/lodicule/stamen primordia	Yang et al., 2017
pHvPLT1::HvPLT1-mVENUS	Mirrors auxin distribution	Auxin signailling downstream gene HvPLT	C-terminal mVENUS	Barley	Root		Kirschner et al., 2018
CaV35S::DII-VENUS-NLS	Monitors auxin signalling input by switching off the signal in the presence of auxin	Aux/IAA auxin-interaction domain (termed domain II; DII)	VENUS	Arabidopsis		Complementary with DR5-VENUS signals	Brunoud et al., 2012; Vernoux et al., 2011

R2D2 (ratiometric version of two DIIs) RPS5A:: DII-n3VENUS fused with RPS5A::mDII-ntdTomato	Quantitatively measures 'auxin input'	DII and mDII (lack auxin-dependent degradation)	Nuclear tandem Tomato or nuclear 3×eGFP	Arabidopsis	Root		Liao et al., 2015
Auxin transport							
AUX1::GUS	Traces auxin influx	AUX1 is a representative influx carrier of auxin	GUS	Arabidopsis	Major tissue of root		Marchant et al., 1999
PIN1::GUS	Traces auxin efflux		GUS	Arabidopsis	Lateral root		Benková et al., 2003
PIN1::PIN1-GFP		PIN proteins are polar localised in cells, indicaitors of auxin concentration gradient.	GFP	Arabidopsis	Root	Embryo, floral meristem, organ primordia, nucellus of young ovule	Benková et al., 2003; Pagnussat et al., 2009; Gallavotti et al., 2008
ZmPIN1a::PIN1a-YFP			YFP	Maize		Nucellus cell, antipodal cells	Chetoor and Evans, 2015
SoPIN1: SoPIN1-Citrine			Citrine (a variant of YFP)	Brachypodium		Spikelet meristem and lemma primordia	O'Connor et al., 2014
HvpPIN1a:HvPIN1amVENUS			C-terminal cVENUS	Barley	Root		Kirschner et al., 2018
PIN2::GFP			GFP	Arabidopsis	Root	Nucellus	Blilou et al., 2005; Pagnussat et al., 2009
PIN4::GFP			GFP	Arabidopsis	Root	Nucellus	Blilou et al., 2005; Pagnussat et al., 2009

PIN5::GUS	GUS	Arabidopsis	Root		Mravec et al., 2009
PIN6::GFP	GFP	Arabidopsis		Nectary and stamen	Bender et al., 2013
PIN7::GFP	GFP	Arabidopsis	Root		Blilou et al., 2005
PIN8::GFP	GFP	Arabidopsis		Pollen specific	Bosco et al., 2012

Table 2: Transcript abundance of TIR/AFB, ARF and Aux/IAA genes in different barley tissues.

ID	Gene	Leaf	Root	Int	Inf 5mm	Inf 15mm	Car 5DAP	Car 15 DAP	Emb 4DAG
HvTIR1	HORVU1Hr1G021550	10.7	17.2	24.2	52.3	80.5	43.4	6.2	28.4
HvAFB2	HORVU2Hr1G070800	24.3	28.7	42.2	110.6	148.6	33.9	21.2	48.1
HvAFB3	HORVU5Hr1G075620	3.8	4.6	8	8.8	12.7	8.5	3.6	5.9
HvAFB4	HORVU6Hr1G077570	12.8	18.9	34.7	65.6	54.2	28.5	5	32.3
HvAFB5	HORVU4Hr1G078120	3.2	6.9	3.9	24.1	21.3	6.7	1.9	13.3
HvARF1	HORVU3Hr1G032230	0.4	8.8	0.1	0.4	1.8	13.6	3.5	4.9
HvARF2	HORVU1Hr1G087460	11.6	8.8	36.1	49.6	61.3	25.5	2	18.6
HvARF3	HORVU3Hr1G072340	6.3	10.6	32.8	29.2	65.3	45.4	4.8	16.8
HvARF4a	HORVU3Hr1G097200	52.6	31	48.7	197	293	56.1	31.9	35.4
HvARF4b	HORVU3Hr1G096410	2.5	2.8	0.7	7.6	9.4	1.8	0.6	2.3
HvARF4c	HORVU3Hr1G096510	84.3	68.4	70.4	334.1	524.5	123.9	29.8	70.9
HvARF5	HORVU6Hr1G020330	11	5.1	24.2	12.3	12.8	1	0.6	5.9
HvARF6	HORVU6Hr1G026730	13	13.8	30.1	37.4	56.3	7.3	4.7	19.6
HvARF8	HORVU6Hr1G058890	4.1	0.7	4.5	3.4	1.1	5.4	0.5	2
HvARF9	HORVU2Hr1G076920	92.8	100.7	77.9	120.7	115.9	53.6	23.6	67.1
HvARF10a	HORVU2Hr1G089670	4.1	6.9	25.1	3.1	2.9	18.5	2.2	7.7
HvARF10b	HORVU2Hr1G089660	0	0	0.3	0	0.1	0.4	0.1	0.1
HvARF11	HORVU2Hr1G109650	0.4	1.2	0.3	42.3	38.8	0.4	3	1.7
HvARF12	HORVU2Hr1G121110	15.1	17.3	82.4	128.4	79.7	50	3.6	42.3
HvARF13	HORVU2Hr1G125740	0	0	0	0	0.5	2.3	1.1	0
HvARF14	HORVU1Hr1G076690	1.4	1.8	1.8	32.3	47.7	6.6	3	3.6
HvARF16	HORVU7Hr1G033820	10.2	4.8	12.9	21.8	17.1	19.1	5.6	11.8
HvARF17	HORVU7Hr1G106280	34	22.1	101.7	127.6	145.1	68.9	11.8	50.9
HvARF18	HORVU7Hr1G101270	24.8	14.4	29.3	7.8	10.8	46.3	6.2	15.5
HvARF19	HORVU7Hr1G096460	10.2	12	17.5	17.8	19.4	7.2	1.4	9.8
HvARF21	HORVU7Hr1G051930	30	26.3	125.4	45.4	47.9	16.3	3	42.8
HvARF22	HORVU1Hr1G041770	7.3	7.5	28	7.5	13.2	83.3	5.7	12.9
HvARF25	HORVU5Hr1G009650	8.3	14.8	31.9	125.2	111	75	6.1	30.9
HvIAA1	HORVU3Hr1G022540	26.2	27.7	446.8	13	17.9	63.6	8.2	26.7
HvIAA2	HORVU3Hr1G019750	11	12.8	48.6	21.6	12.2	37.3	0.8	21.5
HvIAA3	HORVU3Hr1G031460	108.7	78.9	263	127	169.5	102.2	11	103.1
HvIAA4	HORVU1Hr1G017770	2.8	0.3	2.1	0	0	0.9	0.1	0.2
HvIAA5a	HORVU3Hr1G062160	1.5	0.8	0.7	2.5	3.9	1.3	1	0.8
HvIAA5b	HORVU3Hr1G088810	1.5	2.9	2.3	2.4	3.9	1.5	1.4	3.1
HvIAA6	HORVU3Hr1G070620	25.6	14.9	7	14	6.2	0.4	0.8	13.8
HvIAA9	HORVU6Hr1G088140	0.6	1.8	1.3	0.1	0.2	0.1	0	2
HvIAA10	HORVU6Hr1G091260	44.2	14.3	96.1	29.6	43.9	6.7	1.3	11.2
HvIAA11	HORVU5Hr1G093580	2.2	38.5	20.4	1	1.6	23	1.1	32.1
HvIAA12	HORVU5Hr1G093640	21.3	73.6	301	2.4	1.1	2.9	0.6	110.4
HvIAA13	HORVU5Hr1G094220	0.2	0.1	0	0	0.3	0.1	0.2	0.2

HvIAA14	HORVU5Hr1G106350	17.1	3.7	22.5	1.9	2.2	40.5	3.7	8.8
HvIAA15	HORVU1Hr1G025670	25.3	20.3	92.2	12	20.7	13.4	2.6	22.6
HvIAA16	HORVU1Hr1G028170	1.3	3.6	0.1	21.3	20.5	0.4	0.3	4.5
HvIAA19	HORVU1Hr1G086070	13.7	10.5	19.6	29	21.1	1.7	0.4	18.8
HvIAA20	HORVU7Hr1G026970	0	7	0	0	0	0	0	1.6
HvIAA21	HORVU0Hr1G021630	225.4	53	906.7	112.7	190.5	166.6	28	52.5
HvIAA22	HORVU7Hr1G077110	2.1	0.9	8.3	3.8	4.7	2.1	0.3	0.7
HvIAA23	HORVU7Hr1G084940	10.1	19	28.9	16.8	2.4	0.2	0.7	27.5
HvIAA26	HORVU5Hr1G081180	0	0.4	0	2.4	1.1	0	0.2	4.3
HvIAA27	HORVU4Hr1G016160	1.2	4.5	5.8	5.2	5.5	0	0.2	7.1
HvIAA28	HORVU4Hr1G016110	0	0	0	0	0	114.9	0	0
HvIAA30	HORVU5Hr1G014300	87.2	82.2	320.2	30.3	42	104.3	3.3	167.5
HvIAA31	HORVU5Hr1G014290	116.6	69.9	731.1	13.1	17.3	38.9	0.9	156
HvIAA33	HORVU2Hr1G112440	3	0.4	0	0.2	0.9	0	0.1	2

Transcript abundance for the predicted TIR/AFB, ARF and Aux/IAA genes in eight tissues from barley, as determined by RNAseq. Values show TPM and are extracted from public datasets (IBGS 2012). Grey boxes indicate highest TPM value for a given gene. Tissues: Internodes (Int), inflorescences (Inf), caryopsis (Car), embryo (Emb). Days after pollination (DAP); Days after germination (DAG).

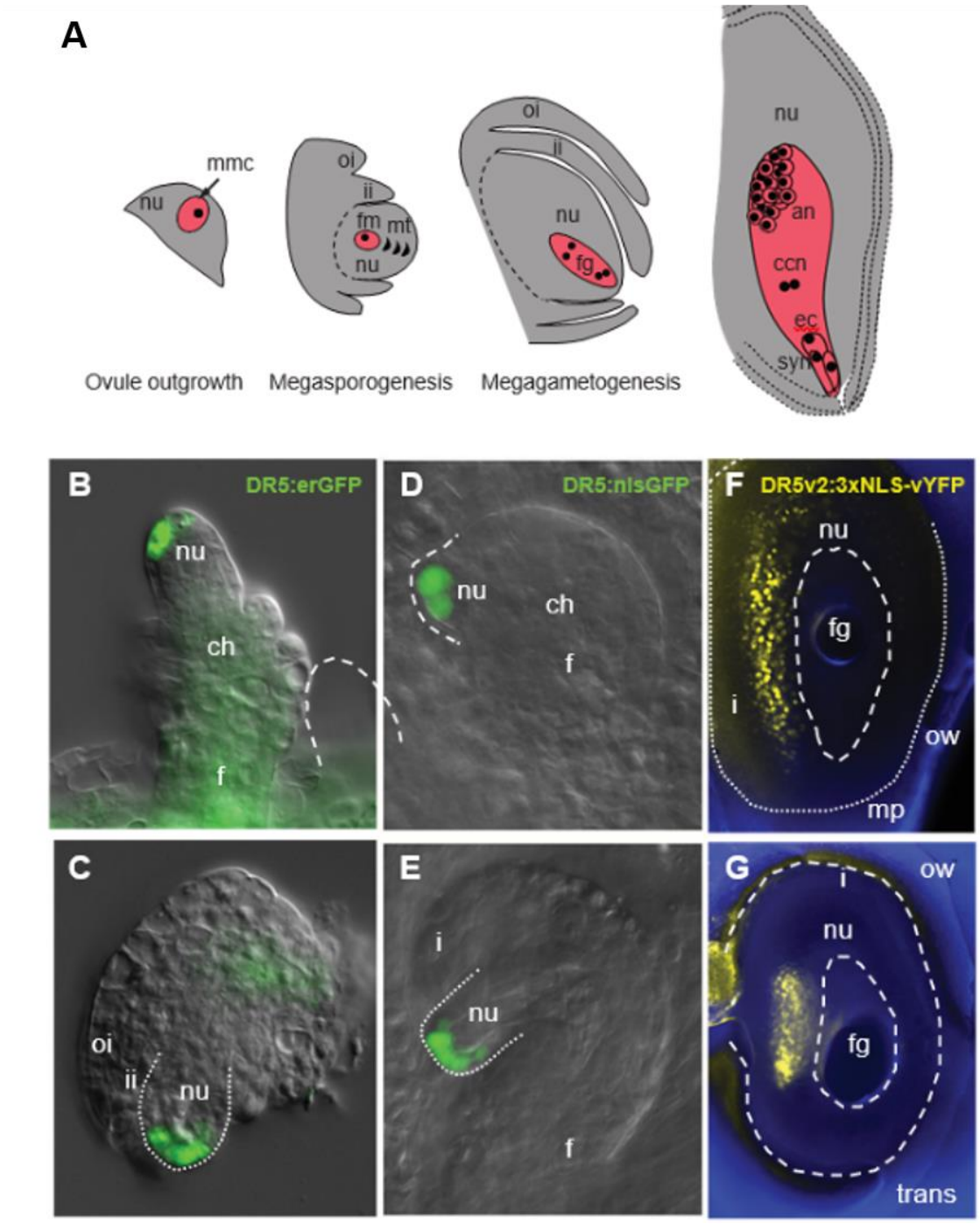

Figure 1: Patterns of auxin accumulation during ovule development. (**A**) Schematic representation of ovule development in barley. Four stages are shown including ovule initiation, megasporogenesis, megagametogenesis and ovule maturity at anthesis. nu, nucellus; mmc, megaspore mother cell; oi, outer integument; ii, inner integument; fm, functional megaspore; fg, female gametophyte; mt, meiotic tetrad; an, antipodals; ccn, central cell nuclei; ec, egg cell; syn, synergids. (**B, C**) DR5:erGFP accumulation in Arabidopsis during megaspore mother cell expansion and after meiosis. ch, chalaza; f, funiculus. (**D, E**) DR5:nlsGFP accumulation in *Hieracium* during megaspore mother cell initiation and expansion (adapted from Tucker et al. 2012). (**F, G**) DR5v2:3xnlsvYFP expression in mature barley ovules. Panels show a longitudinal and transverse view. ow, ovary wall.

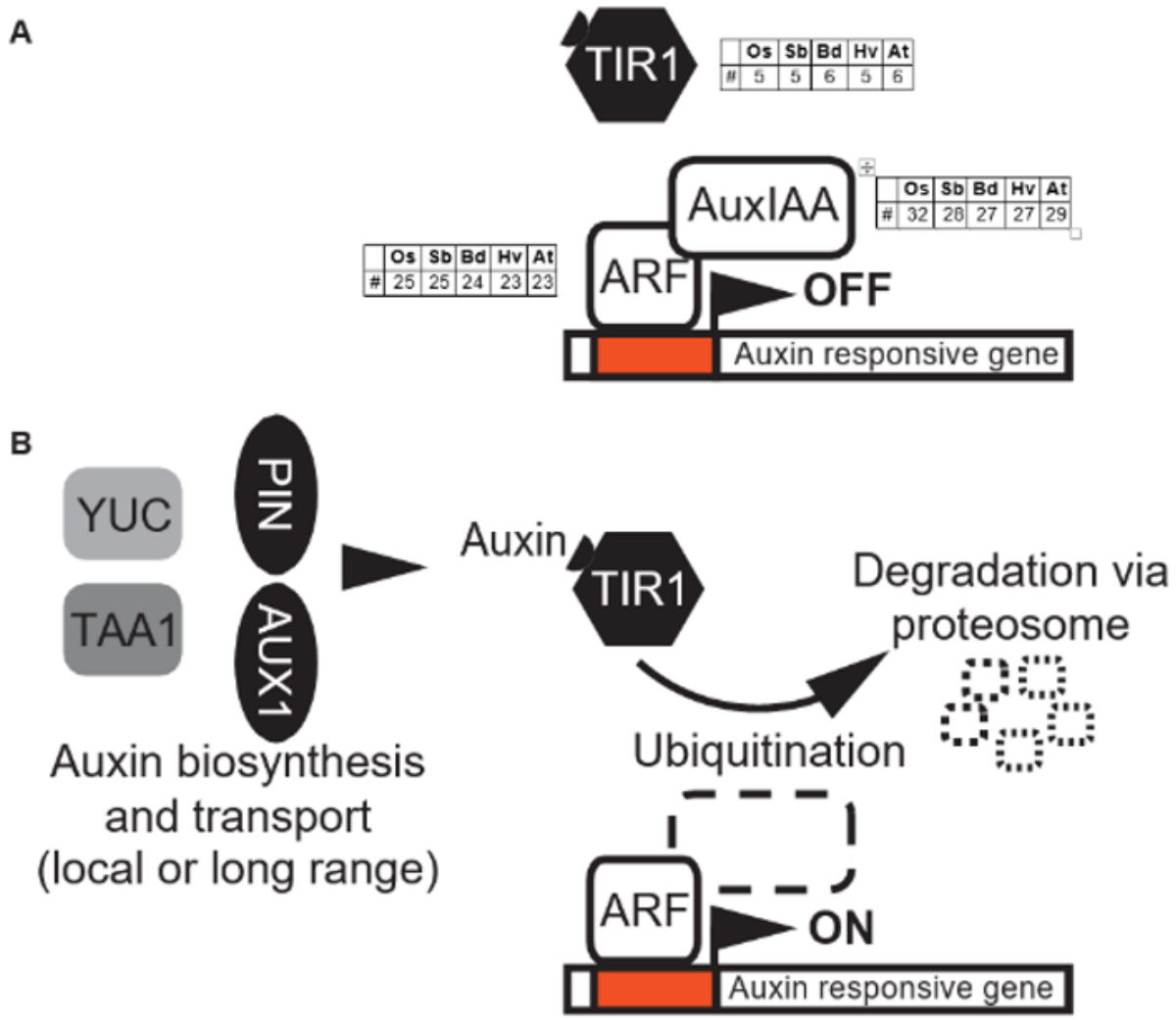

Figure 2: A schematic representation of auxin signalling pathway. (**A**) In the absence of auxin or at low auxin levels, Aux/IAA proteins limit the activity of ARF proteins through recruitment of co-repressors. (**B**) Synthesis of auxin is facilitated by TAA1 and YUC proteins and is transported via diffusion, AUX1 and PIN proteins. The TIR1 protein binds auxin to form a complex which leads to degradation of Aux/IAA and de-repression of ARF target genes. The number of *TIR1*/*AFB*, *ARF* and *Aux*/*IAA* genes in *Oryza sativa* (rice), *Sorghum bicolor*, *Brachypodium distachyon*, *Hordeum vulgare* (barley) and *Arabidopsis thaliana* are indicated.

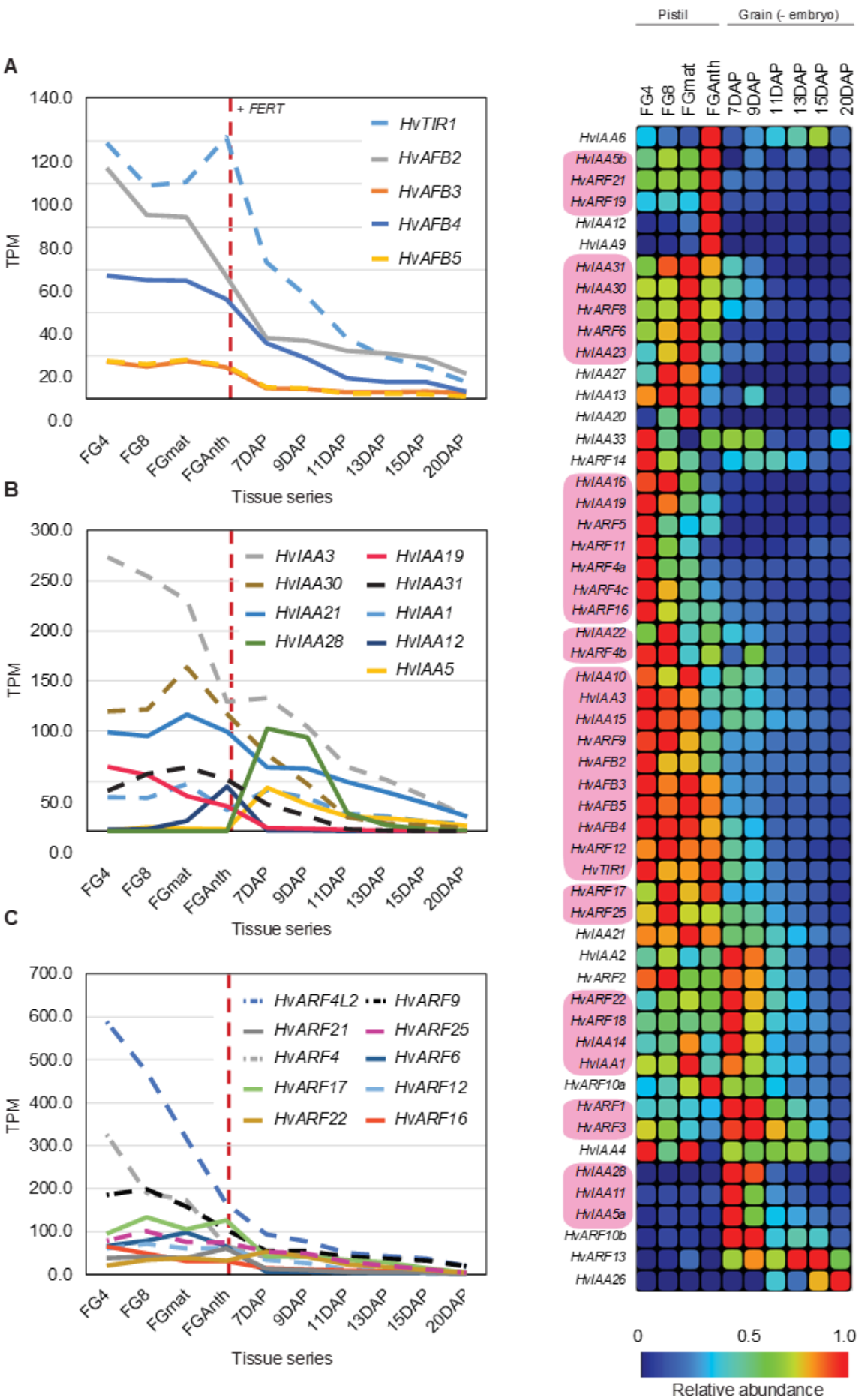
A
TPM
+ FERT
HvTIR1
HvAFB2
HvAFB3
HvAFB4
HvAFB5
FG4 FG8 FGmat FGAnth 7DAP 9DAP 11DAP 13DAP 15DAP 20DAP
Tissue series
B
HvIAA3
HvIAA30
HvIAA21
HvIAA28
HvIAA19
HvIAA31
HvIAA1
HvIAA12
HvIAA5
C
HvARF4L2
HvARF21
HvARF4
HvARF17
HvARF22
HvARF9
HvARF25
HvARF6
HvARF12
HvARF16
Pistil
Grain (- embryo)
HvIAA6
HvIAA5b
HvARF21
HvARF19
HvIAA12
HvIAA9
HvIAA31
HvIAA30
HvARF8
HvARF6
HvIAA23
HvIAA27
HvIAA13
HvIAA20
HvIAA33
HvARF14
HvIAA16
HvIAA19
HvARF5
HvARF11
HvARF4a
HvARF4c
HvARF16
HvIAA22
HvARF4b
HvIAA10
HvIAA3
HvIAA15
HvARF9
HvAFB2
HvAFB3
HvAFB5
HvAFB4
HvARF12
HvTIR1
HvARF17
HvARF25
HvIAA21
HvIAA2
HvARF2
HvARF22
HvARF18
HvIAA14
HvIAA1
HvARF10a
HvARF1
HvARF3
HvIAA4
HvIAA28
HvIAA11
HvIAA5a
HvARF10b
HvARF13
HvIAA26
0 0.5 1.0
Relative abundance

Figure 3: Transcript dynamics of the *TIR*, *ARF* and *Aux*/*IAA* (*IAA*) gene families in barley extracted from publically available pistil and seed RNAseq datasets (Aubert et al., 2018). (**A**) TIR1 family. (**B**) ARF family. (**C**) IAA family. In **B** and **C**, only genes showing a transcript value of at least 50TPM in at least one stage are included. The dashed line indicates the approximate timing of fertilisation (FERT). (**D**) Hierarchical cluster analysis of all barley *TIR*, *ARF* and *IAA* genes during pistil and seed development. Values were normalised relative to the highest expression (in TPM) in the dataset. Pink boxes highlight gene clusters showing similar accumulation patterns according to hierarchical clustering.

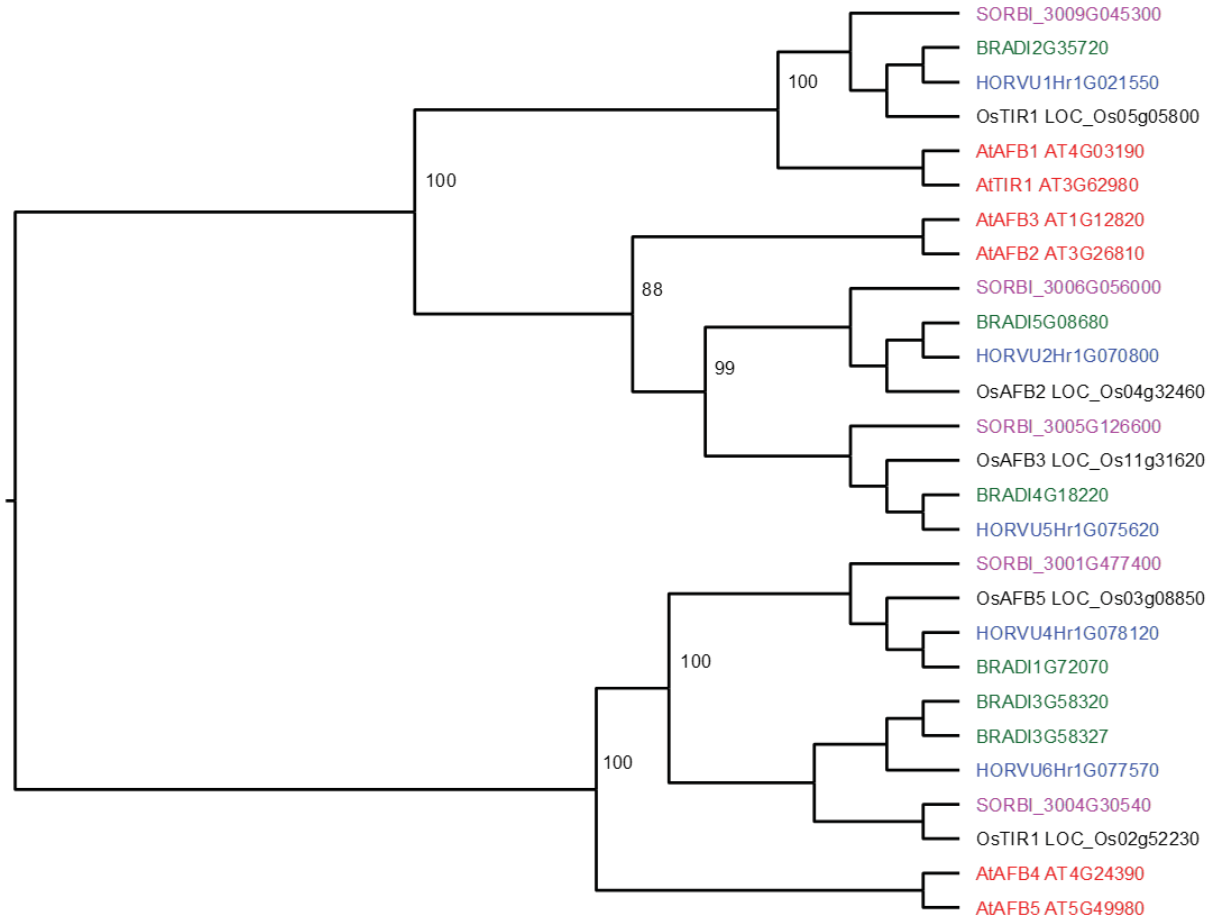

Figure 4: Phylogenetic analysis of the TIR1/AFB family from rice, sorghum, Brachypodium, barley and Arabidopsis. Arabidopsis sequences were obtained from the TAIR website (https://www.arabidopsis.org/). Barley, sorghum, rice and Brachypodium were downloaded from the Ensembl Plants Biomart website (http://plants.ensembl.org/biomart/martview/) using appropriate PFAM (Finn et al., 2014) parameters (Aux/IAA=PFAM02309, Fig 5; ARF=PFAM2309, Fig 6), from the Rice Genome Annotation Project (http://rice.plantbiology.msu.edu/index.shtml) and by BLAST at NCBI (https://blast.ncbi.nlm.nih.gov/Blast.cgi). For each gene family, the coding sequences were curated using the FGENESH+ application (Solovyev, 2007) then aligned by translation after which a tree was constructed in Geneious Pro 8.1.3 ((Biomatters Ltd. Level 2 76 Anzac Avenue Auckland 1010 New Zealand) using RaXML (Stamatakis, 2006) with the GTRGAMMA substitution model and 1000 bootstrap iterations.

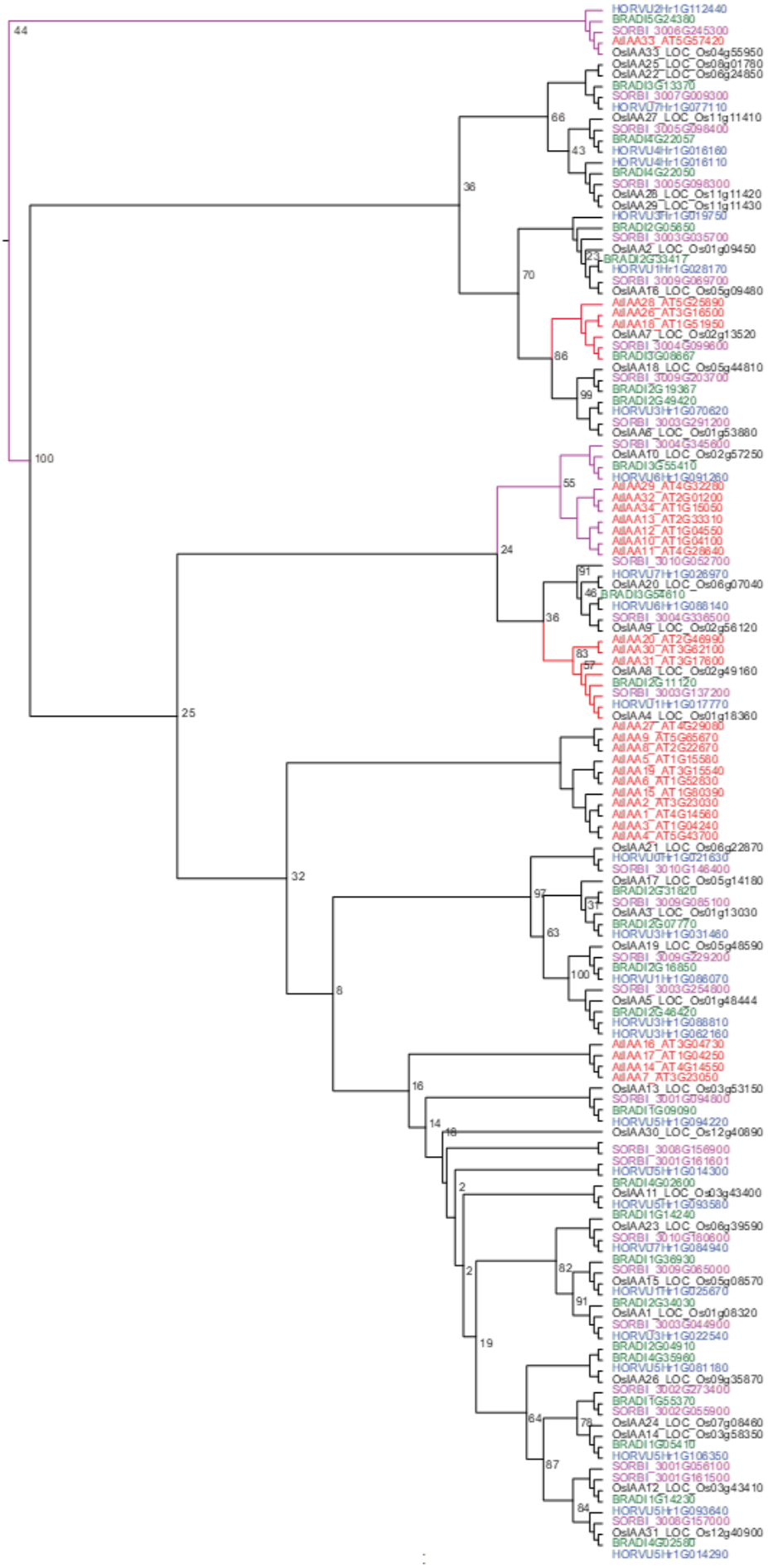
HORVU2Hr1G112440
BRADI5G24380
SORBI_3006G245300
AtIAA33_AT5G57420
OsIAA33_LOC_Os04g55950
OsIAA25_LOC_Os08g01780
OsIAA22_LOC_Os06g24850
BRADI3G13370
SORBI_3007G009300
HORVU7Hr1G077110
OsIAA27_LOC_Os11g11410
SORBI_3005G098400
BRADI4G22057
HORVU4Hr1G016160
HORVU4Hr1G016110
BRADI4G22050
SORBI_3005G098300
OsIAA28_LOC_Os11g11420
OsIAA29_LOC_Os11g11430
HORVU3Hr1G019750
BRADI2G05650
SORBI_3003G035700
OsIAA2_LOC_Os01g09450
BRADI2G33417
HORVU1Hr1G028170
SORBI_3009G069700
OsIAA16_LOC_Os05g09480
AtIAA28_AT5G25890
AtIAA26_AT3G16500
AtIAA18_AT1G51950
OsIAA7_LOC_Os02g13520
SORBI_3004G099600
BRADI3G08667
OsIAA18_LOC_Os05g44810
SORBI_3009G203700
BRADI2G19367
BRADI2G49420
HORVU3Hr1G070620
SORBI_3003G291200
OsIAA6_LOC_Os01g53880
SORBI_3004G345600
OsIAA10_LOC_Os02g57250
BRADI3G55410
HORVU6Hr1G091260
AtIAA29_AT4G32280
AtIAA32_AT2G01200
AtIAA34_AT1G15050
AtIAA13_AT2G33310
AtIAA12_AT1G04550
AtIAA10_AT1G04100
AtIAA11_AT4G28640
SORBI_3010G052700
HORVU7Hr1G026970
OsIAA20_LOC_Os06g07040
BRADI3G54610
HORVU6Hr1G088140
SORBI_3004G336500
OsIAA9_LOC_Os02g56120
AtIAA20_AT2G46990
AtIAA30_AT3G62100
AtIAA31_AT3G17600
OsIAA8_LOC_Os02g49160
BRADI2G11120
SORBI_3003G137200
HORVU1Hr1G017770
OsIAA4_LOC_Os01g18360
AtIAA27_AT4G29080
AtIAA9_AT5G65670
AtIAA8_AT2G22670
AtIAA5_AT1G15580
AtIAA19_AT3G15540
AtIAA6_AT1G52830
AtIAA15_AT1G80390
AtIAA2_AT3G23030
AtIAA1_AT4G14560
AtIAA3_AT1G04240
AtIAA4_AT5G43700
OsIAA21_LOC_Os06g22870
HORVU0Hr1G021630
SORBI_3010G146400
OsIAA17_LOC_Os05g14180
BRADI2G31820
SORBI_3009G085100
OsIAA3_LOC_Os01g13030
BRADI2G07770
HORVU3Hr1G031460
OsIAA19_LOC_Os05g48590
SORBI_3009G229200
BRADI2G16850
HORVU1Hr1G086070
SORBI_3003G254800
OsIAA5_LOC_Os01g48444
BRADI2G46420
HORVU3Hr1G088810
HORVU3Hr1G062160
AtIAA16_AT3G04730
AtIAA17_AT1G04250
AtIAA14_AT4G14550
AtIAA7_AT3G23050
OsIAA13_LOC_Os03g53150
SORBI_3001G094800
BRADI1G09090
HORVU5Hr1G094220
OsIAA30_LOC_Os12g40890
SORBI_3008G156900
SORBI_3001G161601
HORVU5Hr1G014300
BRADI4G02600
OsIAA11_LOC_Os03g43400
HORVU5Hr1G093580
BRADI1G14240
OsIAA23_LOC_Os06g39590
SORBI_3010G180600
HORVU7Hr1G084940
BRADI1G36930
SORBI_3009G065000
OsIAA15_LOC_Os05g08570
HORVU1Hr1G025670
BRADI2G34030
OsIAA1_LOC_Os01g08320
SORBI_3003G044900
HORVU3Hr1G022540
BRADI2G04910
BRADI4G35960
HORVU5Hr1G081180
OsIAA26_LOC_Os09g35870
SORBI_3002G273400
BRADI1G55370
SORBI_3002G355900
OsIAA24_LOC_Os07g08460
OsIAA14_LOC_Os03g58350
BRADI1G05410
HORVU5Hr1G106350
SORBI_3001G056100
SORBI_3001G161500
OsIAA12_LOC_Os03g43410
BRADI1G14230
HORVU5Hr1G093640
SORBI_3008G157000
OsIAA31_LOC_Os12g40900
BRADI4G02580
HORVU5Hr1G014290

Figure 5: Phylogenetic analysis of the Aux/IAA family from rice, sorghum, Brachypodium, barley and Arabidopsis. See Figure 4 legend for construction details. The full-length Aux/IAA gene RAXML tree produced a number of poorly supported nodes with and without partitioning codon position. Because of this, the gene sequence coding for just the PFAM (PF02309) associated with the gene family was extracted and used in a translation alignment. A RAXML tree without codon partitioning was created. A marginal improvement in bootstrap support values was achieved. Red clades are “well supported” and purple clades are poorly supported.

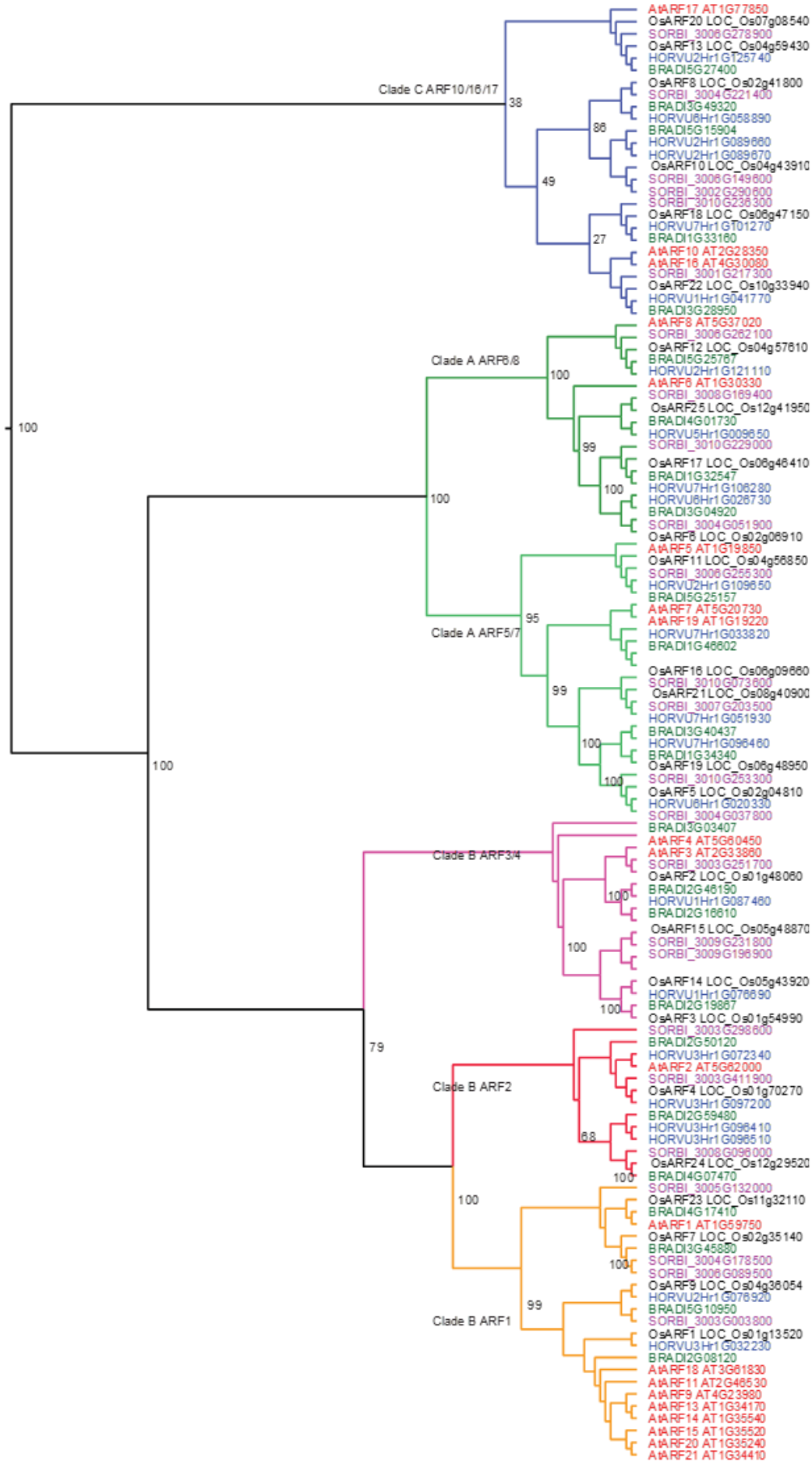
Clade C ARF10/16/17
Clade A ARF6/8
Clade A ARF5/7
Clade B ARF3/4
Clade B ARF2
Clade B ARF1
AtARF17 AT1G77850
OsARF20 LOC_Os07g08540
SORBI_3006G278900
OsARF13 LOC_Os04g59430
HORVU2Hr1GT25740
BRADI5G27400
OsARF8 LOC_Os02g41800
SORBI_3004G221400
BRADI3G49320
HORVU6Hr1G058890
BRADI5G15904
HORVU2Hr1G089660
HORVU2Hr1G089670
OsARF10 LOC_Os04g43910
SORBI_3006G149600
SORBI_3002G290600
SORBI_3010G236300
OsARF18 LOC_Os06g47150
HORVU7Hr1GT01270
BRADI1G33160
AtARF10 AT2G28350
AtARF16 AT4G30080
SORBI_3001G217300
OsARF22 LOC_Os10g33940
HORVU1Hr1G041770
BRADI3G28950
AtARF8 AT5G37020
SORBI_3006G262100
OsARF12 LOC_Os04g57610
BRADI5G25767
HORVU2Hr1G121110
AtARF6 AT1G30330
SORBI_3008G169400
OsARF25 LOC_Os12g41950
BRADI4G01730
HORVU5Hr1G009650
SORBI_3010G229000
OsARF17 LOC_Os06g46410
BRADI1G32547
HORVU7Hr1G106280
HORVU6Hr1G026730
BRADI3G04920
SORBI_3004G051900
OsARF6 LOC_Os02g06910
AtARF5 AT1G19850
OsARF11 LOC_Os04g56850
SORBI_3006G255300
HORVU2Hr1G109650
BRADI5G25157
AtARF7 AT5G20730
AtARF19 AT1G19220
HORVU7Hr1G033820
BRADI1G46602
OsARF16 LOC_Os06g09660
SORBI_3010G073600
OsARF21 LOC_Os08g40900
SORBI_3007G203500
HORVU7Hr1G051930
BRADI3G40437
HORVU7Hr1G096460
BRADI1G34340
OsARF19 LOC_Os06g48950
SORBI_3010G253300
OsARF5 LOC_Os02g04810
HORVU6Hr1G020330
SORBI_3004G037800
BRADI3G03407
AtARF4 AT5G60450
AtARF3 AT2G33860
SORBI_3003G251700
OsARF2 LOC_Os01g48060
BRADI2G46190
HORVU1Hr1G087460
BRADI2G16610
OsARF15 LOC_Os05g48870
SORBI_3009G231800
SORBI_3009G196900
OsARF14 LOC_Os05g43920
HORVU1Hr1G076690
BRADI2G19867
OsARF3 LOC_Os01g54990
SORBI_3003G298600
BRADI2G50120
HORVU3Hr1G072340
AtARF2 AT5G62000
SORBI_3003G411900
OsARF4 LOC_Os01g70270
HORVU3Hr1G097200
BRADI2G59480
HORVU3Hr1G096410
HORVU3Hr1G096510
SORBI_3008G096000
OsARF24 LOC_Os12g29520
BRADI4G07470
SORBI_3005G132000
OsARF23 LOC_Os11g32110
BRADI4G17410
AtARF1 AT1G59750
OsARF7 LOC_Os02g35140
BRADI3G45880
SORBI_3004G178500
SORBI_3006G089500
OsARF9 LOC_Os04g36054
HORVU2Hr1G078920
BRADI5G10950
SORBI_3003G003800
OsARF1 LOC_Os01g13520
HORVU3Hr1G032230
BRADI2G08120
AtARF18 AT3G61830
AtARF11 AT2G46530
AtARF9 AT4G23980
AtARF13 AT1G34170
AtARF14 AT1G35540
AtARF15 AT1G35520
AtARF20 AT1G35240
AtARF21 AT1G34410
100
38
86
49
27
100
100
99
100
95
99
100
100
100
79
100
100
100
100
68
100
100
99

Figure 6: Phylogenetic analysis of the ARF family from rice, sorghum, Brachypodium, barley and Arabidopsis. See Fig 4 legend for construction details. Different clades are indicated (Finet et al., 2012) that generally separate activators (Clade A) from repressors (Clades B and C).

Appendix IV

Candidature Milestones

ꕥ • ꕥ

Date	Milestone
December 2014	Offered and Accepted a University of Adelaide Divisional Scholarship
	Offered and Accepted a GRDC Grains Industry Research Scholarship
January 2015	Admitted into PhD program at The University of Adelaide
February 2015	Started PhD
August 2015	Completed the "Core Component of the Structured Program"
September 2015	Volunteered with the School of Agriculture, Food and Wine at the Royal Adelaide Show
November 2015	Poster presentation at the ARC Centre of Excellence in Plant Cell Walls Centre Retreat. Adelaide, Australia
February 2016	Completed the "Major Review of Progress for Doctoral Programs"
March 2016	Presentation at the GRDC Barley Breeders Meeting. Adelaide, Australia
	Presentation at the ARC Centre of Excellence in Plant Cell Walls Centre Meeting. Melbourne, Australia
June 2016	Poster presentation at the 12th International Barley Genetics Symposium. Minneapolis, Minnesota USA
July 2016	Started Volunteering for the Why Waite outreach program
September 2016	Volunteered with Why Waite and the School of Agriculture, Food and Wine at the Royal Adelaide Show
	Presentation at the School of Agriculture, Food and Wine 2016 Post-Graduate Symposium. Adelaide, Australia
	Awarded the ARC Centre of Excellence in Plant Cell Walls prize for Best Presentation in Plant Cell Biology
	Speaker in the GRDC "Celebrating 25 years of Grains RD&E" video presented at the GRDC Gala dinner at the Australian National Arboretum in Canberra
October 2016	Poster presentation at the ARC Centre of Excellence in Plant Cell Walls Centre Retreat. Adelaide, Australia
November 2016	Poster presentation at the 6th Australia and New Zealand Society for Cell and Developmental Biology (ANZSCDB) Adelaide Meeting. Adelaide, Australia
	Awarded an Outstanding Student Poster Presentation Prize at the 6th ANZSCDB Adelaide Meeting. Adelaide, Australia
May 2017	Poster presentation at the University Council Lunch at Waite, Adelaide, Australia
August 2017	Presentation at the ARC Centre of Excellence in Plant Cell Walls Centre Meeting. Brisbane, Australia
September 2017	Poster presentation at the 18th Australian Barley Technical Symposium. Hobart, Australia
	Awarded a Poster Award at the 18th Australian Barley Technical Symposium. Hobart, Australia
October 2017	Poster presentation at COMBIO 2017. Adelaide, Australia
November 2017	Completed the "Pre-Submission Review"

December 2017	Volunteered at Science Alive with Why Waite and the School of Agriculture, Food and Wine
February 2018	Poster presentation at the GRDC Grains Research Update. Adelaide, Australia
	Invited to participate in the Environment Institute Leadership Development Program for Early Career Researchers at the University of Adelaide
April 2018	Presented an original Dragon's Den style research project pitch to a panel of industry leaders as part of the Environment Institute Leadership Development Program for Early Career Researchers
	Completed the Environment Institute Leadership Development Program for Early Career Researchers
July 2018	First research paper as first author accepted in Scientific Reports
September 2018	Submitted "Notification of Intention to Submit" to Adelaide Graduate Centre
November 2018	Submitted thesis to Adelaide Graduate Centre
	Thesis accepted and doctorate conferred